DE GRUYTER

Victor K. Andreev, Yuri A. Gaponenko,
Olga N. Goncharova, Vladislav V. Pukhnachev

MATHEMATICAL MODELS OF CONVECTION

2ND EDITION

STUDIES IN MATHEMATICAL PHYSICS 5

Victor K. Andreev, Yuri A. Gaponenko, Olga N. Goncharova, and Vladislav Pukhnachev
Mathematical Models of Convection

De Gruyter Studies in Mathematical Physics

Edited by
Michael Efroimsky, Bethesda, Maryland, USA
Leonard Gamberg, Reading, Pennsylvania, USA
Dmitry Gitman, São Paulo, Brazil
Alexander Lazarian, Madison, Wisconsin, USA
Boris Smirnov, Moscow, Russia

Volume 5

Victor K. Andreev, Yuri A. Gaponenko,
Olga N. Goncharova, and Vladislav Pukhnachev

Mathematical Models of Convection

2nd edition

DE GRUYTER

Physics and Astronomy Classification 2010
02.20.Sv, 02.30.Hq, 02.30.Ik, 02.30.Jr, 02.30.Mv, 02.30.Nw, 47.10.ab, 47.10.ad, 47.11.Bc, 47.55.dm, 47.55.nb, 47.55.P-, 47.55.pb, 47.55.pd, 47.55.pf, 44.25.+f

Authors

Prof. Dr. Victor K. Andreev
Institute of Computational Modeling
SD RAS
Siberian Federal University
Akademgorodok Bld. 50
Krasnoyarsk 660036
Russian Federation
andr@icm.krasn.ru

Dr. Yuri A. Gaponenko
University Libre de Bruxelles
Microgravity Research Center
Avenue Franklin Roosevelt 50
1050 Brussels
Belgium
ygaponen@ulb.ac.be

Prof. Dr. Olga N. Goncharova
Altai State University
Institute of Mathematics and Information Technologies
Lenin Ave. 61
Barnaul 656049
Russian Federation
gon@math.asu.ru

Prof. Dr. Vladislav Pukhnachev
Lavrentyev Institute of Hydrodynamics
SD RAS
Novosibirsk State University
Lavrentyev Ave. 15
Nowosibirsk 630090
Russian Federation
pukhnachev@gmail.com

ISBN 978-3-11-065378-6
e-ISBN (PDF) 978-3-11-065546-9
e-ISBN (EPUB) 978-3-11-065394-6
ISSN 2194-3532

Library of Congress Control Number: 2020939559

Bibliographic information published by the Deutsche Nationalbibliothek
The Deutsche Nationalbibliothek lists this publication in the Deutsche Nationalbibliografie; detailed bibliographic data are available on the Internet at http://dnb.dnb.de.

Typesetting: VTeX UAB, Lithuania
Printing and binding: CPI books GmbH, Leck

www.degruyter.com

Contents

Preface —— ix

Preface to the second edition —— xv

1 Equations of fluid motion —— 1
1.1 Basic hypotheses of continuum —— **1**
1.2 Two methods for the continuum description. Translation formula —— **4**
1.3 Integral conservation laws. Equations of continuous motion —— **7**
1.4 Thermodynamics aspects —— **13**
1.5 Classical models of liquids and gases —— **16**

2 Conditions on the interface between fluids and on solid walls —— 25
2.1 Notion of the interface —— **25**
2.2 Kinematic condition —— **26**
2.3 Dynamic condition —— **26**
2.4 Elements of thermodynamics of the interface —— **32**
2.5 Conditions of continuity —— **34**
2.6 Energy transfer across the interface —— **36**
2.7 Free surfaces —— **40**
2.8 Additional conditions —— **42**

3 Models of convection of an isothermally incompressible fluid —— 45
3.1 Isothermally incompressible fluid —— **45**
3.2 Equations of thermal convection of an isothermally incompressible fluid —— **47**
3.3 Model of linear thermal expansion —— **48**
3.4 Some submodels —— **50**
3.5 On boundary conditions —— **51**
3.6 Two problems of convection —— **53**

4 Hierarchy of convection models in closed volumes —— 61
4.1 Initial relations —— **61**
4.2 Similarity criteria —— **63**
4.3 Transition to dimensional variables —— **65**
4.4 Expansion in the small parameter —— **68**
4.5 Equations of microconvection of an isothermally incompressible fluid —— **71**
4.6 Oberbeck–Boussinesq equations —— **74**
4.7 Linear model of the transitional process —— **75**
4.8 Some conclusions —— **78**

4.9 Convection of nonisothermal liquids and gases under microgravity conditions —— **81**
4.10 Convection of a thermally inhomogeneous weakly compressible fluid —— **88**
4.11 Exact solutions in an infinite band —— **92**
4.12 Analysis of well-posedness of the initial-boundary problem for equations of convection of a weakly compressible fluid —— **104**

5 Invariant submodels of microconvection equations —— 113
5.1 Basic model and its group properties —— **113**
5.2 Optimal subsystems of the subalgebras Θ_1 and Θ_2, factor-systems, and some solutions —— **116**
5.3 On one steady solution of microconvection equations in a vertical layer —— **124**
5.4 Solvability of a nonstandard boundary-value problem —— **134**
5.5 Unsteady solution of microconvection equations in an infinite band —— **140**
5.6 Invariant solutions of microconvection equations that describe the motion with an interface —— **147**

6 Group properties of equations of thermodiffusion motion —— 153
6.1 Lie group of thermodiffusion equations —— **153**
6.2 Group properties of two-dimensional equations —— **169**
6.3 Invariant submodels and exact solutions of thermodiffusion equations —— **174**

7 Stability of equilibrium states in the Oberbeck–Boussinesq model —— 193
7.1 Convective instability of a horizontal layer with oscillations of temperature on the free boundary —— **193**
7.2 Instability of a liquid layers with an interface —— **201**
7.3 Convection in a rotating fluid layer under microgravity conditions —— **211**

8 Small perturbations and stability of plane layers in the microconvection model —— 221
8.1 Equations of small perturbations —— **221**
8.2 Stability of the equilibrium state of a plane layer with solid walls —— **225**
8.3 Emergence of microconvection in a plane layer with a free boundary —— **235**
8.4 Stability of a steady flow in a vertical layer —— **245**

9 Numerical simulation of convective flows under microgravity conditions — 257
9.1 Numerical methods used for calculations — **257**
9.2 Numerical study of unsteady microconvection in canonical domains with solid boundaries — **268**
9.3 Numerical study of steady microconvection in domains with free boundaries — **284**
9.4 Study of convection induced by volume expansion — **300**
9.5 Convection in miscible fluids — **320**

10 Convective flows in tubes and layers — 341
10.1 Group-theoretical nature of the Birikh solution and its generalizations — **341**
10.2 An axial convective flow in a rotating tube with a longitudinal temperature gradient — **349**
10.3 Unsteady analogs of the Birikh solutions — **357**
10.3.1 Introduction — **357**
10.3.2 Plane motion in a horizontal band — **358**
10.3.3 Layered motion of immiscible fluids — **361**
10.3.4 Unsteady axial convection in a rotating tube — **363**
10.3.5 Motion of immiscible fluids in a rotating tube — **364**
10.3.6 Three-dimensional analogs of the Birikh solution — **366**
10.3.7 On the Ostroumov solutions — **369**
10.3.8 Concluding remarks — **370**
10.4 Model of viscous layer deformation by thermocapillary forces — **371**
10.5 Convective flow in a horizontal channel with non-Newtonian surface rheology under time-dependent longitudinal temperature gradient — **394**
10.5.1 Formulation of the problem — **394**
10.5.2 Limiting steady flow — **397**
10.5.3 Unsteady convection — **398**

Bibliography — 401

Index — 413

Preface

Convection (originating from the Latin word *convectio*, which means delivery) is understood as displacements of macroscopic volumes of the fluid (gas or liquid), resulting in transfer of mass, heat, and other physical quantities. Two types of convection are distinguished: natural or free convection induced by medium inhomogeneity (gradients of temperature, density, and concentration) and forced convection induced by external mechanical actions on the medium (e. g., vibrations). Thus, owing to the presence of density gradients in the fluid, the potential gravitational energy transforms to the energy of motion under the action of buoyancy forces. Changes in fluid density can be caused by fluid heating or by the difference in concentration in mixtures, such as salt solutions. The importance of such flows cannot be overestimated. We can recall the circulation of air masses in the Earth atmosphere, which cannot be explained without taking into account convective motion induced by air heating by the Sun. On the Sun itself, free convection arises in the form of granulation, i. e., granular structures (granules) of the photosphere, which can be seen through a telescope. The granules have sizes from 500 to 1000 km and cover the entire solar disk; an individual granule forms and decomposes during 5–10 minutes. The development of space technologies gave rise to studies of thermocapillary convection or Marangoni convection. This convection arises because surface tension depends on temperature, which changes along the free boundary of the fluid or along the interface between two fluids. Under onground conditions, the Marangoni effect is usually localized in the vicinity of the free surface. In layers approximately 1 mm thick, however, thermocapillary convection becomes a dominating form of the convective fluid flow.

The range of problems dealing with flows that involve natural or free convection has been extended recently. Natural convection is one of the forms of macroscopic motion, which is intensely studied in modern basic research. Though observations and qualitative descriptions of natural convection date back to far–off times, the development of quantitative models was started at the end of the 19th century. Based on experimental and theoretical investigations of natural convection, it was identified as a separate field of fluid mechanics.

Natural convection mechanisms determine various processes that have numerous applications and a cognitive value. As high technologies were developed, the applied significance of results obtained increased. Achievements in studying natural convection are applied in power engineering, metallurgy, environmental science, meteorology, geo- and astrophysics, aeronautics and space engineering, chemistry, crystal physics, etc. Owing to the increased accuracy of measurements and detailed mathematical models, it is possible to pose and successfully solve new problems in this field, e. g., obtaining superpure materials under microgravity conditions.

In studying the fluid properties (it can be water, solution of a chemical reagent, or metal melt) it is necessary to examine its internal state. Thus, for a quiescent fluid, it

https://doi.org/10.1515/9783110655469-201

is important to formulate the laws of interaction of external factors capable of making the fluid lose its mechanical equilibrium stability under certain conditions. Problems of convection in liquids are of considerable interest for applications. The dynamics of flow structure development depends substantially on the boundary conditions or internal sources. Moreover, internal interfaces, chemical reaction fronts, heat fluxes, and admixtures can also exert significant effects.

The above-mentioned processes in the fluid are usually unsteady and nonlinear; for this reason, studying these phenomena involves many problems. The difficulties in experimental investigations of these problems are mainly caused by difficulties in reconstruction of conditions in which the phenomenon is observed, necessity of providing high-accuracy measurements in the entire examined region, and significant consumption of energy and other resources. Therefore, methods of mathematical modeling are now considered as an important alternative for studying an extremely wide range of convective flow problems.

It is also important to choose a correct mathematical model for studying a particular phenomenon. In this way, it is possible to determine in advance those problem parameters where particular processes prevail. For instance, the Oberbeck–Boussinesq model, which is often used to study natural convection problems, becomes inapplicable under microgravity conditions or in microscopic-scale problems.

Another important aspect is the methodology of examining the mathematical model proper. The development of numerical schemes and construction of optimal computational algorithms, as well as performing calculations of flows with a complicated internal structure should be directly related to analytical properties of model equations determining asymptotic and limiting solutions of general equations.

Convective flow modeling comprises a set of problems arising in predicting natural phenomena and dynamics of various engineering processes. Studying velocity fields near interfaces and in surface layers allows one to take into account temperature and admixture transfer and to determine the forms of the affecting factors. To describe such processes, one should use new mathematical models of thermal and concentration convection, where the density depends not only on temperature, but also on pressure and concentration. It was the main challenge of this book to perform a comprehensive study of convection origination mechanisms, flow structure, and flow stability to perturbations on the interface with due allowance for deformations of the interface itself. Let us give a brief outline of the book.

Chapter 1. *Equations of fluid motion.* The goal of this chapter is to formulate equations of fluid motion under the action of mass and internal forces, as well as heat sources. A number of formulas used in subsequent chapters are derived. As a whole, this chapter dealing with the basic notions of hydrodynamics is written to make the book consistent and logical.

Chapter 2. *Conditions on the interface between fluids and on the solid walls.* A problem of motion of two immiscible fluids with a common interface is formulated. Details of derivation of dynamic and energetic conditions from integral conservation laws are

given. An important notion of the free boundary and conditions on it are formulated. Additional conditions associated with the presence of solid walls and moving contact boundaries are discussed.

Chapter 3. *Models of convection of an isothermally incompressible fluid*. In this chapter, we consider convection in a situation where the viscosity and thermal conductivity coefficients are temperature-dependent, and the density is a function of temperature only. Based on the general thermodynamic relations, it is demonstrated that the specific volume is always a linear function of temperature if the specific heat is constant. Various possible formulations of initial-boundary problems for the system of equations obtained are discussed. It turns out that the velocity, pressure, and temperature fields at the initial time can be arbitrarily specified in the general case (they should only be consistent with the boundary conditions). If the small term with the derivative of pressure with respect to time in the energy equation is neglected, the initial pressure distribution cannot be specified arbitrarily. Moreover, it turns out that elastic properties of the container should be taken into account in the problem of convection in a closed volume, which allows the influence of the wall on the convective flows to be described correctly. Properties of some models that include deformations of the flow domain boundary are also considered.

Chapter 4. *Hierarchy of convection models in closed volumes*. Models that describe natural convection of the fluid in closed volumes with constant transfer coefficients are studied. A theorem of existence and uniqueness is proved for the microconvection model. Possible generalizations and corollaries of formulations of initial-boundary problems are discussed. Based on a hyposonic flow approximation, a comprehensive analysis of the influence of changes in thermophysical parameters as functions of temperature and pressure and the work of pressure forces on the formation of natural convection in a weakly nonisothermal medium under conditions of extremely small external forces is performed. The limits of applicability of the Oberbeck–Boussinesq approximation for the description of convection of this kind are determined. An asymptotically exact mathematical model for convection in weak force fields with allowance for small changes in medium properties is constructed. Unique solvability of the basic boundary-value problems is established, and the problem of local exact controllability is studied. A model of convection in a thermally nonuniformly weakly compressible fluid is presented, where all transfer coefficients are nonlinear functions. The local theorem of existence of the smooth solutions of the initial-boundary problem for the equations of convection of a weakly compressible fluid is proved. Exact solutions of the equations of convection of a weakly compressible fluid in an infinite band are constructed. For comparison, the trajectories of fluid particles predicted by the classical Oberbeck–Boussinesq model of convection and by the microconvection model are presented.

Chapter 5. *Invariant submodels of microconvection equations*. This chapter deals with group properties of the microconvection model equations. Optimal systems of the subalgebras Θ_1 and Θ_2 are constructed, and all factor-systems are given. For some of

them, initial-boundary problems are formulated and solved. The issue of invariance of conditions on the interface and on the free boundary is considered. Solvability of the non-standard initial-boundary problems of the microconvection equations is studied in the classes of Holder functions. The unsteady solutions of the microconvection equations in an infinite band are constructed.

Chapter 6. *Group properties of equations of thermodiffusion motion.* Group properties of equations of nonisothermal motion of binary mixtures are studied in this chapter. The basic Lie algebras and equivalence transformations are found, and the problem of group classification is solved. A classification of invariant solutions is performed: optimal systems of subalgebras of the first and second orders are constructed for an infinite-dimensional algebra of operators admitted by equations of plane motion. New classes of exact solutions and generalizations of the previously known solutions of equations of thermal diffusion motion are constructed. Subgroups of continuous transformations are identified, for which the conditions on the interface or on the free boundary remain invariant.

Chapter 7. *Stability of equilibrium states in the Oberbeck–Boussinesq model.* Conditions of origination of convective flows in layers with a free boundary, interface, and solid walls are considered in this chapter. A finite-thickness layer with a free upper boundary and a solid lower boundary is examined. The temperature of the lower boundary is assumed to be constant, and the temperature of the upper boundary varies periodically with time. As a result, an equilibrium temperature gradient, which is nonuniform over the layer thickness and periodic in time, is formed; the influence of this gradient is studied numerically. Convective stability of the equilibrium state of a system of two immiscible fluids with similar densities is studied. A generalized Boussinesq approximation is constructed, which allows interface deformations to be correctly taken into account. Stability of the equilibrium state of a system of two fluids in a horizontal layer with a vertical temperature gradient is investigated. The existence of several instability mechanisms is found: long-wave and cellular monotonic perturbations, and oscillatory perturbations. The influence of boundary deformability on instability characteristics is examined. It is demonstrated that an increase in deformability leads to a change in instability mechanisms. A problem of destabilization of a rotating fluid owing to a temperature gradient is considered.

Chapter 8. *Small perturbations and stability of plane layers in the microconvection model.* Equations of small perturbations of arbitrary motions of the fluid in the microconvection model are derived. Stability of the equilibrium state of a plane layer bounded by solid walls or by a solid wall and a free boundary is studied with the use of these equations. The asymptotic behavior of the complex decrement in the cases of long-wave and short-wave perturbations is found. Results obtained by solving the full spectral problem for a silicon melt are presented. In contrast to the classical Oberbeck–Boussinesq model, the perturbations in the problem considered here are nonmonotonic because the boundary-value problem is not self-adjoint. For small Boussinesq numbers, the spectrum of this problem is demonstrated to approximate the spectra of

the corresponding problems for a viscous heat-conducting fluid or for thermal gravitational convection with a finite Rayleigh number. Stability of steady flows in a plane layer with linear and exponential distributions of temperature across the layer is studied. The flows are found to be stable to long-wave perturbations. Neutral curves are constructed numerically, and critical Grashof numbers for a silicon melt are obtained. Instability in the microconvection model is shown to occur at lower values of the wave number. This effect is caused by fluid compressibility.

Chapter 9. *Numerical simulation of convective flows under microgravity conditions*. This chapter describes the basic numerical methods used to calculate convective flows. In addition, adaptation of these methods to convection models is considered. Based on the microconvection model, problems of the influence of unsteady and also spatially nonuniform heating in canonical domains with solid and free boundaries for a single-species fluid and for a binary fluid are considered. Typical flow structures, trajectories of particle motion, and kinematic parameters of particles are determined as functions of the fluid properties, boundary conditions, and computational domain geometry. Quantitative and qualitative differences in flow characteristics calculated within the framework of the classical model and the microconvection model of an isothermally incompressible fluid are confirmed. For miscible fluids, a problem of the influence of transitional zone thickness nonuniformity on convection formation is studied. This problem is considered in the full formulation and also for a model problem with a smaller spatial dimension. It is shown that initial perturbations of the thickness propagate along the entire transitional zone, which affects the flow structure and kinematic characteristics.

Chapter 10. *Convective flows in tubes and layers*. Solutions of equations of thermal gravitational and thermocapillary convection, which describe three-dimensional nonisothermal motions of the fluid, are constructed on the basis of the group-theoretical approach. The Oberbeck-Boussinesq equations admit solutions where the temperature and pressure are linear functions of one Cartesian coordinate, while all three components of velocity are independent of this coordinate. These solutions are interpreted as flows in infinitely long tubes with an arbitrary cross section. They generalize the known Birikh's solution of a plane problem of convection in a horizontal band. Another example of reduction of a three-dimensional problem to a two-dimensional one is the problem of an axial convective flow in a circular rotating tube with a streamwise temperature gradient and transverse gravity force. To use these solution for an approximate description of convection in finite-length tubes, with the tube length being much greater than its diameter, it is necessary to specify the flow rate through the tube cross section as a function of time. Thus, there arises an inverse problem, which is effectively solved in plane and axisymmetric cases. In the same cases, it is also possible to construct exact solutions of problems of a convective flow of a two-layer system of immiscible fluids. The thermocapillary effect on the interface is taken into account. The problem of deformation of a plane layer of a viscous incompressible fluid by thermocapillary forces is considered in the last section of this chapter. In this case, the

buoyancy forces are ignored, and the source of motion is a nonuniform distribution of temperature on the free boundaries of the layer. If the temperature is a quadratic function of the streamwise coordinates, the initial-boundary problem for the Navier-Stokes equations reduces to a one-dimensional problem with an unknown boundary for a system of integrodifferential parabolic equations. The last problem can be effectively studied by analytical and numerical methods.

By virtue of the facts discussed above, the book is appreciably different from previous books [10, 16, 42, 43, 45, 71, 140, 141, 149, 168] mainly dealing with only one aspect of convection.

This book is an appreciably enlarged version of the book [20] published in Russian in 2008. The English version has seven new sections and a considerably extended list of references.

Chapters 1, 3, 4 (Sections 4.9 and 4.10), 5 (Sections 5.1–5.3 and 5.6), 6, 7 (Sections 7.1 and 7.2), and 8 were written by V. K. Andreev; Chapter 9 (Sections 9.1, 9.4, and 9.5) were written by Yu. A. Gaponenko; Chapters 4 (Sections 4.11 and 4.12), 5 (Sections 5.4 and 5.5), and 9 (Sections 9.2 and 9.3) were written by O. N. Goncharova; Chapters 2, 4 (Sections 4.1–4.8), 7 (Section 7.3), and 10 were written by V. V. Pukhnachev.

The work on this book was supported by Grant No. 116 (2009–2011) of the Siberian Branch of the Russian Academy of Sciences.

Russian Academy of Sciences
Siberian Branch
Institute of Computational Modelling
Lavrentyev Institute of Hydrodynamics
Altai State University

Preface to the second edition

The first edition of the book "Mathematical Models of Convection" was published in 2012 (see [21] in the list of references). In the second edition, Section 10.5 is added to Chapter 10, the list of references is supplemented and noticed typos are corrected.

The recent experiments (Birikh et al. 2011, Mizev et al. 2011) showed that in narrow channels at a local surfactant egress onto the surface the Marangoni convection occurs only at a fairly high surfactant concentration gradient. The delay of the onset of the surface motion can also be observed, when thermocapillary convection is excited by a point heat source in a horizontal channel with a bounded free surface, if only its surface has not been thoroughly cleaned. The threshold nature of the convection onset is attributed to the presence of an uncontrolled surfactant film kept by the channel walls. In this connection, it seems helpful to develop the models of thermocapillary convection in the presence of a temperature gradient along the free surface with the threshold excitation of the convection flow. One of possible models of this phenomenon is presented in Section 10.5.

https://doi.org/10.1515/9783110655469-202

1 Equations of fluid motion

Equations of fluid motion under the influence of external and internal forces as well as of thermal sources are formulated. This area of continuum mechanics, which has long been a classical science, has been described in various textbooks [208, 225, 154, 64, 128]. This chapter briefly gives the basic notions of hydrodynamics, with the aim of makes the material presented in this book more concise.

1.1 Basic hypotheses of continuum

Continuum mechanics is actually based on three postulates:
1) the classical Newtonian mechanics is valid;
2) the classical thermodynamics is valid;
3) the continuity hypothesis is valid.

The first postulate implies that motion velocities are small compared to the light speed, and that the study is focused on macroscopic objects, the sizes of which are substantially greater than the microcosm size.

The second postulate implies that the medium in a certain vicinity of each point is in the thermodynamically equilibrium state or close to it; for this reason, the laws of classical thermodynamics can be applied.

The third postulate implies that the real medium with a discrete molecular structure is replaced by a model with a continuous distribution of matter over the volume considered. The possibility of this replacement is called the continuity hypothesis.

Elementary particle

Let us identify a certain volume of the medium $\delta\Omega$ bounded by the surface $\delta\Sigma$, and assume that this volume has a mass δm. The average density of the medium is $\varrho_{\text{av}} = \delta m/\delta\Omega$. If the volume $\delta\Omega$ is sufficiently large, then the average density depends on the volume value by virtue of medium inhomogeneity. As the volume $\delta\Omega$ decreases, the mass distribution becomes increasingly homogeneous, and ϱ_{av} gradually reaches a constant value. As soon as the linear size of this volume becomes commensurable with the molecule size, the average density again experiences violent oscillations [29], because it may contain different numbers of molecules. It is therefore necessary to define an elementary particle (or simply a particle). The size of such a particle should be negligibly small relative to characteristic scales of the phenomenon being studied, so that the volume-averaged characteristics of the medium could be considered to be constant. On the other hand, the particle size should be large enough for the molecular structure of the fluid to be ignored. What is meant in this case is an infinitely small volume of the medium which is effectively equal to zero. The particle definition formu-

https://doi.org/10.1515/9783110655469-001

lated above allows the value to be assigned at a certain point to continuum characteristics. A principal difference between an elementary particle shrunk to a point and a point in space should be noted: a *point* is a place in space, while a *particle* is a small portion of a material volume.

A set of the same particles remaining during their motion within one contour, surface, or volume is called a moving contour, a moving surface, or a moving volume, respectively.

Thus, using the continuity hypothesis as a basis for the mathematical description of material behavior (in a wide sense) means that the functions characterizing the state of the material should be sufficiently smooth, i. e., continuous and differentiable in space and time. Violations of continuity are admitted only at individual points, lines, or surfaces.

Density

Let us proceed to the definition of some basic quantities of continuum mechanics. The density of the medium at a given point is found as the limit (which exists in accordance with the continuity hypothesis):

$$\varrho = \lim_{\delta\Omega\to 0} \varrho_{\text{av}} = \lim_{\delta\Omega\to 0} \frac{\delta m}{\delta\Omega}. \tag{1.1}$$

Thus, density is a function of the variables $(x_1, x_2, x_3) = \mathbf{x} \in \mathbb{R}^3$ and time t. In the international system of units (SI), the dimension of density is $[\varrho] = \text{kg/m}^3$; engineering applications often involve the specific weight $\gamma = \varrho g$, where g is the acceleration due to gravity ($[\gamma] = \text{N/m}^3$).

Volume and surface forces

The forces acting on a continuous medium are classified into two types: *volume* and *surface* forces.

Volume (or mass) forces include, for example, gravity forces and inertial forces, in particular centrifugal forces. Mass forces of a different nature are not considered here. Volume forces act at each point of the elementary volume of the continuum.

Let $\delta\mathbf{f}$ be the principal vector of volume forces acting in the volume $\delta\Omega$. We then introduce the concept of the distribution density of volume forces in the form of the limit

$$\mathbf{f} = \lim_{\delta\Omega\to 0} \frac{\delta\mathbf{f}}{\varrho\delta\Omega} \tag{1.2}$$

and $\mathbf{f} = \mathbf{f}(\mathbf{x}, t)$. The dimension of $\mathbf{f}$ is the dimension of acceleration ($[\mathbf{f}] = \text{m/s}^2$); the weight is described by the equality $\mathbf{f} = \mathbf{g}$, where $\mathbf{g}$ is the acceleration due to gravity.

Surface forces are forces acting on a surface element (part of the boundary surface or any internal surface). Examples of surface forces are pressure forces, internal friction (viscosity) forces, and forces of contact interaction between bodies.

Let $\delta\mathbf{p}_n$ be the principal vector of forces applied from the medium to a certain small area $\delta\Sigma_n$ identified in the medium. The subscript n means that the force acts on the area $\delta\Sigma_n$ arbitrarily oriented in the medium rather than the force projection. Similar to eq. (1.2), surface forces are defined in terms of *stress*:

$$\mathbf{p}_n = \lim_{\delta\Sigma_n \to 0} \frac{\delta\mathbf{p}_n}{\delta\Sigma_n}. \tag{1.3}$$

A principal difference between the vectors $\mathbf{f}$ and $\mathbf{p}_n$ should be noted: the vector $\mathbf{f}$ is a one-valued vector function of space points and time, i. e., it forms a *vector field*, while the vector $\mathbf{p}_n$ takes an infinite number of values at each point in space, depending on the *orientation of the area* $\delta\Sigma_n$ to which this stress is applied; thus, *no vector field is formed*.

In accordance with the third Newton law (see Postulate 1), eq. (1.3) yields $\mathbf{p}_n = -\mathbf{p}_{-n}$. Following Cauchy, the dependence of the stress vector on the normal can be substantially refined. For this purpose, we consider an elementary volume in the form of a tetrahedron with three faces being parallel to the coordinate axes and the fourth face being arbitrarily oriented (Figure 1.1). The face areas are indicated by $\delta\Sigma_{x_1}$, $\delta\Sigma_{x_2}$, $\delta\Sigma_{x_3}$, and $\delta\Sigma_n$; the geometrical meaning is clear from the figure. The area orientation is uniquely determined by the unit normal $\mathbf{n} = (\cos(n, x_1)\cos(n, x_2), \cos(n, x_3))$; then, we have $\delta\Sigma_{x_1} = \cos(n, x_1)\delta\Sigma_n$, $\delta\Sigma_{x_2} = \cos(n, x_2)\delta\Sigma_n$, and $\delta\Sigma_{x_3} = \cos(n, x_3)\delta\Sigma_n$. Let the tetrahedron height from the point $\mathcal{M}$ onto $\delta\Sigma_n$ be ε; then, the tetrahedron volume is $\delta\Omega = \varepsilon\delta\Sigma_n/3$. Applying the second Newton law (Postulate 1) to the elementary volume $\delta\Omega$, we obtain the equation of motion

$$\frac{1}{3}\varepsilon\delta\Sigma_n\varrho\mathbf{a} = \frac{1}{3}\varepsilon\delta\Sigma_n\varrho\mathbf{f} + \mathbf{p}_n\delta\Sigma_n - \mathbf{p}_{x_1}\delta\Sigma_{x_1} - \mathbf{p}_{x_2}\delta\Sigma_{x_2} - \mathbf{p}_{x_3}\delta\Sigma_{x_3},$$

where $\mathbf{a}$ is the acceleration of the center of mass of the tetrahedron.

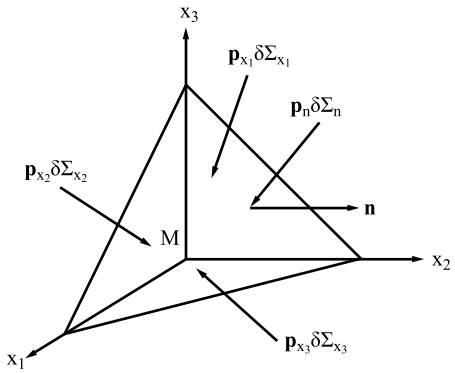

Figure 1.1: Elementary areas for mass point *M* with elementary forces.

Passing to the limit (as $\varepsilon \to 0$) in accordance with the continuity hypothesis, we obtain the following relation at the point M:

$$\mathbf{p}_n = \mathbf{p}_{x_1} \cos(n, x_1) + \mathbf{p}_{x_2} \cos(n, x_2) + \mathbf{p}_{x_3} \cos(n, x_3). \tag{1.4}$$

This is the Cauchy formula (derived in 1822), which states that the stresses on the faces form a system of mutually balancing stresses. Thus, eq. (1.4) yields

$$\mathbf{p}_n = \mathcal{P} \cdot \mathbf{n}, \tag{1.5}$$

where

$$\mathcal{P} = \begin{pmatrix} \mathcal{P}_{11} & \mathcal{P}_{12} & \mathcal{P}_{13} \\ \mathcal{P}_{21} & \mathcal{P}_{22} & \mathcal{P}_{23} \\ \mathcal{P}_{31} & \mathcal{P}_{32} & \mathcal{P}_{33} \end{pmatrix} \equiv (\mathbf{p}_{x_1}, \mathbf{p}_{x_2}, \mathbf{p}_{x_3}) \tag{1.6}$$

is the tensor of the second rank, which is called the *stress tensor*. Equations (1.4)–(1.6) mean that the stress state at an arbitrary point of a continuous medium is characterized by nine components $\mathcal{P}_{ij}$ $(i, j = 1, 2, 3)$.

1.2 Two methods for the continuum description. Translation formula

Let $(x_1, x_2, x_3) \in \mathbb{R}^3$ be a rectangular coordinate system, which is assumed to be inertial. An arbitrary triad of numbers (x_1, x_2, x_3) is identified with a point in space and is denoted by $\mathbf{x}$. Let us consider a particle moving together with the medium. Let this particle be located at the point $\boldsymbol{\xi} = (\xi_1, \xi_2, \xi_3)$ at the time $t = 0$, and at the point $\mathbf{x} = (x_1, x_2, x_3)$ at the time t. Therefore, the following mapping characterizing the medium motion is defined:

$$\mathbf{x} = \mathbf{x}(\boldsymbol{\xi}, t). \tag{1.7}$$

If $\boldsymbol{\xi}$ is fixed, then eq. (1.7) specifies the trajectory of the particle initially located at the point $\boldsymbol{\xi}$. On the other hand, for a fixed t, equality (1.7) determines the mapping of the area occupied by the medium at the initial time $t = 0$ to the area occupied by the medium at the time t.

The inverse mapping is assumed to exist:

$$\boldsymbol{\xi} = \boldsymbol{\xi}(\mathbf{x}, t). \tag{1.8}$$

It is assumed everywhere that $\mathbf{x}(\boldsymbol{\xi}, t)$ and $\boldsymbol{\xi}(\mathbf{x}, t)$ are sufficiently smooth vector functions of their arguments.

Remark 1.1. Instead of the Cartesian coordinates of the initial location of the point, it is possible to use any other curvilinear coordinates $\mathbf{a} = (a_1, a_2, a_3)$ related to $\boldsymbol{\xi} = (\xi_1, \xi_2, \xi_3)$ by the expression $\boldsymbol{\xi} = \boldsymbol{\xi}(\mathbf{a})$, with the transformation Jacobian being $\partial(\boldsymbol{\xi})/\partial(\mathbf{a}) \neq 0$.

The variables $(\boldsymbol{\xi}, t)$ (or $(\mathbf{a}, t)$) are called the *Lagrange variables*, and $(\mathbf{x}, t)$ are called the *Euler variables*. The motion descriptions in the Lagrange and Euler coordinates basically differ by the fact that x_1, x_2, and x_3 in the first case are the variable coordinates of moving fluid particles; in the second case, they are the coordinates of fixed points in space traversed by different fluid particles at a given time. In the Lagrangian description, the particle motion velocity $\mathring{\mathbf{v}}$ is expressed via the radius vector derivative as

$$\mathring{\mathbf{v}}(\boldsymbol{\xi}, t) = \frac{d\mathbf{x}(\boldsymbol{\xi}, t)}{dt} = \frac{\partial \mathbf{x}(\boldsymbol{\xi}, t)}{\partial t},$$

and the acceleration is expressed via the velocity derivative as

$$\mathring{\mathbf{w}}(\boldsymbol{\xi}, t) = \frac{d\mathring{\mathbf{v}}(\boldsymbol{\xi}, t)}{dt} = \frac{\partial^2 \mathbf{x}(\boldsymbol{\xi}, t)}{\partial t^2}.$$

During differentiation, the parameters ξ_1, ξ_2, and ξ_3 in these two formulas are fixed, $\mathbf{x}$ and $\mathring{\mathbf{v}}$ are functions of time only, and the differentiation operations d/dt and $\partial/\partial t$ are identical. If the vector function $\mathring{\mathbf{v}}(\boldsymbol{\xi}, t)$ is known, then the particle trajectories are found by using the quadrature

$$\mathbf{x} = \boldsymbol{\xi} + \int_0^t \mathring{\mathbf{v}}(\boldsymbol{\xi}, \tau)\, d\tau.$$

If the mapping (1.7) (and the inverse mapping (1.8)) is known, all functions $F(\mathbf{x}, t)$ of the Euler (Lagrange) variables can be expressed in the Lagrange (Euler) variables

$$F\big(\mathbf{x}(\boldsymbol{\xi}, t), t\big) = \mathring{F}(\boldsymbol{\xi}, t) \quad \big(\mathring{F}\big(\boldsymbol{\xi}(\mathbf{x}, t), t\big) = F(\mathbf{x}, t)\big).$$

Differentiating the first equality with respect to time, we obtain

$$\frac{\partial \mathring{F}}{\partial t} = \frac{\partial F}{\partial t} + \mathbf{v} \cdot \nabla F,$$

where $\mathbf{v}(\mathbf{x}, t) \equiv \mathring{\mathbf{v}}(\boldsymbol{\xi}(\mathbf{x}, t), t)$ is the velocity vector in the Euler variables and $\nabla = (\partial/\partial x_1, \partial/\partial x_2, \partial/\partial x_3)$ is the gradient operator. The differential operator over F is called the operator of *total differentiation with respect to time*, and the expression

$$\frac{dF}{dt} = \frac{\partial F}{\partial t} + \mathbf{v} \cdot \nabla F \tag{1.9}$$

is called the *total derivative* (also called *individual derivative*, *material derivative*, *substantial derivative*, *particle derivative*, and *derivative along the trajectory*) of the function $F(\mathbf{x}, t)$. In particular, at $F = x_i$, $i = 1, 2, 3$, eq. (1.9) yields

$$\frac{d\mathbf{x}}{dt} = \mathbf{v}(\mathbf{x}, t). \tag{1.10}$$

The total derivative of velocity with respect to time is acceleration. In the Euler variables, according to eq. (1.9), we have

$$w_i(\mathbf{x}, t) \equiv \frac{dv_i(\mathbf{x}, t)}{dt} = \frac{\partial v_i}{\partial t} + \mathbf{v} \cdot \nabla v_i,$$

or, in the invariant form,

$$\mathbf{w}(\mathbf{x}, t) = \frac{d\mathbf{v}(\mathbf{x}, t)}{dt} = \frac{\partial \mathbf{v}}{\partial t} + \mathbf{v} \cdot \nabla \mathbf{v}. \tag{1.11}$$

This means that the total acceleration $d\mathbf{v}/dt$ of the particle consists of two parts: *local acceleration* $\partial \mathbf{v}/\partial t$, caused by variations of velocity in time at this point, and *convective acceleration* $\mathbf{v} \cdot \nabla \mathbf{v}$, associated with inhomogeneity of the velocity field in the neighborhood of this point.

Let the velocity vector in eq. (1.10) be known as a function of the Euler coordinates. Then, eq. (1.10) transforms to a system of ordinary differential equations for x_1, x_2, and x_3. Supplementing the system with the initial data at $t = 0$

$$\mathbf{x} = \boldsymbol{\xi}, \tag{1.12}$$

we obtain the Cauchy problem whose solution determines the mapping (1.7) and, correspondingly, the particle trajectories.

Let us introduce the Jacobi matrix $M = \partial(\mathbf{x})/\partial(\boldsymbol{\xi})$ of the mapping (1.7) at a fixed value of t. By virtue of eqs. (1.10) and (1.12), it satisfies the linear Cauchy problem

$$\frac{dM}{dt} = \frac{\partial(\mathbf{v})}{\partial(\mathbf{x})} M, \quad M\big|_{t=0} = E, \tag{1.13}$$

where $\partial(\mathbf{v})/\partial(\mathbf{x})$ is a matrix with the elements $\partial v_i/\partial x_j$, $i, j = 1, 2, 3$, and E is a unit matrix. As the Jacobian of this matrix $J = \det M$ is the Vronsky determinant for system (1.13) [165], there follows the Euler formulas

$$\frac{dJ}{dt} = J \operatorname{div} \mathbf{v}, \tag{1.14}$$

because $Sp(\partial(\mathbf{v})/\partial(\mathbf{x})) = \operatorname{div} \mathbf{v}$.

A *moving* or *material* volume is understood as a volume ω_t consisting of the same particles for all $t \geq 0$; the volume ω_0 is the domain of variation of the Lagrange coordinates $\boldsymbol{\xi}$. For an arbitrary smooth function $F(\mathbf{x}, t)$, the integral

$$\int_{\omega_t} F \, d\omega$$

is a function of time. The *translation formula* yields an expression for the derivative of this function, namely,

$$\frac{d}{dt}\int\limits_{\omega_t} F\,d\omega = \int\limits_{\omega_t}\left(\frac{dF}{dt} + F\operatorname{div}\mathbf{v}\right)d\omega, \tag{1.15}$$

where dF/dt is the total derivative of F from eq. (1.9).

The proof of eq. (1.15) is based on passing to the Lagrange coordinates in the integral in the left-hand side by eq. (1.7). As a result, the domain of integration ω_t transforms to the domain ω_0, which is independent of time, and the integral takes the form

$$\int\limits_{\omega_0} \mathring{F}(\boldsymbol{\xi},t)\mathring{J}(\boldsymbol{\xi},t)\,d\omega_0.$$

Here, $\mathring{J}(\boldsymbol{\xi},t) = J(\mathbf{x}(\boldsymbol{\xi},t),t)$ is the Jacobian of the mapping (1.7) expressed in the Lagrange variables. The derivative of the integrand with respect to t, by virtue of eq. (1.14) and the definition of the total derivative (1.9) is

$$\frac{\partial}{\partial t}(\mathring{F}\mathring{J}) = \frac{d}{dt}(FJ) = \left(\frac{dF}{dt} + F\operatorname{div}\mathbf{v}\right)J.$$

The reverse transition from the Lagrange to the Euler variables yields equation (1.15).

1.3 Integral conservation laws. Equations of continuous motion

The most important characteristics of a material volume are its *mass*, *momentum*, *moment of momentum*, and *total energy*. Being additive functions of sets, these quantities in an arbitrary domain occupied by the medium $\Omega \subset \mathbb{R}^3$ have the form

$$M(\Omega) = \int\limits_{\Omega} \varrho\,d\Omega, \qquad \mathbf{K}(\Omega) = \int\limits_{\Omega} \varrho\mathbf{v}\,d\Omega,$$

$$\mathbf{H}(\Omega) = \int\limits_{\Omega} \varrho(\mathbf{x}\times\mathbf{v})\,d\Omega, \quad E(\Omega) = \int\limits_{\Omega} \varrho\left(\frac{|\mathbf{v}|^2}{2} + U\right)d\Omega,$$

where $\varrho(\mathbf{x},t)$ is the medium density, $\mathbf{v}(\mathbf{x},t)$ is the velocity vector, and $U(\mathbf{x},t)$ is the specific internal energy.

Let $\omega_t \subset \Omega$ be an arbitrary moving volume. The values of $\mathbf{K}$, $\mathbf{H}$, and E during the volume motion are changed under force and energy actions on the volume ω_t (the mass M remains unchanged). These actions are performed through the principal vector of forces

$$\mathbf{F}(\omega_t) = \int\limits_{\omega_t} \varrho\mathbf{f}\,d\omega + \int\limits_{\partial\omega_t} \mathbf{p}_n\,d\Sigma,$$

the principal moment of forces

$$\mathbf{G}(\omega_t) = \int\limits_{\omega_t} \varrho(\mathbf{x} \times \mathbf{f})\, d\omega + \int\limits_{\partial\omega_t} \mathbf{x} \times \mathbf{p}_n\, d\Sigma,$$

and the supplied power

$$N(\omega_t) = \int\limits_{\omega_t} \varrho \mathbf{v} \cdot \mathbf{f}\, d\omega + \int\limits_{\partial\omega_t} \mathbf{v} \cdot \mathbf{p}_n\, d\Sigma + \int\limits_{\partial\omega_t} q_n\, d\Sigma + \int\limits_{\omega_t} \varrho h\, d\omega.$$

Here, $\mathbf{f}(\mathbf{x}, t)$ and $\mathbf{p}_n(\mathbf{x}, t)$ are the densities of mass and surface forces; Σ is the piecewise smooth boundary of ω_t ($\Sigma = \partial\omega_t$), so that the normal vector $\mathbf{n}$ is determined almost at all points of this boundary; $q_n(\mathbf{x}, t)$ is the surface density of the heat flux incoming into the volume through $\partial\omega_t$; and $h(\mathbf{x}, t)$ is the volume density of internal (e. g., radioactive or chemical) heat sources.

The following equalities are valid in a moving continuous medium for an arbitrary moving volume ω_t:

$$\frac{d}{dt} M(\omega_t) = \frac{d}{dt} \int\limits_{\omega_t} \varrho\, d\omega = 0; \tag{1.16}$$

$$\frac{d}{dt} \mathbf{K}(\omega_t) = \frac{d}{dt} \int\limits_{\omega_t} \varrho \mathbf{v}\, d\omega = \int\limits_{\omega_t} \varrho \mathbf{f}\, d\omega + \int\limits_{\partial\omega_t} \mathbf{p}_n\, d\Sigma; \tag{1.17}$$

$$\frac{d}{dt} \mathbf{H}(\omega_t) = \frac{d}{dt} \int\limits_{\omega_t} \varrho(\mathbf{x} \times \mathbf{v})\, d\omega = \int\limits_{\omega_t} \varrho(\mathbf{x} \times \mathbf{f})\, d\omega + \int\limits_{\partial\omega_t} \mathbf{x} \times \mathbf{p}_n\, d\Sigma; \tag{1.18}$$

$$\begin{aligned} \frac{d}{dt} E(\omega_t) = \frac{d}{dt} \int\limits_{\omega_t} \varrho\left(\frac{|\mathbf{v}|^2}{2} + U\right) d\omega &= \int\limits_{\omega_t} \varrho(\mathbf{v} \times \mathbf{f})\, d\omega \\ &+ \int\limits_{\partial\omega_t} \mathbf{v} \times \mathbf{p}_n\, d\Sigma + \int\limits_{\partial\omega_t} q_n\, d\Sigma + \int\limits_{\omega_t} \varrho h\, d\omega. \end{aligned} \tag{1.19}$$

Each of these equalities is usually called the *law of conservation* of the corresponding mechanical quantity.

Generally speaking, it is not obligatory for the functions $\mathbf{p}_n$, q_n, $\mathbf{f}$, and h in the right-hand sides of eqs. (1.17)–(1.19) to be continuous, because this is not required for integral conservation laws to be valid. Nevertheless, the class of motions for which the basic quantities are rather smooth functions is of considerable interest for applications and can be studied using mathematical analysis tools. The medium motion is called *continuous* if the functions ϱ, U, $\mathbf{u}$, $\mathbf{p}_n$, and q_n are continuous and continuously differentiable and if the functions $\mathbf{f}$ and h are continuous within the domain of their definition. For such motions, the system of conservation laws (1.16)–(1.19) turns out to be equivalent to a system of differential equations. Indeed, under the assumption that

$F = \varrho$ in the translation formula (1.15), eq. (1.16) yields

$$\int_{\omega_t} \left(\frac{d\varrho}{dt} + \varrho \operatorname{div} \mathbf{v} \right) d\omega = 0.$$

By virtue of arbitrariness of the volume ω_t, we obtain the equality

$$\frac{d\varrho}{dt} + \varrho \operatorname{div} \mathbf{v} = 0, \tag{1.20}$$

which is called the *continuity equation*. It is equivalent to the law of mass conservation on the class of continuous motions. In turn, using eq. (1.20) we can substantially simplify eq. (1.15), and it takes the form (with the substitution $F \leftrightarrow \varrho F$)

$$\frac{d}{dt} \int_{\omega_t} \varrho F \, d\omega = \int_{\omega_t} \varrho \frac{dF}{dt} \, d\omega, \tag{1.21}$$

which is convenient for transformations of the left-hand sides of eqs. (1.17)–(1.19).

Let us now consider the momentum conservation law (1.17). To transform its left-hand side, we consecutively use eq. (1.21), assuming that $F = v_i$, $i = 1, 2, 3$ in this formula. The surface integral in the right-hand side is transformed by the Gauss–Ostrogradskii formula, based on equality (1.5) for the stress vector. As a result, we obtain

$$\int_{\omega_t} \varrho \frac{d\mathbf{v}}{dt} \, d\omega = \int_{\omega_t} (\operatorname{div} \mathcal{P} + \varrho \mathbf{f}) \, d\omega,$$

where $\operatorname{div} \mathcal{P}$ is the vector with the components

$$(\operatorname{div} \mathcal{P})_i = \sum_{j=1}^{3} \partial \mathcal{P}_{ij} / \partial x_j$$

(see eq. (1.6)). Taking into account the arbitrariness of ω_t, we obtain the equation

$$\varrho \frac{d\mathbf{v}}{dt} = \operatorname{div} \mathcal{P} + \varrho \mathbf{f}, \tag{1.22}$$

which is called the *momentum equation*.

For the integral law of conservation of the moment of momentum (1.18), the left-hand side by virtue of eq. (1.21), (1.10) is

$$\int_{\omega_t} \varrho \left(\mathbf{x} \times \frac{d\mathbf{v}}{dt} \right) d\omega.$$

To transform the surface integral in the right-hand side of eq. (1.18), we use the Cauchy formula (1.4) and the equality $\operatorname{div}\mathcal{P} = \partial\mathbf{p}_{x_1}/\partial x_1 + \partial\mathbf{p}_{x_2}/\partial x_2 + \partial\mathbf{p}_{x_3}/\partial x_3$. We obtain

$$\begin{aligned}
&\int_{\partial\omega_t} \mathbf{x}\times\mathbf{p}_n\, d\Sigma \\
&\quad= \int_{\partial\omega_t} \left[\cos(n,x_1)\mathbf{x}\times\mathbf{p}_{x_1} + \cos(n,x_2)\mathbf{x}\times\mathbf{p}_{x_2} + \cos(n,x_3)\mathbf{x}\times\mathbf{p}_{x_3}\right] d\Sigma \\
&\quad= \int_{\omega_t} \left[\frac{\partial}{\partial x_1}(\mathbf{x}\times\mathbf{p}_{x_1}) + \frac{\partial}{\partial x_2}(\mathbf{x}\times\mathbf{p}_{x_2}) + \frac{\partial}{\partial x_3}(\mathbf{x}\times\mathbf{p}_{x_3})\right] d\omega \\
&\quad= \int_{\partial\omega_t} \left(\mathbf{x}\times\operatorname{div}\mathcal{P} + \frac{\partial\mathbf{x}}{\partial x_1}\times\mathbf{p}_{x_1} + \frac{\partial\mathbf{x}}{\partial x_2}\times\mathbf{p}_{x_2} + \frac{\partial\mathbf{x}}{\partial x_3}\times\mathbf{p}_{x_3}\right) d\omega.
\end{aligned}$$

Therefore, the conservation law (1.18) takes the following form ($\partial\mathbf{x}/\partial x_1 = \mathbf{e}_1$, $\partial\mathbf{x}/\partial x_2 = \mathbf{e}_2$, $\partial\mathbf{x}/\partial x_3 = \mathbf{e}_3$, where $\mathbf{e}_1$, $\mathbf{e}_2$, and $\mathbf{e}_3$ are the unit orths along the x_1, x_2, and x_3 axes):

$$\int_{\omega_t} \left[\mathbf{x}\times\left(\varrho\frac{d\mathbf{v}}{dt} - \operatorname{div}\mathcal{P} - \varrho\mathbf{f}\right) - \mathbf{e}_1\times\mathbf{p}_{x_1} - \mathbf{e}_2\times\mathbf{p}_{x_2} - \mathbf{e}_3\times\mathbf{p}_{x_3}\right] d\omega = 0.$$

Taking into account eq. (1.22), we obtain the equality

$$\mathbf{e}_1\times\mathbf{p}_{x_1} + \mathbf{e}_2\times\mathbf{p}_{x_2} + \mathbf{e}_3\times\mathbf{p}_{x_3} = 0, \tag{1.23}$$

which is valid for all continuous media, independent of the character of application of volume forces. Projecting (1.23) onto the coordinate axes $\mathbf{e}_1$, $\mathbf{e}_2$, and $\mathbf{e}_3$, we verify the validity of the equalities

$$p_{x_1x_2} = p_{x_2x_1}, \quad p_{x_2x_3} = p_{x_3x_2}, \quad p_{x_3x_1} = p_{x_1x_3}, \tag{1.24}$$

($p_{x_1x_1}, p_{x_1x_2}, p_{x_1x_3}$ are the components of the vector $\mathbf{p}_{x_1}$; $p_{x_2x_1}, p_{x_2x_2}, p_{x_2x_3}$ are the components of the vector $\mathbf{p}_{x_2}$; $p_{x_3x_1}, p_{x_3x_2}, p_{x_3x_3}$ are the components of the vector $\mathbf{p}_{x_3}$).

Thus, the stress tensor is symmetric: $\mathcal{P} = \mathcal{P}^*$, $\mathcal{P}_{ij} = \mathcal{P}_{ji}$. Obviously, it is possible to obtain the conservation law (1.18) by applying the inverse transformations to eq. (1.24). In other words, in a continuous medium that has no other internal moments, the *law of conservation of the moment of momentum* (1.18) *is equivalent to stress tensor symmetry*.

The quantities $p_{x_1x_1} = \mathcal{P}_{11}$, $p_{x_2x_2} = \mathcal{P}_{22}$, and $p_{x_3x_3} = \mathcal{P}_{33}$ are called *normal stresses*, and $p_{x_1x_2} = \mathcal{P}_{12}$, $p_{x_2x_3} = \mathcal{P}_{23}$, $p_{x_3x_1} = \mathcal{P}_{31}$, ... are called *shear stresses*.

The essence of equalities (1.24) is the content of the so-called theorem on reciprocation of shear stresses. Now we have

$$(\operatorname{div}\mathcal{P})_i = \sum_{j=1}^{3} \partial\mathcal{P}_{ij}/\partial x_j = \sum_{j=1}^{3} \partial\mathcal{P}_{ji}/\partial x_j,$$

i. e., the order of the subscripts in the coordinate form $\operatorname{div}\mathcal{P}$ is irrelevant.

Let us consider the Cauchy equality (1.4) for the case with no shear stresses, i. e., $\mathcal{P}_{ij} = 0$, $i \neq j$. Then, we obtain $p_{nx_j} = \mathcal{P}_{jj}\cos(n, x_j)$; on the other hand, we have $p_{nx_j} = \mathbf{p}_n \cdot \mathbf{e}_j = p_n \cos(n, x_j)$, where p_n is the projection of the stress vector onto the normal to the area considered. Comparing these formulas, we obtain $\mathcal{P}_{11} = \mathcal{P}_{22} = \mathcal{P}_{33} = p_n$. Let us introduce the notion of *pressure* $p(\mathbf{x}, t)$ in accordance with the equalities

$$p = -p_n = -\mathcal{P}_{11} = -\mathcal{P}_{22} = -\mathcal{P}_{33}.$$

If there are no shear stress, the pressure at a point is a scalar quantity, i. e., it is independent of the orientation of the area passing through the point $M(x_1, x_2, x_3)$. The minus sign means that the pressure considered here is the compressive pressure. The dimension of pressure in the SI system is $[p] = \mathrm{N/m^2}$, $1\,\mathrm{N/m^2} = 1\,\mathrm{Pa}$ (one pascal). Other units of pressure are also used, for instance $1\,\mathrm{kg \cdot s/m^2} = 9.80665\,\mathrm{Pa} \approx 10\,\mathrm{Pa}$, $1\,\mathrm{atm} = 101{,}325\,\mathrm{Pa} \approx 0.1\,\mathrm{MPa}$, $1\,\mathrm{bar} = 10^5\,\mathrm{Pa}$, $1\,\mathrm{mmHg} \approx 133\,\mathrm{Pa}$, $1\,\mathrm{mmH_2O} \approx 10\,\mathrm{Pa}$, as well as multiple and fractional units derived from the pascal: gigapascal ($1\,\mathrm{GPa} = 10^9\,\mathrm{Pa}$), megapascal ($1\,\mathrm{MPa} = 10^6\,\mathrm{Pa}$), kilopascal ($1\,\mathrm{kPa} = 10^3\,\mathrm{Pa}$), millipascal ($1\,\mathrm{mPa} = 10^{-3}\,\mathrm{Pa}$), and picopascal ($1\,\mathrm{pPa} = 10^{-12}\,\mathrm{Pa}$).

Remark 1.2. Continuous media with $\mathcal{P} = -pI$ (I is the unit tensor, $I_{ij} = \delta_{ij}$) are called the *ideal* media.

Using eqs. (1.21), the property of symmetry of the tensor $\mathcal{P}$, and the formulas

$$\int\limits_{\partial\omega_t} \mathbf{v} \cdot \mathbf{p}_n \, d\Sigma = \int\limits_{\partial\omega_t} \mathcal{P}\mathbf{v} \cdot \mathbf{n} \, d\Sigma = \int\limits_{\omega_t} \operatorname{div}(\mathcal{P}\mathbf{v}) \, d\omega,$$

$$\operatorname{div}(\mathcal{P}\mathbf{v}) \equiv \mathbf{v} \cdot \operatorname{div}\mathcal{P} + \mathcal{P} : \mathcal{D},$$

we can write the energy conservation law (1.19) in the form

$$\int\limits_{\omega_t} \varrho\left(\mathbf{v} \cdot \frac{d\mathbf{v}}{dt} + \frac{dU}{dt}\right) d\omega = \int\limits_{\omega_t} (\mathbf{v} \cdot \operatorname{div}\mathcal{P} + \mathcal{P} : \mathcal{D}) \, d\omega + \int\limits_{\omega_t} \varrho\mathbf{v} \cdot \mathbf{f} \, d\omega + \int\limits_{\partial\omega_t} q_n \, d\Sigma + \int\limits_{\omega_t} \varrho h \, d\omega.$$

Using the momentum equation (1.22), we can simplify the previous equality to

$$\int\limits_{\omega_t} \varrho \frac{dU}{dt} \, d\omega = \int\limits_{\omega_t} \mathcal{P} : \mathcal{D} \, d\omega + \int\limits_{\partial\omega_t} q_n \, d\Sigma + \int\limits_{\omega_t} \varrho h \, d\omega, \tag{1.25}$$

where $\mathcal{D}$ is the so-called *strain rate tensor* with the elements

$$\mathcal{D}_{ij} = \frac{1}{2}\left(\frac{\partial v_i}{\partial x_j} + \frac{\partial v_j}{\partial x_i}\right), \quad i, j = 1, 2, 3. \tag{1.26}$$

Researchers often write $\mathcal{D}(\mathbf{v})$ to emphasize its dependence on the velocity vector. The expression $\mathcal{P} : \mathcal{D}$ is called the *convolution of the tensors* $\mathcal{P}$ and $\mathcal{D}$; it has the form

$$\mathcal{P} : \mathcal{D} \equiv \sum_{j=1}^{3} \mathcal{P}_{ij}\mathcal{D}_{ij}. \tag{1.27}$$

The conservation law (1.25) can be written as

$$\int\limits_{\partial\omega_t} q_n \, d\Sigma = \int\limits_{\omega_t} \psi \, d\omega, \tag{1.28}$$

where $\psi = \varrho \, dU/dt - \mathcal{P} : \mathcal{D} - \varrho h$. The density of the heat flux q_n is a function of the variables $\mathbf{x}$, t, and the normal $\mathbf{n}$; we assume that $q_n = q(\mathbf{x}, t, \mathbf{n})$. Let us first demonstrate that $q(\mathbf{x}, t, \mathbf{n}) = -q(\mathbf{x}, t, -\mathbf{n})$. As the domain ω_t has an arbitrary shape, we choose ω_t in the form of a sphere with the center $M(x_1, x_2, x_3)$, having a small radius ε. The plane passing through the point M orthogonally to the vector $\mathbf{n}$ divides this sphere into two hemispheres, ω_{1t} and ω_{2t}, with $\mathbf{n}$ being directed toward ω_{2t}.

Let K_ε be a circle obtained in the section. We apply equality (1.28) to the volumes ω_{1t}, ω_{2t}, and ω_t:

$$\begin{gathered}
\int\limits_{\partial\omega_{1t}} q(\mathbf{x}, t, \mathbf{n}) \, d\Sigma + \int\limits_{K_\varepsilon} q(\mathbf{x}, t, -\mathbf{n}) \, d\Sigma = \int\limits_{\omega_{1t}} \psi \, d\omega, \\
\int\limits_{\partial\omega_{2t}} q(\mathbf{x}, t, \mathbf{n}) \, d\Sigma + \int\limits_{K_\varepsilon} q(\mathbf{x}, t, \mathbf{n}) \, d\Sigma = \int\limits_{\omega_{2t}} \psi \, d\omega, \\
\int\limits_{\partial\omega_{1t} \cup \partial\omega_{2t}} q(\mathbf{x}, t, \mathbf{n}) \, d\Sigma = \int\limits_{\omega_{1t}} \psi \, d\omega
\end{gathered}$$

($\partial\omega_{1t}$ and $\partial\omega_{2t}$ are the hemisphere surfaces, and $\partial\omega_{1t} \cup \partial\omega_{2t} = \partial\omega_t$). By adding the first two equalities and subtracting the third one, we obtain

$$\int\limits_{K_\varepsilon} \left[q(\mathbf{x}, t, \mathbf{n}) + q(\mathbf{x}, t, -\mathbf{n}) \right] d\Sigma = 0.$$

Therefore, by virtue of the continuity of the scalar field q on K_ε, it should be $q(\mathbf{x}, t, \mathbf{n}) = -q(\mathbf{x}, t, -\mathbf{n})$ at point M.

Let us now assume that ω_t is a tetrahedron (see Figure 1.1). With the same notation, equality (1.28) yields the relation

$$\begin{aligned}
&\int\limits_{\delta\Sigma_n} q(\mathbf{x}, t, \mathbf{n}) \, d\Sigma + \int\limits_{\delta\Sigma_{x_1}} q(\mathbf{x}, t, -\mathbf{e}_1) \, d\Sigma \\
&\qquad + \int\limits_{\delta\Sigma_{x_2}} q(\mathbf{x}, t, -\mathbf{e}_2) \, d\Sigma + \int\limits_{\delta\Sigma_{x_3}} q(\mathbf{x}, t, -\mathbf{e}_3) \, d\Sigma = \int\limits_{\omega_t} \psi \, d\omega.
\end{aligned}$$

By virtue of the continuity of the integrands, the integrals on the left have the order of ε^2, and the integrals on the right have the order of ε^3 as $\varepsilon \to 0$. Therefore, the following equality is valid at point M (the formulas $\delta\Sigma_{x_j} = \cos(n, x_j)\delta\Sigma_n$ are taken into account): $q(\mathbf{x}, t, \mathbf{n}) = q(\mathbf{x}, t, \mathbf{e}_1)\cos(n, x_1) + q(\mathbf{x}, t, \mathbf{e}_2)\cos(n, x_2) + q(\mathbf{x}, t, \mathbf{e}_3)\cos(n, x_3)$. In other words, there exists a vector field $\mathbf{q}(\mathbf{x}, t)$ such that

$$q_n = -\mathbf{q} \cdot \mathbf{n}. \tag{1.29}$$

The vector $\mathbf{q}$ is called the *heat flux vector*. The minus sign is used for the vector $\mathbf{q}$ to show the real direction of thermal energy transfer, because $\mathbf{n}$ is the orth of the external normal to the boundary $\partial\omega_t$ of the volume to which the heat flux with the surface density $\mathbf{q}$ is *inserted*. Assuming again in eq. (1.25) that ω_t is an arbitrary material volume, and taking into account eq. (1.29), we obtain the heat inflow equation

$$\varrho\frac{dU}{dt} = \mathcal{P} : \mathcal{D} - \operatorname{div}\mathbf{q} + \varrho h. \tag{1.30}$$

Remark 1.3. The reasoning used above could have also been applied for the derivation of the Cauchy formula (1.4) from the integral law of conservation of momentum (1.17) [225, 154, 64].

The system of eqs. (1.20), (1.22), (1.30) forms the mathematical model for continuous motions of a continuous medium. This model is not closed, because it contains five scalar equations and fourteen (with allowance for symmetry of the stress tensor $\mathcal{P}$) sought functions: ϱ, v_1, v_2, v_3, $\mathcal{P}_{11}$, $\mathcal{P}_{12}$, $\mathcal{P}_{13}$, $\mathcal{P}_{22}$, $\mathcal{P}_{23}$, $\mathcal{P}_{33}$, U, q_1, q_2, and q_3. The mass densities of the external forces $\mathbf{f}$ and the volume heat sources h are assumed to be specified functions; therefore, the problem of "closing" the model arises, which should be solved by analyzing additional information.

1.4 Thermodynamics aspects

Taking into account the thermal energy in model (1.20), (1.22), (1.30) requires application of thermodynamic laws (in the case considered, it would be more exact to say "thermostatic laws"). Thermodynamics deals with relation between thermal energy and other types of energy, firstly with mechanical energy, and establishes the laws of mutual conversion of one type of energy into another.

The basic concept of thermodynamics is the notion of the *state* of the medium. The phenomenological description of the state is given on the basis of the *state parameters*. Such parameters are, for example, the specific internal energy U and the density ϱ (or specific volume $V = 1/\varrho$). Apart from these, other frequently-used state parameters are the *absolute temperature* θ, *specific entropy* s, and pressure p. In the SI system, the temperature is expressed in kelvins, K, $\theta\,\mathrm{K} = 273{,}15 + \theta\,^{\circ}\mathrm{C}$; the entropy dimension is $[s] = \mathrm{J}/(\mathrm{kg}\cdot\mathrm{K})$. Sometimes, it is convenient to use the components of the stress tensor $\mathcal{P}$ or some other quantities as the state parameters. If the set of the state parameters

characterizing a certain medium is already established, the next task is to determine all possible relations between these parameters. These relations should follow from the general physical laws and empirical features which determine the behavior of the examined medium.

Let $Z = (z^1, z^2, \ldots)$ be a set of characteristic state parameters z^k for a certain medium. The set of all admissible values of Z forms the *state space*. The dimension ν of this space equals the minimum number of parameters determining the state of the medium. The medium is called a one-parameter medium if $\nu = 1$, a two-parameter medium if $\nu = 2$, etc.

Two states Z_1 and Z_2 can be connected by directed curves (paths) $l(Z_1, Z_2)$ passing from Z_1 to Z_2. If the states on the curve are physically feasible in principle, then these paths are called the *processes*. The process $l(Z_1, Z_2)$ called *reversible* if the path $l(Z_2, Z_1)$ lying on the same curve is also a process. Otherwise, the process $l(Z_1, Z_2)$ is called *irreversible*.

The thermal energy Q (or the *amount of heat*), defined as the energy of random motion of molecules, is, generally speaking, not a state parameter. It depends on the process $l(Z_1, Z_2)$ transforming the medium from Z_1 to Z_2. If we consider differentiable processes transforming the medium from the state Z to $Z + dZ$, then the amount of heat in this elementary process is calculated

$$\delta Q = \sum_k B_k(Z)\, dz^k.$$

Here, the process-dependence on the path is manifested in the fact that the right-hand side is not the total differential of some function. It is proved in thermodynamics, however, that there exists a state parameter called the absolute temperature θ with which the relation $\delta Q/\theta$ for an arbitrary *reversible* process is the total differential of a certain function called the entropy s. Thus, for any reversible process $l(Z_1, Z_2)$, we have

$$s_2 - s_1 = \int\limits_{l(Z_1, Z_2)} \theta^{-1} \delta Q \quad (ds = \theta^{-1} \delta Q), \tag{1.31}$$

where the curvilinear integral is independent of the path.

If the set of state parameters is formed for such a medium, the next important task is to find all possible relations between the parameters. These relations should follow from the general physical laws and empirical features determining the behavior of the examined medium.

If a certain amount of heat δQ is imparted to the medium in a certain elementary physical process, it performs a mechanical work δA, and the internal energy of the medium is augmented by dU. The *first law of thermodynamics* states that the following equality is always valid:

$$\delta Q = dU + \delta A. \tag{1.32}$$

This physical law, which establishes the equivalence of thermal and mechanical energies, is a thermodynamic expression for the energy conservation law. The use of different notations in eq. (1.32) means that dU is the differential of U, i. e., the linear part of the increment of U, whereas δQ and δA are infinitesimal amounts of heat and work.

The *second law of thermodynamics* states that the entropy of a thermally insulated medium (without heat inflow or outflow) with an arbitrary process inside this medium does not decrease, i. e.,

$$\theta ds \geq \delta Q \tag{1.33}$$

for elementary processes. Such a process is reversible if and only if the equality $\theta ds = \delta Q$ is valid. For such processes, eqs. (1.31) and (1.32) yield the *basic thermodynamic* identity

$$\theta ds = dU + \delta A. \tag{1.34}$$

An important class of media includes the so-called ideal continuous media. For these media, the stress tensor is proportional to the unit tensor: $P = -pI$, $p(\mathbf{x}, t)$ is the pressure. The elementary work is determined by the formula $\delta A = pdV$, and identity (1.34) has the form

$$\theta ds = dU + pdV. \tag{1.35}$$

The state of the "ideal" medium in the general case depends on five parameters:

$$\varrho = 1/V,\ U,\ \theta,\ s,\ p.$$

Let us assume that the "ideal" medium considered is a two-parameter medium. Taking into account that there are total differentials in eq. (1.35), we can find two relations between these five state parameters. Therefore, to obtain a complete description of the thermodynamic state of such a two-parameter medium, it is sufficient to specify one more relation, which is called the *state equation*. State equations of the following types are most frequently used in applications:

1) the internal energy is defined as a function of the parameters V and s:

$$U = U(V, s);$$

2) the heat content (enthalpy) is defined as a function of p and s:

$$i = i(p, s) = U + pV;$$

3) the free energy $F = U - \theta s$ is defined as a function of V and θ:

$$F = F(V, \theta) = U - \theta s;$$

4) the thermodynamic potential $\psi = U - \theta s + pV$ is defined as a function of p and θ:

$$\psi = \psi(p, \theta) = U - \theta s + pV.$$

As the main measure of the amount of heat is temperature, heat fluxes are initiated by a difference in temperature. In thermodynamics, this fact is formulated as the *Fourier law*

$$\mathbf{q} = -k\nabla\theta, \tag{1.36}$$

where k is a new state parameter—*thermal conductivity coefficient*. Now the heat inflow equation (1.30) is transformed to

$$\varrho\frac{dU}{dt} = \mathcal{P} : \mathcal{D} + \operatorname{div}(k\nabla\theta) + \varrho h. \tag{1.37}$$

Complete closure of the system of differential equations of continuum mechanics requires six more equations. These equations, which are also called the *state equations*, relate the stress tensor to motion (or displacement). These relations have different forms for fluids and solids.

1.5 Classical models of liquids and gases

Stokes axioms

Fluids (liquids and gases) are easily moving continuous media that do not retain equilibrium when affected by infinitesimal forces. Therefore, the internal stresses in fluids do not depend on strain directly. As is known from the experience, however, these stresses depend on how rapidly the strain occurs, i. e., on the strain rate. The phenomenological theory offers the following definition: a *liquid* or a *gas* is such a continuous medium in which the stress tensor $\mathcal{P}$ is a function of the strain rate tensor $\mathcal{D}$. In addition, the stress tensor may depend on a certain set of thermodynamic state parameters and, generally speaking, on the point in space $\mathbf{x}$ and time t.

Thus, the following relation is valid for fluids:

$$\mathcal{P} = F(\mathcal{D}, \Pi, \mathbf{x}, t) \tag{1.38}$$

($\Pi = (\varrho, U, \theta, s, p)$ is the set of the state parameters).

The *Stokes axioms* are assumed to be valid for fluids. These axioms specify dependence (1.38):

a) *the medium is homogeneous*: F does not explicitly depend on $\mathbf{x}$, t;
b) *the medium is isotropic*: F is an isotropic tensor function of the strain rate tensor $\mathcal{D}$;
c) *the quiescent medium* is ideal: $F(0, \Pi) = -pI$, p is the pressure.

The isotropic character of the tensor function $F(\mathcal{D})$ means that the following equality is valid for an arbitrary orthogonal transformation O:

$$OF(\mathcal{D})O^* = F(O\mathcal{D}O^*),$$

whence the axiom b) yields the dependence [208, 225, 154, 64, 128, 29]

$$\mathcal{P} = \alpha I + \beta\mathcal{D} + \gamma\mathcal{D}^2. \tag{1.39}$$

Here, α, β, and γ are, generally speaking, functions of the invariants J_1, J_2, and J_3 of the tensor $\mathcal{D}$, and also functions of the thermodynamic state parameters Π. The invariants J_j, $j = 1, 2, 3$, are defined as follows: if $\mathcal{D}_{ij}$ are the components of the tensor $\mathcal{D}$, then

$$\begin{aligned} J_1 &= \operatorname{Sp}\mathcal{D} = \mathcal{D}_{11} + \mathcal{D}_{22} + \mathcal{D}_{33}, \\ J_2 &= \begin{vmatrix} \mathcal{D}_{11} & \mathcal{D}_{12} \\ \mathcal{D}_{12} & \mathcal{D}_{22} \end{vmatrix} + \begin{vmatrix} \mathcal{D}_{11} & \mathcal{D}_{13} \\ \mathcal{D}_{13} & \mathcal{D}_{33} \end{vmatrix} + \begin{vmatrix} \mathcal{D}_{22} & \mathcal{D}_{23} \\ \mathcal{D}_{23} & \mathcal{D}_{33} \end{vmatrix}, \\ J_3 &= \det(\mathcal{D}_{ij}). \end{aligned}$$

The tensor $\mathcal{D}$ satisfies the Cayley–Hamilton identity

$$\mathcal{D}^3 - J_1\mathcal{D}^2 + J_2\mathcal{D} - J_3\mathcal{D} = 0.$$

The thermodynamic state of fluids is fairly well described by eq. (1.35). Certainly, the identity is valid for reversible processes only. The classical thermodynamics deals with medium states close to equilibrium and with mutual conversions of one type of energy to another in these states, which are expressed by identity (1.35). Liquids and gases are usually assumed to be *two-parameter media*, which is valid for considering single-phase one-component motions.

Independent parameters are often taken to be the density ϱ and specific entropy s; then, the specific internal energy $U = U(\varrho, s)$ is prescribed, and eq. (1.35) yields the formulas

$$\theta = \frac{\partial U(\varrho, s)}{\partial s}, \quad p = \varrho^2 \frac{\partial U(\varrho, s)}{\partial \varrho}. \tag{1.40}$$

The thermal conductivity coefficient k involved into the heat inflow equation (1.37) is also assumed to be a known function of the state parameters: $k = k(\varrho, s)$.

Sometimes it is convenient consider the absolute temperature and density as independent parameters; in this case, $U = U(\varrho, \theta)$ is specified. Then, eq. (1.35) yields

$$ds = \frac{1}{\theta} U_\theta d\theta + \frac{1}{\theta}\left(U_\varrho - \frac{p}{\varrho^2}\right) d\varrho,$$

and the expression in the right-hand side of this identity is the total differential if and only if there exists a function $F(\theta, \varrho)$ (free energy) such that

$$U = -\theta^2 \frac{\partial}{\partial \theta}\left(\frac{F}{\theta}\right), \quad p = \varrho^2 F_\varrho; \tag{1.41}$$

certainly, now we have $k = k(\varrho, \theta)$.

Of certain practical interest is the *specific heat* of the fluid, i. e., the amount of heat that has to be imparted to a unit mass of the fluid in order to increase its temperature by one degree with a reversible change in its state. The *specific heat* is written as $c = \delta Q/d\theta$. Two *principal* specific heats are identified: specific heats at constant pressure c_p and at constant volume c_V:

$$\begin{aligned} c_p &= \left(\frac{\delta Q}{d\theta}\right)_{p=\text{const}} = \left(\frac{\partial U}{\partial \theta}\right)_p + p\left(\frac{\partial V}{\partial \theta}\right)_p, \\ c_V &= \left(\frac{\delta Q}{d\theta}\right)_{V=\text{const}} = \left(\frac{\partial U}{\partial \theta}\right)_V. \end{aligned} \tag{1.42}$$

The conservation law (1.35) $\delta Q = dU + p\,dV$ is taken into account here. The use of entropy allows obtaining some other expressions for specific heats. Indeed, as $\delta Q = \theta\,ds$, then we have

$$c_p = \theta\left(\frac{\partial s}{\partial \theta}\right)_p, \quad c_V = \theta\left(\frac{\partial s}{\partial \theta}\right)_V. \tag{1.43}$$

To close the system of equations that describe fluid motion, we have to know the dependences of the coefficients in eq. (1.39) on the invariants $J = (J_1, J_2, J_3)$ of the strain rate tensor $\mathcal{D}$ and the state parameters ϱ, s (or others):

$$\begin{aligned} &\alpha = \alpha(J, \varrho, s), \quad \beta = \beta(J, \varrho, s), \\ &\gamma = \gamma(J, \varrho, s), \quad \alpha(0, \varrho, s) = -p. \end{aligned} \tag{1.44}$$

In other aspects, dependences (1.44) should follow either from some general assumptions or from experimental data. Thus, the model consists of eqs. (1.20), (1.22), (1.37), (1.39), and (1.44). It contains five equations (the tensor $\mathcal{P}$ is eliminated by using eq. (1.39)) for five unknown functions: three components of the velocity vector $\mathbf{v}$ and two independent state parameters. Nevertheless, this model is very rarely used in applications, because it requires a very large amount of additional information (see eq. (1.44)).

Newtonian fluids

The most widely used and rather general model is the so-called *classical model* of the fluid. It is based on the fact that the stress tensor dependence (1.39) is linear: $\mathcal{P} = \alpha I + \beta\mathcal{D}$. Such fluids are also called the *Newtonian fluids*. First of all, we have $\gamma = 0$,

$\alpha = -p + \lambda \operatorname{div} \mathbf{v}$ and $\operatorname{div} \mathcal{P} = \nabla(-p + \lambda \operatorname{div} \mathbf{v}) + \operatorname{div}(2\mu\mathcal{D})$, $\mathcal{P} : \mathcal{D} = -p \operatorname{div} \mathbf{v} + \Phi$, where the *dissipative function* is

$$\Phi = \left(\lambda + \frac{2}{3}\mu\right)(\operatorname{div} \mathbf{v})^2 + 2\mu\mathcal{D}' : \mathcal{D}', \tag{1.45}$$

and $\mathcal{D}' = \mathcal{D} - 3^{-1} \operatorname{div} \mathbf{v} I$ is the *deviator* of the tensor $\mathcal{D}$; here, the notation $\mu = \beta/2$ is introduced. Taking into account that

$$\varrho \frac{dU}{dt} = \varrho\theta \frac{ds}{dt} - p \operatorname{div} \mathbf{v},$$

we obtain the fluid motion model

$$\begin{gathered} \varrho_t + \mathbf{v} \cdot \nabla\varrho + \varrho \operatorname{div} \mathbf{v} = 0, \\ \varrho(\mathbf{v}_t + \mathbf{v} \cdot \nabla\mathbf{v}) = \nabla(-p + \lambda \operatorname{div} \mathbf{v}) + \operatorname{div}(2\mu\mathcal{D}) + \varrho\mathbf{f}, \\ \theta\varrho(s_t + \mathbf{v} \cdot \nabla s) = \operatorname{div}(k\nabla\theta) + \Phi + \varrho h, \end{gathered} \tag{1.46}$$

in which λ, μ, and k are assumed to be known functions of two independent state parameters, while p, ϱ, s, and θ are related by two expressions (1.40) or (1.41). Model (1.45), (1.46) is closed, and the coefficients λ and μ are called the *dynamic viscosity coefficients* and reflect the fluid property of resisting shear forces.

Particular models

Model (1.46) serves as the basis for obtaining the well-known Navier–Stokes equations (λ, μ, $k, \varrho = \text{const}$), equations of an ideal incompressible fluid ($\mu = 0$, $\varrho = \text{const}$), and equations of gas dynamics ($\lambda = \mu = k = 0$).

One of the simplest models proven in practice is the *incompressible fluid model*. In this case, the moving volume ω_t remains unchanged at all time instants, i. e.,

$$|\omega_t| \equiv \int\limits_{\omega_t} d\omega = \text{const}.$$

Using equality (1.14), we find

$$\frac{d}{dt}|\omega_t| = \int\limits_{\omega_0} \frac{\partial \mathring{J}}{\partial t} d\omega_0 = \int\limits_{\omega_t} \operatorname{div} \mathbf{v}\, d\omega = 0,$$

whence it follows that the condition of incompressibility is equivalent to *solenoidity* of the velocity vector field:

$$\operatorname{div} \mathbf{v} = 0. \tag{1.47}$$

For such fluids, model (1.46) is now simplified to the following form (here $\mathcal{D}' = \mathcal{D}$):

$$\begin{aligned} &\varrho_t + \mathbf{v}\cdot\nabla\varrho = 0, \quad \operatorname{div}\mathbf{v} = 0,\\ &\varrho(\mathbf{v}_t + \mathbf{v}\cdot\nabla\mathbf{v}) = -\nabla p + \operatorname{div}(2\mu\mathcal{D}) + \varrho\mathbf{f},\\ &\theta\varrho(s_t + \mathbf{v}\cdot\nabla s) = \operatorname{div}(k\nabla\theta) + \Phi + \varrho h. \end{aligned} \tag{1.48}$$

From the basic thermodynamic identity (1.35) and (1.43), we obtain

$$\frac{\theta ds}{dt} = \frac{dU}{dt} + p\frac{dV}{dt} = \frac{dU}{dt} = \frac{dU}{d\theta}\frac{d\theta}{dt} = c_V\frac{d\theta}{dt},$$

because the specific volume is retained in the particle (along the trajectory) by virtue of the first equation of system (1.48). Specific heat should be considered as a known function of the temperature θ, which is determined experimentally. The energy equation in system (1.48) can be written as

$$\varrho c_V(\theta_t + \mathbf{v}\cdot\nabla\theta) = \operatorname{div}(k\nabla\theta) + \Phi + \varrho h. \tag{1.49}$$

Model (1.48) is used to describe *stratified flows* and is called the model of *inhomogeneous fluid* flows.

The assumption about the constant fluid density ($\varrho = \text{const}$, *homogeneous fluids*) can be further simplified. Firstly, the medium becomes a *one-parameter medium* in the thermodynamic aspect. The pressure p disappears from the thermodynamic relations and can no longer be considered as a state parameter. The reason is that the work in eq. (1.35) is $p\,dV = 0$; therefore, there remains one parameter: the temperature θ.

Let us introduce the kinematic viscosity $\nu = \mu/\varrho$. In the general case, $\nu = \nu(\theta)$, but it can be assumed that $\nu = \text{const}$ for the simple model. The term $\operatorname{div}(2\mu\mathcal{D})$ in the momentum equation is transformed as

$$\operatorname{div}(2\mu\mathcal{D}) = 2\mu\operatorname{div}\mathcal{D} \equiv \mu\big[\nabla(\operatorname{div}\mathbf{v}) + \Delta\mathbf{v}\big] = \mu\Delta\mathbf{v},$$

where $\Delta = \sum_{j=1}^{3}\partial^2/\partial x_j^2$ is the Laplace operator. Thus, the model of a *viscous incompressible fluid* is obtained:

$$\begin{aligned} &\operatorname{div}\mathbf{v} = 0,\\ &\mathbf{v}_t + \mathbf{v}\cdot\nabla\mathbf{v} = -\frac{1}{\varrho}\nabla p + \nu\Delta\mathbf{v} + \mathbf{f}. \end{aligned} \tag{1.50}$$

System (1.50) is also called the *Navier–Stokes system*.

It is of interest to note that thermodynamics is altogether not involved in model (1.50). The temperature θ is determined from the heat inflow equation (1.49), which can also be written in the form

$$\theta_t + \mathbf{v}\cdot\nabla\theta = \frac{1}{\varrho c_V}\operatorname{div}(k\nabla\theta) + \Phi' + \frac{h}{c_V}, \tag{1.51}$$

where

$$\Phi' = 2\nu\, c_V^{-1}\, \mathcal{D} : \mathcal{D}.$$

Model (1.50) is fairly simple, because the fluid whose dynamics is studied by solving equations is described only by two quantities: density ϱ and viscosity ν. These constants are determined from experiments. The Navier–Stokes model is widely used for calculating particular motions of the fluid.

Sometimes effects caused by fluid viscosity are insignificant (tsunami, jet flows, waves on water, etc.). In this case, the *model of an ideal fluid* is valid: $\nu = 0$. The system of equations is

$$\begin{gathered} \operatorname{div} \mathbf{v} = 0, \\ \mathbf{v}_t + \mathbf{v} \cdot \nabla \mathbf{v} = -\frac{1}{\varrho} \nabla p + \mathbf{f}. \end{gathered} \tag{1.52}$$

It is called the system of the *Euler equations*. Equation (1.51) for temperature is simplified. If we additionally assume that k and c_V are constants, then we obtain

$$\frac{d\theta}{dt} = \chi \Delta\theta + \frac{h}{c_V},$$

where $\chi = k/\varrho c_V$ is the *thermal diffusivity coefficient*.

In contrast to liquids, *gases* are strongly compressible media, whereas gas viscosity is often insignificant. Moreover, thermal conductivity can also be ignored in considering many fast processes in gases. Assuming that $\lambda = \mu = k = 0$ in eqs. (1.45)–(1.46), we obtain the system of gas-dynamic equations

$$\begin{gathered} \varrho_t + \mathbf{v} \cdot \nabla \varrho + \varrho \operatorname{div} \mathbf{v} = 0, \\ \mathbf{v}_t + \mathbf{v} \cdot \nabla \mathbf{v} + \frac{1}{\varrho} \nabla p = \mathbf{f}, \\ s_t + \mathbf{v} \cdot s = 0, \\ p = f(\varrho, s). \end{gathered} \tag{1.53}$$

The last relation is called the *state equation of the gas* and is determined experimentally.

Energy dissipation

The properties of viscosity and thermal conductivity of liquids and gases are manifested, in particular, as follows: mechanical energy imparted to the medium can be irreversibly converted to thermal energy and scatter in random thermal motion of molecules. This scattering of mechanical energy is called *dissipation*, and the processes accompanied by energy dissipation are called *dissipative processes*.

From the viewpoint of thermodynamics, a dissipative process is irreversible and should be accompanied by an increase in entropy. Vice versa, an increase in entropy of some part of a continuous medium without "pumping" thermal energy from outside indicates that a dissipative process proceeds in this part of the medium.

Let us consider two examples to illustrate that the properties responsible for energy dissipation in liquids and gases are viscosity and thermal conductivity.

The first example is related to the entropy of the moving volume ω_t:

$$S(\omega_t) = \int\limits_{\omega_t} \varrho s \, d\omega.$$

Let us calculate the derivative with respect to time, using the heat inflow equation (1.46), equality (1.36), and the identity

$$\frac{1}{\theta} \operatorname{div}(\mathrm{k}\nabla\theta) = \operatorname{div}\left(\frac{\mathrm{k}}{\theta}\,\nabla\theta\right) + \frac{\mathrm{k}}{\theta^2}\,|\nabla\theta|^2.$$

We have

$$\frac{d}{dt}\,S(\omega_t) = \int\limits_{\omega_t} \frac{1}{\theta}\,\Phi\,d\omega + \int\limits_{\omega_t} \frac{\mathrm{k}}{\theta^2}\,|\nabla\theta|^2\,d\omega + \int\limits_{\partial\omega_t} \frac{1}{\theta}\,q_n\,d\Sigma + \int\limits_{\omega_t} \frac{1}{\theta}\,h\,d\omega. \tag{1.54}$$

Let the volume ω_t be thermally insulated so that $q_n = 0$ and there are no internal heat sources ($h = 0$). Then, the right-hand side of eq. (1.54) is the sum of two quantities generated owing to different factors. The first term is generated by motion, and the second term is generated by a nonuniform distribution of temperature in the volume ω_t. The second law of thermodynamics required the quantity (1.54) to be nonnegative. As the terms in the right-hand side of eq. (1.54) are independent, we obtain the inequalities

$$\Phi \geq 0, \quad \mathrm{k}|\nabla\theta|^2 \geq 0, \quad \theta > 0.$$

From these inequalities, we obtain the inequalities for the coefficients of viscosity and thermal conductivity:

$$\mathrm{k} \geq 0, \quad \mu \geq 0, \quad \lambda + \frac{2}{3}\,\mu \geq 0. \tag{1.55}$$

Certainly, inequalities may be satisfied with the equality sign if $\mathcal{D} = 0$ and $\nabla\theta = 0$. In this case, the medium moves as a solid: $\mathbf{v} = \mathbf{v}_0 + \boldsymbol{\omega} \times \mathbf{x}$ ($\mathbf{v}_0$ and $\boldsymbol{\omega}$ are constant vectors); the temperature is identical at all points. For motions of a general character, equalities (1.55) can be valid only if $\mathrm{k} = \lambda = \mu = 0$. This actually means that the medium is either an inviscid heat-conducting gas or an ideal incompressible fluid.

Therefore, in the general case of motion of liquids and gases, *the entropy of a thermally insulated volume increases*.

The second example is related to the change in kinetic energy of a moving volume for the *Navier–Stokes equations* (1.52).

Model (1.51), (1.52) is usually called the model of motion of a *viscous heat-conducting* fluid. Generally speaking, the temperature and other characteristics of motion are related not only by eq. (1.52), but also by the boundary conditions (see Chapter 2).

The kinetic energy for model (1.52) is

$$E(\omega_t) = \frac{1}{2}\int\limits_{\omega_t} \varrho|\mathbf{v}|^2\, d\omega,$$

whence it follows that

$$\frac{dE}{dt} = \int\limits_{\omega_t} \mathbf{v}\cdot \operatorname{div}\mathcal{P}\, d\omega + \int\limits_{\omega_t} \varrho\mathbf{v}\cdot\mathbf{f}\, d\omega.$$

As $\mathbf{v}\cdot\operatorname{div}\mathcal{P} = \operatorname{div}(\mathcal{P}\mathbf{v}) + p\operatorname{div}\mathbf{v} - \Phi$, then, using the equality $\operatorname{div}\mathbf{v} = 0$ and the Gauss–Ostrogradskii theorem, we obtain

$$\frac{dE}{dt} = -\int\limits_{\omega_t} \Phi\, d\omega + \int\limits_{\partial\omega_t} \mathbf{v}\cdot\mathbf{p}_n\, d\Sigma + \int\limits_{\omega_t} \varrho\mathbf{v}\cdot\mathbf{f}\, d\omega. \tag{1.56}$$

Let us assume that the second and third integrals in eq. (1.56) are equal to zero, i. e., the surface stresses $\mathbf{p}_n$ and external mass forces $\mathbf{f}$ do not perform any work over the volume ω_t as a whole. Then, eq. (1.56) yields the rate of change of kinetic energy

$$\frac{dE}{dt} = -\int\limits_{\omega_t} \Phi\, d\omega. \tag{1.57}$$

Equality (1.57) shows that the kinetic energy of the volume ω_t does not always increase despite the absence of work performed over it. Conservation of $E(\omega_t)$ is equivalent to the equality $\Phi = 0$ in the volume ω_t, which is possible either if $\mathcal{D} = 0$ or if $\mu = 0$. In the first case, the volume ω_t moves as a solid; in the second case, we deal with an ideal fluid. Therefore, except for these cases, *the kinetic energy of a moving volume decreases*. This is manifestation of a dissipative process in a viscous incompressible fluid; a responsible agent for that is the viscosity coefficient μ. The value of the integral in eq. (1.57) yields the kinetic energy dissipation rate. Therefore, we can say that the dissipative function Φ is equal to the *kinetic energy dissipation rate density*. This, in particular, justifies the name "dissipative function" for the quantity Φ.

2 Conditions on the interface between fluids and on solid walls

In this chapter, a problem of motion of two immiscible fluids with a common interface is formulated. Derivation of dynamic and energy conditions from integral conservation laws is described in detail. An important notion of a free boundary and conditions on this boundary are formulated. Additional conditions related to the presence of solid walls and moving contact lines are discussed.

This chapter is based on previous publications [147, 171].

2.1 Notion of the interface

Equations of motion of a homogeneous fluid were formulated in Chapter 1. Applications, however, often involve situations with joint motion of two liquid media (or a liquid and a gas) contacting along a certain surface. If the contacting fluids do not dissolve in each other, they form a more or less clearly expressed interface. A typical example is a water–oil system. The interface between these media is stable as long as the system is in a state close to stable equilibrium (e. g., an oil spot on the water reservoir surface). Even as the interface becomes unstable (which may occur, in particular, during oil displacement by water in capillaries), the description of such a medium as a system of immiscible fluids is often a fairly adequate one, including the range of parameters characterized by changes in the interface topology. It should be noted that this approach is hardly feasible with the development of secondary instability and a further decrease in characteristic scales of the flow; a rational description of the motion of such a system is given in terms of mechanics of heterogeneous media. Such a description is outside the scope of this book.

Problems of motion of viscous fluids with interfaces in the exact formulation have been mathematically studied for about 35 years. A systematic derivation of conditions on the interface of immiscible fluids during their unsteady nonisothermal motion was first given in [171]. This section deals with this kind of derivation. The constructions described here are modifications of considerations discussed in [147].

An important particular case of the interface is a free boundary, i. e., a surface separating a liquid and a gas. The influence of the dynamic characteristics of the gas on liquid motion can be often neglected, and the problem of liquid motion description reduces to solving system (1.46) (for Newtonian fluids) under appropriate boundary and initial conditions. In this case, in addition to the functions ϱ, $\mathbf{v}$, and θ, it is necessary to find the domains of their definition, with the free surface being some part of the boundary (or the entire boundary) of this domain. In the general case, it is necessary to solve a "doubled" system (1.46) under additional conditions including conditions on the interface. Let us now derive these conditions.

https://doi.org/10.1515/9783110655469-002

2.2 Kinematic condition

We consider the motion of a viscous heat-conducting fluid in a material domain $\Omega_t \subset \mathbb{R}^3$ divided by a smooth surface Γ_t into two subdomains Ω_{1t} and Ω_{2t}. Let us assume that sets of functions $\varrho_1, \mathbf{v}_1, \theta_1$, and $\varrho_2, \mathbf{v}_2, \theta_2$ satisfying system (1.46) are defined in each subdomain, respectively. The coefficients of viscosity $\lambda = \lambda_i$, $\mu = \mu_i$ and thermal conductivity $k = k_i$ involved into the system are defined as smooth functions of θ_i, and the free energy $F = F_i$ is defined as a smooth function of ϱ_i and θ_i $(i = 1, 2)$. The acceleration of external forces $\mathbf{f} = \mathbf{f}_i(\mathbf{x}, t)$ can take various values in the domains Ω_{it}; the function $\mathbf{f}_i$ is assumed to be continuous in Ω_{it}.

The motion examined can be treated as a flow of an inhomogeneous fluid the parameters of which change across Γ_t. It seems preferable, however, to consider it as the motion of two fluids with the interface Γ_t. We assume that limiting values of the functions ϱ_i, θ_i, and $\mathbf{v}_i$ and their first derivatives with respect to all variables from the subdomain Ω_{it} $(i = 1, 2)$ exist at each point of Γ_t at each time instant. It turns out that these sets of functions cannot be arbitrary: they should be coupled by some relations following conservation laws and thermodynamic postulates.

The first relations have a purely kinematic character. They are based on the assumption that Γ_t is a moving material surface (in the same sense as the material volume in Section 1.1). Using this assumption, we do not need to consider such processes as evaporation of the fluid from the free boundary or condensation of saturated vapor, dissolution of one contacting fluid in the other, etc.; in other words, mass transfer across the surface Γ_t is not allowed.

Let us denote the unit vector normal to the surface Γ_t and directed into the domain Ω_{2t} by $\mathbf{n}$ and the velocity of motion of the surface Γ_t in the direction of the normal $\mathbf{n}$ by V_n. The material character of this surface is expressed by the equalities

$$\mathbf{v}_1 \cdot \mathbf{n} = \mathbf{v}_2 \cdot \mathbf{n} = V_n, \quad \mathbf{x} \in \Gamma_t. \tag{2.1}$$

Equality (2.1) and the natural assumption that the surface Γ_t has zero mass, together with the continuity equation from system (1.46), ensure the validity of the integral mass conservation law in an arbitrary material subdomain $\overline{\Omega_{1t} \cup \Omega_{2t}}$.

Remark 2.1. If $f(\mathbf{x}, t) = 0$ is an implicit equation of the surface Γ_t, then $V_n = -f_t/|\nabla_x f|$, $\nabla_x f = (f_{x_1}, f_{x_2}, f_{x_3})$.

2.3 Dynamic condition

Let us first introduce some notations. As previously, we assume that $\omega_t \subset \Omega_t$ is an arbitrary liquid volume having a nonempty intersection γ_t with the surface Γ_t, $\partial\omega_t$ is its boundary, and ω_{1t} and ω_{2t} are the parts of ω_t that belong to Ω_{1t} and Ω_{2t}, respectively

(Figure 2.1). Let us denote $\Sigma_{it} = \partial\omega_{it}/\gamma_t$ $(i = 1, 2)$; $\boldsymbol{\nu}_i$ is the unit vector of the external (relative to ω_t) normal to the surface Σ_{it}. The line $\partial\gamma_t$ is the boundary of the domain γ_t; $\boldsymbol{\nu}_\Gamma$, which is the unit vector determined at each point of $\partial\gamma_t$, lies in the tangential plane to the surface γ_t at this point and, simultaneously, in the normal plane to the curve $\partial\gamma_t$ (the direction $\boldsymbol{\nu}_\Gamma$ is external relative to the domain ω_t). The surface γ_t and the curve $\partial\gamma_t$ are assumed to have continuous curvature; $\partial\omega_t$ can be a piecewise-smooth surface.

Let us postulate the integral law of conservation of momentum of the moving volume ω_t in the form

$$\frac{d}{dt}\int\limits_{\omega_{1t}} \varrho_1 \mathbf{v}_1\, d\omega_1 + \frac{d}{dt}\int\limits_{\omega_{2t}} \varrho_2 \mathbf{v}_2\, d\omega_2 \tag{2.2}$$
$$= \int\limits_{\omega_{1t}} \varrho_1 \mathbf{f}_1\, d\omega_1 + \int\limits_{\omega_{2t}} \varrho_2 \mathbf{f}_2\, d\omega_2 + \int\limits_{\Sigma_{1t}} \mathcal{P}_1 \cdot \boldsymbol{\nu}_1\, d\Sigma_1 + \int\limits_{\Sigma_{2t}} \mathcal{P}_2 \cdot \boldsymbol{\nu}_2\, d\Sigma_2 + \int\limits_{\partial\gamma_t} \sigma \boldsymbol{\nu}_\Gamma\, dl.$$

Here, $\mathcal{P}_i$ is the stress tensor in the i-th fluid $(i = 1, 2)$, dl is a linear element of the curve $\partial\gamma_t$, and σ is a scalar function (generally speaking, temperature-dependent), which is called the surface tension coefficient. The thermodynamic meaning of this function will be clarified in the next section.

Let us emphasize that eq. (2.2) principally differs from the integral form of the momentum conservation law (1.17) for a homogeneous fluid by the last term in the right-hand side, which characterizes the total action of forces concentrated on the interface $\partial\gamma_t$ of the contact region of two fluids contained in the moving volume ω_t. The origin of these forces is caused by "elastic properties" of the interface, i. e., properties of resisting its deformations. These forces are called the *capillary forces* or the *surface tension forces*. If the fluid is homogeneous, then we have $\sigma = 0$, and the notion of the interface becomes fictitious. In this case, the surface integrals and the related volume integrals in (2.2) are united into integrals over the surface $\partial\omega_t$ and the volume ω_t, respectively, while equality (2.2) transforms to eq. (1.17).

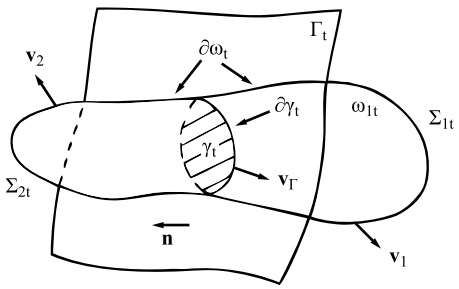

Figure 2.1: Flow domain.

Let us now transform relation (2.2). The first step is based on the identities

$$\frac{d}{dt}\int\limits_{\omega_{it}} \varrho_i \mathbf{v}_i \, d\omega_i - \int\limits_{\omega_{it}} \varrho_i \mathbf{f}_i \, d\omega_i - \int\limits_{\Sigma_{it}} \mathcal{P}_i \cdot \boldsymbol{\nu}_i \, d\Sigma_i = (-1)^{i-1} \int\limits_{\gamma_t} \mathcal{P}_i \cdot \mathbf{n} \, d\gamma \tag{2.3}$$

($i = 1, 2$), which are valid owing to the momentum equations (1.17) satisfied independently in each of the domains ω_{it}, and to the assumption of continuous differentiability of the functions ϱ_i, $\mathbf{v}_i$, and θ_i up to the boundary of the domain ω_{it} and continuity of the functions $\mathbf{f}_i$ in ω_{it}. Together with the previously postulated smoothness of the functions F_i, λ_i, and μ_i, this assumption is sufficient to ensure continuity of the elements of the stress tensor $\mathcal{P}_i = (-p_i + \lambda_i \operatorname{div} \mathbf{v}_i)I + 2\mu_i \mathcal{D}(\mathbf{v}_i)$ in the domain ω_{it}. Using eq. (2.3), we can simplify equality (2.2) to

$$-\int\limits_{\gamma_t} [\mathcal{P} \cdot \mathbf{n}] \, d\gamma + \int\limits_{\partial\gamma_t} \sigma \boldsymbol{\nu}_\Gamma \, dl = 0. \tag{2.4}$$

Here $[\mathcal{P} \cdot \mathbf{n}] = \mathcal{P}_1|_\Gamma \cdot \mathbf{n} - \mathcal{P}_2|_\Gamma \cdot \mathbf{n}$. The symbol $[f]$ is used hereinafter to indicate the difference between the traces $f_1|_\Gamma$ and $f_2|_\Gamma$ of the functions f_1 and f_2 determined in the domains Ω_{1t} and Ω_{2t}, respectively; the subscript t in the surface notation is omitted here.

Before moving further, we define the surface gradient ∇_Γ as a vector operator of the form

$$\nabla_\Gamma = \nabla - \mathbf{n}(\mathbf{n} \cdot \nabla).$$

As $\mathbf{n} \cdot \nabla_\Gamma f = 0$ for an arbitrary smooth scalar function determined in the domain Γ, then it is sufficient to know the values of the function f only at points of this surface to calculate the vector-function $\nabla_\Gamma f$. The "surface divergence" operator $\operatorname{div}_\Gamma$ acts on the vector function $\mathbf{b} = (b_1, b_2, b_3)$ specified on the surface Γ in accordance with the rule

$$\operatorname{div}_\Gamma \mathbf{b} \equiv \nabla_\Gamma \cdot \mathbf{b} = \sum_{i=1}^{3} \left[\frac{\partial}{\partial x_i} - n_i (\mathbf{n} \cdot \nabla) \right] b_i.$$

Finally, if T is a tensor of the second rank with the elements T_{ij} ($i, j = 1, 2, 3$), then $\operatorname{div}_\Gamma T$ is understood to be a vector with the components

$$(\operatorname{div}_\Gamma T)_i = \sum_{j=1}^{3} \left[\frac{\partial}{\partial x_j} - n_j (\mathbf{n} \cdot \nabla) \right] T_{ji}.$$

Using the equality

$$\int\limits_{\partial\gamma_t} \sigma \boldsymbol{\nu}_\Gamma \, dl = -\int\limits_{\partial\gamma_t} \sigma \mathbf{n} \times \mathbf{dl},$$

where **dl** is the oriented element of the tangent line to the curve $\partial\gamma_t$, we transform the curvilinear integral in eq. (2.4). Applying the Stokes formula to the calculation of each component of the vector in the right-hand side of the last equality, we obtain the relation

$$\int_{\partial\gamma_t} \sigma \mathbf{v}_\Gamma \, dl = \int_{\gamma_t} \operatorname{div}_\Gamma(\sigma G_\Gamma) \, d\gamma, \tag{2.5}$$

in which the symbol G_Γ means the tensor

$$G_\Gamma = I - \mathbf{n} \otimes \mathbf{n},$$

where $\otimes$ means dyadic multiplication, $(\mathbf{n} \otimes \mathbf{n})_{ij} = (n_i n_j)_{i,j=1}^3$, n_i are the components of the normal **n**, and I is the unit tensor. By virtue of arbitrariness of the domain $\gamma_t \subset \Gamma$, eqs. (2.4) and (2.5) yield the equality

$$[\mathcal{P} \cdot \mathbf{n}] = \operatorname{div}_\Gamma(\sigma G_\Gamma), \tag{2.6}$$

expressing the law of momentum conservation across the interface. Generally speaking, in accordance with eq. (2.6), the stress vector $\mathcal{P} \cdot \mathbf{n}$ is not continuous on the surface Γ; at first glance, this contradicts the assumption of an "inertia-free" interface. The seeming contradiction disappears if we take into account that the interface has a nonzero surface density of internal energy (see Section 2.4).

The right-hand side of eq. (2.6) can be written in a more convenient form by using an easily verified identity (analog to the vector analysis formula)

$$\operatorname{div}_\Gamma(\sigma G_\Gamma) = \nabla_\Gamma \sigma \cdot G_\Gamma + \sigma \operatorname{div}_\Gamma G_\Gamma.$$

It follows from the definition of the tensor G_Γ and orthogonality of the vector $\nabla_\Gamma \sigma$ and **n** that $\nabla_\Gamma \sigma \cdot G_\Gamma = \nabla_\Gamma \sigma$. As is shown below, we have

$$\operatorname{div}_\Gamma G_\Gamma = 2H\mathbf{n}, \tag{2.7}$$

where H is the mean curvature of the surface Γ (it is assumed that $H > 0$ if the surface Γ is convex outward the domain Ω_{2t}). Based on these considerations, equality (2.6) is transformed to

$$[\mathcal{P} \cdot \mathbf{n}] = 2\sigma H\mathbf{n} + \nabla_\Gamma \sigma. \tag{2.8}$$

Let us prove the validity of equality (2.7). We have a chain of almost obvious relations:

$$\begin{aligned} \operatorname{div}_\Gamma G_\Gamma &= \operatorname{div}_\Gamma(I - \mathbf{n} \otimes \mathbf{n}) = -\operatorname{div}_\Gamma(\mathbf{n} \otimes \mathbf{n}) \\ &= -(\operatorname{div}_\Gamma \mathbf{n})\mathbf{n} - \frac{1}{2} \nabla_\Gamma |\mathbf{n}|^2 = -(\operatorname{div}_\Gamma \mathbf{n})\mathbf{n}. \end{aligned}$$

Equality (2.7) is valid if

$$\operatorname{div}_\Gamma \mathbf{n} = -2H. \tag{2.9}$$

To prove eq. (2.9), we need some notions from differential geometry of surfaces (see, e. g., [49]).

Let the surface $\Gamma = \Gamma_t$ be defined by the parametrization

$$\mathbf{x} = \mathbf{x}(\eta^1, \eta^2, t),$$

where η^1 and η^2 are curvilinear coordinates. The vectors

$$\mathbf{e}_\alpha = \frac{\partial \mathbf{x}}{\partial \eta^\alpha} \quad (\alpha = 1, 2)$$

are covariant vectors of the tangential basis to this surface. The unit vector $\mathbf{n}$ of the normal to Γ can be expressed via $\mathbf{e}_1$ and $\mathbf{e}_2$ by the formula

$$\mathbf{n} = \frac{\mathbf{e}_1 \times \mathbf{e}_2}{\sqrt{g}}. \tag{2.10}$$

Here g is the determinant of the metric tensor of the surface Γ with the elements $g_{\alpha\beta} = \mathbf{e}_\alpha \cdot \mathbf{e}_\beta$ $(\alpha, \beta = 1, 2)$. Formula (2.10) follows from the identity

$$g = g_{11}g_{22} - g_{12}^2 = |\mathbf{e}_1 \times \mathbf{e}_2|^2.$$

Let us denote the Euclidean distance from the point lying outside the surface Γ to this surface by n. As Γ has a continuous curvature, the triple of the numbers (η^1, η^2, n) determines the coordinates of such points, at least, for sufficiently small values of n. With these notations, the operator gradient ∇_Γ is written in the form $\nabla = \nabla_\Gamma + \mathbf{n}\,\partial/\partial n$, and the surface gradient ∇_Γ is written as

$$\nabla_\Gamma = \mathbf{e}^\alpha \frac{\partial}{\partial \eta^\alpha} \tag{2.11}$$

(the sign of summation over repeated Greek superscripts and subscripts is omitted). The symbol $\mathbf{e}^\alpha$ in eq. (2.11) means the vectors of the reciprocal (contravariant) basis on Γ. The relation between the both bases is given by the formulas $\mathbf{e}^\alpha \cdot \mathbf{e}_\beta = \delta^\alpha_\beta$ (δ^α_β is the Kronecker delta).

The vectors $\mathbf{e}^\alpha$, like $\mathbf{e}_\alpha$, are orthogonal to $\mathbf{n}$. Differentiating the identity $\mathbf{e}^\alpha \cdot \mathbf{n} = 0$ with respect to η^β, we obtain

$$\frac{\partial \mathbf{e}^\alpha}{\partial \eta^\beta} \cdot \mathbf{n} + \mathbf{e}^\alpha \cdot \frac{\partial \mathbf{n}}{\partial \eta^\beta} = 0 \quad (\alpha, \beta = 1, 2).$$

The last equality together with eq. (2.11) shows that

$$\operatorname{div}_\Gamma \mathbf{n} = -\frac{\partial \mathbf{e}^\alpha}{\partial \eta^\alpha} \cdot \mathbf{n}. \tag{2.12}$$

Let us note now that

$$\frac{\partial \mathbf{e}^{\alpha}}{\partial \eta^{\beta}} \cdot \mathbf{n} = b^{\alpha}_{\beta},$$

where b^{α}_{β} are the mixed components of the tensor associated with the second quadratic form of the surface Γ [49]. It is known that the trace of this tensor is equal to the doubled mean surface curvature. From here and from eq. (2.12) we obtain the required relation (2.9) and, correspondingly, the dynamic condition on the interface (2.8).

Equality (2.8) has an important corollary: if Γ_t is not a level surface of the function $\sigma(\theta(\mathbf{x}, t))$, then the tangent line to Γ_t, which is the component of the vector $[\mathcal{P} \cdot \mathbf{n}]$, differs from zero. In turn, this means that a system of two fluids with the interface Γ cannot be in equilibrium if $\sigma|_{\Gamma} \neq \text{const}$. If $\theta_i \neq \text{const}$ for $\mathbf{x} \in \Omega_{it}$ $(i = 1, 2)$, the equilibrium state is possible only in exceptional cases. Leaving these cases aside, let us consider the conditions of equilibrium for a system of immiscible *isothermal* fluids. To obtain these conditions, we should substitute the equalities $\mathbf{v}_i = 0$ into the continuity and momentum equations in system (1.46). Thus, we obtain

$$\partial \varrho_i / \partial t = 0; \tag{2.13}$$

$$\varrho_i^{-1} \nabla p_i = \mathbf{f}_i \quad (i = 1, 2). \tag{2.14}$$

By virtue of the equation of state (1.41), equality (2.13), and assumption that $\theta_i = \text{const}$, the left-hand side of eq. (2.14) for each $i = 1, 2$ is a gradient of a certain function independent of t. Thus, the necessary condition of equilibrium is the potentiality of the vectors $\mathbf{f}_i$,

$$\mathbf{f}_i = \nabla \Pi_i \quad (i = 1, 2), \tag{2.15}$$

and their independence of time. The function Π_i involved in eq. (2.15) is called the *potential of acceleration of external forces* (or, more often, simply the *potential of external forces*).

The kinematic condition on the interface (2.1) requires the surface Γ to be steady. The set of the equilibrium conditions becomes closed if eqs. (2.13)–(2.15) are supplemented with eq. (2.8); at $\mathbf{v}_i = 0$ and $\sigma = \text{const}$, the last equation becomes scalar. Let us consider this relation for an important case of *homogeneous incompressible fluids*. If $\varrho_i = \text{const}$ $(i = 1, 2)$, then equality (2.13) is satisfied automatically, and eqs. (2.14) and (2.15) yield $p_i = \varrho_i \Pi_i + c_i$, where $c_i = \text{const}$ (the potential possibility of an arbitrary dependence of c_i on t turns out to be incompatible, by virtue of eq. (2.8), with the condition of steadiness of the surface Γ). Substituting the resultant expressions for p_i and the equalities $\mathbf{v}_i = 0$ and $\sigma = \text{const}$ into condition (2.8), we obtain

$$2\sigma H = -[\varrho \Pi]. \tag{2.16}$$

Equality (2.16) satisfied at the points of the surface Γ is actually a differential equation for determining this surface. For instance, if the surface Γ is uniquely projected onto the plane x_3, i. e., its equation has the form $x_3 = f(x_1, x_2)$, then the mean curvature of Γ is calculated by the formula [49]

$$2H = \nabla_2 \cdot \left(\frac{\nabla_2 f}{\sqrt{1 + |\nabla_2 f|^2}} \right),$$

where ∇_2 is a gradient over the variables x_1 and x_2. In this case, eq. (2.16), which describes the equilibrium shape of the interface in a potential field of external forces, takes the form

$$\sigma \nabla_2 \cdot \left(\frac{\nabla_2 f}{\sqrt{1 + |\nabla_2 f|^2}} \right) = \varrho_2 \Pi_2(x_1, x_2, f) - \varrho_1 \Pi_1(x_1, x_2, f) + c, \tag{2.17}$$

where $c = c_2 - c_1$ is a constant. The shapes of equilibrium of the capillary fluid in vessels, based on eq. (2.17), are determined in [140, 55].

2.4 Elements of thermodynamics of the interface

According to the notions introduced by Gibbs, the interface between two liquids (or a liquid and a gas) is a special thermodynamic medium characterized by additive functions of the sets of this surface: entropy, internal energy, free energy, and others. In this chapter, we consider only "pure" interfaces (i. e., those interfaces that do not contain surface-active agents). This kind of surface is a one-parameter thermodynamic medium with the state parameter usually chosen to be the absolute temperature θ.

Let us denote the specific (per unit area of the interface) surface entropy and internal energy by s and u, respectively. The quantities θ, s, and u are related by the thermodynamic identity

$$\theta \, ds = du. \tag{2.18}$$

Relation (2.18) is similar to the basic thermodynamic identity for another one-parameter medium: incompressible fluid (see Section 1.5) with $dU = \theta \, ds$. At the same time, it should be noted that this equality can be obtained from the first law of thermodynamics (1.35) under the formal assumption $\varrho = \text{const}$. It is difficult to put the analog of identity (1.35) into correspondence to relation (2.18), because the interface is assumed to have no mass; therefore, the notion of density is meaningless for the interface.

Following Gibbs, let us identify the specific free energy of the surface phase with the surface tension coefficient $\sigma(\theta)$. For a two-parameter medium, as follows from

eq. (1.41), the dependence between the free energy F, internal energy u, and entropy s is described by the formula $F = u - \theta s$, which does not contain the second state parameter, i. e., the density ϱ (the first parameter is the temperature). Let us postulate a similar dependence for the interface:

$$\sigma = u - \theta s. \tag{2.19}$$

Then, eqs. (2.18) and (2.19) yield the relation

$$d\sigma + s d\theta = 0, \tag{2.20}$$

which is called the Gibbs–Duhem equation. An equivalent recording of eq. (2.20) is $d\sigma/d\theta = -s$. This relation is similar to the second equality in (1.41), which is valid for two-parameter media.

As it will be demonstrated at the end of this section, the thermodynamic condition of interface stability implies that σ is positive. As the surface entropy is $s > 0$, then the Gibbs–Duhem equation yields the inequality $d\sigma/d\theta < 0$. For the majority of pure interfaces, the relation $\sigma(\theta)$ is adequately approximated by the linear dependence

$$\sigma = \sigma_0 - æ(\theta - \theta_0). \tag{2.21}$$

Here σ_0, θ_0, and æ are positive constants; the latter is called the temperature coefficient of surface tension. (The requirement that both σ and æ should be simultaneously positive restricts the range of temperatures where eq. (2.21) can be used.) For most interfaces, however, the value of æ is rather small, and the considered interval of θ variation is a priori bounded by the melting and boiling temperatures of the fluids. Thus, for the water–air interface at $\theta_0 = 293\,\mathrm{K}$, we have $\sigma = \sigma_0 = 72.8\,\mathrm{dyn/cm}$, whereas $\sigma = 75.7\,\mathrm{dyn/cm}$ at $\theta = 273\,\mathrm{K}$ and $\sigma = 58.8\,\mathrm{dyn/cm}$ at $\theta = 373\,\mathrm{K}$. If we assume that $æ = 0.17\,\mathrm{dyn/cm \cdot deg}$, then the error of determining the values of σ by eq. (2.21) at the extreme points of the above-indicated interval is within 0.7 %. For the linear dependence $\sigma(\theta)$, by virtue of eqs. (2.19) and (2.20), we obtain $s = æ$ and $u = \sigma_0 + æ\theta_0 = \text{const}$. If we define the interface heat capacity c_Γ as $c_\Gamma = du/d\theta$, then we obtain $c_\Gamma = 0$ for interfaces with the dependence of σ on θ of the form (2.21).

Let us recall that the surface tension coefficient was initially introduced in formulating the momentum conservation law for a moving volume containing an interface. The last term in eq. (2.2) induced by the capillary effect characterized the action of linear forces from the side of the supplement of the selected part of the interface γ_t to the entire surface Γ_t. At the same time, the function $\sigma(\theta)$ was axiomatically determined as the free energy of the interface. To check the equivalence of the two definitions of the surface tension coefficient, let us consider a reversible isothermal change in the interface area. Let us denote the element of the interface area increment in this process

by $d\Sigma$ and the corresponding elementary change in the surface energy by dE_Γ. Using eqs. (2.19) and (2.20) and the definition of the specific surface energy $dE_\Gamma = u d\Sigma$, we obtain

$$dE_\Gamma = \left(\sigma - \theta \frac{d\sigma}{d\theta}\right) d\Sigma.$$

The amount of heat δQ absorbed during elementary deformation of the interface is

$$\delta Q = \theta\, ds = -\theta \frac{d\sigma}{d\theta}\, d\Sigma.$$

The difference in the values of dE_Γ and δQ is equal to the work dR performed by capillary forces in the process considered; therefore, we obtain

$$dR = \sigma\, d\Sigma. \tag{2.22}$$

Relation (2.22) corresponds to the formula $dR = -pd(1/\varrho)$ for the elementary work in the case of reversible deformation of a fluid volume with a pressure p, which is characterized by a change in its density $d\varrho$. Thus, there is an obvious analogy between the quantities σ for the interface and $-p$ for the fluid volume. During volume compression ($d\varrho > 0$), the mechanical work performed over this volume is known to be positive. Concerning the work on changing the interface area, the experience shows that it is positive if $d\Sigma > 0$. By virtue of eq. (2.22), this means that $\sigma > 0$.

Let us consider an element dl of the line $\partial\gamma_t$, which bounds the selected part of the interface γ_t. Using dv to denote an elementary displacement of the point of the curve $\partial\gamma_t$ in the direction of the vector $\boldsymbol{\nu}_\Gamma$ (see Figure 2.1), we obtain $d\Sigma = dvdl$. It follows from here and from eq. (2.22) that a force $-\sigma\boldsymbol{\nu}_\Gamma dl$ acts on the element d from the side of the external (relative to $\partial\gamma_t$) part of the interface. This conclusion precisely corresponds to eq. (2.2), thus, supporting the equivalence of the "thermodynamic" and "mechanical" definitions of the quantity $\sigma(\theta)$.

If we assume that $\sigma < 0$, then the forces acting on the curve $\partial\gamma_t$ would tend to increase the area of the surface γ_t, which would finally lead to an unlimited increase in this area, i. e., to complete mixing of two fluids. This is the process observed for the alcohol–water contact: these two fluids mix in arbitrary proportions. Only those fluids for which $\sigma > 0$ do not mix with each other.

2.5 Conditions of continuity

Apart from the conditions following from the mass, momentum, and energy conservation laws, some additional conditions are satisfied on the interface. These conditions

can be called the continuity conditions. One of them is the condition of continuity of the total velocity vector:

$$\mathbf{v}_1 = \mathbf{v}_2, \quad \mathbf{x} \in \Gamma_t. \tag{2.23}$$

Similar to the no-slip condition on the interface between a liquid and a solid (see Section 2.8 below), condition (2.23) is simply postulated in most cases. The following considerations support the natural character of condition (2.23). If a Newtonian fluid were homogeneous, the presence of a velocity discontinuity on a certain surface inside the flow domain would lead, in accordance with the equality $\mathcal{P}_i = -p_i I + 2\mu_i \mathcal{D}(\mathbf{v}_i)$, to infinite values of the stress vector on this surface. The interface is a mathematical idealization of a rather thin layer of the mixture of two fluids. It can be reasonably assumed that the velocity in such a layer changes smoothly; otherwise, the previous rheological relation would give rise to singularities of the stress field as the mixing zone becomes thinner.

Note that eq. (2.23) actually contains only two additional scalar conditions, because the continuity of the normal component of the velocity vector is already implied by condition (2.1).

Another continuity condition follows from the requirement of local thermodynamic equilibrium of contacting media: this is the temperature continuity condition

$$\theta_1 = \theta_2, \quad \mathbf{x} \in \Gamma_t. \tag{2.24}$$

From the viewpoint of the Fourier law, equality (2.24) is as natural as equality (2.23) from the viewpoint of the Stokes postulates. Using eqs. (2.23) and (2.24), we can use $\mathbf{v}$ and θ to denote the coinciding limiting values of the functions $\mathbf{v}_i$ and θ_i ($i = 1, 2$) as the points $\mathbf{x} \in \Omega_{it}$ tend to the point $\mathbf{x}_i \in \Gamma_t$.

A particular case of the interface is the boundary separating two phases of the same substance, e. g., liquid and vapor formed from this liquid. In this case, there arises an additional condition of thermodynamic equilibrium: continuity of the chemical potential on the interface. By definition, the chemical potential is $\Psi = F + p/\varrho$, where F is the free energy. This continuity condition has the form

$$[F + p/\varrho] = 0. \tag{2.25}$$

Nevertheless, the interface between two phases can be considered as a material surface only in some particular situations eliminating the possibility of the phase transition. (In this case, one more condition of phase equilibrium of the form (2.16) is added to conditions (2.24) and (2.25).)

Finally, it should be noted that the limiting values of the fluid densities ϱ_1 and ϱ_2 on the surface Γ_t are not mandatory coupled by some a priori relations.

2.6 Energy transfer across the interface

The study of this issue is based on the integral law of conservation of the total energy of a system of immiscible fluids enclosed in a moving volume ω_t:

$$\begin{aligned}\frac{d}{dt}\int\limits_{\omega_{1t}}\varrho_1\Big(\frac{|\mathbf{v}_1|^2}{2}+U_1\Big)d\omega_1+\frac{d}{dt}\int\limits_{\omega_{2t}}\varrho_2\Big(\frac{|\mathbf{v}_2|^2}{2}+U_2\Big)d\omega_2+\frac{d}{dt}\int\limits_{\gamma_t}u\,d\gamma\\ =\int\limits_{\omega_{1t}}\varrho_1\mathbf{v}_1\cdot\mathbf{f}_1\,d\omega_1+\int\limits_{\omega_{2t}}\varrho_2\mathbf{v}_2\cdot\mathbf{f}_2\,d\omega_2+\int\limits_{\Sigma_1}\mathbf{v}_1\cdot\mathcal{P}_1\cdot\boldsymbol{\nu}_1\,d\Sigma_1\\ +\int\limits_{\Sigma_2}\mathbf{v}_2\cdot\mathcal{P}_2\cdot\boldsymbol{\nu}_2\,d\Sigma_2+\int\limits_{\partial\gamma_t}\mathbf{v}\cdot(\sigma\boldsymbol{\nu}_\Gamma)\,dl-\int\limits_{\Sigma_1}\mathbf{q}_1\cdot\boldsymbol{\nu}_1\,d\Sigma_1\\ -\int\limits_{\Sigma_2}\mathbf{q}_2\cdot\boldsymbol{\nu}_2\,d\Sigma_2+\int\limits_{\omega_{1t}}\varrho_1h_1\,d\omega_1+\int\limits_{\omega_{2t}}\varrho_2h_2\,d\omega_2.\end{aligned}\tag{2.26}$$

Here $\mathbf{v}$ is the common limiting value of the vectors $\mathbf{v}_1$ and $\mathbf{v}_2$ on the surface Γ_t and $\mathbf{q}_i$ ($i=1,2$) is the heat-flux vector in the i-th fluid.

For a homogeneous medium obeying relations (1.5) and (1.29), equality (2.26) turns to eq. (1.25), because the notion of the interface for such a medium becomes fictitious, and we necessarily have $u=0$ and $\sigma=0$ in eq. (2.26). The additional (as compared with eq. (1.25)) term in the left-hand side of eq. (2.26) expresses the rate of energy of the selected part of the interface, whereas the curvilinear integral in the right-hand side of this relation is the power of capillary forces spent on deformation of the mentioned surface.

Equality (2.26) allows considerable simplifications. First of all, let us note that the equations of continuity, momentum, and heat inflow (1.46) are satisfied in each subdomain ω_{it} where the functions $\varrho_i, \mathbf{v}_i$, and θ_i are sufficiently smooth. Therefore, the identities

$$\begin{aligned}\frac{d}{dt}\int\limits_{\omega_{it}}\varrho_i\Big(\frac{|\mathbf{v}_i|^2}{2}+U_i\Big)\,d\omega_i-\int\limits_{\omega_{it}}\varrho_i\mathbf{v}_i\cdot\mathbf{f}_i\,d\omega_i-\int\limits_{\omega_{it}}\varrho_ih_i\,d\omega_i\\ -\int\limits_{\Sigma_i}(\mathbf{v}_i\cdot\mathcal{P}_i\cdot\boldsymbol{\nu}_i-\mathbf{q}_i\cdot\boldsymbol{\nu}_i)\,d\Sigma_i=(-1)^{i-1}\int\limits_{\gamma_t}(\mathbf{v}_i\cdot\mathcal{P}_i\cdot\mathbf{n}_i-\mathbf{q}_i\cdot\mathbf{n})\,d\gamma\end{aligned}\tag{2.27}$$

are valid for $i=1,2$ (cf. eq. (2.3)). In writing the right-hand side of eq. (2.27), we used the notation $\mathbf{v}_i|_\Gamma=\mathbf{v}$ introduced in Section 2.5 based on equality (2.23). Taking into account eqs. (2.26) and (2.27), we obtain

$$\frac{d}{dt}\int\limits_{\gamma_t}u\,d\gamma=\int\limits_{\gamma_t}\big([\mathbf{q}\cdot\mathbf{n}]-\mathbf{v}\cdot[\mathcal{P}\cdot\mathbf{n}]\big)\,d\gamma+\int\limits_{\partial\gamma_t}\sigma\mathbf{v}\cdot\boldsymbol{\nu}_\Gamma\,dl.\tag{2.28}$$

Further transformations are aimed at presenting the left-hand side of eq. (2.28) and the last term in the right-hand side of this equality in the form of certain integrals

over the domain γ_t. The transformation of the first expression is based on an analog of the translation formula (see Section 1.2). Let γ_t be a smooth material surface, and let $f(\mathbf{x}, t)$ be a smooth function determined in a certain neighborhood of this surface. Then, we obtain

$$\frac{d}{dt}\int\limits_{\gamma_t} f\, d\gamma = \int\limits_{\gamma_t}\left(\frac{df}{dt} + f\,\mathrm{div}_\Gamma\,\mathbf{v}\right) d\gamma, \tag{2.29}$$

where df/dt is the total derivative of the function f, and div_Γ is the surface divergence of the vector $\mathbf{v}$, which was determined in Section 2.3.

Similar to the classical translation formula (1.15), relation (2.29) is proved by passing to the Lagrange coordinates. Let the surface γ_0 at $t = 0$ be defined by the parametrization $\mathbf{x} = \mathbf{x}_0(\xi^1, \xi^2)$, where ξ^1 and ξ^2 are curvilinear coordinates, and the coordinate ξ^3 is counted along the normal to the surface γ_0. The triple of the numbers ξ^1, ξ^2, ξ^3 determines the Lagrange coordinates, at least in a certain neighborhood of γ_0. As γ_t is a moving surface, its location at a current time instant t is determined as a constriction of the mapping $\boldsymbol{\xi} \to \mathbf{x}$ formed by solving the Cauchy problem (1.10), (1.12) onto the domain γ_0.

Let us pass to the Lagrange coordinates in the left-hand side of eq. (2.29). Then, the integral whose derivative has to be calculated takes the form

$$\int\limits_{\gamma_0} \mathring{f}(\boldsymbol{\xi}, t)\mathring{J}_\Gamma(\boldsymbol{\xi}, t)\, d\gamma_0,$$

where, as in Section 1.2, $\mathring{f}(\boldsymbol{\xi}, t) = f(\mathbf{x}(\boldsymbol{\xi}, t), t)$, and $\mathring{J}_\Gamma$ is the determinant of the metric tensor of the surface γ_0. Let us note now that the parameters η^1 and η^2 introduced in Section 2.3 to derive eq. (2.9) can be identified with the Lagrange coordinates ξ^1 and ξ^2. Therefore, the following equality is valid:

$$\mathring{J}_\Gamma(\boldsymbol{\xi}, t) = \left[g(\mathbf{x}(\boldsymbol{\xi}, t), t)\right]^{1/2}$$

($g = |\mathbf{e}_1 \times \mathbf{e}_2|$ is the determinant of the metric tensor $(g_{\alpha\beta})$). For a fixed value of $\boldsymbol{\xi}$, the function satisfies the differential equation (see the Euler formula (1.14))

$$\frac{d\mathring{J}_\Gamma}{dt} = \mathring{J}_\Gamma\,\mathrm{div}_\Gamma\,\mathbf{v}. \tag{2.30}$$

Let us prove the validity of eq. (2.30). As $\mathring{J}_\Gamma = (\det g_{\alpha\beta})^{1/2}$, then

$$\frac{d\mathring{J}_\Gamma}{dt} = \frac{1}{2\sqrt{g}}\frac{\partial g}{\partial g_{\alpha\beta}}\frac{dg_{\alpha\beta}}{dt} = \frac{1}{2\sqrt{g}}\, g g^{\beta\alpha}\frac{dg_{\alpha\beta}}{dt}, \tag{2.31}$$

where $g^{\beta\alpha}$ are the elements of a matrix inverse to $g_{\alpha\beta}$. Further, as $g_{\alpha\beta} = (\partial\mathbf{x}/\partial\boldsymbol{\xi}^\alpha)\cdot(\partial\mathbf{x}/\partial\boldsymbol{\xi}^\beta)$, then

$$\frac{dg_{\alpha\beta}}{dt} = \frac{\partial\mathbf{v}}{\partial\xi^\alpha}\cdot\mathbf{e}_\beta + \mathbf{e}_\alpha\cdot\frac{\partial\mathbf{v}}{\partial\xi^\beta} = (\mathbf{e}_\alpha\cdot\nabla_\Gamma\mathbf{v})\cdot\mathbf{e}_\beta + (\mathbf{e}_\beta\cdot\nabla_\Gamma\mathbf{v})\cdot\mathbf{e}_\alpha, \tag{2.32}$$

where $\mathbf{e}_\alpha$ are the covariant vectors of the tangential basis of the surface Γ, and ∇_Γ is the surface gradient determined by eq. (2.11) in which $\eta^\alpha = \xi^\alpha$ should be assumed. The symbol $\nabla_\Gamma \mathbf{v}$ denotes a tensor of the form (summation is performed over the superscript β)

$$\nabla_\Gamma \mathbf{v} = \mathbf{e}^\beta \otimes \frac{\partial \mathbf{v}}{\partial \xi^\beta}.$$

Let $\mathcal{D}_\Gamma$ be the symmetric part of the tensor: $2\mathcal{D}_\Gamma = \nabla_\Gamma \mathbf{v} + (\nabla_\Gamma \mathbf{v})^*$. Then equality (2.32) is rewritten in the form

$$\frac{dg_{\alpha\beta}}{dt} = 2\mathbf{e}_\beta \cdot \mathcal{D}_\Gamma \cdot \mathbf{e}_\alpha.$$

From the last relation and eq. (2.31), we obtain

$$\frac{d\mathring{J}_\Gamma}{dt} = \mathring{J}_\Gamma \mathbf{e}^\alpha \cdot \mathcal{D}_\Gamma \cdot \mathbf{e}_\alpha.$$

To derive eq. (2.30) we have to prove that

$$\mathbf{e}^\alpha \cdot \mathcal{D}_\Gamma \cdot \mathbf{e}_\alpha = \operatorname{div}_\Gamma \mathbf{v}. \tag{2.33}$$

Let us denote the normal component of the vector $\mathbf{v}$ by v^3 (let us recall that the directions of the ξ^3 axis and the normal $\mathbf{n}$ coincide); then we obtain $\mathbf{v} = v^\gamma \mathbf{e}_\gamma + v^3 \mathbf{n} = \mathbf{v}_\Gamma + v^3 \mathbf{n}$. We determine the tensor $\mathcal{D}'_\Gamma$ through the relation $2\mathcal{D}'_\Gamma = \nabla_\Gamma(v^3 \mathbf{n}) + (\nabla_\Gamma(v^3 \mathbf{n}))^*$. Thus, we have an obvious chain of equalities:

$$\begin{aligned}
\mathbf{e}^\alpha \cdot \mathcal{D}'_\Gamma \cdot \mathbf{e}_\alpha &= \frac{1}{2}\, \mathbf{e}^\alpha \cdot \mathbf{e}^\beta \otimes \left(\frac{\partial v^3}{\partial \xi^\beta}\, \mathbf{n} + v^3 \frac{\partial \mathbf{n}}{\partial \xi^\beta} \right) \cdot \mathbf{e}_\alpha \\
&\quad + \frac{1}{2}\, \mathbf{e}^\alpha \cdot \left(\frac{\partial v^3}{\partial \xi^\beta}\, \mathbf{n} + v^3 \frac{\partial \mathbf{n}}{\partial \xi^\beta} \right) \otimes \mathbf{e}^\beta \cdot \mathbf{e}_\alpha \\
&= \frac{1}{2}\, \mathbf{e}^\alpha \cdot \mathbf{e}^\beta \otimes \left(v^3 \frac{\partial \mathbf{n}}{\partial \xi^\beta} \right) \cdot \mathbf{e}^\beta g_{\alpha\beta} + \frac{1}{2}\, \mathbf{e}^\alpha \cdot \left(v^3 \frac{\partial \mathbf{n}}{\partial \xi^\alpha} \right) \\
&= v^3 \operatorname{div}_\Gamma \mathbf{n} + \mathbf{n} \cdot \nabla_\Gamma v^3 = \operatorname{div}_\Gamma (v^3 \mathbf{n}).
\end{aligned}$$

In a similar manner, we find that the following relation is valid for the tensor $\mathcal{D}''_\Gamma = \mathcal{D}_\Gamma - \mathcal{D}'_\Gamma$:

$$\mathbf{e}^\alpha \cdot \mathcal{D}''_\Gamma \cdot \mathbf{e}_\alpha = \operatorname{div}_\Gamma \mathbf{v}_\Gamma.$$

This and previous equalities show that formula (2.33) and, correspondingly, eq. (2.30) are valid. Based on eq. (2.30), we can obtain formula (2.29) by almost completely repeating the considerations of Section 1.2 (with natural replacement of a moving volume by a moving surface and of the operator div by the operator $\operatorname{div}_\Gamma$).

To transform the curvilinear integral in the right-hand side of eq. (2.28), we use the formula

$$\int\limits_{\partial\gamma_t} \mathbf{b}\cdot\boldsymbol{\nu}_\Gamma\, dl = \int\limits_{\gamma_t} \operatorname{div}_\Gamma[\mathbf{b} - (\mathbf{n}\cdot\mathbf{b})\mathbf{n}]\, d\gamma, \tag{2.34}$$

where $\mathbf{b}$ is an arbitrary smooth vector. To prove the validity of eq. (2.34), we note that the following relation holds by virtue of the identity $\boldsymbol{\nu}_\Gamma\, dl = -\mathbf{n}\times d\mathbf{l}$ (which was already used in Section 2.3):

$$\int\limits_{\partial\gamma_t} \mathbf{b}\cdot\boldsymbol{\nu}_\Gamma\, dl = \int\limits_{\partial\gamma_t} (\mathbf{n}\times\mathbf{b})\cdot d\mathbf{l}. \tag{2.35}$$

We transform the integral in the right-hand side of eq. (2.35) on the basis of the Stokes theorem by taking into account the equality

$$\mathbf{n}\cdot[\operatorname{rot}(\mathbf{n}\times\mathbf{b})] = \operatorname{div}[\mathbf{b} - (\mathbf{n}\cdot\mathbf{b})\mathbf{n}]. \tag{2.36}$$

In turn, equality (2.36) follows from the vector analysis formula $\operatorname{rot}(\mathbf{n}\times\mathbf{b}) = \mathbf{b}\cdot\nabla\mathbf{n} - \mathbf{n}\cdot\nabla\mathbf{b} + \mathbf{n}\operatorname{div}\mathbf{b} - \mathbf{b}\operatorname{div}\mathbf{n}$ and from the fact that $\nabla|\mathbf{n}|^2 = 0$ and, therefore, $\mathbf{n}\cdot(\mathbf{b}\cdot\nabla\mathbf{n}) = 0$. Finally, we have $\operatorname{div}[\mathbf{b} - (\mathbf{n}\cdot\mathbf{b})\mathbf{n}] = \operatorname{div}_\Gamma[\mathbf{b} - (\mathbf{n}\cdot\mathbf{b})\mathbf{n}]$, because the vector $\mathbf{b} - (\mathbf{n}\cdot\mathbf{b})\mathbf{n}$ has a zero normal component. The required equality (2.34) follows from here and from eqs. (2.35) and (2.36).

Let us now assume that $f = u$ in eq. (2.29) and $\mathbf{b} = \sigma\mathbf{v}$ in eq. (2.34). Using these formulas, we write both sides of equality (2.28) as integrals over the domain γ_t. We obtain

$$\begin{aligned}\int\limits_{\gamma_t}\left(\frac{du}{dt} + u\operatorname{div}_\Gamma\mathbf{v}\right)d\gamma \\ = \int\limits_{\gamma_t}\left([\mathbf{q}\cdot\mathbf{n}] - \mathbf{v}\cdot[\mathcal{P}\cdot\mathbf{n}] + \operatorname{div}_\Gamma\langle\sigma\{\mathbf{v} - (\mathbf{n}\cdot\mathbf{v})\mathbf{n}\}\rangle\right)d\gamma.\end{aligned} \tag{2.37}$$

As the domain $\gamma_t \subset \Gamma_t$ is arbitrary, it follows from eqs. (2.37) that the integrands in both sides of this equality coincide. In other words,

$$\frac{du}{dt} + u\operatorname{div}_\Gamma\mathbf{v} = [\mathbf{q}\cdot\mathbf{n}] - \mathbf{v}\cdot[\mathcal{P}\cdot\mathbf{n}] + \operatorname{div}_\Gamma(\sigma\mathbf{v}_\Gamma), \tag{2.38}$$

where the notation $\mathbf{v}_\Gamma = \mathbf{v} - (\mathbf{n}\cdot\mathbf{v})\mathbf{n}$ is used.

To find the final form of condition (2.38), we use the following relations: equality

$$u(\theta) = \sigma - \theta\frac{d\sigma}{d\theta},$$

which follows from eqs. (2.19) and (2.20); Fourier law (1.29); dynamic condition on the interface (2.8), which implies that $\mathbf{v}\cdot[\mathcal{P}\cdot\mathbf{n}] = 2\sigma H(\mathbf{n}\cdot\mathbf{v}) + \mathbf{v}_\Gamma\cdot\nabla_\Gamma\sigma$; formula

$\operatorname{div}_\Gamma(\sigma \mathbf{v}_\Gamma) = \sigma \operatorname{div}_\Gamma \mathbf{v}_\Gamma + \mathbf{v}_\Gamma \cdot \nabla_\Gamma \sigma$; equality $\operatorname{div}_\Gamma\{(\mathbf{n} \cdot \mathbf{v})\mathbf{n}\} = -2\sigma H(\mathbf{n} \cdot \mathbf{v})$, which follows from eq. (2.9). Based on all considerations discussed above, we can conclude that

$$-\theta\sigma''(\theta)\frac{d\theta}{dt} = \theta\sigma'(\theta)\operatorname{div}_\Gamma \mathbf{v} - \left[k\frac{\partial\theta}{\partial n}\right], \tag{2.39}$$

where the prime denote differentiation with respect to θ.

Condition (2.39) can be called the *energy condition on the interface* Γ_t of two fluids. It means that the jump of the heat flux into direction of the normal to Γ_t is compensated by the change in the internal energy of this surface. In turn, this change is related both to the change in temperature (and, correspondingly, in the specific internal energy) and to the change in the interface area: this circumstance is responsible for the emergence of the first term in the right-hand side of eq. (2.39). In an important particular case of a linear dependence of σ on θ of the form (2.21), condition (2.39) is simplified to

$$\left[k\frac{\partial\theta}{\partial n}\right] + æ\theta \operatorname{div}_\Gamma \mathbf{v} = 0. \tag{2.40}$$

Finally, if $\sigma = \text{const}$, then eq. (2.39) expresses the continuity of the surface density of the heat flux $q_n = k\partial\theta/\partial n$ across the interface.

To conclude this section, we note that the coefficient $-\theta\sigma''(\theta)$ used as a multiplier ahead of the derivative $d\theta/dt$ in condition (2.39) coincides with the specific heat capacity of the interface $c_\Gamma = du/d\theta$. Physically, the heat capacity is a nonnegative quantity; this condition, together with the positiveness of the absolute temperature θ, yields the inequality $\sigma''(\theta) \le 0$. The following *mathematical* considerations support the fact that the value of c_Γ is nonnegative. If, for the sake of simplicity, we assume that the fluids are incompressible and the surface Γ_t and the velocity fields $\mathbf{v}_1$ and $\mathbf{v}_2$ in the domains Ω_{1t} and Ω_{2t} are specified (these domains are assumed to be compact), then condition (2.39) with $c_\Gamma > 0$ has a dissipative character with respect to the heat conduction operator. Therefore, problem (1.49), (2.24), (2.39), under additional initial conditions and standard (Dirichlet or Neumann) conditions on fixed external boundaries of the domains Ω_{it}, can be considered to be well-posed. (If $c_\Gamma = 0$, then we obtain a well-studied problem of diffraction for parabolic equations.) In the case with $c_\Gamma < 0$, however, the problem discussed here is ill-posed in the sense of Hadamard.

2.7 Free surfaces

Applications often involve liquid–gas contact boundaries. It is known that the dynamic coefficients of viscosity for gases are smaller by one or two orders of magnitude than the corresponding coefficients for liquids. Therefore, in the case of gas motion with moderate velocities, we can assume that the shear stresses arising on the interface from the side of the gas are negligibly small and the normal stresses coincide with

the gas pressure with accuracy to their sign. In this paragraph, the fields of variables that refer to the liquid are described by symbols without subscripts or superscripts, and the gas pressure and temperature are denoted by p_g and θ_g, respectively.

The notion of the free boundary appears when the problem of joint motion of a liquid and a gas is replaced by a simpler problem where the functions p_g and θ_g are assumed to be specified, while the characteristics of the liquid and the interface location have to be determined. It is important to emphasize that the issue of finding the velocity field in the gas does not arise at all in this approach. Therefore, only one condition from (2.1) is relevant here:

$$\mathbf{v} \cdot \mathbf{n} = V_n, \quad \mathbf{x} \in \Gamma_t \tag{2.41}$$

(in this paragraph, $\mathbf{n}$ is used to denote the unit vector of the normal to the surface Γ_t, which is external relative to the domain Ω_t).

The dynamic condition on the free boundary is obtained from eq. (2.8), if we set $\mathcal{P}_g = -p_g I$ in accordance with the discussion above. This yields

$$\mathcal{P} \cdot \mathbf{n} + p_g \mathbf{n} = 2\sigma H \mathbf{n} + \nabla_\Gamma \sigma, \quad \mathbf{x} \in \Gamma_t. \tag{2.42}$$

As the velocity field in the gas is not determined, condition (2.23) becomes meaningless. Formally, conditions (2.42) with a known surface Γ_t (which is material by virtue of eq. (2.41)) and a known temperature field θ in the domain Ω_t are sufficient for the boundary-value problem for $\varrho(\mathbf{x}, t)$, $\mathbf{v}(\mathbf{x}, t)$, and $p(\mathbf{x}, t)$ from system (1.46), which is formulated by adding initial conditions, to become well-posed. (In any case, this follows from considering a linearized version of this problem.) On the other hand, relation (2.41) can be considered as an equation for determining the interface, based on a known velocity field $\mathbf{v}$: $f_t + \mathbf{v} \cdot \nabla f = 0$, $\mathbf{x} \in \Gamma_t$, where $f(\mathbf{x}, t) = 0$ is the equation of Γ_t.

Applying similar considerations to eq. (1.49), we conclude that only one boundary condition for temperature should be imposed on the boundary of the domain Ω_t if the surface Γ_t and the functions ϱ and $\mathbf{v}$ in this domain are specified. In particular, we can simply assume that

$$\theta = \theta_g, \quad \mathbf{x} \in \Gamma_t. \tag{2.43}$$

If $\theta_g = \text{const}$, then eq. (2.43) means *isothermality* of the free surface. Another, less popular option is to use eq. (2.39), with $k_2 \partial\theta_2/\partial n = q_g$ being assumed to be a specified function, as the initial condition instead of eq. (2.24). This yields

$$-\theta\sigma''(\theta)\frac{d\theta}{dt} - \theta\sigma''(\theta)\,\mathrm{div}_\Gamma \mathbf{v} + k\frac{\partial\theta}{\partial n} = q_g. \tag{2.44}$$

At $q_g = 0$, eq. (2.44) transforms to the condition of a thermally insulated free boundary.

The approaches proposed above are vulnerable because the right-hand sides of eqs. (2.43) and (2.44) include the values of temperature or heat flux along the normal

to Γ_t on the free boundary unknown in advance. Therefore, eq. (2.43) or (2.44) is often replaced in practice by the condition

$$k\frac{\partial\theta}{\partial n} + b(\theta - \theta_g) = 0, \quad \mathbf{x} \in \Gamma_t, \tag{2.45}$$

where θ_g is a controlled value of temperature at a certain point of the gas phase (for instance, the value of the gas temperature at infinity for an unbounded domain θ_g external to Ω_t) and b is an empirical function called the *interphase heat-transfer coefficient*.

Determination of the function $b(\mathbf{x}, t)$ depending on the domain geometry, conditions on the external boundaries, etc., is a problem difficult to formalize. An empirical coefficient in condition (2.45) serves as a penalty for the lack of desire (or lack of skills) to solve the problem with a free boundary as a problem of joint motion of a liquid and a gas and heat transfer between them.

2.8 Additional conditions

The problem of motion of immiscible fluids consists of determining the domains Ω_{it} ($i = 1, 2$) and two sets of functions $\varrho_i, \mathbf{v}_i, \theta_i$ satisfying system (1.46) in each domain Ω_{it}. Equations (2.1), (2.8), (2.23), (2.34), and (2.39) should be satisfied on the interface Γ_t. Obviously, these conditions are insufficient to solve the problem under discussion for the mere reason that the union of the domains $\bar{\Omega}_{1t}$ and $\bar{\Omega}_{2t}$ does not necessarily coincide with the entire space $\mathbb{R}^3$. In a typical situation, each domain Ω_{1t}, Ω_{2t} has an "external" boundary S_{it} ($i = 1, 2$) in addition to their common "internal" boundary Γ_t. The case where the boundaries S_{1t} and S_{2t} are solid surfaces is particularly important.

We assume that the surfaces S_{1t} and S_{2t} are specified for all $t \in [0, T]$, where $T > 0$ is a certain number. In addition, we first assume that $\bar{\Gamma}_t \cap \bar{S}_{it} = \varnothing$ for $0 \le t \le T$ ($i = 1, 2$); the bar means closure. As the location of the surface Γ_t is not known in advance, it is difficult to verify the last condition. Nevertheless, if it is satisfied at $t = 0$ and the velocity field is continuous in the domains $\bar{\Omega}_{1t}$ and $\bar{\Omega}_{2t}$, then the validity of this condition is guaranteed for sufficiently small values of T. The condition for velocities on the external boundaries of the domains Ω_{it} is usually imposed in the form

$$\mathbf{v}_i = \mathbf{a}_i(\mathbf{x}, t), \quad \mathbf{x} \in S_{it}, \tag{2.46}$$

where $\mathbf{a}_i$ are known functions.

Now let S_{it} be the surface of a nondeformable solid. The velocity distribution in such a solid is given by the formula $\mathbf{u}_i = \mathbf{U}_i(t) + \boldsymbol{\Omega}_i(t) \times \mathbf{x}$. Let us postulate that the fluid velocity coincides with the boundary velocity on the solid part of the boundary of the domain Ω_{it}. It follows from the last formula and eq. (2.46) that

$$\mathbf{v}_i = \mathbf{U}_i + \boldsymbol{\Omega}_i \times \mathbf{x}, \quad \mathbf{x} \in S_{it}, \tag{2.47}$$

where $\mathbf{U}_i(t)$ is the translational velocity of the i-th solid and $\mathbf{\Omega}_i(t)$ is its instantaneous angular velocity. If the solid boundaries are motionless, eq. (2.47) turns to

$$\mathbf{v}_i = 0, \quad \mathbf{x} \in S_i. \tag{2.48}$$

Condition (2.47) and its particular case (2.48) are called the *no-slip conditions*. If only some part of the surface S_{it} is the fluid–solid boundary, the condition (2.47) is imposed only on this part of the surface. On the remaining part of S_{it}, the function $\mathbf{a}_i$ can be rather arbitrary.

The no-slip condition reflects the fact that there are always molecular adhesion forces between the solid surface and the fluid. These forces capture and arrest fluid particles contacting the wall. In special situations (rarefied gas flow or motion near the line of the liquid contact with a gas and a solid), these forces can be attenuated, which results in modifications of the no-slip conditions. Rarefied gas dynamics issues are not considered here; the flow near the three-phase contact line is considered in [171, 50, 189, 28] (see also the end of this section).

As a condition for temperature on specified components of the interface between the domains Ω_{1t} and Ω_{2t}, one of two equalities should be satisfied, either

$$\theta_i = \theta_{S_i}(\mathbf{x}, t), \quad \mathbf{x} \in S_{it} \tag{2.49}$$

or

$$k_i \frac{\partial \theta_i}{\partial n_i} = q_{S_i}(\mathbf{x}, t), \quad \mathbf{x} \in S_{it}. \tag{2.50}$$

Here θ_{S_i} and q_{S_i} $(i = 1, 2)$ are known functions, which actually are the temperature of the surface S_{it} and the heat flux normal to this surface. The unit vector of the external normal to the surface S_{it} is denoted by $\mathbf{n}_i$, and the operation of differentiation in the direction $\mathbf{n}_i$ is denoted by $\partial/\partial n_i$.

As the values of the vector $\mathbf{v}_i$ on the surface S_i are assumed to be known, let us determine the sets $S_{it} = \{\mathbf{x} \in v_{it}, \mathbf{v}_i \cdot \mathbf{n}_i < U_{n_i}\}$, $i = 1, 2$, where U_{n_i} is the velocity of motion of the surface S_{it} in the direction $\mathbf{n}_i$. (Let us call them the sets or the *inlet segments*.) The differential equation of continuity (the first equation of system (1.46)) can be formally treated as a first-order equation with respect to density. The corresponding system of equations of the characteristics coincides with eq. (1.10). Therefore, an additional condition for the function ϱ_i appears:

$$\varrho_i = \gamma_i(\mathbf{x}, t), \quad \mathbf{x} \in S_{it}^+ \tag{2.51}$$

(γ_i are known functions). Two cases where condition (2.51) is not imposed should be mentioned. If a fluid contacts a solid, then there are no inlet segments owing to the no-slip condition. The second case is the motion of a system of homogeneous incompressible fluids. The continuity equation is replaced here by $\operatorname{div} \mathbf{v}_i = 0$, and the quantities ϱ_i become given constants instead of the sought functions; on the other hand, the functions p_i are added to the list of the sought functions.

Finally, we need to formulate initial conditions for the solution of the evolution problem described as definite. First, we have to impose the initial location of the interface Γ_0. Definition of Γ_0 determines the domains Ω_{10} and Ω_{20}. The initial conditions for system (1.46) have the natural form

$$\mathbf{v}_i = \mathbf{v}_{i0}(\mathbf{x}) \quad \text{at } t = 0; \tag{2.52}$$

$$\boldsymbol{\theta}_i = \boldsymbol{\theta}_{i0}(\mathbf{x}) \quad \text{at } t = 0; \tag{2.53}$$

$$\boldsymbol{\varrho}_i = \boldsymbol{\varrho}_{i0}(\mathbf{x}) \quad \text{at } t = 0. \tag{2.54}$$

The functions $\mathbf{v}_{i0}, \boldsymbol{\theta}_{i0}$, and $\boldsymbol{\varrho}_{i0}$ determined in the domain Ω_{i0} $(i = 1, 2)$ are assumed to be known. If the fluid is incompressible and homogeneous, condition (2.54) is not imposed.

An important class of problems of motion with interfaces also includes steady problems. In such solutions, the surfaces Γ and the sought functions ϱ_i, $\mathbf{v}_i$, and θ_i are independent of time. For steady solutions to exist, it is obvious that the external surfaces S_i should be motionless, and the known functionals $\mathbf{f}_i$, h_i, $\mathbf{a}_i$, etc., which are involved into the equations and boundary conditions, should be also independent of t. The issue of the initial conditions for steady problems is immaterial, although such problems involve additional conditions of another kind: the specified quantities include the values of one or several functionals fixing the flow rates of the fluids, the volume of the domain Ω_1 or Ω_2, etc.

We did not discuss here the issues of the smoothness and compatibility conditions which the input data of the problem discussed for system (1.46) should obey. They may be different in different problems. The example of a model problem of plane isothermal motion of a homogeneous fluid with moving contact points between the free boundary and the solid wall clearly shows that these issues are nontrivial. Generally speaking, it turns out that the condition of continuity of the velocity field at the three-phase contact point is incompatible with the no-slip condition and with the kinematic condition on the free boundary. This incompatibility was first noted by Dussan and Davis [51] (see also [50, 189]). A mathematically well-posed and physically grounded method of closing the problem of motion of immiscible fluids (or the problem with a free boundary) is a disputable issue if the condition $[\Gamma_t] \cap [S_{it}] = \varnothing$ is not satisfied. Alternative approaches for solving this issue are discussed in [28] as well as in the works cited above. An original method for closing the problem of motion of the three-phase contact line, which requires only one empirical constant to be known, was proposed by Voinov [231] (see also [47]). The current state of wetting hydrodynamics was described in [232].

3 Models of convection of an isothermally incompressible fluid

In this chapter, the case of convection with temperature-dependent viscosity and thermal conductivity and with density only as a function of temperature is considered. With the use of the thermodynamic identity, the specific volume at a constant specific heat is demonstrated to be a linear function of temperature. Possible formulations of initial-boundary problems for the systems of equations obtained are discussed. It is shown that elastic properties of the container should be taken into account in the problem of convection in a closed volume, which allows the influence of the container walls on convective fluxes to be described correctly.

The results of this chapter are based on publications [237, 177, 13].

3.1 Isothermally incompressible fluid

It is well known from thermodynamics [132] that a comprehensive description of a certain medium is obtained by defining a state equation of the form $H(V, p, \theta) = 0$; for instance, for a perfect gas, $Vp = R\theta$ is the Clapeyron–Mendeleev equation, where R is the universal gas constant. The caloric equation, which expresses the specific heat at constant pressure c_p via the basic thermodynamic parameters (see eq. (1.43)) is also assumed to be known.

Let the state equation be resolved with respect to the specific volume:

$$V = V(\theta, p). \tag{3.1}$$

It is certainly not always possible to present the state equation in the form (3.1). In fact, the assumption above eliminates the possibility of phase transitions in the substance considered. It is the nonuniqueness, i. e., different values of V at identical values of θ and p, that indicates the existence of different phases, for example, ice–water–steam. Such a multiphase medium is described (though only approximately) by the van der Waals equation [132]

$$\left(p + \frac{an^2}{V^2}\right)(V - bn) = nR\theta,$$

where n is the number of moles; a and b are constants.

Let $F = U - \theta s$ be the free Helmholtz energy, and let $U = U(\theta, p)$ and $s = s(\theta, p)$. Then, the thermodynamic identity (1.35) yields the presentations (the expressions at the differentials $d\theta$ and dp should be equated to each other)

$$s = -pV_\theta - F_\theta - A; \tag{3.2}$$

$$U = -p\theta V_\theta + F - \theta F_\theta + B; \tag{3.3}$$

https://doi.org/10.1515/9783110655469-003

$$F = -pV + \int_{p_0}^{p} V(\theta, \bar{p})\, d\bar{p} + G(\theta) \tag{3.4}$$

with certain constants A, B, p_0, and an arbitrary function $G(\theta)$; in eqs. (3.2)–(3.4), $V(\theta, p)$ is defined by equality (3.1). If, in addition to eq. (3.1), as mentioned above, the dependence $c_p(\theta, p)$ on the temperature θ is defined at least for one value of the pressure p, then, using eqs. (1.35) and (3.2) we can find the function $G(\theta)$ in (3.4) from the equality

$$G_{\theta\theta} = -\int_{p_0}^{p} V_{\theta\theta}(\theta, \bar{p})\, d\bar{p} - \frac{1}{\theta}\, c_p(\theta, p). \tag{3.5}$$

Let us again recall that p in eq. (3.5) is a certain *fixed value of pressure*.

A fluid is called *isothermally incompressible* if its density is independent of pressure, but it may depend on temperature, i. e.,

$$V = V(\theta) \quad (\varrho = V^{-1}(\theta)). \tag{3.6}$$

In this case, eqs. (3.2), (3.3), and (3.5) become the equalities

$$c_p = -p\theta V''(\theta) - \theta G''(\theta); \tag{3.7}$$

$$s = -pV'(\theta) - G'(\theta); \tag{3.8}$$

$$U = -p\theta V'(\theta) + G(\theta) - \theta G'(\theta). \tag{3.9}$$

Without loss of generality, the constants A, B, and p_0 here are replaced by zeroes.

Expression (3.7) for c_p yields a remarkable conclusion: the specific heat at constant pressure for an isothermally incompressible fluid is independent of the pressure p if and only if the specific volume V is a *linear function of temperature*,

$$V(\theta) = V_0(1 + \beta\theta), \tag{3.10}$$

where $\beta > 0$ is the coefficient of thermal (volume) expansion. Choosing a certain value of the temperature θ_0, we can write this volume as

$$V(\theta) = V(\theta_0)[1 + \beta(\theta - \theta_0)]. \tag{3.11}$$

Formulas (3.7)–(3.9) are simplified to

$$c_p = -\theta G''(\theta); \tag{3.12}$$

$$s = -\beta p V_0 - G'(\theta); \tag{3.13}$$

$$U = -\beta\theta p V_0 + G(\theta) - \theta G'(\theta). \tag{3.14}$$

3.2 Equations of thermal convection of an isothermally incompressible fluid

We proceed from system (1.48), assuming that the coefficients λ, μ, and k depend on the absolute temperature θ and pressure p. In addition, we introduce the *coefficient of volume viscosity*

$$\zeta = \lambda + \frac{2}{3}\mu. \tag{3.15}$$

By virtue of the last inequality of system (1.55), we have $\zeta \geq 0$. Another assumption of principal importance is the dynamic validity of eqs. (3.7)–(3.9), which express the dependence of c_p, s, and U on p and θ. In reality, however, not only the particular expressions (3.7)–(3.9), but also the mere fact of the existence of such functional dependences is doubtful. The conditions of applicability of the assumption made above have been little studied. In any case, it is clear that this assumption is valid only in situations where the process is not too far from thermodynamic equilibrium and can be considered to be a quasi-static process.

Let us rewrite the left-hand side of the energy equation (1.48) as

$$\begin{aligned}\varrho\theta\frac{ds}{dt} &= \varrho\theta\left[\left(\frac{\partial s}{\partial\theta}\right)_p\frac{d\theta}{dt} + \left(\frac{\partial s}{\partial p}\right)_\theta\frac{dp}{dt}\right]\\ &= \varrho c_p\frac{d\theta}{dt} + \varrho\theta\left(\frac{\partial s}{\partial p}\right)_\theta\frac{dp}{dt} = \varrho c_p\frac{d\theta}{dt} + \frac{\theta}{\varrho}\left(\frac{\partial\varrho}{\partial\theta}\right)\frac{dp}{dt},\end{aligned}$$

because $\partial s/\partial p = \varrho^{-2}\partial\varrho/\partial\theta$.

Let us now insert eqs. (3.6) and (3.8) into eqs. (1.48) and obtain a *model of convective motion of an isothermally incompressible fluid*

$$V'(\theta)\frac{d\theta}{dt} = V(\theta)\operatorname{div}\mathbf{v}; \tag{3.16}$$

$$\frac{d\mathbf{v}}{dt} = V(\theta)\nabla(-p + \zeta\operatorname{div}\mathbf{v}) + V(\theta)\operatorname{div}\left[2\mu\left(\mathcal{D} - \frac{1}{3}\operatorname{div}\mathbf{v}I\right)\right] + \mathbf{f}; \tag{3.17}$$

$$c_p\frac{d\theta}{dt} - \theta V'(\theta)\frac{dp}{dt} = V(\theta)\Phi + V(\theta)\operatorname{div}(k\nabla\theta) + h, \tag{3.18}$$

where I is the unit tensor in eq. (3.17), c_p is defined by eq. (3.7), and the dissipative function Φ (see eq. (1.47)) is

$$\Phi = \zeta(\operatorname{div}\mathbf{v})^2 + 2\mu\mathcal{D}' : \mathcal{D}'. \tag{3.19}$$

Equations (3.16)–(3.18) with known dependences (3.6) and (3.7) form a closed system for determining v_1, v_2, v_3, θ, and p. If the value of the derivative $d\theta/dt$ from eq. (3.16) is substituted into eq. (3.18), then system (3.16)–(3.18) transforms to a system resolved relative to derivatives with respect to time for the unknown velocity vector $\mathbf{v}$, temperature θ, and pressure p. Thus, the issue of initial conditions is clarified: it is necessary to specify $\mathbf{v}$, θ, and p at the initial time. The issue of boundary conditions is more complicated; it is discussed later in Section 3.5.

3.3 Model of linear thermal expansion

Let us consider the case where the state equation has the form (3.10). As it was demonstrated above, this linear law corresponds exactly to the case where the specific heat c_p is independent of the pressure p. In this case, eqs. (3.12)–(3.14) are valid. We also need to define the caloric equation or, in accordance with eqs. (3.4) and (3.5), the free energy $F(\theta) = G(\theta)$. Let us define it in the simplest form as

$$c_p = \text{const}, \tag{3.20}$$

i. e., c_p is also assumed to be temperature independent. This assumption is justified by the fact that the dependence of specific heat on temperature, and on pressure as well, is much weaker for the majority of *real fluids* than the corresponding dependences of viscosity and thermal conductivity. For example, for water at atmospheric pressure with θ varying from 273 K to 373 K, the deviation of c_p from its mean value does not exceed 1 %.

From eqs. (3.20), (3.5), and (3.4), we find

$$F(\theta) = G(\theta) = -c_p(\theta \ln \theta - \theta) + A\theta + B, \tag{3.21}$$

where A and B are constants. Substitution of eq. (3.21) into eqs. (3.13) and (3.14) yields the relations

$$s = -\beta V_0 p + c_p \ln \theta - A; \tag{3.22}$$

$$U = -\beta V_0 \theta p + B. \tag{3.23}$$

Obviously, the values of the constants A and B are unimportant: they only determine the reference point for calculating the values of s and U.

Equations (3.16)–(3.18) now take the form

$$\beta \frac{d\theta}{dt} = (1 + \beta\theta) \operatorname{div} \mathbf{v}; \tag{3.24}$$

$$\frac{d\mathbf{v}}{dt} = V_0(1 + \beta\theta)\left\{\nabla(-p + \zeta \operatorname{div} \mathbf{v}) \operatorname{div}\left[2\mu\left(\mathcal{D} - \frac{1}{3}\operatorname{div} \mathbf{v} I\right)\right]\right\} + \mathbf{f}; \tag{3.25}$$

$$\frac{d\theta}{dt} - \frac{\beta V_0 \theta}{c_p}\frac{dp}{dt} = \frac{V_0}{c_p}(1 + \beta\theta)[\Phi + \operatorname{div}(k\nabla\theta)] + \frac{h}{c_p}. \tag{3.26}$$

Let us bring system (3.24)–(3.26) to the dimensionless form. There is a certain arbitrariness in choosing the characteristic scales that allow us to pass to dimensionless equations, but common sense suggests which scales should be used in each *particular problem*. The choice of such scales eliminates insignificant variables, so that in the end only the basic variables are left. It is particularly important to choose appropriate basic dimensionless parameters in studying the model of convection in the "limiting" cases where one or several parameters tend to zero (infinity).

Let us introduce some characteristic quantities: l is the length, e. g., the linear size of the domain occupied by the fluid, θ_* is the difference in temperatures, μ_0 is the dynamic viscosity, $\mu = \mu_0\mu'(\theta)$, k_0 is the thermal conductivity, $k = k_0k'(\theta)$, ζ_0 is the volume viscosity, $\zeta = \zeta_0\zeta'(\theta)$, and $\chi_0 = k_0/\varrho_0 c_p$ is the thermal diffusivity, where $\varrho_0 = 1/V_0$. Following the discussion above and the reasoning of [13], we introduce dimensionless (primed) variables by the formulas

$$\mathbf{x} = l\mathbf{x}', \quad t = \frac{l^2}{\chi_0}\,t', \quad \mathbf{v} = \frac{\chi_0}{l}\,\mathbf{v}', \quad p = \frac{\varrho_0\nu_0\chi_0}{l^2}\,p', \quad \theta = \theta_*\theta' \left(\nu_0 = \frac{\mu_0}{\varrho_0}\right). \tag{3.27}$$

Substituting eqs. (3.27) into eqs. (3.24)–(3.26) and omitting the primes, we obtain the system

$$\varepsilon\frac{d\theta}{dt} = (1+\varepsilon\theta)\operatorname{div}\mathbf{v}, \tag{3.28}$$

$$\frac{d\mathbf{v}}{dt} = \operatorname{Pr}(1+\varepsilon\theta)\left\{\nabla(-p+\xi\zeta\operatorname{div}\mathbf{v}) + 2\operatorname{div}\left[\mu\left(\mathcal{D} - \frac{1}{3}\operatorname{div}\mathbf{v}I\right)\right]\right\} + \mathbf{f}_1, \tag{3.29}$$

$$\frac{d\theta}{dt} - \varepsilon\varepsilon_1\theta\frac{dp}{dt} = (1+\varepsilon\theta)\left[\operatorname{div}(k\nabla\theta) + \varepsilon_1\Phi + h_1\right], \tag{3.30}$$

where

$$\varepsilon = \beta\theta_*, \quad \xi = \frac{\zeta_0}{\mu_0}, \quad \operatorname{Pr} = \frac{\nu_0}{\chi_0}, \quad \varepsilon_1 = \frac{\nu_0\chi_0}{l^2c_p\theta_*}, \tag{3.31}$$

$$\mathbf{f}_1 = \frac{l^3}{\chi_0^2}\,\mathbf{f}, \quad h_1 = \frac{l^2h}{c_pk_0\theta_*}, \tag{3.32}$$

ε is the *Boussinesq parameter*, and Pr is the *Prandtl number*. The dimensionless dissipative function is described by the equality

$$\Phi = \xi(\operatorname{div}\mathbf{v})^2 + 2\mathcal{D}' : \mathcal{D}'$$

ε_1 is called the *dissipation parameter*.

Let the field of mass forces depend on time only: $\mathbf{f} = \mathbf{f}(t)$. Then, the replacement (where $\bar{p}$ is the *modified pressure*)

$$p = \bar{p} + \mathbf{x}\cdot\mathbf{f}_1(t)\operatorname{Pr}^{-1} \tag{3.33}$$

allows us to rewrite the equations of momentum (3.29) and energy (3.30) in the form

$$\begin{aligned}\frac{d\mathbf{v}}{dt} = \operatorname{Pr}(1+\varepsilon\theta)\Big\{&\nabla(-\bar{p}+\xi\zeta\operatorname{div}\mathbf{v}) \\ &+ 2\operatorname{div}\left[\mu\left(\mathcal{D} - \frac{1}{3}\operatorname{div}\mathbf{v}I\right)\right]\Big\} - \varepsilon\operatorname{Pr}\theta\boldsymbol{\eta}(t);\end{aligned} \tag{3.29′}$$

$$\frac{d\theta}{dt} - \varepsilon\varepsilon_1\theta\frac{d\bar{p}}{dt} = (1+\varepsilon\theta)\left[\operatorname{div}(k\nabla\theta) + \varepsilon_1\Phi + h_1\right] + \varepsilon\varepsilon_1\operatorname{Pr}^{-1}\theta\frac{d}{dt}\left(\mathbf{x}\cdot\boldsymbol{f}_1(t)\right), \tag{3.30′}$$

$\boldsymbol{\eta}(t) = l^3\mathbf{f}(t)/(\nu_0\chi_0)$ being the *vector parameter of microconvection*. Note that $\varepsilon\boldsymbol{\eta}(t) = \mathbf{Ra}(t)$ is the vector of the *Rayleigh numbers* and the product $\mathrm{Pr}\,\varepsilon\boldsymbol{\eta}(t) = \mathbf{Gr}$ is the vector of the *Grashof numbers*.

Let us assume that $\mathbf{f} = (0, 0, -g)$, where $g = \mathrm{const}$ is the acceleration due to gravity. In this case, convection is called the *thermogravitational convection*, the parameter $\eta = l^3g/(\nu_0\chi_0)$ is simply the microconvection parameter [177], while the Rayleigh and Grashof numbers take the form

$$\mathrm{Ra} = \beta\theta_* l^3 g/(\nu_0\chi_0), \quad \mathrm{Gr} = \beta\theta_* l^3 g/\chi_0^2, \tag{3.34}$$

they play an important role in studying free convection.

To gain a certain idea about possible values of the parameters ξ, ε, ε_1, Pr, and η, let us consider one particular example (more details on dimensionless parameters are given in the Chapter 4). As $g \sim 9.81\,\mathrm{m/s^2}$, $\varrho_0 \sim 10^3\,\mathrm{kg/m^3}$, $\mu_0 \sim 10^{-4}$–$10^{-3}\,\mathrm{kg/(s{\cdot}m)}$, $\chi_0 \sim 14\cdot 10^{-7}\,\mathrm{m^2/s}$, $c_p \sim 10^3\,\mathrm{J/(kg{\cdot}deg)}$, and $\beta \sim 10^{-4}$–$10^{-3}\,\mathrm{deg^{-1}}$ for real fluids [234], the dimensionless parameters can be estimated at $\theta_* = 10\,^\circ\mathrm{C}$ as $\varepsilon \sim 2.1\cdot 10^{-3}$, $\mathrm{Pr} \sim 0.72$, $\eta \sim 7\cdot 10^6 l^3\,\mathrm{m^{-3}}$, $\xi \sim 1$, and $\varepsilon_1 \sim 14\cdot 10^{-13} l^{-2}\,\mathrm{m^2}$. As shown by [13] (see also Chapter 4), this choice of parameters leads to "correct submodels" as $\varepsilon \to 0$, whereas another transition to dimensionless variables should be used in particular calculations. In particular, the time scale is defined in [237] as $(\beta g\theta_* l^{-1})^{-1/2}$. It describes the typical *upfloating* of a hot fluid particle (or submersion of a cold fluid particle); at $\theta_* = 10\,^\circ\mathrm{C}$, the characteristic velocity for a water pool with a depth $l = 10\,\mathrm{m}$ is $v_* = l(\beta g\theta_* l^{-1})^{1/2} \approx 30\,\mathrm{cm/s}$. In this case, however, there arises a singularity in pressure determination when $\varepsilon \to 0$. In other words, there are some difficulties in comparing the results with the "limiting" models.

3.4 Some submodels

At moderate Prandtl numbers and $\varepsilon \to 0$, system (3.28), (3.29′), (3.30′) approximates the system of equations

$$\frac{d\mathbf{v}}{dt} = \mathrm{Pr}\big[-\nabla\bar{p} + 2\,\mathrm{div}(\mu\mathcal{D})\big]; \tag{3.35}$$

$$\mathrm{div}\,\mathbf{v} = 0; \tag{3.36}$$

$$\frac{d\theta}{dt} = \mathrm{div}(k\nabla\theta) + h_1. \tag{3.37}$$

This system is called the *model of convection of a viscous heat-conducting fluid*. It is often used with constant values of μ and k (equal to unity); then, $2\,\mathrm{div}\,\mathcal{D} = \Delta\mathbf{v}$ and $\mathrm{div}\,\nabla\theta = \Delta\theta$ in this model.

Remark 3.1. The velocity and pressure fields in model (3.35)–(3.37) form a closed system. Nevertheless, they can be related to the temperature field by means of the boundary conditions on the interface or free boundary (see Chapter 4, equality (4.147)).

Let $\varepsilon\boldsymbol{\eta}(t) \to \mathbf{Ra}(t) \neq 0$; then, system (3.28), (3.29′), (3.30′) in the limit as $\varepsilon \to 0$ reduces to the system

$$\frac{d\mathbf{v}}{dt} = \Pr\left[-\nabla\bar{p} + 2\operatorname{div}(\mu\mathcal{D})\right] - \Pr\mathbf{Ra}\,\theta; \tag{3.38}$$

$$\operatorname{div}\mathbf{v} = 0; \tag{3.39}$$

$$\frac{d\theta}{dt} = \operatorname{div}(k\nabla\theta) + \varepsilon_1\Phi + h_1. \tag{3.40}$$

At constant μ, k, and $\varepsilon_1 = 0$ (for many processes, ε_1 is negligibly small), we have $\mathbf{Ra} = \operatorname{Ra}\mathbf{e}_3$, and, from eqs. (3.38)–(3.40), we obtain the *classical Oberbeck–Boussinesq model*

$$\frac{d\mathbf{v}}{dt} = \Pr(-\nabla\bar{p} + \Delta\mathbf{v}) - \Pr\ \operatorname{Ra}\theta\mathbf{e}_3; \tag{3.41}$$

$$\operatorname{div}\mathbf{v} = 0; \tag{3.42}$$

$$\frac{d\theta}{dt} = \Delta\theta + h_1. \tag{3.43}$$

Let us assume that $\varepsilon_1 = 0$ and $h_1 = 0$; then, system (3.28), (3.29′), (3.30′) is called the *microconvection model* (see Chapter 4 for more details).

If the Prandtl number is high ($\Pr \gg 1$), and other parameters are fixed, then system (3.28), (3.29′), (3.30′) in the limit as $\Pr \to \infty$ yields a system of equations that describe "creeping" motions:

$$\varepsilon\frac{d\theta}{dt} = (1 + \varepsilon\theta)\operatorname{div}\mathbf{v}; \tag{3.44}$$

$$\left[\nabla(-\bar{p} + \xi\zeta\operatorname{div}\mathbf{v})\right] + 2\operatorname{div}\left[\mu\left(\mathcal{D} - \frac{1}{3}\operatorname{div}\mathbf{v}I\right)\right] = \varepsilon(1 + \varepsilon\theta)^{-1}\theta\boldsymbol{\eta}(t); \tag{3.45}$$

$$\frac{d\theta}{dt} - \varepsilon\varepsilon_1\frac{d\bar{p}}{dt} = (1 + \varepsilon\theta)\left[\operatorname{div}(k\nabla\theta) + \varepsilon_1\Phi + h_1\right]. \tag{3.46}$$

3.5 On boundary conditions

It is well known in hydrodynamics (see Chapter 2) which conditions should be imposed on the solid walls, on the free boundaries, and on the interfaces. Every time, however, that the object under study is a compressible (and capable of expansion) *fluid*, the question arises whether or not it is feasible to formulate the problem for a domain with an impermeable solid boundary in such a case.

In any case, this formulation implies that the fluid volume is constant, which fact may turn out to be incompatible with the condition of compressibility. In the course of fluid motion, its volume can decrease, and then voids (cavities) should appear in a real fluid; the fluid volume can also increase, owing to thermal expansion. Indeed, let

$|\omega_t|$ be a volume consisting of the same particles at all time instants. Then we have

$$\frac{d|\omega_t|}{dt} = \frac{d}{dt}\int\limits_{\omega_t} d\omega = \int\limits_{\omega_t} \operatorname{div}\mathbf{v}\, d\omega. \tag{3.47}$$

(Here, we use the Euler formula (1.14).) Let us assume that $\varepsilon_1 = 0$ and $h_1 = 0$ in the energy equation (3.30′). If we also take eq. (3.28) into account, we obtain the equation of the change in the fluid volume from eq. (3.47):

$$\frac{d|\omega_t|}{dt} = \varepsilon \int\limits_{\partial\omega_t} k\frac{\partial\theta}{\partial n}\, d\Gamma, \tag{3.48}$$

i. e., the rate of change of the volume of a given fluid mass is proportional to the heat flux through its boundary. Obviously, the fluid volume can remain unchanged only in some exclusive cases, e. g., when the boundary is thermally insulated ($\partial\theta/\partial n = 0$). If the boundary $\partial\omega_t$ is isothermal ($\theta = \theta_0(\mathbf{x}, t)$), the volume changes. We therefore conclude that the problem for an isothermally incompressible fluid cannot be formulated in a domain with a time-independent impermeable boundary, not even in a domain with a constant volume. Note that if an infinite domain (e. g., an infinite layer) is considered, it is possible to avoid the contradiction under the assumption that the wall is solid and undeformable. It is also reasonable to solve problems of the fluid flow in a domain with some part of its boundary being free.

Poor or incompatibility of compressibility with the assumption of a constant total volume of the fluid forces us to take the property of deformability of the walls under consideration. The condition that should be imposed on the solid impermeable wall is the velocity (by eqs. (2.46)), and this condition is independent of whether or not the wall is fixed or deforms with time. The free boundary is subjected to the kinematic (2.41) and dynamic (2.42) conditions, and also to one of the two conditions (2.43) or (2.45). The latter conditions are also imposed on the solid walls. An *essentially new factor* is the allowance for the properties of the deformable wall, and this offers many possibilities. Now we need to consider a combined fluid–solid system, write a system of equations for an elastic (or perhaps viscoelastic or plastic) body, and write the conditions on the external part of this body (container) as well as on the fluid–solid interface.

Among these problems, two are worth mentioning:

1) convection of a fluid filling a cavity in an elastic array;
2) convection of a fluid in a container, which is an elastic shell.

We can use, for example, the Marger–Vlasov equation system, with the addition of temperature stresses if necessary. In the case of small deformations, it is also possible to use the linear theory of shells. Both models are rather complicated and have not been thoroughly studied. Therefore, it seems reasonable to consider a simple model for elucidating the role of container elasticity in the problem of convection.

In addition to the unknowns already introduced, we define a function $\zeta(\mathbf{x}, t)$ on the boundary S (solid wall or its part) of the domain Ω. This function describes the normal displacement of the boundary point. Let us assume as a hypothesis that the normal displacement ζ is proportional to the normal stress

$$\mathcal{P}_{nn} = -\gamma\zeta, \tag{3.49}$$

where $\mathcal{P}_{nn} = -p + 2\mu(\mathcal{D} - 3^{-1}\operatorname{div}\mathbf{v}I)\mathbf{n}\cdot\mathbf{n}$, $\mathbf{n}$ is the normal to S and γ is the stiffness coefficient characterizing the boundary and, generally speaking, depending on $\mathbf{x} \in S$. It is positive, and we have $\zeta = 0$ at $\gamma = \infty$, i. e., the case with a nondeformable boundary. Assuming the *displacement ζ to be small*, we obtain a problem for a fixed domain Ω by shifting all boundary conditions (for velocity, temperature, and eq. (3.49)) to the boundary S. Moreover the boundary S should obey the kinematic boundary condition

$$\frac{\partial\zeta}{\partial t} = -\mathbf{v}\cdot\mathbf{n} \tag{3.50}$$

and the no-slip condition for the tangential component of velocity

$$\mathbf{v}\cdot\boldsymbol{\tau} = 0, \tag{3.51}$$

where $\boldsymbol{\tau}$ is the tangential vector to S. Certainly, the boundary deformations due to shear stresses are actually neglected here: in the case of fast rotation of the fluid, equality (3.51) can be violated.

In the formulation considered, the function ζ is involved only into the boundary conditions (3.49) and (3.50). Differentiating eq. (3.49) with respect to time and taking into account eq. (3.50), we obtain a *boundary condition for velocity* in the form

$$\frac{\partial\mathcal{P}_{nn}}{\partial t} = -\gamma\mathbf{v}\cdot\mathbf{n}. \tag{3.52}$$

3.6 Two problems of convection

Mechanical equilibrium

Let us find all possible mechanical equilibrium states for system (3.28), (3.29′), (3.30′), assuming convection to be thermogravitational, i. e., $\mathbf{f} = (0, 0, -g)$, $g = \text{const}$. The condition $\mathbf{v} = 0$ in the convection problem imposes severe constraints on possible temperature and pressure profiles, independent of the boundary conditions. Thus, we assume that $\boldsymbol{v} = 0$ in eqs. (3.28), (3.29′), (3.30′). As $d/dt = \partial/\partial t + (\mathbf{v}\cdot\nabla)$, it follows from eq. (3.28) that θ is independent of time. Equations (3.29′) and (3.30′) take the form

$$\nabla\bar{p} = \frac{\varepsilon\eta\theta}{1+\varepsilon\theta}\mathbf{e}_3, \quad \mathbf{e}_3 = (0, 0, 1), \tag{3.53}$$

$$-\varepsilon\varepsilon_1\theta\frac{\partial\bar{p}}{\partial t} = \operatorname{div}(k\nabla\theta)(1+\varepsilon\theta). \tag{3.54}$$

In deriving the last equation, we take into account that $d\mathbf{x}/dt = \mathbf{v} = 0$ and, for the sake of simplicity, assume that $h_1 = 0$, i. e., there are no internal sources of heat. It follows from eq. (3.53) that $\bar{p} = \bar{p}(z,t)$, $\theta = \theta(z,t)$ and

$$\frac{\partial \bar{p}}{\partial z} = \frac{\varepsilon\eta\theta}{1+\varepsilon\theta}. \tag{3.55}$$

Equation (3.54) reduces to

$$\frac{\partial \bar{p}}{\partial t} = -\frac{1}{\varepsilon\varepsilon_1}\cdot\frac{1+\varepsilon\theta}{\theta}\,\frac{d}{dz}\left(k\frac{d\theta}{dz}\right). \tag{3.56}$$

The right-hand side of eq. (3.56) is independent of time, $\bar{p} = A(z)t + B(z)$, and it follows from eq. (3.55) that $A(z) = A = \text{const}$. Therefore, the modified pressure $\bar{p}$ in the case of mechanical equilibrium is

$$\bar{p}(z,t) = At + B(z), \tag{3.57}$$

where the function $B(z)$ is the solution of the equation

$$\frac{dB}{dz} = \frac{\varepsilon\eta\theta}{1+\varepsilon\theta}. \tag{3.58}$$

In accordance with eqs. (3.57) and (3.56), the temperature satisfies the equation

$$\frac{d}{dz}\left(k\frac{d\theta}{dz}\right) = -\frac{\varepsilon\varepsilon_1 A\theta}{1+\varepsilon\theta}. \tag{3.59}$$

The pressure in the mechanical equilibrium state can increase linearly with time if $\varepsilon_1 > 0$. If $\varepsilon_1 = 0$, then $\bar{p}$ is determined with accuracy to an arbitrary term—a function of time. If $\varepsilon_1 = 0$ (or $\varepsilon_1 > 0$, $A = 0$), eq. (3.59) is integrated. Introducing a function $K(\theta)$ such that $K'(\theta) = k(\theta)$, we obtain from eq. (3.59) at $\varepsilon_1 A = 0$

$$K(\theta) = Cz + \mathcal{D} \tag{3.60}$$

with constants C and $\mathcal{D}$. Note that the function $K(\theta)$ increases strictly monotonically for $k(\theta) > 0$ everywhere. It follows from here that $\theta(z)$ is uniquely found from eq. (3.60) with given C and $\mathcal{D}$. Therefore, the solution of the boundary-value problem for eq. (3.59) with specified values of $\theta(0)$ and $\theta(l)$ at the ends of the interval $(0,l)$, $l > 0$ is unique.

The situation becomes more complicated in the case of the boundary conditions of the second or third kind ($\theta'(0) = q_1$, $\theta'(h) = q_2$ or $\theta'(0) + b_1\theta(0) = q_1$, $\theta'(l) + b_2\theta(l) = q_2$): the solution may even fail to exist. If the boundary is thermally insulated ($\theta'(0) = \theta'(l) = 0$), then the solution is an arbitrary constant.

It is interesting to compare these results for mechanical equilibrium with the results obtained for the Oberbeck–Boussinesq model (3.38)–(3.40) under the same assumptions: $\mathbf{f} = (0,0,-g)$, $h_1 = 0$. The previous conclusion that θ is independent of time

is based on the assumption that $\varepsilon \neq 0$ in eq. (3.28). If $\varepsilon = 0$, however, then at $\mathbf{v} = 0$ it follows from eqs. (3.38)–(3.40) that $\theta(z,t)$ is the solution of the one-dimensional heat-conduction equation

$$\frac{\partial\theta}{\partial t} = \frac{\partial}{\partial z}\left(k\frac{\partial\theta}{\partial z}\right). \tag{3.61}$$

In this case, $\bar{p}$ is determined from eq. (3.55), where it should be assumed that $\varepsilon\eta = \mathrm{Ra}$ (Rayleigh number) in the numerator and $\varepsilon = 0$ in the denominator (the Rayleigh number is assumed to be finite as $\varepsilon \to 0$).

Let us now draw some conclusions

At $\varepsilon_1 > 0$, in the mechanical equilibrium state ($\mathbf{v} = 0$), the modified pressure $\bar{p}$ is determined by equalities (3.57) and (3.58), while the temperature θ is determined by eq. (3.59). For the temperature, a pair of boundary conditions at the ends of the interval $(0,l)$ should be imposed. Moreover, it is necessary to impose two more conditions to fix the constant A and the additive constant, which is the initial condition of the value of the function $B(z)$.

If $\varepsilon = 0$, then the temperature is found from eq. (3.61), and it is necessary to impose two conditions determining the constants C and $\mathcal{D}$. The pressure $\bar{p}$ is found from eq. (3.57), and one more condition is needed to determine the constant of integration.

It was already mentioned that the temperature is uniquely determined at $A = 0$ if the domain boundaries are isothermal. In the general case, it may turn out that the distributions of θ and $\bar{p}$ are reconstructed nonuniquely.

In the case of a non-heat-conducting fluid ($\varepsilon_1 = 0$, $k = 0$), an arbitrary profile of the temperature $\theta(z)$ is possible in mechanical equilibrium, and the pressure is found from eq. (3.55).

Convection of the fluid in a finite cylinder

Let us consider one possible formulation of the problem of free convection in model (3.28), (3.29′), (3.30′) in the case where a fluid fills a cylinder $\Omega = S \times (0,l)$ with horizontal end faces $\Sigma_0 = S \times \{0\}$ and $\Sigma_1 = S \times \{l\}$ (Figure 3.1). We assume that the end faces are solid walls; the bottom Σ_0 is absolutely solid, and the cover Σ_1 is deformable. The side surface $\partial S \times (0,l)$ is assumed to be an absolutely solid, thermally insulated wall.

Thus, after the transition to the dimensionless variables with the use of eqs. (3.27), the boundary conditions for temperature have the form

$$\theta(0) = \bar{\theta}_1, \quad \theta(1) = \bar{\theta}_2, \tag{3.62}$$

with specified constants $\bar{\theta}_j = \theta_j/\theta_*$. On the side surface $\partial S \times (0,1)$, we have

$$\frac{\partial\theta}{\partial n} = 0, \quad \mathbf{v} = 0. \tag{3.63}$$

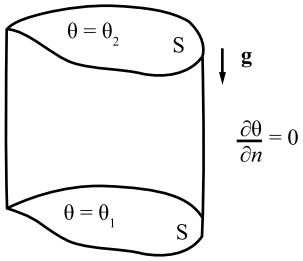

Figure 3.1: Domain of convection.

On the deformable cover $\Sigma_1 = S \times \{1\}$, the tangential components of velocity vanish:

$$v_1 = v_2 = 0; \tag{3.64}$$

in addition, the kinematic and dynamic conditions (3.50) and (3.49) are satisfied (it is taken into account that $v_{1x} = v_{2y} = 0$ at $z = 1$ by virtue of eq. (3.64)):

$$\frac{\partial \zeta}{\partial t} = v_3; \tag{3.65}$$

$$p - \frac{4}{3}\mu \frac{\partial v_3}{\partial z} = \gamma \zeta. \tag{3.66}$$

Here, ζ is the normal displacement (more exactly, the displacement in the z direction) of the boundary point and γ is a positive constant—the stiffness coefficient of the boundary. Conditions (3.65) and (3.66) are written in the dimensionless form. The relationship with dimensional variables is described by the equalities $\zeta' = l\zeta$, $\gamma' = \rho_0 \nu_0 \chi_0 \gamma / l^3$. According to eq. (3.33), the total pressure p is

$$p = \bar{p} - \eta z, \tag{3.67}$$

where $\eta = l^3 g / \nu_0 \chi_0$ is the microconvection parameter. The no-slip condition is satisfied on the solid motionless bottom Σ_0:

$$\mathbf{v} = 0. \tag{3.68}$$

We should also specify the total mass M of the fluid. If Ω_ζ is the domain occupied by the fluid at a given normal displacement $\zeta = \zeta(x, y, t)$ of the cover, we have the equality

$$\int_{\Omega_\zeta} \rho(\mathbf{x}, t)\, dxdydz = \int_{\Omega_\zeta} \frac{dxdydz}{1 + \varepsilon\theta} = M. \tag{3.69}$$

Here, we take into account equality (3.10), written in the form (in dimensionless variables) $\rho = (1 + \varepsilon\theta)^{-1}$; therefore, the dimensional mass is $M\rho_0 l^3$. As ζ is assumed to be

small, the temperature in a layer of thickness $O(\zeta)$ near the cover can be assumed to be constant and equal to $\bar{\theta}_2$, with an error of the order $O(\zeta^2)$. Then the condition of the constant mass (3.69) is rewritten as

$$\int_0^1 \int_S \frac{dxdydz}{1+\varepsilon\theta} + \frac{1}{1+\varepsilon\bar{\theta}_2} \int_S \zeta(x,y,t)\, dxdy = M. \tag{3.70}$$

The boundary conditions (3.62)–(3.66), (3.68), (3.70) together with the initial conditions for $\mathbf{v}$, $\mathbf{p}$, θ, and ζ, and equations (3.28), (3.29′), (3.30′) form the initial-boundary problem which describes the time evolution of the thermohydrodynamic field.

It turns out that the imposed conditions uniquely determine the mechanical equilibrium considered above. To find it, we substitute eqs. (3.67) and (3.57) into eq. (3.66). As eq. (3.65) predicts that ζ is independent of time, then it follows from the resultant equality $At + B(1) - \eta = \gamma\zeta$ that $A = 0$, while $\zeta = \text{const}$ and

$$B(1) - \eta = \gamma\zeta. \tag{3.71}$$

To find the temperature, we use equality (3.60), which takes the following form after the constants C and $\mathcal{D}$ are found from the boundary conditions (3.62):

$$K(\theta) = K(\bar{\theta}_2)z + K(\bar{\theta}_1)(1-z). \tag{3.72}$$

As $K'(\theta) = k(\theta) > 0$, the implicit equation (3.72) uniquely determines the function $\theta_0(z)$, $z \in [0,1]$. In particular, for the case with a constant thermal conductivity we have $k = 1$, and the temperature profile is linear: $\theta_0(z) = z\bar{\theta}_2 + (1-z)\bar{\theta}_1$ (as in the classical meaning).

From the condition of a constant mass (3.70), we find $\zeta = \zeta_0$:

$$\zeta_0 = (1+\varepsilon\bar{\theta}_2)\left[\frac{M}{|S|} - \int_0^1 \frac{dz}{1+\varepsilon\theta_0(z)}\right]. \tag{3.73}$$

In equilibrium, therefore, the cover is shifted over the vertical as a whole. Thus, the question arises: What happens at the cover boundary? We can imagine that the side surface is slightly stretched, as if the cover were attached by elastic springs. In fact, the proposed model certainly does not describe phenomena that occur near the cover boundary and can be used only in cases where this edge effect does not exert any pronounced influence on the fluid flow inside the cylinder.

As the fluid cannot withstand negative pressures (at least, high negative pressures) and $p = \gamma\zeta_0$ at $z = 1$ in accordance with eq. (3.66), the mass M should be large. Otherwise, we obtain ζ_0 in accordance with eq. (3.73), the pressure p is negative, the fluid separates from the cover, and a free surface is formed. The function $\bar{p}_0(z) = B(z)$

is found from eq. (3.58), with the initial condition $B(1) = \eta + \gamma\zeta_0$ (see equality (3.71)); it is equal to

$$\bar{p}_0(z) = \eta + \gamma\zeta_0 - \varepsilon\eta \int_z^1 \frac{\theta_0(z)dz}{1+\varepsilon\theta_0(z)}. \tag{3.74}$$

For convenience, let us note two formulas for the integrals in eqs. (3.73) and (3.74):

$$\int_0^1 \frac{dz}{1+\varepsilon\theta_0(z)} = \frac{1}{m}\int_{\bar{\theta}_1}^{\bar{\theta}_2} \frac{K'(\theta)d\theta}{1+\varepsilon\theta},$$

$$\int_z^1 \frac{\theta_0(z)dz}{1+\varepsilon\theta_0(z)} = \frac{1}{m}\int_{\bar{\theta}_0(z)}^{\bar{\theta}_2} \frac{K'(\theta)\theta}{1+\varepsilon\theta}\,d\theta.$$

They are obtained with the use of the replacement

$$z = \frac{K(\theta_0) - K(\bar{\theta}_1)}{m}, \quad m = K(\bar{\theta}_2) - K(\bar{\theta}_1).$$

Thus, we found that the unique solution corresponds to mechanical equilibrium $\mathbf{v}_0 = 0$, $\bar{p}_0(z)$, $\theta_0(z)$, $\zeta_0 = \text{const}$.

The cover is an elastic plate

Let us consider a physically more exact model, retaining all conditions of the previous problem, except for the rather rough condition (3.66). Instead of that, we assume that the cover is an elastic plate. If it has a thickness h_p and density ρ_p and is fabricated from a material with known Young's modulus E and Poisson's ratio ν, then its dimensional stiffness is [118]

$$\mathcal{D} = \frac{Eh^3p}{12(1-\nu^2)}.$$

The plate deflection $\zeta(x,y,t)$ is assumed to be so small that the linear theory can be used; then, the equation of motion can be written as

$$\rho_p h_p \frac{\partial^2\zeta}{\partial t^2} + \mathcal{D}\Delta^2\zeta = p - \frac{4}{3}\mu\frac{\partial v_3}{\partial z}, \tag{3.75}$$

where Δ^2 is a biharmonic operator over the variables x and y. The dimensional hydrodynamic pressure on the cover $z = l$ is indicated by p. This equation plays the role of the boundary condition replacing eq. (3.66). We only need to pass to dimensionless quantities and fix the boundary condition on the line of cover attachment $\partial S \times \{l\}$. We determine the dimensionless unknown ζ' by assuming that $\zeta = h_p\zeta'$, and we retain

the previously used scales for the remaining variables (see eq. (3.27)). Then, eq. (3.75), which is the boundary condition at $z = 1$, is rewritten in the dimensionless form (the primes are omitted) as

$$\begin{gathered} d\zeta_{tt} + \bar{\mathcal{D}}\Delta^2\zeta = p - \frac{4}{3}\mu\frac{\partial v_3}{\partial z}, \\ p|_{z=1} = \bar{p}(x, y, 1, t) - \eta. \end{gathered} \tag{3.76}$$

Here we use equality (3.67). The parameters d and $\bar{\mathcal{D}}$ have the meaning of the dimensionless density and stiffness of the plate, respectively, and are equal to

$$d = \frac{\rho_p \chi_0}{\rho_0 \nu_0}\left(\frac{h_p}{l}\right)^2, \quad \bar{\mathcal{D}} = \left(\frac{h_p}{l}\right)^4 \frac{l^2 E}{12\rho_0 \nu_0 \chi_0 (1-\nu^2)}.$$

Equation (3.76) should be satisfied in the domain S, and two boundary conditions have to be imposed on the boundary ∂S of this domain. If, for instance, the side boundary is absolutely stiff and the cover is rigidly attached to it, these conditions are

$$\zeta = 0, \quad \frac{\partial \zeta}{\partial n} = 0. \tag{3.77}$$

The initial conditions include specifying the functions ζ and ζ_t everywhere in S at $t = 0$.

Obviously, the boundary condition (3.76) can be further improved by taking into account the geometrical and physical nonlinearity and thermal stresses, by considering a shell instead of a plate, or by introducing this or that property of material viscosity and external friction.

In the case with $d/\bar{\mathcal{D}} \ll 1$, condition (3.76) can be simplified (physically, it means that the period of inherent oscillations of the plate is much smaller than the convective time scale). Equation (3.76) becomes

$$\bar{\mathcal{D}}\Delta^2\zeta = \bar{p}(x, y, 1, t) - \eta - \frac{4}{3}\mu\frac{\partial v_3}{\partial z}(x, y, 1, t) \tag{3.78}$$

and no initial conditions for ζ are needed.

Note that the use of the boundary condition (3.76) or (3.78) in mechanical equilibrium should lead to $\zeta_0 = 0$. Indeed, we have $\bar{p} = \bar{p}(z)$ in the equilibrium state; if $\bar{p}(1) \neq \eta$, then the boundary condition (3.78) (for the equilibrium state, it coincides with eq. (3.76)) cannot be satisfied. Thus, $\zeta_0 = 0$ and $\bar{p}(1) = \eta$ in equilibrium. According to eq. (3.69), the equilibrium state is only possible if the fluid mass is determined by the equality

$$M = |S| \int_0^1 \frac{dz}{1 + \varepsilon\theta_0(z)}. \tag{3.79}$$

Thus, the formulation of the problem of free convection, which is conventional for the Oberbeck–Boussinesq model, is impossible here: with additional heating, the equilibrium is instantly destroyed. It is possible, however, to consider a similar problem, assuming that the extra fluid leaves the container through thin pores.

There are possible variations with regard to the deformable cover. A problem of an absolutely solid cover on springs can be posed, assuming that conditions (3.65) and (3.66) are satisfied, but the normal displacement ζ is independent of x and y, i. e., $\zeta = \zeta(t)$. Another interesting problem can be posed, in which a membrane is used as the cover. In this case, the term $\bar{\mathcal{D}}\Delta^2\zeta$ in eq. (3.76) should be replaced by $-T_m\Delta\zeta$, where T_m is the tension force of the membrane. As a result, the boundary condition (3.76) is replaced by

$$d_m\zeta_{tt} - \bar{T}_m\Delta\zeta = \bar{p} - \eta - \frac{4}{3}\mu\frac{\partial v_3}{\partial z}, \tag{3.80}$$

where d_m and T_m are dimensionless constants:

$$d_m = \frac{\rho_m\chi_0}{l\rho_0\nu_0}, \quad \bar{T}_m = \frac{T_m l}{\rho_0\nu_0\chi_0},$$

and ρ_m is the surface density of the membrane. Equation (3.80) should be supplemented with one more boundary condition on ∂S (of the first, second, or third kind).

4 Hierarchy of convection models in closed volumes

In this chapter, three models that describe natural convection of the fluid in closed volumes with constant transfer coefficients (Sections 4.1–4.8) are considered. The theory of existence and uniqueness is proved for the microconvection model. Possible generalizations and corollaries of resultant initial-boundary problems are discussed [172]. A comprehensive analysis of the comparative influence of temperature- and pressure-induced changes in thermophysical parameters and of the work of pressure forces on formation of natural convection in a weakly nonisothermal medium with extremely small mass forces is performed in Section 4.9 in the subsonic flow approximation. The limits of applicability of the Oberbeck–Boussinesq approximation for the description of this type of convection are determined. An asymptotically exact mathematical model for convection in weak force fields, with allowance for small changes in the medium properties, is developed. One-value solvability of the basic boundary-value problems is formulated, and the problem of local exact controllability is studied [77, 240]. Section 4.10 describes the convection model for a thermally inhomogeneously weakly compressible fluid [139] where all transfer coefficients are nonlinear functions.

4.1 Initial relations

A viscous heat-conducting fluid is assumed to fill a finite vessel Ω whose boundary is a solid nondeformable impermeable wall with a specified heat-flux or temperature distribution. The fluid is subjected to the gravity force with the acceleration $\mathbf{g}$. It is known that the fluid can be in equilibrium under these conditions only if the thermal regime on the boundary is chosen in a special manner. The "general location case" corresponds to the emergence of convection.

In the following, the fluid is considered as a two-parameter thermodynamic medium with the state parameters θ (absolute temperature) and p (pressure). The fluid density ϱ is determined by the state equation (see eq. (3.1))

$$\varrho = R(\theta, p), \tag{4.1}$$

where the function R is specified below. As the basic model, we use model (1.46), where $\mathbf{f} = \mathbf{g}$, $h = 0$, while λ, k, and μ are positive constants. Then, the functions $\mathbf{v}$, p, and θ satisfy the system of equations

$$\frac{d\varrho}{dt} + \varrho \operatorname{div} \mathbf{v} = 0; \tag{4.2}$$

$$\varrho \frac{d\mathbf{v}}{dt} = \nabla(-p + \lambda \operatorname{div} \mathbf{v}) + \mu \Delta \mathbf{v} + \varrho \mathbf{g}; \tag{4.3}$$

$$\varrho\theta \frac{ds}{dt} = k\Delta\theta + \Phi,$$

https://doi.org/10.1515/9783110655469-004

and the dissipative function is determined by equality (1.45). The last equation of this system can be rewritten in a more convenient form (see the beginning of Section 3.2) as

$$\varrho c_p \frac{d\theta}{dt} + \frac{\theta}{\varrho}\left(\frac{\partial \varrho}{\partial \theta}\right)\frac{dp}{dt} = k\Delta\theta + \Phi, \tag{4.4}$$

where $c_p = \theta \partial s/\partial\theta$ is the specific heat at constant pressure.

System (4.1)–(4.4) becomes closed if the dependence of the specific heat c_p on θ and p is known. The simplest form of this dependence, $c_p = \text{const} > 0$ (see eq. (3.20)), is considered below.

Let us now discuss the state equation. The writing of it in the form (4.1) is dictated by the fact that significant variations of temperature (and even greater variations of pressure) in true ("droplet"-type) liquids, in contrast to gases, lead to small variations in density. We can naturally assume that R is a nondecreasing function of p. Eliminating anomalous situations from our consideration (the classical example is water close to the temperature of 273 K, see [144, 226]), we assume that the function $R(\theta, p)$ monotonically decreases with increasing θ. In considering flows initiated by buoyancy forces (they constitute the essence of the theory of thermal gravitational convection), the dependence of ϱ on θ is usually approximated by the linear function

$$\varrho = \varrho_0[1 - \beta_1(\theta - \theta_0) + \beta_2(p - p_0)],$$

where β_1 and β_2 are positive constants, while ϱ_0, θ_0, and p_0 are the characteristic values of density, temperature, and pressure, respectively. In our case, however, we use another approximation of the state equation:

$$\varrho = \varrho_0[1 + \beta_1(\theta - \theta_0)]^{-1}[1 + \beta_2(p - p_0)]. \tag{4.5}$$

From the viewpoint of applications, the fact that dependence (4.5) differs from a linear function is insignificant. Indeed, the relative error here has the order $(\beta_1\theta_*)^2$, where θ_* is the maximum difference in temperature in the motion considered. In particular, its value for water is within 10^{-5}.

System (4.2)–(4.5) is the starting point for further considerations (Sections 4.2–4.8). It can be resolved with respect to the derivatives $d\mathbf{v}/dt$, $d\theta/dt$, and dp/dt; therefore, we need to specify the initial values of all sought functions:

$$\mathbf{v} = \mathbf{v}_0(\mathbf{x}), \quad \mathbf{x} \in \Omega, \quad t = 0; \tag{4.6}$$

$$\theta = \theta_0(\mathbf{x}), \quad \mathbf{x} \in \Omega, \quad t = 0; \tag{4.7}$$

$$p = p_0(\mathbf{x}), \quad \mathbf{x} \in \Omega, \quad t = 0. \tag{4.8}$$

The boundary Σ of the domain Ω is subjected to the no-slip condition for velocity

$$\mathbf{v} = 0, \quad \mathbf{x} \in \Sigma, \quad t > 0, \tag{4.9}$$

and one of two temperature conditions, either

$$k\frac{\partial\theta}{\partial n} = q(\mathbf{x}, t), \quad \mathbf{x} \in \Sigma, \quad t > 0 \tag{4.10}$$

or

$$\theta = h(\mathbf{x}, t), \quad \mathbf{x} \in \Sigma, \quad t > 0, \tag{4.10′}$$

where $\partial/\partial n$ is the derivative along the external normal to Σ.

It is not our purpose here to review the results of how well problems (4.2)–(4.10) and (4.2)–(4.10′) are posed. Note that the theorem of uniqueness of the classical solution of each of these problems is actually contained in [209]. If the functions $\mathbf{v}_0$, θ_0, p_0, q, and h, and the surface Σ are rather smooth, the theorem of existence is also valid for these problems, at least on a small interval of time [218].

4.2 Similarity criteria

Assuming the hypothesis on a constant specific heat c_p and specifying the state equation (4.5), we eliminate functional arbitrariness in the system of hydrodynamic equations. The resultant system (4.2)–(4.5) includes nine dimensional parameters: $g = |\mathbf{g}|$, μ, λ, k, c_p, ϱ_0, β_1, β_2, θ_0, and p_0. These parameters can be combined into six independent dimensionless combinations, and each combination can be considered as a similarity criterion for convective flows. The total set of the governing parameters (and, consequently, similarity criteria) becomes greater if we consider the motion emerging from a given initial state and supported by a specified heat-flux or temperature distribution on the boundary. In particular, setting the flow domain Ω defines the characteristic linear size $l = \operatorname{diam}\Omega$. Other important dimensional characteristics are the characteristic time τ of changes in the functions $f(\mathbf{x}, t)$ or $h(\mathbf{x}, t)$ determining the thermal regime on the boundary and also the characteristic difference in temperature θ_* in the considered flow. The latter quantity has the same order as $(q_{\max} - q_{\min})l/k$ or $h_{\max} - h_{\min}$, where max and min are calculated over the domain $\Sigma \times [0, \bar{t}]$ ($\bar{t}$ is the time interval in which problem (4.2)–(4.10) or (4.2)–(4.10′) is considered).

Considering the quantity θ_* as the characteristic temperature scale, we can form one important similarity criterion (Boussinesq number)

$$\varepsilon = \beta_1\theta_*, \tag{4.11}$$

characterizing the response of density to a change in temperature. Another temperature characteristic of the process θ_0, which is involved into the state equation (4.5), can be identified with the mean temperature of the fluid. Obviously, the parameters θ_* and θ_0 are independent. Another dimensional parameter p_0 in eq. (4.5) can be set to zero without loss of generality, because eqs. (4.2)–(4.4) admit the equivalence transformation $\hat{p} = p - p_0$.

Let us introduce the notations $\nu = \mu/\varrho_0$ (kinematic viscosity coefficient) and $\chi = k/\varrho_0 c_p$ (thermal diffusivity coefficient). They are used to compose two more similarity criteria:

$$\mathrm{Pr} = \nu/\chi, \quad \xi = \lambda/\mu. \tag{4.12}$$

We further assume that the parameters Pr (Prandtl number) and ξ have the order of unity. At the same time, the parameter ε is always small, which serves as a basis for asymptotic expansions used to derive equations of thermal gravitational convection from exact hydrodynamic equations. (The procedure of expansion with respect to the parameter ε in the convection theory was performed for the first time in [133] for the case where the function R in eq. (4.1) is linear with respect to θ and is independent of p.) Now we must determine the characteristic "internal" time scale (it does not necessarily coincide with the previously introduced quantity τ). The so-called convective scale $t_c = (l/g\varepsilon)^{1/2}$ is usually used for this purpose. In order of magnitude, it coincides with the time of up-floating of a hot fluid particle to a height l. As $t_c \to \infty$ when $g \to 0$, while we want to construct a convection model uniformly suitable for arbitrary infinitesimal values of g, we choose the characteristic time in the form $t_f = l^2/\chi$, which is the temperature relaxation time. As the Prandtl number is $\mathrm{Pr} \sim 1$, then the time of relaxation of viscous stresses $t_s = l^2/\nu$ has the same order as t_f.

Using the characteristic time, we can determine two characteristic velocities. One of them, $V_e = \varepsilon\chi/l$, is introduced on the basis of the continuity equation (4.2) and characterizes the velocity of uniform expansion of the fluid owing to the local heat source placed into this fluid. The other velocity, $V_b = g\varepsilon l^2/\nu$, is determined from the momentum equation (4.3) with equated orders of the terms $\mu\Delta\mathbf{v}$ and $\varrho_0\beta_1(\theta - \theta_0)\mathbf{g}$ (the latter term characterizes the contribution of buoyancy forces to the total force balance). Owing to the condition $\mathrm{Pr} \sim 1$, the left-hand side of eq. (4.3) has the same order.

The steady component in the momentum equation (it is also present in the state at rest) is compensated by the hydrostatic pressure $p_{hs}(\mathbf{x})$. Let us consider the function $\bar{p} = p - p_{hs}(\mathbf{x})$. We can naturally assume that the term $\nabla\bar{p}$ has the same order as the remaining dynamic components of forces acting on the fluid particle. This fact determines the characteristic scale of the quantity $\bar{p}$: $\varrho_0 g\varepsilon l$.

Let us denote the ratio of the characteristic velocities V_b and V_e by η. The parameter

$$\eta = \frac{gl^3}{\nu\chi} \tag{4.13}$$

plays an important role in the microconvection theory [177, 176, 161]. It was shown in these papers that the classical Oberbeck–Boussinesq model cannot be used to describe thermal gravitational convection if the parameter η has the order smaller than or equal to unity. The quantity η has a simple physical meaning: it characterizes the

relative contribution of the factors of buoyancy and volume expansion of the fluid to velocity field formation. Our further considerations will involve an important dimensionless quantity

$$\delta = \frac{\beta_2 \varrho_0 \nu\chi}{l^2}, \tag{4.14}$$

which can be called the compressibility parameter.

Two more similarity criteria,

$$\varepsilon_1 = \frac{\nu\chi}{l^2 c_p \theta_*}, \quad \varepsilon_2 = \frac{\nu\chi\beta_1\theta_0}{l^2 c_p \theta_*}, \tag{4.15}$$

characterize the relative contribution of the dissipative function Φ and the term proportional to dp/dt to the energy equation (4.4). Finally, the ratio of the previously introduced characteristic times t_q and τ yields the similarity criterion $\zeta = t_q/\tau$. Note that another possible similarity criterion, which includes p_0, is irrelevant, because p_0 can be eliminated from the state equation (4.5) with the use of the equivalence transformation.

Thus, we have eight similarity criteria: Pr, ξ, ε, η, δ, ε_1, ε_2, and ζ. They are independent and can be called the basic criteria. Certainly, the choice of the basic criteria is not unique. For instance, instead of ε, δ, and ε_1, it is possible to use the parameters $\hat{\varepsilon} = \beta_1\theta_0$, $\varrho_0^{1/3}(\mu g)^{2/3}\beta_2$ (analog to the compressibility parameter), and $c_p\theta_0(\varrho_0/\mu g)^{2/3}$ (dimensionless heat capacity). Then, these three parameters, together with Pr and ξ, form five (i. e., the greatest possible number) "internal" similarity criteria determined only by the fluid properties and by the acceleration due to gravity g. The remaining three parameters η, ε_2, and ζ can be naturally called the external parameters, because they involve the characteristics of the flow domain and the thermal regime on the boundary. The initial choice of the basic similarity criteria, however, is more convenient, because it is these criteria that are formed during nondimensionalization of eqs. (4.2)–(4.5), which will be performed in the next section.

4.3 Transition to dimensional variables

Let us choose the quantities l, l^2/χ, χ/l, $\varrho_0\nu\chi/l^2$, and θ_* as the characteristic scales of length, time, velocity, pressure, and temperature, respectively, and again indicate the differences $\theta - \theta_0$ and $p - p_0$ by θ and p. Note that the characteristic velocity $V = \chi/l$ differs from the previously introduced quantities V_e and V_b. This is caused by our desire, by analogy with [68], to make the characteristic velocity independent of the temperature condition on the domain boundary and thus give "equal rights" to the velocity scale and the length and time scales.

We introduce dimensionless (primed) variables by the formulas (see eqs. (3.27))

$$\mathbf{x} = l\mathbf{x}', \quad t = \frac{l^2}{\chi}t', \quad \mathbf{v} = \frac{\chi}{l}\mathbf{v}', \quad \hat{p} = \frac{\varrho_0\nu\chi}{l^2}p', \quad \theta = \theta_*\theta'. \tag{4.16}$$

We substitute eqs. (4.16) into eqs. (4.2)–(4.5) and omit the primes. The state equation (4.5) in dimensionless variables takes the form

$$\varrho = (1 + \varepsilon\theta)^{-1}(1 + \delta p) \tag{4.17}$$

(the density scale here is ϱ_0). Owing to eqs. (4.16) and (4.17), the dimensionless form of the continuity equation (4.2) is

$$\frac{\delta}{1 + \delta p} \cdot \frac{dp}{dt} - \frac{\varepsilon}{1 + \varepsilon\theta} \cdot \frac{d\theta}{dt} + \operatorname{div} \mathbf{v} = 0, \tag{4.18}$$

and the momentum equation (4.3) becomes

$$\frac{1 + \delta p}{1 + \varepsilon\theta} \cdot \frac{d\mathbf{v}}{dt} = \operatorname{Pr}[\nabla(-p + \xi \operatorname{div} \mathbf{v}) + \Delta\mathbf{v}] + \frac{\eta \operatorname{Pr}(1 + \delta p)}{1 + \varepsilon\theta} \mathbf{e}, \tag{4.19}$$

with the notation $\mathbf{e} = |\mathbf{g}|/g$. Finally, the energy equation (4.4) in dimensionless variables is written in the form

$$\frac{1 + \delta p}{1 + \varepsilon\theta} \cdot \frac{d\theta}{dt} - \frac{\varepsilon_2 + \varepsilon\varepsilon_1\theta}{1 + \varepsilon\theta} \cdot \frac{dp}{dt} = \Delta\theta + \varepsilon_1\Phi, \tag{4.20}$$

where the dimensionless dissipative function Φ is determined by the equality

$$\Phi = \left(\xi + \frac{2}{3}\right)(\operatorname{div} \mathbf{v})^2 + 2D' : D'$$

(here D' is the dimensionless deviator of the strain rate tensor). Equations (4.18)–(4.20) contain seven parameters, which can be divided into four groups in order of decreasing of their typical values. The first group consists of one element η. Under the terrestrial conditions and for usual fluids, the value of η is rather high. Thus, if the vessel diameter is $l = 10^{-2}$ m (this typical size will also be used in what follows), and the fluid filling this vessel is water at a temperature of 293 K, then we have $\eta = 6.9 \cdot 10^7$ for $g = 9.81\,\mathrm{m/s^2}$ in accordance with eq. (4.13). Under the microgravity conditions, however, in the range of small sizes, and also for high-viscosity fluids, the values of η can be of the order of unity, which gives us the grounds to *call* η the *microconvection parameter*.

The second group is formed by the parameters Pr and ξ determined by eqs. (4.12). As was noted above, both these quantities are assumed to be of the order of unity. We are not aware of any liquids with high values of ξ (i. e., the ratio of the coefficients of the second and first viscosities). Concerning the Prandtl number Pr, this parameter varies within wide limits for real liquids (in contrast to gases). Nevertheless, the assumption $\operatorname{Pr} \sim 1$ unites a large group of fluid media, including water, ethyl alcohol, carbon tetrachloride, and all gases.

The third group again consists of one parameter ε (Boussinesq number) determined by eq. (4.11). As the volume coefficient of thermal expansion β for usual liquids

does not exceed $2 \cdot 10^{-3}$ 1/K, the value of ε is small even for the characteristic temperature difference $\theta_* = 50$ K. For $\theta_* = 10$ K (this value of θ_* will also be used for estimating the values of ε_1 and ε_2), however, we have $\varepsilon = 2.1 \cdot 10^{-3}$ for water at room temperature.

Finally, the fourth group of parameters consists of δ, ε_1, and ε_2 determined by eqs. (4.14) and (4.15). Let us first estimate the value of δ. This parameter is proportional to the isothermal compressibility coefficient β_2 involved into the state equation (4.5). For usual liquids, β_2 lies in the interval 10^{-9}–10^{-10} m^2/N. Taking into account that $\beta_2 = 4.9 \cdot 10^{-10}$ m^2/N for water, eq. (4.14) with $l = 10^{-2}$ m yields the value $\delta = 6.9 \cdot 10^{-15}$. The value of the parameter ε_1 under the same conditions is slightly greater (but still small as compared with ε): $\varepsilon_1 = 3.4 \cdot 10^{-14}$, and $\varepsilon_2 = 1.8 \cdot 10^{-15}$ has the same order as δ.

Then, we use the fact that the parameters δ, ε_1, and ε_2 are small for asymptotic simplification of system (4.18)–(4.20). Taking into account that the quantities ε_i ($i = 1, 2$) in typical situations have the same order as δ and wanting to reduce the procedure to expansion in one small parameter, we assume that $\varepsilon_i = \alpha_i \delta$, where $\alpha_i = O(1)$ as $\delta \to 0$. Then, eq. (4.20) can be presented as

$$\frac{1 + \delta p}{1 + \varepsilon\theta} \cdot \frac{d\theta}{dt} - \delta \frac{\alpha_2 + \varepsilon\alpha_1\theta}{1 + \varepsilon\theta} \cdot \frac{dp}{dt} = \Delta\theta + \delta\alpha_1\Phi. \tag{4.20′}$$

The boundary conditions for system (4.18)–(4.20′) are conditions (4.9) and (4.10) or (4.9) and (4.10′) rewritten in dimensionless variables. Retaining the previous notations for the dimensionless heat flux or temperature specified on the domain boundary, we rewrite the boundary conditions in the form

$$\mathbf{v} = 0, \quad \mathbf{x} \in \Sigma, \quad t > 0; \tag{4.21}$$

$$\frac{\partial\theta}{\partial n} = f(\mathbf{x}, \zeta t), \quad \mathbf{x} \in \Sigma, \quad t > 0, \quad \text{or} \tag{4.22}$$

$$\theta = h(\mathbf{x}, \zeta t), \quad \mathbf{x} \in \Sigma, \quad t > 0. \tag{4.22′}$$

We introduce the parameter ζ into the right-hand sides of eqs. (4.22) and (4.22′) because we want to consider situations with appreciably different values of t_q (time of temperature relaxation in the volume Ω) and τ (characteristic time of change in the heat flux or temperature specified on the boundary Σ). For example, let the vessel diameter be $l = 10^{-2}$ m, let the fluid be water at room temperature, and let the temperature on the vessel surface be a periodic function of time with a period $\tau = 14$ s; then, we have $\zeta = t_q/\tau = 50$.

To close the formulation of the problem, we need to rewrite the initial conditions (4.6)–(4.8) in dimensionless variables:

$$\mathbf{v} = \mathbf{v}_0(\mathbf{x}), \quad \mathbf{x} \in \Omega, \quad t = 0; \tag{4.23}$$

$$\theta = \theta_0(\mathbf{x}), \quad \mathbf{x} \in \Omega, \quad t = 0; \tag{4.24}$$

$$p = p_0(\mathbf{x}), \quad \mathbf{x} \in \Omega, \quad t = 0. \tag{4.25}$$

As before, the dimensionless functions determining the initial distributions of velocity, temperature, and pressure again retain their previous notations.

4.4 Expansion in the small parameter

Below, we construct an asymptotic expansion of the solution of system (4.18)–(4.20′) in the compressibility parameter $\delta \to 0$ under the assumption that the remaining parameters involved into this system (ε, Pr, ξ, η, α_1, and α_2) retain finite values.

System (4.18)–(4.20′) is singularly perturbed, because the small parameter δ in the first and third equations of this system is a multiplier at the evolutionary derivative dp/dt. It is clear a priori that the presentation of the solution of this system in the form of series in powers of δ cannot exactly satisfy all required conditions asymptotically. Using this expansion, however, it is possible to satisfy the equations of the system, all boundary conditions, and two first initial conditions (4.23) and (4.24) with an arbitrary power accuracy in terms of the parameter δ. Thus, we seek for the solution of system (4.18)–(4.20′) in the form of formal power series

$$\mathbf{v} = \sum_{k=0}^{\infty} \delta^k \mathbf{v}^{(k)}(\mathbf{x}, t), \quad \theta = \sum_{k=0}^{\infty} \delta^k \theta^{(k)}(\mathbf{x}, t),$$
$$p = \frac{P(t) - 1}{\delta} + \sum_{k=0}^{\infty} \delta^k p^{(k)}(\mathbf{x}, t). \tag{4.26}$$

In contrast to $\mathbf{v}$ and θ, the function p has a singular component when $\delta \to 0$. Its origination has a clear physical meaning. The quantity $\delta^{-1}[P(t) - 1]$ can be identified with the fluid pressure averaged over the domain Ω. If the total heat flux through the boundary Σ of the domain Ω differs from zero, the fluid temperature averaged over Ω changes. As the vessel walls are motionless and impermeable, the mass of the enclosed fluid is retained. By virtue of the state equation (4.17) and the assumption concerning the small value of δ, finite changes in the mean temperature will lead to mean pressure changes of the order of δ^{-1} as $\delta \to 0$.

Substitution of series (4.26) into eqs. (4.18)–(4.20′) yields a recurrent system for the functions $\mathbf{v}^{(k)}$, $\theta^{(k)}$, and $p^{(k)}$ ($k = 0, 1, \dots$). The system satisfied by the functions $\mathbf{v}^{(0)}$, $\theta^{(0)}$, and $p^{(0)}$ is nonlinear. All subsequent triples of the functions $\mathbf{v}^{(j)}$, $\theta^{(j)}$, $p^{(j)}$ ($j = 1, 2, \dots$) are determined from linear systems of equations with homogeneous boundary and initial conditions. As our attention is mainly focused on the principal terms of expansions (4.26), we consider the system satisfied by the functions $\mathbf{v}^{(0)}$, $\theta^{(0)}$, and $p^{(0)}$. Substituting eqs. (4.26) into eqs. (4.18)–(4.20′) and passing to the limit at $\delta \to 0$, we obtain

$$\frac{\dot{P}}{P} - \frac{\varepsilon}{1 + \varepsilon\theta^{(0)}} \left(\theta_t^{(0)} + \mathbf{v}^{(0)} \cdot \nabla\theta^{(0)}\right) + \operatorname{div} \mathbf{v}^{(j)} = 0; \tag{4.27}$$

$$\frac{P}{1 + \varepsilon\theta^{(0)}} \left(\mathbf{v}_t^{(0)} + \mathbf{v}^{(0)} \cdot \nabla\mathbf{v}^{(0)}\right) = \operatorname{Pr}\left[\nabla\left(-p^{(0)} + \xi \operatorname{div} \mathbf{v}^{(0)}\right) + \Delta\mathbf{v}^{(0)}\right] + \frac{\eta \operatorname{Pr} P\mathbf{e}}{1 + \varepsilon\eta^{(0)}}; \tag{4.28}$$

$$\frac{P}{1 + \varepsilon\theta^{(0)}} \left(\theta_t^{(0)} + \mathbf{v}^{(0)} \cdot \nabla\theta^{(0)}\right) - \dot{P} \frac{\alpha_2 + \varepsilon\alpha_1\theta^{(0)}}{1 + \varepsilon\theta^{(0)}} = \Delta\theta^{(0)}, \tag{4.29}$$

where $\dot{P}$ means the derivative of the function $P(t)$.

Let us formulate the initial-boundary problem for system (4.27)–(4.29). In order to be certain, we further assume that a condition of the second kind is imposed for temperature on the surface Σ. By virtue of eqs. (4.21), (4.22), and (4.26), we have

$$\mathbf{v}^{(0)} = 0, \qquad \mathbf{x} \in \Sigma, \qquad t > 0; \tag{4.30}$$

$$\frac{\partial \theta^{(0)}}{\partial n} = q(\mathbf{x}, \zeta t), \quad \mathbf{x} \in \Sigma, \qquad t > 0. \tag{4.31}$$

Conditions (4.23) and (4.24) yield the initial conditions for the functions $\mathbf{v}^{(0)}$ and $\theta^{(0)}$:

$$\mathbf{v}^{(0)} = \mathbf{v}_0(\mathbf{x}), \quad \mathbf{x} \in \Omega, \quad t = 0; \tag{4.32}$$

$$\theta^{(0)} = \theta_0(\mathbf{x}), \quad \mathbf{x} \in \Omega, \quad t = 0. \tag{4.33}$$

The initial condition for the pressure $p^{(0)}$ is not imposed, because system (4.27)–(4.29) is not evolutionary with respect to $p^{(0)}$. Moreover, eqs. (4.27)–(4.33) determine the function $p^{(0)}$ with accuracy to an arbitrary time-dependent summand. (The functions $p^{(j)}$, $j = 1, 2, \dots$ possess similar arbitrariness.) Using this arbitrariness, we can ensure that the relations

$$\int_\Omega p^{(k)}(\mathbf{x}, t)\, dx = 0, \quad k = 0, 1, \dots,$$

are satisfied for all $t \geq 0$. With such normalization of $p^{(k)}$, the value of $\delta^{-1}[P(t) - 1]$ exactly coincides with the mean pressure of the fluid in the domain Ω for all $t \geq 0$.

To close the formulation of the initial-boundary problem, we need to derive an equation determining the function $P(t)$. For this purpose, we multiply eq. (4.27) by P and eq. (4.29) by ε and sum up the resultant equalities. This yields

$$\left[1 - \frac{\varepsilon(\alpha_2 + \varepsilon\alpha_1\theta^{(0)})}{1 + \varepsilon\theta^{(0)}}\right]\dot{P} + \operatorname{div}(P\mathbf{v}^{(0)} - \varepsilon\nabla\theta^{(0)}) = 0.$$

Integrating this relation over the domain Ω and taking into account conditions (4.30) and (4.31), we obtain the required equation:

$$\dot{P}\int_\Omega \left[1 - \frac{\varepsilon(\alpha_2 + \varepsilon\alpha_1\theta^{(0)})}{1 + \varepsilon\theta^{(0)}}\right] dx = \varepsilon\int_\Sigma q\, d\Sigma. \tag{4.34}$$

As the initial condition for eq. (4.34), we choose

$$P(0) = 1, \tag{4.35}$$

which, by virtue of eq. (4.26), is consistent with the natural assumption that the values of the function $p_0(\mathbf{x})$ are finite as $\delta \to 0$.

Problem (4.27)–(4.35) is a rather complicated object for studying. It suffices to tell that eqs. (4.27) and (4.28) in the limiting case with $\varepsilon = 0$ (then, $P = 0$ by virtue of eqs. (4.34) and (4.35)) transform to the Navier–Stokes equations for an incompressible fluid. It is known that the issue of one-value solvability "as a whole" of the initial-boundary problem for this system in the general three-dimensional case is still open. Therefore, local theorems of existence are of interest for problem (4.27)–(4.35). Let us formulate one of them.

Assuming the problem data $(\mathbf{v}_0, \theta_0, q)$ to be rather smooth, we make them comply with the local matching conditions

$$\mathbf{v}_0 = 0, \quad \mathbf{x} \in \Sigma; \tag{4.36}$$

$$q_t(\mathbf{x}, 0) = \frac{\partial G}{\partial n}, \quad \mathbf{x} \in \Sigma; \tag{4.37}$$

$$\left[1 - \frac{\varepsilon(\alpha_2 + \varepsilon\alpha_1\theta_0)}{1 + \varepsilon\theta_0}\right]\dot{P}_0 + \operatorname{div}(\mathbf{v}_0 - \varepsilon\nabla\theta_0) = 0, \quad \mathbf{x} \in \Omega, \tag{4.38}$$

where

$$\dot{P}_0 = \varepsilon\left\{\int\limits_\Omega \left[1 - \frac{\varepsilon(\alpha_2 + \varepsilon\alpha_1\theta_0)}{1 + \varepsilon\theta_0}\right] dx\right\}^{-1} \int\limits_\Sigma q(\mathbf{x}, 0)\, d\Sigma; \tag{4.39}$$

$$G(\mathbf{x}) = (1 + \varepsilon\theta_0)\Delta\theta_0 - \mathbf{v}_0 \cdot \nabla\theta_0 + \dot{P}_0(\alpha_2 + \varepsilon\alpha_1\theta_0) \equiv \theta_t^{(0)}(\mathbf{x}, 0)$$

and a nonlocal condition formulated in terms of the function $\pi_0(\mathbf{x}) = p^{(0)}(\mathbf{x}, 0)$. This function is the solution of the boundary-value problem

$$\operatorname{div}\left[(1 + \varepsilon\theta_0)\nabla\pi_0\right] = \operatorname{div}\mathbf{F} - \operatorname{Pr}^{-1} PH, \quad \mathbf{x} \in \Omega;$$

$$(1 + \varepsilon\theta_0)\frac{\partial\pi_0}{\partial n} = \mathbf{F} \cdot \mathbf{n}, \qquad \mathbf{x} \in \Sigma,$$

where the following notations are introduced:

$$\mathbf{F} = (1 + \varepsilon\theta_0)(\xi\nabla \operatorname{div}\mathbf{v}_0 + \Delta\mathbf{v}_0) + \eta P\mathbf{e}_3 - \operatorname{Pr}^{-1} P\mathbf{v}_0 \cdot \nabla\mathbf{v}_0;$$

$$H = \dot{P}_0\left[G\frac{\varepsilon^2(\alpha_1 - \alpha_2)}{(1 + \varepsilon\theta_0)^2} - \operatorname{div}\mathbf{v}_0\right] - \ddot{P}_0\left[1 - \frac{\varepsilon(\alpha_2 + \varepsilon\alpha_1\theta_0)}{1 + \varepsilon\theta_0}\right] \equiv \operatorname{div}\mathbf{v}_t^{(0)}(\mathbf{x}, 0);$$

$$\ddot{P}_0 = \left\{\int\limits_\Omega \left[1 - \frac{\varepsilon(\alpha_2 + \varepsilon\alpha_1\theta_0)}{1 + \varepsilon\theta_0}\right] dx\right\}^{-1} \left[\varepsilon\int\limits_\Sigma q_t(\mathbf{x}, 0)\, d\Sigma - \dot{P}_0\varepsilon^2(\alpha_1 - \alpha_2)\int\limits_\Omega \frac{G\, dx}{(1 + \varepsilon\theta_0)^2}\right].$$

The required non-local condition has the form

$$(1 + \varepsilon\theta_0)\left[\nabla\pi_0 = (\nabla\pi_0 \cdot \mathbf{n})\mathbf{n}\right] = \mathbf{F} - (\mathbf{F} \cdot \mathbf{n})\mathbf{n}, \quad \mathbf{x} \in \Sigma. \tag{4.40}$$

It is similar to Solonnikov's condition [216] obtained in studying solvability of the initial-boundary problem for the Stokes system in classes of smooth functions.

Statement 4.1. Let the surface Σ belong to the Hölder class $C^{4+\alpha}$, $0 < \alpha < 1$, and let the functions involved into conditions (4.31)–(4.33) satisfy the smoothness requirements $q \in C^{3+\alpha,(3+\alpha)/2}(\Sigma \times [\infty))$, $\mathbf{v}_0 \in C^{2+\alpha}(\bar{\Omega})$, $\theta_0 \in C^{4+\alpha}(\bar{\Omega})$ and the matching conditions (4.36)–(4.40). Then, there exists $N > 0$ such that problem (4.27)–(4.35) has a solution $\mathbf{v}^{(0)} \in C^{2+\alpha,(1+\alpha)/2}(\bar{Q}_N)$, $\theta^{(0)} \in C^{3+\alpha,(3+\alpha)/2}(\bar{Q}_N)$, $\nabla p^{(0)} \in C^{\alpha,\alpha/2}(\bar{Q}_N)$, $P \in C^{(2+\alpha)/2}[0, N]$, where $Q_N = \{\mathbf{x}, t : \mathbf{x} \in \Omega, 0 < t < N\}$. The functions $\mathbf{v}^{(0)}$, $\theta^{(0)}$, and P are uniquely determined, and the function $p^{(0)}$ is uniquely determined under the additional condition

$$\int_{\Omega} p^{(0)}\, dx = 0, \quad 0 \le t \le N. \tag{4.41}$$

In what follows, we refer to eqs. (4.27)–(4.29), (4.34) the *equations of convection of a weakly compressible fluid*. These equations are naturally obtained by generalizing the equations of convection of an isothermally incompressible fluid (see Chapter 3).

Similar to Statement 4.1, the local theorem of existence of a smooth solution of the initial-boundary problem for the equations of convection of a weakly compressible fluid with a general temperature condition of the third kind instead of eq. (4.10) or eq. (4.10′) was proved in [77].

Substitution of the expressions $\mathbf{v} = \mathbf{v}^{(0)}$, $p = \delta^{-1}(P - 1) + p^{(0)}$, and $\theta = \theta^{(0)}$ into system (4.18)–(4.20) yields residues of the order of $O(\delta)$ as $\delta \to 0$. The boundary conditions (4.21) and (4.22) and the initial conditions (4.23) and (4.24) are satisfied exactly in this case. The constructed approximate solution can be expected to approximate the solution of the initial-boundary problem (4.18)–(4.25) at large times with the same order of approximation as $\delta \to 0$.

As the function $\pi_0(\mathbf{x}) = p^{(0)}(\mathbf{x}, 0)$ obtained by solving problem (4.27)–(4.35), (4.40) does not necessarily coincide with the function $p_0(\mathbf{x})$ specifying the initial pressure distribution in the initial problem, the formal asymptotics (4.26) does not work at small times. It is extremely difficult to describe the transitional process accompanied by propagation of high-frequency, nonlinear acoustic waves in a viscous heat-conducting fluid, and this has not yet been done. A certain idea about this process can be obtained by studying its linear model.

4.5 Equations of microconvection of an isothermally incompressible fluid

This is term for a fluid whose density depends on temperature only. We write the state equation of an isothermally incompressible fluid in the form (see eq. (3.10))

$$\varrho = \varrho_0(1 + \varepsilon\theta)^{-1}. \tag{4.42}$$

Equality (4.42) is obtained from eq. (4.17) in the limit as $\delta \to 0$. As was already noted in Section 4.1, owing to the small value of the Boussinesq number $\varepsilon = \beta\theta_*$ (here we

assume that $\beta_1 \equiv \beta$), the differences between approximations of the state equation $\varrho(\theta)$ by a linear function or by a function of the form (4.42) are insignificant. At the same time, among numerous possible approximations of the function $\varrho(\theta)$, the dependence (4.42) has some wonderful properties, which were noted in [177, 237] (see also Chapter 3). In particular, the specific heat at constant pressure c_p of an isothermally incompressible fluid is independent of pressure if and only if the state equation has the form (4.42). Another important property of the chosen state equation is the possibility of drastic simplifications of the equations of convection of an isothermally incompressible fluid. Before applying these simplifications, we obtain the condition of solvability of the initial-boundary problem for such equations. Assuming that $\delta = 0$ in eqs. (4.18)–(4.20) (which corresponds to the case where density is independent of pressure), we obtain

$$-\frac{\varepsilon}{1+\varepsilon\theta}\cdot\frac{d\theta}{dt} + \operatorname{div}\mathbf{v} = 0; \tag{4.43}$$

$$\frac{1}{1+\varepsilon\theta}\cdot\frac{d\mathbf{v}}{dt} = \operatorname{Pr}\big[\nabla(-p+\xi\operatorname{div}\mathbf{v}) + \Delta\mathbf{v}\big] + \frac{\eta\operatorname{Pr}}{1+\varepsilon\theta}\,\mathbf{e}; \tag{4.44}$$

$$\frac{1}{1+\varepsilon\theta}\cdot\frac{d\theta}{dt} = \Delta\theta. \tag{4.45}$$

System (4.43)–(4.45) is supplemented with the boundary conditions (4.21) and (4.22) and with the initial conditions (4.23) and (4.24).

It follows from eqs. (4.43) and (4.45) that

$$\operatorname{div}(\mathbf{v} - \varepsilon\nabla\theta) = 0. \tag{4.46}$$

Integrating the last equality over the domain Ω and using conditions (4.21) and (4.22), we find

$$\int_\Sigma q\, d\Sigma = 0, \quad t \geq 0. \tag{4.47}$$

This is the necessary condition for the solvability of problem (4.43)–(4.45), (4.21)–(4.24). The physical treatment of condition (4.47) is rather obvious. For an isothermally incompressible fluid which completely fills a bounded domain, a nonzero total heat flux through its boundary induces a mass flux, which is impossible if the domain boundary is a nondeformable impermeable wall.

The same reasoning shows that the problem of convection of an isothermally incompressible fluid in a closed volume becomes only conditionally well-posed if condition (4.22) for temperature is replaced by the condition of the first kind (4.22′) or by a condition of the third kind. The model of convection of a weakly compressible fluid does not have this drawback. It should also be noted that the satisfaction of condition (4.47) leads to the exact coincidence of eqs. (4.43)–(4.45) with eqs. (4.27)–(4.29), which are satisfied by the principal terms of expansion (4.26). In this case, according

to eqs. (4.34), (4.35), we have $P = 1$, and there is no singular component in expansion (4.26) for pressure.

Let us return to system (4.43)–(4.45). Equality (4.46), which follows from this system, means that the vector $\mathbf{v} - \varepsilon\nabla\theta$ is a solenoidal vector. This fact suggests that we can pass to new sought functions $\mathbf{w}$ and q in the system considered. These functions are determined by the relations

$$\mathbf{w} = \mathbf{v} - \varepsilon\nabla\theta, \quad \bar{q} = p - \varepsilon(1 + \xi - \mathrm{Pr}^{-1})\Delta\theta. \tag{4.48}$$

In the new variables, system (4.43) takes the form

$$\begin{aligned}\mathbf{w}_t + \mathbf{w}\cdot\nabla\mathbf{w} + \varepsilon\big[\nabla\theta\cdot\nabla\mathbf{w} + (\mathbf{w}\cdot\nabla)\nabla\theta - \nabla(\mathbf{w}\cdot\nabla\theta)\big] \\ + \varepsilon^2\big[(\nabla\theta\cdot\nabla)\nabla\theta + \Delta\theta\nabla\theta - \nabla(|\nabla\theta|^2)\big] \\ = \mathrm{Pr}(1+\varepsilon\theta)(-\nabla\bar{q} + \Delta\mathbf{w}) + \eta\,\mathrm{Pr}\,\mathbf{e}_3; \qquad (4.49)\end{aligned}$$

$$\mathrm{div}\,\mathbf{w} = 0; \tag{4.50}$$

$$\theta_t + \mathbf{w}\cdot\nabla\theta + \varepsilon|\nabla\theta|^2 = (1+\varepsilon\theta)\Delta\theta. \tag{4.51}$$

Equations (4.49)–(4.51) were derived in [133] and were later called the microconvection equations. Andreev et al. [17] demonstrated that the momentum equation (4.49) can be transformed to a more compact form:

$$\begin{aligned}\mathbf{w}_t + \mathbf{w}\cdot\nabla\mathbf{w} + \varepsilon\,\mathrm{rot}\,\mathbf{w}\times\nabla\theta + \varepsilon^2\,\mathrm{div}(\nabla\theta\otimes\nabla\theta - |\nabla\theta|^2 I) \\ = \mathrm{Pr}(1+\varepsilon\theta)(-\nabla\bar{q} + \Delta\mathbf{w}) + \eta\,\mathrm{Pr}\,\mathbf{e}_3. \qquad (4.52)\end{aligned}$$

If we replace θ in eqs. (4.50)–(4.52) by c (concentration of the passive admixture), we obtain equations that describe the concentration convection under microgravity conditions or at microscales. These equations were derived in [161].

The most natural problem for system (4.50)–(4.52) is the initial-boundary problem

$$\mathbf{w} = -\varepsilon\nabla\theta, \qquad \mathbf{x}\in\Sigma, \quad t > 0; \tag{4.53}$$

$$\frac{\partial\theta}{\partial n} = q(\mathbf{x},\zeta t), \quad \mathbf{x}\in\Sigma, \quad t > 0; \tag{4.54}$$

$$\mathbf{w} = \mathbf{w}_0(\mathbf{x}), \qquad \mathbf{x}\in\Omega, \quad t = 0; \tag{4.55}$$

$$\theta = \theta_0(\mathbf{x}), \qquad \mathbf{x}\in\Omega, \quad t = 0. \tag{4.56}$$

The boundary condition (4.53) is the no-slip condition rewritten in terms of the modified velocity $\mathbf{w}$. The function $\mathbf{w}_0(\mathbf{x})$ involved into the initial condition (4.55) is equal to $\mathbf{v}_0(\mathbf{x}) - \varepsilon\nabla\theta_0(\mathbf{x})$ by virtue of eqs. (4.23) and (4.48).

We further assume that $\mathbf{w}_0 = \varepsilon\mathbf{u}_0$, where the function $\mathbf{u}_0$ is independent of ε. In this case, the initial velocity field $\mathbf{v}_0 = \varepsilon(\mathbf{u}_0 + \nabla\theta_0)$ as $\varepsilon \to 0$ has the same order as the characteristic velocity of up-floating of a nonuniformly heated fluid in the gravity field as well as the characteristic velocity of uniform expansion of the fluid induced by

a local heat source (let us recall that the two last quantities have an identical order at $\eta \sim 1$). The assumption made above allows us to seek the solution of problem (4.50)–(4.56) in the form of series in powers of the small parameter ε (Boussinesq number):

$$\theta = \sum_{i=0}^{\infty} \varepsilon^i \theta^{(i)}(\mathbf{x}, t), \quad \mathbf{w} = \sum_{i=1}^{\infty} \varepsilon^i \mathbf{w}^{(i)}(\mathbf{x}, t),$$
$$q = \eta \mathbf{e}_3 \cdot \mathbf{x} + \sum_{i=1}^{\infty} \varepsilon^i q^{(i)}(\mathbf{x}, t). \tag{4.57}$$

The function $\theta^{(0)}$ (here, it has a different meaning from that in the previous paragraph) is determined as the solution of the second initial-boundary problem for the linear homogeneous equation of heat conduction. The functions $\mathbf{w}^{(i)}$ and $q^{(i)}$ and the functions $\theta^{(i)}$ ($i = 1, 2, \ldots$) are found from the consecutively solved first initial-boundary problem for the Stokes system and second initial-boundary problem for the linear inhomogeneous heat-conduction equation.

The results of Solonnikov and his colleagues [216, 116] imply the solvability of the problems arising in the Holder class if the natural conditions of smoothness and matching imposed on the surface Σ and the functions q, $\mathbf{w}_0$, and θ_0 are satisfied. These conditions are similar to those indicated in the formulation of Statement 4.1. The functions $\mathbf{w}^{(i)}$ and $\theta^{(i)}$ are determined in a unique manner, and for one-value determination of the functions it is sufficient to require that the mean value of these functions over the domain Ω is equal to zero for any $t > 0$. Convergence of expansions (4.57) in suitable Holder norms at small values of the parameter ε was established in [183]. A key role in proving convergence belongs to the solenoidal nature of the modified velocity vector $\mathbf{w}$. The same property allows us to use the "stream function—vorticity" variables for constructing effective algorithms of the numerical solution of two-dimensional problems of microconvection. Some problems of this kind were studied numerically in [79, 80, 81]. The results of these works revealed not only quantitative, but also qualitative differences in the behavior of velocity fields calculated by the microconvection model and by the conventional Oberbeck–Boussinesq model in the case where the microconvection parameter $\eta = gl^3/\nu\chi$ is of the order of unity.

To conclude this section, we should note that eqs. (4.50)–(4.52) admit a large group of transformations [17]. On this basis, a number of exact solutions of microconvection equations was constructed in [77, 176, 30, 197] (see Chapter 5).

4.6 Oberbeck–Boussinesq equations

In the previous sections, based on exact equations of motion of a viscous compressible heat-conducting fluid (4.18)–(4.20′) we formulated two approximate models of convection. One of them (system (4.27)–(4.29), (4.34)) was derived under the assumption of weak compressibility of the fluid. In this case, high-frequency acoustic oscillations

were "filtered" in the resulting equations (they should be taken into account only at the initial stage of motion), and the contribution of compressibility was of an integral character. If we assume that $P = 1$ in system (4.27)–(4.29), which corresponds to an isothermally incompressible fluid, and pass to the modified velocity and pressure in accordance with eqs. (4.48), we obtain the microconvection equations (4.50)–(4.52). As a result, there arises a certain hierarchy of models (under the assumptions made in Section 4.1) in the convection theory. The third chain of this hierarchy is the classical Oberbeck–Boussinesq model. The equations of this model can be readily derived from eqs. (4.50)–(4.52) with the use of the limiting transition $\varepsilon \to 0$, $\eta \to \infty$.

The continuity equation (4.50) retains the previous form

$$\operatorname{div} \mathbf{w} = 0, \tag{4.58}$$

and eq. (4.51) in the limit $\varepsilon \to 0$ transforms to the heat-transfer equation for an incompressible fluid

$$\theta_t + \mathbf{w} \cdot \nabla\theta = \Delta\theta, \tag{4.59}$$

which contains no term with the dissipative function (the assumption of smallness of this term is one of the basic assumptions in the classical convection theory). In the momentum equation, we first use the substitution $\bar{q} = \eta \mathbf{e}_3 \cdot \mathbf{x} + r$ (i. e., identify the hydrostatic component of pressure) and then make ε tend to zero and the parameter η tend to infinity, so that their product $\varepsilon\eta = \beta\theta_* g l^3/\nu\chi$ (Rayleigh number) retains a constant positive value. As a result, we obtain

$$\mathbf{w}_t + \mathbf{w} \cdot \nabla\mathbf{w} = \Pr(-\nabla r + \Delta\mathbf{w} - \operatorname{Ra} \theta\, \mathbf{e}). \tag{4.60}$$

With accuracy to notations, system (4.58)–(4.60) coincides with the Oberbeck–Boussinesq system of equations (3.41)–(3.43), where $h_1 = 0$. Let us also note that the modified velocity $\mathbf{w}$ at $\varepsilon = 0$ turns by virtue of eq. (4.48) to the usual variable $\mathbf{v}$; the same refers to the modified pressure.

4.7 Linear model of the transitional process

As was noted in Section 4.4, the approximate solution of system (4.18)–(4.20′) constructed there does not satisfy the initial condition for pressure, because the function $p_0(\mathbf{x})$ involved into it does not generally coincide with the function $\pi_0(\mathbf{x}) = p^{(0)}(\mathbf{x}, 0)$ (the latter is determined from the initial values of velocity $\mathbf{v}_0(\mathbf{x})$ and temperature $\theta_0(\mathbf{x})$ as a solution of the elliptical boundary-value problem formulated in Section 4.4). If we assume, however, that the function $\Pi_0(\mathbf{x}) = p_0(\mathbf{x}) - \pi_0(\mathbf{x})$ is small and take into account that the initial conditions for velocity and temperature in the approximate solution are

exactly satisfied, we can linearize eqs. (4.18)–(4.20′) in the vicinity of the isothermal equilibrium state and consider the following linear initial-boundary problem:

$$\delta\Pi_t - \varepsilon\Xi_t + \operatorname{div}\mathbf{U} = 0, \qquad \mathbf{x}\in\Omega, \quad t>0; \tag{4.61}$$

$$\mathbf{U}_t = \operatorname{Pr}[\Delta(-\Pi + \xi\operatorname{div}\mathbf{U}) + \Delta\mathbf{U}], \qquad \mathbf{x}\in\Omega, \quad t>0; \tag{4.62}$$

$$\Xi_t - \delta\alpha_2\Pi_t = \Delta\Xi, \qquad \mathbf{x}\in\Omega, \quad t>0; \tag{4.63}$$

$$\mathbf{U} = 0, \qquad \mathbf{x}\in\Sigma, \quad t>0; \tag{4.64}$$

$$\frac{\partial\Xi}{\partial n} = 0, \qquad \mathbf{x}\in\Sigma, \quad t>0; \tag{4.65}$$

$$\mathbf{U} = 0, \qquad \mathbf{x}\in\Omega, \quad t=0; \tag{4.66}$$

$$\Xi = 0, \qquad \mathbf{x}\in\Omega, \quad t=0; \tag{4.67}$$

$$\Pi = \Pi_0(\mathbf{x}), \qquad \mathbf{x}\in\Omega, \quad t=0. \tag{4.68}$$

Here, the symbols $\mathbf{U}$, Ξ, and Π indicate perturbations of velocity, temperature, and pressure, respectively. In the following, we assume that $\Pi_0 \in W_2^2(\Omega)$.

Despite its linearity, problem (4.61)–(4.68) is still rather complicated because of the presence of the small parameter δ at the derivative Π_t. Nevertheless, an idea about its qualitative behavior as $\delta \to 0$ can be obtained by using decomposition of the vector $\mathbf{U}$ into the potential and solenoidal components:

$$\mathbf{U} = \nabla\varphi + \mathbf{V}, \quad \operatorname{div}\mathbf{V} = 0.$$

Omitting simple calculations, we write relations satisfied by the function φ:

$$\delta\frac{\partial}{\partial t}\left[\frac{\partial}{\partial t} - (\xi+1)\Delta\right][(1-\alpha_2\varepsilon)\varphi_t - \Delta\varphi] - \left(\frac{\partial}{\partial t} - \Delta\right)\Delta\varphi = 0, \qquad \mathbf{x}\in\Omega, \quad t>0; \tag{4.69}$$

$$\frac{\partial\varphi}{\partial n} = 0, \quad \frac{\partial\Delta\varphi}{\partial n} = 0, \qquad \mathbf{x}\in\Sigma, \quad t>0; \tag{4.70}$$

$$\varphi = 0, \quad \varphi_t = -\Pi_0(\mathbf{x}), \quad \varphi_{tt} = -(\xi+1)\Delta\Pi_0, \qquad \mathbf{x}\in\Omega, \quad t=0. \tag{4.71}$$

For a known value of φ, the functions Π and Ξ are described by the explicit relations

$$\Pi = (\xi+1)\Delta\varphi - \varphi_t, \quad \Xi = \varepsilon^{-1}\left\{\delta[(\xi+1)\Delta\varphi - \varphi_t] + \int_0^t \Delta\varphi\, d\tau\right\}.$$

The solution of problem (4.69)–(4.71) is sought in the form of the Fourier series

$$\varphi = \sum_{k=1}^{\infty} A_k(t)\varphi_k(\mathbf{x}),$$

where $\{\varphi_k\}$ is the system of eigenfunctions of the Laplace operator with the Neumann condition, which is orthonormalized to $L_2(\Omega)$, i. e., $\Delta\varphi_k = -\mu_k^2\varphi_k$, $\mathbf{x}\in\Omega$; $\partial\varphi_k/\partial n =$

0, $\mathbf{x} \in \Sigma$, and $-\mu_k^2$ are the corresponding eigenvalues, $0 < \mu_1 < \mu_2 < \cdots$. Without loss of generality, we can assume that the value of the function Π_0 averaged over Ω is equal to zero. In this case, the expansion for φ has no term with the function $\varphi = \text{const}$ corresponding to the eigenvalue $\mu_0 = 0$. The functions $A_k(t)$ are found from the solution of the Cauchy problem for the third-order linear ordinary equation with constant coefficients whose solution is found in the form $A_k = e^{\lambda t}$. The characteristic equation for λ has the following form (it follows from eq. (4.69)):

$$\delta\lambda[\lambda + (\xi + 1)\mu_k^2][(1 - \alpha_2\varepsilon)\lambda + \mu_k^2] + (\lambda + \mu_k^2)\mu_k^2 = 0. \tag{4.72}$$

Equation (4.72) contains two small parameters, δ and ε. If $\varepsilon = 0$, it decomposes into a linear and a quadratic equation. This permits us to obtain a presentation of the roots of eq. (4.72) in the form

$$\lambda_{1,2} = \left\{-\frac{(\xi + 1)^2\mu_k^2}{2} \pm \mu_k\left[\frac{(\xi + 1)^2\mu_k^2}{4} - \frac{1}{\delta}\right]^{1/2}\right\}[1 + O(\varepsilon)],$$
$$\lambda_3 = -\mu_k^2[1 + O(\varepsilon)].$$

The root $\lambda_3 < 0$ corresponds to the thermal mode, and the roots λ_1 and λ_2 correspond to the acoustic modes. As $\delta \to 0$, the calculations show that the contribution of the thermal mode to the amplitude $A_k(t)$ of each harmonic over which the function φ is expanded has the order of δ, whereas the acoustic modes make the main contribution $O(\delta^{1/2})$. The decrement of thermal mode decay is independent of δ as $\delta \to 0$. The dependence of the characteristic numbers λ_1 and λ_2 on δ is rather significant. If $\delta < \delta_0 = 4[(\xi + 1)\mu_1]^{-2}$, where $-\mu_1^2$ is the Laplace operator eigenvalue with the smallest absolute value, then there exists a natural $n = n(\delta)$ such that the roots $\lambda_{1,2}$ at $k < n$ have a nonzero imaginary part, while $\operatorname{Im}\lambda_{1,2} = O(\delta^{-1/2})$, and $\operatorname{Re}\lambda_{1,2} < 0$, and also $\operatorname{Re}\lambda_{1,2} = O(1)$ as $\delta \to 0$. If $k \geq n$, then the roots λ_1 and λ_2 are real and negative, with $\lambda_2 = O(\delta^{-1})$ as $\delta \to 0$, whereas the estimate of the first root uniform with respect to $k \geq n$, which cannot be improved, has the form $\lambda_1 = O(1)$, but the contribution of the corresponding mode to the amplitude $A_k(t)$ has the order of δ as $\delta \to 0$.

Thus, the solution to problem (4.69)–(4.71) admits the presentation

$$\varphi = \sum_{k=1}^{n} B_k(t)\varphi_k(\mathbf{x}) + \omega(\mathbf{x}, t),$$

where B_k are rapidly oscillating functions of t, and the norm of the function $\omega(\mathbf{x}, \cdot)$ in the space $W_2^2(\Omega)$ (or its stronger norm if the function $\Pi_0(\mathbf{x})$ possesses greater smoothness) is estimated as $C\delta\exp(æt)$ uniformly over $t \geq 0$, where the positive constants æ and C are independent of δ as $\delta \to 0$. In this case, $n(\delta) \to \infty$ as $\delta \to 0$. Each of the functions $B_k(t)$ exponentially decreases as $t \to \infty$, but these functions have no pointwise limits as δ tends to zero: in this sense, they are rather similar to the functions $\exp(-a_k t) \times \sin(b_k\delta^{-1/2}t)$, where a_k and b_k are independent of δ. Nevertheless, as

$\delta \to 0$, there exists a weak limit of constriction of the functions $B_k(t)$ to an arbitrary interval $[0, N]$, and this limit is equal to zero.

Thus, we determined the potential component of the vector $\mathbf{U}$ and as well as the functions Π and Ξ. To satisfy the no-slip condition (4.66), we introduce a solenoidal component of $\mathbf{V}$ and a corresponding pressure Q. These functions form the solution of the Stokes system

$$\mathbf{V}_t = \Pr(-\nabla Q + \Delta \mathbf{V}), \quad \operatorname{div} \mathbf{V} = 0, \quad \mathbf{x} \in \Omega, \quad t > 0, \tag{4.73}$$

for which the following initial-boundary problem is posed:

$$\mathbf{V}_t = \mathbf{a}(\mathbf{x}, t), \quad \mathbf{x} \in \Sigma, \quad t > 0; \tag{4.74}$$

$$\mathbf{V} = 0, \quad \mathbf{x} \in \Omega, \quad t = 0. \tag{4.75}$$

The function $\mathbf{a}$ is determined by the equality $\mathbf{a} = -\nabla\varphi|_\Sigma$ and, by virtue of eq. (4.70), has a zero normal component on the surface Σ. From here and from eqs. (4.73) and (4.75), it follows that the function $Q(\mathbf{x}, 0)$ as a solution of the homogeneous Neumann problem for the Laplace equation is constant; without loss of generality, this constant can be taken equal to zero. Therefore, the total pressure in the linearized problem $\Pi + Q$ satisfies the original initial condition (4.68).

The solution of problem (4.73)–(4.75) can be obtained in the form of an expansion in eigenfunctions of the Stokes operator [114] after introduction of an auxiliary function $\mathbf{b}(\mathbf{x}, t)$ that ensures a solenoidal continuation of the vector $\mathbf{a}$ to the domain Ω. Leaving out the details, we only mention that rapid oscillations of the function $\mathbf{a}$ in time at small values of δ give rise to oscillations of the functions $\mathbf{V}$ and Q. These oscillations, however, are dampened by viscosity. This is manifested not only in a comparatively slow decay of the solution of problem (4.73)–(4.75) with time, but also in localization of high-frequency oscillations near the boundary of the domain Ω (the characteristic thickness of the unsteady boundary layer has the order of $\delta^{1/4}$ as $\delta \to 0$).

Remark 4.1. The last chain of this hierarchy is the model of a viscous heat-conducting fluid (3.35)–(3.37). It is obtained from eqs. (4.50)–(4.52) as $\varepsilon \to 0$ and other parameters being fixed.

4.8 Some conclusions

Let us now draw some conclusions from Sections 4.1–4.7.

1. As was noted above, the asymptotic solution of the linear problem (4.61)–(4.68) has no pointwise limit as $\delta \to 0$. Nevertheless, it can be considered to be the principal term of the internal (i. e., describing the initial stage of convection) expansion of the solution of linearized equations of motion (4.18)–(4.20′), if the traditional principle of

matching of asymptotic expansions is extended to matching on functionals. Indeed, as $\delta \to 0$, the following relation is valid for an arbitrary test function $\sigma(t) \in C_0^\infty[0,\infty)$:

$$\int_0^\infty \sigma(t) W(\mathbf{x},t)\, dt = O(\delta), \quad \mathbf{x} \in \Omega.$$

In this relation, W can be taken to be the components U_k $(k = 1,2,3)$ of the vector $\mathbf{U}$, $\Pi + Q$, or Ξ.

2. The reason for the emergence of high-frequency acoustic oscillations considered in Section 4.7 is the disagreement between the initial pressure distribution $p_0(\mathbf{x})$ and the distribution that will be obtained in the course of solving problem (4.27)–(4.35), (4.40), i. e., $\pi_0(\mathbf{x}) = p^{(0)}(\mathbf{x},0)$. To avoid these oscillations, it suffices to set $p_0(\mathbf{x}) = \pi_0(\mathbf{x})$. This will lead to a differential relation between the functions $\mathbf{v}_0$, θ_0, and p_0 defining the initial state of the fluid, which also involves the values of the functions $q(\mathbf{x},0)$ and $q_t(\mathbf{x},0)$ averaged over the surface Σ. In the simplest case of homogeneous initial conditions (4.23)–(4.25), this relation is satisfied if

$$\int_\Sigma q_t(\mathbf{x},0)\, d\Sigma = 0,$$

i. e., if the heating of the initially quiescent fluid with constant temperature and pressure begins smoothly.

3. It should be noted that the procedure of "sound filtration" in the convection equations was also performed previously [159, 151, 44, 120]. In these works, however, convection in gases was considered, where the assumption of weak compressibility of the medium is not natural. It is therefore difficult to give an asymptotic meaning to the operation of dividing the pressure into a component averaged over the flow domain (which leads to the emergence of the "source" term in the continuity equation of the type of the expression $P^{-1}\dot{P}$ in eq. (4.27)) and an inhomogeneous component (analog to the function $p^{(0)}$ in the momentum equation (4.28)).

4. Relations (4.34) and (4.35) yield the presentation for the mean pressure $P(t)$ involved into the equations of convection of a weakly compressible fluid (4.27)–(4.29)

$$P = 1 + \frac{\varepsilon}{|\Omega|} \int_0^t \left(\int_\Sigma q\, d\Sigma \right) dt' + O(\varepsilon^2)$$

as $\varepsilon \to 0$ (here, $|\Omega|$ indicates the volume of the domain Ω). This permits the simplification of the above-mentioned equations, if only terms of the zero-th and first orders with respect to ε are retained. Let us recall that the parameter ε in typical situations (see Section 4.3) has the order of 10^{-3}; therefore, the neglect of the quantities $O(\varepsilon^2)$ is more than justified from the viewpoint of applications.

5. In Section 4.4, we considered the initial-boundary problem for system (4.27)–(4.29) with the boundary condition of the second kind for temperature (4.31). The problem with the condition of the first kind (eq. (4.22′)) is more difficult to study. In this case, the right-hand side of eq. (4.34) should be replaced by

$$\varepsilon \int_{\Sigma} \frac{\partial \theta^{(0)}}{\partial n}\, d\Sigma \equiv H[P(t)],$$

where H is an operator that puts into correspondence the function $P(t)$ and the mean (with accuracy to a constant factor) value of the heat flux on the surface Σ calculated at the time t, based on the solution of problem (4.27)–(4.30), (4.22), (4.32)–(4.35). The operator H is continuous (and even compact) in the space $C^{(1+\beta)/2}[0, N]$ if the value of N is rather small. This allows us to prove local one-valued solvability of the problem considered.

6. In contrast to that, the unsteady problem for equations of microconvection of an isothermally incompressible fluid with the boundary condition of the first kind for temperature (4.22′) has no solution for an arbitrarily specified function h, because it is impossible to ensure *a priori* the necessary condition of its solvability

$$\int_{\Sigma} \frac{\partial \theta}{\partial n}\, d\Sigma = \int_{\Sigma} q\, d\Sigma = 0, \quad t > 0, \tag{4.76}$$

following from eqs. (4.46) and (4.21). At the same time, the steady problem for microconvection equations is well posed with temperature conditions of both the second and first kinds on the boundary of the domain Ω.

Let us here give the basic results of [178] under this aspect. We consider a steady analog of system (4.49)–(4.51): the functions $\mathbf{w}$, $\bar{q}$, and θ are independent of time. For this system, we pose the boundary-value problem (4.53), (4.54), which is called problem A, or (4.53), (4.22′), which is called problem B (the functions q and h are independent of t).

Statement 4.2. Let the boundary Σ of the domain Ω belong to the Hölder class $C^{3+\beta}$, $0 < \beta < 1$, the function q belong to $C^{2+\beta}(\Sigma)$, and eq. (4.76) be satisfied. There exists $\varepsilon_0 > 0$ such that problem A has a solution $\mathbf{w} \in C^{2+\alpha}(\bar{\Omega})$, $\theta \in C^{3+\alpha}(\bar{\Omega})$, $\bar{q} \in C^{1+\alpha}(\bar{\Omega})$ for $\varepsilon \in (0, \varepsilon_0]$. This solution is unique with accuracy to adding a constant to $\bar{q}$ in a certain sphere with the center at the zero product of the spaces $C^{2+\alpha}(\bar{\Omega}) \times C^{3+\alpha}(\bar{\Omega}) \times C^{1+\alpha}(\bar{\Omega})$. In addition, the solution of problem A is an analytical vector-function of the parameter ε at the point $\varepsilon = 0$.

Statement 4.3. Let the conditions $\Sigma \in C^{3+\alpha}$ and $h(x) \in C^{3+\alpha}(\Sigma)$ be satisfied. There exists $\varepsilon_0 > 0$ such that problem B has a solution $\mathbf{w} \in C^{2+\alpha}(\bar{\Omega})$, $\theta \in C^{3+\alpha}(\bar{\Omega})$, $\bar{q} \in C^{1+\alpha}(\bar{\Omega})$ for $\varepsilon \in (0, \varepsilon_0]$. This solution is isolated if the mean value of the function $\bar{q}$ in the domain Ω is fixed and is an analytical vector-function of the parameter ε at the point $\varepsilon = 0$.

These statements are proved by expanding the solution into series of the form (4.57) and by estimating the series terms. Note that condition (4.76) should also be satisfied for problem B, but no additional relations for the function h are required.

7. Well-posedness of the initial-boundary problem for equations of an isothermally incompressible fluid can be provided by changing its formulation, as was mentioned in Chapter 3.

4.9 Convection of nonisothermal liquids and gases under microgravity conditions

Let us consider natural convective flows under conditions where external mass forces are rather small and there are no large drops of temperature and pressure in the medium. The characteristic size of the domain where convection occurs is assumed not to be too large. The equations that describe the motion and heat transfer in the Newtonian fluid have the form

$$\begin{gathered}\frac{d\varrho}{dt}+\varrho\,\mathrm{div}\,\mathbf{v}=0,\quad \varrho\frac{d\mathbf{v}}{dt}=-\nabla p+\mathrm{div}(\mu\mathbf{T})+\varrho g\mathbf{e}_3,\\ \varrho c_p\frac{d\theta}{dt}-\beta\theta\frac{dp}{dt}=\mathrm{div}(k\nabla\theta)+\mu\Phi,\\ \varrho=\varrho(\theta,p),\quad \mu=\mu(\theta,p),\quad k=k(\theta,p),\quad \beta=\beta(\theta,p),\quad c_p=c_p(\theta,p).\end{gathered}\tag{4.77}$$

For convenience, we indicate $\mathbf{T}=2\mathcal{D}(\mathbf{v})-2\,\mathrm{div}\,\mathbf{v}I/3$; then, $\Phi=\mathbf{T}:\mathbf{T}/2$; the volume viscosity is assumed to be equal to zero, and there are no internal heat sources.

It is more convenient to write the continuity equation in the following form with the use of the energy equation:

$$\frac{1}{\varrho}\frac{\partial\varrho}{\partial\theta}\frac{1}{\varrho c_p}\left(\beta\theta\frac{dp}{dt}+\mathrm{div}(k\nabla\theta)+\mu\Phi\right)+\frac{1}{\varrho}\frac{\partial\varrho}{\partial p}\frac{dp}{dt}=-\,\mathrm{div}\,\mathbf{v}.\tag{4.78}$$

Let us now simplify the initial full equations step by step. For a weakly nonisothermal medium with small variations of pressure *far from the stagnation point and in the absence of such phenomena as the thermal anomaly*, it is possible to use linearized equations determining the changes in the thermophysical parameters of the medium

$$\begin{aligned}V&=V_0(1+\beta_0(\theta-\theta_0)-f_{\varrho 0}(p-p_0)),\\ \mu&=\mu_0(1+e_{\mu 0}(\theta-\theta_0)+f_{\mu 0}(p-p_0)),\\ k&=k_0(1+e_{k0}(\theta-\theta_0)+f_{k0}(p-p_0)),\\ \beta&=\beta_0(1+e_{\beta 0}(\theta-\theta_0)+f_{\beta 0}(p-p_0)),\\ c_p&=c_{p0}(1+e_{c0}(\theta-\theta_0)+f_{c0}(p-p_0)),\end{aligned}\tag{4.79}$$

where $V = 1/\varrho$ is the specific volume; the subscript 0 refers to quantities in the state θ_0, p_0 (θ_0 and p_0 are the characteristic (constant) values of temperature and pressure in the system). For convenience, we introduce one more notation for isothermal compressibility: $\alpha_0 = f_{\varrho 0}$, and we also indicate $\varrho_0 = 1/V_0$.

The flows under considerations are characterized by extremely low velocities. To describe convection for velocities much smaller than the velocity of sound, it is reasonable to use the approximation of essentially subsonic flows [120]. Owing to this approximation, the analysis of the comparative influence of physical effects and resultant equations can be substantially simplified.

Let us consider the variables whose variations definitely occur in an interval of the order of unity. The corresponding scales for velocity and time will be refined later; for the moment, they are assumed to be equal to a certain characteristic value of the flow velocity u_* and characteristic time t_*. Let the convection occur in a domain with a characteristic size l, and let the characteristic difference of temperatures have a value of the order of θ_*. The scales for density, viscosity, thermal conductivity, volume expansion coefficient, and specific heats at constant pressure and constant volume are chosen to be ϱ_0, μ_0, k_0, β_0, c_{p0}, and c_{v0}, respectively; the scale for the acceleration of external mass forces is taken as a certain characteristic (constant) value of this quantity equal to g_0. We assume that

$$\begin{gathered} \mathbf{x} = l\mathbf{x}', \quad t = t_* t', \quad \mathbf{v} = u_* \mathbf{v}', \quad \mathbf{T} = \frac{u_*}{l}\,\mathbf{T}', \\ \theta - \theta_0 = \theta_* T', \quad \Phi = \frac{u_*^2}{l^2}\,\Phi'. \end{gathered} \tag{4.80}$$

The dimensionless pressure p/p_0 in subsonic flows changes only weakly. Following [120], we introduce a dynamic pressure normalized to $\mu_0 u_*/l$, which definitely changes in an interval of the order of unity, independent of the flow Mach number. At the same time, as is seen from eq. (4.78) integrated over the considered domain, the domain-averaged pressure is proportional to the total heat flux through the domain boundary. We assume that

$$p - p_0 = \frac{\varrho_0 c_0^2}{\gamma_0}\left(AP' + \frac{\gamma_0 M^2}{\mathrm{Re}}\,\Pi'\right) \equiv \frac{\beta_0 q}{k_0 l \alpha_0}\,P' + \frac{\mu_0 u_*}{l}\,\Pi', \tag{4.81}$$

where $c_0^2 = \gamma_0(\partial p/\partial \varrho)_\theta \equiv \gamma_0/\varrho_0\alpha_0$ is the squared velocity of sound in the medium, $\gamma_0 = c_{p0}/c_{v0}$, $M = u_*/c_0$ is the Mach number, $A = \beta_0 q/(k_0 l)$ is a parameter characterizing the rate of change of the mean pressure, $q = \int_\Sigma k_0 \nabla\theta \cdot \mathbf{n}\, d\Sigma$ is the total heat flux through the boundary Σ of the domain Ω, and $\mathrm{Re} = \varrho_0 u_* l/\mu_0$ is the Reynolds number. The factor A is introduced for more exact normalization of the pressure P' (see eq. (4.87)).

The changes in the parameters due to variations of hydrostatic pressure (in particular, hydrostatic compressibility) are ignored, because the acceleration of external mass forces is assumed to be rather small, so that the condition $f_{j0}\varrho_0 g_0 l \ll 1$ ($j = \varrho, \mu, k, \beta, c$) is satisfied.

As a result, system (4.77)–(4.79) is written in the following form (the dimensionless quantities are primed):

$$
\begin{aligned}
&\mathrm{Sh}\,\frac{\partial \varrho'}{\partial t'} + \mathbf{v}'\cdot\nabla'\varrho' = -\varrho'\,\mathrm{div}\,\mathbf{v}',\\
&\mathrm{Re}\Big(\mathrm{Sh}\,\varrho'\frac{\partial \mathbf{v}'}{\partial t'} + \varrho'\mathbf{v}'\cdot\nabla'\mathbf{v}'\Big) = -\nabla'\Pi' - \frac{\mathrm{Re}\,A}{\gamma_0 M^2}\,\nabla' P' + \mathrm{div}(\mu'\mathbf{T}') + \frac{\mathrm{Re}}{\mathrm{Fr}}\,\varrho' g'\mathbf{e}_3,\\
&\mathrm{Sh}\,\varrho' c_p'\frac{\partial T'}{\partial t'} + \varrho' c_p'\mathbf{v}'\cdot\nabla' T' = \frac{1}{\mathrm{Re}\,\mathrm{Pr}}\,\mathrm{div}(k'\nabla' T')\\
&\qquad + \frac{B}{\varepsilon_T}\,\beta'(1+\varepsilon_T T')\Big[A\Big(\mathrm{Sh}\,\frac{\partial P'}{\partial t'} + \mathbf{v}'\cdot\nabla' P'\Big)\\
&\qquad\qquad + \frac{\gamma_0 M^2}{\mathrm{Re}}\Big(\mathrm{Sh}\,\frac{\partial \Pi'}{\partial t'} + \mathbf{v}'\cdot\nabla'\Pi'\Big)\Big]\\
&\qquad - \frac{\gamma_0 M^2}{\mathrm{Re}}\,\frac{B}{\varepsilon_\varrho}\,\mu'\Phi',\\
&\varrho' = \Big[1 - \varepsilon_\varrho T' - \varphi_\varrho\Big(P' + \frac{\gamma_0 M^2}{\mathrm{Re}\,A}\,\Pi'\Big)\Big]^{-1},\\
&\mu', k', \beta', c_p' = 1 + \varepsilon_{\mu,k,\beta,c}\,T' + \varphi_{\mu,k,\beta,c}\Big(P' + \frac{\gamma_0 M^2}{\mathrm{Re}\,A}\,\Pi'\Big).
\end{aligned}
\tag{4.82}
$$

Here,

$$
\begin{gathered}
\mathrm{Sh} = \frac{l}{u_* t_*},\quad \mathrm{Re} = \frac{\varrho_0 u_* l}{\mu_0},\quad M^2 = \frac{u_*^2}{c_0^2},\quad \mathrm{Fr} = \frac{u_*^2}{g_0 l},\quad \mathrm{Pr} = \frac{\mu_0}{\varrho_0\chi_0},\\
\varepsilon_T = \frac{\theta_*}{\theta_0},\quad A = \frac{\beta_0 q}{k_0 l},\quad B = \frac{\beta_0}{\alpha_0 c_{p0}\varrho_0},\quad \varepsilon_j = e_{j0}\theta_*,\\
\varphi_j = \frac{f_{j0}}{\alpha_0}\,\frac{\beta_0 q}{k_0 l}\quad (j = \varrho,\mu,k,\beta,c).
\end{gathered}
$$

In the case of a perfect gas, we have $B = (\gamma_0 - 1)/\gamma_0$; $\beta'(1+\varepsilon_T T') \equiv 1$; $\varepsilon_\varrho = -\varepsilon_T$.

Passing to the limit as $\gamma_0 M^2/\mathrm{Re} \to 0$ in eqs. (4.82) and returning to dimensional quantities, we obtain

$$
\begin{aligned}
&\beta_0\big(1 + e_{c0}(\theta-\theta_0) + f_{c0}(P-P_0)\big)^{-1}\\
&\quad\times\Big\{\frac{\beta_0}{\varrho_0 c_{p0}}\,[1 + e_{\beta 0}(\theta-\theta_0) + f_{\beta 0}(P-P_0)]\theta\frac{dP}{dt}\\
&\qquad + \chi_0[1 + e_{k0}(\theta-\theta_0) + f_{k0}(P-P_0)]\Delta\theta + \chi_0 e_{k0}\nabla\theta\cdot\nabla\theta\Big\}\\
&\quad - [1 + \beta_0(\theta-\theta_0) - \alpha_0(P-P_0)]^{-1}\alpha_0\frac{dP}{dt} = \mathrm{div}\,\mathbf{v};\\
&\frac{\partial \mathbf{v}}{\partial t} + \mathbf{v}\cdot\nabla\mathbf{v} = [-\beta_0(\theta-\theta_0) + \alpha_0(P-P_0)]g\mathbf{e}_3 + [1 + \beta_0(\theta-\theta_0) - \alpha_0(P-P_0)]
\end{aligned}
\tag{4.83}
$$

$$\times \left\{ -\frac{1}{\varrho_0} \nabla \Pi_* + \nu_0 [1 + e_{\mu 0}(\theta - \theta_0) + f_{\mu 0}(P - P_0)] \operatorname{div} \mathbf{T} + \nu_0 e_{\mu 0} \nabla\theta \cdot \mathbf{T} \right\}; \tag{4.84}$$

$$\frac{\partial \theta}{\partial t} + \mathbf{v} \cdot \nabla\theta = \frac{1 + \beta_0(\theta - \theta_0) - \alpha_0(P - P_0)}{1 + e_{c0}(\theta - \theta_0) + f_{c0}(P - P_0)}$$
$$\times \left\{ \frac{\beta_0}{\varrho_0 c_{p0}} [1 + e_{\beta 0}(\theta - \theta_0) + f_{\beta 0}(P - P_0)] \theta \frac{dP}{dt} \right.$$
$$\left. + \chi_0 [1 + e_{k0}(\theta - \theta_0) + f_{k0}(P - P_0)] \Delta\theta + \chi_0 e_{k0} \nabla\theta \cdot \nabla\theta \right\}. \tag{4.85}$$

Here, $P = P(t)$, $\Pi^* = \Pi - \varrho_0 g \mathbf{e}_3 \cdot \mathbf{x}$; $\nu_0 = \mu_0/\varrho_0$; $\chi_0 = k_0/(\varrho_0 c_{p0})$.

Thus, within the framework of the subsonic flow approximation, the total pressure p is presented as the sum of a spatially homogeneous thermodynamic component $P(t)$ and a component that takes into account the dynamic and hydrostatic effects $\Pi(\mathbf{x}, t)$. The influence of viscous dissipation of kinetic energy is ignored here.

System (4.83)–(4.85) is closed by the relation determining the evolution of $P(t)$. In the case of convection in a domain bounded by solid walls, integration over the considered domain Ω of the continuity equation (4.83) yields

$$\frac{dP}{dt} \int_\Omega \left\{ -\frac{\beta_0^2 \theta [1 + e_\beta(\theta - \theta_0) + f_\beta(P - P_0)]}{c_{p0}[1 + e_c(\theta - \theta_0) + f_c(P - P_0)]} + \frac{\alpha_0 \varrho_0}{1 + \beta_0(\theta - \theta_0) - \alpha_0(P - P_0)} \right\} d\mathbf{x}$$
$$= \int_\Omega \frac{\beta_0 \operatorname{div}\{k_0[1 + e_k(\theta - \theta_0) + f_k(P - P_0)]\nabla\theta\}}{c_{p0}[1 + e_c(\theta - \theta_0) + f_c(P - P_0)]} d\mathbf{x} - \int_\Sigma \varrho_0 \mathbf{v} \cdot \mathbf{n} \, d\Sigma. \tag{4.86}$$

For a domain opened into the atmosphere or into one rather large reservoir, it can be assumed that $P(t) = P_0$, where P_0 is the ambient pressure.

Note, if $A \le O(\gamma_0 M^2/\mathrm{Re})$, then the dependence of the parameters on pressure and the work of pressure forces are not reflected by the resultant system; this case will be considered in detail below. The dependence of the parameter on pressure, however, cannot be always neglected, e. g., if convection in a domain bounded by solid impermeable walls with a given power of external heat sources is considered. According to eq. (4.82), the full system (4.77) should be used in such cases; this system involves, in particular, viscous dissipation of kinetic energy.

Let the values of e_{j0}, f_{j0} ($j = \varrho, \mu, k, \beta, c$), $\theta - \theta_0$, $P - P_0$, and g_0, as well as the velocity on the boundaries of the domain occupied by the fluid be rather small at the initial time, so that the characteristic values of flow velocities and acceleration are also small. In the case where convection is a closed domain bounded by solid impermeable walls, the time evolution of the pressure P is determined by eq. (4.86), which has the following form in the principal order: $dP/dt = B|\Omega|/(1 - \beta_0\theta_0 B)q$ ($|\Omega| = \int_\Omega d\mathbf{x}$ is the volume of the domain Ω). The value of $B\beta_0\theta_0$ is usually smaller than unity; for instance, 0.29 for air and $3.2 \cdot 10^{-3}$ for water. We therefore choose Bq/l^3 as a scale for the rate of change of thermodynamic pressure $(dP/dt)_*$. For time, it seems natural to choose a scale corresponding to molecular thermal conductivity, because convection

is rather weak: $t_* = l^2/\chi_0$. Then the scale for thermodynamic pressure variations is determined as

$$P_* = \left(\frac{dP}{dt}\right)_* t_* = \frac{A}{\alpha_0} \tag{4.87}$$

in accordance with eq. (4.81). Using eqs. (4.83)–(4.85), we can estimate the contributions of the changes in density u_ϱ, viscosity u_μ, thermal conductivity u_k, and specific heat u_c induced by small variations of temperature (indicated by the superscript (T)) and pressure (indicated by the superscript (P)) and the contribution of the work of pressure forces u_P to formation of the velocity field. From the continuity equation (4.83) (or from eq. (4.86)), we obtain the following estimates: $u_\varrho^{(T)} = \beta_0\theta_*\chi_0/l$, $u_{1P} = \alpha_0(dP/dt)_* l$, $u_{2P} = \beta_0^2\theta_0(dP/dt)_* l/(\varrho_0 c_{p0})$. From the momentum equation (4.84), we have $u_\mu^{(T)} = e_{\mu 0}\theta_*\nu_0/l$, $u_\mu^{(P)} = f_{\mu 0}P_*\nu_0/l$, $u_{\varrho 2}^{(T)} = \beta_0\theta_*\nu_0/l$, $u_{\varrho 2}^{(P)} = \alpha_0 P_*\nu_0/l$. From the energy equation (4.85), we obtain $u_P = \beta_0\theta_0(dP/dt)_* l/(\varrho_0 c_{p0}\theta_*)$, $u_k^{(T)} = e_{k0}\theta_*\chi_0/l$, $u_k^{(P)} = f_{k0}P_*\chi_0/l$, $u_c^{(T)} = e_{c0}\theta_*\chi_0/l$, $u_c^{(P)} = f_{c0}P_*\chi_0/l$, $u_{\varrho 3}^{(T)} = \beta_0\theta_*\chi_0/l$, $u_{\varrho 3}^{(P)} = \alpha_0 P_*\chi_0/l$. The contribution of the pressure forces to velocity field formation is estimated as u_P, because $u_{2P}/u_P = \beta_0\theta_* \ll 1$; $u_{1P}/u_P = \varepsilon_T/B$. The contribution of the buoyancy forces u_b to the velocity field at low Rayleigh numbers is estimated in a standard manner: $u_b = \beta_0\theta_* g_0 l^2/\nu_0$ (the scale $(\beta_0\theta_* g_0 l)^{1/2}$ is less appropriate at low velocities).

Obviously, if one of the conditions

$$\frac{u_b}{u_j^{(T)}} \le O(1), \quad \frac{u_b}{u_j^{(P)}} \le O(1) \quad (j = \varrho, \mu, k, c), \quad \frac{u_b}{u_P} \le O(1), \tag{4.88}$$

which have the following form in terms of the basic governing parameters (Rayleigh number $\mathrm{Ra} = \beta_0\theta_* g_0 l^3/(\nu_0\chi_0)$, ε_j, and φ_j):

$$\mathrm{Ra} \le \varepsilon_j \quad (j = \varrho, k, c), \quad \mathrm{Ra} \le \mathrm{Pr}\,\varepsilon_j \quad (j = \varrho, \mu); \tag{4.89}$$

$$\mathrm{Ra} \le \varphi_j \quad (j = \varrho, k, c), \quad \mathrm{Ra} \le \mathrm{Pr}\,\varphi_j \quad (j = \varrho, \mu); \tag{4.90}$$

$$\mathrm{Ra} \le \frac{AB}{\varepsilon_T}, \tag{4.91}$$

is satisfied, then the Oberbeck–Boussinesq approximation is inapplicable for the description of thermal convection. The condition $\mathrm{Ra} \le \varepsilon_\varrho$ reflecting the influence of changes in density was obtained in [177]. Note that other conditions (4.89), for example, those reflecting the change in viscosity and thermal conductivity, $\mathrm{Ra} \le \mathrm{Pr}\,\varepsilon_\mu$ and $\mathrm{Ra} \le \varepsilon_k$, can be much less rigorous than those in [177] (e. g., for water at a temperature $\theta_0 = 15\,°\mathrm{C}$ and pressure $P_0 = 1\,\mathrm{atm}$, we have $\varepsilon_\varrho/(\mathrm{Pr}\,\varepsilon_\mu) = 6.9 \cdot 10^{-4}$ and $\varepsilon_\varrho/\varepsilon_k = -8.8 \cdot 10^{-2}$). Under conditions (4.88), it is not only the Oberbeck–Boussinesq approximation proper that is invalid, but also its various generalizations with constant thermophysical parameters, except for density.

In some cases of practical importance, thermodynamic pressure is almost constant. Let us consider the case with $P = P_0 = \text{const}$. We nondimensionalize the equations so that the values of all field variables change within intervals of the order of unity. The scales for the spatial variables, temperature, and pressure were defined in eqs. (4.80) and (4.81). The scale for velocity should be related to the motion intensity: the scales related to the molecular diffusion characteristics, ν_0/l and χ_0/l, are not suitable for this purpose [89]. In accordance with estimates (4.88)–(4.91), one of the quantities u_ϱ, u_μ, u_k, or u_c should be chosen as the scale of velocity of the microconvective flow. Let us assume that $u_* = \varepsilon\chi_0/l$, where $\varepsilon = \max_j(|\varepsilon_j|)$ $(j = \varrho, \mu, k, c)$. As the time scale, it seems reasonable to take the characteristic time of heat diffusion $t_* = l^2/\chi_0$, because it is smaller than the convective time scale l/u_*. In this case, we have

$$\mathrm{Sh} = \frac{1}{\varepsilon}, \quad \mathrm{Re} = \frac{\varepsilon}{\mathrm{Pr}}, \quad \mathrm{Fr} = \frac{\varepsilon^2\chi_0^2}{g_0 l^3}, \quad \frac{\gamma_0 M^2}{\mathrm{Re}} = \frac{\varepsilon\varrho_0\alpha_0\nu_0\chi_0}{l^2}.$$

For microconvective flows, we have $\gamma_0 M^2/\mathrm{Re} \ll \varepsilon_j$. Thus, $\gamma_0 M^2\,\mathrm{Re}^{-1} = \varepsilon \cdot 7.3 \cdot 10^{-16}\,\mathrm{cm}^2/l^2$ for water at a temperature $\theta_0 = 15\,^\circ\mathrm{C}$ and pressure $P_0 = 1\,\mathrm{atm}$ and $\gamma_0 M^2\,\mathrm{Re}^{-1} = \varepsilon \cdot 3.5 \cdot 10^{-11}\,\mathrm{cm}^2/l^2$ for air. Let us assume that $\varepsilon \ll 1$ and $\gamma_0 M^2/\mathrm{Re} \ll \varepsilon_j$. Omitting terms of the order of smallness greater than $O(\varepsilon_j)$ in eqs. (4.82) (automatically passing to the limit of the subsonic flow approximation $\gamma_0 M^2/\mathrm{Re} \to 0$), we obtain

$$\begin{aligned}
&-\frac{\varepsilon_\varrho}{\varepsilon}\left[(1+\varepsilon_k T' - \varepsilon_c T')\Delta T' + \varepsilon_k \nabla' T' \cdot \nabla' T'\right] = \operatorname{div}\mathbf{v}',\\
&\mathrm{Pr}^{-1}\left(\frac{\partial \mathbf{v}'}{\partial t'} + \varepsilon \mathbf{v}' \cdot \nabla' \mathbf{v}'\right) = \frac{T'_\Sigma - T'}{1-\varepsilon_\varrho T'_\Sigma}\, G g' \mathbf{e}_3 - (1-\varepsilon_\varrho T')\nabla'\Pi_*\\
&\qquad\qquad + (1+\varepsilon_\mu T' - \varepsilon_\varrho T')\operatorname{div}\mathbf{T}' + \varepsilon_\mu \nabla' T' \cdot \mathbf{T}',\\
&\frac{\partial T'}{\partial t} + \varepsilon \mathbf{v}' \cdot \nabla' T' = (1+\varepsilon_k T' - \varepsilon_\varrho T' - \varepsilon_c T')\Delta T' + \varepsilon_k \nabla' T' \cdot \nabla' T',
\end{aligned} \tag{4.92}$$

where $T'_\Sigma = (\theta_\Sigma - \theta_0)/\theta_*$; $\Pi_* = \Pi' - \Pi'_\Sigma$.

In many cases, specific heat changes with temperature to a smaller extent than viscosity, thermal conductivity, or density. At $\varepsilon_c = 0$, instead of a nonsolenoidal velocity field, we can determine a new solenoidal vector field $\mathbf{w} = \mathbf{v}' + (\varepsilon_\varrho/\varepsilon)(\nabla' T' + \varepsilon_k T' \nabla' T')$, which simplifies studying some aspects of the problem. In the case with $\varepsilon_c = \varepsilon_k = \varepsilon_\mu = 0$, system (4.92) coincides with eqs. (4.49)–(4.51) in natural variables.

Based on the principle of compressive mappings, by analogy with [183], solvability of the basic boundary-value problems for system (4.92) with rather small values of ε is proved (it is assumed that ϱ_0, μ_0, k_0, and c_{p0} are positive, and $\beta_0 \geq 0$). Let us give here the following results. We consider a boundary-value problem for the steady system of equations (4.92) in the case with $\varepsilon_c = 0$, which is posed in a bounded domain Ω of the Euclidean space $\mathbb{R}^3$ with a smooth boundary Σ and with the following conditions on this boundary:

$$\mathbf{v}' = \mathbf{a}(\mathbf{x}), \quad (1+\varepsilon_k T')\nabla T' \cdot \mathbf{n} = \Gamma(\mathbf{x}), \quad \mathbf{x} \in \Sigma$$

($\mathbf{a} = (a_1, a_2, a_3)$ and Γ are known functions of the variable $\mathbf{x}$). This problem (let us call it problem A) corresponds to the model of convection in a reservoir with solid impermeable walls with a specified heat-flux distribution on them. The following statement is valid.

Statement 4.4. Let $\Sigma \in C^{l+3}$, $\Gamma \in C^{l+2}(\Sigma)$, $a_i \in C^{l+2}(\Sigma)$ ($C^l(\Sigma)$ and $C^l(\bar{\Omega})$ indicate the corresponding Holder classes of functions); let $l > 0$ be an integer number, and let the condition $\int_\Sigma (\mathbf{n} \cdot \mathbf{a} + (\varepsilon_\varrho/\varepsilon)\Gamma)\, d\Sigma = 0$ be satisfied. Then, there exists $\varepsilon_0 > 0$ such that problem A at $\varepsilon \in [0, \varepsilon_0]$ has a unique solution with $v_i' \in C^{l+2}(\bar{\Omega})$, $\partial\Pi_*/\partial x_i \in C^l(\bar{\Omega})$, $T' \in C^{l+3}(\bar{\Omega})$. This solution is an analytical vector function of the parameter ε at the point $\varepsilon = 0$.

The proof of this statement involves the estimates of solutions of systems elliptical in the Douglis–Nirenberg sense in the Hölder classes. It can be easily demonstrated that the Hölder norms of the difference between the components of the solutions of problem A and the corresponding problem for the Boussinesq equation tend to zero as $\varepsilon \to 0$. Convective effects at finite values of ε, however, can exert a significant influence on microconvection formation.

In the functional spaces $L_{p\,x\,t}^{2l,l}(\bar{D}_4)$ and $L_p^{2l+2-2/p}(\mathbb{R}^3)$ (see the definitions in [215]), we consider the Cauchy problem for system (4.92) in the case with $\varepsilon_c = 0$ in the domain $D_4 = \{(\mathbf{x}, t) : \mathbf{x} \in \mathbb{R}^3,\ t > 0\}$ with the initial conditions (problem B)

$$\mathbf{v}' = \mathbf{v}'_0(\mathbf{x}), \quad T' = T'_0(\mathbf{x}) \quad (t' = 0); \quad \operatorname{div} \mathbf{v}'_0 = 0,$$

where T'_0 and $\mathbf{v}'_0$ are specified functions.

Statement 4.5. Let $T'_0 \in L_p^{2l+2-2/p}(\mathbb{R}^3)$, $v'_{0i} \in L_p^{2l+2-2/p}(\mathbb{R}^3)$, $g_i' \in L_{p\,x\,t}^{2l,l}(\bar{D}_4)$ ($l \geq 0$ is an integer number). Then, there exists $\varepsilon_0 > 0$ such that problem B at $\varepsilon \in [0, \varepsilon_0]$ has a unique solution with $v_i' \in L_{p\,x\,t}^{2l+2,l+1}(\bar{D}_4)$, $\partial\Pi_*/\partial x_i \in L_{p\,x\,t}^{2l,l}(\bar{D}_4)$, $T' \in L_{p\,x\,t}^{2l+2,l+1}(\bar{D}_4)$. This solution is an analytical vector-function of the parameter ε at the point $\varepsilon = 0$.

The proof involves the estimates of the solutions of the Cauchy problem for the heat-conduction equation and the linearized Navier–Stokes equations.

One-valued solvability of the boundary-value problems for the linearized system (4.92) in various functional spaces is established with the use of well-known methods.

By analogy with [58], we can obtain results on local exact controllability by system (4.92) for the control distributed over the boundary. In the case with $\varepsilon_c = 0$, we perform the following replacement in eqs. (4.92): $\mathbf{w} = \mathbf{v}' + (\varepsilon_\varrho/\varepsilon) \times (\nabla' T' + \varepsilon_k T' \nabla' T')$; the system of the transformed equations is denoted by (4.92′).

Statement 4.6. Let a solution $\mathbf{w}_* \in H^{1,2(2)}(Q)$, $T \in W^{1,2(2)}(Q)$, $\nabla q \in L_2(0, \tau; W_2^2(\Omega))$ of eqs. (4.92′), such that $\int_\Sigma \mathbf{n} \cdot \mathbf{w}\, d\Sigma = 0$ be given, as well as the initial conditions for which $\mathbf{w}_0 \in H^1(\Omega)$, $T_0 \in W_2^1(\Omega)$, $\int_\Sigma \mathbf{n} \cdot \mathbf{w}_0\, d\Sigma = 0$ and $||\mathbf{w}_* - \mathbf{w}_0||_{H^1(\Omega)} + ||T_* - T_0||_{H^1(\Omega)} < \varepsilon$, where $\varepsilon > 0$ is a rather small quantity (notations of the functional spaces can be found in [58]). There then exists a boundary control $(u_w, u_T) \in (L_2(\Sigma))^3 \times L_2(\Sigma)$ such that the

solution of problem (4.92′)

$$\mathbf{w} = \mathbf{w}_0(\mathbf{x}), \quad T = T_0(\mathbf{x}) \quad (t = 0);$$
$$\mathbf{w} = \mathbf{u}_w, \quad (1 + \varepsilon_k T')\nabla T' \cdot \mathbf{n} = u_T \quad (\mathbf{x} \in \Sigma),$$

(where T_0' and $\mathbf{v}'_0$ are given functions) exists and satisfies the condition

$$\mathbf{w}(\tau, \mathbf{x}) \equiv \mathbf{w}_*(\tau, \mathbf{x}), \quad T(\tau, \mathbf{x}) \equiv T_*(\tau, \mathbf{x}).$$

4.10 Convection of a thermally inhomogeneous weakly compressible fluid

Here we describe the convection model proposed and studied in [139]. The initial system is the general system of hydrodynamic equations (1.46) in which $\mathbf{f} = \mathbf{g} + \mathbf{F}$ (the acceleration of the gravity force $\mathbf{g}$ is singled out) and the left-hand side of the last equation (energy equation) is replaced by $\varrho c_p d\theta/dt + \theta\varrho^{-1}\varrho_\theta dp/dt$:

$$\frac{d\varrho}{dt} + \varrho \operatorname{div}\mathbf{v} = 0; \tag{4.93}$$

$$\varrho\frac{d\mathbf{v}}{dt} = \nabla(-p + \zeta \operatorname{div}\mathbf{v}) + 2\operatorname{div}(\mu\mathcal{D}') + \mathbf{g} + \mathbf{F}; \tag{4.94}$$

$$\varrho c_p\frac{d\theta}{dt} + \frac{\theta}{\varrho}\varrho_\theta\frac{dp}{dt} = \operatorname{div}(k\nabla\theta) + \zeta(\operatorname{div}\mathbf{v})^2 + 2\mu\mathcal{D}' : \mathcal{D}' + h \tag{4.95}$$

($\zeta = \lambda + 2\mu/3$ is the volume viscosity coefficient, eq. (3.15), and $\mathcal{D}' = \mathcal{D} - \operatorname{div}\mathbf{v}I/3$ is the deviator of the strain rate tensor $\mathcal{D}$).

Let us write system (4.93)–(4.95) in an arbitrary curvilinear coordinate system $Oq_1q_2q_3$ fitted to the Cartesian coordinate system through one-to-one dependences $\mathbf{x} = \mathbf{x}(q_1, q_2, q_3)$. Let $\mathbf{e}_1, \mathbf{e}_2$, and $\mathbf{e}_3$ be the unit vectors of the system $Oq_1q_2q_3$, $\mathbf{v} = v_1\mathbf{e}_1 + v_2\mathbf{e}_2 + v_3\mathbf{e}_3$. We introduce the Lamé parameters $H_i = |\mathbf{x}_{q_i}|$, $i = 1, 2, 3$, $H = H_1H_2H_3$. Then, we have [110]

$$\nabla = \sum_{i=1}^{3}\frac{\mathbf{e}_i}{H_i}\frac{\partial}{\partial q_i}, \quad \operatorname{div}\mathbf{v} = \frac{1}{H}\sum_{i=1}^{3}\frac{\partial}{\partial q_i}\left(v_i\frac{H}{H_i}\right),$$
$$\operatorname{div}\mathcal{P} = \frac{1}{H}\sum_{i=1}^{3}\frac{\partial}{\partial q_i}\left(\mathcal{P}_{ij}\frac{H}{H_i}\mathbf{e}_j\right), \quad \Delta = \operatorname{div}\nabla; \tag{4.96}$$

$$\frac{\partial\mathbf{e}_j}{\partial q_i} = \frac{\mathbf{e}_i}{H_j}\frac{\partial H_i}{\partial q_j} - \delta_{ij}\sum_{k=1}^{3}\frac{\mathbf{e}_k}{H_k}\frac{\partial H_j}{\partial q_k}, \quad \delta_{ij} = \begin{cases} 1, & i = j, \\ 0, & i \neq j; \end{cases}$$

$$\mathcal{D}'_{ij} = \frac{H_i}{H_j}\frac{\partial}{\partial q_j}\left(\frac{v_i}{H_i}\right) + \frac{H_j}{H_i}\frac{\partial}{\partial q_i}\left(\frac{v_j}{H_j}\right) + 2\delta_{ij}\sum_{k=1}^{3}\frac{v_k}{H_iH_k}\frac{\partial H_i}{\partial x'_k}. \tag{4.97}$$

In new variables, the form of the scalar equations (4.93) and (4.95) is not changed (certainly ∇ and div have to be written in accordance with eqs. (4.96)). Concerning the momentum equation (4.94), it becomes

$$\varrho\frac{d\mathbf{v}}{dt} = 2\mu\,\mathrm{div}\,\mathcal{D}' + 2\mathcal{D}'\nabla\mu + \mu\mathbf{S} + \nabla(-p + \zeta\,\mathrm{div}\,\mathbf{v}) + \varrho(\mathbf{g} + \mathbf{F}), \tag{4.98}$$

where the elements $\mathcal{D}'$ are determined by eq. (4.97), and the projections of the vector $\mathbf{S}$ onto the axes $\mathbf{e}_i$ $(i = 1, 2, 3)$ are

$$S_i = \frac{2}{H_i}\sum_{j=1}^{3}\left[\mathcal{D}'_{ij}\left(\frac{1}{H}\frac{\partial H}{\partial q_i} - \frac{1}{H_i}\frac{\partial H_i}{\partial q_j} + \frac{1}{H_j}\frac{\partial H_i}{\partial q_j}\right) - \frac{\mathcal{D}'_{jj}}{H_j}\frac{\partial H_j}{\partial q_j}\right]. \tag{4.99}$$

To close this system, as was already noted in Chapter 1, it is necessary to set $\varrho = \varrho(\theta, p)$ (state equation), $\mu = \mu(\theta, p)$, $\zeta = \zeta(\theta, p)$, $c_p = c_p(\theta, p)$, and $k = k(\theta, p)$. Following [139], the fluid is called *weakly compressible* if the following conditions are satisfied:

1) the functions

$$\begin{gathered}\varrho = \varrho(\varepsilon_1\theta, \varepsilon_2 p), \quad \mu = \mu(\varepsilon_1\theta, \varepsilon_2 p), \quad \zeta = \zeta(\varepsilon_1\theta, \varepsilon_2 p),\\ c_p = c_p(\varepsilon_1\theta, \varepsilon_2 p), \quad k = k(\varepsilon_1\theta, \varepsilon_1|\nabla\theta|, \varepsilon_2 p)\end{gathered} \tag{4.100}$$

are positive and continuously differentiable; ε_1 and ε_2 are small nonnegative parameters;

2)

$$\frac{\partial\varrho(\xi,\eta)}{\partial\xi} < 0, \quad \frac{\partial\varrho(\xi,\eta)}{\partial\eta} > 0; \tag{4.101}$$

3)

$$\frac{\partial\mu(\xi,\eta)}{\partial\xi} < 0, \quad \frac{\partial\mu(\xi,\eta)}{\partial\eta} > 0; \tag{4.102}$$

4)

$$\frac{\partial c_p(\xi,\eta)}{\partial\xi} > 0, \quad \frac{\partial c_p(\xi,\eta)}{\partial\eta} < 0 \tag{4.103}$$

for all admissible ξ and μ.

If all of these functions are independent of p ($\varepsilon_2 = 0$), then the fluid is called *thermally inhomogeneous and weakly compressible*.

In the linear approximation, we have $\varrho = \varrho_0(1 - \varepsilon_1\theta + \varepsilon_2 p)$, and the parameters ε_1 and ε_2 are actually the coefficients of thermal expansion (β_1) and isothermal compressibility (β_2) (see Section 4.1).

To identify the characteristic quantities providing unified information about the convection process, we introduce the following dimensionless quantities in eqs. (4.93), (4.95), and (4.98):

$$\mathbf{x}' = \frac{\mathbf{x}'}{l}, \quad t' = \frac{\mu_0}{\varrho_0 l^2}\, t, \quad \mathbf{v}' = \frac{l\varrho_0}{\mu_0}\,\mathbf{v}, \quad p' = \frac{\varrho_0 l^2}{\mu_0^2}\, p, \quad \theta' = \frac{l^3|\mathbf{g}|\varrho_0^2\varepsilon_1}{\mu_0^2}\,\theta,$$
$$\varrho' = \frac{\varrho}{\varrho_0}, \quad c_p' = \frac{c_p}{c_{p_0}}, \quad k' = \frac{k}{c_{p_0}\mu_0}, \quad \mu' = \frac{\mu}{\mu_0}, \quad \mathbf{g}' = \frac{\mathbf{g}}{|\mathbf{g}|},$$
$$\varepsilon_1' = \frac{\mu_0^2}{l^3|\mathbf{g}|\varrho_0^2}, \quad \varepsilon_2' = \frac{\mu_0^2\varepsilon_2}{l^2\varrho_0} = l|\mathbf{g}|\varepsilon_1'\varepsilon_2, \quad \varepsilon_3' = \frac{l|\mathbf{g}|\varepsilon_1}{c_{p_0}},$$
$$\mathbf{F}' = \frac{\varrho_0^2 l^3}{\mu_0^2}\,\mathbf{F}\Big(l\mathbf{x}', \frac{\varrho_0 l^2}{\mu_0}\,t'\Big), \quad h' = |\mathbf{g}|\varrho_0^3 l^5\varepsilon_1 h\Big(l\mathbf{x}', \frac{\varrho_0 l^2}{\mu_0}\,t', \frac{\mu_0^2}{l^3|\mathbf{g}|\varrho_0^2\varepsilon_1}\,\theta'\Big).$$

In these equations, $\varrho_0 = \varrho(0,0)$, $\mu_0 = \mu(0,0)$, $c_{p_0} = c_p(0,0)$, $\zeta_0 = \zeta(0,0)$. We also introduce the notation $\xi = \xi_0/\mu_0$.

Remark 4.2. For real fluids [234], $|\mathbf{g}| \sim 10\,\mathrm{m\cdot s^2}$, $\varrho_0 \sim 10^3\,\mathrm{kg/m^3}$, $c_p \sim 10^3\,\mathrm{J/(kg\cdot deg)}$, $\mu_0 \sim 10^{-4}$–$10^{-3}\,\mathrm{kg/(m\cdot s)}$, $\varepsilon_1 \sim 10^{-4}$–$10^{-3}\,\mathrm{deg^{-1}}$, $\varepsilon_2 \sim 10^{-10}$–$10^{-8}\,\mathrm{m^2\cdot N^{-1}}$ ($\varepsilon_2 \ll \varepsilon_1$), and the dimensionless parameter ε_1', ε_2', and ε_3' are estimated as $\varepsilon_1' \sim 10^{-15}$–$10^{-13}l^{-3}$, $\varepsilon_2' \sim 10^{-23}$–$10^{-17}l^{-2}$, $\varepsilon_3' \sim 10^{-6}$–$10^{-5}l$.

Omitting the primes, we can write eqs. (4.93), (4.95), and (4.98) in the dimensionless form as the system

$$\frac{d\varrho}{dt} + \varrho\,\mathrm{div}\,\mathbf{v} = 0; \tag{4.104}$$
$$\varrho\frac{d\mathbf{v}}{dt} = 2\nu\,\mathrm{div}\,\mathcal{D}' + \frac{2}{\varrho}\,\mathcal{D}'\nabla\mu - \frac{1}{\varrho}\,\nabla q + \frac{\mathbf{g}}{\varepsilon_1}\Big(1 - \frac{1}{\varrho}\Big) + \frac{\xi}{\varrho}\,\nabla(\zeta\,\mathrm{div}\,\mathbf{v}) + \nu\mathbf{S} + \mathbf{F}; \tag{4.105}$$
$$\varrho c_p\frac{d\theta}{dt} = \mathrm{div}(k\nabla\theta) + \varepsilon_3\Big[2\mu\mathcal{D}' : \mathcal{D}' + \xi\zeta(\mathrm{div}\,\mathbf{v})^2 - \frac{\theta}{\varrho}\,\frac{\partial\varrho}{\partial\theta}\,\frac{dp}{dt}\Big] + h, \tag{4.106}$$

where ϱ, $\nu = \mu/\varrho$, μ, ζ, and c_p are known functions of two variables $\varepsilon_1\theta$ and $\varepsilon_2 p$, which are equal to unity at the point $(0,0)$ and satisfy conditions (4.101)–(4.103); $k = k(\varepsilon_1\theta, \varepsilon_1|\nabla\theta|, \varepsilon_2 p)$, $k(0,0,0) = K = \mathrm{const} > 0$, $q = p - p_0$, p_0 is the dimensionless hydrostatic pressure: $\nabla p_0 = \varepsilon_1^{-1}\mathbf{g}$.

From eqs. (4.104)–(4.106), neglecting terms of the order of $\varepsilon_i\varepsilon_j$ $(i,j = 1,2,3)$, we obtain a system that describes convection of a viscous weakly compressible fluid

$$\mathrm{div}\,\mathbf{v} = \varepsilon_1 a_1\frac{d\theta}{dt} - \varepsilon_2 a_2\frac{dq}{dt} - \frac{\varepsilon_2}{\varepsilon_1}\,a_2\mathbf{v}\cdot\mathbf{g}; \tag{4.107}$$
$$\frac{d\mathbf{v}}{dt} = 2\nu\,\mathrm{div}\,\mathcal{D}' + 2\Big(-\varepsilon_1 a_3\nabla\theta + \varepsilon_2 a_4\nabla q + \frac{\varepsilon_2}{\varepsilon_1}\,a_4\mathbf{g}\Big)\mathcal{D}'$$
$$+ \xi\nabla\Big(\varepsilon_1 a_1\frac{d\theta}{dt} - \varepsilon_2 a_2\frac{dq}{dt} - \varepsilon_2 a_2\mathbf{v}\cdot\mathbf{g}\Big)$$

$$+\frac{\mathbf{g}}{\varepsilon_1}\left(1-\frac{1}{\varrho}\right)-\frac{1}{\varrho}\nabla q+\nu\mathbf{S}+\mathbf{F}; \tag{4.108}$$

$$\varrho c_p\frac{d\theta}{dt}=\operatorname{div}(k\nabla\theta)+2\varepsilon_3\mathcal{D}':\mathcal{D}'+h, \tag{4.109}$$

where $a_1=-\varrho_\xi(0,0)$, $a_2=\varrho_\eta(0,0)$, $a_3=-\mu_\xi(0,0)$, and $a_4=\mu_\eta(0,0)$ are known positive constants.

For a thermally inhomogeneous ($\varepsilon_2=0$) weakly compressible fluid, system (4.107)–(4.109) is simplified:

$$\operatorname{div}\mathbf{v}=\varepsilon_1 a_1\frac{d\theta}{dt}; \tag{4.110}$$

$$\frac{d\mathbf{v}}{dt}=2\nu\operatorname{div}\mathcal{D}'-2\varepsilon_1 a_3\mathcal{D}'\nabla\theta+\varepsilon_1 a_1\xi\nabla\frac{d\theta}{dt}+\nu\mathbf{S}-\frac{\mathbf{g}}{\varepsilon_1}\mathcal{P}(\varepsilon_1\theta)-\frac{1}{\varrho}\nabla q+\mathbf{F}; \tag{4.111}$$

$$\varrho c_p\frac{d\theta}{dt}=\operatorname{div}(k\nabla\theta)+2\varepsilon_3\mathcal{D}':\mathcal{D}'+h, \tag{4.112}$$

here $\varrho=\varrho(\varepsilon_1\theta)$, $\nu=\nu(\varepsilon_1\theta)$, $c_p=c_p(\varepsilon_1\theta)$, $k=k(\varepsilon_1\theta,\varepsilon_1|\nabla\theta|)$, $\varrho(0)=\nu(0)=c_p(0)=1$, $k(0,0)=K$, $\mathcal{P}=\varrho^{-1}-1$.

Remark 4.3. If ε_2 is a quantity of the order of ε_1^2, then terms with the coefficient $\varepsilon_4=\varepsilon_2\varepsilon_1^{-1}$ have to be retained in this system.

Remark 4.4. According to eqs. (4.101) and (4.103), we have

$$\dot\varrho(\xi)<0,\quad \dot c_p>0. \tag{4.113}$$

Inequalities (4.113) together with $\varrho(0)=c_p(0)=1$ allow us to assume that

$$\varrho(\varepsilon_1\theta)c_p(\varepsilon_1\theta)=1+O(\varepsilon_1^2), \tag{4.114}$$

and we can set $\varrho c_p=1$ in eq. (4.112) (note that eq. (4.114) is valid for $-\dot\varrho(0)=\dot c_p(0)$).

If eq. (4.114) is not satisfied, i. e.,

$$\varrho(\varepsilon_1\theta)c_p(\varepsilon_1\theta)=1+\varepsilon_1 a\theta+O(\varepsilon_1^2),\quad 1+\varepsilon_1 a\theta>0,\quad a=\text{const}, \tag{4.115}$$

then, introducing a new variable $\tau=\theta+\varepsilon_1 a\theta^2/2$, we obtain

$$\theta=\frac{1}{a\varepsilon_1}\left(\sqrt{1+2a\varepsilon_1\tau}-1\right),\quad 1+2a\varepsilon_1\tau>0,$$

$$(1+\varepsilon_1 a\theta)\frac{d\theta}{dt}=\frac{d\tau}{dt},\quad \varepsilon_1 a_3\nabla\theta=\varepsilon_1 a_3\nabla\tau+O(\varepsilon_1^2),$$

$$\mathcal{P}(\varepsilon_1\theta)=\mathcal{P}\left(\frac{1}{a}\left(\sqrt{1+2a\varepsilon_1\tau}-1\right)\right)\equiv\widetilde{\mathcal{P}}(\varepsilon_1\tau),$$

$$\operatorname{div}(k\nabla\theta) = \operatorname{div}(\widetilde{k}\nabla\tau),$$

$$\widetilde{k}(\varepsilon_1\theta, \varepsilon_1|\nabla\theta|) = \frac{1}{\sqrt{1+2a\varepsilon_1\tau}}\, k\left(\frac{\sqrt{1+2a\varepsilon_1\tau}-1}{a}, \frac{\varepsilon_1|\nabla\tau|}{\sqrt{1+2a\varepsilon_1\tau}}\right).$$

Therefore, we again obtain system (4.110)–(4.112) with the coefficient at $d\tau/dt$ in eq. (4.112) being equal to unity.

Remark 4.5. System (4.110)–(4.112) refines and generalizes the Oberbeck–Boussinesq equations (4.58)–(4.60); it is more rigorous and physical, because the change in density is taken into account in all equations of this system. On the other hand, the Oberbeck–Boussinesq model is obtained from this system by the limiting transition as $\varepsilon_1 \to 0$ and $\varepsilon_3 \to 0$ under the condition that

$$\lim_{\xi\to 0} \frac{\mathcal{P}(\xi)}{\xi} = 1.$$

The global theorems of existence and uniqueness of weak solutions for various initial-boundary problems of convection with axial symmetry (Oberbeck–Boussinesq problem, problem for a viscous incompressible fluid with energy dissipation, and problem (4.110)–(4.112)) were proved in [139]. In the general three-dimensional case, theorems such as these were established for the modified Oberbeck–Boussinesq model and for the problem of convection of a weakly compressible fluid under the condition of small initial data. For all of these problems, the theorems of a continuous dependence of the generalized solutions on the problem data and on their asymptotic stability were proved, and a priori estimates characterizing the decay of the solutions with time were obtained.

4.11 Exact solutions in an infinite band

A mathematical model of fluid convection under microgravity conditions is considered. The equation of state is used in a form that allows the fluid to be considered as a weakly compressible medium. Based on the previously proposed mathematical model of convection of a weakly compressible fluid, unsteady convective motion in a vertical band, with a heat flux periodic in time set on the solid boundaries of this band, is considered. This model of convection allows the study of the problem with the boundary thermal regime oscillating in an antiphase rather than in-phase mode, while the latter was required for the model of microconvection of an isothermally incompressible fluid (see Section 5.5).

Exact solutions for velocity components and temperature are derived, and the trajectories of fluid particles are constructed. For comparison, the trajectories predicted by the classical Oberbeck–Boussinesq model of convection and by the microconvection model are presented.

Let us consider the system of equations for a weakly compressible fluid (4.27)–(4.29) rewritten as follows:

$$\frac{P}{1+\varepsilon T}(\mathbf{V}_t + \mathbf{V}\cdot\nabla\mathbf{V}) = \Pr\left[\nabla(-p + \bar{\xi}\,\mathrm{div}\,\mathbf{V}) + \Delta\mathbf{V}\right] + \frac{\eta\,\Pr P}{1+\varepsilon T}\,\mathbf{g}_0, \tag{4.116}$$

$$\frac{\dot{P}}{P} - \frac{\varepsilon}{1+\varepsilon T}(T_t + \mathbf{V}\cdot\nabla T) + \mathrm{div}\,\mathbf{V} = 0, \tag{4.117}$$

$$\frac{P}{1+\varepsilon T}(T_t + \mathbf{V}\cdot\nabla T) - \dot{P}\frac{\alpha_2 + \varepsilon\alpha_1 T}{1+\varepsilon T} = \Delta T. \tag{4.118}$$

Here $\dot{P} = dP(t)/dt$, the function $P(t)$ satisfies the equation

$$\dot{P}\int\limits_{\Omega}\left[1 - \frac{\varepsilon(\alpha_2 + \varepsilon\alpha_1 T)}{1+\varepsilon T}\right]dx = \varepsilon\int\limits_{\Sigma} f\,d\Sigma \tag{4.119}$$

and the initial condition

$$P(0) = 1. \tag{4.120}$$

The initial-boundary problem for system (4.116)–(4.118) is formulated as follows. We consider the no-slip conditions for the velocity vector

$$\mathbf{V} = 0, \quad x \in \Sigma, \quad t > 0,$$

and the conditions of the second kind for temperature, which define the heat flux at the boundary of the domain Σ:

$$\frac{\partial T}{\partial n} = f(x,t), \quad x \in \Sigma, \quad t > 0. \tag{4.121}$$

At the initial time, we set the velocity vector and the temperature:

$$\mathbf{V} = \mathbf{V}_0(x), \quad T = T_0(x), \quad x \in \Omega, \quad t = 0.$$

It was noted that the equations of convection of a weakly compressible fluid (4.116)–(4.118) admit a group with addition of an arbitrary function of time to pressure. Let us construct the solutions of these equations, which are invariant with respect to the operator $\frac{\partial}{\partial y} + \varphi(t)\frac{\partial}{\partial p}$, where $\varphi(t)$ is an arbitrary function of time. The construction is performed in a manner similar to that in [17, 18].

We denote the Cartesian coordinates in space by x, y, z. Let the coordinate system be chosen so that $\vec{g}_0 = (0, -1, 0)$, and the fluid fill the layer $|x| \le 1$ with the heat flux according to eq. (4.121) being set at the solid boundaries of this layer. Let the heat-flux value be independent of z. The invariant solutions should have the form

$$\mathbf{V} = (u, v), \quad u = u(x,t), \quad v = v(x,t),$$
$$T = T(x,t), \quad p = \varphi(t)y + r(x,t).$$

Then, system (4.116)–(4.118) transforms to

$$\frac{\dot{P}}{P} - \frac{\varepsilon}{1+\varepsilon T}(T_t + uT_x) + u_x = 0, \tag{4.122}$$

$$\frac{P}{1+\varepsilon T}(u_t + uu_x) = \Pr(-r_x + \bar{\bar{\xi}}u_{xx}), \tag{4.123}$$

$$\frac{P}{1+\varepsilon T}(v_t + uv_x) = \Pr\left(-\varphi + v_{xx} - \frac{\eta}{1+\varepsilon T}\right), \tag{4.124}$$

$$\frac{P}{1+\varepsilon T}(T_t + uT_x) - \dot{P}\frac{\alpha_2 + \varepsilon\alpha_1 T}{1+\varepsilon T} = T_{xx}. \tag{4.125}$$

Here $\bar{\bar{\xi}} = \bar{\xi}+1$. We assume that the functions u, v, and $\dot{P}$ are functions of the order of the Boussinesq number ε, and the temperature T is a function of the order of unity, i. e., $u = \varepsilon U(x,t)$, $v = \varepsilon V(x,t)$, and $\dot{P} = \varepsilon f(t)$. In other words, the expansions of the functions u and v into series in powers of the small parameter ε begin from the first-order terms U and V, and the expansions of the functions T and P begin from the zeroth-order terms T^0 and 1, respectively. Then, the corollary of eq. (4.122) is the relation

$$f(t) - T^0_t + U_x = 0,$$

and the corollary of the heat transfer equation (4.125) is the relation

$$T^0_t = T^0_{xx}, \tag{4.126}$$

hence

$$U_x = T^0_{xx} - f(t),$$

or

$$U = T^0_x - xf(t) + b(t).$$

According to the no-slip conditions, we have $U(1,t) = U(-1,t) = 0$, so we first consider the case where

$$T^0_x(-1,t) = a_-(t), \quad T^0_x(1,t) = a_+(t), \quad a_-(t) = a_+(t) = a(t).$$

In this case, $f = 0$, which corresponds to the condition of the zero total heat flux (see the situation described in [17, 18, 81]).

Let now $a_-(t) = -a_+(t) = a(t)$. Then, we have $b = 0$ and

$$U = T^0_x - xf(t), \tag{4.127}$$

$$T^0_x(-1,t) = a(t), \quad T^0_x(1,t) = -a(t), \tag{4.128}$$

with, e. g., $a(t) = \mathcal{A}\sin\omega t$.

Thus, T^0 is the solution of eq. (4.126) in the domain $|x| \le 1$, $t \in [0, t_{\text{end}}]$, with condition (4.128) fulfilled at the boundary, and the following initial condition can be set at the initial time:

$$T^0(x,0) = T_0(x), \quad |x| \le 1. \tag{4.129}$$

The function U is found from eq. (4.127). Note that because of condition (4.128) we have $f(t) = -a(t)$. Equation (4.123) now determines the function $r(x,t)$ with accuracy to an arbitrary function of time:

$$r_x = -\frac{1}{\text{Pr}} U_t + \bar{\bar{\xi}} U_{xx}.$$

Equation (4.124) for the function $V(x,t)$ involves the function $\varphi(t)$, which is found from the condition of the zero flow rate of the fluid through an arbitrary cross section of the band $y = \text{const}$ (see [176]).

For this purpose, we differentiate the condition $\int_{-1}^{1} \rho v \, dx = 0$ with respect to t and use eqs. (4.122), (4.124), and the equation of state $\rho = \frac{P(t)}{1+\varepsilon T}$ in the situation considered. Then we obtain

$$\rho_t v = \frac{\varepsilon P}{(1+\varepsilon T)^2} T_x u v - \frac{P}{1+\varepsilon T} u_x v,$$

$$\rho v_t = \frac{P}{1+\varepsilon T} v_t = \text{Pr}\left[-\varphi + v_{xx} - \frac{\eta}{1+\varepsilon T} \right] - \frac{P}{1+\varepsilon T} u v_x,$$

and, as a consequence, we determine the function

$$\varphi(t) = \frac{1}{2}\left[v_x(1,t) - v_x(-1,t) \right] - \frac{\eta}{2} \int_{-1}^{1} \frac{dx}{1+\varepsilon T^0}. \tag{4.130}$$

Now eq. (4.124), with allowance for eq. (4.130), enables us to determine $V(x,t)$ as

$$V_t = -\,\text{Pr}\,\tilde{\varphi} + \text{Pr}\, V_{xx} + \text{Pr}\,\eta T^0,$$

where

$$\tilde{\varphi} = \frac{1}{2}[V_x]\Big|_{-1}^{1} + \frac{\eta}{2} \int_{-1}^{1} T^0 dx,$$

and hence

$$V_t = \text{Pr}\left[-\frac{1}{2}\left[V_x(1,t) - V_x(-1,t) \right] + V_{xx} + \eta T^0 - \frac{\eta}{2} \int_{-1}^{1} T^0 dx \right]. \tag{4.131}$$

For this equation, we consider the following initial and boundary conditions:

$$V(x,0) = V_0(x), \quad |x| \le 1, \tag{4.132}$$

$$V(-1,t) = 0, \quad V(1,t) = 0, \quad t \in [0, t_{\text{end}}]. \tag{4.133}$$

Each of the problems (4.126), (4.128), (4.129), and (4.131)–(4.133) is solved using the Fourier method. Let us consider periodic solutions of these problem, where the initial conditions are not set, the boundary conditions are described by the function $a(t) = \mathcal{A}\sin\omega t$, and the functions T^0 and V have the form

$$T^0 = T_s(x)\sin\omega t + T_c(x)\cos\omega t, \tag{4.134}$$

$$V = V_s(x)\sin\omega t + V_c(x)\cos\omega t. \tag{4.135}$$

Then, from the functions U and V we determine the components of dimensionless velocity $u = \varepsilon U(x,t)$ and $v = \varepsilon V(x,t)$. In further comparisons with the results of the classical Oberbeck–Boussinesq model, we should bear in mind that the velocity component u in the invariant solution is constant at each time instant (and can be set equal to zero with allowance for satisfaction of the initial condition). The second velocity component v is determined by the relations written above.

Solution of problem for temperature

Let us consider the equation

$$T^0_t = T^0_{xx}$$

in an infinite band $-1 \le x \le 1$ and consider the boundary conditions that determine the heat flux in antiphase at the band boundaries:

$$T^0_x(-1,t) = a(t), \quad T^0_x(1,t) = -a(t).$$

Here $a(t) = \mathcal{A}\sin\omega t$. The search for a solution in the form (4.134) yields the following problem for T_c:

$$T_c^{(IV)} + \omega^2 T_c = 0, \tag{4.136}$$

$$T_c'(-1) = 0, \quad T_c'(1) = 0, \quad T_c'''(-1) = \omega\mathcal{A}, \quad T_c'''(1) = -\omega\mathcal{A}, \tag{4.137}$$

whereas T_s is determined in terms of T_c as

$$T_s = T_c''/\omega$$

and the following boundary conditions are satisfied for T_s:

$$T_s'(-1) = \mathcal{A}, \quad T_s'(1) = -\mathcal{A}.$$

We introduce the notation $\vartheta = \sqrt{\omega/2}$, $\kappa = \sqrt{\omega/(2\,\mathrm{Pr})}$, where $\mathrm{Pr} \neq 1$. The solution of problem (4.136), (4.137) yields a linear system of algebraic equations of the form

$$\begin{aligned} -DC_1 + CC_2 - BC_3 + AC_4 &= \mathcal{A}\omega/(2\vartheta^3),\\ DC_1 + CC_2 - BC_3 - AC_4 &= -\mathcal{A}\omega/(2\vartheta^3),\\ AC_1 + BC_2 + CC_3 + DC_4 &= 0,\\ -AC_1 + BC_2 + CC_3 - DC_4 &= 0. \end{aligned}$$

The coefficients of the system are determined as

$$\begin{aligned} A &= -\sinh\vartheta\cos\vartheta + \cosh\vartheta\sin\vartheta, \quad B = \sinh\vartheta\sin\vartheta + \cosh\vartheta\cos\vartheta,\\ C &= \cosh\vartheta\cos\vartheta - \sinh\vartheta\sin\vartheta, \quad D = -(\cosh\vartheta\sin\vartheta + \sinh\vartheta\cos\vartheta), \end{aligned} \tag{4.138}$$

and the solution of problem (4.136), (4.137) is the function

$$T_c = C_1\cosh\vartheta x\cos\vartheta x + C_4\sinh\vartheta x\sin\vartheta x,$$

where

$$\begin{aligned} C_1 &= \frac{\mathcal{A}\omega}{4\vartheta^3}\,\frac{\cosh\vartheta\sin\vartheta + \sinh\vartheta\cos\vartheta}{\sinh^2\vartheta\cos^2\vartheta + \cosh^2\vartheta\sin^2\vartheta},\\ C_4 &= \frac{\mathcal{A}\omega}{4\vartheta^3}\,\frac{-\sinh\vartheta\cos\vartheta + \cosh\vartheta\sin\vartheta}{\sinh^2\vartheta\cos^2\vartheta + \cosh^2\vartheta\sin^2\vartheta}. \end{aligned} \tag{4.139}$$

The function T_s has the form

$$T_s = [-C_1\sinh\vartheta x\sin\vartheta x + C_4\cosh\vartheta x\cos\vartheta x].$$

Solution of problem for velocity

We consider the problem of finding a periodic solution of the form (4.135) for system (4.131)–(4.133), which can be rewritten in the following form for convenience:

$$V_t = \mathrm{Pr}\,V_{xx} - \frac{\mathrm{Pr}}{2}\big[V_x(1,t) - V_x(-1,t)\big] - \frac{\mathrm{Pr}\,\eta}{2}\int_{-1}^{1} T^0 + \mathrm{Pr}\,\eta T^0,$$

$$V(-1,t) = 0, \quad V(1,t) = 0, \quad t \in [0, t_{\mathrm{end}}].$$

The function V_c is found by solving the inhomogeneous ordinary differential equation

$$V_c^{(IV)} + \frac{\omega^2}{\mathrm{Pr}^2}V_c = \frac{1}{2}\big[V_c'''(1) - V_c'''(-1)\big] - \eta\,T_c'' + \frac{\eta\omega}{\mathrm{Pr}}\,T_s + \frac{\eta\omega}{2\,\mathrm{Pr}}\,I_1. \tag{4.140}$$

The function V_s is determined from the relation

$$V_s = \frac{\mathrm{Pr}}{\omega}V_c'' - \frac{\mathrm{Pr}}{2\omega}\big[V_c'(1) - V_c'(-1)\big] - \frac{\mathrm{Pr}\,\eta}{2\omega}I_2 + \frac{\mathrm{Pr}\,\eta}{\omega}T_c.$$

Here

$$I_1 = \int_{-1}^{1} T_s(x)\,dx, \quad I_2 = \int_{-1}^{1} T_c(x)\,dx.$$

The solution of eq. (4.140) is constructed as the sum of the general solution of the homogeneous equation and the partial solution determined by the right side of eq. (4.140):

$$V_c = \bar{C}_1 \cosh \kappa x \cos \kappa x + \bar{C}_2 \cosh \kappa x \sin \kappa x + \bar{C}_3 \sinh \kappa x \cos \kappa x + \bar{C}_4 \sinh \kappa x \sin \kappa x + \tilde{V},$$
$$\tilde{V} = G_0 + G_1 \sinh \vartheta x \sin \vartheta x + G_2 \cosh \vartheta x \cos \vartheta x.$$

With allowance for the boundary conditions

$$V_c(-1) = 0, \quad V_c(1) = 0, \quad V_s(-1) = 0, \quad V_s(1) = 0$$

the coefficients $\bar{C}_1$, $\bar{C}_2$, $\bar{C}_3$, and $\bar{C}_4$ are found as the solutions of the linear algebraic system

$$\begin{aligned} &\tilde{A}\bar{C}_1 + \tilde{B}\bar{C}_2 + \tilde{C}\bar{C}_3 + \tilde{D}\bar{C}_4 = \tilde{E}, \quad \tilde{A}\bar{C}_1 - \tilde{B}\bar{C}_2 - \tilde{C}\bar{C}_3 + \tilde{D}\bar{C}_4 = \tilde{E}, \\ &K\bar{C}_1 + L\bar{C}_2 + M\bar{C}_3 + N\bar{C}_4 = F, \quad K\bar{C}_1 - L\bar{C}_2 - M\bar{C}_3 + N\bar{C}_4 = F. \end{aligned} \tag{4.141}$$

The coefficients of this system are determined as follows:

$$\tilde{A} = \bar{A} + \bar{\Phi}_1, \quad \bar{A} = \cosh \kappa \cos \kappa, \quad \tilde{D} = \bar{D} + \bar{\Phi}_4, \quad \bar{D} = \sinh \kappa \sin \kappa,$$
$$\tilde{B} = \bar{B} = \cosh \kappa \sin \kappa, \quad \tilde{C} = \bar{C} = \sinh \kappa \cos \kappa,$$
$$\tilde{E} = -(\Phi_0 + G_1 \sinh \vartheta \sin \vartheta + G_4 \cosh \vartheta \cos \vartheta),$$
$$K = -2\kappa^2 \bar{D}\frac{\mathrm{Pr}}{\omega} - \kappa(\bar{C} - \bar{B})\frac{\mathrm{Pr}}{\omega}, \quad L = 2\kappa^2 \bar{C}\frac{\mathrm{Pr}}{\omega},$$
$$M = -2\kappa^2 \bar{B}\frac{\mathrm{Pr}}{\omega}, \quad N = 2\kappa^2 \bar{A}\frac{\mathrm{Pr}}{\omega} - \kappa(\bar{C} + \bar{B})\frac{\mathrm{Pr}}{\omega},$$
$$F = \frac{\mathrm{Pr}\,\eta}{2\omega} I_2 - \frac{\mathrm{Pr}\,\eta}{\omega}(C_1\bar{\Phi}_c + C_4\bar{\Phi}_s) - \frac{\mathrm{Pr}}{\omega}\vartheta(G_1 D + G_4 A) - \mathrm{Pr}(G_1\bar{\Phi}_c - G_4\bar{\Phi}_s).$$

The coefficients A and D are calculated by formulas (4.138), and the coefficients C_1 and C_4 are calculated by formulas (4.139). Here we calculate

$$I_1 = \frac{2\vartheta}{\omega}(C_4 - C_1)\cosh \vartheta \sin \vartheta + \frac{2\vartheta}{\omega}(C_4 + C_1)\sinh \vartheta \cos \vartheta,$$
$$I_2 = \frac{1}{\vartheta}(C_1 + C_4)\cosh \vartheta \sin \vartheta + \frac{1}{\vartheta}(C_1 - C_4)\sinh \vartheta \cos \vartheta,$$

and introduce the following notation for convenience:

$$\Phi_0 = \frac{\eta\omega}{8\,\mathrm{Pr}\,\kappa^4} I_1, \quad \bar{\Phi}_1 = \frac{\Phi_1}{4\kappa^4}, \quad \bar{\Phi}_4 = \frac{\Phi_4}{4\kappa^4},$$

$$\bar{\Phi}_c = \cosh\vartheta\cos\vartheta, \quad \bar{\Phi}_s = \sinh\vartheta\sin\vartheta,$$
$$\Phi_1 = (-2\kappa^3)(\cosh\kappa\sin\kappa + \sinh\kappa\cos\kappa),$$
$$\Phi_4 = (-2\kappa^3)(\sinh\kappa\cos\kappa - \cosh\kappa\sin\kappa),$$
$$G_0 = \Phi_0 + \bar{\Phi}_1\bar{C}_1 + \bar{\Phi}_4\bar{C}_4, \quad G_1 = \frac{F_1}{4(\kappa^4 - \vartheta^4)}, \quad G_4 = \frac{F_4}{4(\kappa^4 - \vartheta^4)},$$
$$F_1 = -\eta(-2\vartheta^2 C_1) + \frac{\eta\omega}{\mathrm{Pr}}(-C_1),$$
$$F_4 = -\eta(2\vartheta^2 C_4) + \frac{\eta\omega}{\mathrm{Pr}}(C_4).$$

The solution of system (4.141) has the form

$$\bar{C}_1 = \bar{\Delta}_1/\bar{\Delta}, \quad \bar{C}_4 = \bar{\Delta}_4/\bar{\Delta}, \quad \bar{C}_2 = \bar{C}_3 = 0,$$

where the denominator is determined as

$$\bar{\Delta} = (\bar{A} + \bar{\Phi}_1)\frac{\mathrm{Pr}}{\omega}\left(2\kappa^2\bar{A} - \kappa(\bar{C} + \bar{B})\right) - (\bar{D} + \bar{\Phi}_4)\frac{\mathrm{Pr}}{\omega}\left(-2\kappa^2\bar{D} - \kappa(\bar{C} - \bar{B})\right),$$

and the numerators are written as

$$\bar{\Delta}_1 = -(\Phi_0 + G_1\sinh\vartheta\sin\vartheta + G_4\cosh\vartheta\cos\vartheta)\frac{\mathrm{Pr}}{\omega}\left(2\kappa^2\bar{A} - \kappa(\bar{C} + \bar{B})\right)$$
$$- \frac{\mathrm{Pr}}{\omega}\left(\frac{\eta}{2}I_2 - \eta(C_1\bar{\Phi}_c + C_4\bar{\Phi}_s) - \vartheta(G_1 D + G_4 A) - 2\vartheta^2(G_1\bar{\Phi}_c - G_4\bar{\Phi}_s)\right)(\bar{D} + \bar{\Phi}_4),$$
$$\bar{\Delta}_4 = (\bar{A} + \bar{\Phi}_1)\frac{\mathrm{Pr}}{\omega}\left(\frac{\eta}{2}I_2 - \eta(C_1\bar{\Phi}_c + C_4\bar{\Phi}_s) - \vartheta(G_1 D + G_4 A) - 2\vartheta^2(G_1\bar{\Phi}_c - G_4\bar{\Phi}_s)\right)$$
$$+ \frac{\mathrm{Pr}}{\omega}\left(-2\kappa^2\bar{D} - \kappa(\bar{C} - \bar{B})\right)(\Phi_0 + G_1\sinh\vartheta\sin\vartheta + G_4\cosh\vartheta\cos\vartheta),$$

and hence, we have

$$V_c(x) = \bar{C}_1\cosh\kappa x\cos\kappa x + \bar{C}_4\sinh\kappa x\sin\kappa x + \tilde{V}(x),$$
$$\tilde{V}(x) = G_0 + G_1\sinh\vartheta x\sin\vartheta x + G_4\cosh\vartheta x\cos\vartheta x.$$

The following relation is valid for the function V_s:

$$V_s(x) = \frac{\mathrm{Pr}}{\omega}[-2\bar{C}_1\kappa^2\sinh\kappa x\sin\kappa x + 2\bar{C}_4\kappa^2\cosh\kappa x\cos\kappa x$$
$$+ 2\vartheta^2(G_1\cosh\vartheta x\cos\vartheta x - G_4\sinh\vartheta x\sin\vartheta x)]$$
$$- \frac{\mathrm{Pr}}{\omega}[\kappa\bar{C}_1(\bar{C} - \bar{B}) + \kappa\bar{C}_4(\bar{C} + \bar{B}) - \vartheta(G_1 D + G_4 A)] - \frac{\mathrm{Pr}\,\eta}{2\omega}I_2$$
$$+ \frac{\mathrm{Pr}\,\eta}{\omega}[C_1\cosh\vartheta x\cos\vartheta x + C_4\sinh\vartheta x\sin\vartheta x].$$

Thus, we determine the functions V_c and V_s, and simultaneously, $V(x,t)$ of the form (4.135).

Note, in real situations, the Boussinesq numbers ε are small. The present analysis of the linearized problem is fairly justified because its solution is given by the main term of the asymptotic solution as $\varepsilon \to 0$ (see a similar justification for the microconvection model in [17, 18]).

Trajectory calculations

The components of the physical (dimensional) velocity are determined as $v_1 = v_* u$ and $v_2 = v_* v$, where $u = \varepsilon U$, $v = \varepsilon V$, $v_* = \chi/l$, and formulas (4.135) and (4.127) are used for U and V. Knowing the functions v_1 and v_2, we can calculate the trajectories of fluid particles. For this purpose, we have to solve the Cauchy problem

$$\frac{dx}{dt} = v_1(x,t), \quad \frac{dy}{dt} = v_2(x,t), \quad t > 0; \quad x(0) = x_0, \quad y(0) = 0. \tag{4.142}$$

Note that in constructing trajectories of fluid particles by the Oberbeck–Boussinesq model we must use $v_1 = 0$, whereas the expression for v_2 remains unchanged.

The objective of the present work was to determine the trajectories of fluid particles from the calculation results based on the model of convection of a weakly compressible fluid. The differences from the results predicted by the classical convection model allow us to conclude that there are non-Boussinesq effects and allow us justify the use of new mathematical models of convection. In addition, the problem of comparing the results with the data obtained by the model of microconvection of an isothermally incompressible fluid is posed. Formulation of the initial-boundary problem for microconvection equations implies setting the boundary heat flux under the condition that the integral heat flux equals zero. In the problem of convection of a heat-conducting fluid in an infinite band, this is manifested in the phase changes in the boundary thermal mode, i. e., one lateral boundary is heated and the other lateral boundary is simultaneously cooled. It became possible to consider the boundary heat flux periodic in time and to change in antiphase in simulating convection under microgravity conditions, owing to the new mathematical model of convection of a weakly compressible fluid.

Projections of the integral curves of system (4.142) onto the plane (x, y), which were calculated by the microconvection model with the parameters $\varepsilon = 0.01$ and 0.02, $\omega = 0.5$ and $2\,\mathrm{sec}^{-1}$, are given in [17, 18] and demonstrate the helical (the main coil is an ellipse) periodic motion of the fluid particle. As was noted in [17], it is rather difficult to analyze the behavior of the trajectories because of the variety of dimensionless parameters that affect the solution of the Cauchy problem (4.142). Nevertheless, we can assume that, under conditions of applicability of the microconvection model and with the use of the model of convection of a weakly compressible fluid under the same conditions, the intensity of periodic motion and the particle drift are primarily determined by the values of the angular frequency ω, the Boussinesq parameter ε, and, naturally, by the position of the point (x_0, y_0) relative to the lateral boundaries of the domain. These assumptions were validated in [81].

Table 4.1: Basic parameters of the problem (4.142).

Calculation variant	Pr	η	ε	ν cm^2/sec	χ cm^2/sec	g cm/sec^2	β deg^{-1}	ω sec^{-1}
1	0.75	1.0	0.01; 0.5	0.150	0.2	0.030	0.0003	0.5; 2.5; 5
2	0.01	0.4	0.01; 0.5	0.015	1.5	0.009	0.0006	0.5; 2.5; 5
3	0.10	0.4	0.02; 0.5	0.150	1.5	0.090	0.0006	0.5; 5

The main parameters of the problem are listed in Table 4.1 and are conventionally presented by three models of fluid media and physical situations with different values of Pr, η, and g, similarly to that considered in [81]. The characteristic velocities, Reynolds numbers, and times of the process are also different. To demonstrate the behavior of the trajectories, whose time evolution is rather complicated, we choose the values $\varepsilon = 0.5$ and 0.02, $\omega = 0.5$ and $5\,sec^{-1}$. The value $\varepsilon = 0.5$ is chosen in order to demonstrate the dependence on the Boussinesq number, which is most important for trajectory development, and to obtain illustrative results.

The calculations were performed for $\mathcal{A} = -1$ (see the boundary condition (4.138)), which implies heating of the right boundary $x = 1$ both in the microconvection model and in the model of a weakly compressible fluid. This allows simple comparisons with the results described in [17, 18, 81].

Figures 4.1–4.3 for variants 1–3, respectively, show the trajectories of fluid particles calculated by three convection models. The trajectories calculated by the classical Oberbeck–Boussinesq model are shown as vertical segments of straight lines, and the trajectories calculated by the microconvection model display helical motion. They are marked by the dashed curves. The trajectories calculated by the model of convection of a weakly compressible fluid are also of the helical type and are marked by the solid curves. Figures 4.1 and 4.2 for $\varepsilon = 0.5$ and $\omega = 5\,sec^{-1}$ show the trajectories in the time interval from 0 to 24 sec, for the fluid particle located at the initial time $t = 0$ at the

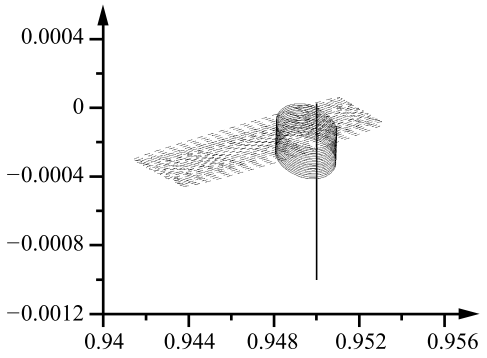

Figure 4.1: Trajectory of the fluid particle for variant 1 with $t = 0$–24 sec, $x_0 = 0.95$, $y_0 = 0$, $\varepsilon = 0.5$, $\omega = 5\,sec^{-1}$, and $\mathcal{A} = -1$.

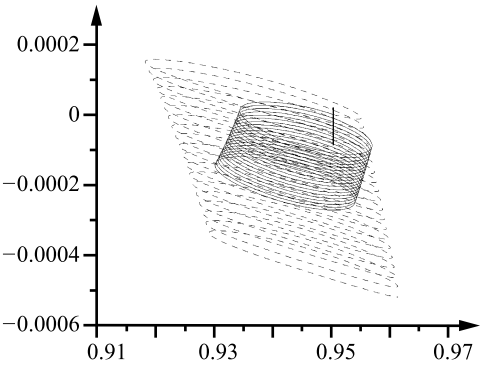

Figure 4.2: Trajectory of the fluid particle for variant 2 with $t = 0$–24 sec, $x_0 = 0.95$, $y_0 = 0$, $\varepsilon = 0.5$, $\omega = 5\,\text{sec}^{-1}$, and $\mathcal{A} = -1$.

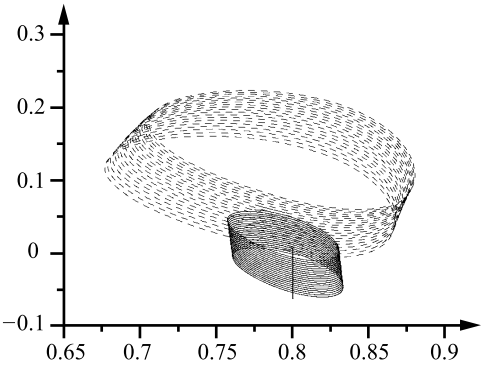

Figure 4.3: Trajectory of the fluid particle for variant 3 with $t = 0$–240 sec, $x_0 = 0.8$, $y_0 = 0$, $\varepsilon = 0.5$, $\omega = 0.5\,\text{sec}^{-1}$, and $\mathcal{A} = -1$.

point $x_0 = 0.95$, $y_0 = 0$. For $\varepsilon = 0.5$ and $\omega = 0.5\,\text{sec}^{-1}$, Figure 4.3 shows the trajectories of the fluid particle in the time interval from 0 to 240 sec (at the initial time $t = 0$, the particle is located at the point $x_0 = 0.8$, $y_0 = 0$). The Oberbeck–Boussinesq model describes the motion over the vertical segment of the straight line $x = 0.95$ (Figures 4.1 and 4.2) or $x = 0.8$ (Figure 4.3).

Figure 4.4 shows the calculation results for variant 2 for $\varepsilon = 0.5$ and $\omega = 2.5\,\text{sec}^{-1}$ the fluid particle at the initial time is located at the point $(0.95, 0)$. The particle drift is tracked in the time interval from 0 to 600 sec. This figure shows the complicated helical motion in accordance with the model of convection of a weakly compressible fluid. Figure 4.5 shows the particle trajectory for $\mathcal{A} = 1$ (see condition (4.138)), which corresponds to cooling of the right boundary $x = 1$. For comparison with the microconvection model, we should say that the particle-drift direction changes in the model of a weakly compressible fluid and remains unchanged in the microconvection model (see Figure 4.4: the downward motion is replaced by the upward motion).

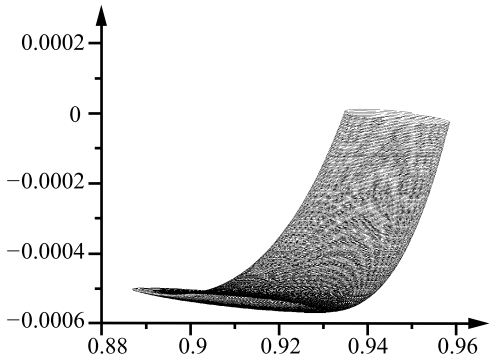

Figure 4.4: Trajectory of the fluid particle for variant 2 with $t = 0$–600 sec, $x_0 = 0.95$, $y_0 = 0$, $\varepsilon = 0.5$, $\omega = 2.5\ \text{sec}^{-1}$, and $\mathcal{A} = -1$.

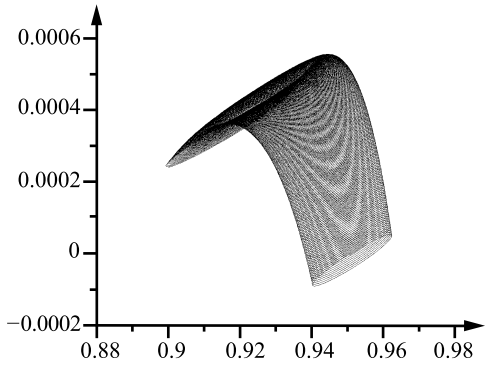

Figure 4.5: Trajectory of the fluid particle for variant 2 with $t = 0$–600 sec, $x_0 = 0.95$, $y_0 = 0$, $\varepsilon = 0.5$, $\omega = 2.5\ \text{sec}^{-1}$, and $\mathcal{A} = 1$.

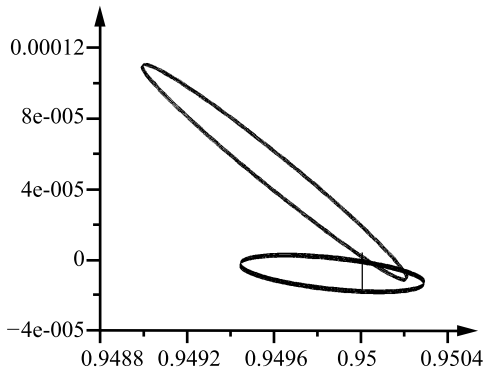

Figure 4.6: Trajectory of the fluid particle for variant 3 with $t = 0$–24 sec, $x_0 = 0.95$, $y_0 = 0$, $\varepsilon = 0.02$, $\omega = 5\ \text{sec}^{-1}$, and $\mathcal{A} = -1$.

Figure 4.6 shows the trajectories calculated for variant 3 in the time interval from 0 to 24 sec for $\varepsilon = 0.02$ and $\omega = 5\,\text{sec}^{-1}$. At the initial time, the fluid particle is located at the point $(0.95, 0)$. By comparing the trajectories, we note that the microconvection model predicts a helical trajectory with a larger diameter than that in calculations by the model of a weakly compressible fluid.

All calculations were performed until the final time $t_{\text{end}} = 2400$ sec. The Cauchy problem for the system of ordinary differential equations (4.142) was numerically examined using the Runge–Kutta method [103].

4.12 Analysis of well-posedness of the initial-boundary problem for equations of convection of a weakly compressible fluid

The theorem of existence of a smooth solution proved in this section refers to the so-called local theorems and is satisfied for small values of the Boussinesq number. The proof is based on constructing the problem solution in the form of series in the small parameter ε (Boussinesq number) and proving the solvability of the resultant recurrent problems. The third initial-boundary problem for a linear inhomogeneous heat conduction equation, the Cauchy problem for an ordinary differential equation, and the first initial-boundary problem for an unsteady Stokes system are all solved consecutively. The known Solonnikov's results on solvability of the problems mentioned above in classes of the Hölder functions are used. A principal issue is using the velocity representation (for each approximation) in the form of the sum of the solenoidal and gradient parts and finding the potential (for each approximation) as a solution of the Neumann problem for the Poisson equation. The convergence of the chosen expansions in the powers of the parameter ε is established in suitable Hölder norms at small values of ε.

Let us rewrite the system of equations for a weakly compressible fluid (4.27)–(4.29) with the zero subscript being omitted:

$$P\,(\mathbf{v}_t + \mathbf{v}\cdot\nabla\mathbf{v}) = \Pr(1+\varepsilon T)\left[\nabla(-p + \bar{\xi}\ \operatorname{div}\mathbf{v}) + \Delta\mathbf{v}\right] + \eta\,\Pr P\,\mathbf{g}_0, \tag{4.143}$$

$$(1+\varepsilon T)\,\dot{P} - \varepsilon\,P\,(T_t + \mathbf{v}\cdot\nabla T) + P\,(1+\varepsilon T)\operatorname{div}\mathbf{v} = 0, \tag{4.144}$$

$$P\,(T_t + \mathbf{v}\cdot\nabla T) - \dot{P}\,(\alpha_2 + \varepsilon\alpha_1 T) = (1+\varepsilon T)\,\Delta T. \tag{4.145}$$

We consider the following initial-boundary problem for system (4.143)–(4.145). The no-slip condition for velocity is imposed on the boundary Σ of the domain Ω at all time instants:

$$\mathbf{v}(x,t) = 0, \quad x \in \Sigma, \quad t > 0. \tag{4.146}$$

For the temperature on the boundary Σ, we consider the boundary condition of the third kind

$$\frac{\partial T}{\partial n} + \varkappa T = f(x,t), \quad x \in \Sigma, \quad t > 0, \tag{4.147}$$

where the dimensionless coefficient κ is expressed via the coefficients of heat transfer of the fluid and heat exchange with the ambient medium.

At the initial time $t = 0$, the velocity vector and temperature are prescribed as

$$\mathbf{v}(x,0) = \mathbf{v}_0(x), \quad T(x,0) = T_0(x), \quad x \in \Omega. \tag{4.148}$$

The function $P(t)$ satisfies the equation

$$\dot{P} \int_\Omega \left[1 - \frac{\varepsilon(\alpha_2 + \varepsilon\alpha_1 T)}{1 + \varepsilon T}\right] dx = \varepsilon \int_\Sigma (f - \kappa T)\, d\Sigma. \tag{4.149}$$

The initial condition for eq. (4.149) has the form

$$P(0) = 1. \tag{4.150}$$

We seek for the solution of system (4.143)–(4.145) in the form of formal power series in the small parameter ε:

$$\begin{aligned} &\mathbf{v} = \sum_{n=1}^{\infty} \varepsilon^n \mathbf{v}^{(n)}(x,t), \quad p = \sum_{n=0}^{\infty} \varepsilon^n p^{(n)}(x,t) \quad \left(p^{(0)}(x,t) = \eta \mathbf{g}_0 \cdot \mathbf{x}\right), \\ &T = \sum_{n=0}^{\infty} \varepsilon^n T^{(n)}(x,t), \quad P = \sum_{n=0}^{\infty} \varepsilon^n P^{(n)}(t) \qquad \left(P^{(0)}(t) = 1\right). \end{aligned} \tag{4.151}$$

Substituting expansions (4.151) into eqs. (4.143), (4.144), (4.145), we obtain a recurrent system for the functions $\mathbf{v}^{(n)}$, $p^{(n)}$, $T^{(n)}$, and $P^{(n)}$. The principal terms of the expansions $\mathbf{v}^{(1)}$, $p^{(1)}$, $T^{(0)}$, and $P^{(1)}$ are solutions of the linear initial-boundary problems given below.

The function $T^{(0)}$ is a solution of the initial-boundary problem for the homogeneous heat-conduction equation

$$T_t^{(0)} = \Delta T^{(0)}, \tag{4.152}$$

where the initial and boundary conditions are imposed on the basis of eqs. (4.147), (4.148):

$$T^{(0)}(x,0) = T_0(x), \quad x \in \Omega, \tag{4.153}$$

$$\frac{\partial T^{(0)}}{\partial n} + \kappa T^{(0)} = f(x,t), \quad x \in \Sigma, \quad t > 0. \tag{4.154}$$

The function $P^{(1)}$ is found as a solution of the Cauchy problem for the first-order ordinary differential equation

$$\dot{P}^{(1)} = \frac{1}{|\Omega|} \int_\Sigma (f - \kappa T^{(0)}) d\Sigma, \quad P^{(1)}(0) = 0. \tag{4.155}$$

The pair of the functions $(\mathbf{v}^{(1)}, p^{(1)})$ satisfies the unsteady inhomogeneous system of equations

$$\begin{aligned} \mathbf{v}^{(1)}{}_t &= -\operatorname{Pr}\nabla p^{(1)} + \operatorname{Pr}\Delta\mathbf{v}^{(1)} + \mathbf{F}_v{}^1(p^0, T^{(0)}, P^{(1)}), \\ \operatorname{div}\mathbf{v}^{(1)} &= F_d{}^1(T^{(0)}, P^{(1)}), \end{aligned} \tag{4.156}$$

with the notation

$$\begin{aligned} F_d{}^1(T^{(0)}, P^{(1)}) &= T_t{}^{(0)} - \dot{P}^{(1)}, \\ \mathbf{F}_v{}^1(p^{(0)}, T^{(0)}, P^{(1)}) &= -\operatorname{Pr} T^{(0)}\nabla p^{(0)} + \operatorname{Pr}\bar{\xi}\,\nabla\left[T_t{}^{(0)} - \dot{P}^{(1)}\right] + \operatorname{Pr}\eta\mathbf{g}_0 P^{(1)}. \end{aligned} \tag{4.157}$$

The function $\mathbf{v}^{(1)}$ satisfies the initial and boundary conditions of the form (see eqs. (4.146) and (4.148))

$$\begin{aligned} &\mathbf{v}^{(1)}(x,0) = \mathbf{v}_0(x), \quad x \in \Omega, \\ &\mathbf{v}^{(1)}(x,t) = 0, \quad x \in \Sigma, \quad t > 0. \end{aligned} \tag{4.158}$$

Note that the necessary condition of solvability of problem (4.156)–(4.158) is satisfied by virtue of eq. (4.155).

To make further considerations more convenient, we introduce the notations

$$\begin{aligned} &F_T{}^n(\mathbf{v}^{(1)}, \dots, \mathbf{v}^{(n)}; T^{(0)}, \dots, T^{(n-1)}; P^{(1)}, \dots, P^{(n)}) \\ &\quad = -\sum_{j=1}^{n}\mathbf{v}^{(j)}\nabla T^{(n-j)} - \left[\sum_{j=1}^{n-1}P^{(j)}C_{n-j} + P^{(n)}T_t^{(0)}\right] \\ &\qquad + \left[\alpha_2\dot{P}^{(n)} + \alpha_1\sum_{j=0}^{n-2}T^{(j)}\dot{P}^{(n-1-j)}\right] \\ &\qquad + \sum_{j=0}^{n-1}T^{(j)}\Delta T^{(n-1-j)} \quad (n \geq 2); \end{aligned} \tag{4.159}$$

$$\begin{aligned} &F_d{}^n(\mathbf{v}^{(1)}, \dots, \mathbf{v}^{(n-1)}; T^{(0)}, \dots, T^{(n-1)}; P^{(1)}, \dots, P^{(n)}) \\ &\quad = -\dot{P}^{(n)} - \sum_{j=0}^{n-2}T^{(j)}\dot{P}^{(n-1-j)} + \left[\sum_{j=1}^{n-2}C_jP^{(n-1-j)} + P^{(n-1)}T_t{}^{(0)}\right] \\ &\qquad - \sum_{j=1}^{n-1}A_j\operatorname{div}\mathbf{v}^{(n-j)} \quad (n \geq 2); \end{aligned} \tag{4.160}$$

$$\begin{aligned} &\mathbf{F}_v{}^n(p^{(0)}, \dots, p^{(n-1)}; \mathbf{v}^{(1)}, \dots, \mathbf{v}^{(n-1)}; T^{(0)}, \dots, T^{(n-1)}; P^{(n)}) \\ &\quad = -\sum_{j=1}^{n-1}\mathbf{v}^{(j)}\nabla\mathbf{v}^{(n-j)} - \sum_{j=1}^{n-1}P^{(j)}B_{n-j} - \operatorname{Pr}\sum_{j=0}^{n-1}\nabla p^{(j)}T^{(n-1-j)} \\ &\qquad + \operatorname{Pr}\bar{\xi}\left[\nabla\operatorname{div}\mathbf{v}^{(n)} + \sum_{j=0}^{n-2}T^{(j)}\nabla\operatorname{div}\mathbf{v}^{(n-1-j)}\right] \end{aligned}$$

$$+ \operatorname{Pr} \sum_{j=0}^{n-2} T^{(j)} \Delta \mathbf{v}^{(n-1-j)} + \operatorname{Pr} \eta \mathbf{g}_0 P^{(n)} \quad (n \geq 2), \tag{4.161}$$

where

$$\begin{gathered} C_n = T_t{}^{(n)} + \sum_{j=1}^{n} \mathbf{v}^{(j)} \nabla T^{(n-j)} \quad (n \geq 2), \quad C_1 = T_t{}^{(1)} + \mathbf{v}^{(1)} \nabla T^{(0)}; \\ A_n = P^{(n)} + T^{(n-1)} + \sum_{j=1}^{n-1} P^{(j)} T^{(n-1-j)} \quad (n \geq 2), \quad A_1 = P^{(1)} + T^{(0)}; \\ B_n = \mathbf{v}_t{}^{(n)} + \sum_{j=1}^{n-1} \mathbf{v}^{(j)} \nabla \mathbf{v}^{(n-j)} \quad (n \geq 2), \quad B_1 = \mathbf{v}_t{}^{(1)}. \end{gathered} \tag{4.162}$$

The recurrent system of equations determining the functions $\mathbf{v}^{(n)}$, $p^{(n)}$, $T^{(n)}$, and $P^{(n)}$ looks as follows. Let us start from the Cauchy problem of finding the function $P^{(n)}$, namely

$$\dot{P}^{(n)} E_0 + \sum_{j=1}^{n-1} \dot{P}^{(j)} E_{n-j} = -\kappa \int_{\Sigma} T^{(n-1)} d\Sigma, \quad P^{(n)}(0) = 0 \quad (n \geq 2), \tag{4.163}$$

where

$$\begin{gathered} E_n = (\alpha_2 - \alpha_1) \int_{\Omega} T^{(n-2)} dx + \alpha_1 \int_{\Omega} \sum_{j=0}^{n-3} T^{(j)} T^{(n-3-j)} dx \quad (n \geq 3), \\ E_0 = |\Omega|, \quad E_1 = -\alpha_2 E_0, \quad E_2 = (\alpha_2 - \alpha_1) \int_{\Omega} T^{(0)} dx. \end{gathered} \tag{4.164}$$

Then, we consider the initial-boundary problem for finding the n-th term of the temperature expansion

$$\begin{gathered} T_t{}^{(n)} = \Delta T^{(n)} + F_T{}^n\big(\mathbf{v}^{(1)}, \dots, \mathbf{v}^{(n)}; T^{(0)}, \dots, T^{(n-1)}; P^{(1)}, \dots, P^{(n)}\big) \quad (n \geq 1), \\ T^{(n)}(x, 0) = 0, \quad x \in \Omega, \\ \frac{\partial T^{(n)}}{\partial n} + \kappa T^{(n)} = 0, \quad x \in \Sigma, \quad t > 0. \end{gathered} \tag{4.165}$$

Finally, the unsteady inhomogeneous system of equations for determining the functions $\vec{v}^{(n)}$ and $p^{(n)}$ has the form

$$\begin{aligned} \mathbf{v}_t{}^{(n)} &= -\operatorname{Pr} \nabla p^{(n)} + \operatorname{Pr} \Delta \mathbf{v}^{(n)} \\ &\quad + F_v{}^n\big(p^{(0)}, \dots, p^{(n-1)}; \mathbf{v}^{(1)}, \dots, \mathbf{v}^{(n-1)}; T^{(0)}, \dots, T^{(n-1)}; P^{(n)}\big), \\ \operatorname{div} \mathbf{v}^{(n)} &= F_d{}^n\big(\mathbf{v}^{(1)}, \dots, \mathbf{v}^{(n-1)}; T^{(0)}, \dots, T^{(n-1)}; P^{(1)}, \dots, P^{(n)}\big) \quad (n \geq 2). \end{aligned} \tag{4.166}$$

The following initial and boundary conditions are imposed for system (4.166):

$$\begin{aligned} \mathbf{v}^{(n)}(x,0) &= 0, \quad x \in \Omega, \\ \mathbf{v}^{(n)}(x,t) &= 0, \quad x \in \Sigma, \quad t > 0. \end{aligned} \tag{4.167}$$

It should be noted that the necessary condition of solvability of problem (4.166), (4.167) is satisfied, at which $\int_\Omega {F_d}^n dx = 0$. This condition is valid by virtue of eqs. (4.163) and (4.165).

Let us now consider solvability of problems (4.152)–(4.154); (4.155); (4.156)–(4.158); (4.163); (4.165); (4.166), (4.167) in the spaces of the functions $C^{l+\alpha,(l+\alpha)/2}$ whose elements have continuous derivatives in accordance to Hölder. The notations for continuous functions in accordance to Hölder, the norms in these spaces, and the properties of the functions can be found, for instance, in [25, 116, 216].

As in [172], we assume that the initial data for problem (4.143)–(4.150) are sufficiently smooth and obey the local compatibility conditions

$$\mathbf{v}_0(x) = 0, \quad x \in \Sigma, \tag{4.168}$$

$$f(x,0) = \frac{\partial T_0}{\partial n} + \kappa T_0, \quad f_t(x,0) = \frac{\partial F}{\partial n} + \kappa F, \quad x \in \Sigma, \tag{4.169}$$

where

$$F(x) = (1 + \varepsilon T_0)\Delta T_0 - \mathbf{v}_0 \cdot \nabla T_0 + \dot{P}_0(\alpha_2 + \varepsilon \alpha_1 T_0).$$

Moreover, we have

$$\operatorname{div}(\mathbf{v}_0 - \varepsilon \nabla T_0) + \left[1 - \frac{\varepsilon(\alpha_2 + \varepsilon\alpha_1 T_0)}{1 + \varepsilon T_0}\right]\dot{P}_0 = 0, \quad x \in \Omega, \tag{4.170}$$

where

$$\dot{P}_0 = \varepsilon \frac{\int_\Sigma (f(x,0) - \kappa T_0)\, d\Sigma}{\int_\Omega [1 - \frac{\varepsilon(\alpha_2 + \varepsilon\alpha_1 T_0)}{1+\varepsilon T_0}]\, dx}.$$

We also make the initial data obey the nonlocal compatibility condition in terms of the function $\pi_0(x) = p(x,0)$ [172]

$$\begin{aligned} \operatorname{div}[(1 + \varepsilon T_0)\nabla \pi_0] &= H - \frac{1}{\mathrm{Pr}} D - \frac{1}{\mathrm{Pr}} \operatorname{div}(\mathbf{v}_0 \cdot \nabla \mathbf{v}_0), \quad x \in \Omega, \\ (1 + \varepsilon T_0)\frac{\partial \pi_0}{\partial n} &= \mathbf{G} \cdot \vec{n}, \quad x \in \Sigma, \end{aligned}$$

where the following notations are used:

$$\mathbf{G} = (1 + \varepsilon T_0)(\tilde{\xi} \nabla \operatorname{div} \mathbf{v}_0 + \Delta \mathbf{v}_0) + \eta\, \mathbf{g}_0 - \frac{1}{\mathrm{Pr}} \mathbf{v}_0 \cdot \nabla \mathbf{v}_0,$$

$$D = \dot{P}_0\left[F\frac{\varepsilon^2(\alpha_1-\alpha_2)}{(1+\varepsilon T_0)^2} - \operatorname{div}\mathbf{v}_0\right] - \ddot{P}_0\left[1 - \frac{\varepsilon(\alpha_2+\varepsilon\alpha_1 T_0)}{1+\varepsilon T_0}\right] + \varepsilon\Delta F,$$

$$H = \varepsilon^2\nabla T_0\cdot\nabla\left(\tilde{\xi}\dot{P}_0\frac{\alpha_2+\varepsilon\alpha_1 T_0}{1+\varepsilon T_0} + \Delta T_0\right)$$

$$+ (1+\tilde{\xi})\varepsilon(1+\varepsilon T_0)\Delta\left(\dot{P}_0\frac{\alpha_2+\varepsilon\alpha_1 T_0}{1+\varepsilon T_0} + \Delta T_0\right),$$

$$\ddot{P}_0 = \frac{\varepsilon\int_\Sigma (f_t(x,0)-\kappa F)\,d\Sigma + \dot{P}_0\varepsilon^2(\alpha_1-\alpha_2)\int_\Omega \frac{F}{(1+\varepsilon T_0)^2}dx}{\int_\Omega[1-\frac{\varepsilon(\alpha_2+\varepsilon\alpha_1 T_0)}{1+\varepsilon T_0}]\,dx}.$$

Then, the required nonlocal condition has the form

$$(1+\varepsilon T_0)\big[\nabla\pi_0 - (\nabla\pi_0\cdot\mathbf{n})\mathbf{n}\big] = \mathbf{G} - (\mathbf{G}\cdot\mathbf{n})\mathbf{n}, \quad x\in\Sigma. \tag{4.171}$$

Let the following assumptions be satisfied:

(i) the surface Σ belongs to the Hölder class $C^{4+\alpha}$, $0<\alpha<1$,

(ii) the functions involved into conditions (4.146)–(4.148) satisfy the smoothness conditions

$$f(x,t)\in C^{3+\alpha,1+(1+\alpha)/2}(\Sigma\times[0,t_*]),$$
$$\mathbf{v}_0(x)\in C^{2+\alpha}(\bar{\Omega}), \quad T_0(x)\in C^{4+\alpha}(\bar{\Omega})$$

and the compatibility conditions (4.168)–(4.171).

Then, based on the results of [116, 216], we can demonstrate that there exists a value of t_0, $0<t_0<t_*$ such that problems (4.152)–(4.154), (4.155), (4.156)–(4.158) have the following solution:

$$\mathbf{v}^{(1)}\in C^{2+\alpha,1+\alpha/2}(\bar{Q}_{t_0}), \quad \nabla p^{(1)}\in C^{\alpha,\alpha/2}(\bar{Q}_{t_0}),$$
$$T^{(0)}\in C^{4+\alpha,2+\alpha/2}(\bar{Q}_{t_0}), \quad P^{(1)}\in C^{2+(1+\alpha)/2}([0,t_0]).$$

Unique solvability of problem (4.152)–(4.154) follows from [116], and the following estimate of the norm of the solution $T^{(0)}$ is valid:

$$\big|T^{(0)}\big|^{4+\alpha,2+\alpha/2} \le c_1\big[|T_0|^{4+\alpha} + |f|^{3+\alpha,1+(1+\alpha)/2}\big] = C_T.$$

Here, c_1 depends on the domain Ω, t_* and the coefficient κ.

We note that the right-hand side of the ordinary differential equation (4.155) belongs to the class $C^{1+(1+\alpha)/2}([0,t_0])$ and conclude that the Cauchy problem (4.155) is uniquely solvable in the class $C^{2+(1+\alpha)/2}([0,t_0])$, in accordance, for instance, with [105, 222], and

$$\big|P^{(1)}\big|^{2+(1+\alpha)/2} \le c_2\big[|f|^{3+\alpha,1+(1+\alpha)/2} + \big|T^{(0)}\big|^{4+\alpha}\big]$$
$$\le c_2\big[|f|^{3+\alpha,1+(1+\alpha)/2} + C_T\big] = C_P,$$

where c_2 depends on Ω, t_*, and κ.

Belonging of the functions $T^{(0)}$ and $P^{(1)}$ to the classes $C^{4+\alpha,2+\alpha/2}(\bar{Q}_{t_0})$ and $C^{2+(1+\alpha)/2}([0,t_0])$, respectively, guarantees belonging of the right-hand side ${F_d}^1$ in the second equation of system (3.17) to the class $C^{2+\alpha,1+\alpha/2}(\bar{Q}_{t_0})$. Then, $\nabla {F_d}^1$ in the right-hand-side of the first equation of system (4.156) is a function of the class $C^{1+\alpha,(1+\alpha)/2}(\bar{Q}_{t_0})$.

Let us represent the vector $\mathbf{v}^1$ as the sum $\mathbf{v}^1 = \mathbf{u} + \mathbf{w}$, where $\operatorname{div}\mathbf{u} = 0$, and $\mathbf{w} = \nabla\varphi$; for finding φ, we have the following Neumann problem for the Poisson equation:

$$\Delta\varphi = {F_d}^1(x,t), \quad x \in \Omega, \quad t \in [0,t_0], \tag{4.172}$$

$$\frac{\partial\varphi}{\partial n} = 0, \qquad x \in \Sigma, \quad t \in [0,t_0], \tag{4.173}$$

$$\int\limits_{\Omega} \varphi(x,t)\,dx = 0, \qquad t \in [0,t_0]. \tag{4.174}$$

Note that the condition of solvability of this problem is satisfied; therefore, in accordance with [115, 237], problem (4.172)–(4.174) has a unique solution. This solution is characterized by the same properties of smoothness in terms of the variable t as the right-hand side ${F_d}^1$ and belongs at least to the class $C^{4+\alpha,1+\alpha/2}(\bar{Q}_{t_0})$. Therefore, the function $\mathbf{w} = \nabla\varphi$ belongs to the class $C^{3+\alpha,1+\alpha/2}(\bar{Q}_{t_0})$; hence, $\mathbf{w}_t$ and $\Delta\mathbf{w}$ are functions at least of the class $C^{\alpha,\alpha/2}(\bar{Q}_{t_0})$.

To determine the functions $\mathbf{u}$ and $\nabla p^{(1)}$, we have an initial-boundary problem for the system of the Stokes equations, which looks as follows with allowance for eqs. (4.156)–(4.158):

$$\begin{gathered}\mathbf{u}_t = -\operatorname{Pr}\nabla p^{(1)} + \operatorname{Pr}\Delta\mathbf{u} + \mathbf{F}_u(p^{(0)}, T^{(0)}, P^{(1)}, \mathbf{w}),\\ \operatorname{div}\mathbf{u} = 0,\\ \mathbf{u}(x,0) = \mathbf{u}_0(x), \quad x \in \Omega,\end{gathered} \tag{4.175}$$

$$\mathbf{u}(x,t) = 0, \quad x \in \Sigma, \quad t > 0, \tag{4.176}$$

where

$$\mathbf{F}_u(p^{(0)}, T^{(0)}, P^{(1)}, \mathbf{w}) = -\mathbf{w}_t + \operatorname{Pr}\Delta\mathbf{w} - \operatorname{Pr} T^{(0)}\nabla p^{(0)} + \operatorname{Pr}\bar{\xi}\nabla {F_d}^1 + \operatorname{Pr}\eta\,\mathbf{g}_0\,P^{(1)},$$
$$\mathbf{u}_0(x) = \mathbf{v}_0(x) - \mathbf{w}_0(x), \quad \mathbf{w}_0(x) = \nabla\varphi(x,0).$$

Solvability of problem (4.175), (4.176) for the pair of the functions $(\mathbf{u}, \nabla p^{(1)})$ (and, therefore, also for $(\mathbf{v}^{(1)}, \nabla p^{(1)})$) in the classes of functions $C^{2+\alpha,1+\alpha/2}(\bar{Q}_{t_0})$ and $C^{\alpha,\alpha/2}(\bar{Q}_{t_0})$, respectively, follows from the results of [216], and the following estimates are valid:

$$\begin{aligned}\left|\mathbf{v}^{(1)}\right|^{2+\alpha,1+\alpha/2} &\le c_3\left[\left|T^{(0)}\right|^{4+\alpha,2\alpha/2} + \left|P^{(1)}\right|^{2+(1+\alpha)/2} + |\mathbf{v}_0|^{2+\alpha}\right]\\ &\le c_3\left[C_T + C_P + |\mathbf{v}_0|^{2+\alpha}\right] = C_v,\\ \left|\nabla p^{(1)}\right|^{\alpha,\alpha/2} &\le C_v,\end{aligned}$$

where c_3 depends on the domain Ω, t_*, and the parameters Pr, $\bar{\xi}$, η, and g_0.

Note that the function $\mathbf{v}^{(1)}$ is determined uniquely, and the function $p^{(1)}$ is determined uniquely under the additional condition $\int_\Omega p^{(1)} dx = 0$.

Solvability of the initial-boundary problems (4.163), (4.165), (4.166)–(4.167) for an arbitrary value of n can be demonstrated by induction, based on the results of [116, 216], with allowance for satisfaction of eqs. (4.168)–(4.171) for obtaining appropriate compatibility conditions. In this case, we have

$$T^{(n)} \in C^{4+\alpha,2+\alpha/2}(\bar{Q}_{t_0}), \quad P^{(n)} \in C^{2+(1+\alpha)/2}([0,t_0]).$$

The initial-boundary problem for $(\mathbf{v}^{(n)}, \nabla p^{(n)})$ reduces to the first initial-boundary problem for the system of the Stokes equations, similar to that described for the principal term of the expansion $(\mathbf{v}^{(1)}, \nabla p^{(1)})$. In this case, we have $\mathbf{v}^{(n)} \in C^{2+\alpha,1+\alpha/2}(\bar{Q}_{t_0})$ and $\nabla p^{(n)} \in C^{\alpha,\alpha/2}(\bar{Q}_{t_0})$. The functions $p^{(n)}$ are uniquely determined under the additional condition $\int_\Omega p^{(n)} dx = 0$.

To verify the convergence of series (4.151) at sufficiently small values of $\varepsilon > 0$, we consider simultaneously, as was done in [183], the power series with constant coefficients

$$\begin{gathered}
\vartheta = \vartheta_0 + \varepsilon\vartheta_1 + \varepsilon^2\vartheta_2 + \sum_{j=3}^{\infty} \varepsilon^j \vartheta_j, \\
U = \varepsilon U_1 + \varepsilon^2 U_2 + \sum_{j=3}^{\infty} \varepsilon^j U_j, \quad q = q_0 + \varepsilon q_1 + \varepsilon^2 q_2 + \sum_{j=3}^{\infty} \varepsilon^j q_j, \\
Q = Q_0 + \varepsilon Q_1 + \varepsilon^2 Q_2 + \sum_{j=3}^{\infty} \varepsilon^j Q_j.
\end{gathered} \tag{4.177}$$

Note that the series with constant coefficients (4.177) are majorant for series obtained from the corresponding series (4.151) with the functions $\mathbf{v}^{(n)}$, $\nabla p^{(n)}$, $T^{(n)}$, and $P^{(n)}$ being replaced by their norms in the Hölder spaces $C^{2+\alpha,1+\alpha/2}$, $C^{\alpha,\alpha/2}$, $C^{4+\alpha,2+\alpha/2}$, and $C^{2+(1+\alpha)/2}$, respectively.

It is shown further that there exists $\varepsilon_0 > 0$ such that, for an arbitrary value of $\varepsilon \in [0, \varepsilon_0]$, series (4.177) converge to a positive solution (ϑ, U, q, Q) of the system

$$\begin{aligned}
&\vartheta - \vartheta_0 - \varepsilon\vartheta_1 - \varepsilon^2\vartheta_2 \\
&= \varepsilon^3 c_1 \{\vartheta(\vartheta - \vartheta_0 - \varepsilon\vartheta_1) + U\vartheta + (Q - Q_0)(\vartheta - \vartheta_0 + U\vartheta) \\
&\qquad + (Q - Q_0 - \varepsilon Q_1 - \varepsilon^2 Q_2)\vartheta_0 + \alpha_2(Q - Q_0 - \varepsilon Q_1 - \varepsilon^2 Q_2) \\
&\qquad + \alpha_1(\vartheta - \vartheta_0)(Q - Q_0)\} \\
&U - \varepsilon U_1 - \varepsilon^2 U_2 \\
&= \varepsilon^3 c_3 \{U^2 + (Q - Q_0)(U + U^2) \\
&\qquad + \Pr q\vartheta + \Pr\bar{\xi}[\vartheta(Q - Q_0) + (Q - Q_0)(\vartheta - \vartheta_0 + 2U\vartheta) \\
&\qquad + (Q - Q_0 - \varepsilon Q_1)\vartheta_0 + U(Q - Q_0 + 2\vartheta + 2(Q - Q_0)\vartheta)]
\end{aligned} \tag{4.178}$$

$$
\begin{aligned}
&+ \Pr(\bar{\xi}+1)\vartheta U + \Pr \eta g_0 \left(Q - Q_0 - \varepsilon Q_1 - \varepsilon^2 Q_2\right) \\
&+ (1+\Pr)\big[Q - Q_0 - \varepsilon Q_1 - \varepsilon^2 Q_2 + \vartheta\,(Q - Q_0) \\
&+ (\vartheta - \vartheta_0 + U\,\vartheta)\,(Q - Q_0) \\
&+ \vartheta_0 (Q - Q_0 - \varepsilon Q_1) + \left(Q - Q_0 + \vartheta + (Q - Q_0)\,\vartheta\right) U\big]\}; \qquad (4.179)
\end{aligned}
$$

$$
\begin{aligned}
&q - q_0 - \varepsilon q_1 - \varepsilon^2 q_2 \\
&= \varepsilon^3 c_3 \{U^2 + (Q - Q_0)\left(U + U^2\right) + \Pr q\,\vartheta \\
&\quad + \Pr \bar{\xi}\big[\vartheta\,(Q - Q_0) + (Q - Q_0)(\vartheta - \vartheta_0 + 2U\,\vartheta) \\
&\quad + (Q - Q_0 - \varepsilon Q_1)\,\vartheta_0 + U\big(Q - Q_0 + 2\vartheta + 2(Q - Q_0)\,\vartheta\big)\big] \\
&\quad + \Pr(\bar{\xi}+1)\vartheta U + \Pr \eta g_0 \left(Q - Q_0 - \varepsilon Q_1 - \varepsilon^2 Q_2\right) \\
&\quad + (1+\Pr)\big[Q - Q_0 - \varepsilon Q_1 - \varepsilon^2 Q_2 \\
&\qquad\quad + \vartheta\,(Q - Q_0) + (\vartheta - \vartheta_0 + U\,\vartheta)\,(Q - Q_0) \\
&\qquad\quad + \vartheta_0 (Q - Q_0 - \varepsilon Q_1) \\
&\qquad\quad + \left(Q - Q_0 + \vartheta + (Q - Q_0)\,\vartheta\right) U\big]\}; \qquad (4.180)
\end{aligned}
$$

$$
\begin{aligned}
&Q - Q_0 - \varepsilon Q_1 - \varepsilon^2 Q_2 \\
&= \varepsilon^3 c_2 \{(Q - Q_0)\left[|\alpha_2 - \alpha_1|\,|\Omega|\,\vartheta + \alpha_1\,|\Omega|\,\vartheta^2\right] \\
&\quad + \kappa\,|\Sigma|\,(\vartheta - \vartheta_0 - \varepsilon\vartheta_1)\}. \qquad (4.181)
\end{aligned}
$$

Here, we have

$$
\begin{aligned}
&\vartheta_0 = |T^{(0)}|^{4+\alpha,2+\alpha/2}, \quad \vartheta_1 = |T^{(1)}|^{4+\alpha,2+\alpha/2}, \quad \vartheta_2 = |T^{(2)}|^{4+\alpha,2+\alpha/2}, \\
&U_1 = |v^{(1)}|^{2+\alpha,1+\alpha/2}, \quad U_2 = |v^{(2)}|^{2+\alpha,1+\alpha/2}, \\
&q_0 = |\nabla p^{(0)}|^{\alpha,\alpha/2}, \quad q_1 = |\nabla p^{(1)}|^{\alpha,\alpha/2}, \quad q_2 = |\nabla p^{(2)}|^{\alpha,\alpha/2}, \\
&Q_0 = |P^{(0)}|^{2+(1+\alpha)/2}, \quad Q_1 = |P^{(1)}|^{2+(1+\alpha)/2}, \quad Q_2 = |P^{(2)}|^{2+(1+\alpha)/2}.
\end{aligned}
$$

In accordance with the theorem of the implicit function [54], system (4.178)–(4.181) has a unique solution at $\varepsilon \in [0, \varepsilon_0]$ in the neighborhood $(\vartheta_0, 0, q_0, Q_0)$. This solution is analytical in terms of ε and can be represented as series (4.177). Therefore, series (4.151) converge to the solution of problem (4.143)–(4.150) if $\varepsilon \in [0, \varepsilon_0]$.

Thus, we obtain the following theorem.

Theorem 4.1. *Let the surface* Σ *belong to the Hölder class* $C^{4+\alpha}$ $(0 < \alpha < 1)$*, and let the functions involved into conditions* (4.147)–(4.149) *satisfy requirements (i), (ii) and compatibility conditions* (4.168)–(4.171)*. Let also* $0 \le \varepsilon \le \varepsilon_0$*, where* ε_0 *is determined by the solution of eqs.* (4.178)–(4.181)*. Then, problem* (4.143)–(4.150) *has a solution* $\mathbf{v} \in C^{2+\alpha,1+\alpha/2}(\bar{Q}_{t_0})$, $\nabla p \in C^{\alpha,\alpha/2}(\bar{Q}_{t_0})$, $T \in C^{4+\alpha,2+\alpha/2}(\bar{Q}_{t_0})$, $P \in C^{2+(1+\alpha)/2}([0, t_0])$*. This solution is an analytical function of the parameter* ε *at the point* $\varepsilon = 0$*.*

The issue of uniqueness of the solution of problem (4.143)–(4.150) can be studied separately with the use of the proof by contradiction.

5 Invariant submodels of microconvection equations

This chapter describes group properties of equations of a new micrconvection model proposed by Pukhnachov [177]. Optimal systems of subalgebras θ_1 and θ_2 are constructed; all factor-systems are written. For some of them, initial-boundary problems are posed and solved. The issue of invariance of conditions on the interface and free boundary is considered.

5.1 Basic model and its group properties

The overall system of differential equations of motion consists of the following equations:

– mass conservation equation

$$\frac{d\rho}{dt} + \rho \operatorname{div} \mathbf{u} = 0; \tag{5.1}$$

– momentum conservation equation

$$\rho \frac{d\mathbf{u}}{dt} = \nabla(-p + \lambda \operatorname{div} \mathbf{u}) + \operatorname{div}(2\mu D) + \rho \mathbf{g}; \tag{5.2}$$

– energy conservation equation

$$\rho c_p \frac{d\theta}{dt} + \frac{\theta}{\rho}\left(\frac{\partial \rho}{\partial \theta}\right)\frac{dp}{dt} = \operatorname{div}(k\nabla\theta) + \Phi. \tag{5.3}$$

Here $\mathbf{u} = (u_1, u_2, u_3)$ is the velocity vector, p is the pressure, θ is the absolute temperature, ρ is the fluid density, $d/dt = \partial/\partial t + \mathbf{u} \cdot \nabla$ is the total derivative with respect to time, λ and μ are the dynamic coefficients of the first and second viscosities, D is the strain rate tensor with the elements

$$D_{ij} = \frac{1}{2}\left(\frac{\partial u_i}{\partial x_j} + \frac{\partial u_j}{\partial x_i}\right), \quad i, j = 1, 2, 3,$$

$\mathbf{g}$ is the density of external mass forces, c_p is the specific heat at constant pressure, $\Phi = \lambda(\operatorname{div} \mathbf{u})^2 + 2\mu D : D$ is the dissipative function, and k is the thermal conductivity coefficient.

Let us take the pressure p and the absolute temperature θ as the basic thermodynamic variables. Then, the dependence

$$\rho = \rho(p, \theta) \tag{5.4}$$

determines the equations of state of the fluid, while c_p and the transfer coefficients λ, μ, and k are given functions of p and θ. We assume that $c_p > 0$ and $\rho > 0$, the functions

https://doi.org/10.1515/9783110655469-005

μ and k are nonnegative, and $\lambda + 2\mu/3 \geq 0$. The function $\mathbf{g}$ is a known function of the variables x_1, x_2, x_3, and t.

Let $\mathbf{g} = \mathbf{g}(t)$ and (a) the fluid is isothermally incompressible, and the dependence of density on temperature has the form

$$\rho = \rho_0(1 + \beta T)^{-1}, \tag{5.5}$$

where $T = \theta - \theta_0$, θ_0 is the characteristic temperature, and β is the coefficient of volume expansion, (b) the contribution of the dissipative function and the pressure forces to the heat inflow equation (5.3) is negligibly small, and (c) μ, k, and c_p have constant values.

Under these assumptions, the following system of equations was obtained in [177] from the exact equations of motion (5.1)–(5.3):

$$\begin{aligned} \mathbf{w}_t + \mathbf{w}\nabla\mathbf{w} + \beta\chi(\nabla T \cdot \mathbf{w} - \nabla\mathbf{w} \cdot \nabla T) + \beta^2\chi^2(\Delta T \nabla T - \nabla|\nabla T|^2/2) \\ = (1 + \beta T)(-\nabla q + \nu\Delta\mathbf{w}) + \mathbf{g}; \end{aligned} \tag{5.6}$$

$$\operatorname{div}\mathbf{w} = 0; \tag{5.7}$$

$$T_t + \mathbf{w} \cdot \nabla T + \beta\chi|\nabla T|^2 = (1 + \beta T)\chi\Delta T. \tag{5.8}$$

The new functions $\mathbf{w}$ and q are related to the true velocity and pressure as

$$\begin{gathered} \mathbf{w} = \mathbf{u} - \beta\chi\nabla T, \\ q = \rho_0^{-1}(p - \lambda \operatorname{div}\mathbf{u}) - \beta(\nu - \chi)\chi\Delta = T\rho_0^{-1}p - \beta\chi(\rho_0^{-1}\lambda + \nu - \chi)\Delta T \end{gathered} \tag{5.9}$$

($\chi = k/(c_p\rho_0)$ is the thermal diffusivity).

If we use the dependence $\rho = \rho_0(1 + \beta T)$ instead of eq. (5.5) and assume that the velocity field is solenoidal and the change in density is taken into account only in the buoyancy force, we obtain the classical Oberbeck–Boussinesq model [101, 133]. As was shown in [177], however, the Oberbeck–Boussinesq approximation is inapplicable to describing convection if $\eta = \max|\mathbf{g}(t)|l^3/(\nu\chi) < 1$, where l is the characteristic scale. The parameter η is smaller than unity in weak force fields, at microscales, and in fluids with a large product of the viscosity coefficient and thermal diffusivity.

Note that system (5.6)–(5.8) can be written in a more compact form as [9]

$$\mathbf{w}_t + \mathbf{w}\nabla\mathbf{w} + \beta\chi \operatorname{rot}\mathbf{w} \times \nabla\theta + \beta^2\chi^2(\nabla\theta \otimes \nabla\theta - |\nabla\theta|^2 I) = (1 + \beta\theta)(-\nabla q + \nu\Delta\mathbf{w}) + \mathbf{g}; \tag{5.10}$$

$$\operatorname{div}\mathbf{w} = 0; \tag{5.11}$$

$$\theta_t + \mathbf{w} \cdot \nabla\theta + \beta\chi|\nabla\theta|^2 = (1 + \beta\theta)\chi\Delta\theta \tag{5.12}$$

(we returned to the previous notation $T \leftrightarrow \theta$).

The main group of the system was calculated in [196] for $\mathbf{g} = (0, 0, -g)$, $g = \text{const}$. If we apply the substitution $\chi(1 + \beta\theta) \to \theta$, $q \to \chi q$, $\nu \to \chi\nu$ in eqs. (5.10)–(5.12), then the thermal diffusivity χ is eliminated from the equations. Therefore, we can set $\chi = 1$ in system (5.10)–(5.12).

At the first stage of the group analysis of system (5.10)–(5.12), we study the properties of its invariance with respect to transformations of the space of all independent and dependent variables $R^9(t, x, y, z, u, v, w, q, \theta)$. The greatest Lie group of transformations of the space R^9 admitted by this system is infinite-dimensional, because the transformation $q \to q + \varphi(t)$ with an arbitrary function φ conserves the system. The corresponding Lie algebra of the operators is calculated by a standard method [158], and its basis is formed by the following operators:

$$
\begin{aligned}
X_1 &= \partial_x,\\
X_2 &= \partial_y,\\
X_3 &= \partial_z,\\
X_4 &= t\partial_x + \partial_u,\\
X_5 &= t\partial_y + \partial_v,\\
X_6 &= t\partial_z + \partial_w,\\
X_7 &= \partial_t,\\
X_8 &= x\partial_x + y\partial_y + (z + gt^2/2)\partial_z + u\partial_u + v\partial_v + (w + gt)\partial_w + 2\theta\partial_\theta,\\
X_9 &= x\partial_x + y\partial_y + (z - gt^2/2)\partial_z + t\partial_t - gt\partial_w + \theta\partial_\theta - q\partial_q,\\
X_{10} &= (z + gt^2/2)\partial_y - y\partial_z + (w + gt)\partial_v - v\partial_w,\\
X_{11} &= x\partial_z - (z + gt^2/2)\partial_x + u\partial_w - (w + gt)\partial_u,\\
X_{12} &= y\partial_x - x\partial_y + v\partial_u - u\partial_v, \quad X_{13}(\varphi) = \varphi(t)\partial_q
\end{aligned}
\tag{5.13}
$$

(∂_s is the operator of differentiation of the space R^9 with respect to the coordinate s). Let us indicate the Lie algebra of the operators (5.13) by L.

To describe unsteady motion of the fluid in a constant gravity field, we can use the equivalence transformation

$$
z \to z - gt^2/2, \quad w \to w - gt, \tag{5.14}
$$

which simplifies system (5.10)–(5.12) by eliminating the acceleration due to gravity in the first equation. The structure of the equations is not distorted by this replacement. Any exact solution of eqs. (5.10)–(5.13) with $g = 0$ is transformed by the reverse replacement (5.14) to the exact solution of eqs. (5.10)–(5.12) with $g \neq 0$. In what follows, we consider system (5.10)–(5.12) with $g = 0$. The corresponding Lie algebra of the admissible operators (5.13) is simplified: in the basis operators X_8, X_9, X_{10}, X_{11}, it is necessary to set $g = 0$.

5.2 Optimal subsystems of the subalgebras Θ_1 and Θ_2, factor-systems, and some solutions

An optimal system of the subalgebras Θ_1 for eqs. (5.10)–(5.12) has the form [197]

$$\begin{array}{ll}
\varepsilon X_1 + X_6 + X_{13}(\varphi), & \varepsilon X_3 + \delta X_{12} + X_{13}(\varphi), \\
\nu X_6 + X_{12} + X_{13}(\varphi), & X_8 + X_{13}(\varphi), \\
\varepsilon X_1 + X_8 + cX_{12} + X_{13}(\varphi), & \nu X_4 + X_8 + cX_{12} + X_{13}(\varphi), \\
\varepsilon_1 X_6 + X_7 + \varepsilon_2 X_{12}, & \varepsilon X_1 + \nu X_7 + X_8 + cX_{12}, \\
\nu_1 X_4 + \nu_2 X_7 + X_8 + cX_{12}, & \nu X_7 + X_8, \varepsilon X_6 + X_9, \\
\varepsilon_1 X_1 + \varepsilon_2 X_6 + X_9 + cX_{12}, & \nu X_3 + X_8 - X_9, \\
X_8 + bX_9, & \nu X_3 + X_8 - X_9 + cX_{12}, \\
\varepsilon X_3 + \nu X_4 + X_8 - X_9 + cX_{12}, & \varepsilon_1 X_1 + \varepsilon_2 X_4 + X_8 + bX_9 + cX_{12},
\end{array} \tag{5.15}$$

where $\delta = \{0; 1\}$; $\varepsilon, \varepsilon_1, \varepsilon_2 = \{-1; 0; 1\}$; $\nu, \nu_1, \nu_2 = \{-1; 1\}$; $b, c \in R$, $b \neq 0$, $c \neq 0$, and $\varphi(t)$ is an arbitrary smooth function.

Note that eqs. (5.10)–(5.12) with $g \neq 0$ admit the following discrete transformations of their variables:

$$\begin{aligned}
&E_1: \ (t, u, v, w, \theta, q) \to (-t, -u, -v, -w, -\theta, -q), \\
&E_2: \ (x, u) \to (-x, -u), \\
&E_3: \ (y, v) \to (-y, -v), \\
&E_4: \ (t, z, w) \to (t, -z - gt, -w - 2gt),
\end{aligned}$$

though the first transformation has no physical meaning. For system (5.10)–(5.12) with $g = 0$, the transformations E_1, E_2, E_3 are admitted in the same form, while the transformation E_4 is simplified: $(z, w) \to (-z, -w)$.

The optimal system of the second-order subalgebras Θ_2 is given in Table 5.1.

Using the operators of the optimal systems of the subalgebras Θ_1 and Θ_2, we construct several examples of factor-systems in invariant variables [197].

Example 5.1. Let us consider the operators

$$\langle X_9,\ X_6 + X_{13}(c_0 t^{-1}) \rangle = \langle t\partial_t + x\partial_x + y\partial_y + z\partial_z + \theta\partial_\theta - q\partial_q,\ t\partial_z + \partial_w + c_0 t^{-1}\partial_q \rangle,$$

where $c_0 = \text{const}$. Invariants of these operators are the variables $\{xt^{-1}, yt^{-1}, u, v, w - zt^{-1}, \theta t^{-1}, qt - c_0 z t^{-1}\}$. The solution of system (5.10)–(5.12) is sought in the form $(u, v, w, q, \theta) = (U, V, W + zt^{-1}, t^{-1}Q + c_0 z t^{-2}, tT)$, where U, V, W, Q, and T depend

Table 5.1: Optimal system of the subalgebras Θ_2.

No.	$X =$	$Y =$	Comment
1	$\varepsilon_1 X_1 + \varepsilon_2 X_4 + aX_8 + X_9 + bX_{12}$	$y^1 X_1 + y^2 X_2 + y^4 X_4 + y^5 X_5 + +X_{12} + X_{13}(\omega_0 t^{-1})$	$y^1 = \frac{\varepsilon_1 b}{(1+a)^2+b^2}; y^4 = \frac{\varepsilon_2 b}{1+b^2}; y^2 = \frac{-\varepsilon_1(1+a)}{(1+a)^2+b^2}; y^5 = \frac{-\varepsilon_2}{1+b^2}; (\varepsilon_1)^2 + (\varepsilon_2)^2 \neq 0$
2	$\varepsilon_1 X_1 + \varepsilon_2 X_4 + aX_8 + X_9 + bX_{12}$	$X_{13}(t^{\alpha})$	
3	$\varepsilon_1 X_1 + \varepsilon_2 X_4 + aX_8 + X_9 + bX_{12}$	$X_3 + X_{13}(\omega_0 t^{-(a+2)})$	
4	$\varepsilon_1 X_1 + \varepsilon_2 X_4 + aX_8 + X_9 + bX_{12}$	$X_6 + X_{13}(\omega_0 t^{-(a+1)})$	
5	$\varepsilon_1 X_1 + \varepsilon_2 X_4 + aX_8 + X_9 + bX_{12}$	$y^1 X_1 + y^2 X_2 + X_7 + X_{13}(\omega_0 t^{-2})$	$y^1 = \frac{-\varepsilon_2 a}{a^2+b^2}; y^2 = \frac{-\varepsilon_2 b}{a^2+b^2}$
6	$\varepsilon_1 X_1 + \varepsilon_2 X_4 + X_8 + X_9 + bX_{12}$	$y^1 X_1 + y^2 X_2 + bX_6 + X_7 + X_{13}(\omega_0 t^{-2})$	$y^1 = \frac{-\varepsilon_2}{1+b^2}; y^2 = \frac{-\varepsilon_2 b}{1+b^2}$
7	$\varepsilon_1 X_3 + \varepsilon_2 X_4 - X_8 + X_9 + bX_{12}$	$cX_3 + y^4 X_4 + y^5 X_5 + X_{12} + X_{13}(\omega_0 t^{-1})$	$y^4 = \frac{\varepsilon_2 b}{1+b^2}; y^5 = \frac{\varepsilon_2}{1+b^2}$
8	$\varepsilon_1 X_4 - X_8 + X_9 + bX_{12}$	$X_3 + X_{13}(\varepsilon_2 t^{-1})$	
9	$\varepsilon_1 X_3 + \varepsilon_2 X_4 - X_8 + X_9 + bX_{12}$	$X_{13}(t^{-\alpha})$	
10	$\varepsilon_1 X_3 + \varepsilon_2 X_4 - X_8 + X_9 + bX_{12}$	$X_6 + X_{13}(\omega_0)$	
11	$\varepsilon_1 X_3 + \varepsilon_2 X_4 - X_8 + X_9 + bX_{12}$	$y^1 X_1 + y^2 X_2 + X_7 + X_{13}(\omega_0 t^{-2})$	$y^1 = \frac{\varepsilon_2}{1+b^2}; y^2 = \frac{-\varepsilon_2 b}{1+b^2}$
12	$aX_8 + X_9$	$X_{12} + X_{13}(\omega_0 t^{-1})$	
13	$cX_8 + X_9$	$X_3 + X_{13}(\varepsilon t^{-(c+2)})$	
14	$cX_8 + X_9$	$X_6 + X_{13}(\varepsilon t^{-(c+1)})$	
15	$cX_8 + X_9$	$\delta X_7 + X_{13}(\omega_0 t^{-2})$	
16	$X_8 + X_9$	$vX_6 + X_7 + X_{13}(\omega_0 t^{-2})$	
17	$vX_3 - X_8 + X_9$	$kX_1 + mX_3 + X_{13}(\varepsilon t^{-1})$	$k^2 + m^2 \neq 0$
18	$vX_3 - X_8 + X_9$	$kX_4 + \delta X_6 + X_{13}(\varepsilon t^{-1})$	$k^2 + \delta^2 \neq 0$
19	$vX_3 - X_8 + X_9$	$\delta X_7 + X_{13}(\omega_0 t^{-2})$	$\omega_0 = 1$, if $\delta = 0$
20	$X_8 + X_{13}(\varphi_0)$	$X_7 + \varepsilon X_{12}$	
21	$vX_4 + X_8 + bX_{12} + X_{13}(\varphi_0)$	$y^1 X_1 + y^2 X_2 + y^4 X_4 + y^5 X_5 + X_7 + \varepsilon X_{12}$	$y^1 = \frac{-v}{1+b^2}; y^2 = \frac{-vb}{1+b^2}; y^4 = \frac{v\varepsilon b}{1+b^2}; y^5 = \frac{-v\varepsilon}{1+b^2}$
22	$\varepsilon_1 X_1 + X_8 + bX_{12} + X_{13}(\varphi_0)$	$y^1 X_1 + y^2 X_2 + X_7 + \varepsilon_2 X_{12}$	$y^1 = \frac{\varepsilon_1 \varepsilon_2 b}{1+b^2}; y^2 = \frac{-\varepsilon_1 \varepsilon_2}{1+b^2}$
23	$v_1 X_4 + v_2 X_7 + X_8 + bX_{12}$	$y^1 X_1 + y^2 X_2 + y^4 X_4 + y^5 X_5 + +X_{12} + X_{13}(\omega_0)$	$y^1 = \frac{2bv_1 v_2}{(1+b^2)^2}; y^4 = \frac{v_1 b}{1+b^2}; y^2 = \frac{v_1 v_2 (b^2-1)}{(1+b^2)^2}; y^5 = \frac{-v_1 b}{1+b^2}$
24	$v_1 X_4 + v_2 X_7 + X_8 + bX_{12}$	$X_3 + X_{13}(\omega_0 e^{-v_2 t})$	
25	$v_1 X_4 + v_2 X_7 + X_8 + bX_{12}$	$X_{13}(e^{\alpha t})$	

Table 5.1: (continued)

No.	$X =$	$Y =$	Comment
26	$v_1X_1 + v_2X_7 + X_8 + bX_{12}$	$y^1X_1 + y^2X_2 + X_{12} + X_{13}(\omega_0)$	$y^1 = \frac{vb}{1+b^2}; y^2 = \frac{-v}{1+b^2}$
27	$vX_1 + X_8 + bX_{12} + X_{13}(\varphi(t))$	$y^1X_1 + y^2X_2 + X_{12} + X_{13}(\omega(t))$	$y^1 = \frac{vb}{1+b^2}; y^2 = \frac{-v}{1+b^2}$
28	$\varepsilon X_1 + X_8 + bX_{12} + X_{13}(\varphi_0 t^{-1})$	$y^1X_1 + y^2X_2 + X_9 + mX_{12}$	$y^1 = \frac{\varepsilon(1+bm)}{1+b^2}; y^2 = \frac{\varepsilon(b-m)}{1+b^2}$
29	$vX_4 + X_8 + bX_{12} + X_{13}(\varphi(t))$	$y^4X_4 + y^5X_5 + X_{12} + X_{13}(\omega(t))$	$y^4 = \frac{vb}{1+b^2}; y^5 = \frac{-v}{1+b^2}$
30	$vX_4 + X_8 + bX_{12} + X_{13}(\varphi(t))$	$\varepsilon X_3 + X_6$	
31	$vX_4 + X_8 + bX_{12} + X_{13}(\varphi(t))$	X_3	
32	$vX_4 + X_8 + bX_{12} + X_{13}(\varphi(t))$	$X_{13}(\omega(t))$	
33	$vX_4 + X_8 + bX_{12} + X_{13}(\varphi_0 t^{-1})$	$y^4X_4 + y^5X_5 + X_9 + mX_{12}$	$y^4 = \frac{vbm}{1+b^2}; y^5 = \frac{-vb}{1+b^2}$
34	$\varepsilon X_1 + X_8 + bX_{12} + X_{13}(\varphi(t))$	X_6	
35	$\varepsilon X_1 + X_8 + bX_{12} + X_{13}(\varphi(t))$	X_3	
36	$\varepsilon X_1 + X_8 + bX_{12} + X_{13}(\varphi(t))$	$X_{13}(\omega(t))$	
37	$\varepsilon X_1 + vX_7 + X_8 + bX_{12}$	$X_3 + X_{13}(\omega_0 e^{-vt})$	
38	$\varepsilon X_1 + vX_7 + X_8 + bX_{12}$	$X_{13}(e^{\alpha t})$	
39	$vX_7 + X_8$	$X_{12} + X_{13}(\omega_0)$	
40	$vX_7 + X_8$	$X_3 + X_{13}(\omega_0 e^{-vt})$	
41	$vX_7 + X_8$	$X_{13}(e^{\alpha t})$	
42	$vX_7 + X_8$	$X_9 + mX_{12} + X_{13}(\varepsilon)$	
43	$X_8 + X_{13}(\varphi(t))$	$X_{12} + X_{13}(\omega(t))$	
44	$X_8 + X_{13}(\varphi(t))$	$\varepsilon X_1 + X_6$	
45	$X_8 + X_{13}(\varphi(t))$	X_3	
46	$X_8 + X_{13}(\varphi(t))$	$X_{13}(\omega(t))$	
47	$X_8 + X_{13}(\varphi_0(t^{-1}))$	$X_9 + mX_{12}$	
48	$\varepsilon_1X_1 + X_9 + bX_{12}$	$X_6 + X_{13}(\varepsilon_2 t^{-1})$	
49	$\varepsilon_1X_1 + X_9 + bX_{12}$	$mX_3 + X_7 + X_{13}(\omega_0 t^{-2})$	
50	$vX_1 + \varepsilon X_6 + X_9 + bX_{12}$	$y^1X_1 + y^2X_2 + mX_6 + X_{12} + X_{13}(\omega_0 t^{-1})$	$y^1 = vb/(1+b^2); y^2 = -v/(1+b^2)$
51	$\varepsilon_1X_1 + \varepsilon_2X_6 + X_9 + bX_{12}$	$X_3 + X_{13}(\omega_0 t^{-2})$	

Table 5.1: (continued)

No.	$X =$	$Y =$	Comment
52	$\varepsilon_1 X_1 + \varepsilon_2 X_6 + X_9 + bX_{12}$	$X_{13}(t^{\alpha})$	
53	$\varepsilon X_6 + X_9$	$mX_6 + X_{12} + X_{13}(\omega_0 t^{-1})$	
54	X_9	$X_7 + X_{13}(\varepsilon t^{-2})$	
55	$\varepsilon X_6 + X_7 + vX_{12}$	$X_3 + X_{13}(\omega_0)$	
56	$\varepsilon X_6 + X_7 + vX_{12}$	$X_{13}(e^{\alpha t})$	
57	$\varepsilon_1 X_6 + X_7$	$\varepsilon_2 X_3 + X_{12} + X_{13}(\omega_0)$	
58	$\varepsilon_1 X_6 + X_7$	$X_{13}(e^{\alpha} t)$	
59	$vX_6 + X_7$	$mX_1 + \delta X_3 + X_{13}(\omega_0)$	
60	X_7	$X_3 + X_{13}(\varepsilon)$	
61	$vX_6 + X_{12} + X_{13}(\varphi(t))$	$X_3 + \varepsilon X_6 + X_{12} + X_{13}(\omega(t))$	
62	$vX_6 + X_{12} + X_{13}(\varphi(t))$	$X_{13}(\omega(t))$	
63	$\varepsilon X_3 + X_{12} + X_{13}(\varphi(t))$	$X_6 + X_{13}(\omega(t))$	
64	$\varepsilon X_3 + X_{12} + X_{13}(\varphi(t))$	$X_{13}(\omega(t))$	
65	$X_{12} + X_{13}(\varphi(t))$	$X_3 + X_{13}(\omega(t))$	
66	$vX_1 + X_6 + X_{13}(\varphi(t))$	$kX_1 + mX_3 + nX_4 + X_5 + X_{13}(\omega(t))$	
67	$vX_1 + X_6 + X_{13}(\varphi(t))$	$kX_2 + mX_3 + X_4 + X_{13}(\omega(t))$	
68	$vX_1 + X_6 + X_{13}(\varphi(t))$	$kX_1 + mX_2 + X_3 + X_{13}(\omega(t))$	
69	$vX_1 + X_6 + X_{13}(\varphi(t))$	$kX_1 + X_2 + X_{13}(\omega(t))$	
70	$vX_1 + X_6 + X_{13}(\varphi(t))$	$\delta X_1 + X_{13}(\omega(t))$	
71	$X_6 + X_{13}(\varphi(t))$	$kX_2 + vX_3 + X_4 + X_{13}(\omega(t))$	
72	$X_6 + X_{13}(\varphi(t))$	$\varepsilon X_2 + X_4 + X_{13}(\omega(t))$	
73	$X_6 + X_{13}(\varphi(t))$	$kX_1 + X_3 + X_{13}(\omega(t))$	
74	$X_6 + X_{13}(\varphi(t))$	$\delta X_1 + X_{13}(\omega(t))$	
75	$X_3 + X_{13}(\varphi(t))$	$\delta X_1 + X_{13}(\omega(t))$	
76	$X_{13}(\varphi(t))$	$X_{13}(\omega(t))$	

Note. $a, b, c, k, m, n, \alpha, \omega_0$, and φ_0 are constants; $a \neq \{0; -1\}$, $b \neq 0$, and $c \neq 0$; $\varepsilon, \varepsilon_1, \varepsilon_2 = \{0; \pm 1\}$; $v, v_1, v_2 = \{\pm 1\}$; $\delta = \{0; 1\}$; $\varphi(t)$ and $\omega(t)$ are arbitrary smooth functions.

on $\xi = xt^{-1}$, $\eta = yt^{-1}$. The factor-system is written as

$$\begin{gathered}(U-\xi)U_\xi + (V-\eta)U_\eta + (U_\eta - V_\xi)T_\eta + T_\xi T_{\eta\eta} - T_\eta T_{\xi\eta} = T(-Q_\xi + \nu(U_{\xi\xi} + U_{\eta\eta})),\\ (U-\xi)V_\xi + (V-\eta)V_\eta + (V_\xi - U_\eta)T_\xi + T_\eta T_{\xi\xi} - T_\xi T_{\xi\eta} = T(-Q_\eta + \nu(V_{\xi\xi} + V_{\eta\eta})),\\ W + (U-\xi)W_\xi + (V-\eta)W_\eta + W_\xi T_\xi + W_\eta T_\eta = T(-c_0 + \nu(W_{\xi\xi} + W_{\eta\eta})),\\ T + (U-\xi)T_\xi + (V-\eta)T_\eta + {T_\xi}^2 + {T_\eta}^2 = T(T_{\xi\xi} + T_{\eta\eta}), \quad U_\xi + V_\eta + 1 = 0.\end{gathered} \tag{5.16}$$

Let us assume that the functions U, V, W, Q, and T are independent of η. Then, the last equation of system (5.16) yields $U = C_1 - \xi$, $C_1 = \text{const}$. Let us indicate $2\xi - C_1 = h$. The remaining equations are rewritten as

$$\begin{gathered}2TQ_h = -h, \quad -2hV_h + 4V_hT_h = 4\nu TV_{hh},\\ W - 2hW_h + 4W_hT_h = T(-c_0 + 4\nu W_{hh}),\\ T - 2hT_h + 4(T_h)^2 = 4TT_{hh}.\end{gathered} \tag{5.17}$$

Seeking for the solution of the third equation of system (5.17) in the form $T = ah^2 + bh + d$, we obtain

$$T = \frac{3}{8}h^2, \quad Q = C_2 - \frac{4}{3}\ln|h|, \quad V = C_3h^{2/3\nu+1} + C_4.$$

The function W satisfies the Euler equation

$$\frac{3}{2}\nu h^2W_{hh} - hW_h - W = \frac{3}{8}c_0h^2$$

and has the following presentation:

$$\begin{aligned}W &= \left(C_5 + \frac{3c_0}{28}\ln|h|\right)h^2 + C_6h^{-1/3} \quad \text{at} \quad \nu = 1,\\ W &= C_5h^{\lambda_1} + C_6h^{\lambda_2} + \frac{c_0}{8(\nu-1)}h^2 \quad \text{at} \quad \nu \neq 1,\\ \lambda_{1,2} &= \frac{(3\nu+2) \pm \sqrt{(3\nu+2)^2 + 24\nu}}{6\nu}.\end{aligned}$$

Here, C_i, $i = 1, \ldots, 6$ are arbitrary constants.

Example 5.2. Let us consider the following combination of the operators:

$$\begin{aligned}&\langle \alpha X_7 + X_8, X_3 + X_{13}(ce^{-\alpha t})\rangle\\ &\quad = \langle \alpha\partial_t + x\partial_x + y\partial_y + z\partial_z + u\partial_u + v\partial_v + w\partial_w + 2\theta\partial_\theta, \partial_z + ce^{-\alpha t}\partial_q\rangle\end{aligned}$$

($\alpha \neq 0$ and $c = \text{const}$). Invariants of these operators are the variables $\{(x, y, u, v, w) \times e^{-\alpha t}, \theta e^{-2\alpha t}, q - cze^{-\alpha t}\}$. The solution of system (5.10)–(5.12) is sought in the form

$$(u, v, w, q, \theta) = (Ue^{\alpha t}, Ve^{\alpha t}, We^{\alpha t}, Q + cze^{-\alpha t}, Te^{2\alpha t}),$$

where U, V, W, Q, and T depend on $\xi = xe^{-\alpha t}$ and $\eta = ye^{-\alpha t}$. The factor-system is

$$\begin{gathered}
\alpha U + (U - \alpha\xi)U_\xi + (V - \alpha\eta)U_\eta + (U_\eta - V_\xi)T_\eta + T_\xi T_{\eta\eta} - T_\eta T_{\xi\eta} = T(-Q_\xi + \nu(U_{\xi\xi} + U_{\eta\eta})),\\
\alpha V + (U - \alpha\xi)V_\xi + (V - \alpha\eta)V_\eta + (V_\xi - U_\eta)T_\xi + T_\eta T_{\xi\xi} - T_\xi T_{\xi\eta} = T(-Q_\eta + \nu(V_{\xi\xi} + V_{\eta\eta})),\\
\alpha W + (U - \alpha\xi)W_\xi + (V - \alpha\eta)W_\eta + W_\xi T_\xi + W_\eta T_\eta = T(-c + \nu(W_{\xi\xi} + W_{\eta\eta})),\\
\alpha T + (U - \alpha\xi)T_\xi + (V - \alpha\eta)T_\eta + {T_\xi}^2 + {T_\eta}^2 = T(T_{\xi\xi} + T_{\eta\eta}),\\
U_\xi + V_\eta = 0.
\end{gathered} \tag{5.18}$$

As in Example 5.1, we assume that the functions U, V, W, Q, and T are independent of η. Then, the last equation of system (5.18) yields $U = U_0 = \text{const}$. Using the replacement of variables $\alpha\xi - U_0 = h$, we rewrite the remaining equations as

$$\begin{gathered}
TQ_h = -U_0, \quad V - hV_h + \alpha V_h T_h = \nu\alpha T V_{hh},\\
W - hW_h + \alpha W_h T_h = T\left(-\frac{c}{\alpha} + \nu\alpha W_{hh}\right),\\
T - hT_h + \alpha {T_h}^2 = \alpha T T_{hh}.
\end{gathered} \tag{5.19}$$

The solution of the last equation of system (5.19) is sought in the form $T = ah^2 + bh + d$ (a, b, and d are arbitrary constants). Three types of solutions are obtained:

$$T = 0; \quad T = bh - \alpha b^2; \quad T = \frac{1}{2\alpha}h^2 + c.$$

The first case yields a simple solution of system (5.10)–(5.12)

$$u = 0, \quad v = V_0 x, \quad w = W_0 x, \quad q = Q(xe^{-\alpha t}) + cze^{-\alpha t}, \quad \theta = 0,$$

where V_0 and W_0 are arbitrary constants, and $Q(\xi)$ is an arbitrary function.

In the second case ($b \neq 0$), we have

$$\begin{aligned}
Q &= -\frac{U_0}{b}\ln|bh - \alpha b^2| + Q_0,\\
V &= C_1\lambda - C_0\left[e^{-\lambda/\nu\alpha b} - \frac{\lambda}{\nu\alpha b}\int \frac{1}{\lambda}\, e^{-\lambda/\nu\alpha b}\, d\lambda\right].
\end{aligned}$$

In the third case, we obtain

$$\begin{aligned}
Q(h) &= \frac{1}{\sqrt{2c\alpha}}\operatorname{arctg}\frac{h}{\sqrt{2c\alpha}}, && \text{if } 2\alpha > 0,\\
Q(h) &= -\frac{1}{2\sqrt{-2c\alpha}}\ln\left|\frac{\sqrt{-2c\alpha} - h}{\sqrt{-2c\alpha} - h}\right|, && \text{if } 2\alpha < 0,\\
Q(h) &= \frac{2\alpha U_0}{h}, && \text{if } c = 0.
\end{aligned}$$

The functions $V(h)$ and $W(h)$ satisfy second-order ordinary differential equations.

Example 5.3. Let us consider a subalgebra of the operators $\langle \alpha X_3 + X_7, X_1, X_2\rangle = \langle \alpha\partial_z + \partial_t, \partial_x, \partial_y\rangle$, $\alpha = \text{const}$. Invariants of these operators are the variables $\{z - \alpha t, u, v, w, q, \theta\}$. We assume that the functions u, v, w, q, and θ depend on one variable $\zeta = z - \alpha t$. After the substitution, system (5.10)–(5.12) transforms to the factor-system

$$\begin{gathered}(-\alpha + w + \theta')u' = \nu\theta u'', \quad (-\alpha + w + \theta')v' = \nu\theta v'',\\ (-\alpha + w)w' = \theta(-q' + \nu w''), \quad w' = 0,\\ (-\alpha + w + \theta')\theta' = \theta\theta'',\end{gathered} \tag{5.20}$$

where the prime denotes differentiation with respect to the variable ζ.

System (5.20) is integrated and has two variants of solutions:

$$\begin{gathered}u = U_0 + U_1\zeta, \quad v = V_0 + V_1\zeta, \quad w = W_0,\\ q = Q_0, \quad \theta = -(W_0 - \alpha)\zeta + T_1;\end{gathered} \tag{5.21}$$

$$\begin{gathered}u = U_0 + U_1 e^{T_0\zeta/\nu}, \quad v = V_0 + V_1 e^{T_0\zeta/\nu}, \quad w = W_0,\\ q = Q_0, \quad \theta = \frac{W_0 - \alpha}{T_0} + T_1 e^{T_0\zeta}\end{gathered} \tag{5.22}$$

($U_0, U_1, V_0, V_1, W_0, Q_0, T_0$, and T_1 are arbitrary constants; $T_0 \neq 0$).

Returning to natural, physical, functions $\mathbf{v}, p$, and T (velocity, pressure, and temperature) by means of the reverse replacement in eqs. (5.2) and (5.3), we obtain solutions for eqs. (5.21):

$$\begin{gathered}v_1 = U_0 + U_1\zeta, \quad v_2 = V_0 + V_1\zeta, \quad v_3 = \alpha - gt, \quad p = \rho_0\chi Q_0,\\ T = \frac{-(W_0 - \alpha)\zeta + T_1 - \chi}{\chi\beta},\end{gathered}$$

and solutions for eqs. (5.22):

$$\begin{gathered}v_1 = U_0 + U_1 e^{\chi T_0\zeta/\nu}, \quad v_2 = V_0 + V_1 e^{\chi T_0\zeta/\nu}, \quad v_3 = W_0 - gt + T_1 T_0 e^{T_0\zeta},\\ p = \rho_0\chi Q_0 + (\rho_0(\nu - \chi) + \lambda)T_1 {T_0}^2 e^{T_0\zeta},\\ T = \frac{1}{\chi\beta T_0}\left(-\chi T_0 + W_0 - \alpha + T_1 T_0 e^{T_0\zeta}\right).\end{gathered}$$

Here, $T_0 \neq 0$ and $\zeta = z - \alpha t + (gt^2)/2$. Similar solutions can be constructed on the subalgebras $\langle \beta X_1 + X_7, X_2, X_3\rangle$ and $\langle \gamma X_2 + X_7, X_1, X_3\rangle$.

Example 5.4. We construct the solution on the operators $\langle X_2; X_5; X_7; X_3 + X_{13}(\psi_0)\rangle$, $\psi_0 = \text{const}$. Invariants of these operators are the variables $\{x, u, v, w, \theta, q - \psi_0 z\}$; therefore, the partially invariant solution of rank 1 and defect 1 is sought in the form $u = U(x)$, $v = v(t, x, y, z)$, $w = W(x)$, $\theta = \theta(x)$, $q = \psi_0 z + Q(x)$. System (5.10)–(5.12) transforms to the system

$$\begin{gathered} UU_x = \theta(-Q_x + \nu U_{xx}) = 0, \\ v_t + Uv_x + \nu v_y + Wv_z + \chi v_x\theta_x = \nu\theta(v_{xx} + v_{yy} + v_{zz}), \\ UW_x + \chi W_x\theta_x = \theta(-\psi_0 + \nu W_{xx}) - g, \quad U\theta_x + \chi\theta_x^2 = \chi\theta\theta_{xx}, \quad U_x = 0, \end{gathered} \tag{5.23}$$

which yields $U \equiv U_0 = \text{const}$ and $Q \equiv Q_0 = \text{const}$.

System (5.23) is split with respect to the functions θ, W, and v and has two solutions

$$\theta_1(x) = \frac{1}{C_1} + C_2 \exp\left(\frac{C_1 U_0 x}{\chi}\right), \quad \theta_2(x) = \theta_0 - \frac{U_0 x}{\chi},$$

where $C_1,\ C_2,\ \theta_0 = \text{const}$, and $C_1 \neq 0$.

The function $v = \text{const} = 0$ (plane motion) is a solution of system (5.23). This case was considered in detail in [12] (see the next section). The fluid flow in a band $-a \le x \le a$ with a given heat flux on the boundary $\partial\theta/\partial n = \delta(\theta - \theta_{\text{ext}}) = d$ (θ_{ext} is the external temperature of the fluid, i. e., the temperature of the fluid boundary) was studied.

Let us consider the function $\theta_2(x)$; then, the third equation in system (5.23) is integrated:

$$W(x) = \frac{1}{\nu}\left\{\psi_0\frac{x^2}{2} + C_1 x + C_2 + \frac{g\chi^2}{U_0^2}\left(\theta_0 - \frac{U_0 x}{\chi}\right)\left[\ln|\theta_0 - \frac{U_0 x}{\chi}| - 1\right]\right\}.$$

Note that the solution obtained differs substantially from the known solution of the steady problem in the Oberbeck–Boussinesq approximation

$$W_{\text{ob}}(x) = -\frac{gU_0}{6\nu\chi}\, x(a^2 - x^2).$$

Example 5.5. On the operators $\langle \alpha X_1 + X_7; X_2; X_3\rangle$, $\alpha = \text{const}$, the invariant solution is sought in the form

$$u = u(\xi), \quad v = v(\xi), \quad w = w(\xi), \quad q = q(\xi), \quad \theta = \theta(\xi), \quad \xi = x - \alpha t.$$

System (5.10)–(5.12) is rewritten as the factor-system

$$\begin{gathered} u_\xi = 0, \quad (u-\alpha)u_\xi = \theta(-q_\xi + \nu u_{\xi\xi}), \quad (u-\alpha)v_\xi + \chi v_\xi = \nu\theta v_{\xi\xi}, \\ (u-\alpha)w_\xi + \chi w_\xi\theta_\xi = \nu\theta w_{\xi\xi} - g, \quad (u-\alpha)\theta_\xi + \chi\theta_\xi^2 = \chi\theta\theta_{\xi\xi}. \end{gathered} \tag{5.24}$$

Therefore, we have $u \equiv u_0 = \text{const}$ and $q \equiv q_0 = \text{const}$. Let us assume that $u_0 - \alpha = a_0$. Then, we obtain

$$\begin{gathered} a_0 v_\xi + \chi v_\xi\theta_\xi = \nu\theta v_{\xi\xi}, \quad a_0 w_\xi + \chi w_\xi\theta_\xi = \nu\theta w_{\xi\xi} - g, \\ a_0\theta_\xi + \chi\theta_\xi^2 = \chi\theta\theta_{\xi\xi}. \end{gathered} \tag{5.25}$$

The structure of eqs. (5.25) is similar to that of eqs. (5.23), the equation for the function $\theta(\xi)$ is "split off," and, therefore, we have

$$\theta_1(\xi) = \frac{1}{C_1} + C_2 \exp\left(\frac{C_1 a_0 \xi}{\chi}\right), \quad \theta_2(\xi) = \theta_0 - \frac{a_0 \xi}{\chi},$$

where $C_1,\ C_2,\ \theta_0 = \text{const}$, and $C_1 \neq 0$. For the solution $\theta_2(\xi)$, we easily obtain

$$v_2(\xi) = B_1 \xi + B_2, \quad B_1, B_2 = \text{const},$$
$$w_2(\xi) = \frac{1}{\nu}\left\{\varepsilon_1 \xi + \varepsilon_2 + \frac{g\chi^2}{a_0^2}\left(\theta_0 - \frac{a_0 \xi}{\chi}\right)\left(\ln|\theta_0 - \frac{a_0 \xi}{\chi}| - 1\right)\right\}.$$

5.3 On one steady solution of microconvection equations in a vertical layer

1. Solution of the steady problem in the case with a special temperature distribution. Let us choose the coordinate system so that $\mathbf{g} = (0, -g, 0)$. Let the fluid fill a layer $|x| < a$; the boundaries of this layer are solid surfaces with a specified heat flux. If the heat flux value is independent of z, then plane flows in the vertical layer are possible. They occur in the case where the initial velocity and temperature distributions are independent of z, and the velocity component is $v_3 = 0$ at $t = 0$. In what follows, only steady flows in the layer are considered [12].

System (5.10)–(5.12) in the plane case for a steady flow ($\mathbf{w}_t = 0$, $\Theta_t = 0$) admits the operators $\partial/\partial y$ and $\psi\partial/\partial q$, which reflects the system invariance to transformations of shifting along the y axis and addition of an arbitrary constant ψ to the analog of pressure q. The invariant solutions of system (5.10)–(5.12) with respect to the operator $\partial/\partial y + \psi\partial/\partial q$ can be presented as

$$\begin{gathered}\mathbf{w} = (w_1, w_2, 0), \quad w_1(x) \equiv u, \quad w_2(x) \equiv v, \\ \Theta = \Theta(x), \quad q = (\varphi - g)y + r(x),\end{gathered} \tag{5.26}$$

where $\varphi = \psi + g$. The term $-gy$ in the expression for q corresponds to the hydrostatic component in the presentation of the true pressure p. If eq. (5.26) is substituted into system (5.10)–(5.12), the system decomposes into consecutively solved equations of the functions u, v, Θ, and r of the variable x, $\varphi = \text{const}$, $g = \text{const}$ is the acceleration due to gravity, and $w_1(x)$, $w_2(x)$, $\Theta(x)$, $r(x)$, and φ are unknown functions.

It follows from the continuity equation (5.11) that $w_1 = \text{const}$, and $w_2(x)$ is an arbitrary function. Let us assume that $u \equiv w_1 = u_0 = \text{const}$ and $v \equiv w_2$ is an arbitrary function.

The energy equation (5.12) with allowance for eq. (5.26) becomes

$$(u_0 + \beta\chi\Theta_x)\Theta_x = (1 + \beta\Theta)\chi\Theta_{xx}. \tag{5.27}$$

The last equation of the second order has a two-parameter family of steady solutions

$$\Theta(x) = \frac{1}{\beta}\left[\frac{1}{c_1} - 1 + c_2 \exp(c_1 u_0 x/\chi)\right], \quad c_1 \neq 0, \tag{5.28}$$

and a singular solution

$$\Theta_0(x) = \bar{\Theta} - u_0 x/\beta\chi, \quad \bar{\Theta} = \text{const}. \tag{5.29}$$

The boundary condition on the walls $x = \pm a$, $\partial\theta/\partial n = d$ for solution (5.26) takes the form

$$\Theta_x = -u_0/\beta\chi \equiv d. \tag{5.30}$$

Obviously, this condition is satisfied only by the temperature field (5.29) with an arbitrary constant $\bar{\Theta}$.

Projecting eq. (5.10) onto the x axis, we obtain $(1 + \beta\Theta_0)(-r_x) = 0$, i. e., $r = r_0 = \text{const}$. The function $q(x, y)$ is determined with accuracy to a constant, and we can assume that $r_0 \equiv 0$. Projecting eq. (5.10) onto the y yields the equation

$$\begin{aligned}(u_0 + \beta\chi\Theta_{0x})v_x &= (1 + \beta\Theta_0)(\nu v_{xx} - \varphi) + (1 + \beta\Theta_0)g - g \\ &= (1 + \beta\Theta_0)(\nu v_{xx} - \varphi) + \beta\Theta_0 g.\end{aligned} \tag{5.31}$$

According to eq. (5.29), we have $u_0 + \beta\chi\Theta_{0x} = 0$, and eq. (5.31) is simplified to

$$\left(1 + \beta\bar{\Theta} - \frac{u_0 x}{\chi}\right)(\nu v_{xx} - \varphi) + \beta\bar{\Theta} g - \frac{u_0 g}{\chi}\, x = 0. \tag{5.32}$$

Equation (5.32) is a second-order ordinary differential equation, where φ is an unknown constant; therefore, three conditions are needed. As $\nabla\Theta = (\Theta_{0x}, 0)$, we obtain

$$v(x) = 0, \quad x = \pm a. \tag{5.33}$$

To determine $v(x)$ unambiguously, we have to know the constant φ. Using the interpretation of solution (5.26) as a solution that approximately describes convection in the central part of a finite, but rather long closed cavity (as compared with the cavity width $2a$), we impose the condition of a zero mass flow rate of the fluid through any cross section of the layer $y = \text{const}$ onto this solution. In other words, we have

$$\int_{-a}^{a} \rho(x) v_2(x)\, dx = 0, \tag{5.34}$$

where $v_2(x)$ is the true velocity and $\rho(x)$ is the fluid density. In solution (5.26), $v_2(x) = v(x)$; therefore, taking into account the state equation (5.5) accepted in this model, we obtain

$$\int_{-a}^{a} \frac{v(x)}{1 + \beta\Theta_0(x)}\, dx = 0. \tag{5.35}$$

The general solution of eq. (5.32) is

$$v = \frac{1}{\nu}\left[(\varphi - g)\frac{x^2}{2} + c_1 x + c_2 + \frac{g\chi^2}{u_0^2}\left(1 + \beta\bar{\Theta} - \frac{u_0 x}{\chi}\right)\left(\ln\left(1 + \beta\bar{\Theta} - \frac{u_0 x}{\chi}\right) - 1\right)\right] \tag{5.36}$$

with arbitrary constants c_1 and c_2. They are found from eq. (5.33):

$$\begin{aligned} c_1 &= -\frac{g\chi^2}{2au_0^2}\left[\left(1 + \beta\bar{\Theta} - \frac{u_0 a}{\chi}\right)\ln\left(1 + \beta\bar{\Theta} - \frac{u_0 a}{\chi}\right)\right. \\ &\quad \left. - \left(1 + \beta\bar{\Theta} + \frac{u_0 a}{\chi}\right)\ln\left(1 + \beta\bar{\Theta} + \frac{u_0 a}{\chi}\right) + 2\frac{u_0 a}{\chi}\right], \\ c_2 &= \frac{(g - \varphi)a^2}{2} - \frac{g\chi^2}{2u_0^2}\left(\left(1 + \beta\bar{\Theta} - \frac{u_0 a}{\chi}\right)\ln\left(1 + \beta\bar{\Theta} - \frac{u_0 a}{\chi}\right)\right. \\ &\quad \left. + \left(1 + \beta\bar{\Theta} + \frac{u_0 a}{\chi}\right)\ln\left(1 + \beta\bar{\Theta} + \frac{u_0 a}{\chi}\right) - 2(1 + \beta\bar{\Theta})\right). \end{aligned} \tag{5.37}$$

Substituting eq. (5.36) into equality (5.35) and taking into account eq. (5.37), we can determine the constant φ as $\varphi = g + \Phi$, where

$$\begin{aligned} \Phi &= \left[4g\left(\frac{u_0 a}{\chi}\right)^2 + 2g\frac{u_0 a}{\chi}(1 + \beta\bar{\Theta})\ln\left(\frac{1 + \beta\bar{\Theta} - u_0 a/\chi}{1 + \beta\bar{\Theta} + u_0 a/\chi}\right)\right. \\ &\quad + g\left(\frac{u_0 a}{\chi}\right)^2 \ln^2\left(\frac{1 + \beta\bar{\Theta} - u_0 a/\chi}{1 + \beta\bar{\Theta} + u_0 a/\chi}\right) \\ &\quad \left. - g(1 + \beta\bar{\Theta})^2 \ln^2\left(\frac{1 + \beta\bar{\Theta} - u_0 a/\chi}{1 + \beta\bar{\Theta} + u_0 a/\chi}\right)\right] \\ &\quad \times \left[\left(\frac{u_0 a}{\chi}\right)^3 \ln\left(\frac{1 + \beta\bar{\Theta} - u_0 a/\chi}{1 + \beta\bar{\Theta} + u_0 a/\chi}\right)\right]^{-1} + 2\left(\frac{u_0 a}{\chi}\right)^2 (1 + \beta\bar{\Theta}) \\ &\quad - \frac{u_0 a}{\chi}(1 + \beta\bar{\Theta})^2 \ln\left(\frac{1 + \beta\bar{\Theta} - u_0 a/\chi}{1 + \beta\bar{\Theta} + u_0 a/\chi}\right). \end{aligned}$$

Let us compare the resultant solution with the solution of the steady problem in the Oberbeck–Boussinesq approximation. It turns out that the temperature fields in both solutions coincide. Similarly, the horizontal component of velocity is equal to zero in both the classical and new formulations. The difference between these models lies in the vertical component: in the Oberbeck–Boussinesq model, it has the form

$$v = -\frac{gu_0}{6\nu\chi}\, x(a^2 - x^2). \tag{5.38}$$

To compare eqs. (5.36) and (5.38), we write them in the dimensionless form. For this purpose, we choose the unit for distance measurements (the characteristic linear scale $x = \eta a$) and introduce the dimensionless parameters $\gamma = u_0 a/\chi$ and $\varepsilon = \beta\bar{\Theta}$. Passing to the dimensionless variable, we obtain

$$v = -\frac{gu_0}{6\nu\chi}\, a^3\eta(1 - \eta^2).$$

Here, the coefficient $-gu_0a^3/6\nu\chi$ has the dimension [cm/s]. Dividing the expression given above by this coefficient (and denoting the resultant expression by v_b), we obtain

$$v_b = -\frac{6\nu\chi}{gu_0a^3}\, v = \eta - \eta^3. \tag{5.39}$$

Using eq. (5.36), we write the expression for velocity in the new model (denoting it by v_n) in the form

$$v_n = -\frac{\nu}{ga^2}\, v = A(\varepsilon,\gamma)\eta^2 + B(\varepsilon,\gamma)\eta - A - C + \frac{1}{\gamma^2}(1+\varepsilon-\gamma\eta)[\ln(1+\varepsilon-\gamma\eta) - 1], \tag{5.40}$$

where

$$\begin{aligned}
A &= \left\{4g\gamma^2 + 2g\gamma(1+\varepsilon)\ln\left(\frac{1+\varepsilon-\gamma}{1+\varepsilon+\gamma}\right)\right.\\
&\quad \left. + [g\gamma^2 - g(1+\varepsilon)^2]\left[\ln\left(\frac{1+\varepsilon-\gamma}{1+\varepsilon+\gamma}\right)\right]^2\right\}\\
&\quad \times \left\{[2\gamma^3 - 2\gamma(1+\varepsilon)^2]\ln\left(\frac{1+\varepsilon-\gamma}{1+\varepsilon+\gamma}\right) - 4\gamma^2(1+\varepsilon)\right\}^{-1},\\
B &= -\frac{1}{2\gamma^2}\left[(1+\varepsilon)\ln\left(\frac{1+\varepsilon-\gamma}{1+\varepsilon+\gamma}\right) - \gamma[\ln((1+\varepsilon)^2 - \gamma^2) - 2]\right],\\
C &= \frac{1}{2\gamma^2}[\ln((1+\varepsilon)^2 - \gamma^2) - 2] - \gamma\ln\left(\frac{1+\varepsilon-\gamma}{1+\varepsilon+\gamma}\right).
\end{aligned}$$

A comparison of eqs. (5.39) and (5.40) shows that the function v_n loses the property of oddness, which is inherent in the distribution of vertical velocity of a steady stratified convective flow in a vertical layer in accordance with the classical convection model. The velocity profiles are shown in Figure 5.1. It is seen that the value of $v_n(0)$ decreases with increasing difference in temperature, and the velocity profile becomes almost parabolic, as in the Poiseuille flow.

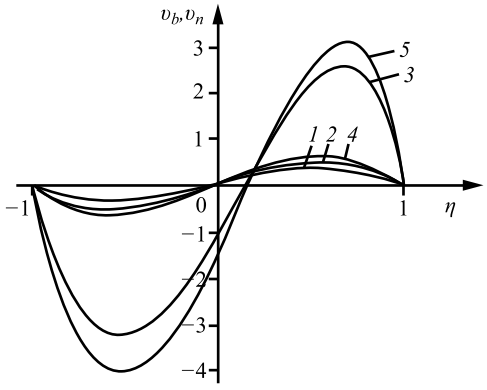

Figure 5.1: Velocity profiles in vertically layer.

Remark 5.1. The motion in a vertical slot with the temperature having the form (5.29) (and also its unsteady variant) was studied in [176], and the boundary conditions were taken in the form (5.30). There are some inaccuracies in the formulas for temperature and, hence, for velocity, and there are no explicit formulas for velocity.

2. Analysis of the steady solution for a specified temperature on the walls

Let us consider the case with the boundary conditions taken in the form $\theta = \theta_w(\mathbf{x}, t)$, $\mathbf{w} + \beta\chi\nabla\theta = 0$, i. e., the temperatures θ_1 and θ_2 are specified on the walls $x = \pm a$. Therefore, we have

$$\Theta|_{x=-a} = \theta_1, \quad \Theta|_{x=a} = \theta_2.$$

From eq. (5.29), we obtain $\theta_1 = \bar{\Theta} + u_0 a/\beta\chi$ è $\theta_2 = \bar{\Theta} - u_0 a/\beta\chi$. Thus, the singular solution (5.29) satisfies these conditions if the constants u_0 and $\bar{\Theta}$ depend on the values of θ_1 and θ_2:

$$\bar{\Theta} = \frac{\theta_1 + \theta_2}{2}, \quad u_0 = \frac{(\theta_1 - \theta_2)\beta\chi}{2a}.$$

It is easily seen that the density is positive ($\beta\bar{\Theta} > -1$) and $\Theta > 0$ in the layer $|x| < a$.

The following conditions should be satisfied on the walls for steady solutions of the form (5.28):

$$\begin{aligned} \frac{1}{\beta}\left[\frac{1}{c_1} - 1 + c_2 \exp\left(-\frac{c_1 u_0 a}{\chi}\right)\right] &= \theta_1, \\ \frac{1}{\beta}\left[\frac{1}{c_1} - 1 + c_2 \exp\left(\frac{c_1 u_0 a}{\chi}\right)\right] &= \theta_2. \end{aligned} \tag{5.41}$$

Subtracting the first equation of system (5.41) from the second equation, we obtain

$$\frac{c_2}{\beta} = \frac{\theta_2 - \theta_1}{\exp(\mu) - \exp(-\mu)}, \tag{5.42}$$

where $\mu = c_1 u_0 a/\chi$.

Let us consider possible variants.

A) If $\theta_1 = \theta_2$, then $c_2 = 0$ and $c_1 = 1/(1 + \beta\theta_1)$, i. e., the temperature in the layer is constant.

B) Let $\theta_1 \neq \theta_2$. We substitute eq. (5.42) into the first equation of system (5.41), perform the replacements

$$\omega = \frac{\beta\chi(\theta_2 - \theta_1)}{u_0 a}, \quad \sigma = (1 + \beta\theta_1)\,\frac{\chi}{u_0 a}$$

and obtain the equation

$$\frac{1}{\mu} + \frac{\omega}{\exp(2\mu) - 1} = \sigma. \tag{5.43}$$

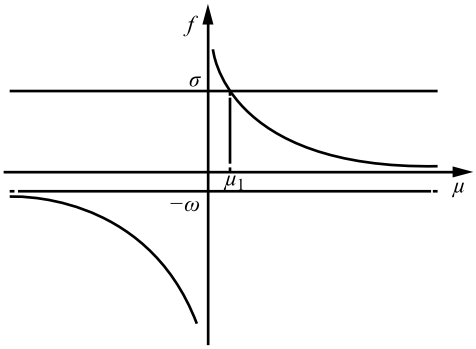

Figure 5.2: Function f vs μ for $\omega > 0$.

Note that $\sigma > 0$ (we assume that $u_0 > 0$). Are there any solutions for eq. (5.43)? Let

$$f(\mu) = \frac{1}{\mu} + \frac{\omega}{\exp(2\mu) - 1}.$$

The derivative of the function $f(\mu)$ is

$$f'(\mu) = -\frac{1}{\mu^2} - \frac{2\omega \exp(2\mu)}{(\exp(2\mu) - 1)^2}. \tag{5.44}$$

B1) At $\omega > 0$ ($\theta_2 > \theta_1$), the function $f(\mu)$ monotonically decreases ($f'(\mu) < 0$) in the domain of its definition. Therefore, there exists a unique solution $f(\mu_1) = \sigma$ and $\mu_1 > 0$, i. e., the only possible constants (Figure 5.2) are

$$c_1 = \frac{\chi}{u_0 a}\,\mu_1 > 0, \quad c_2 = \frac{2\beta(\theta_2 - \theta_1)}{\operatorname{sh}\mu_1}. \tag{5.45}$$

Let $\omega < 0$. As $\mu \to 0$, we have

$$f(\mu) \approx \frac{1}{\mu}\left[1 + \frac{\omega}{2} - \frac{\omega}{2}\,\mu\right],$$

therefore, we have to consider the cases with $1 + \omega/2 = 0$, $-2 < \omega < 0$, and $\omega < -2$.

C) Let $1 + \omega/2 = 0$, i. e., $\omega = -2$. Then, we have $f(+\infty) = 0$, $f(-\infty) = 2$, and $f \to 1$ as $\mu \to \pm 0$. According to eq. (5.44), the derivative $f'(\mu)$ at $\omega = -2$ has the form

$$f'(\mu) = -1/\mu^2 + 4\exp(2\mu)/(\exp(2\mu) - 1)^2.$$

Does the function $f(\mu)$ have local extreme points? We can calculate that $f'(\mu_*) = 0$ if and only if $|\operatorname{sh}\mu_*| = |\mu_*|$. The latter equality is satisfied only at $\mu_* = 0$, but in our case we have $f(0) = 1$ at the point $\mu = 0$. The derivative is $f'(\mu) \le 0$ (it is equal to

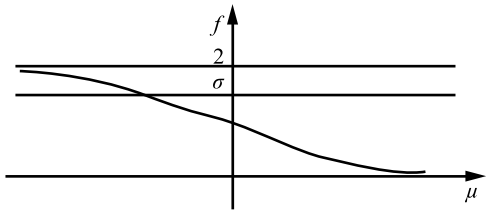

Figure 5.3: Function f vs μ for $\omega = -2$.

zero only at $\mu = 0$); therefore, the function $f(\mu)$ decreases over the entire axis, i. e., the unique solution of eq. (5.43) at $\omega = -2$ is μ_1, and it exists only at $0 < \sigma < 2$. This means that there exist uniquely determined constants c_1 and c_2 for the indicated values of σ (Figure 5.3).

D) Let $1+\omega/2 > 0$, i. e., $\omega > -2$. Then, we have $f(\mu) \sim (1+\omega/2)/\mu$. The function $f(\mu)$ has a discontinuity at the point $\mu = 0$, and $f(\pm 0) = \pm\infty$. If $f'(\mu_*) = 0$, then we consider the following cases: **D1)** $-2 < \omega < 0$ and **D2)** $\omega > 0$. The latter case reduces to the case **B1)**.

In the case **D1)** we have $-\omega = |\omega|$. Let us consider the equation $f'(\mu) = 0$:

$$f'(\mu) = -\frac{1}{\mu^2} + \frac{|\omega|}{2\,\mathrm{sh}^2\,\mu} = 0. \tag{5.46}$$

The derivative is equal to zero only at $\mathrm{sh}^2\,\mu_* = |\omega|\mu_*^2/2$ ($\mu_* \neq 0$). Note that if μ is a solution of eq. (5.46), then $-\mu$ is also a solution for eq. (5.46). We assume that $\mu_* > 0$. Then, we have $\mathrm{sh}\,\mu_* = \sqrt{|\omega|/2}\,\mu_*$. We can easily show that the solution for eq. (5.46) exists only at $|\omega| > 2$; as $-2 < \omega < 0$, the latter equation has no solutions. Thus, $f'(\mu)$ does not change its sign in the domain of its definition, $f'(\mu) < 0$, and $f(\mu)$ decreases. If $0 < \sigma < -\omega$, then eq. (5.43) has two solutions: $\mu_1 > 0$ and $\mu_2 < 0$. Therefore, there exist two pairs of constants (c_1^1, c_2^1) and (c_1^2, c_2^2). If $\sigma \geq -\omega$, then eq. (5.43) has one solution (Figure 5.4).

E) Now let $1 + \omega/2 < 0$, i. e., $\omega < -2$ and $-\omega = |\omega|$. The function is $f(\mu) \sim (1 + \omega/2)/\mu$; as $\mu \to 0$, in accordance with the definition, the functions are $f(+0) \to -\infty$ and

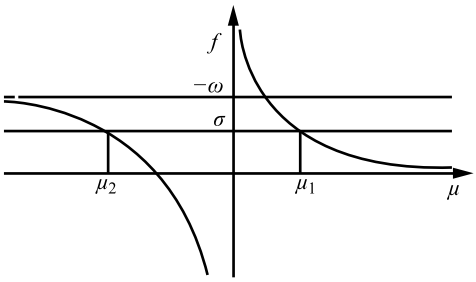

Figure 5.4: Function f vs μ for $-2 < \omega < 0$.

$f(-0) \to +\infty$. We can easily show that the solutions of the equation

$$f'(\mu) = \frac{1}{\mu^2 \operatorname{sh}^2 \mu}\left[\frac{|\omega|}{2}\mu^2 - \operatorname{sh}^2 \mu\right] = 0$$

are $\mu_* > 0, -\mu_*$, if the inequality $|\omega| > 2$ is satisfied.

Thus, we have $f(-\mu_*) = -1/\mu_* - |\omega|(\exp(-2\mu_*) - 1)$ and $f(\mu_*) = \omega(\exp(2\mu_*) - 1) + 1/\mu_*$. Generally speaking, eq. (5.43) at $f(-\mu_*) < f(\mu_*)$ may have four solutions if $f(-\mu_*) < \sigma < f(\mu_*)$. Let us demonstrate that $f(\mu_*) < f(-\mu_*)$. In other words, we have to verify that $2/\mu_* < |\omega| \operatorname{cth} \mu_*$. The latter inequality is equivalent to $\operatorname{th} \mu_* < |\omega|\mu_*/2$ ($\mu_* > 0$). To verify this inequality, we consider the function $h(\mu) = \operatorname{th} \mu - |\omega|\mu/2$. We have $h(0) = 0$, $h'(\mu) = 1/\operatorname{ch}^2 \mu - |\omega|/2$. Let us check the sign of the derivative at the point $\mu = 0$: obviously, $h'(0) = 1 - |\omega|/2 < 0$. Moreover, as $\operatorname{ch} \mu > 1$, we have $h'(\mu) < 0$, i. e., the function $h(\mu)$ decreases. Therefore, we obtain $h(\mu) < 0$ for all values $\mu > 0$, i. e., $\operatorname{th} \mu_* < |\omega|\mu_*/2$ or, which is the same, $f(\mu_*) < f(-\mu_*)$. Thus, if $f(\mu_*) < \sigma < f(-\mu_*)$, then eq. (5.43) has no solutions. If $f(-\mu_*) < \sigma < -\omega$ or $0 < \sigma < f(\mu_*)$, then eq. (5.43) has two solutions. At $\sigma = f(\mu_*)$, $\sigma = f(-\mu_*)$, or $\sigma \geq -\omega$, this equation has one solution (Figure 5.5).

Let us check whether conditions responsible for nonuniqueness of solutions of eq. (5.43) are satisfied. The inequality $\sigma < -\omega$ should be valid for all cases considered:

$$(1 + \beta\theta_1)\frac{\chi}{u_0 a} < -\frac{\beta\chi(\theta_2 - \theta_1)}{u_0 a}, \tag{5.47}$$

whence we obtain $\theta_2 < 0$. Thus, none of the conditions at which eq. (5.43) can have two solutions is satisfied. Therefore, eq. (5.43) has only one solution for all possible values of θ_1 and θ_2. The unique values of c_1 and c_2 are determined from eq. (5.45).

Taking $\Theta(x)$ in the form (5.28) with the indicated values of c_1 and c_2, we project eq. (5.10) onto the y axis. As a result, we obtain the equation for determining the vertical velocity component v:

$$\left(\frac{1}{c_1} + c_2 \exp(kx)\right)\nu v_{xx} - c_1 c_2 u_0 \exp(kx) v_x = f(x), \tag{5.48}$$

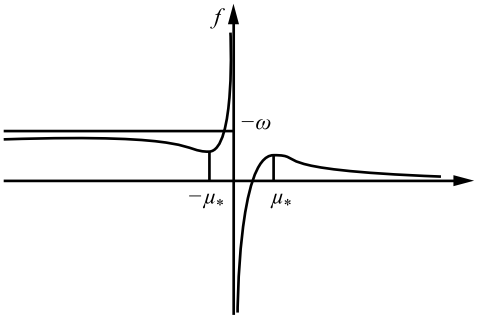

Figure 5.5: Function f vs μ for $\omega < -2$.

$$k = \frac{c_1 u_0}{\chi}, \quad f(x) = \varphi\left(\frac{1}{c_1} + c_2 \exp(kx)\right) - g\left(\frac{1}{c_1} - 1 + c_2 \exp(kx)\right).$$

After the replacement $z = 1 + c_1 c_2 \exp(kx)$, the general solution of eq. (5.48) has the form

$$v = \int_{h_1}^{z} \frac{z^\alpha}{z-1}\left[\frac{\varphi - g}{\nu k^2}\int \frac{dz}{z^\alpha(z-1)} + \frac{g c_1}{\nu k^2}\int \frac{dz}{z^{\alpha+1}(z-1)} + D_1\right]dz + D_2, \tag{5.49}$$

where D_1 and D_2 are constants, $h_1 = 1 + c_1 c_2 \exp(-ak)$, $\alpha = \chi/\nu \equiv 1/\mathrm{Pr}$.

The unknown constant φ is determined from eq. (5.34):

$$\varphi = g(1 - c_1 F_1) - D_1 \nu k^2 F_2, \tag{5.50}$$

$$F_1 = \frac{\int_{h_1}^{h_2} \frac{1}{z}\int_{h_1}^{z} \frac{\sigma^\alpha}{\sigma-1}\int_{h_1}^{\sigma} \frac{d\tau}{\tau^{\alpha+1}(\tau-1)}\, d\sigma dz}{\int_{h_1}^{h_2} \frac{1}{z}\int_{h_1}^{z} \frac{\sigma^\alpha}{\sigma-1}\int_{h_1}^{\sigma} \frac{d\tau}{\tau^{\alpha}(\tau-1)}\, d\sigma dz},$$

$$F_2 = \frac{\int_{h_1}^{h_2} \frac{1}{z}\int_{h_1}^{z} \frac{\sigma^\alpha}{\sigma-1}\, d\sigma dz}{\int_{h_1}^{h_2} \frac{1}{z}\int_{h_1}^{z} \frac{\sigma^\alpha}{\sigma-1}\int_{h_1}^{\sigma} \frac{d\tau}{\tau^{\alpha}(\tau-1)}\, d\sigma dz}.$$

The integration constants D_1 and D_2 are found from the no-slip condition on the motionless solid wall: $D_2 = 0$ and

$$D_1 = \frac{\frac{c_1 F_1}{\nu k^2}\int_{h_1}^{h_2} \frac{z^\alpha}{z-1}\int_{h_1}^{z} \frac{d\sigma}{\sigma^\alpha(\sigma-1)}\, dz - \frac{g c_1}{\nu k^2}\int_{h_1}^{h_2} \frac{z^\alpha}{z-1}\int_{h_1}^{z} \frac{d\sigma}{\sigma^{\alpha+1}(\sigma-1)}\, dz}{\int_{h_1}^{h_2} \frac{z^\alpha}{z-1}\, dz - F_2 \int_{h_1}^{h_2} \frac{z^\alpha}{z-1}\int_{h_1}^{z} \frac{d\sigma}{\sigma^\alpha(\sigma-1)}\, dz},$$

where $h_2 = 1 + c_1 c_2 \exp(ak)$.

To compare the solution obtained for the vertical component with a similar solution of the steady problem in the classical formulation, we write eq. (5.49) in the dimensionless form. For this purpose, we introduce the dimensionless parameter $\gamma_1 = ak$ and, performing the replacement $z = 1 + c_1 c_2 \exp(\gamma_1 \eta)$, obtain

$$v_n = \frac{\nu k^2}{g}\, v(\eta), \ -1 \le \eta \le 1, \tag{5.51}$$

where

$$v(\eta) = \int_{-1}^{\eta} (1 + c_1 c_2 \exp(ak\eta))^\alpha \left[\frac{\varphi - g}{\nu k^2}\int \frac{d\sigma}{(1 + c_1 c_2 \exp(ak\sigma))^\alpha} + H(\eta) + D(\eta)\right]d\eta, \tag{5.52}$$

$$H(\eta) = \frac{g c_1}{\nu k^2}\int \frac{d\sigma}{(1 + c_1 c_2 \exp(ak\eta))^{\alpha+1}},$$

$$D(\eta) = -\frac{1}{\int_{-1}^{1} (1 + c_1 c_2 \exp(ak\eta))^\alpha d\eta}$$

$$\times \left[\frac{\varphi - g}{\nu k^2} \int_{-1}^{1} (1 + c_1 c_2 \exp(ak\eta))^{\alpha} \int_{-1}^{\eta} \frac{d\sigma}{(1 + c_1 c_2 \exp(ak\sigma))^{\alpha}} \, d\eta \right.$$
$$\left. + \frac{g c_1}{\nu k^2} \int_{-1}^{1} (1 + c_1 c_2 \exp(ak\eta))^{\alpha} \int_{-1}^{\eta} \frac{d\sigma}{(1 + c_1 c_2 \exp(ak\sigma))^{\alpha+1}} \, d\eta \right].$$

The velocity profiles are illustrated in Figure 5.6. The solid curves show the velocities for $a = 4$. It is seen that the maximum value $v_{\max}$ increases with increasing temperature difference. A typical feature of eq. (5.51) is the shift of the value $v_{\max}$ toward the heated wall. The calculations were performed for silicon melts with $u_0 = 1$.

The following values were obtained:

1) $a = 4$ and $\Delta\Theta = 10$:

$$c_1 = 9.8741051593 \cdot 10^{-1}, \quad c_2 = 9.4731241528 \cdot 10^{-8},$$
$$\varphi = 1.2338930230 \cdot 10^{-1}, \quad D_1 = 7.4033132577 \cdot 10^{-3};$$

2) $a = 4$ and $\Delta\Theta = 50$:

$$c_1 = 9.8741051596 \cdot 10^{-1}, \quad c_2 = 4.7365620753 \cdot 10^{-7},$$
$$\varphi = 1.2343666848 \cdot 10^{-1}, \quad D_1 = 4.1672399233 \cdot 10^{-2};$$

3) $a = 4$ and $\Delta\Theta = 80$:

$$c_1 = 9.8741051598 \cdot 10^{-1}, \quad c_2 = 7.5784993191 \cdot 10^{-7},$$
$$\varphi = 1.2347011449 \cdot 10^{-1}, \quad D_1 = 7.2380171987 \cdot 10^{-2};$$

4) $a = 2$ and $\Delta\Theta = 10$:

$$c_1 = 9.8741053902 \cdot 10^{-1}, \quad c_2 = 5.3326654478 \cdot 10^{-6},$$

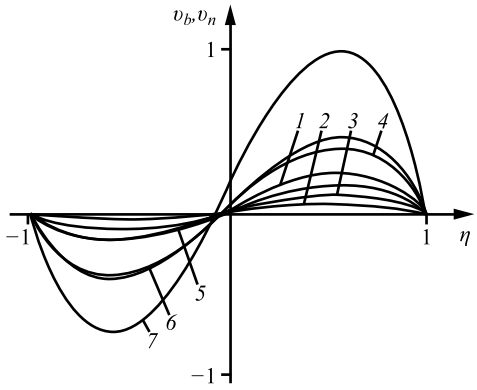

Figure 5.6: Velocity profiles given by (5.40) and (5.32).

$$\varphi = 1.2343236676 \cdot 10^{-1}, \quad D_1 = 1.2276678568 \cdot 10^{-2};$$

5) $a = 2$ and $\Delta\Theta = 50$:

$$c_1 = 9.8741063141 \cdot 10^{-1}, \quad c_2 = 2.6663317178 \cdot 10^{-5},$$
$$\varphi = 1.2364533464 \cdot 10^{-1}, \quad D_1 = 6.7828046692 \cdot 10^{-2};$$

6) $a = 2$ and $\Delta\Theta = 80$:

$$c_1 = 9.8741070070 \cdot 10^{-1}, \quad c_2 = 4.2661295412 \cdot 10^{-5},$$
$$\varphi = 1.2379651505 \cdot 10^{-1}, \quad D_1 = 1.1615778966 \cdot 10^{-1}.$$

5.4 Solvability of a nonstandard boundary-value problem

1. Formulation of the problem

Finding the invariant solution of the microconvection problem (5.6)–(5.8) in a vertical band reduces to solving nonstandard initial-boundary problems. The methods developed in [17, 116, 174] allow us to prove unique solvability of each problem under appropriate conditions of smoothness and compatibility of initial and boundary data.

The initial-boundary problems for the nonlinear heat-conduction equation and the y component of velocity have the form

$$\Pr T_t + \varepsilon(U + T_x)T_x = (1 + \varepsilon T)T_{xx}, \tag{5.53}$$
$$T(x,0) = T_0(x), \quad |x| \le 1; \quad T_x(-1,t) = T_x(2,t) = -U(t), \quad t \ge 0, \tag{5.54}$$
$$v_t + \frac{\varepsilon}{\Pr}(U + T_x)v_x = (1 + \varepsilon T)(v_{xx} - \varphi) + \varepsilon T g, \tag{5.55}$$
$$v(x,0) = v_0(x), \quad |x| \le 1; \quad v(-1,t) = v(1,t) = 0, \quad t \ge 0. \tag{5.56}$$

As the quantity $T_x(\pm 1, t)$ is proportional to the heat flux on the boundary, which is assumed to be given, then, based on problem (5.53), the function $U(t)$ can also be assumed to be given. The function φ satisfies the relation

$$\varphi(t) = \frac{1}{2}\big(v_x(1,t) - v_x(-1,t)\big) + \frac{\varepsilon}{2}\int_{-1}^{1} \frac{T_0}{1 + \varepsilon T_0}\,dx. \tag{5.57}$$

Let the conditions

$$U(t) \in C^{1+\alpha/2}\big([0,t_f]\big), \quad T_0(x) \in C^{3+\alpha}\big([-1,1]\big), \quad v_0(x) \in C^{2+\alpha}\big([-1,1]\big), \tag{5.58}$$

be satisfied for an arbitrary finite value of t_f. We use the compatibility conditions in the form

$$\begin{gathered} -U(0) = T_{0x}(\pm 1), \\ \frac{1}{\mathrm{Pr}}[1+\varepsilon T_0(\pm 1)]T_{0xxx}(\pm 1) + U'(0) = 0, \\ v_0(\pm 1) = 0, \quad (1+\varepsilon T_0(\pm 1))[v_{0xx}(\pm 1) - \varphi(0)] + \varepsilon T_0(\pm 1)g = 0, \\ \varphi(0) = \frac{1}{0}(v_{0x}(1) - v_{0x}(-1)) + \frac{\varepsilon}{2}\int\limits_{-1}^{1} \frac{T_0}{1+\varepsilon T_0}dx. \end{gathered} \tag{5.59}$$

2. Solvability of initial-boundary problems for the heat-conduction equation and loaded equation

If we seek the functions T and v in the form of expansions into series in powers of the small parameter ε, then the expansion of the function T in powers of ε begins from the zero-th-order term, and the expansion of the function v begins from the first-order term:

$$T = \sum_{k=1}^{\infty} \varepsilon^k T^{(k)}, \quad v = \sum_{k=1}^{\infty} \varepsilon^k v^{(k)}. \tag{5.60}$$

The principal terms of the expansions are solutions of the problem

$$\begin{gathered} \mathrm{Pr}\, T_t^{(0)} = T_{xx}^{(0)}, \quad T^{(0)}(x,0) = T_0(x), \\ T_x^{(0)}(-1,t) = T_x^{(0)}(1,t) = -U(t), \end{gathered} \tag{5.61}$$

$$v_t^{(1)} = v_{xx}^{(1)} - \frac{1}{2}\left[v_x^{(1)}(1,t) - v_x^{(1)}(-1,t) + \int\limits_{-1}^{1} T_0 dx\right] + gT^{(0)}, \tag{5.62}$$

$$v^{(1)}(x,0) = v_0(x), \quad v^{(1)}(-1,t) = v^{(1)}(1,t) = 0 \tag{5.63}$$

with compatibility conditions that follow from conditions (5.59) as a result of their splitting in terms of ε.

The function $T^{(0)}$ is a solution of the standard problem for the heat-conduction equation (5.61); the issue of its solvability can be studied with the known approach [116].

For the function $v^{(1)}$, the issue of solvability of problem (5.62), (5.63) in the general case is rather difficult. Similar equations (5.62) have been called in [145] the loaded ones. This problem is nonstandard because of the presence of the derivative of the sought function at the boundary points; it will be studied with an additional representation of $v^{(1)}$ in the form of an expansion into even and odd components.

Note that all remaining functions $T^{(k)}$ and $v^{(k)}$ can be determined in a recurrent manner as solutions of the following boundary-value problems:

$$\Pr T_t^{(k)} = T_{xx}^{(k)} - U(t)T_x^{(k-1)} + \sum_{j=0}^{k-1}\left[T_x^{(j)}T_{xx}^{(k-1-j)} - T_x^{(j)}T_x^{(k-1-j)}\right], \tag{5.64}$$

$$T^{(k)}(x,0) = 0, \quad T_x^{(k)}(-1,t) = T_x^{(k)}(1,t) = 0; \quad k \geq 1,$$

$$\begin{aligned} v_t^{(k)} = v_{xx}^{(k)} &- \frac{1}{4}\left[v_x^{(k)}(1,t) - v_x^{(k)}(-1,t)\right] - \frac{1}{2}\int_{-1}^{1}(-1)^{k-1}T_0^k\,dx \\ &- \frac{1}{\Pr}(U + T_x^{(0)})v_x^{(k-1)} - \frac{1}{2}\sum_{j=0}^{k-2}T^{(j)}v_x^{(k-1-j)}|_{-1}^{1} \\ &- \frac{1}{2}\sum_{j=0}^{k-1}T^{(k-1-j)}\int_{-1}^{1}(-1)^{j-1}T_0^j\,dx - \frac{1}{\Pr}\left[\sum_{j=1}^{k-2}T_x^{(j)}v_x^{(k-1-j)}\right] \\ &+ \sum_{j=0}^{k-2}T^{(j)}v_{xx}^{(k-1-j)} + gT^{(k-1)}, \end{aligned} \tag{5.65}$$

$$v^{(k)}(x,1) = 0, \quad v^{(k)}(-1,t) = v^{(k)}(1,t) = 0; \quad k \geq 2.$$

The necessary compatibility conditions are satisfied thereby as a consequence of conditions (5.59).

Solvability of initial-boundary problems for the principal terms of the expansion

Let us introduce brief notations for some spaces extensively used below:

$$\tilde{C}^m = C^{m+\alpha,(m+\alpha)/2}\left([-1,1]\times[0,t_f]\right), \quad m = 2,3.$$

If conditions (5.58) and compatibility conditions (5.59) are satisfied, the boundary-value problem (5.53) for temperature is solvable, and $T^{(0)} \in \tilde{C}^3$ [116].

Further, let $v^{(1)} = v_1 + v_2$, where v_1 and v_2 are the even and odd components of the velocity $v^{(1)}$ in terms of the variable x. For v_2, we have the classical first boundary-value problem

$$v_{2t} = v_{2xx} + \overline{F}_2(x,t), \quad t \in [0,t_f], \quad x \in [-1,1];$$
$$v_2(x,0) = v_{20}(x), \quad v_2(\pm 1,t) = 0.$$

Here, $\overline{F}_2(x,t)$ and $v_{20}(x)$ are the odd components of the functions $\int_{-1}^{1}T_0(x)dx + gT^{(0)}(x,t)$ and $v_0(x)$, respectively.

Solvability of the problem for v_2 can be proved by using the known procedure [116]. In this case, the function $v_2(x,t)$ belongs at least to the class $\tilde{C}^2$, as $v_{20}(x) \in C^{2+\alpha}([-1,1])$, and $\overline{F}_2(x,t) \in \tilde{C}^3$.

Let us consider the problem for the even component of velocity, where the equation has the nonlocal derivative:

$$v_{1t} = v_{1xx} - v_{1x}(1,t) + \overline{F}_1(x,t), \quad t \in [0,t_f], \quad x \in [-1,1], \tag{5.66}$$

$$v_1(x,0) = v_{10}(x), \quad |x| \le 1, \tag{5.67}$$

$$v_1(-1,t) = v_1(1,t) = 0, \quad t \ge 0. \tag{5.68}$$

Here $\overline{F}_1 = \overline{F}_1(x,t)$ is the even component of the function $\int_{-1}^{1} T_0(x)dx + gT^{(0)}(x,t)$ of the class $\tilde{C}^3$ in eq. (5.62). The initial function $v_{10}(x)$ (even components of the initial velocity) is a function of the class $C^{2+\alpha}([-1,1])$. In this case, in particular, the equality $v_{10}(\pm 1) = 0$ is satisfied, owing to the conditions $v_0(\pm 1) = 0$ (see the corresponding condition (5.59)).

We expand the function v_1 into a generalized Fourier series with due allowance for its evenness, so that the boundary conditions (5.68) are automatically satisfied, namely,

$$v_1 = \sum_{n=0}^{\infty} u_n(t)\cos(\lambda_n x), \quad \lambda_n = \pi\left(n + \frac{1}{2}\right).$$

Taking into account orthonormality of the functions $\cos\lambda_n x$ on the segment $[-1,1]$, we write eq. (5.66) in the form

$$\sum_{n=0}^{\infty} \left[u_n'(t) + \lambda_n^2 u_n(t) + e_n f(t) - F_n(t)\right]\cos\lambda_n x = 0 \tag{5.69}$$

where $f(t)$ is an unknown function of the derivative of the sought function on the boundary $f(t) = v_{1x}(1,t)$. It follows from eq. (5.69) that the following representation is valid for all values of n:

$$u_n(t) = C_n \exp(-\lambda_n^2 t) + \int_0^t \left(-e_n f(\tau) + F_n(\tau)\right)\exp(-\lambda_n^2(t-\tau))\, d\tau. \tag{5.70}$$

The following notations are introduced for the generalized coefficients of the Fourier expansions of the unity, the right-hand side of eq. (5.66), and the initial function (5.67) into a series in $\cos\lambda_n x$:

$$e_n = (-1)^n \frac{2}{\lambda_n}, \quad F_n(t) = 2\int_0^1 \overline{F}_1(x,t)\cos\lambda_n x\, dx,$$

$$C_n = 2\int_0^1 v_{10}(x)\cos\lambda_n x\, dx.$$

The properties of the Fourier coefficients are determined by the properties of the corresponding functions for which expansions are obtained; they will be taken into account below. We should also note that

$$f(t) = \sum_{n=0}^{\infty} (-1)^{n+1} \lambda_n u_n(t), \quad f(0) = \sum_{n=0}^{\infty} (-1)^{n+1} \lambda_n C_n.$$

We multiply each equation of system (5.70) by $(-1)^{n+1}\lambda_n$ and sum up in terms of n from 0 to ∞. Then, for finding the function $f(t)$, we have the integral equation

$$f(t) = 2 \int_0^t f(\tau) \sum_{n=0}^{\infty} \exp(-\lambda_n^2 (t-\tau)) d\tau + Q(t) \tag{5.71}$$

where

$$Q(t) = \sum_{n=0}^{\infty} \left[(-1)^{n+1} \lambda_n \left(C_n \exp(-\lambda_n^2 t) + \int_0^t F_n(\tau) \exp(-\lambda_n^2 (t-\tau))\, d\tau \right) \right]. \tag{5.72}$$

In this case, we have $Q(0) = f(0)$, and the kernel of the integral equation is a function of the form

$$K(z) = \sum_{n=0}^{\infty} \exp(-\lambda_n^2 z); \quad z = t - \tau, \quad \tau \in [0, t], \quad t \in [0, t_f]. \tag{5.73}$$

It should be noted that kernel convergence is equivalent to convergence of the improper integral

$$\int_0^{\infty} \exp\left(-\pi^2 \left(x + \frac{1}{2} \right)^2 z \right) dx = \frac{1}{2\sqrt{\pi z}} - \frac{1}{2\sqrt{\pi z}} \Phi\left(\frac{\pi \sqrt{z}}{2} \right);$$

$$\Phi(\alpha) = \frac{2}{\sqrt{\pi}} \int_0^{\alpha} \exp(-y^2) dy.$$

Here, $\Phi(\alpha)$ is the Laplace function [53]. The second term is a smooth function at $z \geq 0$. Representing series (5.73) as an integral of the stepwise function

$$c(z, x) = c_n, \quad n \leq x < n+1, \ n = 0, 1, \ldots; \quad c_n = \exp\left(-\pi^2 \left(\frac{2n+1}{2} \right)^2 z \right)$$

we can obtain the estimate

$$0 \leq \int_0^{\infty} c(z, x)\, dx - \frac{1}{2\sqrt{\pi z}} + \frac{1}{2\sqrt{\pi z}} \Phi\left(\frac{\pi \sqrt{z}}{2} \right) \leq \frac{1}{\sqrt{\pi z}} \Phi\left(\frac{\pi \sqrt{z}}{2} \right)$$

which allows us to identify a weak singularity of the form $1/\sqrt{z}$ from kernel (5.73) and rewrite eq. (5.71) in the form

$$f(t) = \lambda \int_0^t \frac{f(\tau)}{\sqrt{t-\tau}} d\tau + \overline{Q}(t), \quad \overline{Q}(t) = \int_0^t L(t-\tau) f(\tau) d\tau + Q(t). \tag{5.74}$$

Here, $\lambda = 1/(2\sqrt{\pi})$, and $L(t-\tau)$ is the smooth component of the polar kernel. Equation (5.74) refers to the Volterra integral equations of the second kind of the Abel type [169, 224]. Iteration of the kernel component $\mathcal{K}(t,\tau) = 1/\sqrt{t-\tau}$ of the integral equation (5.74) yields the expression $\mathcal{K}_2(t,\tau) = \int_\tau^t \frac{ds}{\sqrt{t-s}\sqrt{s-\tau}} = \pi$. Using the composition of both sides of eq. (5.74) and the function $\lambda\mathcal{K}(t,\tau)$, we obtain the Volterra equation

$$f(t) = \lambda^2 \pi \int_0^t f(\tau) d\tau + Q_2(t) \tag{5.75}$$

with a bounded kernel consisting of $\mathcal{K}_2(t,\tau)$ and the result of the composition of $\int_0^t L(t-\tau) f(\tau) d\tau$ and $\lambda\mathcal{K}(t,\tau)$, where $Q_2(t) = \overline{Q}(t) + \lambda^2 \int_0^t \frac{\overline{Q}(s)}{\sqrt{t-s}} ds$. Solving eq. (5.75), we obtain a solution of the initial equation (5.74). Note that the Fourier coefficients C_n and $F_n(t)$ of the functions $v_{10}(x) \in C^{2+\alpha}([-1,1])$ ($v_{10}(\pm 1) = 0$) and $\overline{F}_1(x,t) \in \tilde{C}^3$ possess properties that ensure convergence of the integrals in relation (5.72) owing to validity of the inequalities $|C_n| \le M_C/n^3$, $|F_n(t)| \le M_F/n$ [213]. Based on these estimates, we conclude that the series in relation (5.72) converge, because there are converging majorant series of the form $\sum_{n=1}^{\infty} \overline{M}_C/n^2$ and $\sum_{n=1}^{\infty} \overline{M}_F/n^2$, respectively, at $t \ge 0$ and $x \in [-1,1]$, whence it follows that $Q(t) \in C^{2+(1+\alpha)/2}[0, t_f]$ (this is ensured by the properties of the function $\overline{F}_1$).

Thus, the integral equation (5.75) is solvable [224]. The function $f(t)$ belongs at least to the class $C^{1+\alpha/2}([0, t_f])$, which allows us to argue that problem (5.66)–(5.68) is solvable in the class of functions $\tilde{C}^2$, in accordance with the known results [116].

The solution of problem (5.53), (5.55), which can be represented by the power series (5.60), is consecutively determined by the solutions of problems (5.61), (5.62) and (5.64), (5.65). A principally important issue of the proof of solvability of problem (5.66)–(5.68) for the higher approximation in terms of $v^{(1)}$ is the search for the solution in the form of the sum of the odd and even components and the subsequent method of determining the function $f(t)$. The kernel of the integral equation for finding $f(t)$ is determined by the structure of the preceding differential equation, and the properties of smoothness of the sought function mainly depend on smoothness of the corresponding approximation for temperature. By means of induction, solvability of the recurrent boundary-value problems (5.64), (5.65) in the Hölder classes $\tilde{C}^m$ can be proved by the method demonstrated above. We require that the initial temperature $T_0 = T_0(x)$ should satisfy the inequality

$$C_0 = |T_0|^{3+\alpha} \le 1. \tag{5.76}$$

For series (5.60), we can construct majorant power series, which are obtained by replacing $T^{(k)}$ and $v^{(k)}$ by their norms in the spaces $C^{(3+\alpha)}$ and $C^{(2+\alpha)}$, respectively. The series converge if the condition $\varepsilon \in [0, \tilde{\varepsilon}]$ is satisfied. Thus, series (5.60) converges to the solution of problems (5.53), (5.55) only if $\varepsilon \in [0, \tilde{\varepsilon}]$ ($\tilde{\varepsilon}$ is determined during the proof).

Thus, we obtain the following theorem.

Theorem 5.1. *Let conditions* (5.58), (5.59), *and* (5.76) *be satisfied. There then exists* $\tilde{\varepsilon} > 0$ *such that problems* (5.53) *and* (5.55) *at* $0 \le \varepsilon \le \tilde{\varepsilon}$ *have a solution of the form*

$$v^{(1)} \in C^{2+\alpha,1+\alpha/2}([-1,1] \times [0,t_f]), \quad T^{(0)} \in C^{3+\alpha,(3+\alpha)/2}([-1,1] \times [0,t_f])$$

This solution is an analytical function of the parameter ε *at the point* $\varepsilon = 0$.

Uniqueness of the solution can be found by the proof by contradiction.

5.5 Unsteady solution of microconvection equations in an infinite band

Let us consider system (5.6)–(5.8) for the microconvection model. We denote the Cartesian coordinates in space by x, y, z, so that $\mathbf{g} = (0, -g, 0)$, and the fluid is located in the layer $|x| \le a$ with a specified heat flux on the solid boundaries of this layer. If the heat flux value is independent of z, then plane flows can exist in the vertical layer. These flows occur if the initial velocity and temperature distributions are independent of z, and the third velocity component is equal to zero. We consider a special class of solutions of the system of microconvection equations that are invariant with respect to the operator $\partial/\partial y + \varphi(t)\,\partial/\partial q$, where $\varphi(t)$ is an arbitrary function of time (see Section 5.3, where a steady case was studied). Solutions such as these have the form

$$\begin{aligned} &\mathbf{W} = (u, v), \quad u = U(t), \quad v = v(x,t), \\ &\theta = \theta(x,t), \quad q = \big(\varphi(t) - g\big)y + h(x,t). \end{aligned} \tag{5.77}$$

Let us write the problem formulation for the sought functions of velocity v and temperature θ in the dimensionless form, using the characteristic length $l = a$, characteristic time $t_* = l^2/\nu$, characteristic velocity $U_* = \varepsilon\chi/a$, and characteristic temperature T_*, introducing the dimensionless parameters $\mathrm{Pr} = \nu/\chi$ (Prandtl number) and $\varepsilon = \beta T_*$ (Boussinesq number), and indicating the dimensionless temperature by T:

$$v_t + \frac{\varepsilon}{\mathrm{Pr}}(U + T_x)v_x = (1 + \varepsilon T)\big(v_{xx} - \varphi(t)\big) + \varepsilon T g, \tag{5.78}$$

$$\varphi(t) = \frac{1}{2}\big(v_x(1,t) - v_x(-1,t)\big) + \frac{\varepsilon}{2}\int_{-1}^{1} \frac{T_0}{1 + \varepsilon T_0}\,dx,$$

$$v = v_0(x), \quad t = 0, \quad |x| \le 1,$$

$$
\begin{gathered}
v(-1,t) = v(1,t) = 0, \quad t \geq 0. \\
\Pr T_t + \varepsilon(U + T_x)T_x = (1 + \varepsilon T)T_{xx}, \\
T = T_0(x), \quad t = 0, \quad |x| \leq 1, \\
T_x(-1,t) = T_x(1,t) = -U(t), \quad t \geq 0.
\end{gathered} \tag{5.79}
$$

The initial velocity $v_0(x)$ and initial temperature $T_0(x)$ are known functions. The value of T_x, proportional to the heat flux on the interface between the fluid and the solid, is also assumed to be specified. Then, the function $U(t)$ can also be considered as being specified. Independence of the heat flux on the layer boundaries $x = \pm a$ of the coordinate y is conditioned by the structure of the invariant solution. If the problem for temperature is solved, then the coefficients of the linear equation with respect to v are known, and the free term also becomes known if $\varphi(t)$ is specified. The natural problem for this equation is the first initial-boundary problem with conditions that are no-slip conditions for the original physical velocity.

Finding an invariant solution of the problem of convection in a vertical band reduces to solving the second boundary-value problem for the nonlinear heat-conduction equation (5.79) and the subsequent solving of the first boundary-value problem for the linear equation (5.78). Note that eq. (5.78) is not differential in the usual meaning. Solvability of problems (5.78) and (5.79) in classes of the Hölder functions was proved in [77].

To construct the asymptotic solution, we choose the Boussinesq number as a small parameter ε ($T_* = \max_{x\in(-a,a)} T_0$). Then, the principal terms of the expansions $T = \sum_{k=0}^{\infty} \varepsilon^k T^{(k)}$, $v = \sum_{k=1}^{\infty} \varepsilon^k v^{(k)}$ are solutions of the following problems:

$$
\begin{gathered}
\Pr T_t^{(0)} = T_{xx}^{(0)}, \\
T^{(0)}(x,0) = T_0(x), \quad T_x^{(0)}(-1,t) = T_x^{(0)}(1,t) = -U(t).
\end{gathered} \tag{5.80}
$$

$$
\begin{gathered}
v_t^{(1)} = v_{xx}^{(1)} - \frac{1}{2}\left[v_x^{(1)}(1,t) - v_x^{(1)}(-1,t) + \int_{-1}^{1} T_0 dx \right] + gT^{(0)}, \\
v^{(1)}(x,0) = v_0(x), \quad v^{(1)}(-1,t) = v^{(1)}(-1,t) = 0.
\end{gathered} \tag{5.81}
$$

Calculation of trajectories

Following [176, 17], let us consider periodic solutions of problems (5.80) and (5.81). Let $U(t) = \sin \gamma t$. Then, the functions $T^{(0)}$, $v^{(1)}$ have the form

$$
T^{(0)} = T_s(x)\sin \gamma t + T_c(x)\cos \gamma t, \quad v^{(1)} = v_s(x)\sin \gamma t + v_c(x)\cos \gamma t,
$$

and the components of physical velocity (which is now a dimensional quantity for convenience of further discussions) are determined as

$$
v_1 = \varepsilon \bar{v}_1 = \varepsilon(v_{1s}\sin \gamma t + v_{1c}\cos \gamma t),
$$

$$
\begin{aligned}
v_2 &= \varepsilon \bar{v}_2 = \varepsilon(v_{2s}\sin\gamma t + v_{2c}\cos\gamma t),\\
v_{1s} &= \chi a^{-1}\Delta^{-1}(\cosh\lambda a\cos\lambda a\ \cosh\lambda x\cos\lambda x\\
&\quad + \sinh\lambda a\sin\lambda a\sinh\lambda x\sin\lambda x - \Delta),\\
v_{1c} &= \chi a^{-1}\Delta^{-1}(\sinh\lambda\, a\sin\lambda a\cosh\lambda x\cos\lambda x\\
&\quad - \cosh\lambda a\cos\lambda a\sinh\lambda x\sin\lambda x),\\
v_{2s} &= \chi a^{-1}(A\sinh\lambda x\cos\lambda x + B\cosh\lambda x\sin\lambda x\\
&\quad + C\sinh\mu x\cos\mu x + D\cosh\mu x\sin\mu x),\\
v_{2c} &= \chi a^{-1}(A\sinh\lambda x\cos\lambda x - B\cosh\lambda x\sin\lambda x\\
&\quad + C\cosh\mu x\sin\mu x - D\sinh\mu x\cos\mu x).
\end{aligned}
$$

Here, $\lambda = \sqrt{\gamma/2\chi}$, $\mu = \sqrt{\gamma/2\nu}$, and the coefficients δ, Δ, A, B, C, and D are expressed in a rather complicated manner via λ, μ, χ, ν, and a; these coefficients were obtained in [17].

Knowing the functions v_1 and v_2, we can calculate the trajectories of fluid particles. For this, we need to solve the Cauchy problem

$$\frac{dx}{dt} = v_1(x,t), \quad \frac{dy}{dt} = v_2(x,t); \tag{5.82}$$

$$x = x_0, \quad y = 0 \quad \text{at} \quad t = 0. \tag{5.83}$$

Note that we should use $v_1 = 0$ in constructing the trajectories of the fluid particles by the Oberbeck–Boussinesq model, whereas the expression for $v_2 = 0$ remains unchanged. In addition, the dependence of v_2 on x, t is now exact rather than approximate.

The projections of the integral curves of system (5.82) onto the plane x, y at $\varepsilon = 0.01$ and 0.02, and $\gamma = 0.5$ and $2\,\mathrm{s}^{-1}$ [176] demonstrate helical periodic motion (with the main coil being an ellipse) of the fluid particle. As was noted in [176], the analysis of the trajectory behavior is a rather complicated task because of the variety of dimensionless parameters that affect the solution of the Cauchy problem (5.82), (5.83). We can assume, however, that the intensity of periodic motion and particle drift under the conditions of applicability of the microconvection model are primarily determined by the angular frequency γ, Boussinesq parameter ε, and, certainly, location of the point (x_0, y_0) with respect to the lateral boundaries of the domain [81]. If the values of ε are extremely small and the values of γ are commensurable with unity, we can conclude that a typical flow regime is microconvection with a slow drift of fluid particles in the vertical direction. This fact is also confirmed by the analysis of the nontrivial component of motion, which was performed in [77] on the basis of the Krylov–Bogolyubov averaging technique [39]. Let us indicate the mean value of the function f averaged

over the time t by

$$M[f(x,t)] = \lim_{T\to\infty} \frac{1}{T} \int_0^T f(x,t)\, dt.$$

Then, the system of equations in the first approximation (or the averaged system corresponding to system (5.82)) has the form

$$\frac{d\bar{x}}{dt} = \varepsilon M[\bar{v}_1], \quad \frac{d\bar{y}}{dt} = \varepsilon M[\bar{v}_2].$$

This system, however, yields a trivial result because of the zero mean for $\cos \gamma t$ and $\sin \gamma t$. To obtain a nontrivial result, we can write a system of equations in the second approximation [39] corresponding to system (5.82). Thus, for the first equation of system (5.82), the equation in the second approximation is obtained as

$$\frac{d\xi}{dt} = \varepsilon^2 M\left[\left(\tilde{X}\frac{\partial}{\partial \xi}\right)X(t,\xi)\right],$$

with the conventional notations of the averaging theory:

$$X = X_\gamma e^{i\gamma t} + X_{-\gamma} e^{-i\gamma t}, \quad \tilde{X} = \frac{e^{i\gamma t}}{i\gamma} X_\gamma + \frac{e^{-i\gamma t}}{-i\gamma} X_{-\gamma}$$
$$X_\gamma = \left(\frac{v_{1s}}{2i} + \frac{v_{1c}}{2i}\right), \quad X_{-\gamma} = \left(-\frac{v_{1s}}{2i} + \frac{v_{1c}}{2i}\right).$$

The system of equations in the second approximation, which is sometimes called the improvement of the first approximation, finally takes the form

$$\frac{d\xi}{dt} = \frac{\varepsilon^2}{2\gamma}[v_{1c}v'_{1s} - v_{1s}v'_{1c}], \quad \frac{d\zeta}{dt} = \frac{\varepsilon^2}{2\gamma}[v_{2c}v'_{2s} - v_{2s}v'_{2c}]. \tag{5.84}$$

Here, the prime indicates the derivative with respect to ξ. As the second approximation [39], we finally use

$$x = \xi + \varepsilon\frac{1}{\gamma}[v_{1c}(\xi)\sin\gamma t - v_{1s}(\xi)\cos\gamma t];$$
$$y = \zeta + \varepsilon\frac{1}{\gamma}[v_{2c}(\xi)\sin\gamma t - v_{2s}(\xi)\cos\gamma t],$$

where ξ and ζ satisfy the system of equations in the second approximation. These relations allow us to speak about an elliptical trajectory and its transformation both in time and in space. It should be noted that the issue of proximity of the solutions of the averaged and initial systems is rather delicate, because $(\bar{x},\bar{y})$ here depends on t via εt (slow time). According to [134], the proximity of the solution under the minimum assumptions about the right-hand side smoothness that ensures solvability of problem

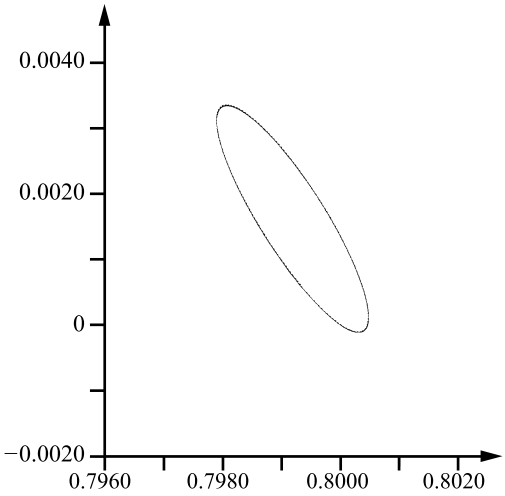

Figure 5.7: Coincidence of the particle trajectories in the time interval [0, 24] s. The particle is initially located at the point (0.8, 0). Model medium $N1$; $\varepsilon = 0.01$ and $\gamma = 0.5$.

(5.82) can be guaranteed within a certain interval of variation of t of the form $[0, t_\varepsilon]$, where $t_\varepsilon = r/L\varepsilon\sqrt{n}$, r is the distance between the initial point and the domain boundary, L is the estimate of the maximum absolute value of the right-hand side, and n is the space dimension.

Figure 5.7 illustrates the coincidence of the trajectory of the particle initially located at the point (0.8, 0), with the trajectory obtained by solving the initial system (5.82) and the system of its second approximation for the model $N1$ (see Table 5.2), but with $\varepsilon = 0.01$ and $\gamma = 0.5$ at the time of 24 s. No coincidence is observed at later times.

The trajectories of motion of fluid particles calculated by the full system (5.82) are presented in what follows. The main parameters of the problem are listed in Table 5.2. They are conventionally classified as three models with different values of Pr, η, and g. The characteristic velocities, Reynolds numbers, and durations of the process are also different (see Table 5.3). For the model $N1$, the characteristic quantities of the process are determined for $\varepsilon = 0.5$ and 0.1. To demonstrate trajectories that differ from those in [176], we choose the values $\varepsilon = 0.5$ and 0.1, $\gamma = \varepsilon$ or ε^2.

Table 5.2: Basic parameters (in the centimeter-gram-second unit system).

	Pr	η	ε	ν	χ	g	β	γ
$N1$	0.75	1	0.5; 0.1	0.15	0.2	0.03	0.0003	2; 0.5; 0.25; 0.1
$N2$	0.01	0.4	0.5	0.015	1.5	0.009	0.0006	0.5; 0.25
$N3$	0.1	0.4	0.5	0.15	1.5	0.09	0.0006	0.5; 0.25

Table 5.3: Characteristic values.

	Re	U_*	t_*
$N1$	0.67/0.13	0.1/0.02	6.67/6.67
$N2$	50	0.75	66.7
$N3$	5	0.75	6.67

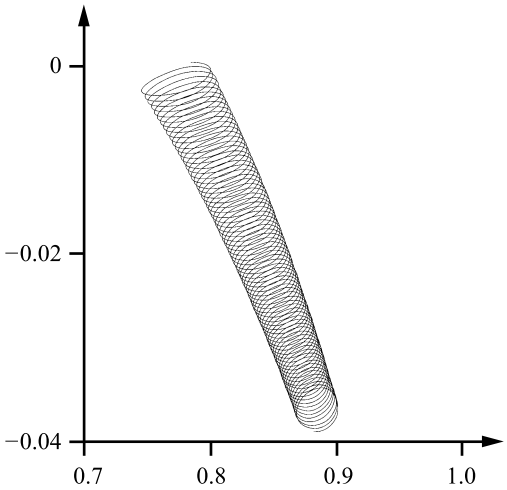

Figure 5.8: Particle trajectory in the time interval [0, 240] s. Model medium $N1$; $\varepsilon = 0.5$ and $\gamma = 2$. The particle is initially located at the point $x_0 = 0.8$; $y_0 = 0$.

Figures 5.8 (for $\varepsilon = 0.5$ and $\gamma = 2$) and 5.9 (for $\varepsilon = \gamma = 0.5$ and for $\varepsilon = 0.5$ and $\gamma = 0.25$) show the trajectories of motion of the fluid particles initially located at the points with the coordinates $x_0 = 0.3$, $y_0 = 0$ or $x_0 = 0.8$, $y_0 = 0$ up to the time $t = 240$ s.

It is of particular interest to trace the particle drift in a rather extended time interval. To demonstrate trajectories that differ from those described in [176], we choose the values $\varepsilon = 0.5$ and 0.1; $\gamma = \varepsilon$ or ε^2.

Let the fluid medium parameters be determined by the model $N1$. Figure 5.10a ($\varepsilon = \gamma = 0.5$) shows the fluid particle trajectory up to the time $t = 2400$ s. The particle is initially located at the point with the coordinates $x_0 = 0.8$; $y_0 = 0$ and demonstrates a vertical drift toward the boundary. For smaller values of ε and γ, the particle drift is less interesting from the viewpoint of differences from the trajectories studied in [176].

Figure 5.10b shows the fluid particle trajectory at the time $t = 2400$ s for $\varepsilon = \gamma = 0.5$ ($x_0 = 0.8$; $y_0 = 0$), for the fluid medium parameters being determined by the model $N2$. Firstly, it should be noted that the vertical drift changes its direction (the upward vertical motion changes to the downward motion). The motion toward the boundary is continued. Secondly, the downward motion can start earlier in time (at $\gamma = 0.25$).

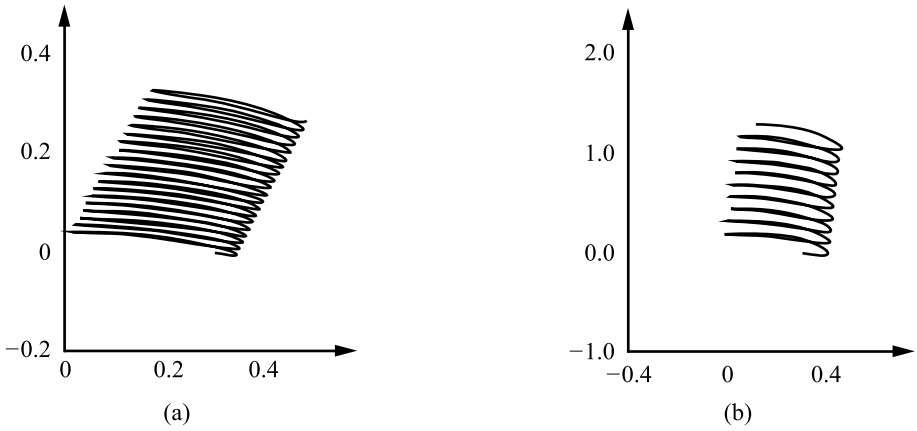

Figure 5.9: Particle trajectory in the time interval [0, 240] s. The particle is initially located at the point $x_0 = 0.3$; $y_0 = 0$. Model medium (a) $N1$; $\varepsilon = 0.5$; $\gamma = 0.5$ and (b) $\gamma = 0.25$.

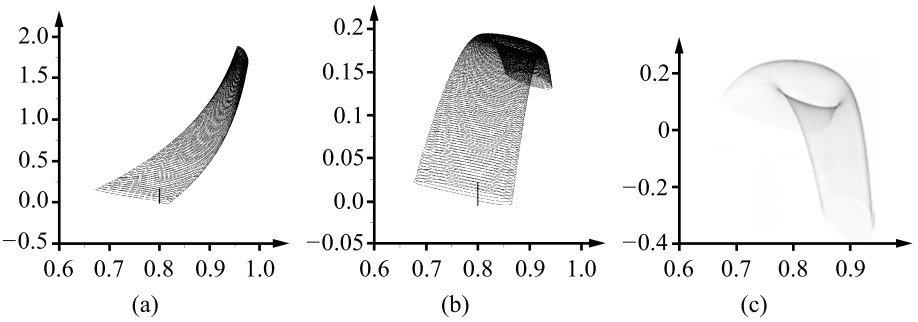

Figure 5.10: Particle trajectories in the time interval [0, 2400] s. (The trajectory calculated by the Oberbeck–Boussinesq model is a segment of the straight line $x = x_0$). The particle is initially located at the point $x_0 = 0.8$; $y_0 = 0$; $\varepsilon = \gamma = 0.5$; (a) model medium $N1$, (b) model medium $N2$, and (c) model medium $N3$.

If the fluid medium parameters are determined by the model $N3$, then the pattern at $\varepsilon = \gamma = 0.5$ is again interesting, and the upward vertical motion again changes to the downward vertical motion; this change, however, occurs much earlier than in the case illustrated in Figure 5.10b. The trajectory is plotted in Figure 5.10c. The downward drift begins immediately at $\gamma = 0.25$.

Note that the trajectories calculated by the Oberbeck–Boussinesq model and shown in Figures 5.10a and b are segments of the straight line $x = x_0$. The trajectories calculated for the linear approximation of the microconvection model demonstrate a much more complicated and versatile drift of the fluid particle.

The Cauchy problem for the systems of ordinary differential equations (5.82), (5.83) were studied numerically by the Runge–Kutta method in [103].

5.6 Invariant solutions of microconvection equations that describe the motion with an interface

1. Governing equations

Let us consider the system of microconvection equations (5.10)–(5.12). We study the motion of two immiscible incompressible fluids that obey the equations of this model and have a common interface Γ. The domains occupied by the fluids are indicated by Ω_j $(j = 1, 2)$; in what follows, the indices "1" and "2" refer to the values of the quantities $\mathbf{w}$, q, θ, and the constants in these domains.

Let the surface tension coefficient σ on the surface Γ be temperature-dependent: $\sigma = \sigma(\theta)$. For the true velocities and pressures on Γ, we have [19]

$$\mathbf{u}_1 = \mathbf{u}_2; \tag{5.85}$$

$$\theta_1 = \theta_2; \tag{5.86}$$

$$\mathbf{u} \cdot \mathbf{n} = V_n; \tag{5.87}$$

$$(T_2 - T_1)\mathbf{n} = 2\sigma K\mathbf{n} + \nabla_{II}\sigma; \tag{5.88}$$

$$k_2\frac{\partial\theta_2}{\partial n} - k_1\frac{\partial\theta_1}{\partial n} = æ\theta\nabla_{II} \cdot \mathbf{u} + \omega(\theta_t + \mathbf{u} \cdot \nabla_{II}\theta). \tag{5.89}$$

In eqs. (5.87)–(5.89), $\mathbf{n}$ is the unit vector of the external normal to Γ, which is directed from Ω_1 to Ω_2, V_n is the velocity of motion of Γ in the direction of $\mathbf{n}$,

$$T_j = -(p_j + \lambda_j \operatorname{div}\mathbf{u}_j)I + 2\rho_j\nu_j D(\mathbf{u}_j) \tag{5.90}$$

are the stress tensors in the fluids, K is the mean curvature of the surface Γ ($K > 0$ if Γ is convex outward the domain Ω_1), $\nabla_{II} = \nabla - (\mathbf{n} \cdot \nabla)\mathbf{n}$ is the surface gradient, and k_j are the constant thermal conductivity coefficients. The velocity vector and temperatures of both fluids on Γ are indicated by $\mathbf{u}$ and θ; these values coincide in pairs by virtue of eqs. (5.85) and (5.86), so that $\nabla_{II} \cdot \mathbf{u}$ is the surface divergence of the vector $\mathbf{u}$. The functions $æ(\theta)$ and $\omega(\theta)$ inserted into eq. (5.89) are determined by the equalities

$$æ = -\frac{d\sigma}{d\theta}, \quad \omega = \frac{d}{d\theta}(\sigma + æ\theta) = \theta\frac{dæ}{d\theta}. \tag{5.91}$$

For many real fluids (e. g., metal melts), the dependence $\sigma(\theta)$ in a wide range is adequately approximated by the linear function $\sigma(\theta) = \sigma_0 - \sigma_T(\theta - \theta_0)$, where $\sigma_T = \text{const} > 0$ is the temperature coefficient of surface tension. In this case, we have $æ = \sigma_T$ and, according to eq. (5.91), $\omega = 0$.

Remark 5.2. Instead of eq. (5.89), many researchers use the condition of identical heat fluxes

$$k_1\frac{\partial\theta_1}{\partial n} = k_2\frac{\partial\theta_2}{\partial n}, \tag{5.92}$$

because the contributions of the terms in the right-hand side of eq. (5.89) are usually small [184].

Remark 5.3. If Γ is implicitly defined by the equation $f(\mathbf{x}, t) = 0$, then we have

$$\mathbf{n} = \frac{\nabla f}{|\nabla f|}, \quad V_n = -\frac{f_t}{|\nabla f|}$$

and the kinematic condition (5.87) takes the following form on Γ:

$$f_t + \mathbf{u} \cdot \nabla f = 0. \tag{5.93}$$

Let the fluid indicated by "1" be a gas with the pressure p_0 and temperature θ_0. Neglecting the transport processes in the gas (passive gas), we assume that $T_1 = -p_0 I$ in eq. (5.88) and replace eq. (5.89) by the thermal contact condition

$$k_2 \frac{\partial \theta_2}{\partial n} + \delta(\theta_2 - \theta_0) = 0. \tag{5.94}$$

Here, $\delta \geq 0$ is the interphase heat-transfer coefficient, which is assumed to be constant. In this case, the surface Γ is called the free boundary.

We now need to perform the replacement in relations (5.85)–(5.90), (5.93) in accordance with eq. (5.9). As $\operatorname{div} \mathbf{w}_j = 0$, we obtain

$$\begin{aligned} p_j &= \rho_{0j} q_j + \lambda_j \operatorname{div} \mathbf{u}_j + \beta_j \rho_{0j} (\nu_j - \chi_j) \chi_j \Delta\theta_j \\ &= \rho_{j0} q_j + \lambda_j \beta_j \chi_j \Delta\theta_j + \beta_j \rho_{0j} (\nu_j - \chi_j) \chi_j \Delta\theta_j = \rho_{0j} q_j + \gamma_j \Delta\theta_j, \end{aligned}$$

where $\gamma_j = \beta_j \chi_j [\lambda_j + \rho_{0j}(\nu_j - \chi_j)]$. From eq. (5.90) we find the relations for the stress tensors

$$T_j = -[\rho_{0j} q_j + (\beta_j \chi_j \lambda_j + \gamma_j) \Delta\theta_j] I + 2\mu_j [D(\mathbf{w}_j) + \beta_j \chi_j D(\nabla\theta_j)].$$

Thus, the conditions on the interface Γ in the new variables take the form

$$\mathbf{w}_1 + \beta_1 \chi_1 \nabla\theta_1 = \mathbf{w}_2 + \beta_2 \chi_2 \nabla\theta_2; \tag{5.95}$$

$$\theta_1 = \theta_2; \tag{5.96}$$

$$\begin{aligned} &\{[\rho_{01} q_1 - \rho_{02} q_2 + (\beta_1 \chi_1 \lambda_1 + \gamma_1) \Delta\theta_1 - (\beta_2 \chi_2 \lambda_2 + \gamma_2) \Delta\theta_2] I \\ &\quad + 2\mu_2 [D(\mathbf{w}_2) + \beta_2 \chi_2 D(\nabla\theta_2)] - 2\mu_1 [D(\mathbf{w}_1) + \beta_1 \chi_1 D(\nabla\theta_1)]\} \mathbf{n} \\ &= 2\sigma(\theta) K \mathbf{n} + \nabla_{II} \sigma(\theta); \end{aligned} \tag{5.97}$$

$$f_t + (\mathbf{w}_1 + \beta_1 \chi_1 \nabla\theta_1) \cdot \nabla f = 0. \tag{5.98}$$

By virtue of the equalities

$$\nabla_{11} \cdot \mathbf{u} = \nabla_{11} \cdot \mathbf{u}_2 = \beta_2 \chi_2 \Delta\theta_2 - \mathbf{n} \cdot \frac{\partial \mathbf{w}_2}{\partial n} - \beta_2 \chi_2 \mathbf{n} \cdot \frac{\partial}{\partial n} \nabla\theta_2$$

the energy condition (5.89) transforms to

$$k_2\frac{\partial\theta_2}{\partial n} - k_1\frac{\partial\theta_1}{\partial n} = æ\theta\Big[\beta_2\chi_2\Delta\theta_2 - \mathbf{n}\cdot\Big(\frac{\partial\mathbf{w}_2}{\partial n} + \beta_2\chi_2\frac{\partial\nabla\theta_2}{\partial n}\Big)\Big] + \omega[\theta_t + (\mathbf{w}_2 + \beta_2\chi_2\nabla\theta_2)\cdot\nabla_{II}\theta]. \tag{5.99}$$

If the energy condition on Γ is taken in the form (5.92), it remains unchanged.

For problems with the free boundary, the dynamic condition transforms to

$$[p_0 - \rho_{20}q_2 - (\beta_2\chi_2\lambda_2 + \gamma_2)\Delta\theta_2]\mathbf{n} + 2\mu_2[D(\mathbf{w}_2) + \beta_2\chi_2 D(\nabla\theta_2)]\mathbf{n} = 2\sigma(\theta)K\mathbf{n} + \nabla_{II}\sigma(\theta). \tag{5.100}$$

In further considerations of problems with the free boundary, the index "2" is omitted.

Remark 5.4. If there is a solid wall Σ_j, then the conditions on it are

$$\mathbf{w}_j + \beta_j\chi_j\nabla\theta_j = \mathbf{v}_{jcm}; \tag{5.101}$$

$$\theta_j = \theta_{jcm} \quad \text{or} \quad \frac{\partial\theta_j}{\partial n} = Q_j, \tag{5.102}$$

where $\mathbf{v}_{jcm}$ is the wall velocity and Q_j is the heat flux.

2. Basic Lie algebra

Here, we assume that the vector of external mass forces in eq. (5.10) depends only on time:

$$\mathbf{g} = -\big(g_1(t), g_2(t), g_3(t)\big), \tag{5.103}$$

with known functions $g_1(t)$, $g_2(t)$, and $g_3(t)$. Then, the transformation

$$\begin{aligned} \bar t = t, \quad \bar x &= x + \iint g_1(t)\,dtd\tau, \quad \bar u = u + \int g_1(t)\,dt, \\ \bar y &= y + \iint g_2(t)\,dtd\tau, \quad \bar v = v + \int g_2(t)\,dt, \\ \bar z &= z + \iint g_3(t)\,dtd\tau, \quad \bar w = w + \int g_3(t)\,dt \end{aligned} \tag{5.104}$$

is an equivalence transformation, and we can assume that $\mathbf{g} = 0$ in system (5.10)–(5.12).

Remark 5.5. In many situations, $\mathbf{g} = (0, 0, -g)$; then, $\bar t = t$, $\bar x = x$, $\bar y = y$, $\bar u = u$, $\bar v = v$, $\bar z = z + gt^2/2$, $\bar w = w + gt$ is an equivalence transformation.

System (5.10)–(5.12) with $\mathbf{g} = 0$ admits the following basic Lie algebra of operators ($\mathbf{w} = (u, v, w)$; see eq. (5.13) with $\mathbf{g} = 0$):

$$\begin{gathered}
X_1 = \partial_x, \quad X_2 = \partial_y, \quad X_3 = \partial_z, \quad X_4 = t\partial_x + \partial_u, \\
X_5 = t\partial_y + \partial_v, \quad X_6 = t\partial_z + \partial_w, \quad X_7 = \partial_t, \\
X_8 = x\partial_x + y\partial_y + z\partial_z + u\partial_u + v\partial_v + w\partial_w + \frac{2}{\beta}(1 + \beta\theta)\partial_\theta, \\
X_9 = x\partial_x + y\partial_y + z\partial_z + t\partial_t + \frac{1}{\beta}(1 + \beta\theta)\partial_\theta - q\partial_q, \\
X_{10} = z\partial_y - y\partial_z + w\partial_v - v\partial_w, \quad X_{11} = x\partial_z - z\partial_x + u\partial_w - w\partial_u, \\
X_{12} = y\partial_x - x\partial_y + v\partial_u - u\partial_v, \quad X_{13}(\varphi) = \varphi(t)\partial_q.
\end{gathered} \tag{5.105}$$

The Lie algebra (5.105) is infinite-dimensional by virtue of the presence of the operator $X_{13}(\varphi)$ with an arbitrary function $\varphi(t) \in C^\infty$. Let us explicitly write groups of transformations in the space R^9 of the variables $(t, x, y, z; u, v, w; q; \theta)$ (only the transformed variables are indicated):

$$\begin{aligned}
X_1:&\quad \bar{x} = x + a_1; \\
X_2:&\quad \bar{y} = y + a_2; \\
X_3:&\quad \bar{z} = z + a_3; \\
X_4:&\quad \bar{x} = x + a_4 t, \quad \bar{u} = u + a_4; \\
X_5:&\quad \bar{y} = y + a_5 t, \quad \bar{v} = v + a_5; \\
X_6:&\quad \bar{z} = z + a_6 t, \quad \bar{w} = w + a_6; \\
X_7:&\quad \bar{t} = t + a_7; \\
X_8:&\quad \bar{x} = e^{a_8} x, \quad \bar{y} = e^{a_8} y, \quad \bar{z} = e^{a_8} z, \quad \bar{u} = e^{a_8} u, \quad \bar{v} = e^{a_8} v, \\
&\quad \bar{w} = e^{a_8} w, \quad \bar{\theta} = -\frac{1}{\beta} + \left(\frac{1}{\beta} + \theta\right) e^{2a_8}; \\
X_9:&\quad \bar{x} = e^{a_9} x, \quad \bar{y} = e^{a_9} y, \quad \bar{z} = e^{a_9} z, \quad \bar{t} = e^{a_9} t, \quad \bar{q} = e^{-a_9} q, \\
&\quad \bar{\theta} = -\frac{1}{\beta} + \left(\frac{1}{\beta} + \theta\right) e^{a_9}; \\
X_{10}:&\quad \bar{y} = \cos a_{10} y + \sin a_{10} z, \quad \bar{z} = \cos a_{10} z - \sin a_{10} y, \\
&\quad \bar{v} = \cos a_{10} v + \sin a_{10} w, \quad \bar{w} = \cos a_{10} w - \sin a_{10} v; \\
X_{11}:&\quad \bar{x} = \cos a_{11} x - \sin a_{11} z, \quad \bar{z} = z \cos a_{11} z + \sin a_{11} x, \\
&\quad \bar{u} = \cos a_{11} u - \sin a_{11} w, \quad \bar{w} = \cos a_{11} w + \sin a_{11} u; \\
X_{12}:&\quad \bar{x} = \cos a_{12} x + \sin a_{12} y, \quad \bar{y} = \cos a_{12} y - \sin a_{12} x, \\
&\quad \bar{u} = \cos a_{12} u + \sin a_{12} v, \quad \bar{v} = \cos a_{12} v - \sin a_{12} u; \\
X_{13}:&\quad \bar{q} = q + a_{13} \varphi(t)
\end{aligned} \tag{5.106}$$

($a_1, \dots, a_{13}$ are group constants). In what follows, this group is indicated by G^j (the index j refers to the flow domain).

3. Invariance of conditions on the interface

The action of the external forces (5.103) is assumed to be identical in the domains Ω_j. In this case, the boundary conditions (5.95)–(5.100), (5.94) are invariant with respect to the equivalence transformation (5.104). Let us demonstrate this with an example of the boundary condition (5.98).

Let

$$f(\mathbf{x}, t) = f\left(\bar{\mathbf{x}} - \iint \mathbf{g}(t)\, dt d\tau, t\right) = \bar{f}(\bar{\mathbf{x}}, \bar{t}) = 0$$

be the interface equation, then we obtain

$$\begin{aligned} f_t + \mathbf{u} \cdot \nabla_x f &= \bar{f}_{\bar{t}} + \nabla_{\bar{x}} \bar{f} \cdot \frac{d\bar{\mathbf{x}}}{dt} + \left(\bar{\mathbf{u}} - \int \mathbf{g}(t)\, dt\right) \cdot \nabla_{\bar{x}} \bar{f} \\ &= \bar{f}_{\bar{t}} + \bar{\mathbf{u}} \cdot \nabla_{\bar{x}} \bar{f} = 0. \end{aligned}$$

Therefore, the usual notations of the dependent and independent variables $\mathbf{x}$, f, $\mathbf{w}$, q, and θ can be used in the boundary conditions on the interface.

Remark 5.6. Condition (5.101) on the solid wall is not invariant with respect to transformations (5.98):

$$\bar{\mathbf{w}}_j - \int \mathbf{g}(t)\, dt + \beta_j \chi_j \nabla \theta_j = \mathbf{v}_{jcm}.$$

Let us choose the following set of operators:

$$\langle X_1^j, X_2^j, X_3^j, X_4^j, X_5^j, X_6^j, X_7^j, X_{10}^j, X_{11}^j, X_{12}^j \rangle.$$

This forms the basis for the Lie algebra generating a ten-parameter group G_{10}^j, which is the Galileo group ($j = 1, 2$).

Statement 5.1. Let H be an intransitive subgroup of the Galileo group G_{10}^j, and let the interface Γ be a nonsingular invariant manifold of the group H in the space $\{t, x, y, z\}$. Then, conditions (5.95)–(5.99), which are satisfied on this surface, are also invariant with respect to H.

The proof is performed directly by formulas (5.106) corresponding to the group G_{10}^j [173].

Note that the group G_{10}^j acts identically in the spaces R_1^9 and R_2^9; therefore, the index j for the subgroup H can be omitted.

In the general case, in formulating Statement 5.1, the group G_{10}^j cannot be replaced by a wider subgroup of the group G^j of transformations (5.106). There are, however, some particular cases where such an extension is possible.

The first case corresponds to identical densities $\rho_{01} = \rho_{02}$. Statement 5.1 remains valid if $H \subset G^j_{10} \otimes G^j_\varphi$, where G^j_φ is an infinite group generated by the operators $X^j_{13}(\varphi) = \varphi(t)\partial_{q_j}$.

The boundary conditions (5.95) and (5.98) are obviously invariant with respect to transformations generated by the operators X_8 and X_9. Concerning the equality of temperatures (5.96) on Γ, we should have $\beta_1 = \beta_2$. In this case, the dynamic condition (5.97) is invariant with respect to X_8, if the dependence $\sigma(\theta)$ has the form

$$\sigma(\theta) = \left(\frac{1}{\beta_1} + \theta\right)^{1/2} c_1$$

($c_1 > 0$ is a constant). Invariance of eq. (5.97) with respect to X_9 is possible only if $\sigma(\theta) = \sigma_0 = \text{const}$; here, the right-hand side of the energy condition (5.99) is equal to zero (condition (5.92) is satisfied), and this permits a transformation related to X_9. If the condition of identical heat fluxes (5.92) is satisfied, then it is invariant with respect to the operator X_8. For other dependences $\sigma(\theta)$, invariance of eq. (5.99) is violated for the group related to the operator X_8.

Thus, extension to the group $G^j_{X_8}$ occurs if $\beta_1 = \beta_2$, $\sigma(\theta) = (1/\beta_1 + \theta)^{1/2} c_1$, and the energy condition (5.92) is satisfied. For the group $G^j_{X_9}$, the boundary conditions are invariant only at $\beta_1 = \beta_2$ and $\sigma(\theta) = \sigma_0 = \text{const}$.

In considering the problem with the free boundary, it is necessary to know the properties of invariance of conditions (5.98), (5.94), and (5.100), where the indices "1" and "2" should be omitted. Let us assume that $\theta_0 = \text{const}$ and $p_0 = p_0(t)$; then, applying the replacement

$$\rho_0 q \to \rho_0 q + p_0(t), \quad \theta \to \theta + \theta_0,$$

we can assume that $p_0 = 0$ and $\theta_0 = 0$.

Thus, we can formulate the following statement.

Statement 5.2. If the free boundary Γ is invariant with respect to the subgroup H of the Galileo group G_{10}, then conditions (5.94), (5.98), and (5.100) with $p_0 = 0$ and $\theta_0 = 0$ are also invariant with respect to H.

In formulating this statement, the Galileo group can be replaced by a wider group if two conditions are satisfied simultaneously:

$$\sigma = 0, \quad \sigma(\theta) = c_1(1/\beta_1 + \theta)^{1/2}$$

or

$$\sigma = 0, \quad \sigma(\theta) = \sigma_0 = \text{const}.$$

The resultant group is $G_{10} \otimes G_{X_8}$ in the first case and $G_{10} \otimes G_{X_9}$ in the second case.

The above-formulated statements allow finding invariant and partially invariant solutions, which are correlated in advance with conditions on the interface and on the free boundary. Certainly, if the problem includes solid walls and external mass forces, it is necessary to take into account Remark 5.6 in analyzing the exact solution.

6 Group properties of equations of thermodiffusion motion

In this chapter, group properties of equations of nonisothermal motion of binary mixtures are studied. The basic Lie algebras and equivalence transformations are found; the problem of the group classification is solved. The classification of invariant solutions is performed; optimal systems of first- and second-order subalgebras are constructed for an infinite-dimensional algebra of operators admitted by the equations of plane motions. New classes of exact solutions and generalizations of previously known solutions of equations of thermodiffusion motion are constructed. Subgroups of continuous transformations to which the conditions on the interface or free boundary remain invariant are identified. This chapter is based on previous publications [6, 22, 200, 201, 202, 203, 204].

6.1 Lie group of thermodiffusion equations

Equations of convection of a binary mixture

Thermodiffusion is understood to be the molecular transport of matter induced by a temperature gradient in the medium (liquid solution or gas mixture). In the case of thermodiffusion, the species have different concentrations in areas with elevated and reduced temperatures. The presence of a concentration gradient leads to the emergence of conventional diffusion. The steady state is established when the balance of diffusion and thermodiffusion processes is reached, i. e., the process of mixing of the species in the mixture is compensated by the process of their separation. Normal thermodiffusion, where the heavy species tend to pass to colder areas and the light species tend to pass to more heated areas, is often observed in practice. In some cases, abnormal thermodiffusion with the opposite directions of motion of the species is observed. Thermodiffusion in solutions is also called the *Soret effect*.

Thermodiffusion is often encountered in nature; there are also numerous applications in engineering. Combined with thermal convection, this effect is used to separate isotopes in liquid and gaseous mixtures [190, 191]. Separation is performed in a thermodiffusion column, which consists of two coaxial tubes heated to different temperatures. Thermodiffusion is used to determine the oil composition and separate its components [233], to deposit various coatings onto metallic articles, and to grow crystals. Another example of the application of the effect considered here is a heat pump [40]. Thermodiffusion also affects currents in seas and oceans, where salt water masses experience various heating regimes [97, 223].

The model of thermodiffusion of a binary mixture is based on the Navier–Stokes equations, supplemented with equations of heat and mass transfer. The Oberbeck–Boussinesq approximation derived to describe convective flows under natural Earth's

https://doi.org/10.1515/9783110655469-006

conditions is used. The mixture density is assumed to be a linear function of temperature and concentration of the light species:

$$\rho = \rho_0(1 - \beta_1 T - \beta_2 C).$$

Here, ρ_0 is the density of the mixture at mean values of temperature and concentration, T and C are small deviations from the mean values, β_1 is the coefficient of thermal expansion of the mixture, and β_2 is the concentration coefficient of density ($\beta_2 > 0$, because C is the concentration of the light species). The motion of the mixture is described by the system of equations [68, 210]

$$\boldsymbol{u}_t + (\boldsymbol{u} \cdot \nabla)\boldsymbol{u} = -\frac{1}{\rho_0}\nabla p + \nu\Delta\boldsymbol{u} - \mathbf{g}(\beta_1 T + \beta_2 C), \tag{6.1}$$

$$T_t + \boldsymbol{u} \cdot \nabla T = \chi\Delta T, \tag{6.2}$$

$$C_t + \boldsymbol{u} \cdot \nabla C = d\Delta C + \alpha d\Delta T, \tag{6.3}$$

$$\operatorname{div}\boldsymbol{u} = 0, \tag{6.4}$$

where $\boldsymbol{u}$ is the velocity vector, p is the deviation of the pressure from the hydrostatic pressure, ν is the coefficient of kinematic viscosity, χ is the coefficient of thermal diffusivity, d is the diffusion coefficient, α is the thermodiffusion parameter, and $\mathbf{g}$ = const is the vector of acceleration due to gravity. All characteristics of the medium are assumed to be constant and correspond to the mean values of temperature and concentration. The thermodiffusion parameter has the form $\alpha = -d_T/d\,T_0$, where d_T is the thermodiffusion coefficient and T_0 is the mean temperature. The values $\alpha < 0$ and $\alpha > 0$ refer to normal and abnormal thermodiffusion, respectively.

In a particular case ($C = 0$ and $\alpha = 0$), system (6.1)–(6.4) transforms into a system of equations of free convection of a homogeneous fluid (Oberbeck–Boussinesq model). A fairly large number of exact solutions are known for this model; many of them can be found in [68, 71]. These works contain studies of the stability of various types of convective flows as well as mechanical equilibrium. Group properties of free convection equations were examined in [76] for the plane case and in an earlier publication [106] for steady plane flows (see also [18]). A number of exact solutions were constructed in those publications; some of these solutions had been previously found by other methods.

Exact solutions of equations of convection in a binary mixture were considered in [72, 235], which mainly deal with investigations of the stability of the corresponding motions. Results of studying the stability of mechanical equilibrium of a binary mixture, with due allowance for thermodiffusion, can be found in [68]. Stability of thermodiffusion motion in a vertical layer with a transverse difference in temperature was considered in [73]; the same problem, complicated by the presence of a streamwise gradient of concentration, was examined in [150]. Instability of a plane horizontal

layer of an incompressible binary gas mixture under the action of a transverse temperature gradient modulated in time was studied in [214]. We should also note the publication [65], in which the stability of a horizontal layer under the action of vibrations and with allowance for thermodiffusion was considered.

The authors of the these works found exact solutions of eqs. (6.1)–(6.4), which describe the main flow. Methods of group analysis of differential equations were not used. As it will be demonstrated in this chapter, however, all of these solutions have group nature.

Group properties of model equations

In system (6.1)–(6.4), let us assume that $\boldsymbol{x} = (x^1, x^2, x^3)$ is the coordinate vector, $\boldsymbol{u} = (u^1, u^2, u^3)$ is the velocity vector, $\mathbf{g} = (0, 0, -\mathrm{g})$, and g is the acceleration due to gravity (the x^3 axis is directed vertically upward). Let us pose the problem of finding an admissible Lie algebra of operators for system (6.1)–(6.4). In our calculations, we assume that the parameters α, β_1, and β_2 can vanish, which means the absence of the corresponding terms in the equations. This approach allows us to study the problem, taking into account or ignoring the dependence of the group properties of the model on various effects in constructing the model (thermodiffusion, dependence of density on temperature and concentration). Note that, from the viewpoint of the group analysis, the case with $\mathbf{g} = 0$ is equivalent to the case with $\beta_1 = \beta_2 = 0$. Therefore, the vector of acceleration due to gravity and the constants χ and d are further assumed to differ from zero. The formulated problem is a problem of the group classification of system (6.1)–(6.4) with respect to the parameters involved.

Let $f(t, \boldsymbol{x})$ be a certain function; its derivatives are then indicated in accordance with the equalities

$$\frac{\partial f}{\partial t} = f_t, \quad \frac{\partial f}{\partial x^i} = f_i, \quad \frac{\partial^2 f}{\partial t\, \partial x^i} = f_{ti}, \quad \frac{\partial^2 f}{\partial x^i \partial x^j} = f_{ij}, \quad i, j = 1, 2, 3, \quad i \le j.$$

Using these equalities, we write system (6.1)–(6.4) in the coordinate form:

$$u^1_t + u^1 u^1_1 + u^2 u^1_2 + u^3 u^1_3 + \frac{1}{\rho_0} p_1 - \nu(u^1_{11} + u^1_{22} + u^1_{33}) = 0; \tag{6.5}$$

$$u^2_t + u^1 u^2_1 + u^2 u^2_2 + u^3 u^2_3 + \frac{1}{\rho_0} p_2 - \nu(u^2_{11} + u^2_{22} + u^2_{33}) = 0; \tag{6.6}$$

$$u^3_t + u^1 u^3_1 + u^2 u^3_2 + u^3 u^3_3 + \frac{1}{\rho_0} p_3 - \nu(u^3_{11} + u^3_{22} + u^3_{33}) - \mathrm{g}(\beta_1 T + \beta_2 C) = 0; \tag{6.7}$$

$$T_t + u^1 T_1 + u^2 T_2 + u^3 T_3 - \chi(T_{11} + T_{22} + T_{33}) = 0; \tag{6.8}$$

$$C_t + u^1 C_1 + u^2 C_2 + u^3 C_3 - d(C_{11} + C_{22} + C_{33}) - \alpha d(T_{11} + T_{22} + T_{33}) = 0; \tag{6.9}$$

$$u^1_1 + u^2_2 + u^3_3 = 0. \tag{6.10}$$

We seek the infinitesimal operator admitted by the system in the form

$$X = \xi^t \frac{\partial}{\partial t} + \xi^i \frac{\partial}{\partial x^i} + \eta^i \frac{\partial}{\partial u^i} + \eta^p \frac{\partial}{\partial p} + \eta^T \frac{\partial}{\partial T} + \eta^C \frac{\partial}{\partial C}, \tag{6.11}$$

assuming that its components depend upon all dependent and independent variables (summation over the repeated index $i = 1, 2, 3$ is implied). To form the governing equations, we need to apply the extended operator $\underset{2}{X}$ to eqs. (6.5)—(6.10) and pass to the manifold defined by the system. The equations considered here, however, are not in involution, which complicates identification of external and internal variables. Let us supplement the system with its differential corollary [212]

$$\begin{aligned} &(u_1^1)^2 + (u_2^2)^2 + (u_3^3)^2 + 2(u_2^1 u_1^2 + u_3^1 u_1^3 + u_3^2 u_2^3) \\ &\quad + \frac{1}{\rho_0}(p_{11} + p_{22} + p_{33}) - \mathrm{g}(\beta_1 T_3 + \beta_2 C_3) = 0, \end{aligned} \tag{6.12}$$

obtained by differentiating eqs. (6.5), (6.6), and (6.7) with respect to x^1, x^2, and x^3, respectively, and by using eq. (6.10). In passing to the manifold, we also take into account the differential corollaries of eq. (6.10):

$$u_{t1}^1 + u_{t2}^2 + u_{t3}^3 = 0, \quad u_{1i}^1 + u_{2i}^2 + u_{3i}^3 = 0, \quad i = 1, 2, 3. \tag{6.13}$$

System (6.5)—(6.10), (6.12), (6.13) is in involution. Now we can easily identify the external variables: u_{11}^1, u_{11}^2, u_{11}^3, p_{11}, T_{11}, C_{11}, u_{t3}^3, u_{13}^3, u_{23}^3, u_{33}^3, and u_1^1. Applying the operator $\underset{2}{X}$ to the system and substituting the expressions for the external variables into the resultant equations, we obtain the system of the governing equations. After rather long transformations, the solution of this system is presented as

$$\begin{gathered} \xi^t = 2c_4 t + c_0, \quad \xi^1 = c_4 x^1 + c_1 x^2 + c_2 x^3 + f^1(t), \\ \xi^2 = -c_1 x^1 + c_4 x^2 + c_3 x^3 + f^2(t), \quad \xi^3 = -c_2 x^1 - c_3 x^2 + c_4 x^3 + f^3(t), \\ \eta^1 = -c_4 u^1 + c_1 u^2 + c_2 u^3 + f_t^1(t), \quad \eta^2 = -c_1 u^1 - c_4 u^2 + c_3 u^3 + f_t^2(t), \\ \eta^3 = -c_2 u^1 - c_3 u^2 - c_4 u^3 + f_t^3(t), \\ \eta^p = \rho_0 [c_5 \mathrm{g}\beta_1 x^3 + c_6 \mathrm{g}\beta_2 x^3 - f_{tt}^1(t) x^1 - f_{tt}^2(t) x^2 - f_{tt}^3(t) x^3] - 2c_4 p + f^0(t), \\ \eta^T = c_7 T + c_9 C + c_5, \quad \eta^C = c_8 C + c_{10} T + c_6. \end{gathered} \tag{6.14}$$

Here, $c_0, \ldots, c_{10}$ are the group constants and $f^i(t) \in T^\infty$, $i = 0, 1, 2, 3$, are arbitrary smooth functions. The group constants are related to the parameters α, β_1, β_2, χ, and d by the system of the classifying equations

$$\begin{gathered} \beta_1(c_7 + 3c_4) + \beta_2 c_{10} = 0, \quad \beta_2(c_8 + 3c_4) + \beta_1 c_9 = 0, \\ \alpha d(c_8 - c_7) + (\chi - d)c_{10} = 0, \quad (\chi - d)c_9 = 0, \\ \alpha c_9 = 0, \quad \beta_1 c_2 = 0, \quad \beta_1 c_3 = 0, \quad \beta_2 c_2 = 0, \quad \beta_2 c_3 = 0. \end{gathered} \tag{6.15}$$

Using eqs. (6.14) and system (6.15), we find the algebras of operators admitted by the system, depending on the values of the parameters involved. The results of the group classification are summarized in Table 6.1.

The first three columns show the values of the constants α, β_1, and β_2; the fourth column contains the basis operators, and the fifth column shows additional operators admitted by the system in the case with $d = \chi$. If all constants differ from zero (last row of the table), then the system admits the operator R_1 at the indicated value of the parameter α.

The operators have the form

$$
\begin{gathered}
X_0 = \frac{\partial}{\partial t}, \quad X_{ij} = x^i \frac{\partial}{\partial x^j} - x^j \frac{\partial}{\partial x^i} + u^i \frac{\partial}{\partial u^j} - u^j \frac{\partial}{\partial u^i}, \\
H_i(f^i(t)) = f^i(t) \frac{\partial}{\partial x^i} + f^i_t(t) \frac{\partial}{\partial u^i} - \rho_0 x^i f^i_{tt}(t) \frac{\partial}{\partial p}, \quad i,j = 1,2,3, \quad i < j, \\
H_0(f^0(t)) = f^0(t) \frac{\partial}{\partial p}, \quad Z = 2t \frac{\partial}{\partial t} + \sum_{i=1}^{3} \left(x^i \frac{\partial}{\partial x^i} - u^i \frac{\partial}{\partial u^i} \right) - 2p \frac{\partial}{\partial p}, \\
U_1 = \rho_0 g x^3 \frac{\partial}{\partial p} + \frac{1}{\beta_1} \frac{\partial}{\partial T}, \quad U_2 = \rho_0 g x^3 \frac{\partial}{\partial p} + \frac{1}{\beta_2} \frac{\partial}{\partial C}, \\
T^1 = T \frac{\partial}{\partial T}, \quad T^2 = C \frac{\partial}{\partial T}, \quad T^3 = \frac{\partial}{\partial T}, \\
C^1 = C \frac{\partial}{\partial C}, \quad C^2 = T \frac{\partial}{\partial C}, \quad C^3 = \frac{\partial}{\partial C}, \\
R = T^1 + C^1, \quad R_1 = T^1 - \frac{\beta_1}{\beta_2} C^2, \quad R_2 = C^1 - \frac{\beta_2}{\beta_1} T^2, \\
Z_1 = Z - 3T^1, \quad Z_2 = Z - 3C^1, \quad Z_3 = Z - 3R, \\
L = \left[\alpha T + (1 - \chi/d) C \right] \frac{\partial}{\partial C}.
\end{gathered}
\tag{6.16}
$$

Note that the transformations of equivalence of the parameters are ignored in this problem of the group classification. The reason is the necessity of knowing the group

Table 6.1: Results of the group classification of the three-dimensional model.

α	β_1	β_2	Operators	$d = \chi$
0	0	0	$X_0, X_{ij}, H_i, H_0, Z, T^1, T^3, C^1, C^3$	T^2, C^2
0	0	$\neq 0$	$X_0, X_{12}, H_i, H_0, Z_2, U_2, T^1, T^3$	T^2
0	$\neq 0$	0	$X_0, X_{12}, H_i, H_0, Z_1, U_1, C^1, C^3$	C^2
0	$\neq 0$	$\neq 0$	$X_0, X_{12}, H_i, H_0, Z_3, U_1, U_2$	R_1, R_2
$\neq 0$	0	0	$X_0, X_{ij}, H_i, H_0, Z, R, L, T^3, C^3$	
$\neq 0$	0	$\neq 0$	$X_0, X_{12}, H_i, H_0, Z_3, U_2, T^3$	
$\neq 0$	$\neq 0$	0	$X_0, X_{12}, H_i, H_0, Z_3, U_1, C^3, L$	
$\neq 0$	$\neq 0$	$\neq 0$	$X_0, X_{12}, H_i, H_0, Z_3, U_1, U_2$	
			$\alpha = \beta_1(d-\chi)/\beta_2 d$, $d \neq \chi$: R_1	

properties of the model, including all necessary physical parameters for construction of exact solutions and their physical interpretation. The solution of the problem of the group classification with allowance for equivalence transformations will be described in the next section.

Let us describe transformations of one-parameter subgroups generated by the operators from Table 6.1. The shift in time t corresponds to the operator X_0, and rotation by an identical angle in the planes x^i, x^j and u^i, u^j corresponds to the operators X_{ij}. The operators H_i express the property of invariance of the equations with respect to the transition to a coordinate system moving along the x^i axis with acceleration that is an arbitrary function of time. Addition of an arbitrary function of time to pressure corresponds to the operator H_0. The final formulas of these transformations are well known [18] and are not shown here. The transformations generated by the remaining operators have the form

$$
\begin{gathered}
Z: \ \tilde{t} = e^{2a}t, \quad \widetilde{x^i} = e^a x^i, \quad \widetilde{u^i} = e^{-a}u^i, \quad \tilde{p} = e^{-2a}p; \\
U_1: \ \tilde{p} = p + a\rho_0 g x^3, \quad \tilde{T} = T + \frac{a}{\beta_1}; \\
U_2: \ \tilde{p} = p + a\rho_0 g x^3, \quad \tilde{C} = C + \frac{a}{\beta_2}; \\
T^1: \ \tilde{T} = e^a T; \quad T^2: \ \tilde{T} = T + aC; \quad T^3: \ \tilde{T} = T + a; \\
C^1: \ \tilde{C} = e^a C; \quad C^2: \ \tilde{C} = C + aT; \quad C^3: \ \tilde{C} = C + a; \\
R_1: \ \tilde{T} = e^a T, \quad \tilde{C} = C + \frac{\beta_1}{\beta_2}(1 - e^a)T; \\
R_2: \ \tilde{C} = e^a C, \quad \tilde{T} = T + \frac{\beta_2}{\beta_1}(1 - e^a)C; \\
R: \ \tilde{T} = e^a T, \quad \tilde{C} = e^a C; \\
L: \ \tilde{C} = \left(C + \frac{\alpha d}{d - \chi}T\right)e^{(1-\chi/d)a} - \frac{\alpha d}{d - \chi}T.
\end{gathered}
\tag{6.17}
$$

The variables whose transformation principle is not indicated are transformed identically (this is also implied in what follows). In eqs. (6.17), a is a real parameter of the one-parameter subgroup, which is specific for each operator. Transformations generated by the operators Z_1, Z_2, and Z_3 are obtained by extension of the one-parameter subgroup corresponding to the operator Z with the use of the following transformations:

$$
Z_1: \tilde{T} = e^{-3a}T; \quad Z_2: \ \tilde{C} = e^{-3a}C; \quad Z_3: \ \tilde{T} = e^{-3a}T, \quad \tilde{C} = e^{-3a}C.
$$

Note that the operators U_1, U_2, T^i, C^i, R, R_1, R_2, L, and Z_i are specific for the equations of convection of a binary mixture with allowance for thermodiffusion, in contrast to the operators X_0, X_{ij}, H_i, and H_0 admitted by many models of hydrodynamics.

Equivalence transformations

Before finding the equivalence transformations for thermodiffusion equations, we should establish one other useful fact. We consider a system of differential equations defined by the equality

$$E(x, u, \underset{1}{u}, \ldots, \underset{k}{u}, c) = 0. \tag{6.18}$$

Here, x is the vector of independent variables, u is the vector of dependent variables, $\underset{s}{u}$ is the set of derivatives of u with respect to x of the order $s = 1, \ldots, k$, and c is the vector of parameters (constants). In the following, the vector s is assumed to take the values indicated above.

Let X be an infinitesimal operator of the form

$$X = \xi \cdot \frac{\partial}{\partial x} + \eta \cdot \frac{\partial}{\partial u} + \tau \cdot \frac{\partial}{\partial c}.$$

If system (6.18) admits the operator X, then this operator generates a one-parameter group of equivalence transformations for this system. Since constants should transform to constants in equivalence transformations, the components of the operator X have the form $\xi = \xi(x, u, c)$, $\eta = \eta(x, u, c)$, $\tau = \tau(c)$. We can easily prove the following statement.

Statement 6.1. If system (6.18) admits the operator X, then this system also admits the operator FX with an arbitrary function $F = F(c)$.

It follows from Statement 6.1 that the operator of the group of equivalence transformations of constants is determined with accuracy to a factor arbitrarily depending on these constants. For particular equations, this fact was established in [98, 113]. The group of equivalence transformations was found for Navier–Stokes equations in [98] and for a modified Burgers equation depending on two parameters in [113]. We should also note [157], where the equivalence transformations for constants were found for a system of equations equivalent to gas dynamics equations with barochronous motion of the gas. In the case considered there, the solution of the governing equations did not include arbitrary functions of constants involved into the system. This happened because the conditions of zero derivatives of the constants with respect to independent variables were not added to the system during the calculations. The infinitesimal operator components corresponding to constants were assumed to be functions of those constants, as well as of dependent and independent variables. The condition that these components depend only on constants was imposed only after the solution of the governing equations was found.

Let us now calculate the equivalence transformations for the thermodiffusion equations (6.1)–(6.4). We seek for the infinitesimal operator of the group in the form

$$\widetilde{X} = X + \eta^{\alpha} \frac{\partial}{\partial \alpha} + \eta^{\beta_1} \frac{\partial}{\partial \beta_1} + \eta^{\beta_2} \frac{\partial}{\partial \beta_2} + \eta^{\chi} \frac{\partial}{\partial \chi} + \eta^{d} \frac{\partial}{\partial d} + \eta^{\rho_0} \frac{\partial}{\partial \rho_0} + \eta^{\nu} \frac{\partial}{\partial \nu} + \eta^{\mathrm{g}} \frac{\partial}{\partial \mathrm{g}},$$

assuming that its components depend on all dependent and independent variables, and also on the parameters involved into the system (here, X is an operator of the form (6.11)). Note that eqs. (6.1)–(6.4) should be supplemented with the conditions of zero derivatives of α, β_1, β_2, χ, d, ρ_0, ν, and g with respect to the variables t, x^i, u^i, p, T, and C, $i = 1, 2, 3$. The components of the extended operator $\widetilde{X}_2$ are calculated by the formulas derived in [129, 130]. Applying the extended operator to the system and passing to the corresponding manifold, we obtain the governing equations. It follows from these equations that the components of the operator $\widetilde{X}$ corresponding to the parameters are independent of the variables t, x^i, u^i, p, T, and C. The solution of the governing equations is given by the formulas

$$
\begin{aligned}
&\xi^t = (2c_4 + \eta^\nu \nu^{-1})t + c_0,\\
&\xi^1 = (c_4 + \eta^\nu \nu^{-1})x^1 + c_1 x^2 + c_2 x^3 + f^1(t),\\
&\xi^2 = -c_1 x^1 + (c_4 + \eta^\nu \nu^{-1})x^2 + c_3 x^3 + f^2(t),\\
&\xi^3 = -c_2 x^1 - c_3 x^2 + (c_4 + \eta^\nu \nu^{-1})x^3 + f^3(t),\\
&\eta^1 = -c_4 u^1 + c_1 u^2 + c_2 u^3 + f_t^1(t), \quad \eta^2 = -c_1 u^1 - c_4 u^2 + c_3 u^3 + f_t^2(t),\\
&\eta^3 = -c_2 u^1 - c_3 u^2 - c_4 u^3 + f_t^3(t),\\
&\eta^p = \rho_0 (c_5 \mathrm{g}\beta_1 x^3 + c_6 \mathrm{g}\beta_2 x^3 - f_{tt}^1(t)x^1 - f_{tt}^2(t)x^2 - f_{tt}^3(t)x^3) + (\eta^{\rho_0}\rho_0^{-1} - 2c_4)p + f^0(t),\\
&\eta^T = c_7 T + c_9 C + c_5, \quad \eta^C = c_8 C + c_{10} T + c_6,\\
&\eta^\alpha = (c_8 - c_7)\alpha + c_{10}(\chi d^{-1} - 1),\\
&\eta^{\beta_1} = -(3c_4 + c_7 + \eta^\nu \nu^{-1} + \eta^{\mathrm{g}} \mathrm{g}^{-1})\beta_1 - c_{10}\beta_2,\\
&\eta^{\beta_2} = -(3c_4 + c_8 + \eta^\nu \nu^{-1} + \eta^{\mathrm{g}} \mathrm{g}^{-1})\beta_2 - c_9 \beta_1,\\
&\eta^\chi = \chi\, \eta^\nu \nu^{-1}, \quad \eta^d = d\, \eta^\nu \nu^{-1},
\end{aligned}
$$

and the following conditions should be satisfied:

$$
(\chi - d)c_9 = \alpha c_9 = 0, \quad \beta_1 c_2 = \beta_1 c_3 = \beta_2 c_2 = \beta_2 c_3 = 0. \tag{6.19}
$$

In these formulas, the quantities c_i, $i = 1, \ldots, 10$, and also the components η^ν, η^{ρ_0}, and η^{g} are arbitrary functions of the parameters α, β_1, β_2, χ, d, ρ_0, ν, and g. Moreover, the functions $f^i(t)$, $i = 0, 1, 2, 3$, also depend on these parameters in an arbitrary manner. According to Statement 6.1, the quantities c_i can be considered as constants without loss of generality, and the undetermined components of the infinitesimal operator can be chosen as $\eta^\nu = c_{11}\nu$, $\eta^{\rho_0} = c_{12}\rho_0$, $\eta^{\mathrm{g}} = c_{13}\mathrm{g}$, where c_{11}, c_{12}, and c_{13} are arbitrary constants. Further, the constant c_4 can be eliminated from the expressions for η^{β_1} and η^{β_2} by introducing new constants $\widetilde{c_7} = 3c_4 + c_7$ and $\widetilde{c_8} = 3c_4 + c_8$. Then, the

operators generating one-parameter groups of equivalence transformations are written as

$$
\begin{aligned}
E_1 &= T\frac{\partial}{\partial T} - \alpha\frac{\partial}{\partial \alpha} - \beta_1\frac{\partial}{\partial \beta_1},\\
E_2 &= C\frac{\partial}{\partial C} + \alpha\frac{\partial}{\partial \alpha} - \beta_2\frac{\partial}{\partial \beta_2},\\
E_3 &= C\frac{\partial}{\partial T} - \beta_1\frac{\partial}{\partial \beta_2},\\
E_4 &= T\frac{\partial}{\partial C} + (\chi d^{-1} - 1)\frac{\partial}{\partial \alpha} - \beta_2\frac{\partial}{\partial \beta_1},\\
E_5 &= t\frac{\partial}{\partial t} + x^i\frac{\partial}{\partial x^i} - \beta_1\frac{\partial}{\partial \beta_1} - \beta_2\frac{\partial}{\partial \beta_2} + \chi\frac{\partial}{\partial \chi} + d\frac{\partial}{\partial d} + \nu\frac{\partial}{\partial \nu},\\
E_6 &= p\frac{\partial}{\partial p} + \rho_0\frac{\partial}{\partial \rho_0},\\
E_7 &= \beta_1\frac{\partial}{\partial \beta_1} + \beta_2\frac{\partial}{\partial \beta_2} - \mathrm{g}\frac{\partial}{\partial \mathrm{g}}.
\end{aligned}
$$

The equivalence transformations defined by these operators are

$$
\begin{aligned}
&E_1: \ \widetilde{\alpha} = e_1\alpha, \quad \widetilde{\beta_1} = e_1\beta_1;\\
&E_2: \ \widetilde{\alpha} = e_2^{-1}\alpha, \quad \widetilde{\beta_2} = e_2\beta_2;\\
&E_3: \ \widetilde{\beta_2} = \beta_2 - e_3\beta_1;\\
&E_4: \ \widetilde{\alpha} = \alpha + e_4(\chi d^{-1} - 1), \quad \widetilde{\beta_1} = \beta_1 - e_4\beta_2;\\
&E_5: \ \widetilde{\beta_1} = e_5\beta_1, \quad \widetilde{\beta_2} = e_5\beta_2, \quad \widetilde{\chi} = e_5^{-1}\chi, \quad \widetilde{d} = e_5^{-1}d, \quad \widetilde{\nu} = e_5^{-1}\nu;\\
&E_6: \ \widetilde{\rho_0} = e_6\rho_0;\\
&E_7: \ \widetilde{\beta_1} = e_7\beta_1, \quad \widetilde{\beta_2} = e_7\beta_2, \quad \widetilde{\mathrm{g}} = e_7^{-1}\mathrm{g}.
\end{aligned}
\tag{6.20}
$$

Here, $e_i > 0$, $i = 1, 2, 5, 6, 7$, $e_3, e_4 \in \mathbb{R}$ are the group parameters of equivalence transformations. According to conditions (6.19), the operator E_3 (and the corresponding transformation) is admitted only if $\alpha = 0$ and $d = \chi$.

Let us now move on to the problem of the group classification of thermodiffusion equations. Firstly, it should be noted that the use of the transformations E_5, E_6, and E_7 allows us to assume that $\nu = 1$, $\rho_0 = 1$, and $\mathrm{g} = 1$. Let us consider the classifying equations (6.15). As it follows from these equations, independent of the values of the parameters, system (6.1)–(6.4) admits the operators (see eq. (6.16))

$$
X_0,\ X_{12},\ H_1,\ H_2,\ H_3,\ H_0. \tag{6.21}
$$

We can demonstrate that operators (6.21) form the Lie algebra. Let find possible extensions of this algebra.

A. Let us assume that $d \neq \chi$. In this case, using the transformation E_4 with the parameter $e_4 = \alpha d/(d-\chi)$, we can obtain $\alpha = 0$. Then, eqs. (6.15) yield $c_9 = c_{10} = 0$. After that, we consider possible values of the constants β_1 and β_2. If any of these constants is not equal to zero, then the use of the transformations E_1 or E_2 allows us to take its value to be equal to unity. In this case, from the classifying equations it follows that $c_2 = c_3 = 0$.

1. Let $\beta_1 \neq 0$ and $\beta_2 \neq 0$; then, we can assume that $\beta_1 = \beta_2 = 1$. Equations (6.15) yield $c_8 = c_7 = -3c_4$. The list (6.21) is supplemented with the operators Z_3, U_1, and U_2. In the last two operators, we should assume that $\beta_1 = \beta_2 = 1$ and $\rho_0 = \mathrm{g} = 1$ (this is also implied in what follows).
2. If $\beta_1 \neq 0$ and $\beta_2 = 0$, we assume that $\beta_1 = 1$; then, we have $c_7 = -3c_4$, and algebra (6.21) is extended by the operators Z_1, U_1, C^1, and C^3.
3. If $\beta_1 = 0$ and $\beta_2 \neq 0$, then, assuming that $\beta_2 = 1$, we obtain $c_8 = -3c_4$. Here, the additional operators are Z_2, U_2, T^1, and T^3.
4. Let $\beta_1 = \beta_2 = 0$. Then, algebra (6.21) is extended by the operators X_{13}, X_{23}, Z, T^1, T^3, C^1, and C^3.

B. Now let $d = \chi$ and $\alpha \neq 0$. The classifying equations yield $c_8 = c_7$ and $c_9 = 0$.

1. If $\beta_2 \neq 0$, then, by applying the transformations E_4, E_2, and E_1, we can obtain $\beta_1 = 0, \beta_2 = 1$, and $\alpha = \pm 1$, respectively. Then, we have $c_8 = c_7 = -3c_4$ and $c_{10} = 0$; the list (6.21) is supplemented with the operators Z_3, U_2, and T^3.
2. Let $\beta_2 = 0$ and $\beta_1 \neq 0$. The use of the transformations E_1 and E_2 allows us to assume that $\beta_1 = 1$ and $\alpha = \pm 1$, respectively. As a result, we obtain $c_8 = c_7 = -3c_4$. Here, the additional operators are Z_3, U_1, C^2, and C^3.
3. If $\beta_1 = \beta_2 = 0$, by applying the transformation E_2, we can obtain $\alpha = \pm 1$, and algebra (6.21) is extended by the operators $X_{13}, X_{23}, Z, R, T^3, C^2$, and C^3.

C. Let us consider the case with $d = \chi$ and $\alpha = 0$.

1. Let $\beta_2 \neq 0$. Using the transformations E_4 and E_2, we can obtain $\beta_1 = 0$ and $\beta_2 = 1$. Then, eqs. (6.15) yield $c_8 = -3c_4$ and $c_{10} = 0$; the list of additional operators consists of Z_2, U_2, T^1, T^2, and T^3.
2. If $\beta_2 = 0$ and $\beta_1 \neq 0$, then, assuming that $\beta_1 = 1$, we obtain $c_7 = -3c_4$ and $c_9 = 0$. As a result, algebra (6.21) is extended by the operators Z_1, U_1, C^1, C^2, and C^3.
3. If $\beta_1 = \beta_2 = 0$, the following additional operators are obtained: $X_{13}, X_{23}, Z, T^1, T^2$, T^3, C^1, C^2, and C^3.

The results of the group classification are summarized in Tables 6.2 and 6.3. The first two columns show the values of the constants β_1 and β_2, the third column contains the admitted operators, and the fourth column shows additional operators admitted in the case with $d = \chi$ (Table 6.2). The operators listed in the tables have the form (6.16), where $\beta_1 = \beta_2 = \rho_0 = \mathrm{g} = 1$ should be assumed. Let us consider the following case in more detail: the parameters α, β_1, and β_2 in system (6.1)–(6.4) are not equal to zero, and

Table 6.2: Results of the classification in the case with $\alpha = 0$.

β_1	β_2	Operators	$d = \chi$
0	0	$X_0, X_{ij}, H_i, H_0, Z, T^1, T^3, C^1, C^3$	T^2, C^2
0	1	$X_0, X_{12}, H_i, H_0, Z_2, U_2, T^1, T^3$	T^2
1	0	$X_0, X_{12}, H_i, H_0, Z_1, U_1, C^1, C^3$	C^2
1	1	$X_0, X_{12}, H_i, H_0, Z_3, U_1, U_2$	

Table 6.3: Results of the classification in the case with $\alpha = \pm 1$ and $d = \chi$.

β_1	β_2	Operators
0	0	$X_0, X_{ij}, H_i, H_0, Z, R, T^3, C^2, C^3$
0	1	$X_0, X_{12}, H_i, H_0, Z_3, U_2, T^3$
1	0	$X_0, X_{12}, H_i, H_0, Z_3, U_1, C^2, C^3$

$d \neq \chi$ (thus, the thermodiffusion effect and the dependence of density on temperature and concentration are taken into account).

It follows from the results of the group classification that the system in the case considered can be brought to the form

$$\begin{aligned} \boldsymbol{u}_t + (\boldsymbol{u}\cdot\nabla)\boldsymbol{u} &= -\nabla p + \Delta\boldsymbol{u} + (T + C)\,\boldsymbol{\gamma}, \\ T_t + \boldsymbol{u}\cdot\nabla T &= \chi\Delta T, \\ C_t + \boldsymbol{u}\cdot\nabla C &= d\Delta C, \\ \operatorname{div}\boldsymbol{u} &= 0, \end{aligned} \tag{6.22}$$

where $\boldsymbol{\gamma} = (0, 0, 1)$. The transformation of dependent variables, which allows the term $\alpha d\Delta T$ in eq. (6.3) to be eliminated, is generated by the operator E_4 and is described by the formula

$$C = \widetilde{C} + \frac{\alpha d}{\chi - d}\,T.$$

This transformation reduces the diffusion equation to a homogeneous equation with respect to the function $\widetilde{C}$ (the bar in eqs. (6.22) is omitted).

System (6.22) admits the Lie algebra of operators with the basis

$$\begin{gathered} X_0 = \frac{\partial}{\partial t}, \quad X_{12} = x^1\frac{\partial}{\partial x^2} - x^2\frac{\partial}{\partial x^1} + u^1\frac{\partial}{\partial u^2} - u^2\frac{\partial}{\partial u^1}, \\ Z_3 = 2t\frac{\partial}{\partial t} + \sum_{i=1}^{3}\left(x^i\frac{\partial}{\partial x^i} - u^i\frac{\partial}{\partial u^i}\right) - 2p\frac{\partial}{\partial p} - 3T\frac{\partial}{\partial T} - 3C\frac{\partial}{\partial C}, \\ U_1 = x^3\frac{\partial}{\partial p} + \frac{\partial}{\partial T}, \quad U_2 = x^3\frac{\partial}{\partial p} + \frac{\partial}{\partial C}, \end{gathered}$$

$$H_i(f^i(t)) = f^i(t)\frac{\partial}{\partial x^i} + f^i_t(t)\frac{\partial}{\partial u^i} - x^i f^i_{tt}(t)\frac{\partial}{\partial p}, \quad i = 1,2,3,$$
$$H_0(f^0(t)) = f^0(t)\frac{\partial}{\partial p}.$$

Let $\boldsymbol{u}(t,\boldsymbol{x},\chi,d)$, $p(t,\boldsymbol{x},\chi,d)$, $T(t,\boldsymbol{x},\chi,d)$, $C(t,\boldsymbol{x},\chi,d)$ be a solution of system (6.22). The corresponding solution of system (6.1)–(6.4) is obtained by replacing the dependent and independent variables, and also the parameters χ and d by the following formulas:

$$t \to \frac{t}{\nu}, \quad \boldsymbol{x} \to \frac{\boldsymbol{x}}{\nu}, \quad \chi \to \frac{\chi}{\nu}, \quad d \to \frac{d}{\nu}, \quad \boldsymbol{u} \to \boldsymbol{u}, \quad p \to \rho_0 p,$$
$$T \to \frac{\chi - d}{\nu g(\beta_1(\chi - d) + \beta_2 \alpha d)}\, T, \tag{6.23}$$
$$C \to \frac{1}{\nu g \beta_2}\, C + \frac{\alpha d}{\nu g(\beta_1(\chi - d) + \beta_2 \alpha d)}\, T.$$

These formulas mean that t should be replaced by t/ν in the solution; instead of the function p, it is necessary to take the function $\rho_0 p$, etc. Note that the equivalence transformations allow the initial system of equations to be substantially simplified.

Let $\beta_1 = \beta_2 = 0$ (or $\mathbf{g} = 0$) in system (6.1)–(6.4). Then, eqs. (6.1), (6.4) form a system of Navier–Stokes equations whose solution is described by the functions $\boldsymbol{u}(t,\boldsymbol{x}) = (u^1(t,\boldsymbol{x}), u^2(t,\boldsymbol{x}), u^3(t,\boldsymbol{x}))$, $p(t,\boldsymbol{x})$. Substituting this solution into eqs. (6.2), (6.3), we obtain the system

$$T_t + \boldsymbol{u}(t,\boldsymbol{x}) \cdot \nabla T = \chi \Delta T; \tag{6.24}$$
$$C_t + \boldsymbol{u}(t,\boldsymbol{x}) \cdot \nabla C = d\Delta C + \alpha d \Delta T. \tag{6.25}$$

It is of interest to consider the following issue: Which transformations are admitted by this system, depending on the form of the function $\boldsymbol{u}(t,\boldsymbol{x})$? Thus, there arises the problem of the group classification of the diffusion and heat conduction equations with respect to comparatively arbitrary elements: velocity vector components u^1, u^2, u^3. This problem in the full formulation is not considered here. We only study the group properties of eqs. (6.24), (6.25) in the case where $\boldsymbol{u}(t,\boldsymbol{x})$ is an *arbitrary solution of Navier–Stokes equations*.

The results of the group classification are summarized in Table 6.4. The operators T^0 and C^0 have the form $T^0 = T^0(t,\boldsymbol{x})(\partial/\partial T)$ and $C^0 = C^0(t,\boldsymbol{x})(\partial/\partial C)$, where the functions T^0 and C^0 are arbitrary solutions of eqs. (6.24) and (6.25).

Table 6.4: Group properties of the diffusion and heat conduction equations.

α	Operators	$d = \chi$
0	T^1, C^1, T^0, C^0	T^2, C^2
$\neq 0$	R, L, T^0, C^0	

Let us now consider the case with where $\alpha = 0$, and the constants β_1 and β_2 can differ from zero. In particular, if $\beta_1 = 0$ and $\beta_2 \neq 0$ ($\beta_1 \neq 0$ and $\beta_2 = 0$), eqs. (6.1), (6.3), (6.4) [(6.1), (6.2), (6.4)] form a closed system whose solution is given by the functions $\boldsymbol{u}(t, \boldsymbol{x})$, $p(t, \boldsymbol{x})$, $C(t, \boldsymbol{x})$ [$T(t, \boldsymbol{x})$] and can be found independent of eq. (6.2) [(6.3)]. Let us study the group properties of the latter equations. It follows from Table 6.4 (case with $\alpha = 0$) that eq. (6.24) admits the operators T^1 and T^0, while eq. (6.25) admits the operators C^1 and C^0 under similar assumptions about the function $\boldsymbol{u}(t, \boldsymbol{x})$.

Optimal systems of the subalgebras ΘL^4 and ΘL^5

As is seen from Table 6.1, system (6.1)–(6.4) in the case considered admits an infinite-dimensional Lie algebra of operators L. This algebra corresponds to an infinite-dimensional group of transformations that leave the system unchanged. For the convenience of further calculations, we introduce new notations for the operators. The algebra L can be presented in the form of a subdirect sum $L = L^5 \oplus L^\infty$, where the finite-dimensional subalgebra L^5 is formed by the operators

$$
\begin{gathered}
X_1 = \frac{\partial}{\partial t}, \quad X_2 = \rho_0 g x^3 \frac{\partial}{\partial p} + \frac{1}{\beta_2}\frac{\partial}{\partial C}, \quad X_3 = \rho_0 g x^3 \frac{\partial}{\partial p} + \frac{1}{\beta_1}\frac{\partial}{\partial T}, \\
X_4 = 2t\frac{\partial}{\partial t} + \sum_{i=1}^{3}\left(x^i \frac{\partial}{\partial x^i} - u^i \frac{\partial}{\partial u^i}\right) - 2p\frac{\partial}{\partial p} - 3T\frac{\partial}{\partial T} - 3C\frac{\partial}{\partial C}, \\
X_5 = x^1 \frac{\partial}{\partial x^2} - x^2 \frac{\partial}{\partial x^1} + u^1 \frac{\partial}{\partial u^2} - u^2 \frac{\partial}{\partial u^1},
\end{gathered}
\tag{6.26}
$$

and the infinite-dimensional ideal L^∞ has the basis

$$
\begin{gathered}
H_i(f^i(t)) = f^i(t)\frac{\partial}{\partial x^i} + f_t^i(t)\frac{\partial}{\partial u^i} - \rho_0 x^i f_{tt}^i(t)\frac{\partial}{\partial p}, \quad i = 1, 2, 3, \\
H_0(f^0(t)) = f^0(t)\frac{\partial}{\partial p}.
\end{gathered}
\tag{6.27}
$$

If the constants included into the system are related as $\alpha = \beta_1(d - \chi)/\beta_2 d$, $d \neq \chi$, then the system is also invariant with respect to the operator

$$
R_1 = T\frac{\partial}{\partial T} - \frac{\beta_1}{\beta_2} T \frac{\partial}{\partial C}.
$$

In what follows, this particular case is not considered (it is assumed that the above-indicated relation is not satisfied, and the operator R_1 is not admitted). Note that the algebra of operators admitted by the initial system with $\alpha = 0, \beta_1 \neq 0, \beta_2 \neq 0$, and $d \neq \chi$ (the thermodiffusion effect is ignored) coincides with the algebra L (see Table 6.1). Thus, all the results obtained below are also valid for this case.

Let us start constructing an optimal system for the Lie algebra $L = L^5 \oplus L^\infty$ admitted by the thermodiffusion equations. Note that finding optimal systems requires large

Table 6.5: Optimal system of the subalgebras ΘL^4.

$p.q$	Basis R^{pq}	Nor R^{pq}	$p.q$	Basis R^{pq}	Nor R^{pq}
4.1	1, 2, 3, 4	= 4.1	2.6	1, 4	= 2.6
3.1	1, 2, 3	4.1	2.7	2, 4	= 2.7
3.2	1, 2, 4	= 3.2	2.8	$\lambda 2 + 3$, 4	= 2.8
3.3	2, 3, 4	= 3.3	1.1	1	4.1
3.4	1, $\lambda 2 + 3$, 4	= 3.4	1.2	2	4.1
2.1	1, 2	4.1	1.3	$\lambda 2 + 3$	4.1
2.2	2, 3	4.1	1.4	1 + 2	3.1
2.3	1, $\lambda 2 + 3$	4.1	1.5	$1 + \lambda 2 + 3$	3.1
2.4	$1 + 2$, $\lambda 1 + 3$	3.1	1.6	4	= 1.6
2.5	$1 + 3$, 2	3.1	0.1	0	4.1

amounts of analytical calculations, and a detailed description of the work performed would take a large number of pages. The optimal system ΘL^4 is given in Table 6.5.

The first column shows the subalgebra number, which has the form $p.q$, where p is the subalgebra dimension and q is the ordinal number of the subalgebra of dimension p. Subalgebra bases written symbolically with the numbers of the corresponding operators are listed in the second column. The symbol $\lambda 2 + 3$ means $\lambda X_2 + X_3$, etc. The constant λ can take any real value. The third column shows the number of the subalgebra normalizer in L^4; the sign of equality indicates self-normalized subalgebras. The optimal system ΘL^5 is given in Table 6.6. Here, the constant λ also takes any real values, and the constant μ is equal to or greater than zero ($\mu \geq 0$).

Optimal system of the first-order subalgebras

In this section, we construct an optimal system $\Theta_1 L$ for the algebra L. Finding this system reduces to the classification of subalgebras of two classes:

$$1) \quad \{H(\boldsymbol{f}) + H_0(f^0)\}, \qquad 2) \quad \{K_i + H(\boldsymbol{f}) + H_0(f^0)\}, \tag{6.28}$$

where $\{K_i\} \in \Theta_1 L^5$, $i = 1, \ldots, 10$. The first class lies in the ideal L^∞, and the second class has a zero intersection with the ideal L^∞. The following notation is used here:

$$H(\boldsymbol{f}) = H_1(f^1) + H_2(f^2) + H_3(f^3), \quad \boldsymbol{f} = (f^1, f^2, f^3).$$

In what follows, we assume that $f^0, f^1, f^2, f^3 \in C^n(t_0, t_1)$, where $-\infty \leq t_0 < t_1 \leq \infty$, $n \in \mathbb{N} \cup \{\infty\}$. The following lemmas are used in the classification of subalgebras [59].

Lemma 6.1. *Let $f \in C^n(t_0, t_1)$. Then, there exists a solution $h \in C^n(t_0, t_1)$ of the equation $th_t + h + f = 0$.*

Lemma 6.2. *Let $f \in C^n(t_0, t_1)$. Then, there exists a solution $h \in C^n(t_0, t_1)$ of the equation $2th_t - h + f = 0$.*

Table 6.6: Optimal system of the subalgebras ΘL^5.

$p.q$	Basis K^{pq}	Nor K^{pq}	$p.q$	Basis K^{pq}	Nor K^{pq}
5.1	1, 2, 3, 4, 5	= 5.1	2.7	1 + 2, 5	4.1
4.1	1, 2, 3, 5	5.1	2.8	$1 + \lambda 2 + 3$, 5	4.1
4.2	1, 2, 3, $4 + \mu 5$, $\mu \geq 0$	5.1	2.9	1 + 5, 2	4.1
4.3	1, 2, 4, 5	= 4.3	2.10	1, 2 + 5	4.1
4.4	1, $\lambda 2 + 3$, 4, 5	= 4.4	2.11	1 + 5, $\lambda 2 + 3$	4.1
4.5	2, 3, 4, 5	= 4.5	2.12	1, $\lambda 2 + 3 + 5$	4.1
3.1	1, 2, 3	5.1	2.13	2 + 5, 3	4.1
3.2	1, 2, 5	5.1	2.14	2, 3 + 5	4.1
3.3	$1, \lambda 2 + 3$, 5	5.1	2.15	$1 + 2 + \mu 5$, $\lambda 1 + 3, \mu \geq 0$	4.1
3.4	2, 3, 5	5.1	2.16	$1 + 2$, $\lambda 1 + 3 + \mu 5, \mu > 0$	4.1
3.5	1 + 5, 2, 3	4.1	2.17	$1 + 3 + \mu 5$, 2, $\mu \geq 0$	4.1
3.6	1, 2 + 5, 3	4.1	2.18	1 + 3, $2 + \mu 5$, $\mu > 0$	4.1
3.7	1, 2, 3 + 5	4.1	2.19	1, $4 + \mu 5$, $\mu \geq 0$	3.13
3.8	1 + 2, $\lambda 1 + 3$, 5	4.1	2.20	2, $4 + \mu 5$, $\mu \geq 0$	3.14
3.9	1 + 3, 2, 5	4.1	2.21	$\lambda 2 + 3$, $4 + \mu 5$, $\mu \geq 0$	3.15
3.10	1, 2, $4 + \mu 5$, $\mu \geq 0$	4.3	2.22	4, 5	= 2.22
3.11	$1, \lambda 2 + 3, 4 + \mu 5, \mu \geq 0$	4.4	1.1	1	5.1
3.12	2, 3, $4 + \mu 5$, $\mu \geq 0$	4.5	1.2	2	5.1
3.13	1, 4, 5	= 3.13	1.3	$\lambda 2 + 3$	5.1
3.14	2, 4, 5	= 3.14	1.4	5	5.1
3.15	$\lambda 2 + 3$, 4, 5	= 3.15	1.5	1 + 5	4.1
2.1	1, 2	5.1	1.6	$1 + 2 + \mu 5$, $\mu \geq 0$	4.1
2.2	1, $\lambda 2 + 3$	5.1	1.7	$1 + \lambda 2 + 3 + \mu 5$, $\mu \geq 0$	4.1
2.3	1, 5	5.1	1.8	2 + 5	4.1
2.4	2, 3	5.1	1.9	$\lambda 2 + 3 + 5$	4.1
2.5	2, 5	5.1	1.10	$4 + \mu 5$, $\mu \geq 0$	2.22
2.6	$\lambda 2 + 3$, 5	5.1	0.1	0	5.1

Lemma 6.3. *Let $f^1, f^2 \in C^n(t_0, t_1)$ and $\mu \in \mathbb{R}$. Then, there exists a solution $h^1, h^2 \in C^n(t_0, t_1)$ of the system of equations*

$$2th_t^1 - h^1 + \mu h^2 + f^1 = 0, \quad 2th_t^2 - h^2 - \mu h^1 + f^2 = 0. \tag{6.29}$$

Note that subalgebras obtained as a result of the classification, whose basis depends on nondetermined functions, may include similar subalgebras. For instance, by consecutive actions of the automorphisms $A_1(a_1)$, $A_4(a_4)$, and $A_1^d(\delta_1)$ and a linear transformation of the basis, the subalgebra $\{X_5 + H_0(f^0)\}$ can be brought to the form $\{X_5 + H_0(\widetilde{f^0})\}$, where

$$\widetilde{f^0}(t) = (-1)^{\delta_1} e^{-2a_4} f^0\big(e^{-2a_4}(t - a_1)\big), \tag{6.30}$$

the resultant subalgebra is similar to the initial one. Here, $A_i(a_i)$ are the automorphisms corresponding to the basis operators X_i, and $A_i^d(\delta_i)$ correspond to the discrete

Table 6.7: Optimal system of the subalgebras $\Theta_1 L$.

i	Basis	Comment	Similarity transformation
1	X_1		
2	$X_1 + X_5$		
3	$X_4 + \mu X_5$	$\mu \geq 0$	
4	$X_1 + X_2 + \mu X_5$	$\mu \geq 0$	
5	$X_1 + \lambda X_2 + X_3 + \mu X_5$	$\mu \geq 0$	
6	$H_0(f^0)$		$\widetilde{f^0}(t) = cf^0(at+b)$
7	$X_5 + H_0(f^0)$	$f^0 \not\equiv 0$	$\widetilde{f^0}(t) = (-1)^\delta a f^0(at+b)$
8	$X_2 - X_3 + H_0(f^0)$	$f^0 \not\equiv 0$	$\widetilde{f^0}(t) = (-1)^\delta a^{-1/2} f^0(at+b)$
9	$X_2 - X_3 + X_5 + H_0(f^0)$	$f^0 \not\equiv 0$	$\widetilde{f^0}(t) = (-1)^\delta f^0(t+b)$
10	$X_5 + H_3(f^3)$		$\widetilde{f^3}(t) = (-1)^\delta a^{-1/2} f^3(at+b)$
11	$X_2 + X_5 + H_3(f^3)$		$\widetilde{f^3}(t) = f^3(t+b)$
12	$\lambda X_2 + X_3 + X_5 + H_3(f^3)$		$\widetilde{f^3}(t) = f^3(t+b)$
13	$H(\boldsymbol{f})$		$\widetilde{\boldsymbol{f}}(t) = D(\delta_1,\delta_2,\delta_3)R(\gamma)\, c\boldsymbol{f}(at+b)$
14	$X_2 + H(\boldsymbol{f})$		$\widetilde{\boldsymbol{f}}(t) = D(\delta_1,\delta_2,0)R(\gamma)\, a^{-2}\boldsymbol{f}(at+b)$
15	$\lambda X_2 + X_3 + H(\boldsymbol{f})$		$\widetilde{\boldsymbol{f}}(t) = D(\delta_1,\delta_2,0)R(\gamma)\, a^{-2}\boldsymbol{f}(at+b)$

symmetries d_i:

$$d_1:\ \widetilde{x^1} = -x^1,\quad \widetilde{u^1} = -u^1;\quad d_2:\ \widetilde{x^2} = -x^2,\quad \widetilde{u^2} = -u^2;$$
$$d_3:\ \widetilde{x^3} = -x^3,\quad \widetilde{u^3} = -u^3,\quad \widetilde{T} = -T,\quad \widetilde{C} = -C.$$

Thus, the action of internal automorphisms and linear transformations of the basis divides each subalgebra in the optimal system $\Theta_1 L$ into classes of similar subalgebras. Note that only those transformations that do not change the finite-dimensional component of the basis operators should be considered here. Each class is uniquely determined by a particular form of functions on which these basis operators depend and includes subalgebras in which these functions are related by a certain expression, for instance, eq. (6.30). This expression, which is independent of the form of the functions, is called the *similarity transformation*. The optimal system $\Theta_1 L$ is given in Table 6.7. For convenience of presentation of results, some changes were made in the classification. In particular, the pair of the subalgebras $\{H(\boldsymbol{f})\}$, $\boldsymbol{f} \not\equiv 0$, and $\{H_0(f^0)\}$ was replaced by an equivalent pair $\{H(\boldsymbol{f})\}$ and $\{H_0(f^0)\}$, $f^0 \not\equiv 0$. A similar replacement was performed in the pair of the subalgebras with the numbers 7 and 10. In the subalgebra No. 8, we can assume that $f^0 \not\equiv 0$, referring the case with $f^0 \equiv 0$ to the subalgebra No. 15, where $\lambda = -1$ and $\boldsymbol{f} = 0$ should be assumed. Similar considerations are also applicable to the pair of the subalgebras with the numbers 9 and 12.

The similarity transformations found in this work are shown in the fourth column of the table. The following notations are used: $a > 0$, $b \in \mathbb{R}$, $c \neq 0$ are arbitrary

constants,

$$R(\gamma) = \begin{pmatrix} \cos\gamma & -\sin\gamma & 0 \\ \sin\gamma & \cos\gamma & 0 \\ 0 & 0 & 1 \end{pmatrix},$$

$$D(\delta_1, \delta_2, \delta_3) = \begin{pmatrix} (-1)^{\delta_1} & 0 & 0 \\ 0 & (-1)^{\delta_2} & 0 \\ 0 & 0 & (-1)^{\delta_3} \end{pmatrix},$$

and the parameter δ takes the values $\{0, 1\}$.

6.2 Group properties of two-dimensional equations

Group classification

In this paragraph, we consider the group analysis of equations of two-dimensional (plane) thermodiffusion motion

$$\begin{gathered} \boldsymbol{u}_t + (\boldsymbol{u}\cdot\nabla)\boldsymbol{u} = -\frac{1}{\rho_0}\nabla p + \nu\Delta\boldsymbol{u} - \mathbf{g}(\beta_1 T + \beta_2 C), \\ T_t + \boldsymbol{u}\cdot\nabla T = \chi\Delta T, \\ C_t + \boldsymbol{u}\cdot\nabla C = d\Delta C + \alpha d\Delta T, \\ \operatorname{div}\boldsymbol{u} = 0. \end{gathered} \tag{6.31}$$

The necessity of a separate study of the two-dimensional case is conditioned by the following considerations. As the system dimension decreases, the number of the basis operators of the admitted Lie algebra, which is infinite-dimensional, also decreases. Construction of optimal systems for such subalgebras is a rather complicated and laborious task which often cannot be fully solved. As demonstrated below, the smaller number of the basis operators (seven against nine for three-dimensional equations in the case with the constants α, β_1, and β_2 simultaneously being other than zero) allows construction of an optimal system of subalgebras not only of the first, but also of the second order. Subalgebras of dimension 2 yield invariant submodels of rank 1 of the initial system (6.1)–(6.4). These submodels are systems of ordinary differential equations and serve as a source of numerous physically meaningful exact solutions. In addition, using a comparatively simple example of two-dimensional equations, we need to clarify which types of solutions can be constructed by using the model symmetry properties. In the following, the possibility of generalizing these solutions to the three-dimensional case will be considered.

Calculations show that the results of the group analysis of three-dimensional equations can be transferred to the two-dimensional case by restricting the action of the admitted group on the corresponding space of dependent and independent

variables. Under this aspect, it is convenient to use the following notations: coordinate vector $\boldsymbol{x} = (x^1, x^3)$, velocity vector $\boldsymbol{u} = (u^1, u^3)$, and acceleration due to gravity $\mathbf{g} = (0, -\mathrm{g})$. In this section we describe the results of the group classification of the two-dimensional equations (6.31) with respect to the parameters included into the system (it is assumed that the constants α, β_1, and β_2 can vanish).

In the coordinate form, system (6.31) is written as

$$u^1_t + u^1 u^1_1 + u^3 u^1_3 + \frac{1}{\rho_0} p_1 - \nu(u^1_{11} + u^1_{33}) = 0; \tag{6.32}$$

$$u^3_t + u^1 u^3_1 + u^3 u^3_3 + \frac{1}{\rho_0} p_3 - \nu(u^3_{11} + u^3_{33}) - \mathrm{g}(\beta_1 T + \beta_2 C) = 0; \tag{6.33}$$

$$T_t + u^1 T_1 + u^3 T_3 - \chi(T_{11} + T_{33}) = 0; \tag{6.34}$$

$$C_t + u^1 C_1 + u^3 C_3 - d(C_{11} + C_{33}) - \alpha d(T_{11} + T_{33}) = 0; \tag{6.35}$$

$$u^1_1 + u^3_3 = 0. \tag{6.36}$$

These equations are supplemented with their differential corollaries

$$(u^1_1)^2 + (u^3_3)^2 + 2u^1_3 u^3_1 + \frac{1}{\rho_0}(p_{11} + p_{33}) - \mathrm{g}(\beta_1 T_3 + \beta_2 C_3) = 0; \tag{6.37}$$

$$u^1_{t1} + u^3_{t3} = 0, \quad u^1_{11} + u^3_{13} = 0, \quad u^1_{13} + u^3_{33} = 0. \tag{6.38}$$

The infinitesimal operator admitted by the system is sought in the form

$$X = \xi^t \frac{\partial}{\partial t} + \xi^1 \frac{\partial}{\partial x^1} + \xi^3 \frac{\partial}{\partial x^3} + \eta^1 \frac{\partial}{\partial u^1} + \eta^3 \frac{\partial}{\partial u^3} + \eta^p \frac{\partial}{\partial p} + \eta^T \frac{\partial}{\partial T} + \eta^C \frac{\partial}{\partial C}.$$

The governing equations are obtained by applying the extended operator $\underset{2}{X}$ to system (6.32)–(6.38) and passing to the corresponding manifold. The quantities u^1_{11}, u^3_{11}, p_{11}, T_{11}, C_{11}, u^3_{t3}, u^3_{13}, u^3_{33}, and u^1_1 are used as the external variables. The solution of the governing equations is given by the formulas

$$\begin{gathered}
\xi^t = 2c_4 t + c_0, \quad \xi^1 = c_4 x^1 + c_2 x^3 + f^1(t), \\
\xi^3 = -c_2 x^1 + c_4 x^3 + f^3(t), \\
\eta^1 = -c_4 u^1 + c_2 u^3 + f^1_t(t), \quad \eta^3 = -c_2 u^1 - c_4 u^3 + f^3_t(t), \\
\eta^p = \rho_0(c_5 \mathrm{g}\beta_1 x^3 + c_6 \mathrm{g}\beta_2 x^3 - f^1_{tt}(t)x^1 - f^3_{tt}(t)x^3) - 2c_4 p + f^0(t), \\
\eta^T = c_7 T + c_9 C + c_5, \quad \eta^C = c_8 C + c_{10} T + c_6,
\end{gathered} \tag{6.39}$$

where $c_0, c_2, c_4, c_5 - c_{10}$ are group constants and $f^i(t) \in C^\infty$, $i = 0, 1, 3$ are arbitrary smooth functions. The system of the classifying equations relating the group constants to the parameters α, β_1, β_2, χ, and d has the form

$$\begin{gathered}
\beta_1(c_7 + 3c_4) + \beta_2 c_{10} = 0, \quad \beta_2(c_8 + 3c_4) + \beta_1 c_9 = 0, \\
\alpha d(c_8 - c_7) + (\chi - d)c_{10} = 0, \quad (\chi - d)c_9 = 0, \\
\alpha c_9 = 0, \quad \beta_1 c_2 = 0, \quad \beta_2 c_2 = 0.
\end{gathered} \tag{6.40}$$

Table 6.8: Results of the group classification of the two-dimensional model.

α	β_1	β_2	Operators	$d = \chi$
0	0	0	$X_0, H_i, H_0, X_{13}, Z, T^1, T^3, C^1, C^3$	T^2, C^2
0	0	$\neq 0$	$X_0, H_i, H_0, Z_2, U_2, T^1, T^3$	T^2
0	$\neq 0$	0	$X_0, H_i, H_0, Z_1, U_1, C^1, C^3$	C^2
0	$\neq 0$	$\neq 0$	$X_0, H_i, H_0, Z_3, U_1, U_2$	R_1, R_2
$\neq 0$	0	0	$X_0, H_i, H_0, X_{13}, Z, R, L, T^3, C^3$	
$\neq 0$	0	$\neq 0$	$X_0, H_i, H_0, Z_3, U_2, T^3$	
$\neq 0$	$\neq 0$	0	$X_0, H_i, H_0, Z_3, U_1, C^3, L$	
$\neq 0$	$\neq 0$	$\neq 0$	$X_0, H_i, H_0, Z_3, U_1, U_2$	
			$\alpha = \beta_1(d-\chi)/\beta_2 d,\ d \neq \chi : R_1$	

The algebras of operators admitted by system (6.31), depending on the values of the parameters, are obtained by analyzing eqs. (6.40) and using formulas (6.39). The results of the group classification are summarized in Table 6.8. The first three columns show the values of the constants α, β_1, and β_2, the fourth column contains the basis operators, and the fifth column shows additional operators admitted by the system in the case with $d = \chi$. If all constants differ from zero (last row of the table), then the operator R_1 is admitted for the indicated value of the parameter α. Note that only one rotation operator X_{13} admitted in the case with $\beta_1 = \beta_2 = 0$ is left in the two-dimensional case.

$$
\begin{gathered}
X_0 = \frac{\partial}{\partial t}, \quad X_{13} = x^1\frac{\partial}{\partial x^3} - x^3\frac{\partial}{\partial x^1} + u^1\frac{\partial}{\partial u^3} - u^3\frac{\partial}{\partial u^1}, \\
H_i(f^i(t)) = f^i(t)\frac{\partial}{\partial x^i} + f^i_t(t)\frac{\partial}{\partial u^i} - \rho_0 x^i f^i_{tt}(t)\frac{\partial}{\partial p}, \quad i = 1, 3, \\
H_0(f^0(t)) = f^0(t)\frac{\partial}{\partial p}, \\
Z = 2t\frac{\partial}{\partial t} + x^1\frac{\partial}{\partial x^1} + x^3\frac{\partial}{\partial x^3} - u^1\frac{\partial}{\partial u^1} - u^3\frac{\partial}{\partial u^3} - 2p\frac{\partial}{\partial p}, \\
U_1 = \rho_0 g x^3\frac{\partial}{\partial p} + \frac{1}{\beta_1}\frac{\partial}{\partial T}, \quad U_2 = \rho_0 g x^3\frac{\partial}{\partial p} + \frac{1}{\beta_2}\frac{\partial}{\partial C}, \\
T^1 = T\frac{\partial}{\partial T}, \quad T^2 = C\frac{\partial}{\partial T}, \quad T^3 = \frac{\partial}{\partial T}, \quad C^1 = C\frac{\partial}{\partial C}, \\
C^2 = T\frac{\partial}{\partial C}, \quad C^3 = \frac{\partial}{\partial C}, \quad R = T^1 + C^1, \\
R_1 = T^1 - \frac{\beta_1}{\beta_2}C^2, \quad R_2 = C^1 - \frac{\beta_2}{\beta_1}T^2, \quad Z_1 = Z - 3T^1, \\
Z_2 = Z - 3C^1, \quad Z_3 = Z - 3R, \quad L = \big[\alpha T + (1-\chi/d)C\big]\frac{\partial}{\partial C}.
\end{gathered}
\tag{6.41}
$$

It should be noted that the results obtained at $\alpha = 0$, $\beta_1 \neq 0$, and $\beta_2 = 0$ agree with the results of the group analysis of the Oberbeck–Boussinesq equations in the two-

Table 6.9: Results of the classification in the case with $\alpha = 0$.

β_1	β_2	Operators	$d = \chi$
0	0	$X_0, H_i, H_0, X_{13}, Z, T^1, T^3, C^1, C^3$	T^2, C^2
0	1	$X_0, H_i, H_0, Z_2, U_2, T^1, T^3$	T^2
1	0	$X_0, H_i, H_0, Z_1, U_1, C^1, C^3$	C^2
1	1	$X_0, H_i, H_0, Z_3, U_1, U_2$	

Table 6.10: Results of the classification in the case with $\alpha = \pm 1$, $d = \chi$.

β_1	β_2	Operators
0	0	$X_0, H_i, H_0, X_{13}, Z, R, T^3, C^2, C^3$
0	1	$X_0, H_i, H_0, Z_3, U_2, T^3$
1	0	$X_0, H_i, H_0, Z_3, U_1, C^2, C^3$

dimensional case [76, 106]. These equations admit the Lie algebra of operators with the basis $X_0, H_1, H_3, H_0, Z_1, U_1$.

The group of equivalence transformations of parameters for the two-dimensional equations (6.31) coincides with the corresponding group for the three-dimensional case (see eqs. (6.20)). Repeating the reasoning described in Section 6.1 (with the system of the classifying equations being considered), we obtain a solution of the group classification problem with allowance for equivalence transformations. The corresponding results are listed in Tables 6.9 and 6.10. The first two columns show the values of the constants β_1 and β_2, the third column contains the admitted operators, and the fourth column shows additional operators admitted in the case with $d = \chi$ (Table 6.9). The operators listed in the tables have the form (6.40), (6.41), where $\beta_1 = \beta_2 = \rho_0 = \mathrm{g} = 1$ should be assumed.

Remark 6.1. In describing the results of the group analysis of the two-dimensional equations (6.31), we retained the notations used in the three-dimensional case (e. g., for the extension operator Z). To emphasize the analogy between the plane and spatial cases, this principle is also used in the following. The discussion is nonetheless unambiguous, because it is clear from the context of the section which case is considered.

Optimal system of the first-order subalgebras

Here we consider the two-dimensional system (6.31), which takes into account the thermodiffusion effect and the linear dependence of density on temperature and concentration perturbations (thus, the parameters α, β_1, and β_2 differ from zero). According to the results of the group classification, system (6.31) in this case admits the infinite-dimensional Lie algebras of operators $\overline{L}$. The expansion $\overline{L} = L^4 \oplus \overline{L}^{\infty}$ into a

subdirect sum of the finite-dimensional subalgebra L^4 with the basis

$$X_1 = \frac{\partial}{\partial t}, \quad X_2 = \rho_0 g x^3 \frac{\partial}{\partial p} + \frac{1}{\beta_2}\frac{\partial}{\partial C}, \quad X_3 = \rho_0 g x^3 \frac{\partial}{\partial p} + \frac{1}{\beta_1}\frac{\partial}{\partial T},$$
$$X_4 = 2t\frac{\partial}{\partial t} + x^1\frac{\partial}{\partial x^1} + x^3\frac{\partial}{\partial x^3} - u^1\frac{\partial}{\partial u^1} - u^3\frac{\partial}{\partial u^3} - 2p\frac{\partial}{\partial p} - 3T\frac{\partial}{\partial T} - 3C\frac{\partial}{\partial C} \tag{6.42}$$

and an infinite-dimensional ideal $\overline{L}^{\infty}$ formed by the operators

$$H_1(f^1(t)) = f^1(t)\frac{\partial}{\partial x^1} + f^1_t(t)\frac{\partial}{\partial u^1} - \rho_0 x^1 f^1_{tt}(t)\frac{\partial}{\partial p},$$
$$H_3(f^3(t)) = f^3(t)\frac{\partial}{\partial x^3} + f^3_t(t)\frac{\partial}{\partial u^3} - \rho_0 x^3 f^3_{tt}(t)\frac{\partial}{\partial p}, \tag{6.43}$$
$$H_0(f^0(t)) = f^0(t)\frac{\partial}{\partial p}$$

is valid for this algebra. For convenience of further calculations, we introduce new notations for the operators here. If the constants involved into the system are related as $\alpha = \beta_1(d-\chi)/\beta_2 d$, $d \neq \chi$, then the basis (6.42), (6.43) is supplemented with the operator

$$R_1 = T\frac{\partial}{\partial T} - \frac{\beta_1}{\beta_2}T\frac{\partial}{\partial C}.$$

In the following, this particular case is not considered, and the above-given relation is assumed to be not satisfied.

Equations (6.31) also possess discrete symmetry:

$$d_1: \widetilde{x^1} = -x^1, \quad \widetilde{u^1} = -u^1; \quad d_3: \widetilde{x^3} = -x^3,$$
$$\widetilde{u^3} = -u^3, \quad \widetilde{T} = -T, \quad \widetilde{C} = -C. \tag{6.44}$$

Let us now pass to constructing the optimal system of subalgebras for the Lie algebra $\overline{L}$. Firstly, we construct the optimal system ΘL^4 for the algebra L^4. This system was found in Section 6.1 (see Table 6.5). The optimal system $\Theta_1\overline{L}$ is given in Table 6.11. The subalgebra number has the form $r.i$, where r is the subalgebra dimension and i is its ordinal number. For convenience sake in the presentation of the results, some changes were made in the classification described here. In particular, the pair of the subalgebras $\{H(\boldsymbol{f})\}$, $\boldsymbol{f} \neq 0$, and $\{H_0(f^0)\}$ was replaced by an equivalent pair $\{H(\boldsymbol{f})\}$ and $\{H_0(f^0)\}$, $f^0 \neq 0$. Further, we can assume that $f^0 \neq 0$ in the subalgebra 1.6, referring the case $f^0 \equiv 0$ to the subalgebra 1.9, where $\lambda = -1$ and $f^1 = f^3 = 0$ should be assumed. The similarity transformations of the subalgebras are listed in the fourth column. The following notations are used: $a > 0$, $b \in \mathbb{R}$, $c \neq 0$ are arbitrary constants, and the parameter δ takes the values $\{0, 1\}$.

To construct the second-order optimal system $\Theta_2\overline{L}$, we have to classify subalgebras from three classes:

Table 6.11: Optimal system of the subalgebras $\Theta_1\overline{L}$.

r.i	**Basis**	**Comment**	**Similarity transformation**
1.1	X_1		
1.2	$X_1 + X_2$		
1.3	$X_1 + \lambda X_2 + X_3$		
1.4	X_4		
1.5	$H_0(f^0)$	$f^0 \not\equiv 0$	$\widetilde{f^0}(t) = cf^0(at+b)$
1.6	$X_2 - X_3 + H_0(f^0)$	$f^0 \not\equiv 0$	$\widetilde{f^0}(t) = (-1)^\delta a^{-1/2} f^0(at+b)$
1.7	$H_1(f^1) + H_3(f^3)$		$\widetilde{f^1}(t) = (-1)^\delta cf^1(at+b)$
			$\widetilde{f^3}(t) = cf^3(at+b)$
1.8	$X_2 + H_1(f^1) + H_3(f^3)$		$\widetilde{f^1}(t) = (-1)^\delta a^{-2} f^1(at+b)$
			$\widetilde{f^3}(t) = a^{-2} f^3(at+b)$
1.9	$\lambda X_2 + X_3 + H_1(f^1) + H_3(f^3)$		$\widetilde{f^1}(t) = (-1)^\delta a^{-2} f^1(at+b)$
			$\widetilde{f^3}(t) = a^{-2} f^3(at+b)$

1) $\{H(\boldsymbol{f}) + H_0(f^0),\ H(\boldsymbol{g}) + H_0(g^0)\}$,
2) $\{R_i + H(\boldsymbol{f}) + H_0(f^0),\ H(\boldsymbol{g}) + H_0(g^0)\}$,
3) $\{P_j + H(\boldsymbol{f}) + H_0(f^0),\ Q_j + H(\boldsymbol{g}) + H_0(g^0)\}$,

where $\{R_i\} \in \Theta_1 L^4$, $\{P_j,\ Q_j\} \in \Theta_2 L^4$, $i = 1, \ldots, 6$, $j = 1, \ldots, 8$. Here, the first class belongs to the ideal $\overline{L}^\infty$, while the second and third classes have one-dimensional and zero intersections with the ideal $\overline{L}^\infty$, respectively.

The optimal system $\Theta_2\overline{L}$ is given in Table 6.12. Here, we use the same principle of subalgebra numeration as that in Table 6.11. The constants λ, μ, γ, and σ take any real values if not stated otherwise. The arbitrary functions in the subalgebras with the numbers 2.42–2.58 satisfy the conditions indicated in the third column. Some of these conditions are ordinary differential equations whose solution is written explicitly. These equations, however, can be resolved with respect to various functions, which involves rather cumbersome transformations. Therefore, the presentation of the results used in this table is preferable.

6.3 Invariant submodels and exact solutions of thermodiffusion equations

Standard notations of the coordinate vector $\boldsymbol{x} = (x, y)$ and velocity vector $\boldsymbol{u} = (u, v)$ are used in constructing invariant submodels of two-dimensional equations. Correspondingly, system (6.31) takes the form

$$u_t + uu_x + vu_y = -\frac{1}{\rho_0} p_x + \nu(u_{xx} + u_{yy}); \tag{6.45}$$

Table 6.12: Optimal system of the subalgebras $\Theta_2\bar{L}$.

r.i	**Basis**	**Comment**
2.1	X_1, $H_0(1)$	
2.2	X_1, $H_3(1)$	
2.3	X_1, $H_1(1) + H_0(1)$	
2.4	X_1, $H_1(1) + H_3(\lambda)$	$\lambda \geq 0$
2.5	X_1, $H_0(e^{\pm t})$	
2.6	X_1, $H_3(e^{\pm t})$	
2.7	X_1, $H_1(e^{\pm t}) + H_3(\lambda e^{\pm t})$	$\lambda \geq 0$
2.8	X_1, X_2	
2.9	X_1, $X_2 \pm H_3(1)$	
2.10	X_1, $X_2 + H_1(1) + H_3(\mu)$	
2.11	X_1, $\lambda X_2 + X_3$	
2.12	X_1, $\lambda X_2 + X_3 \pm H_3(1)$	
2.13	X_1, $\lambda X_2 + X_3 + H_1(1) + H_3(\mu)$	
2.14	X_1, $X_2 - X_3 + H_0(1)$	
2.15	X_1, $X_2 - X_3 + H_1(1) + H_0(\lambda)$	$\lambda > 0$
2.16	X_1, X_4	
2.17	X_4, $H_0(t^\gamma)$	
2.18	X_4, $H_3(t^\gamma)$	
2.19	X_4, $H_1(t^\gamma) + H_3(\mu t^\gamma)$	$\mu \geq 0$
2.20	X_4, $H_3(\sqrt{t}) + H_0(\lambda/t)$	$\lambda > 0$
2.21	X_4, $H_1(\sqrt{t}) + H_3(\mu\sqrt{t}) + H_0(\lambda/t)$	$\lambda > 0, \mu \geq 0$
2.22	X_4, X_2	
2.23	X_4, $\lambda X_2 + X_3 + H_0(\mu\sqrt{t})$	$\mu \geq 0$
2.24	X_4, $\lambda X_2 + \sigma X_3 + H_3(t^2)$	$\lambda^2 + \sigma^2 \neq 0$
2.25	X_4, $\lambda X_2 + \sigma X_3 + H_1(t^2) + H_3(\mu t^2)$	$\lambda^2 + \sigma^2 \neq 0, \mu \geq 0$
2.26	X_4, $\lambda X_2 + (\frac{9}{4\mathrm{g}} - \lambda)X_3 + H_3(t^2) + H_0(\mu\sqrt{t})$	$\mu > 0$
2.27	$X_1 + X_2$, $H_0(1)$	
2.28	$X_1 + X_2$, $H_1(1) + H_0(\lambda)$	$\lambda \geq 0$
2.29	$X_1 + X_2$, $H_1(\lambda) + H_3(1) + H_0(\rho_0 \mathrm{g} t)$	$\lambda \geq 0$
2.30	$X_1 + \lambda X_2$, $H_0(e^{\pm t})$	$\lambda > 0$
2.31	$X_1 + \lambda X_2$, $H_1(e^{\pm t})$	$\lambda > 0$
2.32	$X_1 + \lambda X_2$, $H_1(\mu e^{\pm t}) + H_3(e^{\pm t}) + H_0(\lambda\rho_0 \mathrm{g} t e^{\pm t})$	$\lambda > 0, \mu \geq 0$
2.33	$X_1 + \lambda X_2 + X_3$, $H_0(1)$	
2.34	$X_1 + \lambda X_2 + X_3$, $H_1(1) + H_0(\mu)$	$\mu \geq 0$
2.35	$X_1 + \lambda X_2 + X_3$, $H_1(\mu) + H_3(1) + H_0(\rho_0 \mathrm{g}(\lambda+1)t)$	$\mu \geq 0$
2.36	$X_1 + \lambda X_2 + \mu X_3$, $H_0(e^{\pm t})$	$\mu > 0$
2.37	$X_1 + \lambda X_2 + \mu X_3$, $H_1(e^{\pm t})$	$\mu > 0$
2.38	$X_1 + \lambda X_2 + \mu X_3$, $H_1(\sigma e^{\pm t}) + H_3(e^{\pm t}) + H_0(\rho_0 \mathrm{g}(\lambda+\mu) t e^{\pm t})$	$\mu > 0, \sigma \geq 0$
2.39	$X_1 + X_2$, $X_1 + X_3 + H_1(\lambda) + H_0(\mu)$	$\lambda \geq 0, \mu \neq 0$
2.40	$X_1 + X_2$, $\lambda X_1 + X_3 + H_1(\mu) + H_3(\sigma) + H_0(\sigma\rho_0 \mathrm{g} t)$	$\mu \geq 0$
2.41	$X_1 + X_3$, $X_2 + H_1(\lambda) + H_3(\mu) + H_0(\mu\rho_0 \mathrm{g} t)$	$\lambda \geq 0$
2.42	$H_0(f^0)$, $H_0(g^0)$	
2.43	$H_1(f^1) + H_3(f^3)$, $H_0(g^0)$	

Table 6.12: (continued)

r.i	**Basis**	**Comment**
2.44	$H_3(f^3), H_3(g^3) + H_0(g^0)$	$f^3_{tt}g^3 - f^3g^3_{tt} = 0$, $g^3 \neq cf^3$, $g^0 \neq 0$
2.45	$H_1(f^1) + H_3(\lambda f^1), H_1(g^1) + H_3(\lambda g^1) + H_0(g^0)$	$f^1_{tt}g^1 - f^1g^1_{tt} = 0$, $g^1 \neq cf^1$, $g^0 \neq 0, \lambda \geq 0$
2.46	$H_1(f^1) + H_3(f^3), H_1(g^1) + H_3(g^3)$	$f^1_{tt}g^1 - f^1g^1_{tt} + f^3_{tt}g^3 - f^3g^3_{tt} = 0$
2.47	$X_2 + H_1(f^1), H_0(g^0)$	
2.48	$X_2 + H_1(f^1) + H_3(f^3), H_1(g^1) + H_3(g^3) + H_0(g^0)$	$f^1_{tt}g^1 - f^1g^1_{tt} = 0$, $(f^3_{tt} - \mathrm{g})g^3 - f^3g^3_{tt} = 0$, $f^1g^3 - f^3g^1 = 0$, $f^3, g^0 \neq 0$
2.49	$X_2 + H_1(f^1) + H_3(f^3), H_1(g^1) + H_3(g^3)$	$f^1_{tt}g^1 - f^1g^1_{tt} + (f^3_{tt} - \mathrm{g})g^3 - f^3g^3_{tt} = 0$
2.50	$X_2 - X_3 + H_0(f^0), H_0(g^0)$	
2.51	$X_2 - X_3 + H_0(f^0), H_1(g^1) + H_3(g^3)$	$f^0 \neq 0$
2.52	$X_2 - X_3 + H_1(f^1), H_1(g^1) + H_0(g^0)$	$f^1_{tt}g^1 - f^1g^1_{tt} = 0$, $f^1,\ g^0 \neq 0$
2.53	$\lambda X_2 + X_3 + H_1(f^1), H_0(g^0)$	$\lambda \neq -1$
2.54	$\lambda X_2 + X_3 + H_1(f^1) + H_3(f^3)$, $H_1(g^1) + H_3(g^3) + H_0(g^0)$	$f^1_{tt}g^1 - f^1g^1_{tt} = 0$, $(f^3_{tt} - \mathrm{g}(\lambda+1))g^3 - f^3g^3_{tt} = 0$, $f^1g^3 - f^3g^1 = 0, f^3,\ g^0 \neq 0$
2.55	$\lambda X_2 + X_3 + H_1(f^1) + H_3(f^3), H_1(g^1) + H_3(g^3)$	$f^1_{tt}g^1 - f^1g^1_{tt} + (f^3_{tt} - \mathrm{g}(\lambda+1))g^3 - f^3g^3_{tt} = 0$
2.56	$X_2 + H_1(f^1), X_3 + H_1(f^1) + H_0(g^0)$	$g^0 \neq 0$
2.57	$X_2 + H_1(f^1) + H_3(f^3)$, $X_3 + H_1(g^1) + H_3(g^3) + H_0(g^0)$	$f^1_{tt}g^1 - f^1g^1_{tt} = 0$, $(f^3_{tt} - \mathrm{g})g^3 - f^3(g^3_{tt} - \mathrm{g}) = 0$, $f^1g^3 - f^3g^1 = 0, f^3, g^0 \neq 0$
2.58	$X_2 + H_1(f^1) + H_3(f^3), X_3 + H_1(g^1) + H_3(g^3)$	$f^1_{tt}g^1 - f^1g^1_{tt} + (f^3_{tt} - \mathrm{g})g^3 - f^3(g^3_{tt} - \mathrm{g}) = 0$

$$v_t + uv_x + vv_y = -\frac{1}{\rho_0}p_y + \nu(v_{xx} + v_{yy}) + \mathrm{g}(\beta_1 T + \beta_2 C); \tag{6.46}$$

$$T_t + uT_x + vT_y = \chi(T_{xx} + T_{yy}); \tag{6.47}$$

$$C_t + uC_x + vC_y = d(C_{xx} + C_{yy}) + \alpha d(T_{xx} + T_{yy}); \tag{6.48}$$

$$u_x + v_y = 0. \tag{6.49}$$

The operators (6.42) and (6.43) admitted by the system are written as

$$X_1 = \frac{\partial}{\partial t}, \quad X_2 = \rho_0 \mathrm{g} y\frac{\partial}{\partial p} + \frac{1}{\beta_2}\frac{\partial}{\partial C}, \quad X_3 = \rho_0 \mathrm{g} y\frac{\partial}{\partial p} + \frac{1}{\beta_1}\frac{\partial}{\partial T},$$
$$X_4 = 2t\frac{\partial}{\partial t} + x\frac{\partial}{\partial x} + y\frac{\partial}{\partial y} - u\frac{\partial}{\partial u} - v\frac{\partial}{\partial v} - 2p\frac{\partial}{\partial p} - 3T\frac{\partial}{\partial T} - 3C\frac{\partial}{\partial C},$$

$$
\begin{aligned}
H_1(f) &= f\frac{\partial}{\partial x} + f_t\frac{\partial}{\partial u} - \rho_0 x f_{tt}\frac{\partial}{\partial p},\\
H_3(g) &= g\frac{\partial}{\partial y} + g_t\frac{\partial}{\partial v} - \rho_0 y g_{tt}\frac{\partial}{\partial p},\\
H_0(h) &= h\frac{\partial}{\partial p},
\end{aligned}
\tag{6.50}
$$

where $f = f(t)$, $g = g(t)$, and $h = h(t)$ are arbitrary smooth functions. These operators form the Lie algebra $\overline{L}$.

Submodels of ranks 2 and 1 are constructed on the basis of subalgebras from the optimal systems $\Theta_1\overline{L}$ and $\Theta_2\overline{L}$, respectively (see Tables 6.11 and 6.12). The numeration of these submodels coincides with the numeration of the corresponding subalgebras in the tables. Note that some subalgebras do not satisfy the necessary condition of existence of invariant solutions [157], but the number of the remaining subalgebras (34) is still rather large. Therefore it seems reasonable to start the analysis from considering submodels corresponding to steady and self-similar solutions. Steady solutions are invariant with respect to the shift in time (operator X_1), and self-similar solutions are invariant with respect to extension of dependent and independent variables (operator X_4). These classes of solutions are of undoubted physical interest owing to numerous applications [68, 71].

We should note another class of invariant solutions generated by subalgebras from the optimal systems. This class is formed by solutions where the temperature or concentration is a linear function of time. As an example, let us consider the submodel 1.3 generated by the subalgebra with the operator

$$
X_1 + \lambda X_2 + X_3 = \frac{\partial}{\partial t} + \rho_0 \mathrm{g}(\lambda+1)y\frac{\partial}{\partial p} + \frac{1}{\beta_1}\frac{\partial}{\partial T} + \frac{\lambda}{\beta_2}\frac{\partial}{\partial C}.
$$

Invariants of the corresponding subgroup are

$$
x,\ y,\ u,\ v,\ p - \rho_0 \mathrm{g}(\lambda+1)yt, \quad T - \frac{t}{\beta_1}, \quad C - \frac{\lambda t}{\beta_2}.
$$

The invariant solution has the following presentation:

$$
\begin{gathered}
u = u(x,y), \quad v = v(x,y), \quad p = P(x,y) + \rho_0 \mathrm{g}(\lambda+1)yt,\\
T = T'(x,y) + \frac{t}{\beta_1}, \quad C = C'(x,y) + \frac{\lambda t}{\beta_2}.
\end{gathered}
$$

Obviously, such solutions can describe a certain physical process only on a finite time interval (as the functions T and C are small deviations from the mean values of temperature and concentration and should be bounded). Examples of such solutions are provided by the submodel 1.2 and also by those submodels from the list 2.27–2.41 for which the condition of existence of invariant solutions is satisfied. These submodels are not considered in the present study.

Table 6.13: Subalgebras from the optimal system $\Theta_2\overline{L}$.

r.i	**Basis**	**Comment**
2.2	X_1, $H_3(1)$	
2.3	X_1, $H_1(1) + H_0(1)$	
2.4	X_1, $H_1(1) + H_3(\lambda)$	$\lambda \geq 0$
2.6	X_1, $H_3(e^{\pm t})$	
2.7	X_1, $H_1(e^{\pm t}) + H_3(\lambda e^{\pm t})$	$\lambda \geq 0$
2.9	X_1, $X_2 \pm H_3(1)$	
2.10	X_1, $X_2 + H_1(1) + H_3(\mu)$	
2.12	X_1, $\lambda X_2 + X_3 \pm H_3(1)$	
2.13	X_1, $\lambda X_2 + X_3 + H_1(1) + H_3(\mu)$	
2.15	X_1, $X_2 - X_3 + H_1(1) + H_0(\lambda)$	$\lambda > 0$
2.16	X_1, X_4	
2.18	X_4, $H_3(t^\gamma)$	
2.19	X_4, $H_1(t^\gamma) + H_3(\mu t^\gamma)$	$\mu \geq 0$
2.20	X_4, $H_3(\sqrt{t}) + H_0(\lambda/t)$	$\lambda > 0$
2.21	X_4, $H_1(\sqrt{t}) + H_3(\mu\sqrt{t}) + H_0(\lambda/t)$	$\lambda > 0, \mu \geq 0$
2.24	X_4, $\lambda X_2 + \sigma X_3 + H_3(t^2)$	$\lambda^2 + \sigma^2 \neq 0$
2.25	X_4, $\lambda X_2 + \sigma X_3 + H_1(t^2) + H_3(\mu t^2)$	$\lambda^2 + \sigma^2 \neq 0, \mu \geq 0$
2.26	X_4, $\lambda X_2 + [(9/4g) - \lambda]X_3 + H_3(t^2) + H_0(\mu\sqrt{t})$	$\mu > 0$

Another class of invariant solutions is provided by the submodels 2.42–2.58 generated by subalgebras whose basis operators depend on arbitrary (nonfixed) functions. Here, we have only one variable: time t. Such submodels are also not considered here.

Thus, in the following we study submodels of rank 2 with the numbers 1.1, 1.4, 1.5–1.9 and submodels of rank 1 from the list 2.1–2.26. It should be noted here that the subalgebras 1.5 and 1.6 do not satisfy the necessary condition of existence of invariant solutions. Two-dimensional subalgebras that satisfy this condition are listed in Table 6.13. We should also note one important circumstance. It was demonstrated in Section 6.1 that the transformation $C = \widetilde{C} + \alpha d T/(\chi - d)$ allows the term $\alpha d(T_{xx} + T_{yy})$ to be eliminated from eq. (6.48); as a result, this equation becomes homogeneous with respect to $\widetilde{C}$. It follows from here that the function

$$C - \widetilde{C} = \frac{\alpha d}{\chi - d} T \tag{6.51}$$

is a particular solution of eq. (6.48) under the condition that T satisfies eq. (6.47). This fact is widely used in constructing invariant solutions.

Thermodiffusion in plane layers

Let us give a physical interpretation of two solutions obtained by integrating invariant submodels of rank 1.

1. *Thermodiffusion in a vertical layer.* Let us consider the submodel 2.12.

The basis operators of the subalgebra are

$$X_1 = \frac{\partial}{\partial t},$$
$$\lambda X_2 + X_3 \pm H_3(1) = \pm\frac{\partial}{\partial y} + \rho_0 g(\lambda+1)y\frac{\partial}{\partial p} + \frac{1}{\beta_1}\frac{\partial}{\partial T} + \frac{\lambda}{\beta_2}\frac{\partial}{\partial C}.$$

The invariants of the subgroup are

$$x,\ u,\ v,\ p \mp \frac{\rho_0 g}{2}(\lambda+1)y^2, \quad T \mp \frac{y}{\beta_1},\ C \mp \frac{\lambda y}{\beta_2}.$$

The solution is presented as

$$u = u(x), \quad v = v(x), \quad p = P(x) \pm \frac{\rho_0 g}{2}(\lambda+1)y^2,$$
$$T = T'(x) \pm \frac{y}{\beta_1}, \quad C = C'(x) \pm \frac{\lambda y}{\beta_2}.$$

The factor-system is

$$\begin{gathered} u = u_0, \quad P = p_0, \quad vv_{xx} - u_0 v_x + g(\beta_1 T' + \beta_2 C') = 0, \\ \chi T'_{xx} - u_0 T'_x \mp \frac{v}{\beta_1} = 0, \quad dC'_{xx} - u_0 C'_x + \alpha d T'_{xx} \mp \frac{\lambda v}{\beta_2} = 0. \end{gathered} \tag{6.52}$$

If $u_0 = 0$, then system (6.52) takes the form

$$vv_{xx} + g(\beta_1 T' + \beta_2 C') = 0; \tag{6.53}$$
$$\chi T'_{xx} \mp \frac{v}{\beta_1} = 0; \tag{6.54}$$
$$dC'_{xx} + \alpha d T'_{xx} \mp \frac{\lambda v}{\beta_2} = 0. \tag{6.55}$$

We express the function v from eq. (6.54) and substitute it into eq. (6.55). Then, the last equation is integrated:

$$v = \pm\beta_1\chi T'_{xx}, \quad C' = \left(\frac{\lambda\beta_1\chi}{\beta_2 d} - \alpha\right)T' + \widetilde{c_1}x + \widetilde{c_2}. \tag{6.56}$$

Substituting the resultant expressions for v and C' into eq. (6.53), we obtain

$$T'_{xxxx} \pm \frac{g(d(\beta_1 - \beta_2\alpha) + \lambda\beta_1\chi)}{\beta_1 v\chi d}T' \pm \frac{\beta_2 g}{\beta_1 v\chi}(\widetilde{c_1}x + \widetilde{c_2}) = 0. \tag{6.57}$$

Let us introduce a formula for the coefficient at T':

$$a = \pm\frac{g(d(\beta_1 - \beta_2\alpha) + \lambda\beta_1\chi)}{\beta_1 v\chi d}.$$

Equation (6.57) has three different solutions for the cases with $a < 0$, $a > 0$, and $a = 0$ [239]. The functions v and C' are determined by eqs. (6.56). Let us write the solutions of the initial system for all three cases.

1) $a < 0$, $\gamma = \pm\sqrt[4]{-a}$:

$$\begin{gathered} u = 0, \quad p = p_0 \pm \frac{\rho_0 \mathrm{g}}{2}(\lambda+1)y^2, \\ v = \pm\beta_1\chi\gamma^2(c_3\cosh\gamma x + c_4\sinh\gamma x - c_5\cos\gamma x - c_6\sin\gamma x), \\ T = c_3\cosh\gamma x + c_4\sinh\gamma x + c_5\cos\gamma x + c_6\sin\gamma x + \beta_2(c_1x+c_2) \pm \frac{y}{\beta_1}, \\ C = \left(\frac{\lambda\beta_1\chi}{\beta_2 d} - \alpha\right)(c_3\cosh\gamma x + c_4\sinh\gamma x + c_5\cos\gamma x + c_6\sin\gamma x) \\ - \beta_1(c_1x+c_2) \pm \frac{\lambda y}{\beta_2}. \end{gathered} \tag{6.58}$$

2) $a > 0$, $\gamma = \pm\sqrt[4]{a/4}$:

$$\begin{gathered} u = 0, \quad p = p_0 \pm \frac{\rho_0 \mathrm{g}}{2}(\lambda+1)y^2, \\ v = \pm 2\beta_1\chi\gamma^2(c_4\sinh\gamma x\cos\gamma x - c_3\sinh\gamma x\sin\gamma x \\ + c_6\cosh\gamma x\cos\gamma x - c_5\cosh\gamma x\sin\gamma x), \\ T = c_3\cosh\gamma x\cos\gamma x + c_4\cosh\gamma x\sin\gamma x + c_5\sinh\gamma x\cos\gamma x \\ + c_6\sinh\gamma x\sin\gamma x + \beta_2(c_1x+c_2) \pm \frac{y}{\beta_1}, \\ C = \left(\frac{\lambda\beta_1\chi}{\beta_2 d} - \alpha\right)(c_3\cosh\gamma x\cos\gamma x + c_4\cosh\gamma x\sin\gamma x \\ + c_5\sinh\gamma x\cos\gamma x + c_6\sinh\gamma x\sin\gamma x) - \beta_1(c_1x+c_2) \pm \frac{\lambda y}{\beta_2}. \end{gathered} \tag{6.59}$$

Solutions (6.58), (6.59) involve new constants c_1 and c_2 introduced by the formula

$$c_i = -\frac{d}{d(\beta_1 - \beta_2\alpha) + \lambda\beta_1\chi}\,\widetilde{c_i}, \quad i = 1, 2.$$

3) $a = 0$, $\lambda = d(\beta_2\alpha - \beta_1)(\beta_1\chi)^{-1}$:

$$\begin{gathered} u = 0, \quad v = \beta_1\chi\left(\frac{c_5}{6}x^3 + \frac{c_4}{2}x^2 \pm c_3x \pm c_2\right), \\ p = p_0 \pm \rho_0\mathrm{g}\frac{d(\beta_2\alpha - \beta_1) + \beta_1\chi}{2\beta_1\chi}y^2, \\ C = -\frac{\beta_1}{\beta_2}\left(\pm\frac{c_5}{120}x^5 \pm \frac{c_4}{24}x^4 + \frac{c_3}{6}x^3 + \frac{c_2}{2}x^2 + c_1x + c_0\right) \\ - \frac{\beta_1\nu\chi}{\beta_2\mathrm{g}}(c_5x + c_4) \pm \frac{d(\beta_2\alpha - \beta_1)}{\beta_1\beta_2\chi}y, \\ T = \pm\frac{c_5}{120}x^5 \pm \frac{c_4}{24}x^4 + \frac{c_3}{6}x^3 + \frac{c_2}{2}x^2 + c_1x + c_0 \pm \frac{y}{\beta_1}. \end{gathered} \tag{6.60}$$

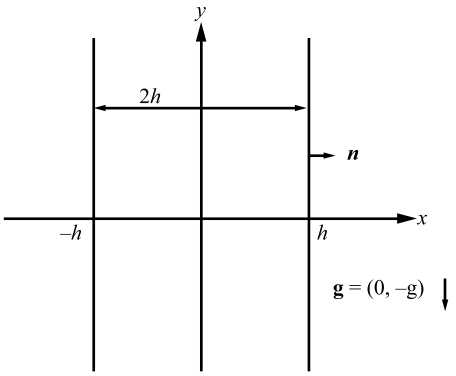

Figure 6.1: Definition sketch for vertically layer flow.

These equations involve new constants c_5 and c_4 in accordance with the formulas

$$c_5 = -\frac{\beta_2 \mathrm{g}}{\beta_1 \nu\chi}\,\widetilde{c_1}, \quad c_4 = -\frac{\beta_2 \mathrm{g}}{\beta_1 \nu\chi}\,\widetilde{c_2}.$$

For interpretation of the model 2.12, we pose the following steady problem. We consider an infinite vertical fluid layer of thickness $2h$ between two solid walls with a unit normal vector $\boldsymbol{n}$ (Figure 6.1). A linear distribution of temperature in the y direction is imposed on the walls. In addition, there is a constant difference in temperatures of the boundaries 2Θ in all cross sections of the layer. The no-slip condition and the absence of the matter flux through the boundary should be satisfied on the walls.

Thus, the boundary conditions at $x = \pm h$ have the form

$$u = v = 0, \quad T = Ay \pm \Theta, \quad -d\left(\frac{\partial C}{\partial \boldsymbol{n}} + \alpha\frac{\partial T}{\partial \boldsymbol{n}}\right) = 0. \tag{6.61}$$

Let us assume that there is also an asymptotically constant vertical gradient of the light species concentration in the layer:

$$\lim_{l\to\infty} \frac{1}{2l} \int_{-l}^{l} \frac{\partial C}{\partial y}\, dy = B. \tag{6.62}$$

We assume that the flow rate of the fluid through an arbitrary cross section of the layer is equal to zero. In the Oberbeck–Boussinesq approximation, this condition is written as

$$\int_{-h}^{h} v\, dx = 0. \tag{6.63}$$

Condition (6.63) is satisfied in a closed finite-length layer. Instead of this layer, we consider here an infinite layer in the vertical direction. This approximation is allowed if

the length of the layer is much greater than its thickness. The solution of the posed problem provides an approximate description of fluid motion in the central part of the closed finite layer.

Note that the choice of one of the three solutions (6.58)–(6.60) depends on the values of parameters involved into the equations and boundary conditions. The discussion below refers to solution (6.58) (the remaining cases are considered in a similar manner). This solution includes an arbitrary parameter λ, which determines the coefficient at y in the expression for the concentration. A similar coefficient in the expression for temperature is fixed. Setting the expressions for the temperature gradient A and concentration gradient B, however, requires two arbitrary parameters determining the coefficients at y in formulas for T and C. The necessary parameter can be introduced into the solution by applying a transformation determined by the extension operator X_4. This transformation is described by the formula

$$\begin{gathered}\tilde{x} = e^{a}x, \quad \tilde{y} = e^{a}y, \quad \tilde{u} = e^{-a}u, \quad \tilde{v} = e^{-a}v,\\ \tilde{p} = e^{-2a}p, \quad \tilde{T} = e^{-3a}T, \quad \tilde{C} = e^{-3a}C\end{gathered} \tag{6.64}$$

and transforms any solution of the system again into a solution. Let $a = -1/4 \ln \mu$ and $\mu > 0$; then, transformations (6.64) can be presented in the form

$$\begin{gathered}x \to \mu^{-1/4}x, \quad y \to \mu^{-1/4}y, \quad u \to \mu^{1/4}u, \quad v \to \mu^{1/4}v,\\ p \to \mu^{1/2}p, \quad T \to \mu^{3/4}T, \quad C \to \mu^{3/4}C.\end{gathered} \tag{6.65}$$

These formulas mean that x in the solution should be replaced by $\mu^{-1/4}x$; the function $\mu^{1/4}u$ should be considered instead of u, etc. In the solution thus obtained, the replacement $\pm\lambda\mu \to \lambda$, $\pm\mu \to \mu$ is performed, and formulas (6.58) take the form

$$\begin{gathered}u = 0, \quad p = p_0 + \frac{\rho_0 \mathrm{g}}{2}(\lambda + \mu)y^2,\\ v = \frac{\beta_1 \chi \gamma^2}{\mu}(c_3 \cosh \gamma x + c_4 \sinh \gamma x - c_5 \cos \gamma x - c_6 \sin \gamma x),\\ T = c_3 \cosh \gamma x + c_4 \sinh \gamma x + c_5 \cos \gamma x + c_6 \sin \gamma x + \beta_2(c_1 x + c_2) + \frac{\mu}{\beta_1}y,\\ C = \left(\frac{\lambda\beta_1\chi}{\mu\beta_2 d} - \alpha\right)(c_3 \cosh \gamma x + c_4 \sinh \gamma x + c_5 \cos \gamma x + c_6 \sin \gamma x) - \beta_1(c_1 x + c_2) + \frac{\lambda}{\beta_2}y,\\ \gamma = \pm\sqrt[4]{-\frac{\mathrm{g}(\mu d(\beta_1 - \beta_2\alpha) + \lambda\beta_1\chi)}{\beta_1 \nu \chi d}}, \quad \mu d(\beta_1 - \beta_2\alpha) + \lambda\beta_1\chi < 0.\end{gathered} \tag{6.66}$$

Here, the coefficients at y in the expressions for T and C are determined by two independent parameters μ and λ, respectively, and $\mu \neq 0$. Note that the replacement of the constants p_0 and c_i, $i = 1, \ldots, 6$ is also performed during this transformation.

For determining the unknown constants, the initial system of equations, boundary conditions, and solution (6.66) are rewritten in the dimensionless form. We introduce the characteristic scales of distance h, velocity $g\beta_1\Theta h^2/\nu$, pressure $\rho_0 g h \beta_1 \Theta$, temperature Θ, and concentration $\beta_1\Theta/\beta_2$. In the dimensionless variables, the steady equations (6.31) take the form

$$\begin{gathered} \mathrm{Gr}(\boldsymbol{u}\cdot\nabla)\boldsymbol{u} = -\nabla p + \Delta\boldsymbol{u} + (T+C)\,\boldsymbol{\gamma}, \\ \mathrm{Gr}(\boldsymbol{u}\cdot\nabla T) = \frac{1}{\mathrm{Pr}}\,\Delta T, \\ \mathrm{Gr}(\boldsymbol{u}\cdot\nabla C) = \frac{1}{\mathrm{Sc}}\,(\Delta C - \varepsilon\Delta T), \\ \operatorname{div}\boldsymbol{u} = 0, \end{gathered} \tag{6.67}$$

where $\boldsymbol{x} = (x, y)$, $\boldsymbol{u} = (u, v)$, and $\boldsymbol{\gamma} = (0, 1)$ should be assumed. The system contains four dimensionless parameters: Grashof number Gr, Prandtl number Pr, Schmidt number Sc, and parameter ε responsible for the thermodiffusion effect:

$$\mathrm{Gr} = \frac{g\beta_1\Theta h^3}{\nu^2}, \quad \mathrm{Pr} = \frac{\nu}{\chi}, \quad \mathrm{Sc} = \frac{\nu}{d}, \quad \varepsilon = -\frac{\alpha\beta_2}{\beta_1}. \tag{6.68}$$

The boundary conditions (6.61) at $x = \pm 1$ are written as

$$u = v = 0; \tag{6.69}$$

$$T = \frac{\mathrm{Ra}}{\mathrm{Gr}\,\mathrm{Pr}}\,y \pm 1; \tag{6.70}$$

$$\frac{\partial C}{\partial x} - \varepsilon\frac{\partial T}{\partial x} = 0. \tag{6.71}$$

Equalities (6.62) and (6.63) take the form

$$\lim_{l\to\infty}\frac{1}{2l}\int_{-l}^{l}\frac{\partial C}{\partial y}\,dy = \frac{\mathrm{Ra}_d}{\mathrm{Gr}\,\mathrm{Sc}}, \quad \int_{-1}^{1} v\,dx = 0. \tag{6.72}$$

Here, we have two new dimensionless parameters: Rayleigh number Ra and concentration Rayleigh number Ra_d, which are determined from the vertical gradients of temperature and concentration, respectively:

$$\mathrm{Ra} = \frac{g\beta_1 A h^4}{\nu\chi}, \quad \mathrm{Ra}_d = \frac{g\beta_2 B h^4}{\nu d}. \tag{6.73}$$

Solution (6.66) in the dimensionless variables is described by the formulas

$$\begin{gathered} u = 0, \quad p = p_0 + \frac{A'+B'}{2}\,y^2, \\ v = \frac{\gamma^2}{A'\,\mathrm{Gr}\,\mathrm{Pr}}\,(c_3\cosh\gamma x + c_4\sinh\gamma x - c_5\cos\gamma x - c_6\sin\gamma x), \\ T = c_3\cosh\gamma x + c_4\sinh\gamma x + c_5\cos\gamma x + c_6\sin\gamma x + c_1 x + c_2 + A' y, \\ C = \left(\frac{B'\,\mathrm{Sc}}{A'\,\mathrm{Pr}} + \varepsilon\right)(c_3\cosh\gamma x + c_4\sinh\gamma x + c_5\cos\gamma x + c_6\sin\gamma x) - c_1 x - c_2 + B' y, \\ \gamma = \pm\sqrt[4]{-\mathrm{Gr}\big(A'\,\mathrm{Pr}(\varepsilon+1) + B'\,\mathrm{Sc}\big)}, \end{gathered} \tag{6.74}$$

where $A'\,\mathrm{Pr}(\varepsilon+1)+B'\,\mathrm{Sc}<0$, $A'=\mu h\,(\beta_1\Theta)^{-1}$, $B'=\lambda h\,(\beta_1\Theta)^{-1}$. The constants c_1–c_6 are determined from conditions (6.69)–(6.71), after which the last condition in eqs. (6.72) is satisfied identically. Further, eqs. (6.70), (6.72), and (6.74) yield

$$A'=\frac{\mathrm{Ra}}{\mathrm{Gr}\,\mathrm{Pr}},\quad B'=\frac{\mathrm{Ra}_d}{\mathrm{Gr}\,\mathrm{Sc}};\tag{6.75}$$

then, we have $\gamma=\pm\sqrt[4]{-\mathrm{Ra}(\varepsilon+1)-\mathrm{Ra}_d}$, and the condition $\mathrm{Ra}(\varepsilon+1)+\mathrm{Ra}_d<0$ should be satisfied. Applying similar considerations to solutions (6.59) and (6.60) of the submodel 2.12, we find that these solutions correspond to the values $\mathrm{Ra}(\varepsilon+1)+\mathrm{Ra}_d>0$ and $\mathrm{Ra}(\varepsilon+1)+\mathrm{Ra}_d=0$, respectively. Let us write the solutions of the posed problem for all three cases (the velocity component $u=0$ is omitted).

1) Let $\mathrm{Ra}(\varepsilon+1)+\mathrm{Ra}_d<0$.

$$\begin{gathered}
v=\frac{\gamma^2(\varepsilon+1)}{D}\left[\frac{\sinh\gamma x}{\sinh\gamma}-\frac{\sin\gamma x}{\sin\gamma}\right],\quad p=p_0+\frac{1}{2}\left[\frac{\mathrm{Ra}}{\mathrm{Gr}\,\mathrm{Pr}}+\frac{\mathrm{Ra}_d}{\mathrm{Gr}\,\mathrm{Sc}}\right]y^2,\\
T=\frac{\mathrm{Ra}(\varepsilon+1)}{D}\left[\frac{\sinh\gamma x}{\sinh\gamma}+\frac{\sin\gamma x}{\sin\gamma}\right]+\frac{\gamma\,\mathrm{Ra}_d}{D}(\cot\gamma+\coth\gamma)x+\frac{\mathrm{Ra}}{\mathrm{Gr}\,\mathrm{Pr}}y,\\
C=\frac{(\mathrm{Ra}\,\varepsilon+\mathrm{Ra}_d)(\varepsilon+1)}{D}\left[\frac{\sinh\gamma x}{\sinh\gamma}+\frac{\sin\gamma x}{\sin\gamma}\right]-\frac{\gamma\,\mathrm{Ra}_d}{D}(\cot\gamma+\coth\gamma)x+\frac{\mathrm{Ra}_d}{\mathrm{Gr}\,\mathrm{Sc}}y,\\
\gamma=\sqrt[4]{-\mathrm{Ra}(\varepsilon+1)-\mathrm{Ra}_d},\quad D=2\,\mathrm{Ra}(\varepsilon+1)+\gamma\,\mathrm{Ra}_d(\cot\gamma+\coth\gamma).
\end{gathered}\tag{6.76}$$

2) Let $\mathrm{Ra}(\varepsilon+1)+\mathrm{Ra}_d>0$.

$$\begin{gathered}
v=\frac{4\gamma^2(\varepsilon+1)}{D}(\sin\gamma\cosh\gamma\cos\gamma x\sinh\gamma x-\cos\gamma\sinh\gamma\sin\gamma x\cosh\gamma x),\\
p=p_0+\frac{1}{2}\left[\frac{\mathrm{Ra}}{\mathrm{Gr}\,\mathrm{Pr}}+\frac{\mathrm{Ra}_d}{\mathrm{Gr}\,\mathrm{Sc}}\right]y^2,\\
T=\frac{2\,\mathrm{Ra}(\varepsilon+1)}{D}(\cos\gamma\sinh\gamma\cos\gamma x\sinh\gamma x+\sin\gamma\cosh\gamma\sin\gamma x\cosh\gamma x)\\
+\frac{\gamma\,\mathrm{Ra}_d}{D}(\sin2\gamma+\sinh2\gamma)x+\frac{\mathrm{Ra}}{\mathrm{Gr}\,\mathrm{Pr}}y,\\
C=\frac{2(\mathrm{Ra}\,\varepsilon+\mathrm{Ra}_d)(\varepsilon+1)}{D}(\cos\gamma\sinh\gamma\cos\gamma x\sinh\gamma x+\sin\gamma\cosh\gamma\sin\gamma x\cosh\gamma x)\\
-\frac{\gamma\,\mathrm{Ra}_d}{D}(\sin2\gamma+\sinh2\gamma)x+\frac{\mathrm{Ra}_d}{\mathrm{Gr}\,\mathrm{Sc}}y,\\
\gamma=\sqrt[4]{\frac{\mathrm{Ra}(\varepsilon+1)+\mathrm{Ra}_d}{4}},\\
D=\mathrm{Ra}(\varepsilon+1)(\cosh2\gamma-\cos2\gamma)+\gamma\,\mathrm{Ra}_d(\sin2\gamma+\sinh2\gamma).
\end{gathered}\tag{6.77}$$

3) Let $\mathrm{Ra}(\varepsilon+1)+\mathrm{Ra}_d=0$.

$$\begin{gathered} v=\frac{15(\varepsilon+1)}{2\,\mathrm{Ra}(\varepsilon+1)-90}(x^3-x),\quad p=p_0+\frac{\mathrm{Ra}}{2\mathrm{Gr}\,\mathrm{Pr}}\left(1-\frac{\mathrm{Pr}}{\mathrm{Sc}}(\varepsilon+1)\right)y^2,\\ T=\frac{\mathrm{Ra}(\varepsilon+1)}{8\,\mathrm{Ra}(\varepsilon+1)-360}(3x^5-10x^3+15x)-\frac{45}{\mathrm{Ra}(\varepsilon+1)-45}x+\frac{\mathrm{Ra}}{\mathrm{Gr}\,\mathrm{Pr}}y,\\ C=-\frac{\mathrm{Ra}(\varepsilon+1)}{8\,\mathrm{Ra}(\varepsilon+1)-360}(3x^5-10x^3+15x)-\frac{45\varepsilon}{\mathrm{Ra}(\varepsilon+1)-45}x-\frac{\mathrm{Ra}(\varepsilon+1)}{\mathrm{Gr}\,\mathrm{Sc}}y. \end{gathered} \tag{6.78}$$

In cases 1 and 2, the form of the solution is independent of the sign of the parameter γ (therefore, we chose the plus sign for certainty). Note that the assumption $\mu\neq 0$ in solution (6.66) leads to $\mathrm{Ra}\neq 0$ (see eqs. (6.74) and (6.75)). If we assume that $\mathrm{Ra}=0$ in the solutions (absence of the temperature gradient), we obtain the following formulas:

1) Let $\mathrm{Ra}_d<0$, $\gamma=\sqrt[4]{-\mathrm{Ra}_d}$.

$$\begin{gathered} v=\frac{\gamma(\varepsilon+1)(\sin\gamma\sinh\gamma x-\sinh\gamma\sin\gamma x)}{\mathrm{Ra}_d(\sin\gamma\cosh\gamma+\cos\gamma\sinh\gamma)},\\ p=p_0+\frac{\mathrm{Ra}_d}{2\mathrm{Gr}\,\mathrm{Sc}}y^2,\quad T=x,\\ C=\frac{(\varepsilon+1)(\sin\gamma\sinh\gamma x+\sinh\gamma\sin\gamma x)}{\gamma(\sin\gamma\cosh\gamma+\cos\gamma\sinh\gamma)}-x+\frac{\mathrm{Ra}_d}{\mathrm{Gr}\,\mathrm{Sc}}y. \end{gathered} \tag{6.79}$$

2) Let $\mathrm{Ra}_d>0$, $\gamma=\sqrt[4]{\mathrm{Ra}_d/4}$.

$$\begin{gathered} v=\frac{4\gamma(\varepsilon+1)}{\mathrm{Ra}_d(\sin 2\gamma+\sinh 2\gamma)}(\sin\gamma\cosh\gamma\cos\gamma x\sinh\gamma x-\cos\gamma\sinh\gamma\sin\gamma x\cosh\gamma x),\\ p=p_0+\frac{\mathrm{Ra}_d}{2\mathrm{Gr}\,\mathrm{Sc}}y^2,\quad T=x,\\ C=\frac{2(\varepsilon+1)}{\gamma(\sin 2\gamma+\sinh 2\gamma)}(\cos\gamma\sinh\gamma\cos\gamma x\sinh\gamma x+\sin\gamma\cosh\gamma\sin\gamma x\cosh\gamma x)\\ -x+\frac{\mathrm{Ra}_d}{\mathrm{Gr}\,\mathrm{Sc}}y, \end{gathered} \tag{6.80}$$

3) Let $\mathrm{Ra}_d=0$.

$$v=-\frac{1}{6}(\varepsilon+1)(x^3-x),\quad p=p_0,\quad T=x,\quad C=\varepsilon x. \tag{6.81}$$

Solution (6.80) was considered in [72, 150], where its stability to small perturbations was studied. In [72], the thermodiffusion effect was ignored ($\varepsilon=0$). Stability of solution (6.81) was studied in [73]. Moreover, if we assume that $\mathrm{Ra}_d=\varepsilon=0$ in eqs. (6.76)–(6.77), the resultant solution describes the motion of a homogeneous fluid in a vertical channel with a streamwise gradient of temperature [71]. We should also

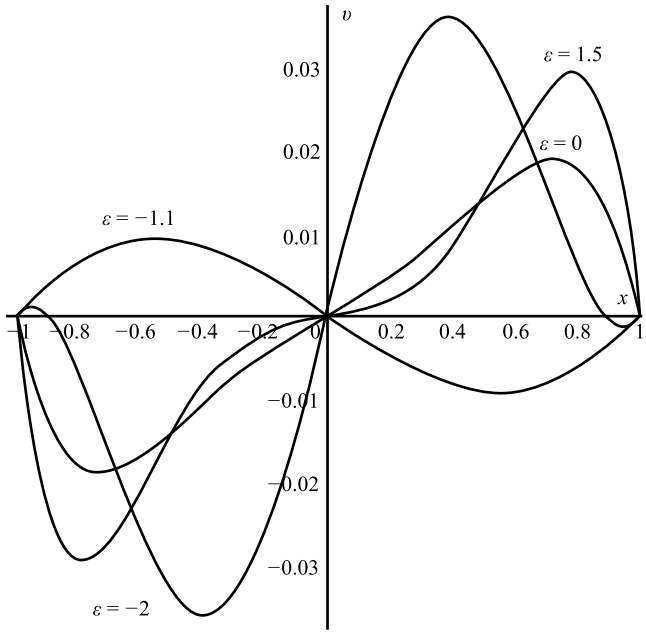

Figure 6.2: Velocity profiles given by (6.74) for Ra = 300, $\mathrm{Ra}_d = 0$.

note the publication [235], which deals with the stability of solutions (6.76)–(6.78) in the cases with $\varepsilon = 0$, Ra > 0, and $\mathrm{Ra}_d > 0$. Thus, these solutions generalize some previously known solutions to the case of thermodiffusion motion of a binary mixture in a vertical layer under various boundary conditions.

It is seen from the derived formulas that the velocity vanishes in all cases at $\varepsilon = -1$, while the temperature and concentration distributions become linear along the x coordinate. Thus, mechanical equilibrium in the system is possible. Moreover, the temperature and concentration gradients (or appropriate numbers Ra and Ra_d) in solutions (6.76) and (6.77) can be chosen in such a manner that the pressure in the layer is constant with accuracy to the hydrostatic pressure. Note that these solutions are not determined for all values of parameters. For example, the velocity v in solution (6.78) at $\mathrm{Ra}(\varepsilon + 1) = 45$ turns to infinity. As demonstrated in [71, 235], however, the steady flow at such values of parameters is unstable and does not occur in practice.

Let us now give an example of velocity, temperature, and concentration profiles in the cross section $y = 0$ for different values of the thermodiffusion parameter (Figure 6.2). These profiles correspond to the Rayleigh numbers Ra $= 300$ and $\mathrm{Ra}_d = 0$. The functions v, T, and C at $y = 0$ are uniquely determined by setting the parameters mentioned above.

In the absence of thermodiffusion (curve $\varepsilon = 0$), the fluid moves upward near the heated boundary and moves downward near the cold boundary. In this case, there

are no concentration inhomogeneities ($C = 0$). If the parameter ε is positive, then normal thermodiffusion occurs, and the light species diffuses toward the heated boundary. This leads to an increase in velocity (curve $\varepsilon = 1.5$). At negative values of the thermodiffusion parameter, abnormal thermodiffusion takes place. The light species moves toward the cold boundary; as a result, the motion velocity decreases. At $\varepsilon = -1$, mechanical equilibrium occurs. A further decrease in the thermodiffusion parameter leads to inversion of the velocity profile (curve $\varepsilon = -1.1$). The concentration of the light species near the cold boundary becomes high enough for the fluid to begin moving upward near this boundary and to move downward near the heated boundary. With a further decrease in the thermodiffusion parameter, velocity profile inversion is again observed (curve $\varepsilon = -2$). The fluid moves upward and downward near the cold and heated boundaries, respectively, and the motion direction in the remaining part of the layer changes to the opposite. Significant inhomogeneities of temperature and concentration in the layer are observed.

2. *Thermodiffusion in an inclined layer with a free boundary*. Let us now consider the submodel 2.4. The basis operators of the subalgebra are

$$X_1 = \frac{\partial}{\partial t}, \quad H_1(1) + H_3(\lambda) = \frac{\partial}{\partial x} + \lambda \frac{\partial}{\partial y}, \quad \lambda \geq 0.$$

The invariants of the subgroup are

$$y - \lambda x,\ u,\ v,\ p,\ T,\ C.$$

The solution is presented as

$$\xi = y - \lambda x, \quad u = u(\xi), \quad v = v(\xi), \quad p = p(\xi),\ T = T(\xi), \quad C = C(\xi).$$

The factor-system is

$$v = \lambda u + v_0, \quad v(\lambda^2 + 1)u_{\xi\xi} - v_0 u_\xi + \frac{\lambda \mathrm{g}}{\lambda^2 + 1}(\beta_1 T + \beta_2 C) = 0,$$
$$\chi(\lambda^2 + 1)T_{\xi\xi} - v_0 T_\xi = 0, \quad d(\lambda^2 + 1)(C_{\xi\xi} + \alpha T_{\xi\xi}) - v_0 C_\xi = 0,$$
$$p_\xi = \frac{\rho_0 \mathrm{g}}{\lambda^2 + 1}(\beta_1 T + \beta_2 C).$$

The solution in the case with $v_0 = 0$ is

$$\begin{aligned} u &= -\frac{\lambda \mathrm{g}}{6\nu(\lambda^2 + 1)^2}((\beta_1 c_1 + \beta_2 c_3)\xi^3 + 3(\beta_1 c_2 + \beta_2 c_4)\xi^2) + c_5\xi + c_6, \\ p &= \frac{\rho_0 \mathrm{g}}{2(\lambda^2 + 1)}((\beta_1 c_1 + \beta_2 c_3)\xi^2 + 2(\beta_1 c_2 + \beta_2 c_4)\xi) + p_0, \\ v &= \lambda u, \quad T = c_1\xi + c_2, \quad C = c_3\xi + c_4, \quad \xi = y - \lambda x. \end{aligned} \tag{6.82}$$

In this solution, all sought functions retain constant values on the straight lines $\xi = y - \lambda x = \mathrm{const}$, which suggests a possible physical interpretation.

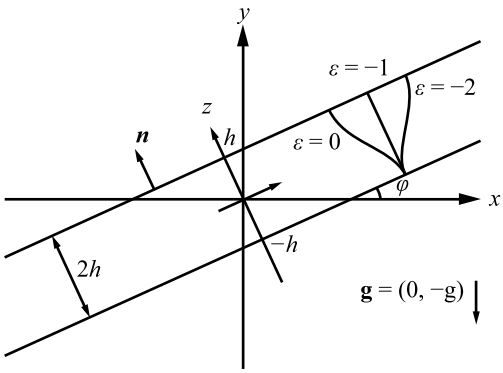

Figure 6.3: Inclined layer of the fluid.

We consider a fluid layer of thickness $2h$, which is aligned at an angle $0 \le \varphi < 90°$ to the horizon. The fluid is bounded from the bottom and from the top by a heated solid wall and a free boundary, respectively. These boundaries are straight lines with a unit normal vector $\boldsymbol{n}$ (Figure 6.3). It is assumed that there is a constant temperature difference 2Θ between the solid wall and the free boundary in all cross sections; the solid wall and the free boundary also retain a constant temperature. If we assume that $\lambda = \tan\varphi$ in solution (6.82), then the functions sought are constant on straight lines parallel to the layer boundaries, and the problem conditions can be satisfied. For the convenience of further calculations, we introduce a new coordinate system, where one axis is directed along the layer, and another axis (z) is perpendicular to the layer. Taking into account that $\xi = y - x\tan\varphi$ and $v = u\tan\varphi$, we replace the variables as $z = -x\sin\varphi + y\cos\varphi = \xi\cos\varphi$, $u \to u\cos\varphi + v\sin\varphi = u/\cos\varphi$, $v \to -u\sin\varphi + v\cos\varphi = 0$; as a result, the solution considered takes the form

$$\begin{gathered} u = -\frac{\mathrm{g}\sin\varphi}{6\nu}\left((\beta_1 c_1 + \beta_2 c_3)z^3 + 3(\beta_1 c_2 + \beta_2 c_4)z^2\right) + c_5 z + c_6, \\ p = \frac{\rho_0 \mathrm{g}\cos\varphi}{2}\left((\beta_1 c_1 + \beta_2 c_3)z^2 + 2(\beta_1 c_2 + \beta_2 c_4)z\right) + p_0, \\ v = 0, \quad T = c_1 z + c_2, \quad C = c_3 z + c_4. \end{gathered} \tag{6.83}$$

To avoid using new notations, we retained those of the velocity components and the constants c_i, $i = 1, \ldots, 6$ in the solution. In eqs. (6.83), the function u is the velocity in the direction parallel to the layer axis (there is no motion in the perpendicular direction).

Let us formulate the boundary conditions of the problem considered. On the wall and free boundary, we impose the temperature distribution and the absence of the matter flux:

$$z = \pm h: \quad T = \mp\Theta, \quad -d\left(\frac{\partial C}{\partial \boldsymbol{n}} + \alpha\frac{\partial T}{\partial \boldsymbol{n}}\right) = 0.$$

In addition, the no-slip condition (i. e., $u = 0$ at $z = -h$) should be satisfied on the wall. On the free boundary, we impose the kinematic condition (which is satisfied identically in the case considered) and the dynamic condition

$$z = h: \quad ((p - p_g)E - 2\nu\rho_0 D(\boldsymbol{u}))\boldsymbol{n} = 2\sigma H\boldsymbol{n} + \nabla_\Gamma\sigma.$$

Here p_g is the pressure on the free boundary, E is the unit matrix, $D(\boldsymbol{u})$ is the strain rate tensor, $\boldsymbol{n} = (0,1)$ is the external normal vector, $\sigma = \sigma(T,C)$ is the surface tension coefficient, H is the mean curvature of the free surface, and $\nabla_\Gamma = \nabla - \boldsymbol{n}(\boldsymbol{n}\cdot\nabla)$ is the surface gradient. As the temperature and concentration on the free boundary in solution (6.83) are constant, the surface gradient is equal to zero. The free surface is a straight line; therefore, $H = 0$. Thus, the dynamic condition does not impose constraints on the dependence $\sigma = \sigma(T,C)$. The strain rate tensor for solution (6.83) takes the form

$$D(\boldsymbol{u}) = \begin{pmatrix} 0 & u_z/2 \\ u_z/2 & 0 \end{pmatrix},$$

and the dynamic condition reduces to satisfying the relations

$$z = h: \quad \frac{\partial u}{\partial z} = 0, \quad p = p_g.$$

Let us specify the mean concentration in the cross section and assume that it remains constant along the layer:

$$\frac{1}{2h}\int_{-h}^{h}(C_0 + C)\,dz = C_0.$$

From here, we can easily obtain the condition on the function C, which determines the deviations from the mean value (see below). The transition to the dimensionless variables is performed in the same manner as previously (see eq. (6.67)). Solution (6.83) takes the form

$$u = -\frac{\sin\varphi}{6}\left[(c_1 + c_3)z^3 + 3(c_2 + c_4)z^2\right] + c_5 z + c_6, \tag{6.84}$$
$$p = \frac{\cos\varphi}{2}\left[(c_1 + c_3)z^2 + 2(c_2 + c_4)z\right] + p_0, \quad T = c_1 z + c_2, \quad C = c_3 z + c_4,$$

and the problem condition are written as

$$z = \pm 1: \quad T = \mp 1, \quad \frac{\partial C}{\partial z} - \varepsilon\frac{\partial T}{\partial z} = 0;$$
$$z = -1: \quad u = 0; \quad z = 1: \quad \frac{\partial u}{\partial z} = 0, \quad p = p_g'; \quad \int_{-1}^{1} C\,dz = 0.$$

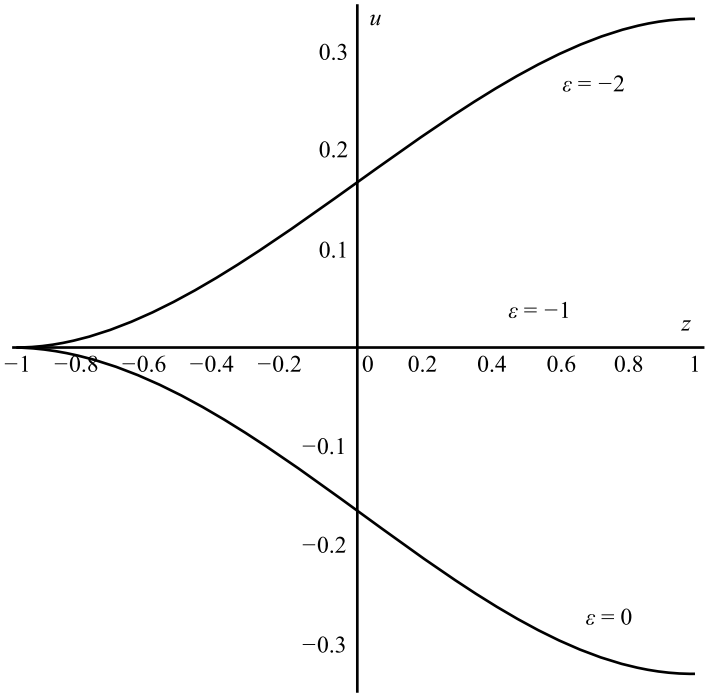

Figure 6.4: Velocity profiles given by (6.84) for $\varphi = 30°$.

Here, ε is the dimensionless parameter determining the thermodiffusion effect and $p'_g = p_g(\rho_0 g h \beta_1 \Theta)^{-1}$. Determining the unknown constants from the boundary conditions, we obtain

$$u = \frac{\sin\varphi}{6}(\varepsilon+1)(z^3 - 3z - 2),$$
$$p = \frac{\cos\varphi}{2}(\varepsilon+1)(-z^2+1) + p'_g, \quad T = -z, \quad C = -\varepsilon z.$$

As is seen from these formulas, the flow intensity increases with increasing angle of inclination.

Figure 6.4 shows the velocity profiles for different values of the thermodiffusion parameter for the angle of inclination $\varphi = 30^\circ$ (see also Figure 6.3). If there is no thermodiffusion (curve $\varepsilon = 0$), the flow moves downward along the layer under the action of the gravity force. In the case of normal thermodiffusion ($\varepsilon > 0$), the concentration of the light species near the heated boundary increases, while the heavy and cold fluid stays on the top. As a result, the motion velocity increases, but its profile is similar to the velocity profile for $\varepsilon = 0$. At negative values of ε, abnormal thermodiffusion occurs. The light species moves toward the cold free boundary, which leads to a decrease in velocity. The value $\varepsilon = -1$ corresponds to mechanical equilibrium.

With a further decrease in the thermodiffusion parameter, the concentration of the light species near the free boundary reaches significant values. As a result, the velocity changes its sign, and the fluid starts moving upward along the layer (curve $\varepsilon = -2$). To conclude, we should note that the problem solution has the following form in the case of heating from above ($T = \pm 1$ at $z = \pm 1$):

$$u = -\frac{\sin\varphi}{6}(\varepsilon + 1)(z^3 - 3z - 2),$$
$$p = \frac{\cos\varphi}{2}(\varepsilon + 1)(z^2 - 1) + p'_g, \quad T = z, \quad C = \varepsilon z,$$

and the motion direction changes to the opposite one.

7 Stability of equilibrium states in the Oberbeck–Boussinesq model

Stability of both equilibrium states and steady flows in the Oberbeck–Boussinesq model has been considered in a large number of works. As an illustration, we cite only three of them [143, 125, 179], in which the conditions of the emergence of convective flows in layers with a free boundary, an interface, and solid walls are examined. A review and analysis of earlier publications can be found in [68]. A finite-depth layer with a free upper boundary and a solid lower boundary is considered in Section 7.1. The temperature of the lower surface is assumed to be constant, and the temperature of the upper surface changes periodically in time. As a result, the equilibrium temperature gradient is nonuniform in terms of depth and periodic in time. The influence of this temperature gradient is studied numerically.

Convective stability of the equilibrium state of a system of two immiscible fluids with close values of density is considered in Section 7.2. A generalized Boussinesq approximation is constructed, which allows interface deformation to be correctly taken into account. Stability of the equilibrium state of a system of two fluids in a horizontal layer with a vertical temperature gradient is studied. Several instability mechanisms are found to exist: long-wave and cellular monotonic perturbations, as well as vibrational perturbations. The influence of interface deformability on instability characteristics is considered. Enhancement of deformability is demonstrated to change instability mechanisms.

The problem of destabilization of a rotating fluid owing to the temperature gradient is considered in Section 7.3.

7.1 Convective instability of a horizontal layer with oscillations of temperature on the free boundary

The problem of the emergence of convection in an infinite horizontal layer of a viscous fluid under the condition of periodic variations of temperature on the free upper boundary is of interest for studying mechanisms which affect the thermal situation in stagnant natural reservoirs. The temperature distribution over the reservoir depth in the absence of forced circulation induced, for example, by the action of wind is determined by free convective motions arising because of nonuniform heating of water masses due to daily and seasonal oscillations of temperature on the surface.

The study of parametric excitation of convective instability in a fluid layer due to periodic changes in the temperature regime was inspired by the publication of Gershuni and Zhukhovitskii [66], who posed and studied the problem of stability of a finite-depth layer with a periodically changing equilibrium temperature gradient. Boundary conditions corresponding to plane free boundaries were considered, which

https://doi.org/10.1515/9783110655469-007

made it possible to perform an analytical study. The case of a layer with solid boundaries was considered in [74], and stability of an infinite-depth layer with periodically changing temperature on the boundary was studied in [67].

The influence of modulation of the boundary temperature on convective stability of a horizontal layer was investigated in [227, 198, 236]. Venezian [227] considered a layer with free boundaries, the temperatures of which oscillate simultaneously with an infinitesimal amplitude. Rosenblat and Herbert [198] studied low-amplitude oscillations of temperature on the lower boundary with finite amplitudes of modulation. Yin and Li [236] considered a layer with solid boundaries with simultaneously oscillating temperatures.

Note that the problem of stability of a fluid layer under the condition of a periodically varying equilibrium temperature gradient is similar to the problem of stability of the layer in a field of external volume forces periodic in time [68, 127].

1. Formulation of the problem

Let a viscous incompressible fluid fill an infinite horizontal layer of thickness l. The bottom temperature is constant and equal to θ_1, and the upper surface temperature varies in accordance with the law $\theta_2 + A\sin\Omega t$. The free surface and the bottom are assumed to be nondeformable and solid, respectively. Let us introduce a coordinate system x, y, z, such that the z axis is directed vertically upward, while the x and y axes are in the plane of the lower boundary of the layer. Let us count temperature from θ_2 and use l, χl^{-1}, $l^2\chi^{-1}$, $|\theta_1 - \theta_2|$, and $\varrho\nu\chi l^{-2}$ as scales of length, velocity, time, temperature, and pressure, respectively. Here, ϱ, χ, and ν are the constant density, thermal diffusivity, and kinematic viscosity of the fluid, respectively.

The free convection equations in the Oberbeck–Boussinesq approximation have the following form in the dimensionless variables:

$$\begin{gathered}\frac{1}{\mathrm{Pr}}\left(\frac{\partial \boldsymbol{v}}{\partial t} + \boldsymbol{v}\cdot\nabla\boldsymbol{v}\right) = -\nabla p + \Delta\boldsymbol{v} + \mathrm{Ra}\,\theta\boldsymbol{e}_3,\\ \operatorname{div}\boldsymbol{v} = 0, \quad \frac{\partial\theta}{\partial t} + \boldsymbol{v}\cdot\nabla\theta = \Delta\theta.\end{gathered} \tag{7.1}$$

Here, $\boldsymbol{v} = (u, v, w)$ is the velocity vector, θ is the temperature, p is the deviation of pressure from the hydrostatic value, $\boldsymbol{e}_3$ stand for the z axes, Pr and Ra are the Prandtl and Reynolds numbers, respectively,

$$\mathrm{Pr} = \frac{\nu}{\chi}, \quad \mathrm{Ra} = \frac{g\beta|\theta_1 - \theta_2|l^3}{\nu\chi},$$

where g is the acceleration due to gravity and β is the coefficient of thermal expansion of the fluid.

The boundary conditions for temperature and velocity on the lower solid boundary and on the upper free boundary have the respective forms

$$\theta = c, \quad \boldsymbol{v} = 0; \tag{7.2}$$

$$\theta = a\sin\omega t, \quad \frac{\partial u}{\partial z} = \frac{\partial v}{\partial z} = w = 0, \quad a = \frac{A}{|\theta_1 - \theta_2|}, \quad \omega = \frac{\Omega l^2}{\chi}, \tag{7.3}$$

where $c = \pm 1$ is the dimensionless temperature of the lower boundary, and a and ω are the dimensionless amplitude and frequency of temperature oscillations on the free boundary, respectively.

2. Equations for perturbations

The boundary-value problem (7.1)–(7.3) has a solution corresponding to conductive heat transfer, i. e., to the quiescent state of the fluid ($\boldsymbol{v}_0 = 0$). The periodically varying temperature distribution can be found from a boundary-value problem of the form

$$\frac{\partial \theta_0}{\partial t} = \frac{\partial^2 \theta_0}{\partial z^2}, \quad \theta_0|_{z=0} = c, \quad \theta_0|_{z=1} = a\sin\omega t, \tag{7.4}$$

whose solution is well known [112].

After determining $\theta_0(z,t)$, we find the function of pressure $p_0(z,t)$ by integrating the equation

$$\frac{\partial p_0}{\partial z} = \mathrm{Ra}\,\theta_0.$$

The final solution of problem (7.1)–(7.3), which corresponds to the conductive heat-transfer mode, has the form

$$\begin{gathered} \boldsymbol{v}_0 = 0, \\ p_0 = \mathrm{Ra}\left[cz\left(1 - \frac{1}{2}z\right) + \frac{a}{2}z^2\sin\omega t - \sum_{n=1}^{\infty}(-1)^n \frac{2a\omega}{(\pi n)^4 + \omega^2} \right. \\ \left. \times \left(\cos\omega t + \frac{\omega}{(\pi n)^2}\sin\omega t\right)\cos\pi n z\right] + C(t), \\ \theta_0 = c(1-z) + az\sin\omega t + \sum_{n=1}^{\infty}(-1)^n \frac{2a\omega}{(\pi n)^4 + \omega^2}\left(\pi n\cos\omega t + \frac{\omega}{\pi n}\sin\omega t\right)\sin\pi n z. \end{gathered} \tag{7.5}$$

The excess pressure distribution $p_0(z,t)$ is determined with accuracy to an arbitrary function of time $C(t)$, which can be assumed to have a zero value.

Substituting $\boldsymbol{v}_0 + \boldsymbol{V}$, $p_0 + P$, and $\theta_0 + T$ into the system (7.1)–(7.3), we obtain equations for perturbations of V, P, and T in the conductive mode (7.5):

$$\begin{gathered} \frac{1}{\mathrm{Pr}}\left(\frac{\partial \boldsymbol{V}}{\partial t} + \boldsymbol{V}\cdot\nabla\boldsymbol{V}\right) = -\nabla P + \Delta\boldsymbol{V} + \mathrm{Ra}\,T\boldsymbol{e}_3, \\ \mathrm{div}\,\boldsymbol{V} = 0, \quad \frac{\partial T}{\partial t} + \boldsymbol{V}\cdot\nabla T = \Delta T - \theta_0'(z,t)\boldsymbol{V}\cdot\boldsymbol{e}_3, \\ \theta_0'(z,t) = -c + a[1 + 2\omega^2\psi_\omega(z)]\sin\omega t - 2a\omega\psi_\omega''(z)\cos\omega t, \end{gathered} \tag{7.6}$$

$$\psi_\omega(z) = \sum_{n=1}^{\infty} (-1)^n \frac{1}{(\pi n)^4 + \omega^2} \cos \pi n z.$$

In the following, the prime denotes differentiation with respect to the z coordinate.

The boundary conditions for perturbations are imposed on the solid bottom and free surface:

$$T = 0, \quad \boldsymbol{V} = 0; \tag{7.7}$$

$$T = 0, \quad \frac{\partial U}{\partial z} = \frac{\partial V}{\partial z} = W = 0. \tag{7.8}$$

3. Linearization

To answer the question on stability of the ω-periodic solution (7.5) of problem (7.1)–(7.3), we use the method of linearization [238]. The linearized problem for small perturbations of the conductive mode (7.5) has the form

$$\begin{aligned} \frac{1}{\mathrm{Pr}} \frac{\partial \boldsymbol{V}}{\partial t} &= -\nabla P + \Delta \boldsymbol{V} + \mathrm{Ra}\, T \boldsymbol{e}_3, \quad \operatorname{div} \boldsymbol{V} = 0, \\ \frac{\partial T}{\partial t} &= \Delta T - \theta_0'(z,t) \boldsymbol{V} \cdot \boldsymbol{e}_3. \end{aligned} \tag{7.9}$$

Note that, in contrast to [66, 74], the equilibrium temperature gradient in system (7.6) depends not only on time, but also on the spatial coordinate z. For convenience when analyzing the results, we write $\theta_0'(z,t)$ in the form

$$\theta_0'(z,t) = -c + a\left[1 + 2\xi\omega^2 \psi_\omega(z)\right] \sin \omega t - 2a\xi\omega\psi_\omega''(z) \cos \omega t. \tag{7.10}$$

Presentation (7.10) contains a formal parameter ξ. At $\xi = 0$, we have a problem with modulation of the gradient of equilibrium temperature or gravity force field [74, 127]; at $\xi = 1$, we obtain problem (7.7)–(7.9) of interest.

For the linear system with periodic coefficients (7.7)–(7.9), we find the Floquet solution with the increment λ under the usual assumptions on the spatial periodicity of perturbations along the layer with the absolute value of the wave vector $\boldsymbol{k} = (\alpha_1, \alpha_2)$. Presenting the unknown functions in system (7.7)–(7.9) in the form

$$\begin{pmatrix} \boldsymbol{V} \\ T \\ P \end{pmatrix} (x,y,z,t) = \begin{pmatrix} \boldsymbol{V} \\ T \\ P \end{pmatrix} (z,t)\, \mathrm{e}^{\lambda t + i(\alpha_1 x + \alpha_2 y)},$$

where the amplitudes $(\boldsymbol{V}, T, P)(z,t)$ are functions periodic in time, we obtain a spectral problem with respect to the parameter λ

$$\begin{aligned} &\frac{1}{\mathrm{Pr}} \dot{W} = -P' + W'' - (k^2 + \lambda) W + \mathrm{Ra}\, T, \\ &\frac{1}{\mathrm{Pr}} \dot{F} = k^2 P + F'' - (k^2 + \lambda) F, \quad W' = -F, \end{aligned} \tag{7.11}$$

$$\dot{T} = T'' - (k^2 + \lambda)T - W\theta_0'(z,t).$$

Here, the dot signifies differentiation with respect to time. The boundary conditions (7.7) and (7.8) take the form

$$T = W = F = 0; \tag{7.12}$$

$$T = W = F' = 0. \tag{7.13}$$

Eliminating the pressure, we can present system (7.11)–(7.8) in the form

$$q\mathcal{L}\dot{W} = (\mathcal{L} - \lambda)\mathcal{L}\,W - k^2\,\mathrm{Ra}\,T, \quad \dot{T} = (\mathcal{L} - \lambda)T - \theta_0'(z,t)W; \tag{7.14}$$

$$W = \mathcal{D}W = T = 0; \tag{7.15}$$

$$W = \mathcal{D}^2W = T = 0, \tag{7.16}$$

where $q = \mathrm{Pr}^{-1}$; $\mathcal{L} = \mathcal{D}^2 - k^2$, $\mathcal{D} = d/dz$ is the operator of differentiation. System (7.14) can be reduced to one equation

$$q\mathcal{L}\ddot{W} - (1+q)(\mathcal{L} - \lambda)\mathcal{L}\dot{W} + (\mathcal{L} - \lambda)^2\mathcal{L}W - k^2\,\mathrm{Ra}\,\theta_0'(z,t)W = 0. \tag{7.17}$$

From the boundary conditions (7.15) and (7.16), we obtain, respectively,

$$W = \mathcal{D}W = (\mathcal{D}^2 - 2k^2 - \lambda)\mathcal{D}^2W - q\mathcal{D}^2\dot{W} = 0; \tag{7.18}$$

$$W = \mathcal{D}^2W = \mathcal{D}^4W = 0. \tag{7.19}$$

The critical regime of heat transfer is determined by the condition $\mathrm{Re}(\lambda) = 0$ or, in the case of monotonic instability of solution (7.5), by the condition $\lambda = 0$.

4. Galerkin method and Fourier method

Let us present the spectral problem (7.14)–(7.16) in the operator-matrix form as

$$\boldsymbol{B}\dot{u} = \mathrm{e}^{i\omega t}\boldsymbol{A}_1\boldsymbol{u} + \boldsymbol{A}_0\boldsymbol{u} + \mathrm{e}^{-i\omega t}\bar{\boldsymbol{A}}_1\boldsymbol{u}, \tag{7.20}$$

$$\boldsymbol{u} = \begin{pmatrix} W \\ T \end{pmatrix}(z,t), \quad \boldsymbol{B} = \begin{pmatrix} q\mathcal{L} & 0 \\ 0 & 1 \end{pmatrix},$$

$$\boldsymbol{A}_1 = \begin{pmatrix} 0 & 0 \\ \Phi(z) & 0 \end{pmatrix}, \quad \boldsymbol{A}_0 = \begin{pmatrix} (\mathcal{L} - \lambda)\mathcal{L} & -k^2\,\mathrm{Ra} \\ c & \mathcal{L} - \lambda \end{pmatrix},$$

which involves the presentation of the conductive temperature gradient (7.10) as an ω-periodic function of time:

$$\begin{aligned} \theta_0'(z,t) &= -c - \Phi(z)\,\mathrm{e}^{i\omega t} - \bar{\Phi}(z)\,\mathrm{e}^{-i\omega t}, \\ \Phi(z) &= a\xi\omega\psi_\omega''(z) + i\frac{a}{2}\left[1 + 2\xi\omega^2\psi_\omega(z)\right]. \end{aligned} \tag{7.21}$$

We look for the solution of eq. (7.20) in the form

$$\boldsymbol{u}(z,t) = \sum_{m=1}^{M} u_m(t)\boldsymbol{\phi}_m(z), \tag{7.22}$$

where the basis vector functions $\boldsymbol{\phi}_m(z) : \boldsymbol{R} \to \boldsymbol{R}^2$ satisfy the boundary conditions

$$\boldsymbol{\phi}_m(0) = \boldsymbol{\phi}_m(1) = 0, \quad \mathcal{D}\boldsymbol{\phi}_{m,1}(0) = \mathcal{D}^2\boldsymbol{\phi}_{m,1}(1) = 0. \tag{7.23}$$

To determine a nontrivial set of the functions $u_m(t)$, we have the Galerkin system of equations

$$\begin{aligned}\sum_{m=1}^{M} (\boldsymbol{B}\boldsymbol{\phi}_m, \boldsymbol{\phi}_j)\dot{u}_m(t) = \sum_{m=1}^{M} (\boldsymbol{A}_0\boldsymbol{\phi}_m, \boldsymbol{\phi}_j)u_m(t) \\ + \mathrm{e}^{i\omega t}\sum_{m=1}^{M} (\boldsymbol{A}_1\boldsymbol{\phi}_m, \boldsymbol{\phi}_j)u_m(t) + \mathrm{e}^{-i\omega t}\sum_{m=1}^{M} (\bar{\boldsymbol{A}}_1\boldsymbol{\phi}_m, \boldsymbol{\phi}_j)u_m(t),\end{aligned} \tag{7.24}$$

$j = 1, \dots, M$. Here, we use a scalar product in $\boldsymbol{L}_2$:

$$(\boldsymbol{f}, \boldsymbol{g}) = \int_0^1 [f_1(z)q_1(z) + f_2(z)q_2(z)]\, dz.$$

Seeking the ω-periodic (in time) solution of system (7.24) in the form

$$u_m(t) = \sum_{n=-\infty}^{\infty} u_{mn}\, \mathrm{e}^{i\omega n t}, \tag{7.25}$$

we obtain a homogeneous infinite system of linear algebraic equations

$$\begin{gathered}\sum_{m=1}^{M} a_{mnj}u_{m,n-1} + b_{mnj}u_{mn} + \bar{a}_{mnj}u_{m,n+1} = 0, \\ b_{mnj} = (\boldsymbol{A}_0\boldsymbol{\phi}_m, \boldsymbol{\phi}_j) + i\omega n(\boldsymbol{B}\boldsymbol{\phi}_m, \boldsymbol{\phi}_j), \\ j = 1, 2, \dots, M, \quad n = 1, \pm 1, \pm 2, \dots.\end{gathered} \tag{7.26}$$

Below, we consider the simplest case where the basis functions have the form

$$\boldsymbol{\phi}_1(z) = \begin{pmatrix} f(z) \\ 0 \end{pmatrix}, \quad \boldsymbol{\phi}_2(z) = \begin{pmatrix} 0 \\ g(z) \end{pmatrix}.$$

We write system (7.26) as

$$\begin{gathered}b_{1n1}u_{1,n} + b_{2n1}u_{2,n} = 0, \\ a_{1n2}u_{1,n-1} + b_{1n2}u_{1,n} + \bar{a}_{1n2}u_{1,n+1} + b_{2n2}u_{2,n} = 0, \\ n = 0, \pm 1, \pm 2, \dots.\end{gathered}$$

Eliminating $u_{2,n}$ from the first equation, we obtain a homogeneous infinite system of linear algebraic equations with a three-diagonal matrix

$$\begin{aligned} &A_n u_{1,n-1} + B_n u_{1,n} + \bar{A}_n u_{1,n+1} = 0, \quad A_n = k^2 \operatorname{Ra}(f,g)(f\Phi,g), \\ &\quad B_n = ck^2 \operatorname{Ra}(f,g)^2 - q(\omega n)^2(\mathcal{L}f,f)(g,g) \\ &\qquad + \big((\mathcal{L}-\lambda)\mathcal{L}f,f\big)\big((\mathcal{L}-\lambda)g,g\big) \\ &\qquad - i\omega n\big[((\mathcal{L}-\lambda)\mathcal{L}f,f)(g,g) + q((\mathcal{L}-\lambda)g,g)(\mathcal{L}f,f)\big], \end{aligned} \tag{7.27}$$

where $(f,g) = \int_0^1 f(z)g(z)\,dz$.

In the case of monotonic instability ($\lambda = 0$), we obtain the following expressions for the coefficients B_n:

$$\begin{aligned} B_n = {} & ck^2 \operatorname{Ra}(f,g)^2 + q(\omega n)^2(||\mathcal{D}f||^2 + k^2||f||^2)||g||^2 \\ & - ||\mathcal{L}f||^2(||\mathcal{D}g||^2 + k^2||g||^2) - i\omega n\big[||\mathcal{L}f||^2||g||^2 \\ & + q(||\mathcal{D}g||^2 + k^2||g||^2)(||\mathcal{D}f||^2 + k^2||f||^2)\big]. \end{aligned}$$

The coefficients of system (7.27) depend on the parameters of problem (7.10)–(7.13) λ, Ra, Pr, k^2, a, and ω. To determine their critical values providing the existence of a nontrivial solution of system (7.27), we use the reduction method [104] based on truncated systems.

Another approach to studying the linearized problem (7.11)–(7.13) can also be used. As the solution for problem (7.11)–(7.13) is ω-periodic in time, we can expand the unknown functions into the Fourier series of the form

$$\begin{pmatrix} W \\ F \\ T \\ P \end{pmatrix}(z,t) = \sum_{n=-\infty}^{\infty} \begin{pmatrix} W_n \\ F_n \\ T_n \\ P_n \end{pmatrix}(z)\,\mathrm{e}^{i\omega n t}.$$

As a result, we obtain a spectral boundary value problem for an infinite system of ordinary differential equations

$$\begin{aligned} &W_n'' - \left(k^2 + \lambda + i\frac{n\omega}{\mathrm{Pr}}\right)W_n - P_n' + \operatorname{Ra} T_n = 0, \quad n = 0, \pm1, \pm1, \dots \\ &F_n'' - \left(k^2 + \lambda + i\frac{n\omega}{\mathrm{Pr}}\right)F_n + k^2 P_n = 0, \quad W_n' = -F_n, \\ &T_n'' - (k^2 + \lambda + in\omega)T_n + cW_n + \Phi(z)W_{n-1} + \bar{\Phi}(z)W_{n+1} = 0, \end{aligned} \tag{7.28}$$

with the boundary conditions

$$W_n = F_n = T_n = 0; \tag{7.29}$$

$$W_n = F_n' = T_n = 0. \tag{7.30}$$

For a fixed value of n, the spectral problem (7.28)–(7.30) can be studied numerically.

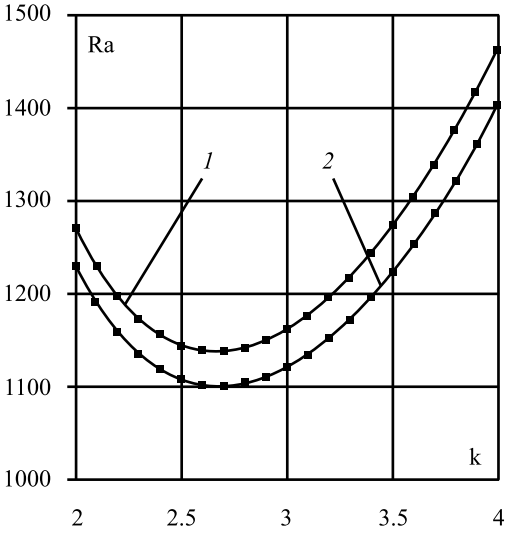

Figure 7.1: Neutral curves for monotone disturbances for Pr = 7 and $\omega = 10$, $a = 0.1$.

5. Numerical results

The neutral curves Ra(k) of monotonic instability were calculated on the basis of the truncated systems (7.27) and (7.28)–(7.30). The values Pr = 7 and $\omega = 10$ were used in all cases.

The results obtained for $a = 0.1$ are shown in Table 7.1 and Figure 7.1. For equations (7.27), we considered truncated systems up to the 11th order, which were studied with the Maple package for analytical computations. The coordinate functions $f(z) = z^2(z-1)(2z-3)$ and $g(z) = z(1-z)$ were used. The computed results are shown in column I of Table 7.1 and by curve 1 in Figure 7.1. For equations (7.28), we considered truncated spectral problems up to the 30th order, which were studied by the shooting method. The computed results are shown in column II of Table 7.1 and by curve 2 in Figure 7.1.

Column III of Table 7.1 shows the critical values obtained at $\xi = 0$ in equation (7.10), which corresponds to the case of modulation of the equilibrium temperature gradient. The last column (column IV) shows, for comparison, the data of the Rayleigh–Benard problem for the solid lower surface and the free upper surface of the layer [142]. It is seen that the numerical values from columns II–IV of Table 7.1 on curve 2 in Figure 7.1 cannot be distinguished.

Obviously, the calculation of the neutral curve on the basis of the truncated systems (7.27) with the basis functions (7.30) yields overpredicted results, although the character of the curve remains the same. Columns I–III of Table 7.2 and curves 1–3 in Figure 7.2 show the results calculated for the amplitude modulation values $a = 0.1$, $a = 0.5$, and $a = 0.9$, respectively. An increase in the amplitude of temperature mod-

Table 7.1: Rayleigh number Ra vs wave number k for different shortened equations (7.28).

Ra(k)				
k	I	II	III	IV
2	1269.5	1230.6	1230.7	1230.3
2.2	1197.5	1160.1	1160.2	1159.8
2.4	1156.7	1119.6	1119.8	1119.4
2.6	1139.8	1102.3	1102.6	1102.1
2.8	1142.4	1103.8	1104	1103.6
3	1161.6	1121.1	1121.3	1120.8
3.2	1195.5	1152.5	1152.7	1152.2
3.4	1243.1	1197.1	1197.1	1196.6
3.6	1303.8	1253.5	1254	1253.5
3.8	1377.4	1323.2	1323.1	1322.5
4	1463.9	1403.9	1404.5	1403.8

Table 7.2: Rayleigh number Ra vs wave number k for $\alpha = 0.1$, $\alpha = 0.5$, $\alpha = 0.9$ respectively.

Ra(k)			
k	I	II	III
2	1230.6	1237.3	1247.7
2.2	1160.1	1166.5	1175.2
2.4	1119.6	1126	1132.7
2.6	1102.3	1108.6	1113.5
2.8	1103.8	1109.9	1112.1
3	1121.1	1127.2	1125.8
3.2	1152.5	1158.6	1152.7
3.4	1197.1	1202.9	1192.1
3.6	1253.5	1259.6	1242.7
3.8	1323.2	1328.5	1304.5
4	1403.9	1409.4	1377.9

ulation on the free boundary leads to insignificant stabilization of conductive heat transfer with respect to perturbations with wave numbers smaller than, at least, the minimum critical wave number. For $a = 0.9$, the neutral curve is less steep; at wave numbers greater than a certain value, it lies lower than the neutral curves corresponding to $a = 0.1$ and $a = 0.5$.

7.2 Instability of a liquid layers with an interface

An important class of problems of the convective stability theory includes problems arising in studying two-layer systems. The majority of these studies are performed under the assumption that the interface is nondeformable (see, e. g., [33, 69, 70]). In many

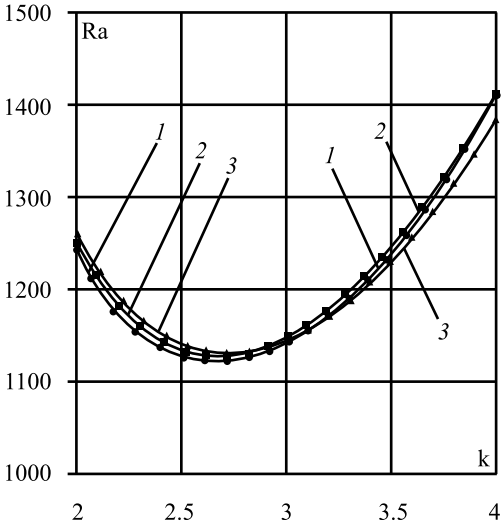

Figure 7.2: Neutral curves for monotone disturbances for Pr = 7, $\omega = 10$, $a = 0.1$ (curve 1), $a = 0.5$ (curve 2), $a = 0.9$ (curve 3).

situations this assumption is well justified, because the influence of interface deformability on convective stability is rather small for accelerations, due to gravity typical for Earth conditions and for sufficiently different fluid densities. At the same time, the assumption on interface nondeformability appreciably simplifies the procedure of finding the problem solution, taking into account that interface deformability is of principal importance from the viewpoint of studying new mechanisms of instability. Convective stability with allowance for interface deformability within the Boussinesq approximation has been studied by various authors (see, e. g., [46, 99, 192, 193]). Nevertheless, the assumption of interface deformability contradicts the standard Boussinesq approximation (see the analysis in [148]) and can lead to physically invalid results. The objective of this section is to construct a more correct approximation.

1. Generalized Boussinesq approximation

Let us consider the gravitational thermal convection in a system of two immiscible fluids with a deformable interface. We write the equations of fluid motion and heat conduction, assuming that the density is a function of temperature only ("Boussinesq fluid") and that the coefficients of dynamic viscosity and thermal conductivity are constant:

$$\varrho_j \frac{\partial \boldsymbol{v}_j}{\partial t} + \varrho_j (\boldsymbol{v}_j \nabla)\boldsymbol{v}_j = -\nabla p_j + \mu_j \Delta \boldsymbol{v}_j - \varrho_j g \boldsymbol{e}_3; \tag{7.31}$$

$$\varrho_j c_{pj} \left[\frac{\partial \theta_j}{\partial t} + (\boldsymbol{v}_j \nabla)\theta_j \right] = \kappa_j \Delta \theta_j; \tag{7.32}$$

$$\frac{\partial \varrho_j}{\partial t} + \operatorname{div}(\varrho_j \boldsymbol{v}_j) = 0. \tag{7.33}$$

Here we use the standard notations; $\boldsymbol{e}_3$ is the unit vector directed vertically upward. The fluids are marked by the subscript j; the fluid with $j = 1$ is located at the bottom. On the interface $z = \zeta(x, y, t)$ (z is the vertical Cartesian coordinate), we impose the usual conditions of continuity of velocity, normal and tangential stresses, temperature, and heat flux, as well as the kinematic condition

$$\begin{aligned} &[\boldsymbol{v}] = 0, \quad -[p]\boldsymbol{n} + [\mathcal{D}]\boldsymbol{n} = 2\sigma H \boldsymbol{n}, \\ &[\theta] = 0, \quad [\kappa \nabla\theta]\boldsymbol{n} = 0, \quad \frac{\partial \zeta}{\partial t} + \boldsymbol{v} \cdot \nabla\zeta = \mathbf{v} \cdot \boldsymbol{e}_3. \end{aligned} \tag{7.34}$$

Here $[f]$ is the jump of the value of f on the interface, i. e., $[f] = f_1 - f_2$, $\mathcal{D}$ is the viscous stress tensor, $\boldsymbol{n}$ is the normal vector to the interface between the fluids, σ is the surface tension coefficient, and H is the mean curvature of the surface.

Problem (7.31)–(7.34), supplemented with appropriate conditions on external boundaries, is characterized by a number of dimensionless parameters. Among these parameters, we now consider the parameter of density inhomogeneity $\beta_* \theta$ and the parameter characterizing the gravity force $\mathrm{Ga} = g l_*^3 / \nu_*^2$. Here, β_* is the characteristic value of the coefficient of volume expansion $\beta = -(1/\varrho)\, d\varrho/dt$, θ_* is the characteristic temperature difference, ν_* is the characteristic coefficient of kinematic viscosity, and l_* is the characteristic size.

Investigations of convection problems are usually based on the Boussinesq approximation [68], where the dependence of density on temperature is neglected everywhere except for the term with the gravity force in the equation of motion (7.31). Formally, this means performing the limiting transition $\beta_* \theta_* \to 0$ and $\mathrm{Ga} \to \infty$; the product $\beta_* \theta_*$ whereby Ga remains finite. Generally speaking, this kind of limiting transition leads to the requirement of interface nondeformability. Indeed, in this transition, the main terms in the equation of motion (7.31) determine the hydrostatic pressure $p_j = -\varrho_j g z + \mathrm{const}$. Then, the main terms in the balance condition for normal stresses yield $[\varrho] g \zeta = \mathrm{const}$. This means that the interface remains flat and horizontal. It follows from the kinematic condition that $\boldsymbol{v} \cdot \boldsymbol{e}_3 = 0$ on the interface, i. e., the condition of impermeability is satisfied.

In the next order in terms of $1/\mathrm{Ga}$ and $\beta_* \theta_*$, the equations of motion and heat conduction transform to the conventional equations of thermal convection in the Boussinesq approximation:

$$\frac{\partial \boldsymbol{v}_j}{\partial t} + (\boldsymbol{v}_j \nabla)\boldsymbol{v}_j = -\frac{1}{\varrho_{0j}} \nabla p_j + \nu_j \Delta \boldsymbol{v}_j + g \beta_j \theta_j \boldsymbol{e}_3; \tag{7.35}$$

$$\frac{\partial \theta_j}{\partial t} + (\boldsymbol{v}_j \nabla)\theta_j = \chi_j \Delta \theta_j, \quad \operatorname{div} \boldsymbol{v}_j = 0. \tag{7.36}$$

Here, p_j is the additive to the hydrostatic pressure; the point from which the temperature is counted is chosen so that ϱ_{0j} is the density of the j-th fluid at $\theta = 0$.

In the next order in terms of $1/\mathrm{Ga}$, the shape of interface perturbations can be found from the stress balance condition, but this does not affect the solution of the convective problem (7.35)–(7.36). Thus, in the conventional Boussinesq approximation, *convective motion is not affected by interface deformation*.

The physical meaning of this result is extremely simple: in the case of a large gravity force and a finite difference in densities, the gravity forces suppress perturbations of the horizontal interface. This conclusion is invalid if the difference in the fluid densities is small. If the difference in the fluid densities is comparable to the difference in the densities due to nonisothermality, the interface can be expected to deform significantly, and these deformations have a significant effect on convective phenomena. Thus, it becomes clear which method should be used to generalize the Boussinesq approximation to the case of a deformable interface. Simultaneously with the limiting transition $\mathrm{Ga} \to \infty$, it is necessary to direct to zero not only $\beta_* \theta_*$, i. e., the relative temperature inhomogeneity of density, but also the relative difference in the fluid densities

$$\varepsilon = (\varrho_{01} - \varrho_{02})/(\varrho_{01} + \varrho_{02}). \tag{7.37}$$

At such a limiting transition, the products $\mathrm{Ga}\,\beta_* \theta_*$ and $\mathrm{Ga}\,\varepsilon$ should remain finite. The use of equations of free convection of a compressible fluid does not seem reasonable because they are too cumbersome. Moreover, they contain certain phenomena that are not relevant for our analysis and do not permit the effective study of many problems of practical importance.

The procedure described above for limiting transition yields thermal convection equations that coincide with equations (7.35)–(7.36); however, now we have $\varrho_{01} = \varrho_{02} = \varrho_0$ in equation (7.35).

The boundary conditions (7.34) remain unchanged, except for the balance condition of stresses on the interface, which acquires the following form:

$$-[p]\boldsymbol{n} + [\mathcal{D}]\boldsymbol{n} + [\varrho] g \zeta \boldsymbol{n} = 2\sigma H \boldsymbol{n}. \tag{7.38}$$

Thus, the difference in the fluid densities $\varrho_{01} - \varrho_{02}$ is taken into account only in one place: in the term containing the gravity force in condition (7.38).

2. Stability of convective equilibrium of a two-layer system

Let us consider a system of two immiscible fluids bounded by two horizontal solid surfaces $z = \pm h$. The boundaries have different constant temperatures θ_{10} and θ_{20}. The convection equations and boundary conditions on the interface formulated above admit a steady solution corresponding to the mechanical equilibrium of the fluids with a flat horizontal interface. Let the fluids occupy identical fractions of the system volume, so that $\zeta = 0$ in equilibrium. The temperature distributions in the layers are

determined by thermal conduction:

$$\begin{aligned}
\theta_1 &= \theta_{10} + (h+z)A_1,\\
\theta_2 &= \theta_{20} + (h-z)A_2,\\
A_1 &= \kappa_2(\theta_{20}-\theta_{10})/[h(\kappa_1+\kappa_2)],\\
A_2 &= \kappa_1(\theta_{20}-\theta_{10})/[h(\kappa_1+\kappa_2)],
\end{aligned} \tag{7.39}$$

whereby the velocity is $\boldsymbol{v}_j = 0$.

Let us formulate the problem of stability of mechanical equilibrium to small perturbations. Linearizing the full problem, we obtain the following boundary-value problem for perturbations of velocity, temperature, and pressure in each fluid:

$$\begin{gathered}
\frac{1}{\mathrm{Pr}}\frac{\partial \boldsymbol{V}_j}{\partial t} = -\nabla \mathcal{P}_j + \nu_j \Delta \boldsymbol{V}_j + \mathrm{Ra}\,\beta_j T_j \boldsymbol{e}_3,\\
\frac{\partial T_j}{\partial t} = \chi_j \Delta T_j + A_j \boldsymbol{V}_j \cdot \boldsymbol{e}_3, \quad \operatorname{div} \boldsymbol{V}_j = 0;\\
z = \pm 1: \quad \boldsymbol{V} = 0, \quad T = 0,\\
z = 0: \quad \boldsymbol{V}_1 = \boldsymbol{V}_2, \quad -A_1 N + T_1 = -A_2 N + T_2,
\end{gathered} \tag{7.40}$$

$$\begin{gathered}
\kappa_1 \frac{\partial T_1}{\partial z} = \kappa_2 \frac{\partial T_2}{\partial z}, \quad \nu_1 \frac{\partial V_{1\tau}}{\partial z} = \nu_2 \frac{\partial V_{2\tau}}{\partial z},\\
-(p_1 - p_2) - \mathrm{Ga}\,N + 2\left(\nu_1 \frac{\partial V_{1z}}{\partial z} - \nu_2 \frac{\partial V_{2z}}{\partial z}\right) = \mathrm{We}\,\Delta_2 N,\\
\frac{\partial N}{\partial t} = \boldsymbol{V} \cdot \boldsymbol{e}_3.
\end{gathered} \tag{7.41}$$

Here, Δ_2 is the Laplace operator in the variables x, y. Equations (7.40)–(7.41) are written in the dimensionless form. The following scales are used: h for distance, h^2/χ_* for time, χ_*/h for velocity, $\chi_*\nu_*\varrho_0/h^2$ for pressure, and $\theta = (\theta_{10} - \theta_{20})/2$ for temperature. The scales for the coefficients of kinematic viscosity ν_*, thermal diffusivity χ_*, thermal conductivity κ_*, thermal expansion β_*, and equilibrium temperature gradients A_* are their mean arithmetic values.

The boundary-value problem (7.40)–(7.41) also involves the following dimensionless parameters: Prandtl number Pr, Rayleigh number Ra, Weber number We, and Galileo number Ga:

$$\mathrm{Pr} = \frac{\nu_*}{\chi_*}, \quad \mathrm{Ca} = \frac{g\beta\Theta h^3}{\nu_*\chi_*}, \quad \mathrm{We} = \frac{\sigma h}{\nu_*\chi_*\varrho_0}, \quad \mathrm{Ga} = \frac{(\varrho_2 - \varrho_1)gh^3}{\mu_*\chi_*}.$$

The Galileo number Ga is defined so that the positive value refers to the case where the heavier fluid is located above the less heavy fluid, i. e., stratification is potentially unstable. With this choice of the scales, the following relations are satisfied:

$$\begin{gathered}
\nu_1 + \nu_2 = 2, \quad \beta_1 + \beta_2 = 2, \quad \chi_1 + \chi_2 = 2, \quad \kappa_1 + \kappa_2 = 2,\\
A_1 + A_2 = 2, \quad A_1\kappa_1 = A_2\kappa_2.
\end{gathered}$$

Thus, the problem is characterized by seven independent dimensionless parameters; if the fluid parameters are fixed, the following three independent parameters are left: Ra, Ga, and We.

Let us consider normal perturbations proportional to $\exp(\lambda t + i\boldsymbol{k}\cdot\boldsymbol{x})$, where λ is the increment and k is the wave vector. For the amplitudes of normal perturbations, we obtain the spectral boundary-value problem

$$\begin{gathered}
\frac{\lambda}{\mathrm{Pr}}\,U_j = -ikQ_j + \nu_j L U_j,\\
\frac{\lambda}{\mathrm{Pr}}\,W_j = -Q_j' + \nu_j L W_j + \mathrm{Ra}\,\beta_j T_j,\\
\lambda T_j = \chi_j L T_j + A_j W_j, \quad W_j' + ikU_j = 0;
\end{gathered} \tag{7.42}$$

$$\begin{gathered}
z = \pm 1:\ U_j = W_j = 0, \quad T_j = 0,\\
z = 0:\ U_1 = U_2, \quad W_1 = W_2 = \lambda N,\\
T_1 - A_1 N = T_2 - A_2 N, \quad \kappa_1 T_1' = \kappa_2 T_2', \quad \nu_1 U_1' = \nu_2 U_2',\\
-(Q_1 - Q_2) - \mathrm{Ga}\,N + 2(\nu_1 W_1' - \nu_2 W_2') = -\,\mathrm{We}\,k^2 N.
\end{gathered} \tag{7.43}$$

Here, we use the following notations for the amplitudes of normal perturbations: U, W, T, and Q are the projections of velocity, vertical components of velocity, temperatures, and pressures onto the wave vector direction. The prime denotes differentiation with respect to the z coordinate, and $L = d^2/dz^2 - k^2$. The eigenvalues of the spectral problem (7.42)–(7.43) are the increments λ as functions of the problem parameters and the wave number k.

3. Long-wave instability of equilibrium

Problem (7.42)–(7.43) does not permit an analytical solution for arbitrary values of the parameters. Nevertheless, there is an important particular case which does permit a fairly deep analytical analysis: long-wave perturbations.

At $k = 0$, the problem has a solution which describes neutral monotonic perturbations corresponding to the shifting of the horizontal interface as a whole along the vertical coordinate:

$$U_j = 0, \quad W_j = 0, \quad T_j = (\kappa_2 - \kappa_1) A_j N\bigl(z - (-1)^j\bigr)/2. \tag{7.44}$$

We can see that all remaining perturbations at $k = 0$ are decaying. In passing to small non-zero wave numbers, the perturbations, generally speaking, are no longer neutral. Let us present the solution of the spectral problem (7.42)–(7.43) in the form of series in the small parameter k:

$$\begin{aligned}
\lambda &= k\lambda_1 + k^2\lambda_2 + \cdots, & U_j &= kU_{1j} + k^2 U_{2j} + \cdots,\\
W_j &= kW_{1j} + k^2 W_{2j} + \cdots, & T_j &= T_{0j} + kT_1 j + \cdots,\\
N &= N_0 + kN_1 + \cdots.
\end{aligned}$$

The calculations show that $\lambda_1 = 0$; for λ_2, we have the expression

$$\lambda_2 = \frac{12[\nu] + 56[\kappa] - 56[\beta] - 3[\kappa][\beta][\nu]}{480(16 - 3[\nu]^2)}\,[\kappa]\,\mathrm{Ra} + \frac{2\,\mathrm{Ga}}{3(16 - 3[\nu]^2)}. \tag{7.45}$$

The correction to the increment λ_2 depends linearly on the Rayleigh number Ra and Galileo number Ga; it also depends in a more complicated manner on the ratios of viscosities ν_1/ν_2, thermal conductivities κ_1/κ_2, and volume expansion coefficients β_1/β_2. The Prandtl number Pr, the Weber number We, and the thermal diffusivities of the fluids χ_1 and χ_2 do not affect the stability of the system under long-wave perturbations. The coefficient at Ga is positive, i. e., as could be expected, the excess of the density of the lower fluid over the density of the upper fluid is a stabilizing factor. At identical thermal conductivities, long-wave instability is absent (at $\mathrm{Ga} < 0$); the mechanism of instability is possibly related to the difference in the temperature gradients in different fluids. In the particular case of identical viscosities, we have

$$\lambda_2 = 7\,\mathrm{Ra}[\kappa]([\kappa] - [\beta])/960 + \mathrm{Ga}\,/24. \tag{7.46}$$

Long-wave instability can occur under heating both from below and from above, depending on the ratios of the coefficients of thermal conductivity and volume expansion. The expression for the increment (7.45) determines the boundary of long-wave instability on the plane determined by the Galileo number Ga and the Rayleigh number Ra. This boundary is a straight line passing through the origin; the domain of instability is located to the right of the boundary (at large values of Ga). To the left of this boundary the long-wave perturbations decay, but cellular perturbations with a finite wavelength can increase.

4. Instability of cellular perturbations

The analysis of instability at finite wave numbers requires numerical calculations. To analyze the boundary-value problem (7.42)–(7.43), we constructed a system of independent partial solutions satisfying the conditions on the solid boundaries $z = \pm 1$. Requiring the boundary conditions on the interface to be satisfied, we obtain a characteristic equation which allows us to determine the boundaries of system stability. Detailed calculations in the full statement were performed for a system consisting of formic acid and transformer oil. Stability of this two-layer system was previously studied in [69] under the assumption that the interface is nondeformable. The system has the following parameters: $[\kappa] = -0.838$, $[\chi] = -0.334$, $[\nu] = 1.756$, and $[\beta] = -0.393$. The Prandtl number for this pair of fluids is 176. The boundary-value problem (7.42)–(7.43) was solved numerically by the differential sweep method.

Figures 7.3–7.5 show the neutral curves $\mathrm{Ga}(k)$ for the Weber number $\mathrm{We} = 0$ and different values of the Rayleigh number. It follows from the structure of the general

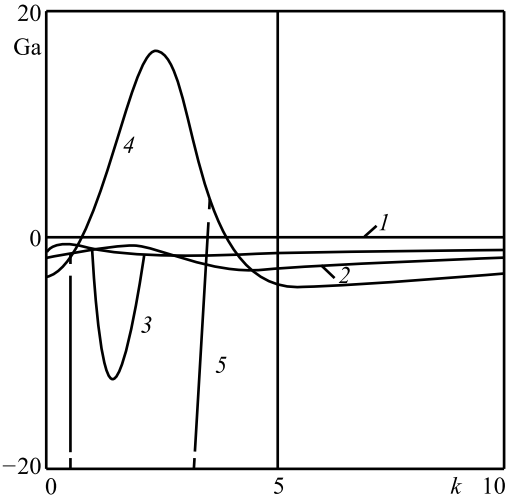

Figure 7.3: Neutral curves Ga vs wave number k for Weber number We = 0 and different values of Rayleigh number Ra.

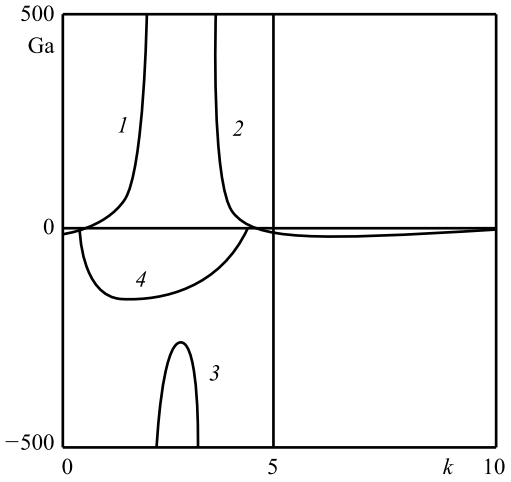

Figure 7.4: Neutral curves Ga vs wave number k for We = 0, Ra = 300.

dispersion relation that the neutral curves of monotonic instability Ga(k) are single-valued. Figure 7.3 shows the neutral curves Ga(k) for Ra = 50 (curve 1), 100 (2 and 3), and 200 (4 and 5) with Ca = 0. Curve 1 is the boundary of stability to monotonic cellular perturbations. The domain of instability is located above the neutral curve. As the Rayleigh number increases, the local maximum on the curve Ga(k) at $k = 0$ turns to a minimum, but long-wave perturbations still remain less dangerous than cellular perturbations (solid curves 2 and 4). A domain of vibrational instability appears in

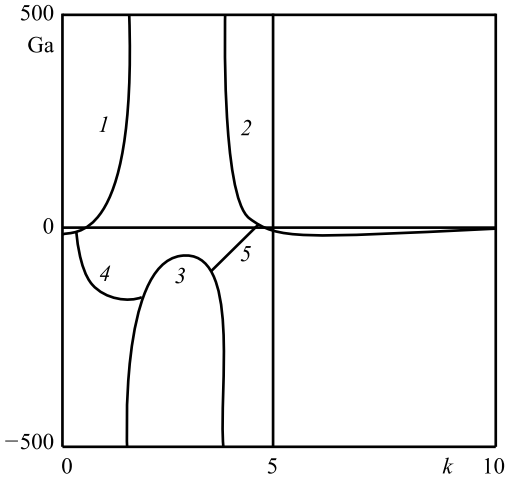

Figure 7.5: Neutral curves Ga(k) for Ca = 0 and Ra = 350; curves 1–3 refer to monotonic perturbations; curves 4 and 5 refer to vibrational perturbations.

the vicinity of the local maximum of the curve Ga(k) (dashed curves 3 and 5). With increasing Ra, the minimums of these curves rapidly decrease in the plane Ga –k, and vibrational perturbations become more dangerous than monotonic perturbations. At high values of Ra, the neutral curve has two discontinuities.

Figure 7.4 shows the neutral curves Ga(k) for Ra = 300 and Ca = 0. Curves 1–3 mark the boundaries of stability to monotonic perturbations. The domains of instability are located above curves 1 and 2 and below curve 3. The neutral curve of vibrational perturbations (curve 4) connects the neutral curves of monotonic perturbations. For this value of Ra, the interval of the values of Ga at which all perturbations decay is bounded both from above and from below. With a further increase in Ra, (Figure 7.5), the interval of stability vanishes, and the equilibrium state is unstable for all values of Ga. The connection of the neutral curves changes: the neutral curve of vibrational perturbations (curves 4 and 5) consists of two components connecting curves 1, 3 and 2, 3. The neutral curves shown here correspond to Ra = 350.

Figure 7.6 shows the pattern of stability in the plane Ga – Ra for We = 0. The boundaries of stability to the most dangerous monotonic (solid curves) and vibrational (dashed curve) perturbations are marked. Curve 1 is the boundary of stability to cellular monotonic perturbations with finite values of k. With increasing |Ga|, curve 1 transforms to a horizontal asymptotic curve Ra $\approx$ 282 (dot-and-dashed curve in Figure 7.6). The wave number of the most dangerous perturbations tends to $k \approx 2.7$. Let us recall that the case with large values of |Ga| corresponds to a nondeformable interface. The asymptotic value of Ra indicated above generally agrees with the results of [69]. The instability mechanism over the entire curve 1 seems to be the same as in the case

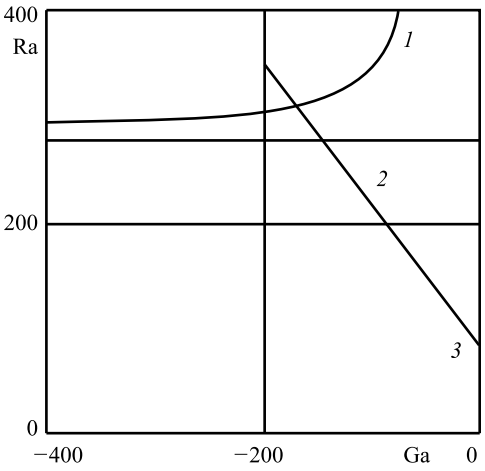

Figure 7.6: General forms of stability for equilibrium state (7.39).

of a nondeformable interface [69]. It is of interest to increase the critical value of Ra with decreasing |Ga| (with increasing interface deformability).

In the range of small values of |Ga|, the most dangerous perturbations are of a different nature: they are traveling waves. The critical values of Ra decrease with decreasing |Ga| (curve 2 bounds the domain of instability from above). The phase velocity of the traveling perturbations is smaller than the phase velocity of gravitational waves on the interface by several orders of magnitude.

In the interval $|\mathrm{Ga}| < 2$, the most dangerous perturbations are again monotonic perturbations. The corresponding boundary of stability in the plane Ga – Ra is almost a straight line (curve 3), which passes through the origin and merges with the axis Ra in the scale used in Figure 7.6. Its angular coefficient is approximately 38.8.

In the case of heating from above ($\mathrm{Ra} < 0$), the domain of instability is bounded on the right by the axis Ra. This result is trivial: if the upper fluid is less heavy ($\mathrm{Ga} < 0$), then stratification is potentially stable in the entire volume. At $\mathrm{Ga} > 0$, the usual Rayleigh–Taylor instability occurs, and the wavelength of the most dangerous perturbations is extremely small. The reason is obvious: at small values of Ga and heating from above, unstable stratification is possible in a small area near the interface, which imposes the spatial scale of the growing perturbations. As $\mathrm{Ga} \to 0$, the wavelength of the most dangerous perturbations tends to zero.

Let us now discuss the effect of capillarity on equilibrium stability. The structure of the boundary-value problem on equilibrium stability is such that the parameter We is involved only within the boundary conditions in the combination $\mathrm{Ga} - k^2\,\mathrm{We}$. It is clear from this how the neutral curves $\mathrm{Ga}(k)$ behave as the Weber number increases: the critical Galileo number also increases; the greater the wave number, the more intense the increase in the Galileo number.

For all values of Ra and rather large values of We, the most dangerous perturbations are the long-wave perturbations for which the minimum critical Rayleigh number is determined by the simple expression $\mathrm{Ra} \approx -68.15\,\mathrm{Ga}$.

At intermediate values of We, the order of the changing of the most dangerous perturbations is determined by the Rayleigh number. At $\mathrm{Ra} < 80$, there is no vibrational instability, and instability to cellular perturbations changes at a certain critical value of We to long-wave instability. As is seen from Figure 7.3, at $\mathrm{Ra} = 50$ this change occurs at $\mathrm{We} \approx 9$. At high values of Ra, when vibrational instability occurs it is also replaced by long-wave monotonic instability.

At $\mathrm{Ra} > 282$, when a discontinuity of the neutral curve appears at $\mathrm{We} = 0$ (see Figure 7.4), the domain of stability vanishes with enhancement of capillarity, i. e., instability is observed for all values of Ga.

For real media and real laboratory conditions, the parameter We is usually rather large; therefore, the domain of stability in the Ga – Ra diagram can be expected to be bounded by two straight lines: $\mathrm{Ra} = 282$ and $\mathrm{Ra} = -68.15\,\mathrm{Ga}$. The numerical calculations performed at $\mathrm{We} = 10^5$ support this conclusion.

7.3 Convection in a rotating fluid layer under microgravity conditions

1. Formulation of the problem

It is known that the state of solid rotation of a viscous incompressible homogeneous fluid possesses a large stability margin. A natural question arises: Is it possible to destabilize this state by cooling the fluid near the axis of revolution and heating the fluid at the periphery? This issue is discussed in this section. It is especially important in studying thermal convection under microgravity conditions.

To simplify the problem formulation, we assume that the field of velocities, pressure, and temperature possesses rotational symmetry. In addition, we assume that the only external mass force acting on the fluid is the centrifugal force. Applying usual assumptions used in deriving the Oberbeck–Boussinesq equations from the full Navier–Stokes equations [68], we can write the equations of momentum, continuity, and energy in the form

$$\begin{gathered} u_t + uu_r + wu_z - 2\omega v - \frac{v^2}{r} = -\frac{1}{\varrho_0} p_r + \nu\left(\Delta u - \frac{u}{r^2}\right) - \omega^2 \beta r\theta, \\ v_t + uv_r + wv_z + 2\omega u + \frac{uv}{r} = \nu\left(\Delta v - \frac{v}{r^2}\right), \\ w_t + uw_r + ww_z = \frac{1}{\varrho_0} p_z + \nu\Delta w, \\ u_r + \frac{u}{r} + w_z = 0, \\ \theta_t + u\theta_r + w\theta_z = \chi\Delta\theta, \end{gathered} \tag{7.47}$$

where

$$\Delta = \frac{\partial^2}{\partial r^2} + \frac{1}{r}\frac{\partial}{\partial r} + \frac{\partial^2}{\partial z^2}$$

means the axisymmetric part of the Laplace operator.

Equations (7.47) are written in a coordinate system rotating with a constant angular velocity ω relative to the initial inertial system. The axis of revolution coincides with the z axis of the cylindrical coordinate system r, θ, z. The radial and axial components of velocity and the deviation of the angular component of the velocity vector from the solid rotation velocity ωr are indicated by u, w, and v, respectively. The quantity p characterizes the deviation of pressure from the equilibrium value, $\varrho_0\ \omega^2 r^2/2$, and θ is the deviation of temperature from a certain mean value.

The next simplification of the problem is related to choosing the geometry of the flow domain Ω. Let Ω be a cylindrical layer $b_1 < r < b_2$, $|z| < a$. The following conditions have to be satisfied: the no-slip condition for velocity on the boundary $\partial\,\Omega$,

$$u = v = w = 0, \quad (r,z) \in \partial\Omega, \quad t \geq 0, \tag{7.48}$$

the condition for temperature on the cylindrical boundaries of the layer

$$\theta = \theta_1, \quad r = b_1, \quad |z| \leq a; \quad \theta = \theta_2, \quad r = b_2, \quad |z| \leq a, \quad t \geq 0 \tag{7.49}$$

(θ_1 and θ_2 are specified constants), and one of the conditions on the flat boundaries:

$$\theta = \gamma(r) \equiv \frac{1}{\ln(b_2/b_1)}\left[(\theta_2 - \theta_1)\ln(r/a) + \theta_1 \ln(b_2/a) - \theta_2 \ln(b_1/a)\right], \quad b_1 \leq r \leq b_2, \quad z = \pm a, \quad t \geq 0 \tag{7.50}$$

(ideally conducting boundaries) or

$$\theta_z = 0, \quad b_1 \leq r \leq b_2, \quad z = \pm a, \quad t \geq 0 \tag{7.51}$$

(thermally insulated boundaries). The problem formulation is closed by the initial conditions

$$u = u_0(r,z), \quad v = v_0(r,z), \quad w = w_0(r,z), \quad \theta = \theta_0(r,z), \quad (r,z) \in \Omega, \quad t = 0. \tag{7.52}$$

Here, we do not discuss the issues of solvability and the qualitative properties of the solution of the initial-boundary problem (7.47)–(7.52) (or (7.47)–(7.49), (7.51), (7.52)); we consider rather its limiting variant with $b_1 \to 0$, $b_2 \to \infty$ below. Here, we only note that system (7.47) for all values of the parameters admits the exact solution

$$u = v = w = 0, \quad p = -\varrho_0 \omega^2 \beta \int_0^r s\gamma(s)ds, \quad \theta = \gamma(r); \tag{7.53}$$

here the function $\gamma(r)$ is determined by equality (7.50). This solution satisfies both the boundary conditions (7.48)–(7.50) and (7.48), (7.50), (7.51).

2. Linear model

Denoting

$$F = \theta - \gamma(r), \quad q = p + \varrho_0 \omega^2 \beta \int_0^r s\gamma(s)\, ds \tag{7.54}$$

and linearizing system (7.47) on its solution (7.53), we obtain

$$\begin{gathered} u_t - 2\omega v = -\frac{1}{\varrho_0} q_r + \nu\left(\Delta u - \frac{u}{r^2}\right) - \omega^2 \beta r\theta, \\ v_t + 2\omega u = \nu\left(\Delta v - \frac{v}{r^2}\right), \quad w_t = -\frac{1}{\varrho_0} q_z + \nu \Delta w, \\ u_r + \frac{u}{r} + w_z = 0, \quad F_t + \frac{Bu}{r} = \chi \Delta F, \end{gathered} \tag{7.55}$$

where $B = (\theta_2 - \theta_1)[\ln(b_2/b_1)]^{-1}$. In what follows, we assume that the planes $z = \pm a$ have an infinite thermal conductivity (this assumption allows further simplifications). Then, it follows from eqs. (7.49), (7.50), and (7.54) that

$$F = 0, \quad (r, z) \in \partial\Omega. \tag{7.56}$$

Seeking for the solution of system (7.55) in the form of normal oscillations, we obtain (by virtue of eqs. (7.48) and (7.56)) a spectral problem for determining the complex (generally speaking) frequency λ and the amplitudes of normal oscillations. We do not write this problem here, but we assume that it satisfies the "principle of monotonicity of perturbations" [68]: $\lambda = 0$. Thus, a complicated spectral problem is replaced by a simpler problem: we need to find the values of the parameter B at which the system

$$\begin{gathered} -2\omega v = -\frac{1}{\varrho_0} q_r + \nu\left(\Delta u - \frac{u}{r^2}\right) - \omega^2 \beta r F, \quad 2\omega u = \nu\left(\Delta v - \frac{v}{r^2}\right), \\ 0 = -\frac{1}{\varrho_0} q_z + \nu \Delta w, \\ u_r + \frac{u}{r} + w_z = 0, \quad \frac{Bu}{r} = \chi \Delta F \end{gathered} \tag{7.57}$$

has a nontrivial solution satisfying the homogeneous conditions (7.48) and (7.56).

Let us demonstrate that there is a linear dependence between the functions F and $\Gamma = rv$ in the solution of the posed problem. Indeed, by virtue of the second equation in (7.57), we have

$$\frac{2\omega u}{r} = \nu \Delta \Gamma$$

and, moreover, $\Gamma = 0$ for $(r, z) \in \partial\Omega$, as it follows from eq. (7.48). It follows from this and from the last equation of system (7.57) that the function $G = Bv\Gamma - 2\omega\chi F$ is an

axisymmetric harmonic function in the domain Ω. As we have $G = 0$ on the boundary of this domain, then $G = 0$ everywhere in Ω; therefore, we obtain

$$F = \frac{B\,\mathrm{Pr}\,\Gamma}{2\omega}, \quad (r,z) \in \Omega, \tag{7.58}$$

where $\mathrm{Pr} = \nu/\chi$ is the Prandtl number.

Let us introduce dimensionless variables, using a, $a\omega$, $\varrho_0\, a\omega^2$, and B as scales of length, velocity, pressure, and temperature, respectively. Then we substitute the expressions $r = a\bar{r}$, $z = a\bar{z}$, $u = a\omega\bar{u}$, $v = a\omega\bar{v}$, $w = a\omega\bar{w}$, $q = \varrho_0 a^2\omega^2\bar{q}$, and $F = B\bar{F}$ into eqs. (7.57) and take into account equality (7.58). Omitting the bar over the dimensionless independent variables and the sought functions, we obtain the system of equations

$$\begin{gathered} \frac{R}{2}\,(\varepsilon\,\mathrm{Pr} - 4)v = -q_r + \Delta u - \frac{u}{r^2}, \quad 2Ru = \Delta v - \frac{v}{r^2}, \\ 0 = -q_z + \Delta w, \quad u_r + \frac{u}{r} + w_z = 0, \end{gathered} \tag{7.59}$$

where $R = a^2\omega/\nu$ is the Reynolds number and $\varepsilon = \beta B$ is the Boussinesq number. The system should be solved in the domain $\Pi = \{r,z : \alpha_1 < r < \alpha_2, |z| < 1\}$ under the conditions

$$u = v = w = 0, \quad (r,z) \in \partial\Pi \tag{7.60}$$

($\alpha_1 = b_1/a$ and $\alpha_2 = b_2/a$).

Let us demonstrate that the boundary-value problem (7.59), (7.60) has no nontrivial solutions if $\varepsilon\,\mathrm{Pr} < 4$. We multiply the first equation in (7.60) by u, the second equation by $(1 - \varepsilon\,\mathrm{Pr}/4)v$, and the third equation by w; then, we sum up the results and integrate the resultant equality over the domain Π with the weight r. After that, we perform integration by parts with the use of the continuity equation (7.59) and the boundary conditions (7.60). Finally, we obtain the relation

$$\int_{\alpha_1}^{\alpha_2}\int_{-1}^{1}\left[u_r^2 + \frac{u^2}{r^2} + u_z^2 + \left(1 - \frac{1}{4}\,\varepsilon\,\mathrm{Pr}\right)\left(v_r^2 + \frac{v^2}{r^2} + v_z^2\right) + w_r^2 + w_z^2\right] r\,dr\,dz = 0,$$

which yields the needed statement. Thus, under the assumption that perturbations are monotonic, we obtain the necessary condition of instability of quasi-solid rotation of the fluid under the action of the radial heat flux along ideally conducting boundaries to axisymmetric perturbations:

$$\varepsilon\,\mathrm{Pr} > 4. \tag{7.61}$$

3. Infinite layer

The last simplification implies that α_1 tends to zero and α_2 tends to infinity. In this case, the domain Π transforms to an infinite layer $\Sigma = \{r, z : r > 0, |z| < 1\}$, and the only possible equilibrium distribution of temperature has the form

$$\theta = A \ln r + C,$$

where A and C are constants. The equations of the spectral problem retain the form (7.59), but they should be solved in the domain Σ; in addition, the definition of the Boussinesq number becomes different: $\varepsilon = \beta A$. System (7.59) is supplemented with the boundary conditions

$$u = v = w = 0, \quad r > 0, \quad z = \pm 1. \tag{7.62}$$

It turns out that problem (7.59), (7.62) has a simple exact solution

$$u = r\xi(z), \quad v = r\eta(z), \quad w = \zeta(z), \quad q = \sigma(z) - kr^2/2, \tag{7.63}$$

where $k = \text{const}$. Substituting eqs. (7.63) into eqs. (7.59), we obtain

$$\begin{aligned} &\frac{R}{2}(\varepsilon \Pr - 4)\eta = -k + \xi'', \quad 2R\xi = \eta'', \\ &2\xi + \zeta' = 0, \quad \zeta'' - \sigma' = 0, \quad |z| < 1, \end{aligned} \tag{7.64}$$

where the prime means differentiation with respect to z. Conditions (7.62) lead to the following boundary conditions for the functions ξ, η, and ζ:

$$\xi = \eta = \zeta = 0, \quad r > 0, \quad z = \pm 1. \tag{7.65}$$

Thus, after numerous simplifications of the initial formulation of the problem, we obtain a very simple, but still meaningful spectral problem (7.64), (7.65).

Eliminating the function η and the constant k from the first two equations of system (7.64), we obtain the equation

$$\xi^{IV} - \mu^4 \xi = 0, \tag{7.66}$$

where $\mu^4 = R^2 (\varepsilon \Pr - 4)$. For this equation, however, it is impossible to formulate a self-adjoint eigenvalue problem. Therefore, we pass from eq. (7.66) to its corollary

$$\xi^{(VI)} - \mu^4 \xi'' = 0. \tag{7.67}$$

The boundary conditions for eq. (7.67) have the form

$$\xi = \xi^{IV} = 0, \quad z = \pm 1, \quad \xi''(-1) = \xi''(1), \quad \xi'''(-1) = \xi'''(1). \tag{7.68}$$

The second condition in system (7.68) is a corollary of eq. (7.66). The condition relating the values of ξ'' at the end points of the segment $[-1, 1]$ follows from the first equation of system (7.64) and from the equalities $\eta(-1) = \eta(1) = 0$. Finally, one more nonlocal condition (the last equality of system (7.68)) is obtained from eq. (7.66) and from the relation

$$\int_{-1}^{1} \xi \, dz = 0,$$

which follows from the third equation of system (7.64) and from the conditions $\zeta(-1) = \zeta(1) = 0$.

It is convenient to divide the eigenfunctions of problem (7.67), (7.68) into two groups: even and odd eigenfunctions. For even values of ξ, we have $\xi = C_0 + C_1 \operatorname{ch} \mu z + C_2 \cos \mu z$, and the corresponding characteristic equation is

$$\operatorname{th} \mu = \operatorname{tg} \mu. \tag{7.69}$$

The smallest positive root of eq. (7.69) is $\mu_{1,e} \approx 3.927$. The presentation of the odd eigenfunctions of problem (7.67), (7.68) has the form $\xi = C_3 \operatorname{sh} \mu z + C_4 \sin \mu z$. They correspond to eigenvalues that are the roots of the equation

$$\sin \mu = 0. \tag{7.70}$$

The smallest positive root of eq. (7.70) is $\mu_{1,0} = \pi < \mu_{1,e}$. Thus, odd perturbations are the most dangerous perturbations in the problem considered.

It is of interest that the spectrum of problem (7.67), (7.68), which is determined by eqs. (7.69), (7.70), exactly coincides with the spectrum of the problem of plane perturbations of the equilibrium state of the fluid between ideally heat-conducting vertical parallel infinite planes [68, 153]. The conditions of stability of the equilibrium state of a nonisothermal rotating layer and a plane vertical layer of a heavy fluid, however, are essentially different.

Recalling the definition of the parameter μ and using the Rayleigh number $\mathrm{Ra} = \varepsilon R^2 \mathrm{Pr}$ in our considerations, we can write the expression for the critical Rayleigh number Ra_* in the form

$$\mathrm{Ra}_* = \pi^4 + 4R^2. \tag{7.71}$$

In the case of a plane layer, the Rayleigh number is defined as $\mathrm{Ra} = ga^3 \beta A / \nu\chi$, where g is the acceleration due to gravity, a is the half-width of the layer, and A is the coefficient in the linear dependence of the temperature of the layer boundaries on the vertical coordinate. In this case, the critical Rayleigh number for plane perturbations is π^4, and it is always possible to surpass this value with a fixed Boussinesq parameter $\varepsilon = \beta A$ by increasing the width of the layer.

Concerning the rotating fluid layer, we can see that it can be destabilized by inducing a radial heat flux from the periphery toward the axis of revolution only if inequality (7.61) is satisfied. A corollary of this inequality is the presence of the term $4R^2$ in eq. (7.71), which characterizes the "stability margin" of solid rotation of the fluid. Inequality (7.61) imposes extremely severe requirements to the fluid nature. It is obviously invalid for media such as air and water. Taking into account that the value of ε usually does not exceed 10^{-3}, we can expect that the condition $\mathrm{Ra} > \mathrm{Ra}_*$ is satisfied only for fluids with extremely high Prandtl numbers.

4. Effectively one-dimensional motions

In this section, we discuss the exact solutions of system (7.47), in which the dependence of the sought function on r has a special form

$$\begin{gathered} u = rf(z,t), \quad v = rg(z,t), \quad w = w(z,t), \\ p = \frac{1}{2}K(t)r^2 + A\varrho_0\beta\omega^2\left(\frac{r^2}{2}\ln\frac{r}{a} - \frac{r^2}{4}\right) + h(z,t), \\ \theta = A\ln\frac{r}{a} + S(z,t), \end{gathered} \tag{7.72}$$

where A and a are the constant dimensions of temperature and length, respectively. Solution (7.72) was obtained in [180] by using the approach proposed there, which allows obtaining new solutions of hydrodynamic equations on the basis of partially invariant solutions.

The system for determining the functions f, g, w, K, h, and S is

$$\begin{gathered} f_t + wf_z - 2\omega g + f^2 - g^2 = -\varrho_0^{-1}K + \nu f_{zz} - \omega^2\beta S, \\ g_t + wg_z + 2\omega f + 2fg = \nu g_{zz}, \quad 2f + \omega_z = 0, \\ S_t + wS_z + Af = \chi S_{zz}, \quad w_t + ww_z = -\varrho_0^{-1}h_z + \nu w_{zz}. \end{gathered} \tag{7.73}$$

The form of solution (7.72) suggests its possible physical interpretation. The fluid fills the layer between the solid planes $z = \pm a$ rotating with the angular velocity ω around the z axis. The no-slip condition is satisfied on these planes. A velocity distribution correlated with eqs. (7.72) is prescribed in the layer at the initial time. Heat sinks or sources with a constant linear density $-2\pi Ak$ (k is the thermal conductivity coefficient of the fluid) are distributed over the axis of revolution. The planes bounding the fluid ensure ideal heat conduction. These conditions induce the following formulation of the initial-boundary problem for system (7.73):

$$\begin{gathered} f = -\frac{1}{2}w_0'(z), \quad g = g_0(z), \quad w = w_0(z), \\ S = S_0(z), \quad |z| \le a, \quad t = 0; \end{gathered} \tag{7.74}$$

$$f = g = 0, \quad w = 0, \quad S = 0, \quad z = \pm a, \quad t > 0 \tag{7.75}$$

(w_0, g_0, and S_0 are given functions of z). Instead of the last condition of system (7.75), it is possible to use the condition $S_z = 0$ at $z = \pm a$, $t > 0$, which means that the planes $z = \pm a$ are thermally insulated.

Let us now transform the equations of system (7.73). Firstly, we have to note that the function h is involved only into the last equation of this system. If w is known, this function is reconstructed by the quadrature and is determined with accuracy to an arbitrary term depending on t only. The function $K(t)$ involved into the first equation of system (7.73) can be also eliminated from considerations. For this purpose, we integrate the equation containing K from $-a$ to a with respect to z and use the equality

$$\int_{-a}^{a} f(z,t)\,dz = 0, \quad t \geq 0,$$

which follows from the third equation of the system and from conditions (7.75) for w. The resultant relation can be written in the form

$$-2\omega\bar{g} + 3\bar{f}^2 - \bar{g}^2 = -\varrho_0^{-1} K + \frac{\nu}{2a}\left[f_z(a,t) - f_z(-a,t)\right] - \omega^2 \beta \bar{S} = 0.$$

The bar over the function means its mean value over z in the interval $[-a, a]$. It follows from here and from the first equation of system (7.73) that

$$f_t - 2f_z \int_{-a}^{z} f(x,t)\,dx - 2\omega(g - \bar{g}) + f^2 - 3\bar{f}^2 - g^2 + \bar{g}^2 = \nu f_{zz} - \frac{\nu}{2a}\left[f_z(a,t) - f_z(-a,t)\right] - \omega^2 \beta(S - \bar{S}). \tag{7.76}$$

In deriving eq. (7.76), we used the equality

$$w(z,t) = -2 \int_{-a}^{z} f(x,t)\,dx, \quad t \geq 0,$$

which follows from the third equation of system (7.73) and from the condition $w(-a,t) = 0$.

Substituting the expression for w into the second and fourth equations of system (7.73), we obtain the relations

$$g_t - 2g_z \int_{-a}^{z} f(x,t)\,dx + 2\omega f + 2fg = \nu g_{zz}; \tag{7.77}$$

$$S_t - 2S_z \int_{-a}^{z} f(x,t)\,dx + Af = \chi S_{zz}. \tag{7.78}$$

Equations (7.76)–(7.78) form a closed system, which should be supplemented with initial and boundary conditions. These conditions are actually contained in system (7.74), (7.75); for continuity of presentation, however, we write them again:

$$f = f_0(z), \quad g = g_0(z), \quad S = S_0(z), \quad |z| \le a, \quad t = 0; \tag{7.79}$$

$$f = g = 0, \quad S = 0, \quad z = \pm a, \quad t > 0 \tag{7.80}$$

(here, we have $f_0 = -w_0'/2$).

System (7.76), (7.77) is not standard because of the presence of the expression $f_z(a,t) - f_z(-a,t)$ in eq. (7.76) rather than because of the presence of integral terms. Nevertheless, the estimates of solutions in the Hölder classes similar to those obtained in [116] are valid for its linearized version. This fact allows us to prove a local theorem of existence of the solution of problem (7.76)–(7.80).

Statement 7.1. Let us assume that the functions f_0, g_0, and S_0 belong to the Hölder class $C^{2+\alpha}[-a,a]$, $0 < \alpha < 1$, and the matching conditions $f_0 = g_0 = 0$, $S_0 = 0$, $g_0'' = 0$, and $S_0'' = 0$ are satisfied at $z = \pm a$,

$$2\omega\bar{g}_0 - 3\bar{f}_0^2 + \bar{g}_0^2 = \nu f_0''(\pm a) - \nu[f'(a) - f'(-a)] + \omega^2 \beta \bar{S}_0.$$

Then, there exists a value of $\tau > 0$ such that problem (7.76)–(7.80) has a solution and this solution is unique: $(f, g, S) \in C^{2+\alpha,1+\alpha/2}([-a,a] \times [0,\tau])$.

The proof of this statement has a routine character and is not presented here.

5. Concluding remarks

The main conclusion is that thermal convection in a rotating cylindrical layer of an imponderous fluid under axisymmetric heating can be excited by perturbations of the same symmetry only if the fluid has a large Prandtl number. In Section 7.2, this statement is proved under the assumption that the flat boundaries of the layer ensure ideal heat conduction. If these boundaries are thermally insulated, then the statement is still valid, but the necessary condition of instability has a more complicated form than eq. (7.61) and is not given here.

It is theoretically possible that nonaxisymmetric perturbations can turn out to be more dangerous than axisymmetric perturbations. By intuition, we can tell that this may happen if the gap between the cylinders is small ($b_2 - b_1 \ll a$) if it is possible at all. It would be interesting to prove this hypothesis or to confirm its validity by numerical experiments. The principle of monotonicity of perturbations also has to be proved, though there are no grounds to doubt its validity for the problem considered here.

The existence of real eigenvalues of problem (7.59), (7.60) deserves special consideration. Here, it may be useful to re-formulate the problem considered in terms of the

stream function ψ as

$$E^3\psi = \mu^4\psi_{zz}, \quad (r,z) \in \Pi; \tag{7.81}$$

$$\psi = 0, \quad (r,z) \in \partial\Pi; \tag{7.82}$$

$$\psi_r = 0, \quad E^2\psi = 0, \quad r = \alpha_1, \quad r = \alpha_2, \quad |z| \le 1; \tag{7.83}$$

$$\psi_z = 0, \quad \alpha_1 \le r \le \alpha_2, \quad z = \pm 1; \tag{7.84}$$

$$E\psi(-1,r) = E\psi(1,r), \quad \alpha_1 \le r \le \alpha_2; \tag{7.85}$$

$$E\psi_z(-1,r) = -E\psi_z(1,r), \quad \alpha_1 \le r \le \alpha_2, \tag{7.86}$$

if ψ is an even function of z or

$$E\psi(-1,r) = -E\psi(1,r), \quad \alpha_1 \le r \le \alpha_2; \tag{7.85′}$$

$$E\psi_z(-1,r) = E\psi_z(1,r), \quad \alpha_1 \le r \le \alpha_2, \tag{7.86′}$$

if ψ is an odd function of z. As previously, we have $\mu^4 = R^2(\varepsilon \operatorname{Pr} -4)$, and E is the Stokes operator:

$$E = r\frac{\partial}{\partial r}\left(\frac{1}{r}\frac{\partial}{\partial r}\right) + \frac{\partial^2}{\partial z^2}.$$

If the solution of problem (7.81)–(7.86) or (7.81)–(7.84), (7.85′), (7.86′) is known, then the velocity field is determined by the formulas

$$u = r^{-1}\psi_z, \quad w = -r^{-1}\psi_r, \quad v = 2R\mu^{-4}\,E^2\psi.$$

The latter comment refers to the nonlinear one-dimensional model of convective flows in an infinite rotating layer (7.76)–(7.80). In addition to obtaining the conditions of solvability of this problem as a whole with respect to time, it is also of interest to perform numerical experiments to trace the evolution of nonlinear perturbations of the trivial solution of the problem in a situation where it is unstable (i. e., at $\mathrm{Ra} > \mathrm{Ra}_*$, where the critical Rayleigh number is determined by eq. (7.71)).

8 Small perturbations and stability of plane layers in the microconvection model

In this chapter, equations of small perturbations of arbitrary motions of the fluid in the microconvection model are derived. Stability of the equilibrium state of a plane layer bounded by solid walls or by a solid wall and a free boundary is studied with the use of these equations. The asymptotic behavior of the complex decrement in the cases of long-wave and short-wave perturbations is found. Results obtained by solving the full spectral problem for a silicon melt are presented. In contrast to the classical Oberbeck–Boussinesq model, the perturbations in the problem considered here are nonmonotonic, because the boundary-value problem is not self-adjoint. For small Boussinesq numbers, the spectrum of this problem is demonstrated in order to approximate the spectra of the corresponding problems for a viscous heat-conducting fluid or for thermal gravitational convection with a finite Rayleigh number.

Stability of steady flows in a plane layer with linear and exponential distributions of temperature across the layer is studied. The flows are found to be stable to long-wave perturbations. Neutral curves are constructed numerically, and critical Grashof numbers for a silicon melt are obtained. Instability in the microconvection model is shown to occur at lower values of the wave number. This effect is caused by fluid compressibility. The results described in this chapter are based on previous publications [9, 11, 13, 31, 14, 23, 15].

8.1 Equations of small perturbations

Let us assume that $\mathbf{w}(\mathbf{x},t) = \mathbf{w}(\mathbf{x},t) + \mathbf{W}(\mathbf{x},t)$, $\tilde{q}(\mathbf{x},t) = q(\mathbf{x},t) + Q(\mathbf{x},t)$, $\tilde{\Theta} = \Theta(\mathbf{x},t) + T(\mathbf{x},t)$, where $\mathbf{W}$, Q, and T are the perturbations and $\mathbf{w}(\mathbf{x},t)$, $q(\mathbf{x},t)$, and $\Theta(\mathbf{x},t)$ form the main solution of the microconvection system (4.49)–(4.51) written in the dimensional form; the functions $\mathbf{w}, \tilde{q}$, and $\tilde{\Theta}$ are the solutions of the same equations. It obvious that

$$\operatorname{div} \mathbf{W} = 0. \tag{8.1}$$

In the linear approximation, we have

$$\begin{aligned}
\tilde{\Theta} \cdot \nabla \mathbf{w} - \nabla \tilde{w} \cdot \nabla \tilde{\Theta} &= (\nabla\Theta + \nabla T) \cdot (\nabla \mathbf{w} + \nabla \mathbf{W}) - (\nabla \mathbf{w} + \nabla \mathbf{W}) \times (\nabla\Theta + \nabla T) \\
&\approx \nabla\Theta \cdot \nabla \mathbf{w} + \nabla\Theta \cdot \nabla \mathbf{W} \\
&\quad + \nabla T \cdot \nabla \mathbf{w} - \nabla \mathbf{w} \cdot \nabla\Theta - \nabla \mathbf{w} \cdot \nabla T - \nabla \mathbf{W} \cdot \nabla\Theta \\
&= (\nabla\Theta \cdot \nabla \mathbf{w} - \nabla \mathbf{w} \cdot \nabla\Theta) \\
&\quad + (\nabla\Theta \cdot \nabla \mathbf{W} - \nabla \mathbf{W} \cdot \nabla\Theta) + (\nabla T \cdot \nabla \mathbf{w} - \nabla \mathbf{w} \cdot \nabla T).
\end{aligned} \tag{8.2}$$

https://doi.org/10.1515/9783110655469-008

Therefore ($\otimes$ means tensor multiplication), we obtain

$$\begin{aligned}\nabla\tilde{\Theta}\otimes\nabla\tilde{\Theta}-\nabla|\nabla\tilde{\Theta}|^2/2&=(\nabla\Theta+\nabla T)(\nabla\Theta+\nabla T)-\nabla|\nabla\Theta+\nabla T|^2/2\\&\approx\nabla\Theta\otimes\nabla\Theta+\nabla\Theta\nabla T\\&\quad+\nabla T\nabla\Theta-\nabla(\nabla\Theta\cdot\nabla T)-\nabla|\nabla\Theta|^2/2\\&=(\nabla\Theta\nabla\Theta-\nabla|\Theta|^2/2)\\&\quad+\nabla\Theta\nabla T+\nabla T\nabla\Theta-\nabla(\nabla\Theta\cdot\nabla T).\end{aligned}$$

The vector analysis formula predicts that

$$\nabla(\mathbf{a}\cdot\mathbf{b})=\mathbf{a}\cdot\nabla\mathbf{b}+\mathbf{b}\cdot\nabla\mathbf{a}+\mathbf{a}\times\operatorname{rot}\mathbf{b}+\mathbf{b}\times\operatorname{rot}\mathbf{a}.$$

If $\mathbf{a}=\nabla\Theta$, $\mathbf{b}=\nabla T$, then $\operatorname{rot}\mathbf{a}=\operatorname{rot}\mathbf{b}=0$; therefore, we obtain

$$\begin{aligned}\nabla\tilde{\Theta}\otimes\nabla\tilde{\Theta}-\nabla|\nabla\tilde{\Theta}|^2/2\approx{}&(\nabla\Theta\otimes\nabla\Theta-\nabla|\Theta|^2/2)+\nabla\Theta\nabla T\\&+\nabla T\nabla\Theta-\nabla\Theta\cdot\nabla(\nabla T)-\nabla T\cdot\nabla(\nabla\Theta)\end{aligned}\tag{8.3}$$

in the same approximation. For the right-hand side of eq. (4.49), we have

$$\begin{aligned}(1+\beta\tilde{\Theta})(-\nabla\tilde{q}+\nu\nabla\tilde{\tilde{w}})&=(1+\beta\Theta+\beta T)(-\nabla q-\nabla Q\\&\quad+\nu\nabla\mathbf{w}+\nu\nabla\mathbf{W})\\&\approx(1+\beta\Theta)(-\nabla q+\nu\nabla\mathbf{w})\\&\quad+(1+\beta\Theta)(-\nabla Q+\nu\nabla\mathbf{W})+\beta T(-\nabla q+\nu\nabla\mathbf{w}).\end{aligned}\tag{8.4}$$

For the energy equation (4.51), we obtain

$$|\nabla\tilde{\Theta}|^2=|\nabla\Theta+\nabla T|^2\approx|\nabla\Theta|^2+2\nabla\Theta\cdot\nabla T;\tag{8.5}$$

$$(1+\beta\Theta+\beta T)(\nabla\Theta+\nabla T)\approx(1+\beta\Theta)\nabla\Theta+(1+\beta\Theta)\nabla T+\beta T\nabla\Theta.\tag{8.6}$$

Now, the equation of momentum in the linear approximation becomes

$$\begin{aligned}&\mathbf{W}_t+\mathbf{w}\cdot\nabla\mathbf{W}+\mathbf{W}\cdot\nabla\mathbf{w}+\beta\chi(\nabla\Theta\cdot\nabla\mathbf{W}-\nabla\mathbf{W}\cdot\nabla\Theta+\nabla T\cdot\nabla\mathbf{w}-\nabla\mathbf{w}\cdot\nabla T)\\&\quad+\beta^2\chi^2\big(\nabla\Theta\nabla T+\nabla T\nabla\Theta-\nabla\Theta\cdot\nabla(\nabla T)-\nabla T\cdot\nabla(\nabla\Theta)\big)\\&=(1+\beta\Theta)(-\nabla Q+\nu\nabla\mathbf{W})+\beta T(-\nabla q+\nu\nabla\mathbf{w}).\end{aligned}\tag{8.7}$$

Here, we take into account that $\mathbf{w}, q$, and Θ form the solution of eq. (4.49) and the "equalities" (8.2)–(8.4).

The energy equation (4.51) in the same approximation, with allowance for eqs. (8.5) and (8.6), takes the form

$$T_t+\mathbf{w}\cdot\nabla T+\mathbf{W}\cdot\nabla\Theta+2\beta\chi\nabla\Theta\cdot\nabla T=(1+\beta\Theta)\chi\nabla T+\beta\chi T\nabla\Theta.\tag{8.8}$$

The boundary condition (4.53) and $\tilde{\theta} = \theta|_{\Sigma}$ (the first boundary condition for temperature) are

$$\mathbf{W} + \beta\chi\nabla T = 0, \quad T = 0. \tag{8.9}$$

We have to add the initial conditions

$$\mathbf{W} = \mathbf{W}_0(\mathbf{x}), \quad \operatorname{div}\mathbf{W}_0 = 0, \quad T = T_0(\mathbf{x}) \quad \text{at} \quad T = 0. \tag{8.10}$$

It should be noted that

$$\begin{aligned}\nabla\Theta\cdot\nabla\mathbf{W} - \nabla\mathbf{W}\cdot\nabla\Theta &= \nabla\Theta\cdot\nabla\mathbf{W} - \nabla\Theta\cdot(\nabla\mathbf{W})^*\\ &= \nabla\Theta\cdot\nabla\mathbf{W} - \nabla\Theta\cdot\mathbf{W} - \nabla\Theta\times\operatorname{rot}\mathbf{W}\\ &= \operatorname{rot}\mathbf{W}\times\nabla\Theta.\end{aligned}$$

Similarly, we have

$$\nabla T\cdot\nabla\mathbf{w} - \nabla\mathbf{w}\cdot\nabla T = \operatorname{rot}\mathbf{w}\times\nabla T$$

(in eq. (4.49), we have $\nabla\Theta\cdot\nabla\mathbf{w} - \nabla\mathbf{w}\cdot\Theta = \operatorname{rot}\mathbf{w}\times\nabla\Theta$).

The identity $\mathbf{a}\cdot(\nabla\mathbf{b})^* = \mathbf{a}\cdot\nabla\mathbf{b} + \mathbf{a}\times\operatorname{rot}\mathbf{b}$ is used here.

Taking into account the last equalities, we write the full problem as

$$\operatorname{div}\mathbf{W} = 0; \tag{8.11}$$

$$\begin{aligned}\mathbf{W}_t + \mathbf{w}\cdot\nabla\mathbf{W} + \mathbf{W}\cdot\nabla\mathbf{w} + \beta\chi(\operatorname{rot}\mathbf{W}\times\nabla\Theta + \operatorname{rot}\mathbf{w}\times\nabla T)\\ + \beta^2\chi^2[\nabla\Theta\nabla T + \nabla T\nabla\Theta - \nabla\Theta\cdot\nabla(\nabla T) - \nabla T\cdot\nabla(\nabla\Theta)]\\ = (1+\beta\Theta)(-\nabla Q + +\nu\nabla\mathbf{W}) + \beta T(-\nabla q + \nu\nabla\mathbf{w});\end{aligned} \tag{8.12}$$

$$T_t + \mathbf{w}\cdot\nabla T + \mathbf{W}\cdot\nabla\Theta + 2\beta\chi\nabla\Theta\cdot\nabla T = (1+\beta\Theta)\chi\nabla T + \beta\chi T\nabla\Theta \tag{8.13}$$

in the domain Ω;

$$\mathbf{W} + \beta\chi\nabla T = 0, \quad T = 0, \tag{8.14}$$

or

$$\mathbf{W} + \beta\chi\nabla T = 0, \quad \frac{\partial T}{\partial \mathrm{n}} + bT = 0 \tag{8.15}$$

on the solid surface Γ.

In eq. (8.12), we can assume that $\nabla\Theta\cdot(\nabla T) - \nabla T\cdot\nabla(\nabla\Theta) = \nabla(\nabla\Theta\cdot\nabla T)$, and the expression at $\beta^2\chi^2$ is (see (4.52))

$$\operatorname{div}[\nabla\Theta\otimes\nabla T + \nabla T\otimes\nabla\Theta - 2I\nabla\Theta\cdot\nabla T].$$

For convenience, we write here the linearized system (8.11)–(8.14) in the coordinates. For this purpose, we use the equalities

$$\begin{aligned}
\operatorname{rot}\mathbf{W} &= (W_{3y} - W_{2z}, W_{1z} - W_{3x}, W_{2x} - W_{1y}) \equiv (\Omega_1, \Omega_2, \Omega_3),\\
\operatorname{rot}\mathbf{w} &= (w_{3y} - w_{2z}, w_{1z} - w_{3x}, w_{2x} - w_{1y}) \equiv (\omega_1, \omega_2, \omega_3),\\
\operatorname{rot}\mathbf{W} \times \nabla\Theta &= (\Omega_2\Theta_z - \Omega_3\Theta_y, \Omega_3\Theta_x - \Omega_1\Theta_z, \Omega_1\Theta_y - \Omega_2\Theta_x)
\end{aligned}$$

and a similar equality for $\operatorname{rot}\mathbf{w} \times \nabla T$ (in the latter equality, we have to use the replacements $\mathbf{W} \leftrightarrow \mathbf{w}$ and $\Theta \leftrightarrow T$).

The system takes the following form:

$$\begin{aligned}
&W_{1t} + w_1W_{1x} + w_2W_{1y} + w_3W_{1z} + W_1w_{1x} + W_2w_{1y} + W_3w_{1z}\\
&\quad + \beta\chi[(W_{1z} - W_{3x})\Theta_z - (W_{2x} - W_{1y})\Theta_y + (w_{1z} - w_{3x})T_z\\
&\qquad - (w_{2x} - w_{1y})T_y] + \beta^2\chi^2[\nabla\Theta T_x + \nabla T\Theta_x - (\nabla\Theta\cdot\nabla T)_x]\\
&\quad = (1 + \beta\Theta)(-Q_x + \nu\nabla W_1) + \beta T(-q_x + \nu\nabla w_1),\\
&W_{2t} + w_1W_{2x} + w_2W_{2y} + w_3W_{2z} + W_1w_{2x} + W_2w_{2y} + W_3w_{2z}\\
&\quad + \beta\chi[(W_{2x} - W_{1y})\Theta_x - (W_{3y} - W_{2z})\Theta_z + (w_{2x} - w_{1y})T_x\\
&\qquad - (w_{3y} - w_{2z})T_z] + \beta^2\chi^2[\nabla\Theta T_y + \nabla T\Theta_y - (\nabla\Theta\cdot\nabla T)_y]\\
&\quad = (1 + \beta\Theta)(-Q_y + \nu\nabla W_2) + \beta T(-q_y + \nu\nabla w_2),\\
&W_{3t} + w_1W_{3x} + w_2W_{3y} + w_3W_{3z} + W_1w_{3x} + W_2w_{3y} + W_3w_{3z}\\
&\quad + \beta\chi[(W_{3y} - W_{2z})\Theta_y - (W_{1z} - W_{3x})\Theta_x + (w_{3y} - w_{2z})T_y\\
&\qquad - (w_{1z} - w_{3x})T_x] + \beta^2\chi^2[\nabla\Theta T_z + \nabla T\Theta_z - (\nabla\Theta\cdot\nabla T)_z]\\
&\quad = (1 + \beta\Theta)(-Q_z + \nu\nabla W_3) + \beta T(-q_z + \nu\nabla w_3),\\
&T_t + w_1T_x + w_2T_y + w_3T_z + W_1\Theta_x + W_2\Theta_y + W_3\Theta_z + 2\beta\chi\nabla\Theta\cdot\nabla T\\
&\quad = (1 + \beta\Theta)\chi\nabla T + \beta\chi T\nabla\Theta, \quad W_{1x} + W_{2y} + W_{3z} = 0.
\end{aligned} \tag{8.16}$$

For two-dimensional flows, the equations of small perturbations in system (8.16) take the form

$$\begin{aligned}
&W_{1t} + w_1W_{1x} + w_2W_{1y} + W_1w_{1x} + W_2w_{1y}\\
&\quad + \beta\chi[-(W_{2x} - W_{1y})\Theta_y - (w_{2x} - w_{1y})T_y]\\
&\quad + \beta^2\chi^2[\nabla\Theta T_x + \nabla T\Theta_x - (\nabla\Theta\cdot\nabla T)_x]\\
&\quad = (1 + \beta\Theta)(-Q_x + \nu\nabla W_1) + \beta T(-q_x + \nu\nabla w_1),\\
&W_{2t} + w_1W_{2x} + w_2W_{2y} + W_1w_{2x} + W_2w_{2y}\\
&\quad + \beta\chi[(W_{2x} - W_{1y}) + (w_{2x} - w_{1y})T_x]\\
&\quad + \beta^2\chi^2[\nabla\Theta T_y + \nabla T\Theta_y - (\nabla\Theta\cdot\nabla T)_y]\\
&\quad = (1 + \beta\Theta)(-Q_y + \nu\nabla W_2) + \beta T(-q_y + \nu\nabla w_2),\\
&T_t + w_1T_x + w_2T_y + W_1\Theta_x + W_2\Theta_y + 2\beta\chi\nabla\Theta\cdot\nabla T\\
&\quad = (1 + \beta\Theta)\chi\nabla T + \beta\chi T\nabla\Theta, \quad W_{1x} + W_{2y} = 0.
\end{aligned} \tag{8.17}$$

These systems are used below to analyze stability of the equilibrium states or motion.

8.2 Stability of the equilibrium state of a plane layer with solid walls

1. Equilibrium state

In the equilibrium state, we have $\boldsymbol{u} = 0$ and $\theta_t = p_t = 0$. Therefore, it follows from eq. (4.48) that

$$\boldsymbol{w}_0 = -\beta\chi\nabla\theta_0,$$

(the zero subscript refers to the equilibrium state); according to eq. (4.50), the temperature is a harmonic function:

$$\Delta\theta_0 = 0. \tag{8.18}$$

Equation (4.51) is satisfied identically, and eq. (4.49) is equivalent to

$$\nabla q_0 = \boldsymbol{g}/(1 + \beta\theta_0). \tag{8.19}$$

Note that by virtue of eqs. (4.48) and (8.18) we have $q_0 = p_0/\varrho_1$. Therefore, the necessary condition of equilibrium has the form $\boldsymbol{g} \cdot \operatorname{rot}\boldsymbol{g} = 0$. This condition is satisfied for a constant vector of external forces, and it follows from eq. (8.19) that

$$\nabla\theta_0 \times \boldsymbol{g} = 0. \tag{8.20}$$

If $\boldsymbol{g} = (0, 0, -g)$ ($g = \text{const} > 0$), then eq. (8.20) is valid only for $\theta_0 = \theta_0(z)$. In this case, we obtain $\theta_0(z) = c_1 z + c_2$ ($c_1, c_2 = \text{const}$) from eq. (8.18). In particular, the equilibrium state of the layer with the solid walls ($|z| = l$) having constant temperatures θ_1 and θ_2 is described by the formulas

$$\begin{gathered}\mathbf{w}_0 = \left(0, 0, \frac{\beta\chi(\theta_2 - \theta_1)}{2l}\right), \quad \theta_0 = \frac{(\theta_1 - \theta_2)z}{2l} + \frac{\theta_1 + \theta_2}{2}, \\ q_0 = -\frac{2lg}{\beta(\theta_1 - \theta_2)} \ln\left(1 + \beta\frac{\theta_1 + \theta_2}{2} + \beta\frac{\theta_1 - \theta_2}{2l} z\right) + c_3, \\ c_3 = \text{const}.\end{gathered} \tag{8.21}$$

In contrast to the classical case, the function $q_0(z)$, which is an analog of pressure, is distributed here *in accordance with a logarithmic rather than linear law*.

Remark 8.1. Equations (8.21) with $\beta \to 0$ yield

$$\begin{gathered}\boldsymbol{w}_0 = \boldsymbol{u}_0 = 0, \quad \theta_0 = \frac{(\theta_1 - \theta_2)z}{2l} + \frac{(\theta_1 + \theta_2)}{2}, \\ q_0 = c_4 - gz, \quad c_4 = \text{const}.\end{gathered} \tag{8.22}$$

As the pressure is $p_0 = q_0\varrho_1$, system (8.22) corresponds to the equilibrium state of a layer of a viscous heat-conducting fluid. It follows from the fact that, in accordance with replacement (4.48), system (4.49)–(4.51) with $\beta \to 0$ approximates the Navier–Stokes equations for a viscous heat-conducting fluid (see Chapter 3, Section 3.4).

Remark 8.2. Retaining terms of the second order of smallness with respect to β in the expression for $q_0(z)$ in system (8.21) and denoting the deviation of pressure from the hydrostatic value by $\bar{p}_0(z)$, we obtain the equilibrium state in the Oberbeck–Boussinesq model (see [68, 119]):

$$\boldsymbol{w}_0 = \boldsymbol{u}_0 = 0, \quad \theta_0 = \frac{\theta_1 - \theta_2}{2l}\, z + \frac{\theta_1 + \theta_2}{2}, \quad \frac{d\bar{p}_0}{dz} = \varrho_1 g\beta\theta_0(z). \tag{8.23}$$

2. Linearized problem of small perturbations for a layer

Let us consider problem (8.16) in the equilibrium case for a layer with solid walls, which is described by eqs. (8.21). Let us introduce the dimensionless variables ($\boldsymbol{W} = (U, V, W) \equiv (W_1, W_2, W_3)$)

$$\xi = \frac{x}{2l}, \quad \eta = \frac{y}{2l}, \quad \zeta = \frac{z}{2l}, \quad \tau = \frac{\chi}{4l^2}\, t,$$
$$U_1 = \frac{2lU}{\chi}, \quad V_1 = \frac{2lV}{\chi}, \quad W_1 = \frac{2lW}{\chi}, \quad Q_1 = \frac{4l^2 Q}{\nu\chi},$$
$$T_1 = \frac{T}{\mu(\theta_1 - \theta_2)} \quad (l_* = 2l, \quad \theta_* = \mu(\theta_1 - \theta_2)),$$

($\mu = 1$ if $\theta_1 > \theta_2$ and $\mu = -1$ if $\theta_1 < \theta_2$). After substitution into eqs. (8.16), we obtain the system (the subscript "1" is omitted)

$$\begin{gathered}
U_\tau - \varepsilon\mu W_\xi - \mu\varepsilon^2 T_{\xi\zeta} = (1 + \beta\theta_0)(-Q_\xi + \Delta U)\,\mathrm{Pr}, \\
V_\tau - \varepsilon\mu W_\eta - \mu\varepsilon^2 T_{\eta\zeta} = (1 + \beta\theta_0)(-Q_\eta + \Delta V)\,\mathrm{Pr}, \\
W_\tau - \varepsilon\mu W_\zeta + \mu\varepsilon^2(T_{\xi\xi} + T_{\eta\eta}) = (1 + \beta\theta_0)(-Q_\zeta + \Delta W)\,\mathrm{Pr} + \frac{\mathrm{Gr}}{1 + \beta\theta_0}\, T, \\
U_\xi + V_\eta + W_\zeta = 0, \\
T_\tau + \varepsilon\mu T_\zeta + \mu W = (1 + \beta\theta_0)\Delta T,
\end{gathered} \tag{8.24}$$

where $\theta_0(\zeta) = (\theta_1 - \theta_2)\zeta + (\theta_1 + \theta_2)/2$, $\varepsilon = \beta|\theta_1 - \theta_2|$ is the Boussinesq parameter; $\mathrm{Gr} = \mu\beta(\theta_1 - \theta_2)(2l)^3 g/\chi^2$ is the Grashof number.

The boundary conditions (8.14) on the solid walls $\zeta = -1/2$ and $\zeta = 1/2$ take the form

$$U + \varepsilon T_\xi = 0, \quad V + \varepsilon T_\eta = 0, \quad W + \varepsilon T_\zeta = 0, \quad T = 0. \tag{8.25}$$

We seek for the solution of the boundary-value problem (8.24), (8.25) in the form of normal waves as

$$(U, V, W, Q, T) = \big(U(\zeta), V(\zeta), W(\zeta), Q(\zeta), T(\zeta)\big) \cdot \exp[i(\alpha_1\xi + \alpha_2\eta - C\tau)]. \tag{8.26}$$

Here, α_1 and α_2 are the dimensionless wave numbers in the x and y directions, respectively, and C is the complex decrement determining the time evolution of the perturbation.

Substituting eq. (8.26) into eqs. (8.24), we obtain a spectral problem with respect to the parameter C for the system of ordinary differential equations

$$-iCU - i\alpha_1\mu\varepsilon W - i\alpha_1\mu\varepsilon^2 T' = (1+\beta\theta_0)[U'' - (\alpha_1^2+\alpha_2^2)U - i\alpha_1 Q]\,\mathrm{Pr}; \tag{8.27}$$

$$-iCV - i\alpha_2\mu\varepsilon W - i\alpha_2\mu\varepsilon^2 T' = (1+\beta\theta_0)[V'' - (\alpha_1^2+\alpha_2^2)V - i\alpha_2 Q]\,\mathrm{Pr}; \tag{8.28}$$

$$-iCW - \mu\varepsilon W' - \left[\mu\varepsilon^2(\alpha_1^2+\alpha_2^2) + \frac{\mathrm{Gr}}{1+\beta\theta_0}\right]T = (1+\beta\theta_0)[W'' - (\alpha_1^2+\alpha_2^2)W - Q']\,\mathrm{Pr}; \tag{8.29}$$

$$i\alpha_1 U + i\alpha_2 V + W' = 0; \tag{8.30}$$

$$-iCT + \mu\varepsilon T' + \mu W = (1+\beta\theta_0)[T'' - (\alpha_1^2+\alpha_2^2)T] \tag{8.31}$$

at $|\zeta| < 1/2$ (the prime means differentiation with respect to ζ).

The boundary conditions (8.25) at $|\zeta| = 1/2$ are

$$U = 0, \quad V = 0, \quad W + \varepsilon T' = 0, \quad T = 0. \tag{8.32}$$

Problem (8.27)–(8.32) can be subjected to the Squire transform [138]. Multiplying eq. (8.27) by $i\alpha_1$ and eq. (8.28) by $i\alpha_2$ and denoting $Z = i\alpha_1 U + i\alpha_2 V$, we obtain the problem

$$-iCZ + \mu\varepsilon k^2 W + \mu\varepsilon^2 k^2 T' = (1+\beta\theta_0)[Z'' - k^2 Z + k^2 Q]\,\mathrm{Pr}; \tag{8.33}$$

$$-iCW - \mu\varepsilon W' - \left(\mu\varepsilon^2 k^2 + \frac{\mathrm{Gr}}{1+\beta\theta_0}\right)T = (1+\beta\theta_0)(W'' - k^2 W - Q')\,\mathrm{Pr}; \tag{8.34}$$

$$Z + W' = 0; \tag{8.35}$$

$$-iCT + \mu\varepsilon T' + \mu W = (1+\beta\theta_0)(T'' - k^2 T), \tag{8.36}$$

where $k = \sqrt{\alpha_1^2 + \alpha_2^2}$ is the modified wave number.

At $|\zeta| = 1/2$, we have

$$Z = 0, \quad W + \varepsilon T' = 0, \quad T = 0. \tag{8.37}$$

For "rough" instability of the equilibrium state (8.21) (i. e., instability in the first approximation), a necessary and sufficient condition is satisfaction of the inequality $\mathrm{Im}\, C > 0$ at least for one eigenvalue.

Remark 8.3. System (8.33)–(8.36) at $C = 0$ can be reduced to one sixth-order equation for the temperature perturbation

$$L^2(xLT - \varepsilon^2 T') + \frac{k^2\,\mathrm{Ra}}{x^2}\,T = 0, \quad T = T' = T'' = 0, \quad x = 1 + \beta\theta_{1,2},$$

where $x = 1 + \beta\theta_0(\zeta)$ and $L = \varepsilon^2 d^2/dx^2 - k^2$. Even in this case, however, the latter equation cannot be explicitly integrated and the critical Rayleigh number Ra in the explicit form cannot be found.

Remark 8.4. As $\mathrm{Gr} = \varepsilon\eta\,\mathrm{Pr}$ ($\eta = (2l)^3 g/\nu\chi$ is the microconvection parameter), the boundary-value problem (8.33)–(8.37) with $\varepsilon \to 0$ at moderate Prandtl numbers approximates the problem of stability of the equilibrium state (8.22) (see Remark 8.1). If $\mathrm{Gr} \to \mathrm{Gr}_0 > 0$ as $\varepsilon \to 0$, then we obtain the problem of stability of the equilibrium state (8.23) in the Oberbeck–Boussinesq model.

3. Asymptotic behavior of long waves

Let us consider the asymptotic behavior of the amplitude equations for $k \to 0$.

As the system involves k^2 everywhere, we assume that

$$Z = Z_0 + k^2 Z_1 + \cdots, \quad W = W_0 + k^2 W_1 + \cdots, \quad Q = Q_0 + k^2 Q_1 + \cdots,$$
$$T = T_0 + k^2 T_1 + \cdots, \quad C = C_0 + k^2 C_1 + \cdots.$$

Substitution of these expressions into eqs. (8.33)–(8.36) in the zeroth approximation yields the system

$$\begin{gathered} -iC_0 Z_0 = (1+\beta\theta_0) Z_0''\,\mathrm{Pr}, \\ -iC_0 W_0 - \mu\varepsilon W_0' - \frac{\mathrm{Gr}}{1+\beta\theta_0}\,T_0 = (1+\beta\theta_0)(W_0'' - Q_0')\,\mathrm{Pr}, \\ Z_0 + W_0' = 0, \\ -iC_0 T_0 + \mu\varepsilon T_0' + \mu W_0 = (1+\beta\theta_0) T_0''. \end{gathered} \tag{8.38}$$

The boundary conditions for Z_i, W_i, Q_i, and T_i ($i = 0, 1$) coincide with eqs. (8.37).

Let us write the equation for Z_0 in the form $Z_0'' = -iC_0 Z_0/[(1+\beta\theta_0)\,\mathrm{Pr}]$. Multiplying it by the complex-conjugate value Z_0^* and integrating over the segment $[-1/2; 1/2]$, we obtain

$$\frac{iC_0}{\mathrm{Pr}} \int\limits_{-1/2}^{1/2} \frac{|Z_0|^2\,d\zeta}{1+\beta\theta_0} = \int\limits_{-1/2}^{1/2} |Z_0'|^2\,d\zeta.$$

It follows from here that the quantity C_0 is imaginary ($C_0 = iC_{oi}$, and $C_{oi} < 0$). Therefore, long-wave perturbations decay monotonically, independent of the sign of the difference $\theta_1 - \theta_2$. The form of C_{oi} can be easily refined. Indeed, the replacement $x =$

$1 + \beta\theta_0(\zeta) = 1 + \beta(\theta_1 - \theta_2)\zeta + \beta(\theta_1 + \theta_2)/2$ yields the equation $xZ_0'' + \mu_0 Z_0 = 0$, where $\mu_0 = iC_0/\Pr\varepsilon^2$; as was proved above, $\mu_0 > 0$. In turn, the last equation has the general solution

$$Z_0 = \sqrt{x}\,[h_1 J_1(2\sqrt{\mu_0 x}) + h_2 Y_1(2\sqrt{\mu_0 x})] \quad (h_1, h_2 = \text{const}),$$

where J_1 and Y_1 are the Bessel functions of the first and second kind. As $Z_0(x_{1,2}) = 0$ ($x_{1,2} = 1 + \beta\theta_{1,2} > 0$), then $\tau = 2\sqrt{\mu_0 x_1}$ is the root of the transcendental equation

$$J_1(\tau)Y_1(\lambda_0\tau) - J_1(\lambda_0\tau)Y_1(\tau) = 0, \quad \lambda_0 = \sqrt{x_2/x_1}.$$

The latter equation has a countable number of roots τ_n [100]. Therefore, we obtain

$$C_{on} = -\frac{\Pr\varepsilon^2\tau_n^2}{4x_1}\,i \equiv iC_{oi}. \tag{8.39}$$

Let us consider the system of the first approximation in terms of k^2. Instead of eqs. (8.38), we obtain the system

$$\begin{gathered}
-i(C_0Z_1 + C_1Z_0) + \varepsilon\mu W_0 + \mu\varepsilon^2 T_0' = (1 + \beta\theta_0)(Z_1'' - Z_0 + Q_0)\Pr, \\
-i(C_0W_1 + C_1W_0) - \mu\varepsilon W_1' - \frac{\mathrm{Gr}}{1 + \beta\theta_0}T_1 - \mu\varepsilon^2 T_0 = (1 + \beta\theta_0)(W_1'' - W_0 - Q_1')\Pr, \\
Z_1 + W_1' = 0, \\
-i(C_1T_0 + C_0T_1) + \mu\varepsilon T_1' + \mu W_1 = (1 + \beta\theta_0)(T_1'' - T_0).
\end{gathered} \tag{8.40}$$

Using eqs. (8.40), we obtain the following boundary-value problem for Z_1:

$$\begin{gathered}
Z_1'' + \frac{iC_0}{\Pr(1 + \beta\theta_0)}\,Z_1 = \frac{1}{\Pr(1 + \beta\theta_0)}\left(-iC_1Z_0 + \mu\varepsilon W_0 + \mu\varepsilon^2 T_0'\right) + Z_0 - Q_0, \\
Z_1(\pm 1/2) = 0.
\end{gathered}$$

For this problem to be solved uniquely, a necessary and sufficient condition is orthogonality of the right-hand side of the last equation and the solution of the homogeneous adjoint equation, i. e., Z_0^*. Thus, we obtain

$$iC_1 = \frac{\int_{-1/2}^{1/2}\left(\frac{\mu\varepsilon W_0 + \mu\varepsilon^2 T_0'}{(1+\beta\theta_0)\Pr} - Q_0 + Z_0\right)Z_0^*\,d\zeta}{\int_{-1/2}^{1/2}\frac{|Z_0|^2}{1+\beta\theta_0}\,d\zeta}. \tag{8.41}$$

It is possible to demonstrate that iC_1 is a real number.

4. Numerical solution of the eigenvalue problem

To find the numerical solution by the method of orthogonalization [75, 1], we convert system (8.33)–(8.36) to the form $\mathbf{y}' = A\mathbf{y}$, where $\mathbf{y}(\xi)$ is the vector of unknowns, $A(\xi)$

is the matrix of coefficients, and $0 \le \xi \le 1$. The following replacement is applied:

$$\begin{gathered} \xi = \zeta + 1/2, \quad y_1 = Z, \quad y_2 = Z', \quad y_3 = Z'', \\ y_4 = W, \quad y_5 = T, \quad y_6 = T'. \end{gathered} \tag{8.42}$$

Eliminating Q from eqs. (8.33)–(8.34), we obtain the following system of equations:

$$\begin{aligned} y_1' &= y_2, \quad y_2' = y_3, \quad y_4' = -y_1, \quad y_5' = y_6, \\ y_3' &= \frac{\varepsilon Ci}{(1+\beta\theta_0)^2\,\mathrm{Pr}}\,y_1 + \left(2k^2 - \frac{Ci}{(1+\beta\theta_0)\,\mathrm{Pr}}\right)y_2 \\ &\quad + \left(k^4 - \frac{k^2 Ci}{(1+\beta\theta_0)\,\mathrm{Pr}} + \frac{\varepsilon k^2(\varepsilon-\mu)}{\mathrm{Pr}(1+\beta\theta_0)^2}\right)y_4 \\ &\quad - \frac{\mu\varepsilon^2 k^2 Ci + k^2\mathrm{Gr}}{(1+\beta\theta_0)^2\,\mathrm{Pr}}\,y_5 + \frac{\varepsilon^3 k^2(1-\mu)}{\mathrm{Pr}(1+\beta\theta_0)^2}\,y_6, \\ y_6' &= \frac{\mu}{1+\beta\theta_0}\,y_4 + \left(k^2 - \frac{Ci}{1+\beta\theta_0}\right)y_5 + \frac{\varepsilon\mu}{(1+\beta\theta_0)}\,y_6. \end{aligned} \tag{8.43}$$

Here, we have $\theta_0 = \theta_2 + (\theta_1 - \theta_2)\xi$. By virtue of replacement (8.42), the boundary conditions (8.37) take the form $y_1 = 0$, $y_4 + \varepsilon y_6 = 0$, and $y_5 = 0$ at $\xi = 0$ and $\xi = 1$.

Thus, a system of the form $\mathbf{y}' = A(\xi)\mathbf{y}$ with the boundary conditions is solved at $\xi = 0$ and $\xi = 1$, $B\mathbf{y}(0) = 0$ and $D\mathbf{y}(1) = 0$, respectively. The matrix A of dimension 6×6 has the following elements:

$$\begin{aligned} &a_{11} = a_{13} = a_{14} = a_{15} = a_{16} = 0, && a_{12} = 1, \\ &a_{21} = a_{22} = a_{24} = a_{25} = a_{26} = 0, && a_{23} = 1, \\ &a_{31} = \frac{\varepsilon Ci}{(1+\beta\theta_0)^2\,\mathrm{Pr}}, && a_{32} = 2k^2 - \frac{Ci}{(1+\beta\theta_0)\,\mathrm{Pr}}, \\ &a_{33} = 0, && a_{34} = k^4 - \frac{k^2 Ci}{(1+\beta\theta_0)\,\mathrm{Pr}} + \frac{\varepsilon k^2(\varepsilon-\mu)}{\mathrm{Pr}(1+\beta\theta_0)^2}, \\ &a_{35} = -\frac{\mu\varepsilon^2 k^2 Ci + k^2\mathrm{Gr}}{(1+\beta\theta_0)^2\,\mathrm{Pr}}, && a_{36} = \frac{\varepsilon^3 k^2(1-\mu)}{\mathrm{Pr}(1+\beta\theta_0)^2}, \\ &a_{41} = -1, && a_{42} = a_{43} = a_{44} = a_{45} = a_{46} = 0, \\ &a_{51} = a_{52} = a_{53} = a_{54} = a_{55} = 0, && a_{56} = 1, \\ &a_{61} = a_{62} = a_{63} = 0, && a_{64} = \frac{\mu}{1+\beta\theta_0}, \\ &a_{65} = k^2 - \frac{Ci}{1+\beta\theta_0}, && a_{66} = \frac{\varepsilon\mu}{(1+\beta\theta_0)}. \end{aligned}$$

The matrices B and D of dimension 3×6 coincide, and their elements have the values

$$b_{11} = d_{11} = b_{24} = d_{24} = b_{35} = d_{35} = 1, \quad b_{26} = d_{26} = \varepsilon.$$

The remaining elements of both matrices are equal to zero.

The solution is sought in the form

$$\mathbf{y} = \sum_{j=1}^{3} p_j \mathbf{y}^j, \tag{8.44}$$

where the coefficients p_j are found from the system $D\mathbf{y}(1) = 0$, and $\mathbf{y}^1$, $\mathbf{y}^2$, and $\mathbf{y}^3$ are linearly independent vectors such that $\mathbf{y}^1(0) = (0, 0, 0, -\varepsilon, 0, 1)$, $\mathbf{y}^2(0) = (0, 1, 0, 0, 0, 0)$, $\mathbf{y}^3(0) = (0, 0, 1, 0, 0, 0)$.

To determine the eigenvalue C, we need two initial approximations, C_0 and C_1, which are chosen from conditions (8.39) and (8.41). We integrate the equations for $\mathbf{y}^1, \mathbf{y}^2$, and $\mathbf{y}^3$ with a given step in terms of ξ over the extreme left segment. The vectors obtained on the right end of the segment are orthogonalized. The solutions for which the initial data are the vectors obtained by means of orthogonalization are integrated over the next segment. The solutions on the right end of the second segment are again orthogonalized. We repeat this procedure until we reach the point $\xi = 1$.

For integration, we use the fourth-order Runge–Kutta–Merson method with automatic selection of the integration step. As the integration step can be specific for each of the vectors $\mathbf{y}^j$, we choose the least integration step among the three values obtained by automatic selection. When we reach the right end of the integration segment, i. e., the point $\xi = 1$, we obtain a system of three equations $D\mathbf{y}(1) = 0$ for finding three unknowns p_j, where $\mathbf{y}$ is taken in the form (8.44). The determinant of the system, which is composed from the coefficients y_i^j ($j = 1, 2, 3$, $i = 1, \ldots, 6$), is taken as the characteristic polynomial $F(C)$. For the system $D\mathbf{y}(1) = 0$ to have a nontrivial solution, a necessary and sufficient condition is the equality of the determinant of the system (in the case considered, $F(C)$) to zero.

Thus, the problem is reduced to solving the nonlinear equation $F(C) = 0$. We solve this equation by the method of secants, using the chosen values of C_0 and C_1 as the initial approximations. The root of the equation $F(C) = 0$ is the sought eigenvalue for a specified wave number k.

We consider long-wave perturbations, i. e., a situation with $k \to 0$. Moving in terms of k from $k = 10^{-5}$, we find the dependence $C(k)$. Based on the sign of the imaginary parts of C, obtained at each step in terms of k, we determine the intervals of stability.

We study stability of a layer with solid walls for a silicon melt with the following parameter values: $\nu = 2.65 \cdot 10^{-3}\,\mathrm{cm}^2/\mathrm{s}$, $\chi = 0.49\,\mathrm{cm}^2/\mathrm{s}$, $\beta = 0.75 \cdot 10^{-5}\,^\circ\mathrm{C}^{-1}$, $\mathrm{Pr} = 5.41 \cdot 10^{-3}$. The calculations are performed for the absolute difference of the wall temperatures $|\theta_1 - \theta_2| = 10$, 100, and 1000 °C. This actually means a change in the dimensionless parameter $\varepsilon = \beta|\theta_1 - \theta_2|$. The linear size of the layer was chosen to satisfy the inequality $(2l)^3 g/\nu\chi < 1$, which is the criterion of applicability of the microconvection model considered (see [176]). The smallness of the parameter $\eta = (2l)^3 g/\nu\chi$ can be reached both by decreasing the length scale and by decreasing the acceleration due to gravity g (e. g., under microgravity conditions with $g \approx (10^{-2}–10^{-3})g_0$, where

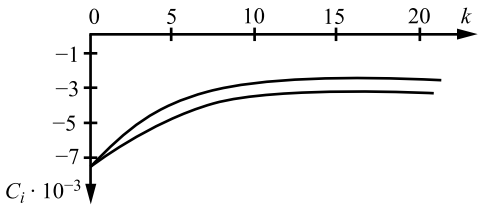

Figure 8.1: Imaginary part of complex decrement vs. wave number k at $\varepsilon = 7.5 \cdot 10^{-5}$, $\mathrm{Ra} = 4.21 \cdot 10^{-4}$.

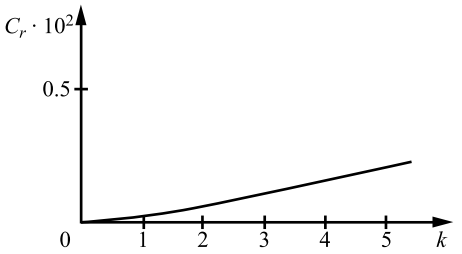

Figure 8.2: Real part of complex decrement vs. wave number k.

$g_0 = 981\,\mathrm{cm/s^2}$ is the acceleration due to gravity near the Earth's surface). In these calculations, we consider $g \sim 10^{-3} g_0$, i. e., $2l < 0.11\,\mathrm{cm}$. For the values of l, β, χ, and ν given above, we find the dependence of the parameters $C_i = \mathrm{Im}\, C$ and $C_r = \mathrm{Re}\, C$ on the wave number k.

Figure 8.1 shows the dependence $C_i(k)$ at $\varepsilon = 7.5 \cdot 10^{-5}$ (which corresponds to $|\theta_1 - \theta_2| = 10\,°\mathrm{C}$) and $\mathrm{Ra} = 4.21 \cdot 10^{-4}$. The dashed and solid curves refer to situations with heating from above ($\theta_1 > \theta_2$) and from below ($\theta_1 < \theta_2$), respectively. In the following, the curves that describe the results in situations with heating from above and from below are indicated by C_i^- and C_i^+, respectively.

Figure 8.2 shows the dependence $C_r(k)$ for the same values of the parameters ε and Ra as those used in Figure 8.1. As the values of $C_r^+(k)$ and $C_r^-(k)$ differ by no more than 10^{-6}, the corresponding curves in Figure 8.2 coincide.

Figure 8.3 shows the dependences C_i^+ and C_i^- (solid and dashed curves, respectively) at $\varepsilon = 7.5 \cdot 10^{-3}$ ($|\theta_1 - \theta_2| = 1000\,°\mathrm{C}$) and $\mathrm{Ra} = 4.21 \cdot 10^{-2}$. Figure 8.4 shows the dependence $C_r(k)$ for the same values of the parameters ε and Ra as those used in Figure 8.3.

Note that the curves $C_i(k)$ change with a greater amplitude and faster increase from the value C_{0i} with increasing ε (i. e., the difference in the wall temperatures).

A typical feature of all curves C_i^- is their slower increase, as compared with the corresponding curves C_i^+. With increasing ε, the absolute value of the difference $|C_i^+ - C_i^-|$ increases. We obtain $C_i < 0$ for all values of k, i. e., the equilibrium state is stable.

A typical feature of all curves C_r is their minor increase with increasing k ($10^{-7} \le k \le 1$). The following conditions are satisfied for all values of ε considered: 1) $C_r > 0$ for

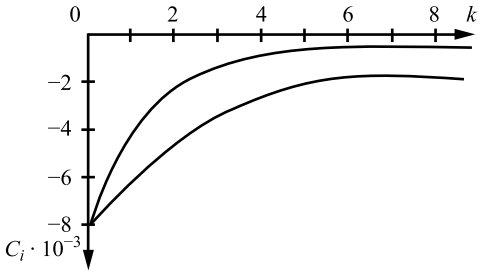

Figure 8.3: Imaginary part of complex decrement vs. wave number k at $\varepsilon = 7.5 \cdot 10^{-3}$, $\mathrm{Ra} = 4.21 \cdot 10^{-2}$.

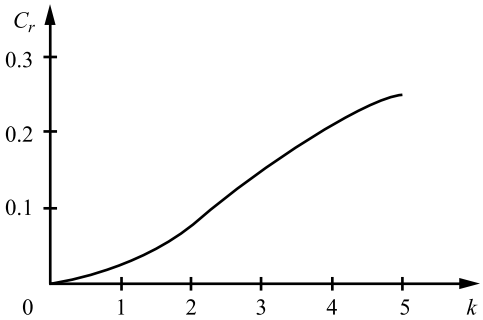

Figure 8.4: Real part of complex decrement vs. wave number k.

all values of k; moreover, the values of C_r are close to zero ($C_r \sim 10^{-12}$) up to $k = 0.05$; 2) the values of C_r are almost unchanged at $k \geq 5$, $|C_r(5) - C_r(20)| \leq 10^{-12}$; 3) all values of C_r^- lie lower than the corresponding values of C_r^+, $|C_r^+(k) - C_r^-(k)| < 10^{-6}$.

Stability of the equilibrium state (8.21) for the silicon melt is not unexpected, because $\mathrm{Pr} = 5.41 \cdot 10^{-3}$ (see Remark 8.4). Assuming that $\varepsilon = 0$ in eqs. (8.33)–(8.37), we obtain a problem of stability of the equilibrium state (8.22) of a viscous heat-conducting fluid

$$-iCZ = (Z'' - k^2 Z + k^2 Q)\,\mathrm{Pr}, \quad -iCW = (W'' - k^2 W - Q')\,\mathrm{Pr},$$
$$-iCT + \mu W = (T'' - k^2 T), \quad Z + W' = 0 \quad (-1/2 < \xi < 1/2),$$
$$Z = W = T = 0 \quad (\xi = \pm 1/2).$$

This spectral problem is easily solved: first, we find Z and W, and then we determine the temperature perturbation. We do not give the explicit expressions here, but we should note that the following integral identity is valid:

$$(k^2 - iC\,\mathrm{Pr}^{-1}) \int_{-1/2}^{1/2} (k^2 |W|^2 + |Z|^2)\, d\xi + \int_{-1/2}^{1/2} (k^2 |W'|^2 + |Z'|^2)\, d\xi = 0.$$

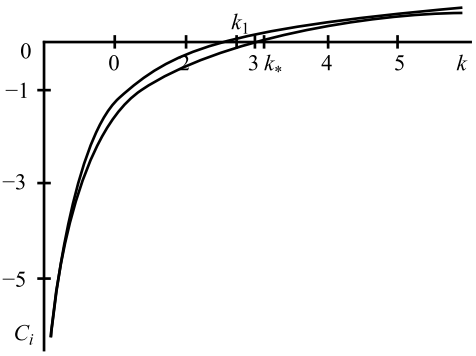

Figure 8.5: Dependence of $C_i(k)$ for microconvection model (solid line) and for Oberbeck–Boussinesq model (dashed line).

It follows from here that $-iC < 0$ is a real number. In other words, the limiting equilibrium state (8.22) as $\beta \to 0$ for eq. (8.21) is always stable. We can demonstrate that the complex decrement is a solution of one of the following equations:

$$x \operatorname{tg} x = -k \operatorname{th}(k/2), \quad (1/x) \operatorname{tg} x = (1/k) \operatorname{th}(k/2)$$

$(x = (iC/\mathrm{Pr} - k^2)^{1/2}/2)$. The last equations have a countable number of real solutions.

It is known that the linearized problem of convective instability of a quiescent fluid in the Oberbeck–Boussinesq model is self-adjoint (in the case of heating from below) [68]; therefore, the real part of the eigenvalue C_r is equal to zero. The perturbations decay or enhance monotonically, and the resultant motion is steady. The equilibrium state (8.23) of a horizontal fluid layer of thickness $2l$ with a downward directed temperature gradient $((\theta_2 - \theta_1)/2l > 0)$ becomes unstable if $\mathrm{Ra} = g\beta(\theta_2 - \theta_1)(2l)^3/(\nu\chi) > \mathrm{Ra}_* = 1708$, and the corresponding dimensionless wave number is $k_* = 3.12$.

It is of interest (see Remarks 8.2 and 8.4) to compare this classical result with the result of the numerical solution of the spectral problem (8.33)–(8.37), with the Rayleigh number $\mathrm{Ra} = \varepsilon\eta$ being finite at $\varepsilon \ll 1$. The calculations are performed for the silicon melt with the same values of the physical parameters and $\theta_2 - \theta_1 = 1000$ °C. As η increases, the curve $C_i(k)$ approaches the axis $C_i = 0$ and crosses this axis for the first time at $k = k_1 = 2.84 < k_*$, at $\eta_1 = 225193.33$. In this case, the Rayleigh number is $\mathrm{Ra}_1 = \varepsilon\eta_1 = 1688.95 < \mathrm{Ra}_*$, and the layer thickness is $2l_1 = 6.68$ cm at $g = 10^{-3}g_0$.

The solid and dashed curves in Figure 8.5 show the dependence $C_i(k)$ for the microconvection model and for the Oberbeck–Boussinesq model, respectively. Thus, in the microconvection model the equilibrium state becomes unstable at smaller wave numbers. Apparently this is caused by the greater mobility (compressibility) of the fluid in the case considered. The values of $C_r(k)$ at $\mathrm{Ra} > 10^3$ for all values of k are close to 10^{-12}, and the spectral problem (8.33)–(8.37) becomes "more self-adjoint." As the Boussinesq parameter ε decreases, the critical values of the Rayleigh number and

wave number increase. Thus, at $\varepsilon = 0.75 \cdot 10^{-4}$ and $\theta_2 - \theta_1 = 10$ °C, we have $k_1 = 2.99$, $\mathrm{Ra}_1 = 1694.54$, which agrees with Remark 8.4.

8.3 Emergence of microconvection in a plane layer with a free boundary

1. Equilibrium state

Let us assume that $f(\mathbf{x}, t) = 0$ is an implicit equation of the free boundary Γ. Then, the following relations are satisfied on this boundary with allowance for replacement (4.48) [11]:

$$f_t + (\mathbf{w} + \beta\chi\nabla\theta) \cdot \nabla f = 0; \tag{8.45}$$

$$[p_{\mathrm{gas}} - \varrho_0 q - \beta\chi\varrho_0(\nu - \chi)\Delta\theta]\mathbf{n} + 2\varrho_0\nu[D(\mathbf{w}) + \beta\chi D(\nabla\theta)]\mathbf{n} = 2\sigma(\theta)H\mathbf{n} + \nabla_{11}\sigma; \tag{8.46}$$

$$k\frac{\partial\theta}{\partial n} + b(\theta - \theta_{\mathrm{gas}}) = Q. \tag{8.47}$$

Equation (8.45) is the kinematic condition, eq. (8.46) is the dynamic condition, and eq. (8.47) defines the heat transfer between the fluid and the gas medium, which is here assumed to be passive (k is the thermal conductivity coefficient of the fluid, $b \geq 0$ is the heat-transfer coefficient, and Q is the heat flux). In eqs. (8.46) and (8.47), p_{gas} and θ_{gas} are the specified pressure and temperature in the gas (in what follows, p_{gas} and θ_{gas} are constants), $\mathbf{n} = \nabla f/|\nabla f|$ is the external normal to Γ, and $\sigma(\theta)$ is approximated by the linear dependence

$$\sigma(\theta) = \sigma_1 - æ(\theta - \theta_1), \tag{8.48}$$

where σ_1 and θ_1 are the values of surface tension and temperature at a certain point of Γ, H is the mean curvature, and $\nabla_{11} = \nabla - \mathbf{n}(\mathbf{n} \cdot \nabla)$ is the surface gradient. In what follows, the free boundary has no common points with the solid wall; therefore, the conditions on the contact line are not considered (see [189, 171]).

In all equations below, we have $\mathbf{g} = (0, 0, -g)$ and $g = \mathrm{const} > 0$. We can easily verify that the fluid can be in the equilibrium state [11] in the layer $0 < z < l$, $|x|, |y| < \infty$; the upper boundary of the layer is the free boundary, and the lower boundary of the layer $z = 0$ is the solid wall. The equilibrium state is described by the equations

$$\begin{gathered}
\mathbf{w}_0 = (0, 0, -\beta\chi\theta_{01}), \quad \theta_0(z) = \theta_{00} + \theta_{01}z, \\
q_0 = -\frac{g}{\beta\theta_{01}}\ln[1 + \beta\theta_0(z)] + c_1, \\
\theta_{01} = \frac{Q + b(\theta_{\mathrm{gas}} - \theta_{00})}{k + bl}, \quad c_1 = \frac{p_{\mathrm{gas}}}{\varrho_0} + \frac{g}{\beta\theta_{01}}\ln[1 + \beta\theta_0(l)],
\end{gathered} \tag{8.49}$$

where $\theta_{00} = \mathrm{const}$ is the temperature of the solid wall; without loss of generality, we assume that $\theta_{00} = 0$. Thus, eqs. (8.49) yield the exact solution of problem (4.49)–(4.51),

(8.45)–(8.48) with a plane free boundary $z = l$. In contrast to the classical case, the function $q_0(z)$ (analog of pressure) is distributed here in accordance with a logarithmic rather than linear law.

From eqs. (8.49) with $\beta \to 0$ and other parameters being fixed, we obtain

$$\mathbf{w}_0 = 0, \quad \theta_0 = \theta_{01} z, \quad q_0 = \frac{p_{\text{gas}}}{\varrho_0} + gl - gz. \tag{8.50}$$

As the pressure is $p_0 = \varrho_0 q_0$, then eqs. (8.50) describe the equilibrium state of a layer of a viscous heat-conducting fluid. This is not surprising, because, in accordance with replacement (4.48), system (4.49)–(4.51) approximates the Navier–Stokes equations for such a fluid in the case considered.

If now we retain terms of the second order of smallness with respect to β in eq. (8.49) for $q_0(z)$ and denote the deviation of pressure from the hydrostatic value by $\bar{p}_0(z) = \varrho_0 \bar{q}_0(z)$ ($\bar{q}_0(z) = q_0(z) + gz$ by virtue of replacement (4.48)), we obtain the equilibrium state of the plane layer in the Oberbeck–Boussinesq model [119]:

$$\mathbf{w}_0 = 0, \quad \theta_0(z) = \theta_{01} z, \quad \bar{p}_0 = p_{\text{gas}} + \frac{\varrho_0 g \beta}{2\theta_{01}} [\theta_0^2(z) - \theta_0^2(l)]. \tag{8.51}$$

The equality for $\bar{p}_0(z)$ is usually written as

$$d\bar{p}_0/dz = \varrho_0 g \beta \theta_0(z).$$

Stability of the equilibrium state (8.49) is studied below in the linear approximation.

2. Small perturbations

Equations of small perturbations for arbitrary solutions of the problem with the free boundary for the microconvection model were obtained in [11]. Here we apply these equations to the equilibrium state (8.49). Let $\mathbf{U}(\mathbf{x}, t) = (U, V, W)$, $T(\mathbf{x}, t)$, $Q(\mathbf{x}, t)$ be perturbations of the basic equilibrium state $\mathbf{w}_0, \theta_0, q_0$ (8.49). We introduce the dimensionless variables

$$\begin{gathered} \mathbf{x}' = \mathbf{x}/l, \quad t' = \nu t/l^2, \quad \mathbf{U}' = l\mathbf{U}/\nu, \\ T' = T/(\mu \theta_{01} l \,\mathrm{Pr}), \quad Q' = l^2 Q/\nu^2, \end{gathered} \tag{8.52}$$

where $\mu = 1$ for $\theta_{01} > 0$ and $\mu = -1$ for $\theta_{01} < 0$.

Substituting eqs. (8.52) into eqs. (8.16), (8.45)–(8.47), we obtain a problem of small perturbations in the dimensionless variables (the primes are omitted):

– at $-\infty < x < \infty$, $-\infty < y < \infty$, $0 < z < 1$,

$$U_t - \frac{\mu\varepsilon}{\mathrm{Pr}} W_x - \frac{\mu\varepsilon^2}{\mathrm{Pr}} T_{xz} = (1 + \mu\varepsilon z)(-Q_x + \Delta U); \tag{8.53}$$

$$V_t - \frac{\mu\varepsilon}{\mathrm{Pr}} W_y - \frac{\mu\varepsilon^2}{\mathrm{Pr}} T_{yz} = (1+\mu\varepsilon z)(-Q_y + \Delta V); \tag{8.54}$$

$$W_t - \frac{\mu\varepsilon}{\mathrm{Pr}} W_z + \frac{\mu\varepsilon^2}{\mathrm{Pr}} (T_{xx} + T_{yy}) = (1+\mu\varepsilon z)(-Q_z + \Delta W) + \frac{\mathrm{Ra}}{1+\mu\varepsilon z}; \tag{8.55}$$

$$T_t + \frac{\mu\varepsilon}{\mathrm{Pr}} T_z + \frac{\mu W}{\mathrm{Pr}} = (1+\mu\varepsilon z)\frac{1}{\mathrm{Pr}} \Delta T; \tag{8.56}$$

$$U_x + V_y + W_z = 0; \tag{8.57}$$

– on the free boundary $z = 1$,

$$\frac{\gamma}{1+\mu\varepsilon} R - Q + \varepsilon\left(\frac{1}{\mathrm{Pr}} - 1\right)\Delta T + 2W_z + 2\varepsilon T_{zz} = \mathrm{We}(R_{xx} + R_{yy}); \tag{8.58}$$

$$U_z + 2\varepsilon T_{xz} + W_x = -\mathrm{M}\left(T + \frac{\mu}{\mathrm{Pr}} R\right)_x; \tag{8.59}$$

$$V_z + 2\varepsilon T_{yz} + W_y = -\mathrm{M}\left(T + \frac{\mu}{\mathrm{Pr}} R\right)_y; \tag{8.60}$$

$$T_z + \mathrm{B}\left(T + \frac{\mu}{\mathrm{Pr}} R\right) = 0; \tag{8.61}$$

$$R_t = W + \varepsilon T_z; \tag{8.62}$$

– on the solid wall $z = 0$,

$$U + \varepsilon T_x = 0, \quad V + \varepsilon T_y = 0, \quad W + \varepsilon T_z = 0, \quad T = 0; \tag{8.63}$$

– at $t = 0$,

$$\begin{gathered} U = U_1(x,y,z), \quad V = V_1(x,y,z), \quad W = W_1(x,y,z); \\ T = T_1(x,y,z), \quad R = R_0(x,y), \quad U_{1x} + V_{1y} + W_{1z} = 0. \end{gathered} \tag{8.64}$$

The following notations are introduced in problem (8.53)–(8.64): Boussinesq parameter $\varepsilon = \mu\theta_{01} l\beta > 0$, Prandtl number $\mathrm{Pr} = \nu/\chi$, Rayleigh number $\mathrm{Ra} = \mu\theta_{01} l^4 \beta g/\nu\chi \equiv \varepsilon\eta$ ($\eta = gl^3/\nu\chi$ is the microconvection parameter), Galileo number $\gamma = gl^3/\nu^2 = \eta/\mathrm{Pr}$, modified Weber number $\mathrm{We} = \sigma(\theta_0(l))l/\varrho_0\nu^2$, Marangoni number $\mathrm{M} = \mu æ\theta_{01} l^2/\varrho_0\nu\chi$, and Biot number $\mathrm{B} = bl/k$.

The function $R(x,y,t)$ describes the perturbation of the free boundary $z = 1$, i. e., deviation from this plane along the normal at each point of the plane.

We seek the solution of problem (8.53)–(8.63) in the form of the normal waves

$$(\mathbf{U}, Q, T, R) = \big(\mathbf{U}(z), Q(z), T(z), R\big) \exp\big[i(\alpha_1 x + \alpha_2 y - Ct)\big], \tag{8.65}$$

where α_1 and α_2 are the dimensionless wave numbers along the x and y axes, respectively; C is the complex decrement determining the time evolution of the perturbation. It is possible to not consider the initial data (8.64). Substituting eq. (8.65) into

eqs. (8.53)–(8.63), we obtain a homogeneous problem with respect to U, V, W, Q, T, and R. It turns out that the Squire transform is applicable to this problem [138]. Namely, if we assume that

$$Z = \alpha_1 U + \alpha_2 V, \quad k^2 = \alpha_1^2 + \alpha_2^2,$$

then we obtain the following boundary-value problem for Z, W, Q, T, R, and the parameter C:

– at $0 < z < 1$,

$$-iCZ - \frac{\mu\varepsilon k^2 i}{\mathrm{Pr}} W - \frac{\mu\varepsilon^2 k^2 i}{\mathrm{Pr}} T' = (1 + \varepsilon\mu z)(Z'' - k^2 Z - ik^2 Q); \tag{8.66}$$

$$-iCW - \frac{\mu\varepsilon}{\mathrm{Pr}} W' - \frac{\mu\varepsilon^2 k^2}{\mathrm{Pr}} T = (1 + \varepsilon\mu z)(W'' - k^2 W - Q') + \frac{\mathrm{Ra}}{1 + \varepsilon\mu z} T; \tag{8.67}$$

$$-iCT + \frac{\mu\varepsilon}{\mathrm{Pr}} T' + \frac{\mu}{\mathrm{Pr}} W = (1 + \varepsilon\mu z)\frac{1}{\mathrm{Pr}}(T'' - k^2 T); \tag{8.68}$$

$$iZ + W' = 0; \tag{8.69}$$

– at $z = 1$,

$$-Q + \frac{\gamma}{1 + \mu\varepsilon} R + 2W' + \varepsilon\left(1 + \frac{1}{\mathrm{Pr}}\right)T'' + \varepsilon k^2\left(1 - \frac{1}{\mathrm{Pr}}\right)T = -\mathrm{We}\, k^2 R; \tag{8.70}$$

$$Z' + 2\varepsilon k^2 iT' + k^2 iW = -\mathrm{M}k^2 i\left(\frac{\mu}{\mathrm{Pr}} R + T\right); \tag{8.71}$$

$$T' + \mathrm{B}\left(T + \frac{\mu}{\mathrm{Pr}} R\right) = 0; \tag{8.72}$$

$$-iCR = W + \varepsilon T'; \tag{8.73}$$

– at $z = 0$

$$Z = T = 0, \quad W + \varepsilon T' = 0. \tag{8.74}$$

The prime here means differentiation with respect to z.

3. Long waves

We find the asymptotic behavior of the spectral problem (8.66)–(8.74) as $k \to 0$. Let us assume that

$$Z = Z_0 + k^2 Z_1 + \cdots, \quad W = W_0 + k^2 W_1 + \cdots, \quad Q = Q_0 + k^2 Q_1 + \cdots,$$
$$T = T_0 + k^2 T_1 + \cdots, \quad C = C_0 + k^2 C_1 + \cdots, \quad R = R_0 + k^2 R_1 + \cdots.$$

In the zeroth approximation, we obtain the problem

$$-iC_0 Z_0 = (1 + \varepsilon\mu z) Z_0'',$$

$$-iC_0W_0 - \frac{\mu\varepsilon}{\mathrm{Pr}}\,W_0' = (1+\varepsilon\mu z)(W_0'' - Q') + \frac{\mathrm{Ra}}{1+\varepsilon\mu z}\,T_0, \tag{8.75}$$

$$-iC_0T_0 + \frac{\mu\varepsilon}{\mathrm{Pr}}\,T_0' + \frac{\mu}{\mathrm{Pr}}\,W_0 = (1+\varepsilon\mu z)\frac{1}{\mathrm{Pr}}\,T_0'',$$

$$iZ_0 + W_0' = 0 \quad (0 < z < 1);$$

$$-Q_0 + \frac{\gamma}{1+\mu\varepsilon}\,R_0 + \varepsilon\left(1+\frac{1}{\mathrm{Pr}}\right)T_0'' = 0,$$

$$Z_0' = 0,\ \mu\,\mathrm{Pr}\,T_0' + \mathrm{B}(\mu\,\mathrm{Pr}\,T_0 + R_0) = 0, \tag{8.76}$$

$$-iC_0R_0 = W_0 + \varepsilon T_0' \quad (z = 1);$$

$$Z_0 = W_0 = T_0 = 0, \quad W_0 + \varepsilon T_0' = 0 \quad (z = 0). \tag{8.77}$$

Clearly, the spectral parameter C_0 is determined from the boundary-value problem for Z_0. As we have

$$iC_0\int_0^1 \frac{|Z_0|^2}{1+\varepsilon\mu z}\,dz = \int_0^1 |Z_0'|^2\,dz,$$

then C_0 is a purely imaginary number and $iC_0 > 0$. We can easily refine the value of C_0. For this purpose, we introduce a new variable $s = 1 + \varepsilon\mu z$; then, we obtain $sZ_{0ss} + d^2Z_0 = 0$, $Z_0(1) = Z_0'(s_1) = 0$, $s_1 = 1 + \varepsilon\mu$, $d^2 = iC/\varepsilon^2 > 0$. The equation for $Z_0(s)$ has the general solution

$$Z_0 = \sqrt{s}\,[h_1J_1(2d\sqrt{s}) + h_2Y_1(2d\sqrt{s})] \quad (h_1, h_2 = \mathrm{const}),$$

where J_1 and Y_1 are the Bessel functions of the first and second kind. The boundary conditions for Z_0 show that $\tau = 2d$ is the root of the transcendental equation

$$J_1(\tau)Y_0(\tau\sqrt{s_1}) - Y_1(\tau)J_0(\tau\sqrt{s_1}) = 0, \tag{8.78}$$

which has a countable number of real roots τ_n [100]. Therefore, we have

$$iC_{0n} = \varepsilon^2\tau_n^2/4, \quad n = 1, 2, \ldots. \tag{8.79}$$

Thus, long-wave perturbations decay monotonically, independent of the sign of θ_{01}.

4. Layer of a viscous heat-conducting fluid

In this case we have $\varepsilon = 0$ ($\beta = 0$), and problem (8.66)–(8.74) is simplified to

$$-iCZ = Z'' - k^2Z - ik^2Q, \quad -iCW = W'' - k^2W - Q',$$
$$-iC\,\mathrm{Pr}\,T + \mu W = T'' - k^2T, \quad iZ + W' = 0 \quad (0 < z < 1); \tag{8.80}$$

$$
\begin{gathered}
-Q + \gamma R + 2W' = -\mathrm{We}\, k^2 R, \quad Z' + ik^2 W = -ik^2 \mathrm{M}\left(\frac{\mu}{\mathrm{Pr}} R + T\right), \\
T' + \mathrm{B}\left(\frac{\mu}{\mathrm{Pr}} R + T\right) = 0, \quad -iCR = W \quad (z = 1);
\end{gathered} \tag{8.81}
$$

$$
Z = W = T = 0 \quad (z = 0). \tag{8.82}
$$

System (8.80) has the general solution

$$
\begin{aligned}
Z &= id(b_1 \cos dz - b_2 \sin dz) + \frac{ik^2}{k^2 + d^2}(a_1 \operatorname{sh} kz + a_2 \operatorname{ch} kz), \\
W &= b_1 \sin dz + b_2 \cos dz + \frac{k}{k^2 + d^2}(a_1 \operatorname{ch} kz + a_2 \operatorname{sh} kz), \\
Q &= a_1 \operatorname{sh} kz + a_2 \operatorname{ch} kz, \\
T &= h_1 \sin qz + h_2 \cos qz + \frac{\mu b_1 \sin dz}{q^2 - d^2} + \frac{\mu b_2 \cos dz}{q^2 - d^2} \\
&\quad + \frac{k\mu}{(k^2 + d^2)(k^2 + q^2)}(a_1 \operatorname{ch} kz + a_2 \operatorname{sh} kz),
\end{aligned} \tag{8.83}
$$

where a_1, a_2, b_1, b_2, h_1, and h_2 are constants; $q^2 = iC\,\mathrm{Pr} - k^2$, $d^2 = iC - k^2$ $(\mathrm{Pr} \neq 1)$.

Let $iC = \tau$, then we have $q^2 + k^2 = \tau\,\mathrm{Pr}$, $k^2 + d^2 = \tau$, $q^2 - d^2 = (\mathrm{Pr} - 1)\tau$, and we obtain the following equations from the boundary conditions (8.82):

$$
b_1 = -\frac{k^2 a_2}{d\tau}, \quad b_2 = -\frac{k a_1}{\tau}, \quad h_2 = \frac{k\mu a_1}{\tau^2\,\mathrm{Pr}(\mathrm{Pr} - 1)}. \tag{8.84}
$$

As $R = -W/\tau$, conditions (8.81) on the free boundary $z = 1$ reduce to the following conditions $(\mu^2 = 1)$:

$$
\begin{gathered}
2W' - Q - (\gamma + k^2\,\mathrm{We})\frac{W}{\tau} = 0, \\
Z' + ik^2 W + i\mu k^2 \mathrm{M}\left(\mu T - \frac{W}{\tau\,\mathrm{Pr}}\right) = 0, \\
\mu\,\mathrm{Pr}\,T' + B\left(\mu\,\mathrm{Pr}\,T - \frac{W}{\tau}\right) = 0.
\end{gathered} \tag{8.85}
$$

System (8.85), together with eqs. (8.84), allows us to determine the complex decrement C at $\mathrm{Pr} \neq 1$. The corresponding characteristic determinant, however, is rather complicated, and problem (8.80)–(8.82) at $\gamma = 0$ was solved numerically in [199] by using the method of orthogonalization. Here we give the dependence of the Marangoni number as $\gamma \neq 0$ for monotonic perturbations with $C = 0$. The calculations show that

$$
\mathrm{M} = -\frac{8\mu k(k - \operatorname{sh} k \operatorname{ch} k)(k \operatorname{ch} k + \mathrm{B} \operatorname{sh} k)}{k^3 \operatorname{ch} k - \operatorname{sh}^3 k - 8k^5 \operatorname{ch} k[\mathrm{Pr}(\gamma + k^2\mathrm{We})]^{-1}}. \tag{8.86}
$$

At $\gamma = 0$, this equation coincides with the expression derived in [199]. At small values of k, eq. (8.86) yields

$$\mathrm{M} \sim -2\mu\gamma\,\mathrm{Pr}(\mathrm{B}+1)/3. \tag{8.87}$$

Performing similar transformations for the Oberbeck–Boussinesq model, we obtain, instead of eq. (8.87),

$$\mathrm{M} \sim -\frac{2}{3}\,\mu\gamma\,\mathrm{Pr}(\mathrm{B}+1) - \frac{11}{60}\,\mathrm{B}\,\mathrm{Ra}, \tag{8.88}$$

where Ra is the Rayleigh number. Note that $\mathrm{Ra} \le 40\gamma(\mathrm{B}+1)/11\mathrm{B} = \mathrm{Ra}_*$ in the case of heating from below ($\mu = -1$), and there is no neutral curve for $\mathrm{Ra} > \mathrm{Ra}_*$. As $\mathrm{B} \to \infty$, the limiting value of Ra_* coincides with that calculated in [99] for $\mathrm{M} = 0$. The case with $\mathrm{B} = \infty$ means that the temperature rather than the heat exchange with the ambient medium is specified on the free surface.

5. Analysis of numerical results

Firstly, we should note that the Boussinesq parameter, the Rayleigh number, and the Marangoni number are proportional to each other, because they depend on a controlled parameter, which is the temperature gradient θ_{01}. Therefore, it is convenient to use new parameters $\alpha = \varrho_0\nu\beta\chi/æl$, $\Gamma = \varrho_0\beta g l^2/\chi$, then $\varepsilon = \alpha\mathrm{M}$, $\mathrm{Ra} = \Gamma\mathrm{M} = \mathrm{Pr}\,\alpha\gamma\mathrm{M}$, and to calculate the Marangoni number. For the Oberbeck–Boussinesq model, stability of the layer with a linear dependence of Ra and M was studied in [32, 95, 99, 162].

Problem (8.66)–(8.74) with arbitrary perturbations was numerically solved by the method of orthogonalization. Expression (8.86) was used as a test in numerically constructing neutral curves. The results calculated for $\alpha = 0$ and $\Gamma \neq 0$ coincide with the numerical data obtained within the framework of the Oberbeck–Boussinesq model in [199].

Figure 8.6 shows the neutral curves constructed at $\gamma = 10^3$, $\mathrm{We} = 10^4$, $\mathrm{Pr} = 5.41 \cdot 10^{-3}$, and $\alpha = 10^{-4}$. Curves 1 and 2 refer to monotonic and oscillatory perturbations, respectively. The asymptotic expressions (8.79) and (8.88) are used to construct

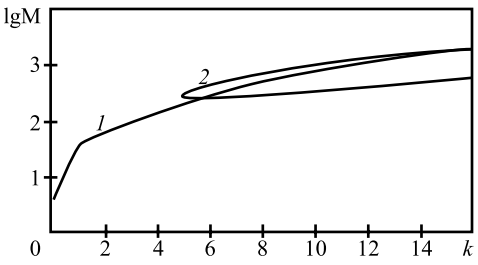

Figure 8.6: Neutral curves vs. wave number k at $\gamma = 10^3$, $\mathrm{We} = 10^4$, $\mathrm{Pr} = 5.41 \cdot 10^{-3}$, $\alpha = 10^{-4}$.

Table 8.1: Minimal values of Marangoni and wave numbers vs. α and γ.

α	γ	M_*	k_*
0	0	224.93	5.35
0	10^3	226.51	5.35
10^{-4}	0	230.88	5.50
10^{-4}	10^3	232.47	5.50

the neutral curve 2. The domain of stability to monotonic perturbations lies above curve 1, and the domain of stability to oscillatory perturbations lies inside curve 2. The calculations show that the qualitative behavior of the neutral curves at small values of the parameters α and Γ coincides with the behavior of the corresponding curves for a viscous heat-conducting fluid ($\alpha = 0$ and $\gamma = 0$) [199]. As was found in [199], curve 1 corresponds to thermocapillary perturbations associated with nonuniformity of fluid heating and curve 2 is the boundary of stability to capillary perturbations induced by deformations of the free boundary.

For several values of α and γ, Table 8.1 shows the minimum values of M_* of the capillary neutral curve (curve 2) and the value of the wave number k_* at which this minimum is reached. Thus, taking into account fluid compressibility ($\alpha \neq 0$), we obtain stabilization of capillary perturbations; even for small values of the parameter α, the values of the critical Marangoni numbers can be noticeably different.

Another specific feature of the model considered is the emergence of new neutral curves with enhancement of gravity forces, which is caused by taking fluid compressibility into account. Perturbations corresponding to the new mechanism of instability grow monotonically, and the domain of instability is located above the corresponding neutral curve.

These new curves are indicated by the numbers 3 to 5 in Figure 8.7, where $\gamma = 10^6$, $\mathrm{Pr} = 5.41 \cdot 10^{-3}$, $\mathrm{We} = 10^4$, and $\alpha = 10^{-4}$; curves 1 and 2 are the same as those in Figure 8.6.

As is seen from Figure 8.8, where $\gamma = 10^7$, capillary perturbations become further stabilized as the gravity force increases, and the threshold of stability for thermo-

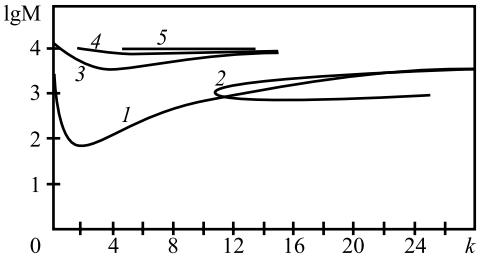

Figure 8.7: New neutral curves 3–5 for $\gamma = 10^6$.

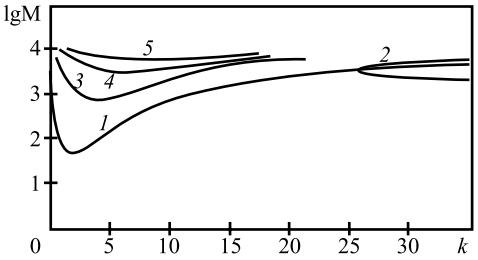

Figure 8.8: New neutral curves 3–5 for $\gamma = 10^7$.

Table 8.2: Minimal values of Marangoni numbers related with neutral curves of Figures 8.1 and 8.2.

γ	M_{*1}	M_{*2}	M_{*3}	M_{*4}	M_{*5}
10^6	74.3	739.3	362.7	8032	9825.6
10^7	49.1	2357	767.3	3214.5	6122

capillary perturbations and new perturbations caused by fluid compressibility decreases. The minimum values of M_{*j} corresponding to j neutral curves in Figures 8.7 and 8.8 are listed in Table 8.2.

Figure 8.9, where $\gamma = 10^7$, We $= 10^4$, M $= 3400$, $\alpha = 10^{-4}$, and Pr $= 5.41 \cdot 10^{-3}$, shows the behavior of the complex decrement of the problem as a function of the wave number. Here, curves 1 and 2 refer to the thermocapillary monotonic and capillary oscillatory modes, respectively. Curves 3 and 4 refer to the new perturbations caused by fluid compressibility. The problem eigenvalues corresponding to the neutral curve 5 (in Figures 8.7 and 8.8) lie in the negative half-plane and are not shown in Figure 8.9.

The influence of the Prandtl number on stability of the equilibrium state is illustrated in Figure 8.10 constructed for $\gamma = 10^6$, Pr $= 1$, We $= 10^4$, and $\alpha = 10^{-4}$; the neutral curves are enumerated in the same manner as in the previous figures. Figure 8.10 does not show the neutral curve for capillary perturbations.

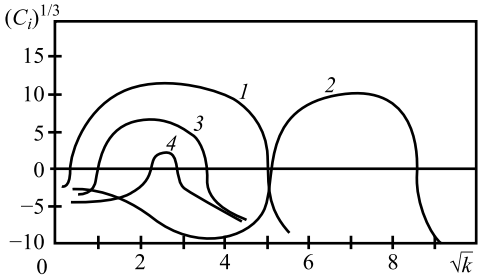

Figure 8.9: Dependence of C_i vs. wave number k for different modes.

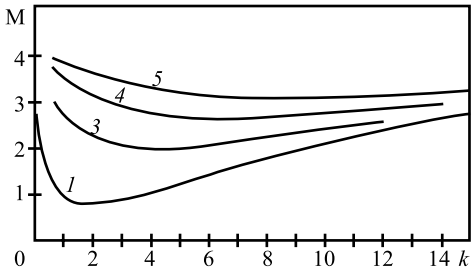

Figure 8.10: Neutral curves vs. wave number k at $\gamma = 10^6$, We $= 10^4$, Pr $= 1$, $\alpha = 10^{-4}$.

Here, the domain of instability is shifted toward extremely short waves with increasing Prandtl number, and the minimum value of the Marangoni number drastically increases. As is seen from the figure, an increase in Pr leads to intense destabilization of monotonic perturbations. The threshold of stability for all perturbations decreases. Thus, the loss of stability with respect to thermocapillary perturbations occurs already at M $= 6.2$.

The influence of deformability of the free boundary on stability of the equilibrium state is illustrated in Table 8.3, composed for $\gamma = 10^6$, Pr $= 5.41 \cdot 10^{-3}$, and $\alpha = 10^{-4}$. As the Weber number decreases, the threshold of stability to capillary perturbations appreciably decreases; correspondingly, the equilibrium state with respect to these perturbations becomes stabilized with increasing We. Capillary instability is absent altogether for We $= 10^6$. For monotonic perturbations, the change in the Weber number has practically no effect on the stability threshold.

Based on the results presented above, we can conclude that the most dangerous perturbations in wide ranges of problem parameters are thermocapillary ones. In the domain of extremely short waves with small values of Pr and We, however, oscillatory capillary perturbations dominate.

Let us estimate the areas of applicability of different models (microconvection, Oberbeck–Boussinesq, and viscous heat-conducting fluid models) in the problem under consideration of stability of the equilibrium state (8.49). The influence of the buoyancy forces is studied with fixed values: $\alpha = 10^{-4}$, Pr $= 5.41 \cdot 10^{-3}$, and We $= 10^4$. The criterion is the relation $\min_k |\mathrm{M}(k) - \mathrm{M}_t(k)|/\mathrm{M}(k) \le 0.05$, where $\mathrm{M}_t(k)$ is the neutral curve constructed within the framework of the viscous heat-conducting fluid model ($\alpha = 0$). The calculations show that allowance for buoyancy forces leads to noticeable

Table 8.3: Minimal values of Marangoni numbers vs. Weber number.

We	M_{*1}	M_{*2}	M_{*3}	M_{*4}	M_{*5}
10^2	74.3	209.8	361.3	8032	9825.6
10^6	74.6	–	373.4	8165.6	9831.7

differences in the Marangoni numbers (more than 5 %) at $\gamma = 8 \cdot 10^5$. The relative error of finding the critical Marangoni number decreases with decreasing γ.

In studying fluid compressibility, the criterion is the relation $\min_k |\mathrm{M}(k) - \mathrm{M}_b(k)|/\mathrm{M}(k) \le 0.05$, where $\mathrm{M}_b(k)$ is the neutral curve constructed within the framework of the Oberbeck–Boussinesq model ($\alpha = 0$ and $\Gamma \neq 0$). The calculations are performed for $\gamma = 10^4$, $\mathrm{Pr} = 5.41 \cdot 10^{-3}$, and $\mathrm{We} = 10^4$. It is demonstrated that allowance for compressibility begins playing a noticeable role at $\alpha > 2 \cdot 10^{-4}$. Here, the relative error again decreases with decreasing α.

8.4 Stability of a steady flow in a vertical layer

1. Main steady motion

We consider the solution of system (4.49)–(4.51) in a vertical layer $-a < x < a$, $-\infty < y < \infty$, $-\infty < z < \infty$ with solid walls $x = \pm a$. The boundary conditions are written as

$$\mathbf{w} + \beta\chi\nabla\theta = 0, \quad \theta = \theta_w(\mathbf{x}, t). \tag{8.89}$$

The first condition is the no-slip condition $\mathbf{u} = 0$ on the motionless solid wall. The second condition defines the temperatures on the walls. We assume that the walls $x = -a$ and $x = a$ are heated to the temperatures θ_1 and θ_2, respectively. Without loss of generality, we assume that $\theta_1 > \theta_2$.

The steady solution of the posed problem is sought in the form

$$\begin{gathered} \mathbf{w} = (u_0, v(x), 0), \quad \theta = \theta_0 - u_0 x/\beta\chi, \quad q = (\varphi - g)y, \\ u_0 = \beta\chi(\theta_1 - \theta_2)/2a, \quad \theta_0 = (\theta_1 + \theta_2)/2, \end{gathered} \tag{8.90}$$

where u_0, θ_0, and φ are constants ($l_* = a$). Interpreting solution (8.90) as a solution that approximately describes convection in the central region of a finite closed cavity, which is still rather long as compared with its width $2a$, we impose the condition of a zero mass flow rate of the fluid through all cross sections of the cavity $y = \mathrm{const}$ onto this solution. As $\varrho = \varrho_1(1 + \beta\theta)^{-1}$, we obtain

$$\int_{-a}^{a} \frac{v(x)}{1 + \beta\theta(x)}\, dx = 0. \tag{8.91}$$

For eqs. (8.90), the true velocity vector is $\mathbf{u} = \mathbf{w} + \beta\chi\nabla\theta = (0, v(x), 0)$, i. e., the motion occurs along the y axis. Solution (8.90) can also be interpreted as a steady flow in a vertical slot with given identical heat fluxes on the solid walls: $\theta_x = -u_0/\beta\chi \equiv -d/k$, where k is the thermal conductivity coefficient and d is the heat flux; therefore, we have $u_0 = \beta\chi d/k$.

Thus, convective circulation occurs: the fluid moves upward near the heated wall $x = -a$ and downward near the cold wall $x = a$. The flow consists of two opposing

convective fluxes; the temperature varies in accordance with the formula

$$\theta = \theta_0 - \theta_* x/a, \quad \theta_* = (\theta_1 - \theta_2)/2. \tag{8.92}$$

Substituting eqs. (8.90) into eqs. (4.49)–(4.51), we can present the function $v(x)$ as

$$v = \frac{1}{\nu}\left\{(\varphi - g)\frac{x^2}{2} + c_1 x + c_2 + \frac{g\chi^2}{u_0^2}(1+\beta\theta)[\ln(1+\beta\theta) - 1]\right\},$$

where the constants c_1, c_2, and φ are determined from the no-slip conditions (8.89) and conditions of a closed flow (8.91)

In what follows, we perform comparisons with the results obtained for the Oberbeck–Boussinesq model in the same situation [8, pp. 301, 302]. It was assumed there that $\theta_2 = -\theta_1$; therefore, $\theta_0 = 0$, and $\theta_* = \theta_1$. Thus, below we have $\theta = -\theta_* x/a = -\theta_1 x/a$.

We use χ/a as the dimensionless velocity and denote the Boussinesq parameter by $\varepsilon = \beta\theta_* = \beta\theta_1$. After certain calculations, we obtain ($x \leftrightarrow x/a$ is the dimensionless variable)

$$v = \frac{\chi}{a}\bar{v}(x) = \frac{\chi}{2a}\,\mathrm{Ra}\left\{\frac{1}{\varepsilon^2}f_3(\varepsilon)(1-x^2) + \frac{1}{\varepsilon^3}[f_1(\varepsilon)x - f_2(\varepsilon) + 2(1-\varepsilon x)(\ln(1-\varepsilon x) - 1)]\right\}; \tag{8.93}$$

$$\begin{aligned} \mathrm{Ra} &= g\beta\theta_1 a^3/\nu\chi = \varepsilon\eta; \\ f_1(\varepsilon) &= (1+\varepsilon)\ln(1+\varepsilon) - (1-\varepsilon)\ln(1-\varepsilon) - 2\varepsilon, \\ f_2(\varepsilon) &= (1+\varepsilon)\ln(1+\varepsilon) + (1-\varepsilon)\ln(1-\varepsilon) - 2, \\ f_3(\varepsilon) &= \frac{4\varepsilon^2 - (1-\varepsilon^2)[\ln(1-\varepsilon) - \ln(1+\varepsilon)]^2}{2\varepsilon + (1-\varepsilon^2)[\ln(1-\varepsilon) - \ln(1+\varepsilon)]}. \end{aligned} \tag{8.94}$$

Here, Ra is the Rayleigh number.

Using eqs. (8.94) for $f_1(\varepsilon)$, $f_2(\varepsilon)$, and $f_3(\varepsilon)$, we can show that

$$v(x) = \frac{\chi\,\mathrm{Ra}}{6a}\left(x^3 - x + O(\varepsilon)\right) = v_b(x) + \frac{\chi\,\mathrm{Ra}}{6a}O(\varepsilon), \tag{8.95}$$

if the Rayleigh number remains finite as $\varepsilon \to 0$. In eq. (8.95), $v_b(x)$ is the velocity along the layer in the Oberbeck–Boussinesq model, i. e., solution (8.90) with $\varepsilon \to 0$ approximates the known solution ([68], p. 302)

$$v_b = \frac{\chi\,\mathrm{Ra}}{6a}(x^3 - x), \quad p = \bar{p} - \rho_1 g a y, \quad y \leftrightarrow \frac{y}{a}, \quad \theta = -\theta_1 x, \tag{8.96}$$

where $\bar{p} = \mathrm{const}$ is the excess of pressure above the hydrostatic value. The velocity profile $v(x)$ (8.93) is not an odd function in terms of x, in contrast to the classical velocity $v_b(x)$ from eqs. (8.96) (see Figure 8.11).

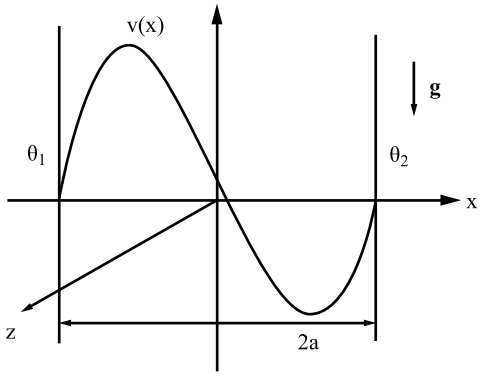

Figure 8.11: Flow pattern: θ_1 and θ_2 are the temperatures on the walls $x = -a$ and $x = a$, respectively; $v(x)$ is the vertical velocity profile. The vector $\mathbf{g}$ has the coordinates $(0, -g, 0)$.

If the parameter η is not too large, then both the velocity profile (8.93) and $v_b(x)$ tend to zero as $\varepsilon \to 0$, i. e., to the equilibrium state in the viscous heat-conducting fluid model:

$$\begin{aligned} &\mathbf{u} \equiv \mathbf{w} = 0, \\ &p = \bar{p} - \rho_1 g a y, \\ &\theta = -\theta_1 x. \end{aligned} \tag{8.97}$$

The flow described by eq. (8.90) is accompanied by convective heat transfer along the layer, and the flux of this heat per unit length along the y axis is

$$Q = \rho_1 c_p \int_{-a}^{a} v(x')\theta(x')\,dx' = -\frac{1}{2}\rho_1 c_p \theta_1 \chi \,\mathrm{Ra} \int_{-1}^{1} \bar{v}(x) x\,dx = \frac{1}{2}\rho_1 c_p \theta_1 \chi \,\mathrm{Ra}\, F(\varepsilon),$$

$$F(\varepsilon) = -\frac{1}{3\varepsilon^3}\left[\left(1 - \frac{1}{\varepsilon^2}\right)\ln\left(\frac{1-\varepsilon}{1+\varepsilon}\right) + \frac{2\varepsilon}{3} - \frac{2}{\varepsilon}\right],$$

where $\bar{v}(x)$ is determined by eq. (8.93), and c_p is the specific heat at constant pressure. We can verify that $F(\varepsilon) \to 4/45$ as $\varepsilon \to 0$; therefore, we have $Q \to Q_b = 2\rho_1 c_p \theta_1 \chi \mathrm{R}/45$ [68].

2. Equations of small perturbations

Let $\mathbf{W} = (U, V)$, T, and Q be perturbations of the main motion (8.90), (8.92). We use the equations of small perturbations (8.17), bearing in mind that $u = u_0 = \mathrm{const}$, $v = v(x)$, $w = 0$, and $q_y = \varphi - g$. We obtain the system of equations

$$\begin{aligned} &U_t + u_0 U_x + vU_y - \beta\chi v_x T_y + \beta^2\chi^2\theta_x T_{yy} = (1+\beta\theta)(-Q_x + v\Delta U), \\ &V_t + u_0 V_x + vV_y + v_x U + \beta\chi[\theta_x(V_x - U_y) + v_x T_x] - \beta^2\chi^2\theta_x T_{xy} \\ &\qquad = (1+\beta\theta)(-Q_y + v\Delta V) + \beta T(g - \varphi + \nu v_{xx}); \end{aligned} \tag{8.98}$$

$$\begin{gathered} U_x + V_y = 0, \\ T_t + u_0 T_x + vT_y + \theta_x U + 2\beta\chi\theta_x T_x = (1+\beta\theta)\chi\Delta T, \\ -a < x < a, \quad -\infty < y < \infty, \\ \mathbf{W} + \beta\chi\nabla T = 0, \quad T = 0, \quad |x| = a. \end{gathered} \tag{8.99}$$

We introduce the dimensionless variables

$$\begin{gathered} t' = \frac{t\chi}{a^2}, \quad \mathbf{x}' = \frac{\mathbf{x}}{a}, \quad \mathbf{W}' = \frac{\mathbf{W}a}{\chi}, \quad T' = \frac{T}{\theta_*} \\ Q' = \frac{Qa^2}{v\chi}, \quad \bar\theta = \frac{\theta}{\theta_*}, \quad \bar v = \frac{va}{\chi}. \end{gathered} \tag{8.100}$$

Substituting eqs. (8.100) into eqs. (8.98), (8.99) and omitting the primes, we obtain the problem

$$\begin{gathered} U_t + \varepsilon U_x + \bar v U_y - \varepsilon\bar v_x T_y + \varepsilon^2\bar\theta_x T_{yy} = (1+\varepsilon\bar\theta)(-Q_x + \Delta U)\,\mathrm{Pr}, \\ V_t + \varepsilon V_x + \bar v V_y + \bar v_x U + \varepsilon\left[\bar\theta_x(V_x - U_y) + \bar v_x T_x\right] - \varepsilon^2\bar\theta_x T_{xy}(1+\varepsilon\bar\theta)(-Q_y + \Delta V)\,\mathrm{Pr} + \frac{\mathrm{Gr}T}{1+\varepsilon\bar\theta}; \end{gathered}$$

$$U_x + V_y = 0, \tag{8.101}$$

$$\begin{gathered} T_t + \varepsilon T_x + \bar v T_y + \bar\theta_x U + 2\varepsilon\bar\theta_x T_x = (1+\varepsilon\bar\theta)\Delta T, \\ -1 < x < 1, \quad -\infty < y < \infty, \quad -\infty < z < \infty, \\ \mathbf{W} + \varepsilon\nabla T = 0, \quad T = 0, \quad |x| = 1, \\ \varepsilon = \beta\theta_*, \quad \mathrm{Pr} = v/\chi, \quad \mathrm{Gr} = \beta\theta_* g a^3/\chi^2 = \varepsilon\eta\,\mathrm{Pr}, \quad \eta = a^3 g/v\chi, \end{gathered} \tag{8.102}$$

where ε is the Boussinesq parameter, Pr is the Prandtl number, Gr is the Grashof number, and η is the microconvection parameter. In transforming system (8.98), we take into account formula (8.90) for u_0 and the relation $vv_{xx} - \varphi + g = g/(1+\beta\theta)$. As it follows from eq. (8.92) that $\bar\theta = \theta_0/\theta_* - x$ in the dimensionless variables, we obtain $\bar\theta_x = -1$.

We seek the solution of the boundary-value problem (8.101)–(8.102) in the form of normal waves

$$(\mathbf{W}, Q, T) = \left(\mathbf{W}(x), Q(x), T(x)\right)\exp\left[i(\alpha y - Ct)\right], \tag{8.103}$$

where α is the wave number along the y axis and C is the complex decrement. Substitution of eq. (8.103) into eqs. (8.101)–(8.102) yields the spectral problem

$$\begin{gathered} \left[i(\alpha\bar v - C) + (1+\varepsilon\bar\theta)\alpha^2\,\mathrm{Pr}\right]U + \varepsilon U' + \left(\varepsilon^2\alpha^2 - \varepsilon\alpha i\bar v_x\right)T = (1+\varepsilon\bar\theta)\,\mathrm{Pr}(-Q' + U''), \\ \left[i(\alpha\bar v - C) + (1+\varepsilon\bar\theta)\alpha^2\,\mathrm{Pr}\right]V + (\bar v_x + \varepsilon i\alpha)U + \left(\varepsilon\bar v_x + \varepsilon^2 i\alpha\right)T' \\ = (1+\varepsilon\bar\theta)\left(V'' - i\alpha Q\right)\mathrm{Pr} + \frac{\mathrm{Gr}T}{1+\varepsilon\bar\theta}; \end{gathered} \tag{8.104}$$

$$\begin{gathered} U' + i\alpha V = 0, \\ \left[i(\alpha\bar v - C) + \alpha^2(1+\varepsilon\bar\theta)\right]T - \varepsilon T' - U = (1+\varepsilon\bar\theta)T'', \quad -1 < x < 1, \\ U + \varepsilon T' = 0, \quad V = 0, \quad T = 0, \quad |x| = 1. \end{gathered} \tag{8.105}$$

3. Long-wave perturbations

Taking into account the mass conservation law, we assume that

$$U = \alpha U_0 + \alpha^2 U_1 + \cdots, \quad V = V_0 + \alpha V_1 + \cdots, \quad Q = Q_0 + \alpha Q_1 + \cdots,$$
$$T = \alpha T_0 + \alpha^2 T_1 + \cdots, \quad C = C_0 + \alpha C_1 + \cdots. \tag{8.106}$$

Substitution into the first equation of system (8.104) yields $Q_0 = \text{const}$. Without loss of generality, we can assume that $Q_0 = 0$. The remaining functions of the zeroth approximation satisfy the boundary-value problem

$$U_0' + iV_0 = 0, \quad -iC_0 V_0 = (1 + \varepsilon\bar{\theta})\,\mathrm{Pr}\, V_0''; \tag{8.107}$$
$$-iC_0 T_0 - \varepsilon T_0' - U_0 = (1 + \varepsilon\bar{\theta}) T_0'', \quad -1 < x < 1;$$
$$T_0 = V_0 = 0, \quad U_0 + \varepsilon T_0' = 0, \quad |x| = 1. \tag{8.108}$$

It is seen from eqs. (8.107) that C_0 is found by solving the problem

$$V_0'' + \frac{iC_0}{\mathrm{Pr}(1 + \varepsilon\bar{\theta})} V_0 = 0, \quad V_0(\pm 1) = 0. \tag{8.109}$$

Obviously, C_0 is purely imaginary, $C_0 = iC_{0i}$:

$$C_{0i} = -\frac{\mathrm{Pr}\,\varepsilon^2 \tau_n^2}{4(1 + \varepsilon)} < 0, \quad n \in N, \tag{8.110}$$

where τ_n is the root of the equation

$$J_1(\tau) Y_1(\lambda_0 \tau) - J_1(\lambda_0 \tau) Y_1(\tau) = 0, \quad \lambda_0 = \sqrt{\frac{1 - \varepsilon}{1 + \varepsilon}}. \tag{8.111}$$

Equation (8.111) has a countable number of real roots. As $C_{0i} < 0$, long-wave perturbations decay monotonically.

The equations of the first approximation are

$$-C_0 U_0 + \varepsilon U_0' = \mathrm{Pr}(1 + \varepsilon\bar{\theta})(U_0'' - Q_1'),$$
$$V_1'' + \frac{iC_0}{\mathrm{Pr}(1 + \bar{\theta}\varepsilon)} V_1 = \frac{1}{\mathrm{Pr}(1 + \varepsilon\bar{\theta})} \left[i(\bar{v} - C_1) V_0 + \bar{v}'(U_0 + \varepsilon T_0') - \frac{\mathrm{Gr} T_0}{1 + \varepsilon\bar{\theta}} \right]; \tag{8.112}$$
$$(1 + \varepsilon\bar{\theta}) T_1'' + iC_0 T_1 + \varepsilon T_1' = i(\bar{v} - C_1) T_0 - U_1, \quad -1 < x < 1,$$
$$V_1 = T_1 = 0, \quad U_1 + \varepsilon T_1 = 0, \quad x = \pm 1. \tag{8.113}$$

Therefore, the first correction to the complex decrement is determined from the condition of solvability of the boundary-value problem for the function V_1:

$$iC_1 = \left\{ i \int_{-1}^{1} \frac{\bar{v} |V_0|^2}{1 + \varepsilon\bar{\theta}}\, dx + \int_{-1}^{1} \frac{1}{1 + \varepsilon\bar{\theta}} \left[\bar{v}'(U_0 + \varepsilon T_0') - \frac{\mathrm{Gr} T_0}{1 + \varepsilon\bar{\theta}} \right] V_0^*\, dx \right\} \left(\int_{-1}^{1} \frac{|V_0|^2}{1 + \varepsilon\bar{\theta}}\, dx \right)^{-1} \tag{8.114}$$

(V_0^* is the complex-conjugate solution of the homogeneous problem (8.109)).

In particular, for the Oberbeck–Boussinesq model ($\varepsilon = 0$, $\mathrm{Gr} > 0$), with allowance for the boundary conditions (8.108), we obtain

$$U_0 = \frac{ia}{\mu}\left[\cos\mu(x+1) - 1\right], \quad V_0 = a\sin\mu(x+1), \quad Q_0 = 0; \tag{8.115}$$

$$a = \mathrm{const}, \quad \mu = n\pi, \quad iC_0 = \mathrm{Pr}\, n^2\pi^2, \quad n \in N; \tag{8.116}$$

$$\mathrm{Pr} \neq 1: \quad T_0 = \frac{ia}{\mu^3}\left[\frac{1}{\mathrm{Pr}} + \frac{\cos\mu(x+1)}{1-\mathrm{Pr}} - \frac{2\,\mathrm{tg}(\mu\sqrt{\mathrm{Pr}})\sin(x+1)}{\mathrm{Pr}(1-\mathrm{Pr})} - \frac{2\cos(\mu\sqrt{\mathrm{Pr}})(x+1)}{\mathrm{Pr}(1-\mathrm{Pr})}\right]; \tag{8.117}$$

$$\mathrm{Pr} = 1: \quad T_0 = \frac{ia}{2\mu^2}\left[\frac{2}{\mu} - (x+1)\sin\mu(x+1) - \frac{2}{\mu}\cos\mu(x+1)\right]. \tag{8.118}$$

Substitution of eqs. (8.115)–(8.118) into eq. (8.114) yields the following presentation for iC_1 (let us recall that $\bar{v}_b = \mathrm{R}(x^3 - x)/6$):

$$\mathrm{Pr} \neq 1: \quad C_1 = -\frac{2\mathrm{Gr}}{\mu^4\,\mathrm{Pr}(1-\mathrm{Pr})^2}\left[\frac{\cos(2\mu\sqrt{\mathrm{Pr}})\cos\mu(2+\sqrt{\mathrm{Pr}})}{\cos(\mu\sqrt{\mathrm{Pr}})} + 2\sqrt{\mathrm{Pr}}\sin(\mu\sqrt{\mathrm{Pr}})\cos\mu(2+\sqrt{\mathrm{Pr}}) - 1\right], \quad \mu = n\pi, \quad n \in N; \tag{8.119}$$

$$\mathrm{Pr} = 1: \quad C_1 = \frac{\mathrm{Gr}}{2\mu^2}. \tag{8.120}$$

Thus, as $\alpha \to 0$, we have

$$C = -i\,\mathrm{Pr}\,\mu^2 + \alpha C_1, \tag{8.121}$$

where C_1 is determined by eqs. (8.119) and (8.120), respectively.

4. Numerical solution of the eigenvalue problem

To find the numerical solution by the method of orthogonalization [75], we convert system (8.104) to the form $\mathbf{y}' = A\mathbf{y}$, where $\mathbf{y}(\xi)$ is the vector of unknowns and $A(\xi)$ is the matrix of coefficients, $0 \le \xi \le 1$. For this purpose, we make the replacement

$$\begin{aligned} &\xi = x/2 + 1/2, \quad y_1 = V, \quad y_2 = V', \quad y_3 = V'', \\ &y_4 = U, \qquad\quad y_5 = T, \quad y_6 = T'. \end{aligned} \tag{8.122}$$

Eliminating Q from eqs. (8.104), we obtain the following system of equations:

$$y_1' = y_2, \quad y_2' = y_3, \quad y_4' = -2i\alpha y_1, \quad y_5' = y_6,$$

$$y_3' = (8i\alpha h_1 + 8\alpha^2 h_4)y_1 + (4i\alpha h_2 + 4\alpha^2)y_2 + \left(8i\alpha h_3 - \frac{8i\alpha h_6}{1+\varepsilon\bar{\theta}}\right)y_4$$

$$+\left\{8i\alpha h_6\left[\frac{i(\alpha\bar v - C)}{1+\varepsilon\bar\theta}+\alpha^2\right]-8i\alpha h_7\right\}y_5+\left(4i\alpha h_5-\frac{4i\alpha h_6\varepsilon}{1+\varepsilon\bar\theta}\right)y_6,$$

$$y_6' = -\frac{4}{1+\varepsilon\bar\theta}\,y_4+4\left[\frac{i(\alpha\bar v - C)}{1+\varepsilon\bar\theta}+\alpha^2\right]y_5-\frac{2\varepsilon}{1+\varepsilon\bar\theta}\,y_6,$$

$$h_1=\frac{\alpha\bar v_\xi(1+\varepsilon\bar\theta)+(\alpha\bar v - C)\varepsilon\bar\theta_\xi}{\mathrm{Pr}\,\alpha(1+\varepsilon\bar\theta)^2},\quad h_2=\frac{(\alpha\bar v - C)}{\mathrm{Pr}\,\alpha(1+\varepsilon\bar\theta)}-i\alpha,$$

$$h_3=-\frac{i\bar v_{\xi\xi}(1+\varepsilon\bar\theta)-i\bar v_\xi\varepsilon\bar\theta_\xi}{\mathrm{Pr}\,\alpha(1+\varepsilon\bar\theta)^2}-\frac{\varepsilon^2\bar\theta_\xi}{\mathrm{Pr}(1+\varepsilon\bar\theta)^2}-\frac{i(\alpha\bar v - C)}{\mathrm{Pr}(1+\varepsilon\bar\theta)}-\alpha^2,$$

$$h_4=-\frac{i\bar v_\xi}{\mathrm{Pr}\,\alpha(1+\varepsilon\bar\theta)},\tag{8.123}$$

$$h_5=-\frac{\varepsilon i\bar v_{\xi\xi}(1+\varepsilon\bar\theta)-\varepsilon^2 i\bar v_\xi\bar\theta_\xi}{\mathrm{Pr}\,\alpha(1+\varepsilon\bar\theta)^2}-\frac{\varepsilon^3\bar\theta_\xi}{\mathrm{Pr}(1+\varepsilon\bar\theta)^2}+\frac{i\mathrm{R}}{\alpha(1+\varepsilon\bar\theta)^2},$$

$$h_6=-\frac{\varepsilon i\bar v_\xi}{\mathrm{Pr}\,\alpha(1+\varepsilon\bar\theta)}+\frac{\varepsilon^2}{\mathrm{Pr}(1+\varepsilon\bar\theta)},\quad h_7=\frac{\varepsilon^2\alpha^2-\varepsilon\alpha i\bar v_\xi}{\mathrm{Pr}(1+\varepsilon\bar\theta)}+\frac{2i\mathrm{R}\varepsilon\bar\theta_\xi}{\alpha(1+\varepsilon\bar\theta)^3},$$

$$\bar\theta=\bar\theta(\xi)=\frac{\theta_0}{\theta_*}-(2\xi-1),\quad \bar\theta_\xi=-1,$$

$$\bar v=\bar v(\xi)=\frac{\mathrm{R}}{2}\left\{\frac{1}{\varepsilon^2}f_3(\varepsilon)\big(-4\xi^2+4\xi\big)+\frac{1}{\varepsilon^3}\left[f_1(\varepsilon)(2\xi-1)-f_2(\varepsilon)\right.\right.$$

$$\left.\left.+2\big(1-\varepsilon(2\xi-1)\big)\big(\ln\big(1-\varepsilon(2\xi-1)\big)-1\big)\right]\right\},$$

$$\bar v_\xi=\mathrm{R}\left\{-\frac{2}{\varepsilon^2}f_3(\varepsilon)(2\xi-1)+\frac{1}{\varepsilon^3}\big[f_1(\varepsilon)-2\varepsilon\ln\big(1-\varepsilon(2\xi-1)\big)\big]\right\},$$

$$\bar v_{\xi\xi}=\mathrm{R}\left\{-\frac{4}{\varepsilon^2}f_3(\varepsilon)+\frac{4}{\varepsilon(1-\varepsilon(2\xi-1))}\right\}\tag{8.124}$$

($f_1(\varepsilon), f_2(\varepsilon)$, and $f_3(\varepsilon)$ are determined from eqs. (8.94)). By virtue of replacement (8.122), the boundary conditions (8.105) take the form

$$y_1=0,\quad y_4+\varepsilon y_6=0,\quad y_5=0\quad(\xi=0,\ \xi=1).\tag{8.125}$$

Thus, we solve a system of the form $\mathbf{y}' = A(\xi)\mathbf{y}$ with the boundary conditions specified at $\xi = 0$ and $\xi = 1$, $B\mathbf{y}(0) = 0$ and $D\mathbf{y}(1) = 0$, respectively. The matrices B and D of dimension 3×6 coincide, and their elements have the following values: $b_{11} = d_{11} = b_{24} = d_{24} = b_{35} = d_{35} = 1$, $b_{26} = d_{26} = \varepsilon$, while the remaining elements of both matrices are equal to zero.

The solution is sought in the form

$$\mathbf{y}=\sum_{j=1}^{3}p_j\mathbf{y}^j,\tag{8.126}$$

where the coefficients p_j are found from the system $D\mathbf{y}(1) = 0$, and $\mathbf{y}^1, \mathbf{y}^2$, and $\mathbf{y}^3$ are linearly independent vectors, such that $\mathbf{y}^1(0) = (0, 0, 0, -\varepsilon, 0, 1)$, $\mathbf{y}^2(0) = (0, 1, 0, 0, 0, 0)$, and $\mathbf{y}^3(0) = (0, 0, 1, 0, 0, 0)$.

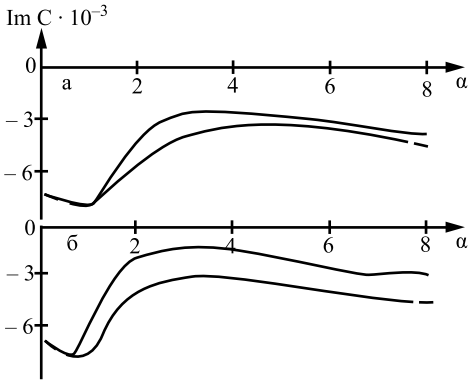

Figure 8.12: Imaginary part of the complex decrement Im C versus the wave number α: a) $\Delta\theta = 10\,°C$; b) $\Delta\theta = 100\,°C$.

To find the eigenvalue C, we have to use two initial approximations C_0 and C_1, which are chosen from conditions (8.110) and (8.119).

We study stability of the layer with the solid walls for the silicon melt SiO_3. The following parameters values are used: $\nu = 2.65 \cdot 10^{-3}$, $\chi = 0.49$, $\beta = 0.75 \cdot 10^{-5}$, and $\mathrm{Pr} = 5.41 \cdot 10^{-3}$. The calculations are performed for the absolute value of the difference in the wall temperatures $|\theta_1 - \theta_2|$ equal to 10 and 100 degrees. This means that variation of the dimensionless parameter $\varepsilon = \beta|\theta_1 - \theta_2|/2$. The linear size of the layer is chosen to satisfy the inequality $\eta = (2a)^3 g/\nu\chi < 1$, which is the criterion of applicability of the microconvection model considered [176]. The smallness of the parameter η can be ensured by decreasing both the length scale and the acceleration due to gravity g (e. g., under microgravity conditions, with g of the order of 10^{-2}–$10^{-3} g_0$, where $g_0 = 981\,\mathrm{cm/s^2}$ is the acceleration due to gravity near the Earth's surface). In these calculations, we consider $g \sim 10^{-3} g_0$, i. e., $2l < 0.11\,\mathrm{cm}$. For the values of a, β, χ, and ν given above, we find the dependence of the imaginary (Im C) and real (Re C) parts on the wave number α.

Figure 8.12 shows the curves Im $C(\alpha)$ for different values of ε and a. The results are presented for $a = 0.025\,\mathrm{cm}$ (dashed curve) and $a = 0.05\,\mathrm{cm}$ (solid curve) for the wall temperature differences $\Delta\theta = 10\,°C$ ($\varepsilon = 3.75 \cdot 10^{-5}$) and $\Delta\theta = 100\,°C$ ($\varepsilon = 3.75 \cdot 10^{-4}$) (Figures 8.12a and b, respectively). The slower variation of the curves Im $C(\alpha)$ corresponding to smaller values of the characteristic size a allows us to speak of a stabilizing effect of viscosity. The values of Re C for the indicated values of the parameters do not exceed 10^{-12}. Thus, for all values of α, we have Im $C < 0$, i. e., the motion is stable. We compared the results of solving the Oberbeck–Boussinesq problem with the numerical solution of the spectral problem (8.104) for the case where the Grashof number $\mathrm{Gr} = \varepsilon\eta\,\mathrm{Pr}$ is finite at $\varepsilon \ll 1$. The calculations are performed for the silicon melt with the same physical parameters and $\theta_2 - \theta_1 = 100\,°C$ (see Figure 8.13).

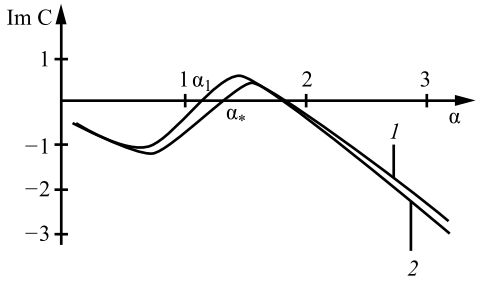

Figure 8.13: Complex decrement Im C vs. the wave number α: curves 1 and 2 refer to the microconvection model ($\alpha_1 = 1.14$) and the Oberbeck–Boussinesq model ($\alpha_* = 1.34$), respectively.

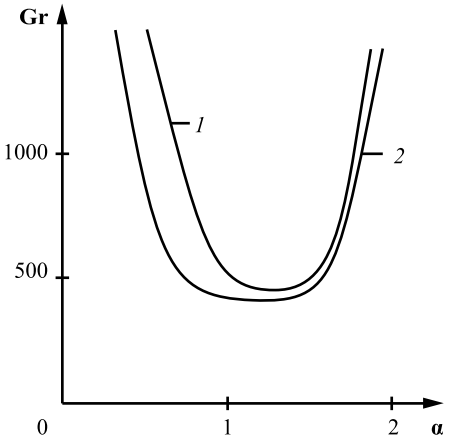

Figure 8.14: Neutral curves for the Oberbeck–Boussinesq model (1) and for the microconvection model (2).

As η increases, the curve Im C approaches the axis Im $C = 0$ and crosses this axis for the first time at $\alpha = \alpha_1 = 1.14$, and $\eta_1 = 2.32409 \cdot 10^8$. At $\alpha_1 < \alpha < 1.80 = \alpha_2$, the curve Im C takes positive values, then vanishes again at the point α_2, and decreases with increasing α. In this case, the Grashof number is $\mathrm{Gr}_1 = \varepsilon\eta_1 \mathrm{Pr} = 471.34 < \mathrm{Gr}_*$, where $\mathrm{Gr}_* = 495.6$ (at $\alpha_* = 1.34$) is the critical Grashof number for the classical problem ([68], p. 321). The layer thickness in this case is $2a = 33.7$ cm for $g = 10^{-3} g_0$. Thus, the motion becomes unstable in the microconvection model at smaller wave numbers, which is apparently attributed to nonsolenoidity of the velocity field.

We also compare the neutral curves (Figure 8.14). Note that the minimum of curve 2 (let us denote it by Gr_{1*}) is shifted to the left along the α axis, i. e., instability occurs at smaller wave numbers, which is also related to nonsolenoidity of the velocity field.

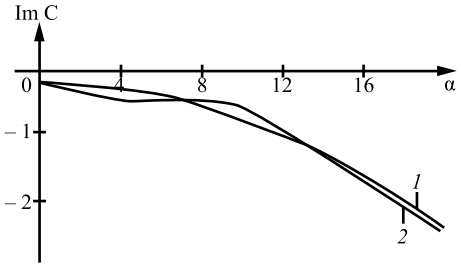

Figure 8.15: Dependences of Im C vs. wave number α at $\varepsilon = 0$ (curve 1) and $\varepsilon = 10^{-7}$ (curve 2).

It was shown in Section 8.1 that solutions (8.93) and (8.96) at $\varepsilon \to 0$ both approximate the equilibrium state of the layer (8.97) of a viscous heat-conducting fluid. Therefore, it seems of interest to study stability of the quiescent state (8.97). For this purpose, it is sufficient to set $\varepsilon = 0$ and $\mathrm{Gr} = 0$ in problem (8.104), (8.105). We obtain the problem

$$(-iC + \alpha^2 \,\mathrm{Pr})U = \mathrm{Pr}(U'' - Q'), \quad U' + i\alpha V = 0,$$
$$(-iC + \alpha^2 \,\mathrm{Pr})V = \mathrm{Pr}(V'' - i\alpha Q); \tag{8.127}$$
$$(-iC + \alpha^2)T - U = T'', \quad -1 < x < 1,$$
$$U = V = T = 0, \quad |x| = 1. \tag{8.128}$$

This spectral problem can be solved in the explicit form. The conclusion about stability of the equilibrium state (8.97) can be easily made on the basis of the integral identity valid for problem (8.127), (8.128):

$$\left(\alpha^2 - \frac{iC}{\mathrm{Pr}}\right) \int_{-1}^{1} (\alpha^2 |U|^2 + |V|^2)\, dx + \int_{-1}^{1} (\alpha^2 |U'|^2 + |V'|^2)\, dx = 0,$$

whence it follows that $-iC$ is real and $-iC < 0$, which means stability.

Figure 8.15 shows the complex decrement $\mathrm{Im}\, C$ as a function of the wave number α. Thus, the spectrum of the problem of stability in the microconvection model approximates the corresponding spectrum for the viscous heat-conducting fluid model. Curve 1 is obtained analytically for a viscous heat-conducting fluid ($\varepsilon = 0$), and curve 2 is obtained by means of numerical integration for the microconvection model ($\varepsilon = 10^{-7}$).

The results of studying stability of the flow in the vertical layer in the microconvection model differ from the results for a similar flow in the classical Oberbeck–Boussinesq model. Here we always have oscillatory perturbations. If the Boussinesq parameter tends to zero ($\varepsilon \to 0$) and the microconvection parameter η is of the order of unity, the flow is always stable. In this case, it is similar to the equilibrium state in the viscous heat-conducting fluid model, which is always stable, as demonstrated above.

At large values of η and $R = \varepsilon\eta \to R_0 < \infty$, as $\varepsilon \to 0$, the values of the decay decrements (or growth increments) of perturbations are close to the corresponding values of $\operatorname{Im} C$ calculated for the Oberbeck–Boussinesq model.

The neutral curves are constructed, and the critical Grashof number Gr_{1*} is found; it turns out that $Gr_{1*} < Gr_*$, where Gr_* is the critical Grashof number for the Oberbeck–Boussinesq model.

9 Numerical simulation of convective flows under microgravity conditions

Heat and mass transfer phenomena in engineering and processing refer to the most important forms of affecting the process medium in those applications where convection should be taken into account. By studying velocity fields arising in various devices, one can effectively take into account the temperature and species transport phenomena and determine the necessary actions on the medium. One direction where convection is studied in order to minimize its action on the production cycle is space material science.

Note that the processes considered in this case occur under specific conditions characterized by weak fields of mass forces and extremely low velocities of the flow (about 1 μm/s). In such situations, the influence of buoyancy forces becomes commensurable with or much smaller than those forces that are usually neglected under standard on-ground conditions. The range of problems to be studied is fairly wide, owing to the existence of alternative fluid models that adequately describe the fluid state under microgravity conditions and mechanisms of convective flow formation that differ from buoyancy forces. The role of numerical simulations of these processes is particularly important, because they allow the most complete modeling of physical experiments, which cannot be performed under on-ground conditions, while real experiments in space laboratories are extremely expensive.

In this chapter, we consider some problems, numerical methods used to solve them, and basic results.

9.1 Numerical methods used for calculations

The numerical methods of fluid flow calculations described in this chapter refer primarily to the microconvection model.

Governing equations

Let the physical system to be considered be an isotropic Newtonian fluid consisting of two nonreacting species located in an external force field.

Let $\mathbf{x} = (x_1, x_2, x_3) \in \mathbf{R}^3$ be the Cartesian coordinates, $\varrho_k(\mathbf{x}, t)$ be the mass density (i. e., the mass of a unit volume) of the species k ($k = 1, 2$) at a point $\mathbf{x}$ at a time t, and $\mathbf{v}_k(\mathbf{x}, t)$ be the velocity of the species k. The state of the system is describes by the field of total density $\varrho(\mathbf{x}, t)$, velocity of the center of mass of the fluid element $\mathbf{v}(\mathbf{x}, t) = (v_1, v_2, v_3)$, pressure $p^* = p^*(\mathbf{x}, t)$, absolute temperature $\theta(\mathbf{x}, t)$, and concentration of mass of one species $c(\mathbf{x}, t)$:

$$\varrho = \varrho_1 + \varrho_2, \quad \mathbf{v} = \frac{\varrho_1 \mathbf{v}_1 + \varrho_2 \mathbf{v}_2}{\varrho}, \quad c = \frac{\varrho_1}{\varrho}.$$

https://doi.org/10.1515/9783110655469-009

The species concentrations and temperature of the mixture are assumed to change weakly, and all physical properties of the mixture except for density are assumed to be constant. The heat flux and the diffusion flux of the substance are linear functions of ∇c and $\nabla\theta$, and the coefficients in these expressions are constant. In particular, the density of the diffusion flux of the substance $\mathbf{J}_c$ is $\mathbf{J}_c = -k_c(\nabla c - \alpha\nabla\theta)$, where the constant coefficients k_c and α characterize the diffusion and thermodiffusion (thus, k_c/ϱ is the coefficient of molecular diffusion). These assumptions allow us to consider the basic properties and mechanisms of the influence of volume expansion of the medium on formation of extremely weak convection in a simple and clear formulation.

Microconvective flows characterized by velocities of the order of 10 μm/s and smaller can be described by the model of essentially subsonic flows with arbitrary variations of density. This model is the limiting case of the full system of Navier–Stokes and heat-transfer equations with the Mach number and the parameter characterizing hydrostatic compressibility tending to zero [120, 44].

In the subsonic flow approximation, the total pressure is presented as a sum of the spatially uniform thermodynamic component $P(t)$ and a component that takes into account the dynamic and hydrostatic effects $p(\mathbf{x}, t)$; the latter is eliminated from the state equation, thus ensuring "filtration" of acoustics. Our analysis is restricted to situations in which the thermodynamic pressure P is constant, which corresponds to an isothermally incompressible fluid. This situation is observed in some typical cases: if the domain occupied by the fluid is open to the atmosphere, or if the total normal heat flux through impermeable solid walls of a closed reservoir is equal to zero (in particular, if the system is insulated). Under the assumptions made above, the system of equations has the form [120]

$$\begin{gathered}\frac{d\varrho}{dt} + \varrho\,\mathrm{div}\,\mathbf{v} = 0, \quad \varrho\frac{d\mathbf{v}}{dt} = -\nabla p' + \mu\,\mathrm{div}\,\mathbf{D} + (\varrho - \varrho_0)g\mathbf{e}_3,\\ \varrho\frac{dc}{dt} = k_c(\Delta c + \alpha\Delta\theta), \quad \varrho c_p\frac{d\theta}{dt} = k(\Delta\theta + \alpha'\Delta c),\\ \varrho = \varrho(\theta, c), \quad p' = p - \varrho_0 g\mathbf{e}_3\cdot\mathbf{x},\\ D_{ij} = \left(\frac{\partial v_i}{\partial x_j} + \frac{\partial v_j}{\partial x_i} - \frac{2}{3}\,\delta_{ij}\,\mathrm{div}\,\mathbf{v}\right).\end{gathered} \tag{9.1}$$

Here, the coefficient k_c characterizes molecular diffusion, α and α' characterize thermodiffusion and the Dufour effect, respectively, $\mathbf{e}_3$ is the unit vector co-directed with the vector of acceleration due to external mass forces, $\mathbf{D}$ is the Cartesian tensor with the components D_{ij}, and δ_{ij} is the unit tensor. The volume viscosity is assumed to be equal to zero.

The state equation is chosen in the form of a linear dependence of the specific volume of the fluid on variations of temperatures and concentrations of the chemical species

$$\varrho = \varrho_0(1 + \beta T + \gamma C)^{-1}, \quad T = \theta - \theta_0, \quad C = c - c_0, \tag{9.2}$$

where θ_0 and c_0 are certain mean values of the temperature and concentration, ϱ_0 is the mean density of the mixture, and β and γ are the constant temperature and concentration coefficients of density.

As a result, the equations of convection of a nonisothermal binary mixture take the form

$$\begin{aligned}
&\operatorname{div}\mathbf{v} = (\beta\chi + \gamma\delta\alpha)\Delta T + (\gamma\delta + \beta\chi\alpha')\Delta C,\\
&\frac{d\mathbf{v}}{dt} = (1 + \beta T + \gamma C)\{-\nabla p''/\varrho_0 + \nu\Delta\mathbf{v}\} - \mathbf{g}(\beta T + \gamma C),\\
&\frac{dC}{dt} = \delta(1 + \beta T + \gamma C)(\Delta C + \alpha\Delta T),\\
&\frac{dT}{dt} = \chi(1 + \beta T + \gamma C)(\Delta T + \alpha'\Delta C),
\end{aligned} \tag{9.3}$$

where $p'' = p - \varrho_0 g\mathbf{l}\cdot x - (\mu/3)\operatorname{div}\mathbf{v}$, $\chi = k/(\varrho_0 c_p)$ is the thermal diffusivity, $\delta = k_c/\varrho_0$ is the diffusion coefficient, and $\nu = \mu/\varrho_0$ is the kinematic coefficient of viscosity.

System (9.2), (9.3) corresponds to the microconvection model (MM) for a single-species fluid [177, 176] (see also [161]) derived from the axioms of mechanics of continuous media by means of a priori assumptions. The MM extends the classical Boussinesq model, which is usually used to describe natural convection.

Numerical methods

In plane cases, the methods of the numerical solution of system (9.2), (9.3) can be conventionally divided into two main groups. The first group involves the stream function ψ and vorticity ω, and the original system of equations is transformed to a system in the variables (ψ, ω). The second group includes methods based on using numerical procedures of calculations in natural variables: velocity and pressure. The basic information on numerical methods can be found in [120, 160, 219, 195, 56, 5, 206, 79, 80, 82, 83, 78, 90, 220]. Numerical methods applicable to flows with the fluid considered in the Oberbeck–Boussinesq model were described in detail in [160, 219, 195, 56, 5, 206].

Let us consider the use of these numerical methods by an example of studying convection in a rectangular domain $0 \le x \le l$, $0 \le y \le h$ bounded by solid walls impermeable for the substance, with no-slip conditions for velocity.

It should be noted that the use of the MM requires the integral heat flux normal to the domain boundary to be equal to zero [177]. Therefore, the heat fluxes on the domain boundaries have to be known in problems considered in the MM approximation. In the general case, the heat flux functions can depend on spatial coordinates and also on time. For certainty, we assume that the vertical boundaries are thermally insulated, and a periodic heat flux is prescribed on the horizontal boundaries.

The boundary conditions for species concentrations are determined by using the expression for the diffusion flux of the substance $\mathbf{J}$. We also assume that $\alpha' = 0$ (the

Dufour effect is ignored). In this case, the boundary conditions can be presented as

$$\begin{aligned} y = 0, l: &\quad \mathbf{v} = 0, \quad T_x = 0, \quad C_x = 0; \\ y = 0, h: &\quad \mathbf{v} = 0, \quad T_y = \Theta\cos(\Omega' t), \quad C_y = -\alpha\Theta\cos(\Omega' t). \end{aligned} \tag{9.4}$$

For numerical simulations in the variables (ψ, ω), we introduce a solenoidal vector field (modified velocity) $\mathbf{w}$ and modified pressure q:

$$\mathbf{w} = (w_1, w_2) = \mathbf{v} - (\beta\chi + \gamma\delta\alpha)\nabla T - \gamma\delta\nabla C; \tag{9.5}$$

$$q = \frac{p''}{\varrho_0} - (\beta\chi + \gamma\delta\alpha)(\nu - \chi)\Delta T - \gamma\delta(\nu - \delta)\Delta C. \tag{9.6}$$

Equations (9.2), (9.3) are written in the variables T (temperature), C (concentration), ω (vorticity), and ψ (stream function) for the field $\mathbf{w}$ as

$$\omega = w_{2x} - w_{1y}, \quad \frac{\partial\psi}{\partial y} = w_1, \quad \frac{\partial\psi}{\partial x} = -w_2.$$

The scale factor for temperature is assumed to be $T_* = \Theta h$. The scale factors for length, velocity, time, modified pressure, and concentration are

$$h, \quad \frac{\chi}{h}, \quad \frac{h^2}{\chi}, \quad \varrho_0\frac{\nu\chi}{h^2}, \quad \frac{\beta}{\gamma}T_*. \tag{9.7}$$

As a result, system (9.2), (9.3) in the dimensionless variables takes the form ($0 \le x \le A$, $0 \le y \le 1$)

$$\Delta\psi = -\omega; \tag{9.8}$$

$$\omega_t + w_1\omega_x + w_2\omega_y = K_\omega\Delta\omega + F_\omega; \tag{9.9}$$

$$C_t + w_1 C_x + w_2 C_y = K_C(\Delta C - s\Delta T) + F_C; \tag{9.10}$$

$$T_t + w_1 T_x + w_2 T_y = K_T\Delta T + F_T; \tag{9.11}$$

$$\begin{aligned} K_\omega &= \mathrm{Pr}(1 + \varepsilon T + \varepsilon C), \quad K_C = \mathrm{Le}(1 + \varepsilon T + \varepsilon C), \quad K_T = (1 + \varepsilon T + \varepsilon C); \\ F_\omega = &-\varepsilon(1 - s\,\mathrm{Le})\{\omega\Delta T + \nabla\omega\cdot\nabla T\} - \varepsilon\,\mathrm{Le}\{\omega\Delta C + \nabla\omega\cdot\nabla C\} \\ &-(\varepsilon - \varepsilon s\,\mathrm{Le})^2\{T_y\Delta T_x - T_x\Delta T_y\} - (\varepsilon\,\mathrm{Le})^2\{C_y\Delta C_x - C_x\Delta C_y\} \\ &-\varepsilon(\varepsilon - \varepsilon s\,\mathrm{Le})\{(C_y\Delta T_x - C_x\Delta T_y) + \mathrm{Le}^2(T_y\Delta C_x - T_x\Delta C_y)\} \\ &+\varepsilon\eta\,\mathrm{Pr}\{l_1 T_y - l_2 T_x\} + \varepsilon\eta\,\mathrm{Pr}\{l_1 C_y - l_2 C_x\} + \varepsilon\,\mathrm{Pr}\{q_x(T_y + C_y) \\ &-q_y(T_x + C_x) + \Delta w_2(T_x + C_x) - \Delta w_1(T_y + C_y)\}; \end{aligned}$$

$$\begin{aligned} F_C &= -\varepsilon\,\mathrm{Le}|\nabla C|^2 - \varepsilon(1 - s\,\mathrm{Le})(\nabla C\cdot\nabla T), \\ F_T &= -\varepsilon(1 - s\,\mathrm{Le})|\nabla T|^2 - \varepsilon\,\mathrm{Le}(\nabla C\cdot\nabla T), \end{aligned}$$

where $A = l/h$ is the aspect ratio, the components of the normalized vector of acceleration due to external forces $\mathbf{e}_3$ are denoted by e_1 and e_2, $\varepsilon = \beta T_*$ is the Boussinesq parameter, $\eta = gh^3/(\nu\chi)$ is the microconvection parameter, $\mathrm{Pr} = \nu/\chi$ is the Prandtl number, $\mathrm{Le} = \delta/\chi$ is the Lewis number, and $s = -\alpha\gamma/\beta$ is the separation ratio.

The approach that involves the vorticity ω and the stream function ψ has the advantage that there is no need to ensure solenoidity of the modified velocity vector, because this condition is satisfied automatically. There are some difficulties, however, in imposing the boundary condition for vorticity on the boundary subjected to no-slip conditions, which is absent in the physical formulation of the problem.

There are many numerical methods for solving system (9.8)–(9.11). These methods differ in the choice of the difference scheme, type of the boundary conditions, and method used to solve Poisson's equation. Specific features of the numerical solution of convective flow problems as applied to the microconvection model that involves the stream function and vorticity variables were considered in [79, 78] for both rectangular geometry and for problems in annular domains with the use of cylindrical coordinates. The majority of algorithms have separate procedures for solving eqs. (9.8)–(9.9) and (9.10)–(9.11). This way of arrangement of calculations is also called the two-field method ([220]).

When the modified velocity $\mathbf{w}$, its stream function ψ, and vorticity ω are used, it is necessary to impose new boundary conditions absent in the physical formulation of the problem. Equation (9.5) defines the components of the modified velocity on the boundary:

$$w_1 = -\varepsilon(1 - s\,\mathrm{Le})T_x - \varepsilon\,\mathrm{Le}C_x, \quad w_2 = \varepsilon(1 - s\,\mathrm{Le})T_y + \varepsilon\,\mathrm{Le}C_y. \tag{9.12}$$

Then the stream function is found by integrating the function (9.12) along the corresponding boundary. Thus, for the domain boundary $y = \mathrm{const}$, the stream function is determined by the equation

$$\psi = \int_{x=0}^{x=l} w_2\,dx.$$

Taking into account the boundary conditions (9.4), we obtain

$$\psi = x\varepsilon\cos(\Omega t), \tag{9.13}$$

where Ω is the dimensionless frequency of heat flux oscillations.

The vorticity on the domain boundary is determined by using the boundary conditions for the tangential component of velocity. Note that this condition is actually an approximate equivalent of the usual no-slip condition. A conventional approach to deriving the boundary condition for vorticity is expanding into a Taylor series along the normal to the boundary. As an example, let us consider the condition for vorticity on

the boundary $y = 0$. Assuming that Δy is small and that all necessary derivatives exist, we expand the stream function at point 1 (point 1 is located at a distance Δy along the y axis from point 0 located on the domain boundary) into the Taylor series:

$$\psi_1 \approx \psi_0 + \Delta y\left(\frac{\partial \psi}{\partial y}\right)_0 + \frac{\Delta y^2}{2}\left(\frac{\partial^2 \psi}{\partial y^2}\right)_0. \tag{9.14}$$

The first derivative of the stream function in eq. (9.14) is determined from eq. (9.12):

$$\left(\frac{\partial \psi}{\partial y}\right)_0 = -\varepsilon(1 - s\,\mathrm{Le})T_x - \varepsilon\,\mathrm{Le}\,C_x. \tag{9.15}$$

Writing Poisson's equation for the stream function, we find (taking into account eq. (9.13) for calculating ψ_{xx})

$$\omega_0 = -\left(\frac{\partial^2 \psi}{\partial x^2}\right)_0 - \left(\frac{\partial^2 \psi}{\partial y^2}\right)_0 = -\left(\frac{\partial^2 \psi}{\partial y^2}\right)_0. \tag{9.16}$$

Substituting eqs. (9.15) and (9.16) into eq. (9.14), we obtain the Thom formula for calculating the vorticity on the domain boundary:

$$\omega_0 = -\frac{2}{\Delta y^2}\left[\psi_1 - \psi_0 + \Delta y(\varepsilon(1 - s\,\mathrm{Le})T_x + \varepsilon\,\mathrm{Le}\,C_x)\right].$$

The Tom formula has the first order of accuracy. Considering the next terms of the series in the Taylor expansion (9.14), we find the expressions for the second order of accuracy (e. g., the Woods formulas [80]). The properties of these and other boundary conditions were studied in [90, 220] for the fluid model in the Boussinesq approximation. Particular attention should be paid to calculating the vorticity on the boundary, because this procedure exerts a considerable effect on computational process stability.

Performing generalization for the problem considered, we can write the boundary conditions in the form

$$\begin{gathered}
x = 0: \quad \psi = 0, \quad \psi_x = \varepsilon(1 - s\,\mathrm{Le})T_y + \varepsilon\,\mathrm{Le}\,C_y, \quad T_x = 0, \quad C_x = 0; \\
x = A: \quad \psi = A\varepsilon\cos(\Omega t), \quad \psi_x = \varepsilon(1 - s\,\mathrm{Le})T_y + \varepsilon\,\mathrm{Le}\,C_y, \quad T_x = 0, \quad C_x = 0; \\
y = 0, 1: \quad \psi = x\varepsilon\cos(\Omega t), \quad \psi_y = -\varepsilon(1 - s\,\mathrm{Le})T_x - \varepsilon\,\mathrm{Le}\,C_x, \\
T_y = \cos(\Omega t), \quad C_y = s\cos(\Omega t).
\end{gathered} \tag{9.17}$$

Let us perform a numerical study of problem (9.8)–(9.11), (9.17), using the approach developed in [80]. Integration is performed by using a class of two-layer implicit difference schemes of the method of alternating directions, which formally has the second order of approximation.

Performing discretization in time with a constant time step τ, we seek for the solution of the system of equations at each time step $t^n = n\tau$, where $n = 1, 2, \ldots$ is the

ordinal number of the time layer. For eqs. (9.9)–(9.11), the calculation scheme is written in the general form as

$$\begin{aligned}\frac{\Phi^{n+1/2}-\Phi^{n}}{\tau/2} &= [\tilde{K}\Phi_x - w_1\Phi]_x^n + [\tilde{K}\Phi_y - w_2\Phi]_y^{n+1/2} + \bar{F}^n,\\ \frac{\Phi^{n+1}-\Phi^{n+1/2}}{\tau/2} &= [\tilde{K}\Phi_x - w_1\Phi]_x^{n+1} + [\tilde{K}\Phi_y - w_2\Phi]_y^{n+1/2} + \bar{F}^n,\end{aligned} \tag{9.18}$$

if $\Phi = \omega$, then $\bar{F} = F_\omega - \varepsilon\,\mathrm{Pr}(\nabla T\cdot\nabla\omega + \nabla C\cdot\nabla\omega)$, $\tilde{K} = K_\omega^n$;
if $\Phi = C$, then $\bar{F} = F_C - \varepsilon\,\mathrm{Le}(\nabla T\cdot\nabla C + |\nabla C|^2) - K_C s\Delta T$, $\tilde{K} = K_C^n$;
finally, if $\Phi = T$, then $\bar{F} = F_T - \varepsilon(\nabla T\cdot\nabla C + |\nabla T|^2)$, $\tilde{K} = K_T^n$.

To solve eq. (9.8), we use the following iterative scheme at each time step t^n:

$$\begin{aligned}\frac{\psi^{m+1/2}-\psi^{m}}{\tau/2} &= \tilde{\lambda}[\psi_{xx}^{m+1/2} + \psi_{yy}^{m} + \omega^{n+1}],\\ \frac{\psi^{m+1}-\psi^{m+1/2}}{\tau/2} &= \tilde{\lambda}[\psi_{xx}^{m+1/2} + \psi_{yy}^{m+1} + \omega^{n+1}]\end{aligned} \tag{9.19}$$

($\tilde{\lambda}$ is the iteration parameter, the choice of which affects the rate of convergence of the iterative process).

For approximating the spatial variables involved into the system of equations, we introduce a grid with the coordinates

$$\begin{aligned}x_i &= (i-1)\Delta x, \quad i = 1,2,\ldots,I; \quad \Delta x = \frac{A}{I-1};\\ y_j &= (j-1)\Delta y, \quad j = 1,2,\ldots,J; \quad \Delta y = \frac{1}{J-1}.\end{aligned}$$

The values of the variables at the point with the coordinates (x_i, y_j) at the time t^n are denoted by $\Phi(t^n, x_i, y_j) = \Phi^n{}_{i,j}$. The spatial derivatives inside the computational domain are approximated during the expansion into the Taylor series by central finite-difference analogs with the second order of accuracy. For example, we have

$$\frac{\partial\Phi}{\partial x} \approx \frac{\Phi_{i+1,j}-\Phi_{i-1,j}}{2\Delta x}, \quad \frac{\partial^2\Phi}{\partial x^2} \approx \frac{\Phi_{i+1,j}-2\Phi_{i,j}+\Phi_{i-1,j}}{\Delta x^2}.$$

Nevertheless, the method of approximation is determined to a large extent by specific features of calculations as well as by the properties of solutions.

Particular attention should be paid to the use of methods of approximations on the computational domain boundary and on their implementation in the computational algorithm. Asymmetric second-order approximations are usually used for this purpose. By calculating the derivatives at the computational domain boundary $y = 0$, we obtain the expressions

$$\left.\frac{\partial\Phi}{\partial x}\right|_{y=0} \approx \frac{-3\Phi_{1,j}+4\Phi_{2,j}-\Phi_{3,j}}{2\Delta x},$$

$$\left.\frac{\partial^2\Phi}{\partial x^2}\right|_{y=0} \approx \frac{-7\Phi_{1,j} + 8\Phi_{2,j} - \Phi_{i,j}}{2\Delta x^2} - \left.\frac{3}{\Delta x}\,\Phi_x\right|_{y=0}.$$

The use of three-point finite-difference approximation of spatial variables leads to a system of linear algebraic equations obtained from eqs. (9.18)–(9.19), which can be presented in the form

$$\begin{aligned} -A^y_{i,j}\Phi^{n+1/2}_{i,j-1} + B^y_{i,j}\Phi^{n+1/2}_{i,j} - C^y_{i,j}\Phi^{n+1/2}_{i,j+1} = D^y_{i,j}, \quad i = 2,\dots,I-1; \\ -A^x_{i,j}\Phi^{n+1}_{i-1,j} + B^x_{i,j}\Phi^{n+1}_{i,j} - C^x_{i,j}\Phi^{n+1}_{i+1,j} = D^x_{i,j}, \quad j = 2,\dots,J-1, \end{aligned}$$

and are solved by the method of consecutive elimination of unknowns with the use of sweeping procedures [205].

The full computational procedure of the transition to the new time layer t^{n+1} is arranged as follows.

1. The transition to the new time layer t^{n+1} begins from calculating the temperature T^{n+1} and concentration C^{n+1} from eqs. (9.10)–(9.11) and the difference scheme (9.18). The values of the modified velocity $\mathbf{w}$ corresponding to the time layer t^n are used in convective terms.

2. Based on the resultant values of T^{n+1} and C^{n+1}, F_ω is calculated. In order to determine the values of q_x and q_y involved into F_ω, we use the momentum conservation equation for the modified velocity, where all values are taken from the time layer t^n (for the sake of simplicity, the superscript n is omitted):

$$\begin{aligned} &\mathbf{w}_t + \mathbf{w}\cdot\nabla\mathbf{w} + \varepsilon(1 - s\,\mathrm{Le})\{\nabla T\cdot\nabla\mathbf{w} - \nabla\mathbf{w}\cdot\nabla T\} + \varepsilon\,\mathrm{Le}\{\nabla C\cdot\nabla\mathbf{w} - \nabla\mathbf{w}\cdot\nabla C\} \\ &\quad + (\varepsilon - \varepsilon s\,\mathrm{Le})^2\left\{\Delta T\nabla T - \frac{1}{2}\nabla|\nabla T|^2\right\} + (\varepsilon\,\mathrm{Le})^2\left\{\Delta C\nabla C - \frac{1}{2}\nabla|\nabla C|^2\right\} \\ &\quad + \varepsilon(\varepsilon - \varepsilon s\,\mathrm{Le})\{\Delta T\nabla C + \mathrm{Le}^2\Delta\nabla T - \mathrm{Le}\,\nabla(\nabla T\cdot\nabla C)\} \\ &\qquad = \varepsilon\eta\,\mathrm{Pr}(T + C) + (1 + \varepsilon T + \varepsilon C)\,\mathrm{Pr}(-\nabla q + \Delta\mathbf{w}). \end{aligned}$$

3. Based on the solution of eq. (9.9) and the difference scheme (9.18), the vorticity ω^{n+1} is found. The values of ψ^n are used in the boundary conditions for ω^{n+1}.

4. To solve eq. (9.8), an internal iterative process of calculating ψ^{m+1} using the difference scheme (9.19) is used. After the iterations are finalized at $m = M$, the values of ψ on the time layer $n+1$ are assumed to be determined with prescribed accuracy ε_ψ: $\psi^{n+1} = \psi^M$. The iterative process is assumed to converge if the convergence criterion

$$\max_{i,j}|\psi^{m+1}_{i,j} - \psi^m_{i,j}| < \varepsilon^{\mathrm{rel}}_\psi \max_{i,j}|\psi^{m+1}_{i,j}|$$

or

$$\max_{i,j}|\psi_{i,j}^{m+1} - \psi_{i,j}^{m}| < \varepsilon_{\psi}^{\text{abs}}$$

(or some other criteria [219, 195, 56, 5, 206]) is satisfied. Here, m is the iteration number; $\varepsilon_{\psi}^{\text{abs}}$ and $\varepsilon_{\psi}^{\text{rel}}$ are the prescribed absolute and relative errors of calculating ψ^{m+1}.

5. The accuracy of satisfying the boundary conditions for the vorticity ε_{ω} is determined. For instance, for the horizontal boundary of the computational domain, we obtain

$$\varepsilon_{\omega} = \max_{i}|\omega_{i,1}(\psi_{i,2}^{n+1}) - \omega_{i,1}(\psi_{i,2}^{n})|.$$

If the prescribed accuracy of calculating ε_{ω} is not reached, the procedure returns to step 3. Otherwise, satisfaction of the prescribed condition means the end of calculating the parameters on the time layer t^{n+1}.

Let us now consider the main procedures of calculating convective flows of a weakly compressible fluid with the use of the "natural" variables of velocity and pressure. System (9.1), with allowance for eqs. (9.7), can be presented as

$$\begin{gathered}
\operatorname{div}\mathbf{v} = \varepsilon(1 - s\,\mathrm{Le})\Delta T + \varepsilon\,\mathrm{Le}\,\Delta C, \\
\mathbf{v}_t + \mathbf{v}\cdot\nabla\mathbf{v} = (1 + \varepsilon T + \varepsilon C)\,\mathrm{Pr}\{-\nabla p + \operatorname{div}\mathbf{D}\} + \varepsilon\eta\,\mathrm{Pr}\,\mathbf{l}\,(T + C), \\
C_t + \mathbf{v}\cdot\nabla C = (1 + \varepsilon T + \varepsilon C)\,\mathrm{Le}(\Delta C - s\Delta T), \\
T_t + \mathbf{v}\cdot\nabla T = (1 + \varepsilon T + \varepsilon C)\Delta T.
\end{gathered} \tag{9.20}$$

The main difficulty in numerical simulations with the use of the "natural" variables is to develop a method of determining the pressure that would ensure sufficiently effective satisfaction of the continuity equation. One possible approach for pressure calculations is the procedure that involves solving Poisson's equation. This method is most frequently used in studying incompressible fluid flows. For this class of problems, the method of markers and cells (MAC method) [94], which was further developed as the SMAC method [3], and their modification [96] were developed and are successfully used. In particular, instead of solving Poisson's equation, it was proposed [96] to use an iterative procedure for determining pressure, which is equivalent to solving Poisson's equation for pressure by the over-relaxation method. In [120], the use of the SMAC method was considered for essentially subsonic flows. As applied to convective flows within the framework of the microconvection model, this method was used in [63].

It should be noted that numerical methods with the use of $(p, \mathbf{v})$ offer appreciable advantages over computational procedures based on the variables (ψ, ω): the major advantages are the simplicity of imposing the boundary conditions and the possibility of calculating three-dimensional flows.

The calculation of the parameters on the time layer t^{n+1} consists of the following stages.

1. The initial velocity $\mathbf{v}_1^{n+1}$ is calculated, which is further used in the iterative procedure as the initial value:

$$\mathbf{v}_1^{n+1} = \mathbf{v}^n + \tau[-\mathbf{v}^n \cdot \nabla \mathbf{v}_1^{n+1} - (1 + \varepsilon T^n + \varepsilon C^n) \operatorname{Pr} \nabla p^n + (1 + \varepsilon T^n + \varepsilon C^n) \operatorname{div} \mathbf{D}_1^{n+1} + \varepsilon \eta \operatorname{Pr} \mathbf{l} (T^n + C^n)].$$

2. The pressure p and refined velocity $\mathbf{v}$ are calculated by the following iterative procedure (m is the iteration number):

$$p_m^{n+1} = p_{m-1}^{n+1} - \gamma^n(\nabla \mathbf{v}_m^{n+1} - \varepsilon(1 - s \operatorname{Le})\Delta T^n - \varepsilon \operatorname{Le} \Delta C^n),$$
$$\mathbf{v}_{m+1}^{n+1} = \mathbf{v}_m^{n+1} - \tau(1 + \varepsilon T^n + \varepsilon C^n) \operatorname{Pr}(\nabla p_m^{n+1} - \nabla p_{m-1}^{n+1}).$$

The iterations are repeated until the inequality $|p_m^{n+1} - p_{m-1}^{n+1}| < \varepsilon_p$ is satisfied (ε_p is the prescribed calculation accuracy). The initial value of pressure for the iterations is $p_1^{n+1} = p^n$. The parameter γ responsible for the rate of process convergence is

$$\gamma^n = \frac{1}{\tau \operatorname{Pr}(1 + \varepsilon T^n + \varepsilon C^n)} \left(\frac{2}{\Delta x^2} + \frac{2}{\Delta y^2} \right)^{-1}.$$

When the iterative procedure is finished, the velocity v and pressure p on the time layer t^{n+1} are assumed to be finally determined.

3. The temperature and concentration on the new time layer are found from the equations

$$T^{n+1} = T^n - \tau \mathbf{v}^{n+1} \cdot \nabla T^{n+1} + \tau(1 + \varepsilon T^n + \varepsilon T^n)\Delta T^{n+1},$$
$$C^{n+1} = C^n - \tau \mathbf{v}^{n+1} \cdot \nabla C^{n+1} + \tau(1 + \varepsilon T^n + \varepsilon C^n) \operatorname{Le}(\Delta C^{n+1} - s\Delta T^{k+1}).$$

The computational procedure for calculating the initial velocity $\mathbf{v}_1^{n+1}$ as well as the temperature T^{n+1} and concentration C^{n+1} involve the class of two-layer implicit difference schemes of the method of alternating directions; as a whole, they are similar to those used for calculating equations in the variables (ψ, ω). A specific feature of the method considered here, however, is the use of the MAC grid [94], which leads to some specific features of the spatial approximation of the equations. A fragment of the MAC grid is shown in Figure 9.1. The MAC grid consists of a system including the basic nodes with the coordinates x_i, y_j and two types of auxiliary nodes: $x_{i+1/2}, y_j$ and $x_i, y_{j+1/2}$, which are shifted with respect to the system of the basic nodes by one half of the grid step in the x and y directions, respectively. The functions of pressure, temperature, and concentration are determined in the nodes of the basic grid.

The auxiliary grids are introduced for the corresponding projections of the velocity vector on the coordinate axes: shifted along the x axis for the horizontal component v_1 and shifted along the y axis for the component v_2 (see Figure 9.1, where the velocity vector components are indicated by $\mathbf{v}(\mathbf{x}, t) = (u, v)$; the same notation is used below

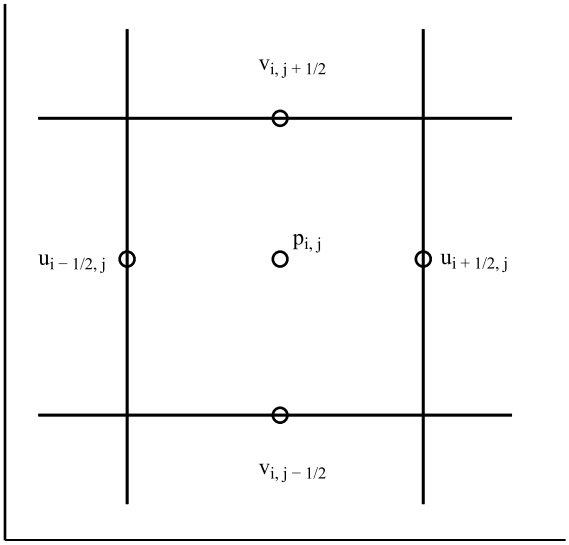

Figure 9.1: Fragment of the MAC grid.

when analyzing the realization of the spatial derivatives and boundary conditions for velocity).

The coordinates of the basic grid are determined by the equations

$$x_i = (i - 1/2)\Delta x, \quad i = 1, 2, \ldots, I; \quad \Delta x = \frac{A}{I};$$
$$y_j = (j - 1/2)\Delta y, \quad j = 1, 2, \ldots, J; \quad \Delta y = \frac{1}{J}.$$

The grid is arranged so that the auxiliary nodes of the first and last lines coincide with the corresponding boundaries of the computational domain.

If the MAC grid is used inside the computational domain, the spatial derivatives are approximated in a standard manner by central differences with the second order of accuracy. The major advantage of using the MAC grid is the use of a smaller grid space in calculating the first derivatives of velocity:

$$\frac{\partial u}{\partial x} \approx \frac{u_{i+1/2,j} - u_{i-1/2,j}}{\Delta x}, \quad \frac{\partial v}{\partial y} \approx \frac{v_{i,j+1/2} - v_{i,j-1/2}}{\Delta y}.$$

The velocity components at the cell center are approximated as

$$u_{i,j} \approx 0.5(u_{i+1/2,j} + u_{i-1/2,j}), \quad v_{i,j} \approx 0.5(v_{i,j+1/2} + v_{i,j-1/2}).$$

A specific feature of using the MAC grid is also observed in approximating the derivatives at the domain boundary, where “dummy” cells outside the computational grid

are used. The heat flux on the domain boundary is specified for the temperature approximation in the considered problems. Therefore, the temperature in the "dummy" cells is determined by the relation $T_{0,j} = T_{1,j} - f\Delta x$, where f is the heat flux specified on the boundary.

In calculating the values in the "dummy" cells, we use the known values of the velocity components on the domain boundaries. For instance, let us determine the values of $u_{i+1/2,0}$ along the horizontal boundaries by using the no-slip condition:

$$u_{i+1/2,1/2} = 0 = (u_{i+1/2,1} + u_{i+1/2,0})/2 \quad \text{or} \quad u_{i+1/2,0} = -u_{i+1/2,1}.$$

These methods and procedures of studying problems of fluid motion in the approximation of the microconvection model as well as their details and specific features are not the only possible and exhaustive ones. For example, such problems can also be solved by using a numerical method with the variables $(\mathbf{w}, q)$, based on the SMAC method [3] for an incompressible fluid.

9.2 Numerical study of unsteady microconvection in canonical domains with solid boundaries

Unsteady regimes of convection under microgravity conditions are studied in domains shaped as a ring and as a rectangle extended in the gravity force direction.

The domain boundary is solid and impermeable, so that the no-slip condition is satisfied for physical velocity. In the case of annular domains, the acceleration induced by the gravity force produces time-periodic oscillations. Convection in an extended rectangle is studied for the case of thermally insulated short sides of the rectangle and a periodic heat flux through the long sides. The condition of the zero total (integral) heat flux through the domain boundary is satisfied in this case.

Mathematical models of convective flows are based on initial-boundary problems for the classical Oberbeck–Boussinesq equations (3.41)–(3.43) and equations of microconvection of an isothermally incompressible fluid (5.6)–(5.8). The solenoidity of the modified velocity $\mathbf{w}$ in the microconvection model permits an analog of the stream function for plane and axisymmetric problems to be introduced, as in the classical equations. The method of alternating directions is used for the numerical solution of equations written for the stream function and vorticity sought. The calculations are performed for model fluids, such as glycerin, silicon, and glass melts, thus, for different values of the Prandtl, Rayleigh, and Boussinesq numbers, and, simultaneously, in the case where the microconvection parameter is rather small. The temperature fields, calculated by different mathematical models and used as one of the most important characteristics of the convective process, do not exhibit significant differences. At the same time, the influence of the nonsolenoidity of the velocity field in the microconvection model could not fail to manifest itself. The calculations confirm the qualitative and quantitative differences in flow characteristics calculated by the two models

mentioned above. In particular, the values of velocity calculated by the new model can exceed those predicted by the conventional model by three orders of magnitude. Moreover, the flow structure, its topology, time evolution, and trajectories of motion of fluid particles are also different.

To illustrate this, we present figures that show the flow topology: fields of velocities, streamlines, and isotherms. The trajectories of fluid particles are also shown.

1. Unsteady microconvection in an extended rectangle

Unsteady microconvection is studied in a domain $0 \le x \le x_0$, $0 \le y \le y_0$ with solid impermeable boundaries. Two boundaries ($x = 0$ and $x = x_0$) are thermally insulated, and the two remaining boundaries are subjected to the condition of a periodic heat flux. The gravity force is directed along the Ox axis. The classical convection and microconvection equations are considered in the variables ω–ψ (ω is the vorticity and ψ is the stream function or modified stream function). The components of the physical or modified velocity are v_1 and v_2. The system of equations in the variables ψ–ω is written as

$$v_1 = \psi_y, \quad v_2 = -\psi_x,$$

$$\omega_t + v_1\omega_x + v_2\omega_y = \tilde{\nu}\Delta\omega + \beta g T_y + F_\omega, \tag{9.21}$$

$$\Delta\psi = -\omega, \tag{9.22}$$

$$T_t + v_1 T_x + v_2 T_y = \tilde{\chi}\Delta T + F_T. \tag{9.23}$$

The following relations are valid for the microconvection model:

$$\tilde{\nu} = (1 + \beta T)\nu, \quad \tilde{\chi} = (1 + \beta T)\chi,$$

$$F_\omega = \beta(-T_x q_y + T_y q_x) + \nu\beta(\Delta v_2 T_x - \Delta v_1 T_y)$$
$$+ (-\beta\chi)(\omega\,\Delta T + \nabla T \cdot \nabla\omega) + (-\beta^2\chi^2)(\Delta T_x\, T_y - \Delta T_y\, T_x),$$

$$F_T = -\beta\chi|\nabla T|^2.$$

For the Oberbeck–Boussinesq model, we have, respectively,

$$\tilde{\nu} = \nu, \quad \tilde{\chi} = \chi, \quad F_\omega = 0, \quad F_T = 0.$$

The boundary conditions for the microconvection model are formulated in terms of the stream function and have the form

$$x = 0: \quad \psi = 0, \quad \psi_x = \beta\chi T_y, \quad T_x = 0; \tag{9.24}$$

$$x = x_0: \quad \psi = \beta\chi x_0 A\sin\gamma t, \quad \psi_x = \beta\chi T_y, \quad T_x = 0; \tag{9.25}$$

$$y = 0: \quad \psi = \beta\chi x A\sin\gamma t, \quad \psi_y = -\beta\chi T_x, \quad T_y = A\sin\gamma t; \tag{9.26}$$

$$y = 1: \quad \psi = \beta\chi x A\sin\gamma t, \quad \psi_y = -\beta\chi T_x, \quad T_y = A\sin\gamma t. \tag{9.27}$$

The boundary conditions for the Oberbeck–Boussinesq model are

$$x = 0: \quad \psi = 0, \quad \psi_x = 0, \quad T_x = 0; \tag{9.28}$$

$$x = x_0: \quad \psi = 0, \quad \psi_x = 0, \quad T_x = 0; \tag{9.29}$$

$$y = 0: \quad \psi = 0, \quad \psi_y = 0, \quad T_y = A \sin \gamma t; \tag{9.30}$$

$$y = 1: \quad \psi = 0, \quad \psi_y = 0, \quad T_y = A \sin \gamma t. \tag{9.31}$$

The initial conditions for both models are

$$t = 0: \quad \omega = 0, \quad \psi = 0, \quad T = T_0. \tag{9.32}$$

Numerical implementation. Calculation scheme

Problems (9.21)–(9.27), (9.32) and (9.21)–(9.23), (9.28)–(9.32) are numerically studied with the use of a longitudinal-transverse finite-difference scheme, which is also known as the method of alternating directions formally having the second order of approximation [126, 207].

The calculation scheme for eqs. (9.21), (9.23) is written in the general form as

$$\begin{aligned} \frac{\Phi^{k+1/2} - \Phi^k}{0.5\tau} &= [\tilde{v}\Phi_x - \nu_1\Phi]_x^k + [\tilde{v}\Phi_y - \nu_2\Phi]_y^{k+1/2} + \bar{F}^k, \\ \frac{\Phi^{k+1} - \Phi^{k+1/2}}{0.5\tau} &= [\tilde{v}\Phi_x - \nu_1\Phi]_x^{k+1} + [\tilde{v}\Phi_y - \nu_2\Phi]_y^{k+1/2} + \bar{F}^k. \end{aligned} \tag{9.33}$$

For the microconvection model, we have the following variants: if $\Phi = \omega$, then $\bar{F} = \beta g T_y + F_\omega - \beta\nu\nabla T \cdot \nabla\omega$; if $\Phi = T$, then $\bar{F} = F_T - \beta\chi|\nabla T|^2$.

For the Oberbeck–Boussinesq model, we assume the following options: if $\Phi = \omega$, then $\bar{F} = \beta g T_y + F_\omega$; if $\Phi = T$, then $\bar{F} = F_T$.

To solve Poisson's equation (9.22), we use the following iterative scheme at each time step $t_k = k\tau$ ($k = 1, 2, \ldots$):

$$\begin{aligned} \frac{\psi^{s+1/2} - \psi^s}{0.5\tau} &= \tilde{\lambda}[\psi_{xx}^{s+1/2} + \psi_{yy}^s + \omega^{k+1}], \\ \frac{\psi^{s+1} - \psi^{s+1/2}}{0.5\tau} &= \tilde{\lambda}[\psi_{xx}^{s+1/2} + \psi_{yy}^{s+1} + \omega^{k+1}] \end{aligned} \tag{9.34}$$

($\tilde{\lambda}$ is the iteration parameter).

To implement the above-described calculation scheme in a standard manner, we introduce the difference grid

$$\begin{aligned} x_n &= (n-1)h_x, \quad n = 1, 2, \ldots, N_1; \quad h_x = x_0/N, \quad N_1 = N + 1; \\ y_m &= (m-1)h_y, \quad m = 1, 2, \ldots, M_1; \quad h_y = y_0/M, \quad M_1 = M + 1. \end{aligned}$$

We use the notation $\Phi^k_{n,m} = \Phi(t_k, x_n, y_m)$. Then, the systems of linear algebraic equations (9.33), (9.34) are presented as

$$\begin{aligned} -a_{n,m}\Phi^{k+1/2}_{n,m-1} + b_{n,m}\Phi^{k+1/2}_{n,m} - c_{n,m}\Phi^{k+1/2}_{n,m+1} &= d_{n,m}, \quad n = 2,\dots,N; \\ -a_{n,m}\Phi^{k+1}_{n-1,m} + b_{n,m}\Phi^{k+1}_{n,m} - c_{n,m}\Phi^{k+1}_{n+1,m} &= d_{n,m}, \quad m = 2,\dots,M, \end{aligned}$$

and are solved by the sweeping method [205]. The following difference approximation for terms of eqs. (9.33) is used:

$$\begin{aligned} [\tilde{\nu}\Phi_x - \psi_y\Phi]_x \approx \bar{\tilde{\nu}}_{n+1}\frac{\Phi_{n+1,m} - \Phi_{n,m}}{h_x^2} - \bar{\tilde{\nu}}_n\frac{\Phi_{n,m} - \Phi_{n-1,m}}{h_x^2} \\ - \frac{(\psi_y)_{n+1,m}\Phi_{n+1,m} - (\psi_y)_{n-1,m}\Phi_{n-1,m}}{2h_x}, \end{aligned}$$

$$(\bar{\tilde{\nu}})_{n+1,m} = 0.5(\tilde{\nu}_{n+1,m} + \tilde{\nu}_{n,m}).$$

The convective terms on the actual layer are approximated by central differences. The first derivatives involved into $\bar{F}^k$ inside the computational domain are approximated in a standard manner by symmetric finite-difference analogs with the second order of accuracy. The first derivatives on the computational domain boundary are also approximated by asymmetric finite-difference analogs of the second order [205, 207]. For example, we have

$$T_x \approx \frac{1}{2h_x}(4T_{2,m} - T_{3,m} - 3T_{1,m}).$$

For approximation of the boundary conditions for temperature, which define the heat flux (see eqs. (9.28)–(9.31)), it is possible to use additionally the heat-transfer equations (9.23). For instance, the following relation is valid for approximation of the boundary condition for temperature at $y = 0$:

$$\left(1 + \frac{h_y^2}{2\chi\tau/2}\right)T^{k+1/2}_{n,1} = T^{k+1/2}_{n,2} - h_y\, A\sin\gamma t^{k+1/2} + \frac{h_y^2}{2\chi\tau/2}T^k_{n,1}.$$

To impose the boundary conditions for vorticity, we derive conditions of the Thom or Woods type [195]. For the microconvection model, these conditions at $y = 0$ have the form

$$\begin{aligned} \omega^{k+1/2}_{n,1} &= -\frac{2}{h_y^2}(\psi^k_{n,2} - \psi^k_{n,1} + h_y(\beta\chi T^{k+1}_x)), \\ \omega^{k+1/2}_{n,1} + \frac{1}{2}\omega^{k+1/2}_{n,2} &= -\frac{3}{h_y^2}(\psi^k_{n,2} - \psi^k_{n,1} + h_y(\beta\chi T^{k+1}_x)); \end{aligned} \tag{9.35}$$

for the Oberbeck–Boussinesq model, respectively, we have

$$\omega^{k+1/2}_{n,1} = -\frac{2}{h_y^2}\psi^k_{n,2} \quad \text{and} \quad \omega^{k+1/2}_{n,1} + \frac{1}{2}\omega^{k+1/2}_{n,2} = -\frac{3}{h_y^2}\psi^k_{n,2}. \tag{9.36}$$

The general scheme of solving the problem consists of the following stages:

1. The transition to the new time layer t^{k+1} begins with the calculation of the temperature T^{k+1}, and only after that is the vorticity ω^{k+1} found from system (9.33). Sweeping in the y direction is performed on the intermediate layer $(k + 1/2)$, and sweeping in the x direction is performed on the basic layer $(k + 1)$. (The starting values are determined by the initial data $T := T_0 = \text{const}$, $\omega := 0$, $\psi := 0$.)
2. On each time layer k, an internal iterative process of calculating ψ^{s+1} by the system (9.34) with an alternated sequence of sweeping is introduced. After the iterations are finalized at $s = S$, the values of ψ on the time layer $(k + 1)$ $(\psi^{k+1} = \psi^S)$ are assumed to be determined with prescribed accuracy ε_ψ.

The iterative process is assumed to converge if the convergence criterion of the form [195, 219]

$$\max_{n,m}|\psi^{s+1}_{n,m} - \psi^s_{n,m}| < \varepsilon_\psi \max_{n,m}|\psi^{s+1}_{n,m}| \tag{9.37}$$

is satisfied (s is the iteration number and ε_ψ is the prescribed accuracy of calculating ψ^{s+1}).

The accuracy of satisfaction of the boundary conditions for vorticity is determined, for example, for conditions (9.35), (9.36) on the basis of the value of $\bar{\varepsilon}$ [195, 219]:

$$\bar{\varepsilon} = \max_n|\omega_{n,1}(\psi^{k+1}_{n,2}) - \omega_{n,1}(\psi^k_{n,2})|. \tag{9.38}$$

Results of the numerical study of microconvection in an extended rectangle

The calculations are performed on a 200×20 grid for a domain $0 \le x \le x_0$; $0 \le y \le y_0$ at $x_0 = 10$ cm and $y_0 = 1$ cm.

The stability of the algorithm and the order of convergence are checked in a numerical experiment on a sequence of grids ($i = 1$: 200×20, $i = 2$: 400×40, $i = 3$: 800×80; $\varepsilon_\psi = 10^{-4}$); the behavior of the quantity r_i is noted, which characterizes the motion intensity $\max_{n,m}|\psi_{n,m}|$ for each grid with the number i or which is the integral norm $\|\psi\| = \sqrt{\Sigma_{n,m}\psi^2_{n,m}h_x h_y}$. The experimentally determined order of convergence r and the approximately determined relative error ϵ are calculated in the following manner, in accordance with the Runge rule (see, e. g., [48, 103, 152]):

$$r = \frac{\ln(|r_2 - r_1|/|r_3 - r_2|)}{\ln 2}, \quad \epsilon = \frac{1}{1 - (1/2)^r} \cdot \left|\frac{r_1 - r_2}{r_2}\right|. \tag{9.39}$$

If the main quantity being observed is the motion intensity, we obtain $r \approx 1.8$ and $\bar{\epsilon} \approx 3\,\%$ (relative error in percent). If the main quantity being observed is the integral L_2-norm of the stream function, then we have $r \approx 2$ and $\bar{\epsilon} \approx 3\,\%$.

The basic values of parameters in the boundary conditions for temperature are assumed to be identical: $T_0 = 35$, $A = 70$, $\gamma = 2$ or $\gamma = 0.5$. The basic parameters of the

Table 9.1: Basic parameters.

	Pr	Re	η	ε	ν	χ	g	β
$N1$	0.75	0.014	1	0.01	0.15	0.2	0.03	0.0003
$N2$	0.01	2.1	0.4	0.02	0.015	1.5	0.009	0.0006
$N3$	0.1	0.21	0.4	0.02	0.15	1.5	0.09	0.0006
$N4$ (*sil*)	0.0054	0.049	0.77	$2.6 \cdot 10^{-5}$	0.00265	0.49	0.001	$7.5 \cdot 10^{-6}$

problem are listed in Table 9.1 (the dimensional quantities are given in the centimeter–gram–second system [226]).

Thus, the calculations are performed for several model fluids ($N1$, $N2$, $N3$, and $N4$) under the action of microaccelerations reachable on an orbital station, i. e., under the condition of a small value of the parameter η, and for different values of g. The models differ in terms of the Prandtl number Pr and Reynolds number $\mathrm{Re} = v_* l/\nu$. The characteristic velocity is taken to be the characteristic rate of volume expansion $v_* = \varepsilon\chi/l$ ($\varepsilon = \beta T_*$ is the Boussinesq number), and $l = y_0 = 1$. The value $t_* = l/v_*$ can be naturally chosen as the characteristic time of the process. It should be noted that the name "model fluid" is rather conventional. Model $N4$ is the silicon melt, while model $N1$ is air (in accordance with the values of the basic parameters) frequently used for real experiments on convection (see [27]).

The calculations performed using the two alternative models demonstrate convincing differences in the behavior of the trajectories of microconvective motion in an extended rectangle. The trajectories of motion of fluid particles are reconstructed as solutions of the Cauchy problem for the system of ordinary differential equations

$$\frac{dx}{dt} = v_1, \quad \frac{dy}{dt} = v_2; \quad x(0) = \bar{x}, \quad y(0) = \bar{y}. \tag{9.40}$$

The calculations are performed by an improved Euler method with the second order of accuracy [103]. Here, v_1 and v_2 are the components of physical velocity.

Figures 9.2–9.7 show the fluid particle trajectories up to the time instant $t = 240$ s. Figure 9.3 shows the particle trajectories at the time $t = 60$ s. The axes give the x and y values multiplied by 10^4.

Figure 9.2 (model $N3$; initial coordinates $(5; 0.1)$; calculation parameters $\mathrm{Pr} = 0.1$, $\varepsilon = 0.02$, $\eta = 0.4$, and $\gamma = 2$), Figure 9.4 (model $N1$; initial coordinates $(5; 0.6)$; calculation parameters $\mathrm{Pr} = 0.75$, $\varepsilon = 0.01$, $\eta = 1$, and $\gamma = 2$), and Figure 9.5 (model $N4$ (*sil*); initial coordinates $(5; 0.6)$; calculation parameters $\mathrm{Pr} = 0.0054$, $\varepsilon = 0.000026$, $\eta = 0.77$, and $\gamma = 2$) illustrate the qualitative differences in the particle trajectories for models $N1$, $N2$, $N3$, and $N4$; the particles in these calculations were located at the same point at the initial time.

Figure 9.3 (model $N3$; initial coordinates $(5; 0.1)$; calculation parameters $\mathrm{Pr} = 0.1$, $\varepsilon = 0.02$, $\eta = 0.4$, and $\gamma = 2$) shows the trajectories of a particle initially located at the

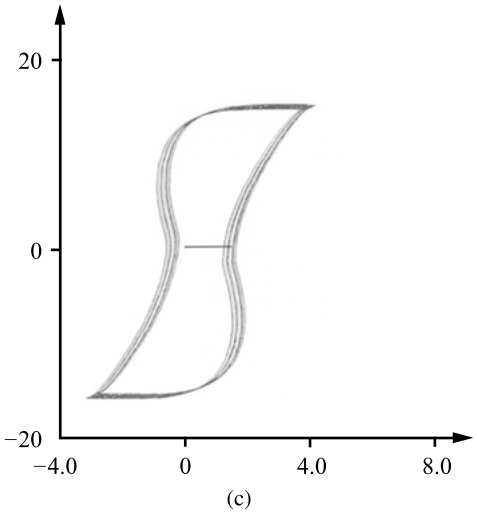

Figure 9.2: Model $N3$; calculation parameters $\mathrm{Pr} = 0.1$, $\varepsilon = 0.02$, and $\eta = 0.4$. Trajectories: $\gamma = 2$; initial coordinates $(5; 0.1)$ (Oberbeck–Boussinesq model: segments of straight lines parallel to Ox).

point $(5; 0.1)$ to illustrate the influence of the amplitude coefficient A in the thermal mode on the boundary: the greater the coefficient A, the more intense the motion.

The trajectories calculated by the Oberbeck–Boussinesq model fill segments of straight lines parallel to Ox; they are shown as bold curves. The trajectories calculated by the microconvection model obviously have a more complicated structure.

Thus, in addition to the differences caused by the use of different mathematical models and to the differences in the behavior of the trajectories as functions of the angular frequency γ and amplitude coefficient A, there are also differences in trajectories of particles initially located at different points: see Figure 9.2 (model $N3$; initial coordinates $(5; 0.1)$; calculation parameters $\mathrm{Pr} = 0.1$, $\varepsilon = 0.02$, $\eta = 0.4$, and $\gamma = 2$), Figure 9.6 (model $N3$; initial coordinates $(9.75; 0.5)$; calculation parameters $\mathrm{Pr} = 0.1$, $\varepsilon = 0.02$, $\eta = 0.4$, and $\gamma = 2$), and Figure 9.7 (model $N3$; initial coordinates $(0.25; 0.1)$; calculation parameters $\mathrm{Pr} = 0.1$, $\varepsilon = 0.02$, $\eta = 0.4$, $\gamma = 2$). For a point located in the vicinity of the thermally insulated short side, Figures 9.6 and 9.7 display qualitatively similar trajectories, but there are significant differences in the amplitudes, which are caused by the difference in the order of velocities, in the direction of motion (see Figure 9.7a) and in the angle of inclination of the curves (see Figure 9.7b).

In addition to the qualitative difference in trajectories predicted by different mathematical models, there are also quantitative differences in velocities. These results are summarized in Table 9.2, together with the characteristic velocities and the time of motion for different models. The velocities calculated by the microconvection model (MM) are greater by one or two orders of magnitude than those predicted by the Oberbeck–Boussinesq model (OBM). The values of the characteristic velocities are consistent

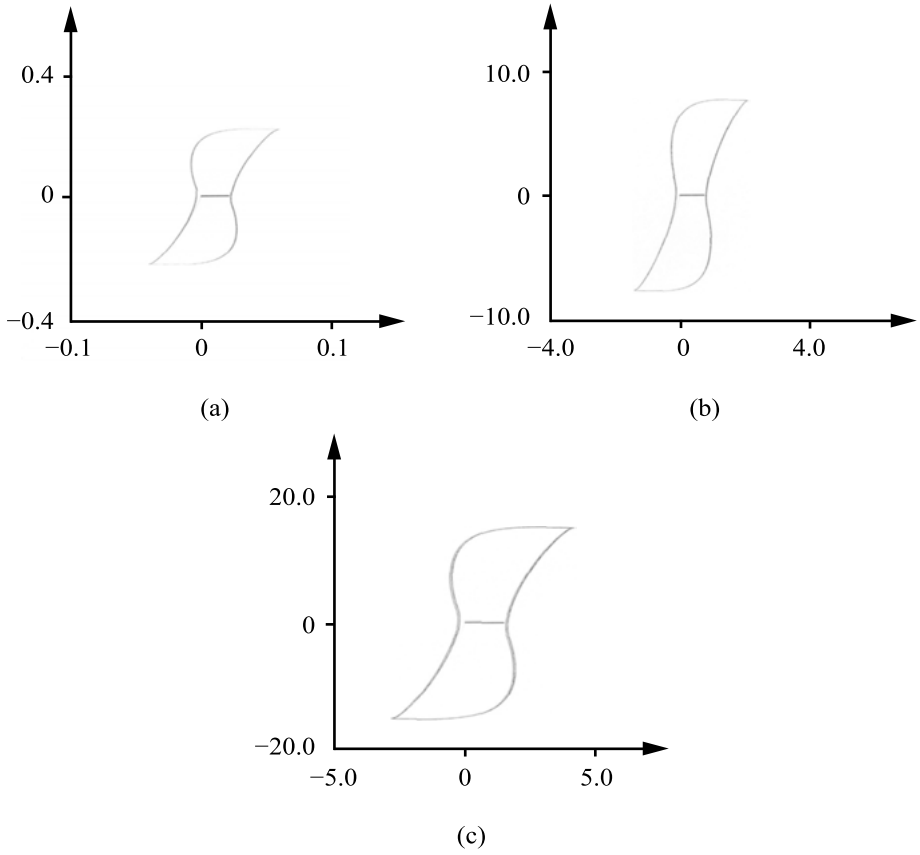

Figure 9.3: (a) Model *N*3; calculation parameters $\mathrm{Pr} = 0.1$, $\varepsilon = 0.02$, $\eta = 0.4$, and $\gamma = 2$; initial coordinates (5; 0.1). Trajectories at $A = 1$ (a), 35 (b), and 70 (c) (Oberbeck–Boussinesq model: segments of straight lines parallel to *Ox*).

Table 9.2: Absolute velocities (maximum orders): (MM/OBM).

	t_*	v_*	$\lvert v_1\rvert$	$\lvert v_2\rvert$
*N*1	476	0.0021	$10^{-4}/10^{-4}$	$10^{-3}/10^{-5}$
*N*2	31	0.0315	$10^{-3}/10^{-4}$	$10^{-2}/10^{-4}$
*N*3	31	0.0315	$10^{-2}/10^{-3}$	$10^{-2}/10^{-4}$
*N*3 ($\gamma = 0.5$)	31	0.0315	$10^{-3}/10^{-4}$	$10^{-2}/10^{-4}$
*N*4 (*sil*)	7774	0.000129	$10^{-5}/10^{-7}$	$10^{-4}/10^{-7}$

with the calculated values. Note that the characteristic times of the process require the calculations to be continued (at least, for models *N*1 and *N*4) for obtaining the real flow pattern and further observations of the trajectories.

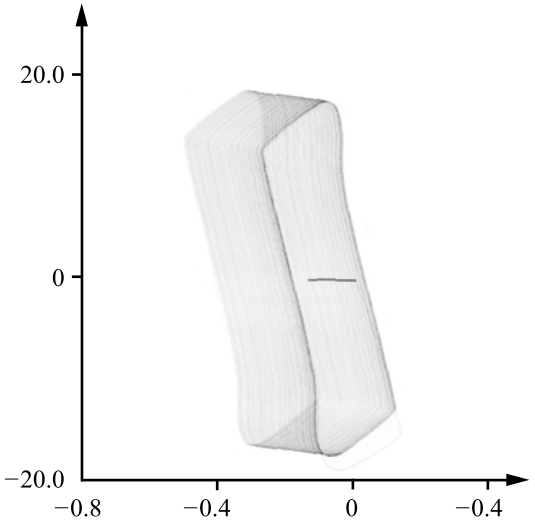

Figure 9.4: Model *N*1; calculation parameters $\mathrm{Pr} = 0.75$, $\varepsilon = 0.01$, $\eta = 1$, and $\gamma = 2$; initial coordinates (5; 0.6). Particle trajectories (Oberbeck–Boussinesq model: segment of a straight line parallel to *Ox*).

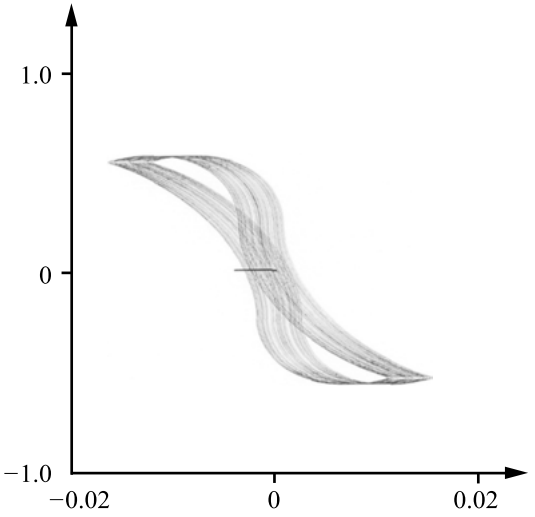

Figure 9.5: Model *N*4 (*sil*); calculation parameters $\mathrm{Pr} = 0.0054$, $\varepsilon = 0.000026$, $\eta = 0.77$, and $\gamma = 2$; initial coordinates (5; 0.6). Particle trajectories (Oberbeck–Boussinesq model: segment of a straight line parallel to *Ox*).

The temperature fields calculated by both models have almost identical qualitative and quantitative characteristics (Table 9.3). The isotherms have the form typical for convection and are almost parallel to the long sides of the rectangle, which confirms

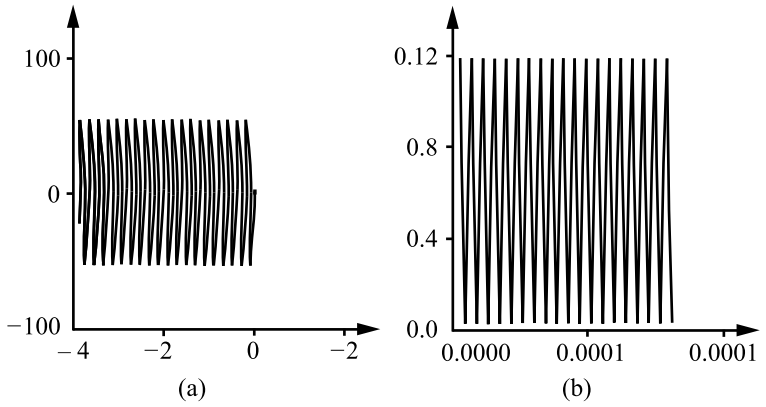

Figure 9.6: Model *N*3; calculation parameters $\mathrm{Pr} = 0.1$, $\varepsilon = 0.02$, $\eta = 0.4$, and $\gamma = 2$; initial coordinates (9.75; 0.5). Particle trajectories calculated by the microconvection model (a) and by the Oberbeck–Boussinesq model (b).

Table 9.3: Change in temperature.

	T **(MM)**	***T*** **(OBM)**
*N*1	11.02–59.83	10.65–59.30
*N*2	11.27–60.69	10.24–59.76
*N*3	11.27–60.70	10.24–59.76
*N*3 ($\gamma = 0.5$)	15.75–54.52	15.63–54.37
*N*4 (*sil*)	7.62–62.41	7.61–62.39

the assumption about the dominating change in temperature in the *Oy* direction and a minor change in the *Ox* direction.

2. Unsteady microconvection in an annular domain

Let us consider unsteady microconvection in an annular domain $R_1 \le r \le R_2$, $0 \le \theta < 2\pi$ under the conditions of a variable gravity field and time-dependent thermal mode on the boundary. The gravity force is directed along the *Oy* axis. Let us write the Oberbeck–Boussinesq equations (3.41)–(3.43) and the microconvection equations (5.6)–(5.8) in polar coordinates for the new sought functions (stream function and vorticity). These equations have the general form

$$\omega_t = \tilde{\nu}\Delta\omega + f_\omega, \tag{9.41}$$

$$\Delta\psi = -\omega, \tag{9.42}$$

$$T_t = \tilde{\chi}\Delta T + f_T, \tag{9.43}$$

where the functions f_ω and f_T, the coefficients $\tilde{\nu}$ and $\tilde{\chi}$, and the initial and boundary conditions are specified for both models as follows.

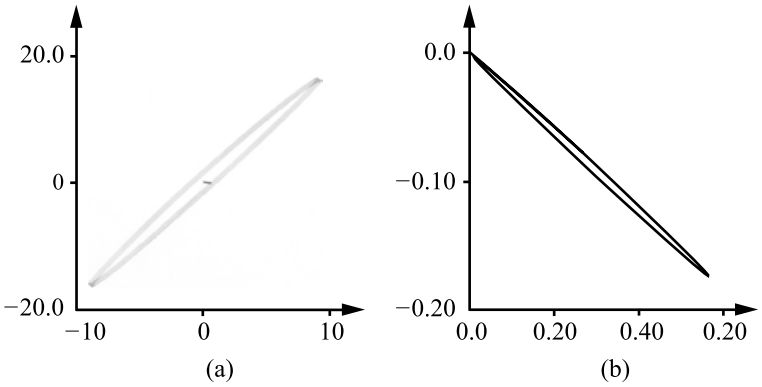

Figure 9.7: Model *N*3; calculation parameters $\mathrm{Pr} = 0.1$, $\varepsilon = 0.02$, $\eta = 0.4$, and $\gamma = 2$; initial coordinates (0.25; 0.1). Particle trajectories calculated by (a) the microconvection model and (b) by the Oberbeck–Boussinesq model.

For the microconvection model, we have

$$
\begin{aligned}
f_\omega = &-\left(v\frac{\partial\omega}{\partial r} + \frac{u}{r}\frac{\partial\omega}{\partial\theta}\right)\\
&+\beta\left[\frac{1}{r}\frac{\partial T}{\partial\theta}\frac{\partial q}{\partial r} - \frac{1}{r}\frac{\partial T}{\partial r}\frac{\partial q}{\partial\theta} + \nu\left(\frac{\partial T}{\partial r}\left(\Delta u - \frac{u}{r^2}\right) - \frac{1}{r}\frac{\partial T}{\partial\theta}\left(\Delta v - \frac{v}{r^2}\right)\right)\right]\\
&+\beta\left(g_\theta\frac{\partial T}{\partial r} - \frac{g_r}{r}\frac{\partial T}{\partial\theta}\right) - \beta\chi\left(\omega\Delta T + \frac{\partial T}{\partial r}\frac{\partial\omega}{\partial r} + \frac{1}{r^2}\frac{\partial T}{\partial\theta}\frac{\partial\omega}{\partial\theta}\right)\\
&-\beta^2\chi^2\left[\frac{1}{r}\left(-\frac{\partial T}{\partial r}\frac{\partial\Delta T}{\partial\theta} + \frac{\partial T}{\partial\theta}\frac{\partial\Delta T}{\partial r}\right)\right],\\
f_T = &-\left(v\frac{\partial T}{\partial r} + \frac{u}{r}\frac{\partial T}{\partial\theta}\right) - \beta\chi|\nabla T|^2.
\end{aligned}
$$

Here, $g_r = g_0\cos(\gamma t)\sin\theta$, $g_\theta = g_0\cos(\gamma t)\cos\theta$, $\tilde{\nu} = (1+\beta T)\nu$, $\tilde{\chi} = (1+\beta T)\chi$. The components of the modified velocity $\mathbf{W} = (v, u)$ are related to the modified stream function ψ as

$$v = \frac{1}{r}\frac{\partial\psi}{\partial\theta}, \quad u = -\frac{\partial\psi}{\partial r}.$$

The initial conditions at $t = 0$ are determined by the state at rest:

$$\omega = 0, \quad \psi = 0, \quad T = T_0.$$

Let us consider two types of the boundary conditions corresponding to two types of the temperature regime:

(a) Case $I = 0$: heat flux through the external boundary of the domain and thermal insulation of the internal boundary;

(b) Case $I = 1$: vice versa — heat flux through the internal boundary of the domain and thermal insulation of the external boundary.

Thus, the boundary conditions for the microconvection model are imposed in the following manner.

– For case $I = 0$, we have

$$\begin{aligned} &\psi = 0, && \frac{\partial \psi}{\partial r} = \beta\chi R_1^{-1}\frac{\partial T}{\partial \theta}, && \frac{\partial T}{\partial r} = 0, && r = R_1,\\ &\psi = -\beta\chi R_2 H(t)\sin\theta, && \frac{\partial \psi}{\partial r} = \beta\chi R_2^{-1}\frac{\partial T}{\partial \theta}, && \frac{\partial T}{\partial r} = H(t)\cos\theta, && r = R_2. \end{aligned}$$

– For case $I = 1$, we have

$$\begin{aligned} &\psi = -\beta\chi R_1 H(t)\sin\theta, && \frac{\partial \psi}{\partial r} = \beta\chi R_1^{-1}\frac{\partial T}{\partial \theta}, && \frac{\partial T}{\partial r} = H(t)\cos\theta, && r = R_1,\\ &\psi = 0, && \frac{\partial \psi}{\partial r} = \beta\chi R_2^{-1}\frac{\partial T}{\partial \theta}, && \frac{\partial T}{\partial r} = 0, && r = R_2. \end{aligned}$$

For the Oberbeck–Boussinesq model, the right-hand sides of eqs. (9.41) and (9.43) have the form

$$\begin{aligned} f_\omega &= -\left(\nu\frac{\partial \omega}{\partial r} + \frac{u}{r}\frac{\partial \omega}{\partial \theta}\right) + \beta\left(g_\theta\frac{\partial T}{\partial r} - \frac{g_r}{r}\frac{\partial T}{\partial \theta}\right),\\ f_T &= -\left(\nu\frac{\partial T}{\partial r} + \frac{u}{r}\frac{\partial T}{\partial \theta}\right). \end{aligned}$$

As previously, we have $g_r = g_0\cos(\gamma t)\sin\theta$ and $g_\theta = g_0\cos(\gamma t)\cos\theta$. In addition, we also have $\tilde{\nu} = \nu$ and $\tilde{\chi} = \chi$. The components of the physical velocity $\mathbf{V} = (v, u)$ are related to the stream function ψ as

$$v = \frac{1}{r}\frac{\partial \psi}{\partial \theta}, \quad u = -\frac{\partial \psi}{\partial r}.$$

The initial conditions at $t = 0$ are also determined by the state at rest:

$$\omega = 0, \quad \psi = 0, \quad T = T_0.$$

The boundary conditions in these two cases are imposed as follows.

– For case $I = 0$, we have

$$\begin{aligned} &\psi = 0, && \frac{\partial \psi}{\partial r} = 0, && \frac{\partial T}{\partial r} = 0, && r = R_1,\\ &\psi = 0, && \frac{\partial \psi}{\partial r} = 0, && \frac{\partial T}{\partial r} = H(t)\cos\theta, && r = R_2. \end{aligned}$$

– For case $I = 1$, we have

$$\begin{aligned} &\psi = 0, && \frac{\partial \psi}{\partial r} = 0, && \frac{\partial T}{\partial r} = H(t)\cos\theta, && r = R_1,\\ &\psi = 0, && \frac{\partial \psi}{\partial r} = 0, && \frac{\partial T}{\partial r} = 0, && r = R_2. \end{aligned}$$

In eqs. (9.41)–(9.43), we use the conventional notations for the differential operators in polar coordinates, namely,

$$\Delta = \frac{1}{r}\frac{\partial}{\partial r} r \frac{\partial}{\partial r} + \frac{1}{r^2}\frac{\partial^2}{\partial \theta^2}, \quad \nabla = \left(\frac{\partial}{\partial r}, \frac{1}{r}\frac{\partial}{\partial \theta}\right)$$

(see the remark at the end of this section on imposing the boundary conditions for doubly connected domains).

Numerical implementation. Calculation scheme

The problem is solved numerically by the method of calculating convective flows in doubly connected domains, which was tested in [229]. The longitudinal-transverse difference scheme for eqs. (9.41)–(9.43) is written in the form

$$\frac{U^{k+1/2} - U^k}{0.5\tau} = \lambda(\Lambda_1 U^k + \Lambda_2 U^{k+1/2}) + F^k,$$
$$\frac{U^{k+1} - U^{k+1/2}}{0.5\tau} = \lambda(\Lambda_1 U^{k+1} + \Lambda_2 U^{k+1/2}) + F^k.$$

Here, $U^k = U(t^k)$, $U = \binom{\omega}{T}$; Λ_1 and Λ_2 are the difference operators approximating, respectively, the differential operators

$$\frac{1}{r}\frac{\partial}{\partial r} r \frac{\partial}{\partial r}, \quad \frac{1}{r^2}\frac{\partial^2}{\partial \theta^2}.$$

Here, λ is determined for vorticity and temperature calculations by $\tilde{\nu}$ and $\tilde{\chi}$, respectively. The convective terms are calculated on the lower time layer and are included into F^k.

To solve Poisson's equation (9.42), we use an iterative scheme with an alternated sequence of sweeping at each time step:

$$\frac{\psi^{s+1/2} - \psi^k}{0.5\tau} = \lambda_s(\Lambda_1 \psi^{s+1/2} + \Lambda_2 \psi^s + \omega^{k+1}),$$
$$\frac{\psi^{s+1} - \psi^{s+1/2}}{0.5\tau} = \lambda_s(\Lambda_1 \psi^{s+1/2} + \Lambda_2 \psi^{s+1} + \omega^{k+1})$$

(λ_s is the iteration parameter). At the end of the iteration cycle, we assume that $\psi^{k+1} = \psi^{s+1}$. The Tom difference boundary conditions relate the functions ω and ψ on the boundaries $r = R_1$ and $r = R_2$. The iterative process is terminated when condition (9.37) is satisfied.

To find $T^{k+1/2}$, $\omega^{k+1/2}$, and ψ^{s+1}, we use cyclic sweeping. The difference equations for ω^{k+1} and $\psi^{s+1/2}$ are solved with the use of the so-called sweeping with parameters [229, 230], which implies that the following presentations are valid:

$$\omega_{n,m} = P_{n,m}\omega_{N+1,m} + Q_{n,m}\omega_{1,m} + R_{n,m},$$
$$\psi_{n,m} = \bar{\psi}_{n,m}\omega_{N+1,m} + \bar{\bar{\psi}}_{n,m}\omega_{1,m} + \bar{\bar{\bar{\psi}}}_{n,m}$$

(the parameters here are the unknown values of vorticity on the domain boundaries). Details of implementation of this method of sweeping with parameters can be found in [229].

To implement the numerical algorithm in the computational domain, we introduce the difference grid

$$r_n = R_1 + (n-1)h, \quad n = 1, \dots, N+1, \quad h = (R_2 - R_1)/N;$$
$$\theta_m = (m-1)\alpha, \quad m = 1, \dots, M+1, \quad \alpha = 2\pi/M;$$
$$t^k = k\tau, \quad k = 1, 2, \dots$$

Results of the numerical study of microconvection in annular domains

Convective flows in a variable field of microaccelerations $g = g_0 \cos(\gamma t)$, $g_0 = 10^{-3}\,\mathrm{cm/s^2}$, $\gamma = 10^{-1}\,1/\mathrm{s}$ are calculated on 21×21, 41×41, and 81×81 grids in the annular domain $R_1 \le r \le R_2$, $0 \le \theta < 2\pi$ at $R_1 = 0.1\,\mathrm{cm}$ and $R_2 = 1.1\,\mathrm{cm}$ for silicon, glycerin, and glass. The values of the Prandtl number Pr, Rayleigh number Ra, and microconvection parameter η are listed in Table 9.4. The heat flux through the external or internal boundary of the domain is

$$\frac{\partial T}{\partial r} = H(t)\cos\theta, \quad H(t) = (T_1 - T_0)\frac{t}{t_1} + T_0, \quad t \le t_1; \quad H(t) = T_1, \quad t > t_1,$$

where

$$t_1 = 60\,c, \quad T_0 = 35\,^\circ\mathrm{C}, \quad T_1 = 70\,^\circ\mathrm{C}.$$

The calculations reveal qualitative differences in the flow patterns calculated by two different models. First of all, these differences are manifested in the flow structure, its topology, and time evolution.

Figures 9.8 and 9.10 show the velocity fields and isotherms for silicon at the instant of time $t = 120\,\mathrm{s}$. The flow topology is also typical for glycerin and glass. Figures 9.8 and 9.9 demonstrate the field of velocities in the silicon melt at the time $t = 120\,\mathrm{s}$

Table 9.4: Basic parameters of the problem.

Substance	Pr	Ra	η
Silicon	10^{-1}	10^{-4}	1
Glycerin	10^{4}	10^{-3}	10^{-1}
Glass	10^{4}	10^{-6}	10^{-2}

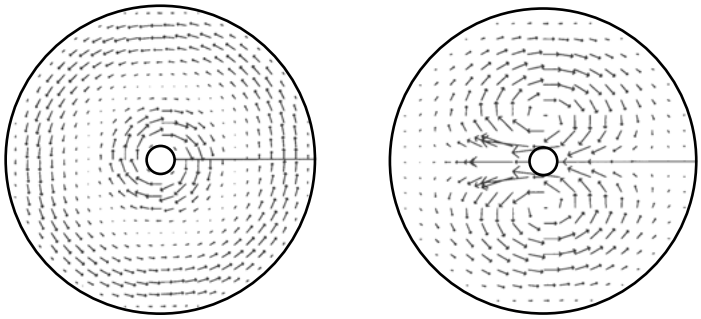

Figure 9.8: Case $I = 0$ (heat flux through the external boundary of the domain and thermal insulation of the internal boundary); velocity field: (a) Oberbeck–Boussinesq model and (b) microconvection model.

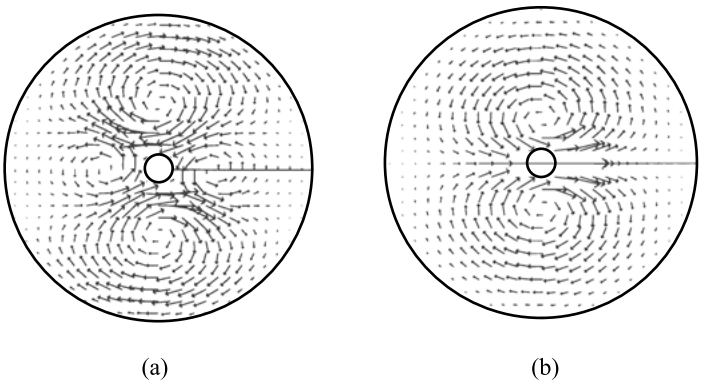

Figure 9.9: Case $I = 1$ (heat flux through the internal boundary of the domain and thermal insulation of the external boundary); velocity field: (a) Oberbeck–Boussinesq model and (b) microconvection model.

for $\eta = 1$, and Figure 9.10 shows the behavior of isotherms for these conditions. Figure 9.8a (Oberbeck–Boussinesq model, $I = 0$) shows the field of velocities, which has the structure of rotational motion with axial symmetry; it should be noted that the external and internal fluid layers rotate in different directions. There are two small symmetric vortices between these layers: in the upper and lower half-circles for silicon and in the right and left half-circles for glycerin and glass. The flow structure in Figure 9.9a (Oberbeck–Boussinesq model, $I = 1$) has four vortices. The domains occupied by the upper and lower vortices are more extended for the case with silicon. For glycerin, the domains occupied by the right and left vortices are more extended. Figure 9.8b (microconvection model, $I = 0$) clearly shows the flow structure with two

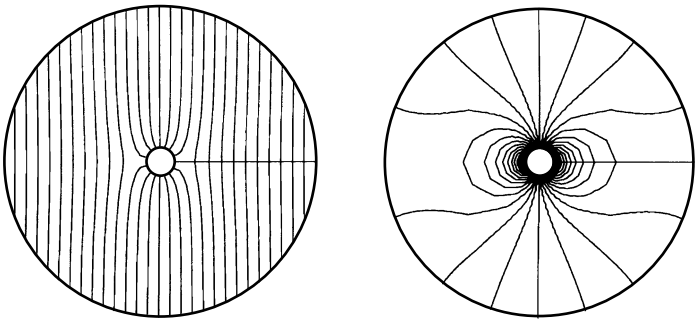

Figure 9.10: Families of isotherms. Oberbeck–Boussinesq model and microconvection model; (a) case $I = 0$ and (b) case $I = 1$.

vortices. The vortices located in the upper and lower half-planes rotate in the clockwise and counterclockwise directions, respectively.

The field of velocities in Figure 9.9b (microconvection model, $I = 1$) has two vortices, as in the case with $I = 0$, but with the opposite direction. The calculations revealed only some quantitative differences in the temperature fields obtained by two different models.

Qualitatively, there are two types of families of isotherms corresponding to two different types of the boundary conditions (Figure 9.10a: $I = 0$ and Figure 9.10b: $I = 1$). The qualitative characteristics, namely, the orders of velocities, are listed for all fluids and two models in Table 9.5 ($t = 120$ s). Here, the Oberbeck–Boussinesq and microconvection models are denoted by OBM and MM, respectively.

Remark 9.1. In the case of a doubly connected domain, the condition $\psi = c(t)$ is imposed on one of the boundary components, for example $r = R_1$. Here, $c(t)$ is an unknown function of time which is determined from a nonlocal condition, as a consequence of the unique value of pressure. This condition has the form

$$\oint\limits_{r=R_1} \frac{\partial \omega}{\partial n} dl = 0$$

Table 9.5: Absolute values of velocities (cm/s).

Substance	OBM	MM
Silicon	10^{-8}–10^{-6}	10^{-5}–10^{-4}
Glycerin	10^{-9}–10^{-8}	10^{-6}–10^{-5}
Glass	10^{-13}–10^{-10}	10^{-7}–10^{-6}

(see, e. g., [217, 221, 228]). In the case of axisymmetric ring considered here, ψ is assumed to be equal to zero on both boundaries, which is possible by virtue of flow symmetry. When the algorithm was tested in [229], it was verified by calculation that $c(t) = 0$.

9.3 Numerical study of steady microconvection in domains with free boundaries

Steady two-dimensional gravitational-thermal convection in a semicircle and in an annular domain with a free boundary is numerically studied with the use of two mathematical models. One boundary is assumed to be solid and impermeable. In the half-circle, the solid (fixed) boundary is the half-circumference. In the annular domain, the solid boundary is one of the circumferences. The other boundary is assumed to be free and subject to a thermocapillary effect. Under microgravity conditions, and in the case where the parameter responsible for free surface deformation by thermocapillary forces (capillary number) is rather small, we consider nondeformable free boundaries, which are approximately determined as capillary equilibrium surfaces. Following [140, 241], we determine the correction to the free boundary from the dynamic condition on it. Both problems with free boundaries are model problems; in physical experiments, thermocapillary convection in a half-circle can be more probably obtained. Numerical experiments are performed for different values of the Prandtl number Pr, Marangoni number M, Rayleigh number Ra, and with due allowance for the drastically changing temperature regime on the boundary in the case of the half-circle. It is known from theoretical investigations that allowance for nonsolenoidity in modeling steady convection yields corrections of the order of the Boussinesq number [178].

In this section we perform a numerical study of the structure of convective flows and analyze situations in which the flow topology can be substantially different. These situations involve additional modeling of large gradients in the thermal regime on the boundary. Quantitative differences in the values of velocities here are less pronounced than in the unsteady case. The calculations are performed by the method approved in studying free convection and microconvection of the fluid in domains with fixed boundaries. The property of velocity vector solenoidity allows us to introduce a stream function for the Oberbeck–Boussinesq equations and an analog of the stream function for the microconvection equations. The second sought function or vorticity is the physical rather than modified vorticity for the microconvection model as well.

1. Microconvection in a semicircle with a free boundary

We write the classical Oberbeck–Boussinesq equations in the dimensionless form, using the characteristic size l, characteristic time of the process t_*, characteristic veloc-

ity v_* (so that $l = v_* t_*$), and characteristic pressure p_* ($p_* = \varrho_0 v_*^2$) for normalization. Then, system (3.41)–(3.43) in the dimensionless form becomes

$$\operatorname{div} \mathbf{V} = 0, \tag{9.44}$$

$$\mathbf{V}_t + \mathbf{V} \cdot \nabla \mathbf{V} = -\nabla p' + \frac{1}{\mathrm{Re}} \Delta \mathbf{V} - \frac{\mathrm{Ra}}{\mathrm{Re}^2 \mathrm{Pr}} \mathbf{g}_0 \, T, \tag{9.45}$$

$$T_t + \mathbf{V} \cdot \nabla T = \frac{1}{\mathrm{Re}\,\mathrm{Pr}} \Delta T. \tag{9.46}$$

Here, p' is used to denote the modified pressure

$$p' = p - \frac{\eta}{\mathrm{Re}^2 \mathrm{Pr}} \mathbf{g}_0 \cdot x,$$

Re is the Reynolds number, and $\mathbf{g}_0 = \mathbf{g}/g$ (the gravity force is directed opposite to the Oy axis). The characteristic quantities for the thermocapillary convection model can be chosen ([241]) as

$$l = R, \quad v_* = \sigma_T T_* / \mu, \quad p_* = \sigma_T T_* / R.$$

Here we assume that the dimensional coefficient of surface tension depends on temperature as $\sigma = \sigma_0 - \sigma_T (T - T_0)$.

The system of microconvection equations (5.6)–(5.8) converted to the dimensionless form is rewritten as

$$\operatorname{div} \mathbf{W} = 0, \tag{9.47}$$

$$\begin{aligned} \mathbf{W}_t + \mathbf{W} \cdot \nabla \mathbf{W} + \frac{\varepsilon}{\mathrm{Re}\,\mathrm{Pr}} (\nabla T \cdot \nabla \mathbf{W} - \nabla \mathbf{W} \cdot \nabla T) + \frac{\varepsilon^2}{\mathrm{Re}^2 \mathrm{Pr}^2} (\Delta T \cdot \nabla T - \nabla |\nabla T|^2) \\ = (1 + \varepsilon T) \left(-\nabla q + \frac{1}{\mathrm{Re}} \Delta \mathbf{W} \right) - \frac{\mathrm{Ra}}{\mathrm{Re}^2 \mathrm{Pr}} \mathbf{g}_0 \, T, \end{aligned} \tag{9.48}$$

$$T_t + \mathbf{W} \cdot \nabla T + \frac{\varepsilon}{\mathrm{Re}\,\mathrm{Pr}} |\nabla T|^2 = (1 + \varepsilon T) \frac{1}{\mathrm{Re}\,\mathrm{Pr}} \Delta T. \tag{9.49}$$

Here, q is the modified pressure

$$q = p' - \left(1 - \frac{\nu'}{\nu} - \frac{1}{\mathrm{Pr}} \right) \frac{\varepsilon}{\mathrm{Re}^2 \mathrm{Pr}} \Delta T,$$

ν' is the second viscosity, and $\mathbf{W} = \mathbf{V} - \frac{\varepsilon}{\mathrm{Re}\,\mathrm{Pr}} \nabla T$ is the dimensionless modified solenoidal velocity.

To formulate the problem, we use the conventional notations for polar coordinates: radial coordinate r and angular coordinate φ. If ω is the vorticity and ψ is the stream function or modified stream function, then $v = 1/r \, \partial\psi/\partial\varphi$ is the radial component of velocity and $u = -\partial\psi/\partial r$ is the tangential component of velocity.

Steady gravitational-thermocapillary convection is studied in the semicircle

$$0 \le r \le R < +\infty, \quad \pi \le \varphi \le 2\pi$$

with the free boundary, which is the diameter of the semicircle

$$\varphi = \pi, \quad \varphi = 2\pi, \quad 0 \le r \le R.$$

The semicircumference $r = R$, $\pi \le \varphi \le 2\pi$ is a solid impermeable boundary with a heat flux through it.

The equations of convection for both models (9.44)–(9.46) and (9.47)–(9.49) can be rewritten in terms of ψ and ω.

Formulation of the problem. Classical Oberbeck–Boussinesq model in terms of ψ and ω (dimensionless form, polar coordinates)

Equations (9.44)–(9.46) considered in the steady case are written in the polar coordinates in the form

$$\Delta\omega - \mathrm{Re}\left(v\frac{\partial\omega}{\partial r} + \frac{u}{r}\frac{\partial\omega}{\partial\varphi}\right) + \frac{\mathrm{Ra}}{\mathrm{M}}\left(\frac{\partial T}{\partial r}\cos\varphi - \frac{1}{r}\frac{\partial T}{\partial\varphi}\sin\varphi\right) = 0, \tag{9.50}$$

$$\Delta\psi + \omega = 0, \tag{9.51}$$

$$\Delta T - \mathrm{M}\left(v\frac{\partial T}{\partial r} + \frac{u}{r}\frac{\partial T}{\partial\varphi}\right) = 0, \tag{9.52}$$

where $\mathrm{M} = \mathrm{Re}\,\mathrm{Pr}$ is the Marangoni number.

To realize rapidly changing temperature fields, we model a local singularity of the heat flux both through the free boundary and through the solid boundary. Thus, we consider three types of the boundary conditions for both models. We conventionally denote them as case II (singularity of the Gaussian type in the thermal regime on the free boundary), case III (local singularity in the thermal regime on the solid boundary), and basic case I with no singularities.

In addition, we can also consider different variations of the temperature regime on the solid boundary, which is reflected in the boundary condition for temperature, namely,

$$\frac{\partial T}{\partial r} = T_G\cos\gamma\varphi, \quad \gamma = \{1,\ 2,\ 4\}. \tag{9.53}$$

– *Case I* (basic case without singularities in the temperature regime on the boundary): The basic case of the boundary conditions is characterized by the absence of "spikes" on the solid and free boundaries. Then, the boundary conditions at $0 \le r \le R$, $\varphi = \pi$, $\varphi = 2\pi$ for the stream function and vorticity are presented as

$$\psi = 0, \quad \omega = \begin{cases} \dfrac{\partial T}{\partial r}, & \varphi = 2\pi, \\ -\dfrac{\partial T}{\partial r}, & \varphi = \pi. \end{cases} \tag{9.54}$$

The boundary condition for temperature characterizes the state of thermal insulation of the free boundary:

$$\frac{\partial T}{\partial \varphi} = 0. \tag{9.55}$$

The boundary conditions for the stream function and vorticity on the solid boundary $r = R$ are natural consequences of the no-slip condition,

$$\psi = 0, \quad \frac{\partial \psi}{\partial r} = 0, \tag{9.56}$$

and the boundary conditions for temperature are considered in the form of eqs. (9.53).

– *Case II* (singularity in the temperature regime on the free boundary): The boundary conditions for the Oberbeck–Boussinesq equations on the free boundary $0 \le r \le R$, $\varphi = \pi$, $\varphi = 2\pi$ can be presented in the form of eqs. (9.54), and the boundary conditions for temperature are modeled as

$$\frac{\partial T}{\partial \varphi} = \begin{cases} 0, & \varphi = \pi, \quad \varphi = 2\pi \quad (r \neq R_*), \\ R_* T_B, & \varphi = 2\pi \qquad\qquad (r = R_*). \end{cases} \tag{9.57}$$

The boundary conditions for the stream function and vorticity on the solid boundary $r = R$ are natural consequences of the no-slip condition and have the form of eqs. (9.56). The boundary conditions for temperature are imposed in accordance with eqs. (9.53).

– *Case III* (singularity in the temperature regime on the solid boundary): In the case of a local singularity ("spike") on the solid boundary and under the assumption of a thermally insulated free boundary, the boundary conditions at $0 \le r \le R$, $\varphi = \pi$, $\varphi = 2\pi$ for the stream function and vorticity can be presented in the form of eqs. (9.54). Equation (9.55) is valid for temperature.

The boundary conditions for the stream function and vorticity on the solid boundary $r = R$ are consequences of the no-slip condition and have the form of eqs. (9.56); for temperature, we impose the conditions

$$\frac{\partial T}{\partial r} = \begin{cases} T_G \cos\varphi, & \varphi \neq \varphi_*, \\ \bar{T}_G \cos\varphi, & \varphi = \varphi_*. \end{cases} \tag{9.58}$$

The boundary conditions on the free boundary are the kinematic and dynamic conditions on the free boundaries written in terms of ψ and ω (see, e. g., [180, 171]).

Thus, for eqs. (9.50)–(9.52), we can consider the boundary-value problems (9.53)–(9.56) (for Case I), (9.53), (9.54), (9.56), (9.57) (for Case II), and (9.54), (9.55), (9.56), (9.58) (for Case III).

Formulation of the problem. Microconvection model in terms of ψ and ω (dimensionless form, polar coordinates)

The dimensionless form of the microconvection equations (9.47)–(9.49) in terms of ψ and ω in the polar coordinates is

$$
\begin{aligned}
&[1+\varepsilon T]\Delta\omega - \mathrm{Re}\left(v\frac{\partial\omega}{\partial r} + \frac{u}{r}\frac{\partial\omega}{\partial\varphi}\right) \\
&\quad + \varepsilon\left\{\frac{1}{r}\frac{\partial T}{\partial\varphi}\frac{\partial\bar{q}}{\partial r} - \frac{1}{r}\frac{\partial T}{\partial r}\frac{\partial\bar{q}}{\partial\varphi} + \left[\frac{\partial T}{\partial r}\left(\Delta u - \frac{u}{r^2}\right) - \frac{1}{r}\frac{\partial T}{\partial\varphi}\left(\Delta v - \frac{v}{r^2}\right)\right]\right\} \\
&\quad + \frac{\mathrm{Ra}}{\mathrm{M}}\left(\frac{\partial T}{\partial r}\cos\varphi - \frac{1}{r}\frac{\partial T}{\partial\varphi}\sin\varphi\right) - \frac{\varepsilon}{\mathrm{Pr}}\left(\omega\Delta T + \frac{\partial T}{\partial r}\frac{\partial\omega}{\partial r} + \frac{1}{r^2}\frac{\partial T}{\partial\varphi}\frac{\partial\omega}{\partial\varphi}\right) \\
&\quad - \frac{\varepsilon^2}{\mathrm{M}\,\mathrm{Pr}}\left(-\frac{1}{r}\frac{\partial T}{\partial r}\frac{\partial\Delta T}{\partial\varphi} + \frac{1}{r}\frac{\partial T}{\partial\varphi}\frac{\partial\Delta T}{\partial r}\right) = 0, \qquad (9.59)
\end{aligned}
$$

$$
\Delta\psi + \omega = 0, \qquad (9.60)
$$

$$
[1+\varepsilon T]\Delta T - \mathrm{M}\left(v\frac{\partial T}{\partial r} + \frac{u}{r}\frac{\partial T}{\partial\varphi}\right) - \varepsilon|\nabla T|^2 = 0. \qquad (9.61)
$$

Here, $\bar{q} = \mathrm{Re}\, q$.

To impose the boundary conditions, we again classify the possible cases of specifying singularities for heat fluxes on the boundaries.

- *Case I* (basic case without singularities in the temperature regime): In the basic case, the boundary conditions on the free boundary $0 \le r \le R$, $\varphi = \pi$, $\varphi = 2\pi$ have the forms of eqs. (9.54), (9.55) for the stream function and vorticity. The condition on the solid boundary $r = R$ follows from the no-slip condition for physical velocity, so that

$$
\psi = -R\,\frac{\varepsilon}{\mathrm{M}}\,T_G\,\frac{1}{\gamma}\sin\gamma\varphi, \quad \frac{\partial\psi}{\partial r} = \frac{1}{R}\,\frac{\varepsilon}{\mathrm{M}}\,\frac{\partial T}{\partial\varphi}. \qquad (9.62)
$$

  For the temperature on the solid boundary, we consider the condition for the heat flux (9.53).
- *Case II* (singularity in the temperature regime on the free boundary): The boundary conditions at $0 \le r \le R$, $\varphi = \pi$, $\varphi = 2\pi$ have the form of eqs. (9.54) for the stream function and vorticity; condition (9.57) is valid for temperature. Conditions (9.62) on the solid boundary $r = R$ are a consequence of the no-slip condition. The heat flux (9.53) is set as the condition for temperature.
- *Case III* (singularity in the temperature regime on the solid boundary): The boundary conditions on the free boundary $0 \le r \le R$, $\varphi = \pi$, $\varphi = 2\pi$ have the form of eqs. (9.54) and (9.55). The conditions on the solid boundary $r = R$ are a consequence of the no-slip condition, i. e.,

$$
\psi = \begin{cases} -R\dfrac{\varepsilon}{\mathrm{M}}\,T_G\sin\varphi, & \varphi \ne \varphi_*, \\ -R\dfrac{\varepsilon}{\mathrm{M}}\,\bar{T}_G\sin\varphi, & \varphi = \varphi_*, \end{cases} \qquad (9.63)
$$

$$\frac{\partial \psi}{\partial r} = \frac{1}{R}\,\frac{\varepsilon}{\mathrm{M}}\,\frac{\partial T}{\partial \varphi}, \tag{9.64}$$

and a "spike" on the solid boundary is modeled by imposing the condition

$$\frac{\partial T}{\partial r} = \begin{cases} T_G \cos\varphi, & \varphi \neq \varphi_*, \\ \bar{T}_G \cos\varphi, & \varphi = \varphi_*. \end{cases} \tag{9.65}$$

For eqs. (9.59)–(9.61), we can consider the boundary-value problems (9.53)–(9.55), (9.62) (for Case I), (9.53), (9.54), (9.57), (9.62) (for Case II), and (9.54), (9.55), (9.63), (9.64), (9.65) (for Case III).

Numerical study. Calculation scheme

The posed problems for systems (9.50)–(9.52) and (9.59)–(9.61) are numerically studied by a time-dependent method, using the longitudinal-transverse finite-difference scheme [207] with the second order of approximation. The convective terms are taken from the previous iteration layer and are approximated upwind. Thus, the first-order scheme is actually used. The method proposed for this study was previously approved on the basis of test problems [229] and calculations of unsteady convection (see, e. g., [79, 80]).

For eqs. (9.50), (9.52) or (9.59), (9.61), the calculation scheme is written in the general form as

$$\begin{aligned} \frac{U^{k+1/2} - U^k}{0.5\tau} &= \tilde{\lambda}_U\left[\Lambda_1 U^k + \Lambda_2 U^{k+1/2}\right] + \lambda_U F^k, \\ \frac{U^{k+1} - U^{k+1/2}}{0.5\tau} &= \tilde{\lambda}_U\left[\Lambda_1 U^{k+1} + \Lambda_2 U^{k+1/2}\right] + \lambda_U F^k, \end{aligned} \tag{9.66}$$

where $U = \binom{\omega}{T}$, $U^k = U(t^k)$; Λ_1 and Λ_2 are the difference operators approximating the differential operators

$$\frac{1}{r}\frac{\partial}{\partial r} r \frac{\partial}{\partial r}, \quad \frac{1}{r^2}\frac{\partial^2}{\partial \varphi^2},$$

respectively. In addition, we have $\tilde{\lambda}_U = \lambda_U$ for the Oberbeck–Boussinesq model and $\tilde{\lambda}_U = \lambda_U(1 + \varepsilon T^k)$ for the microconvection model. Here, λ_U is the iteration parameter, and F^k includes all terms in the left-hand sides of eqs. (9.50), (9.52), (9.59), (9.61), beginning from the second one, which were calculated on the previous layer.

To solve Poisson's equations (9.51) or (9.60), we use the following iterative scheme at each iteration step $t_k = k\tau$ ($k = 1, 2, \ldots$):

$$\begin{aligned} \frac{\psi^{s+1/2} - \psi^s}{0.5\tau} &= \lambda_\psi(\Lambda_1 \psi^{s+1/2} + \Lambda_2 \psi^s + \omega^{k+1}), \\ \frac{\psi^{s+1} - \psi^{s+1/2}}{0.5\tau} &= \lambda_\psi(\Lambda_1 \psi^{s+1/2} + \Lambda_2 \psi^{s+1} + \omega^{k+1}) \end{aligned} \tag{9.67}$$

(λ_ψ is the iteration parameter).

To implement the above-described scheme, we introduce the difference grid

$$r_n = (n-1)h, \quad (n = 1, \dots, N+1), \quad h = R/N;$$
$$\varphi_m = (m-1)\alpha, \quad (m = \bar{m}, \dots, M+1), \quad \alpha = 2\pi/M, \quad (\bar{m}\alpha = \pi).$$

We use the notations $f_{n,m} = f(r_n \text{ and } \varphi_m)$. In this case, we use the conventional presentations for the difference analog of differential operations:

$$\Lambda_1 f = \frac{1}{r_n}\left[r_{n+1/2}\frac{f_{n+1,m} - f_{n,m}}{h^2} - r_{n-1/2}\frac{f_{n,m} - f_{n-1,m}}{h^2}\right],$$
$$\Lambda_2 f = \frac{f_{n,m+1} - 2f_{n,m} + f_{n,m-1}}{r_n^2\alpha^2}.$$

Approximation of the convective terms is based on the idea of upwind approximation

$$-\left[v\frac{\partial f}{\partial r} + \frac{u}{r}\frac{\partial f}{\partial \varphi}\right] \sim -\left[v_{n,m}\frac{f_{n+1,m} - f_{n-1,m}}{2h} + \frac{u_{n,m}}{r_n}\frac{f_{n,m+1} - f_{n,m-1}}{2\alpha}\right]$$
$$+ |v|_{n,m}\frac{f_{n+1,m} - 2f_{n,m} + f_{n-1,m}}{2h} + \left|\frac{u}{r}\right|_{n,m}\frac{f_{n,m+1} - 2f_{n,m} + f_{n,m-1}}{2\alpha}.$$

The first derivatives on the computational domain boundary are approximated by asymmetric finite-difference analogs.

To impose the boundary condition for vorticity on the solid boundary, we derive conditions of the Tom type [195, 219] with the use of the Taylor expansion and Poisson's equation considered on the boundary, for instance,

$$\omega_{N+1,m} = -\frac{2}{h^2}\psi_{N,m},$$
$$\omega_{N+1,m} = -\frac{2}{h^2}\psi_{N,m} - \frac{\varepsilon}{\mathrm{M}}\frac{\partial T}{\partial \varphi}\left(\frac{1}{R^2} + \frac{2}{hR}\right) - \frac{\varepsilon}{\mathrm{M}}T_G \sin\gamma\varphi_m\left(\frac{1}{R}\gamma + \frac{2R}{h^2}\gamma\right).$$

These conditions are written for the classical model and microconvection model, respectively. For Case III, we must replace T_G by $\bar{T}_G$ for $\varphi = \varphi_*$.

The general scheme of solving the problem consists of the following stages:

1. the external iterative process consists of parallel calculations of the functions T^{k+1} and ω^{k+1} by eqs. (9.66). The sweeping is performed in the direction φ on the intermediate layer $(k+1/2)$ and in the direction r on the basic layer $(k+1)$. The starting values are determined by the state at rest $T := T_0 = \text{const}$, $\omega := 0$, $\psi := 0$;
2. on each iteration layer $(k+1)$, we introduce an internal iterative process of calculating ψ^{s+1} from systems (9.67) with an alternated sequence of sweeping. When the iterations are finalized at $s = S$, the values of ψ on the layer $(k+1)$ $(\psi^{k+1} = \psi^S)$ are assumed to be determined with specified accuracy ε_ψ.

The iterative processes are assumed to converge if the convergence criterion of the form (9.37) is satisfied:

$$\max_{n,m}|f_{n,m}^{i+1} - f_{n,m}^{i}| < \varepsilon_f \max_{n,m}|f_{n,m}^{i+1}|$$

(i is the iteration number and ε_f is the prescribed accuracy of calculating the grid function f^{i+1} ([195, 219])).

It should be noted that the external iterative process can also be organized so that an iterative process for ω is introduced on each iteration layer in calculating the temperature T^{l+1}. The steady regimes calculated by the two methods were found to coincide, and the first method was chosen as the basic technique.

In addition to verifying satisfaction of the convergence criterion for the iterative processes, the steady flow is considered to be established if at least K external iterations are performed and

$$\max_{n,m}|f_{n,m}^{K+k} - f_{n,m}^{K}| < \varepsilon_f.$$

We use an additional check of satisfaction of the boundary conditions in terms of the value of $\bar{\varepsilon}$ (9.38):

$$\bar{\varepsilon} = \max_{m}|\omega_{N+1,m}(\psi_{N,m}^{k+1}) - \omega_{N+1,m}(\psi_{N,m}^{k})|.$$

Because obtaining a steady solution is a rather delicate issue, we also checked reaching the steady regime by the method of perturbing the solution. A return to the initial state was observed. Stability of the algorithm was also checked in a computational experiment on a sequence of grids ($\frac{N}{2}\times\frac{N}{2}$, $N\times N$, $2N\times 2N$), and the behavior of the quantity characterizing the motion intensity $\max_{n,m}|f_{n,m}^{k+1}|$ was observed.

We should note that, if necessary, the issues associated with the correction of the free boundary and flow stability can be solved, in accordance with [140, 241]. If $H(x)$ is the deviation of the free boundary from the position $y = 0$, $-R \le x \le R$, then the equation for this correction can be written in the form

$$\delta P - \frac{2}{\mathrm{Re}}\frac{\partial v_2}{\partial y} = -\frac{\sigma}{\mathrm{Ca}\,\mathrm{Re}}H'', \quad H(\pm R) = 0, \quad \int_{-R}^{R} H dx = 0.$$

Here the prime means the derivative with respect to x, v_2 is expressed via the radial and tangential velocity components v and u, δP is the deviation of pressure from the equilibrium level, σ is the surface tension, and Ca is the capillary number ($\mathrm{Ca} = \varrho_0 v_* \nu/\sigma_0$, which is equal to $\sigma_T T_*/\sigma_0$ if the characteristic quantities are chosen in accordance with [241]).

Results of the numerical study of microconvection in a semicircle with a free boundary

We solved the posed problems for model fluids, such as glycerin and glass and silicon melts, which were conventionally called *Glyc*1, *Glyc*3, and *Sil*, under the action of microaccelerations reached on the orbital station, by using both the conventional model and the microconvection model. The basic parameters of the problem can be found in

Table 9.6: Parameters of free boundary problem.

	Pr	M	Re	Ra	η	ε
*Glyc*1	10^4	$3 \cdot 10^2$	$3 \cdot 10^{-2}$	$1.5 \cdot 10^{-3}$	10^{-1}	$1.2 \cdot 10^{-2}$
*Glyc*3	10^4	1	10^{-4}	$1.5 \cdot 10^{-3}$	10^{-1}	$1.5 \cdot 10^{-2}$
Sil	$4 \cdot 10^{-3}$	1	$2.5 \cdot 10^2$	$2 \cdot 10^{-4}$	1	$2 \cdot 10^{-4}$

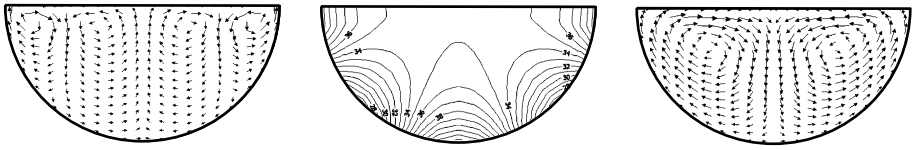

Figure 9.11: Case I; $\gamma = 4$; Oberbeck–Boussinesq model and microconvection model, (a) flow structure for *Glyc*1; (b) family of isotherms for *Glyc*1; (c) flow structure for *Sil*.

Table 9.6. The calculations were performed on the following grids: $(i = 1) : 41 \times 41$, $(i = 2) : 81 \times 81$, and $(i = 3) : 161 \times 161$. The initial data were determined by the semicircle radius $R = 1$ cm. The parameters in the boundary conditions had the following values: $T_B = 70$, $T_B = 150$, $T_0 = 35$, $T_G = 35$, $\bar{T}_G = AT_G$, $A = 10$, $R_* = 0.45$ cm, and $\varphi_* = 1.7\pi$. The necessary dimensionless parameters of the problem are summarized in Table 9.6.

The results for Case I (basic case) *with* $\gamma = 1$ calculated by two alternative models demonstrate only minor quantitative differences and an almost identical qualitative structure of the flow. The steady solution is the structure with one vortex for the fluids *Glyc*3 and *Sil* and the structure with "two small vortices in one" for the fluid *Glyc*1.

During the analysis of Case I, stability of the algorithm and the experimental order of convergence r were checked in a computational experiment by the Runge rule (see [103, 152, 48]) on a sequence of grids. The quantity r_i characterizing the motion intensity for each grid with the number i, or $\max_{n,m} |\psi_{n,m}|$, was calculated. The calculations were performed for the model fluid *Glyc*1: $r_1 = 0.0345$, $r_2 = 0.0303$, and $r_3 = 0.0291$. The experimental order of convergence r and the relative error calculated by eqs. (9.39) were found to be $r \approx 1.8$ and $\bar{\epsilon} \approx 5\,\%$ (relative error in percent).

In the case with $\gamma = 2$, the calculations were performed for *Glyc*1, *Glyc*3, and *Sil*; the flow structure includes two vortices, and the field of isotherms is identical for both mathematical models.

For the case with $\gamma = 4$, Figure 9.11 shows the flow topology and the temperature field. The calculations performed for *Glyc*1 reveal the flow structure with four vortices (Figure 9.11a). Figure 9.11c shows the flow structure with two vortices for the fluid *Sil*. A typical pattern of isotherms is shown in Figure 9.11b. The orders of the dimensionless

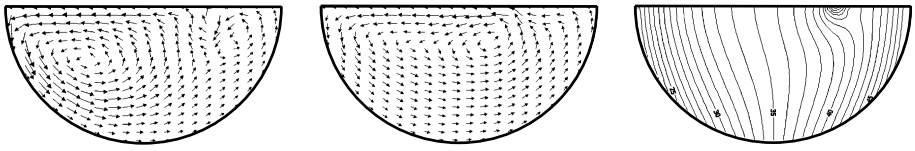

Figure 9.12: Case II; $\gamma = 1$; Oberbeck–Boussinesq model and microconvection model; (a) flow structure for *Sil*; (b) flow structure for *Glyc3*; (c) family of isotherms for *Glyc*3.

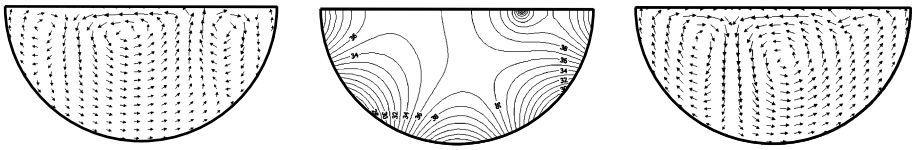

Figure 9.13: Case II; *Sil*; $\gamma = 4$; (a) flow structure; (b) microconvection model and (c) Oberbeck–Boussinesq model; family of isotherms: Oberbeck–Boussinesq model and microconvection model (b).

velocities are $\sim 10^{-2}$ to 10^{0} inside the domain and $\sim 10^{-1}$ on the free surface for *Glyc*1; $\sim 10^{-1}$ to 10^{0} inside the domain and $\sim 10^{0}$ on the free boundary for *Sil*.

Thus, for the basic Case I, there are no qualitative differences in the flow topology predicted by two alternative mathematical models.

Case II includes additional modeling of a rapidly changing temperature field by generating a local singularity of the heat flux on the free boundary.

In the case with $\gamma = 1$, a rather weak singularity of the Gaussian type at $T_B = 70$ is modeled. The differences in results are observed for different fluids. Thus, for *Sil*, we obtained the flow structure with two vortices of the type "two vortices in one," where the small internal vortex is located near the singular point (see Figure 9.12a). For *Glyc*3, both mathematical models demonstrate the flow structure with one vortex (Figure 9.12b). The temperature field calculated for *Glyc*3 is shown in Figure 9.12c. The temperature for *Glyc*3 changes in the interval from 21 to 50 in the Oberbeck–Boussinesq model and from 18.5 to 55 in the microconvection model. The change in temperature for *Sil* occurs in the interval $[25, 45]$ in the Oberbeck–Boussinesq model and in the interval $[21, 50]$ in the microconvection model. The orders of the dimensionless velocities are $\sim 10^{-1}$ to 10^{1} inside the domain and $\sim 10^{1}$ on the free boundary for *Glyc*3; $\sim 10^{-1}$ to 10^{0} inside the domain and $\sim 10^{0}$ on the free boundary for *Sil*.

In the case with $\gamma = 4$, the most pronounced differences in the results predicted by different mathematical models are observed for the fluid *Sil* with the singularity $T_B = 150$. Figure 9.13a shows the flow pattern calculated by the microconvection model. A rather complicated flow structure with two vortices is observed. The large vortex on

the right is the vortex of the "two-vortices-in-one" type. Figure 9.13c shows the flow topology predicted by the Oberbeck–Boussinesq model. In this case, the flow contains two vortices of different sizes, which have approximately identical intensity. The isotherms are plotted in Figure 9.13b. The temperature fields are almost identical. The change in temperature occurs in the interval from 26 to 45 in the Oberbeck–Boussinesq model and from 26 to 49 in the microconvection model. The orders of the dimensionless velocities are $\sim 10^{-2}$ to 10^{0} inside the domain and $\sim 10^{0}$ on the free boundary. The quantitative characteristics obtained by two mathematical models are almost identical. The values of the velocities differ approximately by 15 %.

In considering this Case II, we can conclude that there are certain differences in the results for steady problems predicted by two mathematical models of convection. Modeling of the local singularity of the Gaussian type should be accompanied by a variable temperature regime on the solid boundary (at $\gamma > 1$). The quantitative differences in the flow characteristics calculated by two alternative models are not so significant as in unsteady problems.

The calculations for Case III with a singularity of the heat flux on the solid boundary were performed only for $\gamma = 1$ and $\varphi = 1.7\pi$. There are practically no qualitative differences in the flow structures calculated by two mathematical models. It should be noted that the microconvection model predicts a more intense character of the flow structure with two vortices ("two vortices in one") for the fluid *Glyc*1. For the fluid *Glyc*3, the flow structure with one vortex is obtained in both models, but the vortex center is shifted to the right, toward the "spike" point.

2. Microconvection in an annular domain with a free boundary

Steady gravitational-thermocapillary convection is studied in an annular domain $0 < R_1 \le r \le R_2 < +\infty$, $0 \le \varphi < 2\pi$ for two cases:

- case $I = 0$: the internal circumference $r = R_1$ is the solid boundary with the heat flux through it; the external circumference $r = R_2$ is the free boundary, which is assumed to be thermally insulated;
- case $I = 1$: the external circumference $r = R_2$ is the solid surface with the heat flux through it; the internal circumference $r = R_1$ is the free boundary, which is assumed to be thermally insulated.

The classical Oberbeck–Boussinesq equations of convection and the equations of microconvection of an isothermally incompressible fluid (see eqs. (9.44)–(9.46) and (9.47)–(9.49)) are considered in the dimensionless form in polar coordinates. The characteristic size, velocity, temperature, and pressure are chosen in the form $R_2 - R_1$, $\sigma_T T_* / \mu$, T_*, and $\sigma_T T_* / l$, respectively, where σ_T is the temperature coefficient of surface tension and T_* is the characteristic difference in temperatures (the choice of these characteristic quantities is explained, e. g., in [241]).

Formulation of the problem

For the classical Oberbeck–Boussinesq model, the stream function ψ, vorticity ω, and temperature T in the polar coordinates (r, φ) satisfy system (9.50)–(9.52).

The boundary conditions are formulated in accordance with the cases of considering the domain boundaries.

The boundary conditions in case $I = 0$ have the following form:

1) on the internal boundary of the ring, which is the solid boundary,

$$r = R_1: \quad \psi = 0, \quad \frac{\partial \psi}{\partial r} = 0, \quad \frac{\partial T}{\partial r} = H \cos \varphi, \quad (H = \text{const}), \tag{9.68}$$

2) on the external boundary of the ring, which is the free boundary,

$$r = R_2: \quad \psi = 0, \quad R_2 \omega + 2 \frac{\partial \psi}{\partial r} = -\frac{\partial T}{\partial \varphi}, \quad \frac{\partial T}{\partial r} = 0. \tag{9.69}$$

The boundary conditions in case $I = 1$ have the following form:

1) on the internal boundary of the ring (free boundary),

$$r = R_1: \quad \psi = 0, \quad R_1 \omega + 2 \frac{\partial \psi}{\partial r} = \frac{\partial T}{\partial \varphi}, \quad \frac{\partial T}{\partial r} = 0; \tag{9.70}$$

2) on the external boundary of the ring (solid boundary),

$$r = R_2: \quad \psi = 0, \quad \frac{\partial \psi}{\partial r} = 0, \quad \frac{\partial T}{\partial r} = H \cos \varphi. \tag{9.71}$$

Thus, for system (9.50)–(9.52), we consider the boundary-value problems (9.68), (9.69) or (9.70), (9.71) in cases $I = 0$ or $I = 1$, respectively.

For the microconvection model, the dimensionless equations for the functions ψ, ω, and T in the polar coordinates are written in the form of eqs. (9.59)–(9.61).

The boundary conditions in the microconvection model in case $I = 0$ have the following form:

1) on the internal boundary of the ring, which is the solid boundary,

$$r = R_1: \quad \psi = -R_1 \frac{\varepsilon}{\mathrm{M}} H \sin \varphi,$$
$$\frac{\partial \psi}{\partial r} = \frac{\varepsilon}{\mathrm{M}} \frac{1}{R_1} \frac{\partial T}{\partial \varphi}, \quad \frac{\partial T}{\partial r} = H \cos \varphi, \quad (H = \text{const}); \tag{9.72}$$

2) on the external boundary of the ring, which is the free boundary,

$$r = R_2: \quad \psi = 0, \quad \omega + \frac{2}{R_2} \frac{\partial \psi}{\partial r} = \frac{\partial T}{\partial \varphi} \left(2 \frac{\varepsilon}{\mathrm{M}} \frac{1}{R_2^2} - \frac{1}{R_2} \right), \quad \frac{\partial T}{\partial r} = 0. \tag{9.73}$$

The boundary conditions in case $I = 1$ have the following form:

1) on the internal boundary of the ring (free boundary),

$$r = R_1: \quad \psi = 0, \quad \omega + \frac{2}{R_1}\frac{\partial \psi}{\partial r} = \frac{\partial T}{\partial \varphi}\left(2\frac{\varepsilon}{\mathrm{M}}\frac{1}{R_1^2} - \frac{1}{R_1}\right), \quad \frac{\partial T}{\partial r} = 0; \tag{9.74}$$

2) on the external boundary of the ring (solid boundary),

$$r = R_2: \quad \psi = -R_2\frac{\varepsilon}{\mathrm{M}}H\sin\varphi, \quad \frac{\partial \psi}{\partial r} = \frac{\varepsilon}{\mathrm{M}}\frac{1}{R_2}\frac{\partial T}{\partial \varphi}, \quad \frac{\partial T}{\partial r} = H\cos\varphi. \tag{9.75}$$

For system (9.59)–(9.61), we consider the boundary-value problems (9.72), (9.73) or (9.74), (9.75) for cases $I = 0$ or $I = 1$, respectively.

Corrections to the free boundary can be calculated in the following manner. Let $h(\varphi)$ be the deviation of the free surface from $r = R_1$ (or $r = R_2$); then, at $\mathrm{Ca} = \sigma_T T_*/\sigma_0 \to 0$ and $\mathrm{Ra}/(\mathrm{M}\varepsilon) \to 0$, the condition of the balance of normal stresses on the internal (or external) boundary yields

$$\delta P - 2\frac{\partial v}{\partial r} = \pm\left\{-(T - T_0)\frac{1}{R} - \frac{1}{\mathrm{Ca}}\frac{(h + h'')}{R^2}\right\} - \frac{\mathrm{Ra}}{\mathrm{M}\varepsilon}R\sin\varphi, \quad R = R_1(R_2),$$

where the prime means differentiation with respect to the variable φ, and the quantity δP is the deviation of pressure from the equilibrium level $\delta P_0 = 1/(\mathrm{Ca}\,R)$ at $\sigma_T = 0$ and $g = 0$.

Scheme of the numerical study

For implementation of the numerical algorithm, we introduce a difference grid of the form

$$r_n = R_1 + (n-1)h, \quad n = 1, \ldots, N+1, \quad h = (R_2 - R_1)/N,$$
$$\varphi_m = (m-1)\alpha, \quad m = 1, \ldots, M+1, \quad \alpha = 2\pi/M.$$

The boundary-value problems (9.68), (9.69) and (9.70), (9.71) for systems (9.50)–(9.52) and problems (9.72), (9.73) and (9.74), (9.75) for systems (9.59)–(9.61) are numerically studied by a time-dependent method with the use of a longitudinal-transverse finite-difference scheme similar to (9.66), (9.67). For calculating the temperature (eqs. (9.52) and (9.61)) or vorticity (eqs. (9.50) and (9.59)), the calculation scheme is written in the general form as

$$\frac{U^{k+1/2} - U^k}{0.5\tau} = \tilde{\lambda}_U\left[\Lambda_1 U^k + \Lambda_2 U^{k+1/2}\right] + \lambda_U F^k,$$
$$\frac{U^{k+1} - U^{k+1/2}}{0.5\tau} = \tilde{\lambda}_U\left[\Lambda_1 U^{k+1} + \Lambda_2 U^{k+1/2}\right] + \lambda_U F^k,$$

where the coefficient $\tilde{\lambda}_U$ is equal to the iteration parameter λ_U in the Oberbeck–Boussinesq model and to the iteration parameter multiplied by $(1 + \varepsilon T^k)$ in the microconvection model.

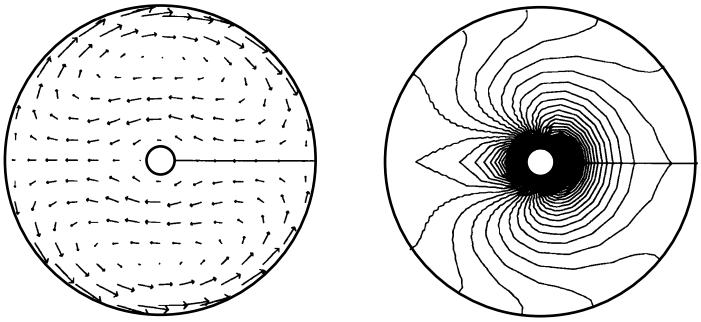

Figure 9.14: Case $I = 0$ (the internal circumference is the solid boundary, and the external circumference is the free boundary).

To solve Poisson's equations (9.51) or (9.60), we use an iterative scheme similar to that described above at each iteration step $t_k = k\tau$ $(k = 1, 2, \ldots)$:

$$\frac{\psi^{s+1/2} - \psi^s}{0.5\tau} = \lambda_\psi(\Lambda_1\psi^{s+1/2} + \Lambda_2\psi^s + \omega^{k+1}),$$
$$\frac{\psi^{s+1} - \psi^{s+1/2}}{0.5\tau} = \lambda_\psi(\Lambda_1\psi^{s+1/2} + \Lambda_2\psi^{s+1} + \omega^{k+1}).$$

This scheme has the iteration parameter λ_ψ and the alternated sequence of sweeping.

We use cyclic sweeping to find $T^{k+1/2}$, $\omega^{k+1/2}$, and ψ^{s+1}, and sweeping with parameters [230, 229] to find ω^{k+1} and $\psi^{s+1/2}$.

Results of the numerical study of microconvection in a ring with a free boundary

The calculations are performed for silicon, glycerin, and glass on 21×21, 41×41, and 81×81 grids. The internal radius is assumed to be $R_1 = 0.1$ cm (in some cases, we used $R_1 = 0.5$ cm), and the external radius is assumed to be $R_2 = 1.1$ cm.

Figures 9.14 and 9.15 show the velocity fields (a) and the families of isotherms (b) for a glycerin-type fluid at $\mathrm{Pr} = 10^4$ and $\mathrm{M} = 3{\cdot}10^2$ $(\mathrm{Re} = 3{\cdot}10^{-2})$. The flow structures and temperature fields presented in these figures are typical for both the microconvection model and for the Oberbeck–Boussinesq model. The calculations show that the velocities predicted by the microconvection model are approximately 20 % higher than the velocities calculated by the Oberbeck–Boussinesq model (the absolute values are compared). For glass-type fluids, and especially for silicon, however, the contours of the isotherms are less deformed and resemble isotherms obtained in calculations of convective flows in domains with fixed boundaries. Figures 9.16 and 9.17 demonstrate the velocity fields (a) and isotherms (b) for silicon, which are typical for both models with the values of the parameters $\mathrm{Pr} = 4 \cdot 10^{-3}$ and $\mathrm{M} = 1$ $(\mathrm{Re} = 2.5 \cdot 10^2)$.

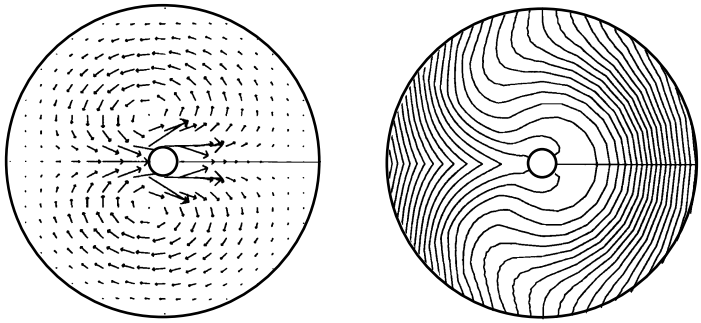

Figure 9.15: Case $I = 1$ (the external circumference is the solid boundary, and the internal circumference is the free boundary).

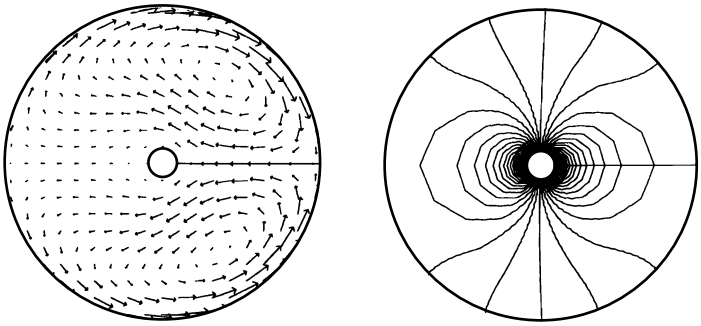

Figure 9.16: Case $I = 0$ (the internal circumference is the solid boundary, and the external circumference is the free boundary).

It is seen from these figures that the vortex centers are shifted to the right in this case.

The dimensionless parameters of the problem are listed in Table 9.7. If the capillary number Ca changes in the interval $10^{-5} \leq \mathrm{Ca} \leq 10^{-2}$ and $\sigma_T \sim 10^{-1}\,\mathrm{g/(s^2{\cdot}K)}$ (see, e. g., [180]), there are only some quantitative differences in flow characteristics calculated by two models.

In all cases, the calculations predict the velocity field structure with two vortices, with a certain displacement of the vortex centers to the left in the cases with glycerin.

Some qualitative and quantitative differences between the calculations performed by two alternative models of convection are manifested at $10^{-5} \leq \mathrm{Ca} \leq 10^{-4}$ and $\sigma_T \sim 10^{-3}$ and $10^{-4}\,\mathrm{g/(s^2{\cdot}K)}$. The parameters used in the numerical simulations are listed in Table 9.8.

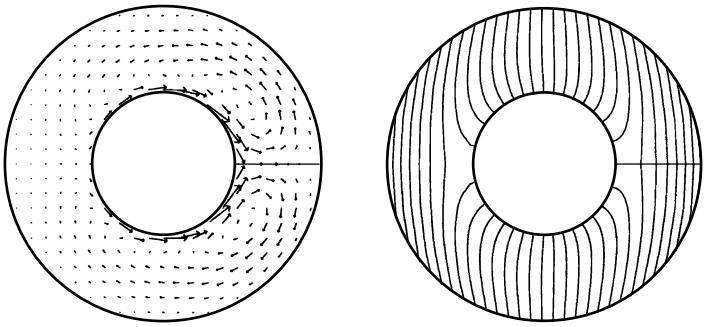

Figure 9.17: Case $I = 1$ (the external circumference is the solid boundary, and the internal circumference is the free boundary).

Figures 9.18 and 9.19 show the velocity fields for $\mathrm{Pr} = 10^4$ and $\mathrm{M} = 1$ ($\mathrm{Re} = 10^{-4}$), which were calculated by two models. For glycerin with the boundary conditions at $I = 0$ (if the external circumference is the free boundary), the microconvection model predicts the structure with two vortices in each semi-circular domain; in contrast to the results predicted by the Oberbeck–Boussinesq model, the vortex centers are shifted toward the internal boundary. At $I = 1$ (Figure 9.19) (if the external circumference is the solid boundary), both models predict a qualitatively identical flow pattern, and there are some quantitative differences, regardless of the internal radius of the computational domain.

It should be noted that the problem of convection stability in domains with free boundaries is a rather interesting one (see, e. g., [140]). The results calculated in [140]

Table 9.7: Basic parameters.

Substance	Pr	M	Re	Ra	η	ε
Glycerin	10^4	$3 \cdot 10^2$	$3 \cdot 10^{-2}$	$1.5 \cdot 10^{-3}$	10^{-1}	$1.5 \cdot 10^{-2}$
Glycerin	10^4	1	10^{-4}	$0.5 \cdot 10^{-5}$	10^{-1}	$0.5 \cdot 10^{-4}$
Glass	10^4	10	10^{-3}	$0.5 \cdot 10^{-6}$	10^{-2}	$4.5 \cdot 10^{-5}$
Silicon	$4 \cdot 10^{-3}$	1	$2.5 \cdot 10^2$	$0.3 \cdot 10^{-7}$	1	$0.3 \cdot 10^{-7}$

Table 9.8: Basic parameters.

Substance	Pr	M	Re	Ra	η	ε
Glycerin	10^4	1	10^{-4}	$1.5 \cdot 10^{-3}$	10^{-1}	$1.5 \cdot 10^{-2}$
Silicon	$4 \cdot 10^{-3}$	1	$2.5 \cdot 10^2$	$2 \cdot 10^{-4}$	1	$2 \cdot 10^{-4}$

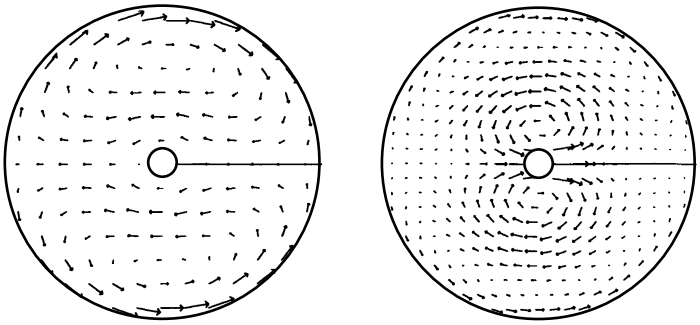

Figure 9.18: Case $I = 0$ (the internal circumference is the solid boundary, and the external circumference is the free boundary). Velocity fields: (a) Oberbeck–Boussinesq model and (b) microconvection model.

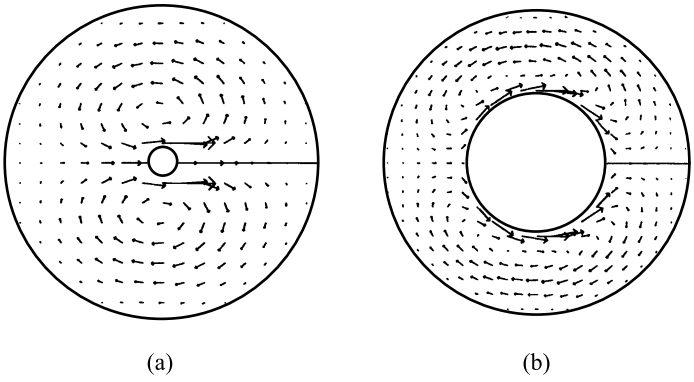

Figure 9.19: Case $I = 1$ (the external circumference is the solid boundary, and the internal circumference is the free boundary); (a) $R_1 = 0.1$ cm, and (b) 0.5 cm.

show that instability can be manifested at greater values of Re and M than those discussed in this section.

9.4 Study of convection induced by volume expansion

Under conditions of weak force fields, the fluid flow structure can form under the action of factors that are insignificant compared to the buoyancy forces under on-ground conditions. In this case, the nature of the forces acting on the fluid can be related to small changes in thermophysical properties of the medium: for example, volume expansion can exert an appreciable effect on fluid convection under certain conditions. A nonuniform distribution of temperature or admixture species in the fluid can induce

actions of this kind and, theoretically, can be the reason for some convective phenomena observed in experiments on board space vehicles [91, 92, 121]. In this section, we consider the results of the numerical study of convection induced by forces of volume expansion of the fluid.

In studying convection under microgravity conditions, research interest in the last decade was aroused by an isothermally incompressible fluid in the case where the dependence of the medium properties on pressure can be neglected. For this case, Pukhnachov [177, 176] determined the limits of applicability of the Oberbeck–Boussinesq approximation at a reduced gravity force with respect to the effect of volume expansion and, using a priori assumptions, constructed a thermal convection model generalizing the Oberbeck–Boussinesq model based on the general principles of mechanics of continuous media (see also [161]). This model became known as the *microconvection model* (MM).

The estimates of the orders of the quantities in the full Navier–Stokes equations and heat transfer equations, as well as the numerical study, show that the contribution of changes in density caused by thermal expansion of the medium to the formation of the velocity field is commensurable with or greater than the contribution of buoyancy forces if the parameter η is rather small, namely [177, 176]

$$\eta = gh^3/(\nu\chi) \le O(1), \tag{9.76}$$

where h is the characteristic linear size, g is the acceleration induced by the external force field, ν is the kinematic viscosity, and χ is the thermal diffusivity of the medium at a certain characteristic temperature. In this case, the Oberbeck–Boussinesq model (OBM) is inapplicable to describe thermal convection. Conditions (9.76) are realistic at a level of microaccelerations reachable on board modern space vehicles. Convective flows formed under conditions (9.76) and usually characterized by velocities of the order of 10 μm/s and smaller are united under the term "microconvection" [176]. Moreover, microconvection can be described by the model of essentially subsonic flows with arbitrary changes in density, which is obtained as the limiting form of the full Navier–Stokes equations and heat transfer equations as the Mach number and the parameter characterizing hydrostatic compressibility tend to zero [120, 44].

In studying microconvection by numerical modeling methods, Goncharova [79, 80] focused her attention on studying the influence of external actions rapidly changing in time, because such actions can induce appreciable changes in the medium density. She considered the flow structure formed in annular [79] and rectangular [80] domains. The results obtained showed that there are significant differences in the predictions of the classical OBM and MM for unsteady regimes. The influence of local spatial singularities of the heat flux through the domain boundary, which model the rapidly changing temperature fields, on gravitational-thermocapillary convection was studied in [82, 78]. Generation of rapidly changing heating conditions was used as a basis

in some experimental investigations on finding and studying the effects of microconvection. Nevertheless, the corresponding methods turned out to be rather complicated and did not allow unique identification of the effect under discussion.

Gaponenko and Zakhvataev [63] proposed the use of spatially nonuniform heating in experiments on microconvection, which allowed them to control the structure and characteristics of convective flows owing to thermal expansion of the medium. Here we consider the influence of spatially periodic heating on formation of microconvection in a rectangular domain and numerically study the dependence of the structure and properties of microconvective flows of this type on physical and geometrical governing parameters.

Microconvection in a single-species fluid with nonuniform heating

We consider two-dimensional microconvective flows of a fluid with an isobaric coefficient of volume expansion β, viscosity μ, thermal conductivity k, and specific heat at constant pressure c_p (the volume viscosity is assumed to be equal to zero); the thermophysical properties mentioned above are assumed to be constant. The fluid fills a rectangular domain $0 \le x \le L$, $0 \le y \le H$ (x, y are the Cartesian coordinates) bounded by impermeable solid walls. The system is located in a constant uniform external force field; the direction of the vector $\mathbf{g}$ of acceleration due to external mass forces coincides with the x axis. The state of the system is described by the density field $\varrho(\mathbf{x}, t)$ at the time t at the point $\mathbf{x} = (x, y)$, velocity field $\mathbf{v}(\mathbf{x}, t) = (v_1, v_2)$, pressure $p(\mathbf{x}, t)$, and deviation of the temperature θ from its characteristic value θ_0 $T(\mathbf{x}, t) = \theta - \theta_0$.

Initially, all walls, except for $y = 0$, are thermally insulated. Beginning from a certain time, a heat flux periodic in space and time

$$T_y = \Theta \cos(\Omega t) \cos(nx\pi/L) \tag{9.77}$$

is instantaneously applied on the domain boundary $y = 0$. Here, Ω is the frequency of variations of the heat flux and n is the number of half-periods of heat flux oscillations. A condition of thermal insulation or condition (9.77) is imposed on the boundary $y = H$. The walls $x = 0, L$ remain thermally insulated.

The state equation is chosen in the form of a linear dependence of specific volume on temperature [177, 176] $\varrho = \varrho_0(1+\beta T)^{-1}$, where $\varrho_0 > 0$ is the characteristic (constant) density and β is the volumetric coefficient of thermal expansion.

The scales of length, velocity, time, and modified pressure and temperature are taken to be h, χ/h, h^2/χ, $\varrho_0\nu\chi/h^2$, and $\Theta H(= \Delta T)$, respectively. As a result, the system of equations in the dimensionless variables takes the form ($0 \le x \le A$, $0 \le y \le 1$):

$$\begin{aligned} \operatorname{div}\mathbf{v} &= \varepsilon\Delta T, \quad \frac{dT}{dt} = (1+\varepsilon T)\Delta T, \\ \frac{d\mathbf{v}}{dt} &= (1+\varepsilon T)\operatorname{Pr}\{-\nabla p + \operatorname{div}\mathbf{D}\} + \varepsilon\eta\operatorname{Pr}\mathbf{e}_3 T, \end{aligned} \tag{9.78}$$

where $\mathrm{Pr} = \nu/\chi$, $A = L/H$ is the aspect ratio, and $\mathbf{D}$ is the Cartesian tensor with the components $D_{ik} = \partial v_i/\partial x_k + \partial v_k/\partial x_i - 2/3\ \delta_{ik}\nabla \cdot \mathbf{v}$; $\mathbf{e}_3 = \mathbf{g}/|\mathbf{g}|$.

Two variants of the boundary conditions for temperature are used. The boundary conditions for one-sided heating have the form

$$x = 0,\ x = A: \quad T_x = 0; \tag{9.79}$$

$$y = 1: \quad qT_y = 0; \quad y = 0: \quad T_y = \cos(\Omega t)\cos(\pi m x/A); \tag{9.80}$$

for two-sided heating, the boundary conditions have the form of eqs. (9.79) and

$$y = 0, 1: \quad T_y = \cos(\Omega t)\cos(\pi m x/A). \tag{9.81}$$

The velocity on the computational domain boundary is subjected to the no-slip condition

$$\mathbf{v} = 0. \tag{9.82}$$

The initial conditions correspond to the equilibrium state

$$t = 0: \quad \mathbf{v} = 0, \quad T = T_0. \tag{9.83}$$

The temperature field is determined by solving the heat-conduction equation $T_{0t} = \Delta T_0$ under the boundary conditions corresponding to the problem considered (9.79)–(9.81).

The results of the numerical study of problem (9.78)–(9.83) are compared with the results for a similar problem in the OBM approximation. The corresponding equations and boundary conditions for the OBM problem can be obtained under the formal assumption $\varepsilon = 0$ in system (9.78), continuity equation, and term $(1 + \varepsilon T)$, in addition to the buoyancy force term.

Equations (9.78) are solved by the finite-difference method, which is described in Section 9.1 and also in [63].

Results of numerical modeling and discussion

The calculations of convective flows are performed for fluids whose parameters are listed in Table 9.9. Model media, such as water H_2O ($N.1$), silicon oils PMS-100 ($N.2$) and PMS-200 ($N.3$) [52] at a temperature of 300 K, and also media with a low Prandtl number, such as melted metal or semiconductor ($N.4$), are considered. The spatial scale H is assumed to be equal to 1 cm. The dimensionless angular frequency ω' of oscillations of the heat flux through the boundary is taken to be equal to unity. The mechanisms of formation of microconvective flows and the dependence of their structure and properties on the governing parameters in the presence of an unsteady spatially periodic distribution of heat fluxes on the boundary of the closed domain occupied by the fluid were studied.

Table 9.9: Physical parameters of model media.

	χ, cm^2/s	β, K^{-1}	Pr
N.1	0.001518	0.0002	5.4
N.2	0.001098	0.001	838
N.3	0.001120	0.001	1625
N.4	0.49	$7.5 \cdot 10^{-6}$	0.0054

The basic parameter of the problem, which reflects the comparative influence of the buoyancy forces and volume expansion, is the Galileo number (microconvection parameter [177, 176]), $\eta = R/\varepsilon$.

Absence of external forces. Basic mechanism

The effect of thermal expansion of the fluid is most pronounced in the absence of external force fields. In this case, the only external factor capable of inducing macroscopic motion is the unsteady nonuniform thermal action on the cavity walls, and the emergence of convection is related only to thermal expansion of the fluid. The mechanism of development of the microconvective flow operates as follows. The effect of thermal expansion reflected by the right-hand side of eq. (9.5), $\beta\chi\Delta T$, induces the emergence of the flow as a necessary condition of mass conservation. In turn, the fact that ΔT differs from zero is caused both by unsteady changes in temperature with time and by the configuration of the temperature and velocity fields such that $\mathbf{v}\cdot\nabla T$ differs appreciably from zero in some parts of the domain occupied by the fluid.

Effect of the microconvection parameter η

In experiments performed on board modern space vehicles, the parameter η can differ from zero. Numerical calculations confirm that the effect of thermal expansion dominates if η is sufficiently small, in accordance with eq. (9.1). Typical flow structures calculated by the MM and OBM are shown in Figure 9.20 for the parameters $\eta = 0.01$, $\varepsilon = 7.5 \cdot 10^{-4}$, and Pr = 0.0054. The figures show the isolines of the temperature field at the initial time (Figure 9.20a), the symmetric velocity field with two vortices, which is typical for the OBM (Figure 9.20b), and the velocity fields predicted the MM at the times t_1 (Figure 9.20c), t_2 (d), and t_3 (Figure 9.20e). The vector of acceleration due to the external force field is directed along the x axis. Figure 9.21 shows the time evolution of the quantity $T_y(x = 0)$ (Figure 9.21a) and of the maximum velocity for the microconvection model (Figure 9.21b).

Figure 9.21 also shows the time instants t_1, t_2, and t_3 corresponding to the flow structures illustrated in Figure 9.20 for the MM. The results show that the MM predicts regimes of a unidirectional flow from the heated to the cooled regions, which are induced by volume expansion (Figure 9.20c, e). Such flows are formed at time instants

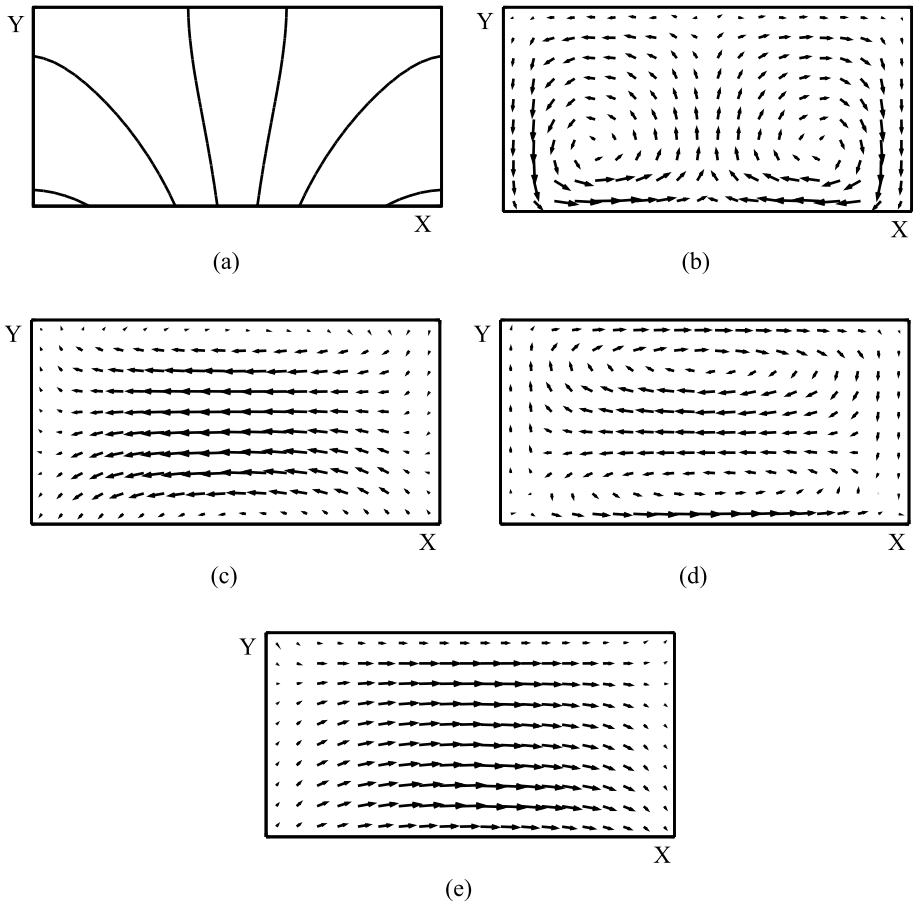

Figure 9.20: Isolines of temperature (a) and velocity fields for the Oberbeck–Boussinesq model (b) and microconvection model (c, d, e) at different time instants.

when the temperature field exhibits the most pronounced dynamic changes and the flow has the maximum velocity (see Figure 9.21). It is only when the time-dependent heat flux through the boundary is close to its extreme value that the flow structure with two vortices is formed (Figure 9.20d), where the compressed fluid leaves the region with a greater density, by virtue of the continuity equation (Figure 9.20c–e). Qualitative differences in the flow structures calculated by the MM and OBM are obvious; in the OBM, a symmetric structure with two vortices (Figure 9.20b) is formed only under the action of buoyancy forces; the vortex centers stay almost at the same place as the temperature field changes with time, but the direction of vortex rotation changes.

In addition, the maximum velocities calculated by these models are appreciably different, especially at low values of η. The maximum velocities for fluid $N.4$ at $A = 2$, $n = 1$, and $\Theta = 100$ K/cm are given in Table 9.10.

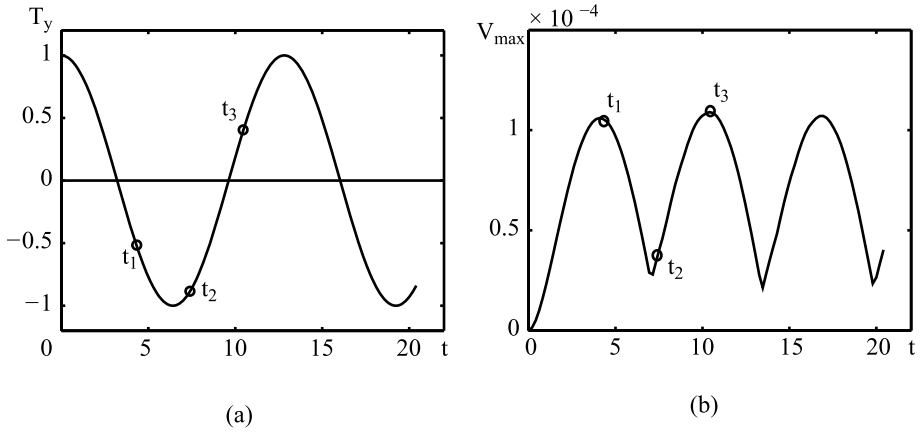

Figure 9.21: Time evolution of the heat flux T_y at $x = 0$ (a) and maximum velocity V_{max} (b).

Table 9.10: Maximum velocity V_{max}, cm/s.

Model	$\eta = 0.01$	$\eta = 1$
MM	$1.09 \cdot 10^{-4}$	$1.10 \cdot 10^{-4}$
OBM	$3.55 \cdot 10^{-9}$	$3.57 \cdot 10^{-7}$

Influence of the spatial structure of the external heat flux on the microconvective flow

The dominating effect on the microconvective flow structure is exerted by the character of spatial nonuniformity of the external temperature field. Let us consider the influence of the number n of half-periods of oscillations of the temperature gradient on the wall on the qualitative and quantitative characteristics of microconvection.

Figure 9.22 shows the results of the calculation of the flow of fluid $N.4$ with the number of half-periods of oscillations of T_y on the wall equal to $n = 5$ at $\eta = 0.01$, $A = 5$, and $\varepsilon = 7.5 \cdot 10^{-4}$.

Figure 9.22 shows the isolines of temperature (a) and the velocity field (b). If the aspect ratio A is sufficiently large, then one half-period of oscillations of T_y usually generates one cell with two vortices in the fluid. Therefore, there are five structures with two vortices in Figure 9.22, each induced by one half-period of oscillations of the heat flux on the boundary. The calculations show that the flow velocity decreases with increasing n. For instance, for fluid $N.4$, we have $V_{max} = 6.05 \cdot 10^{-4}$ ($n = 1$), $1.8 \cdot 10^{-4}$ ($n = 2$), and $1.9 \cdot 10^{-5}$ ($n = 5$) cm/s (note that the maximum difference in temperature over the domain decreases with increasing n).

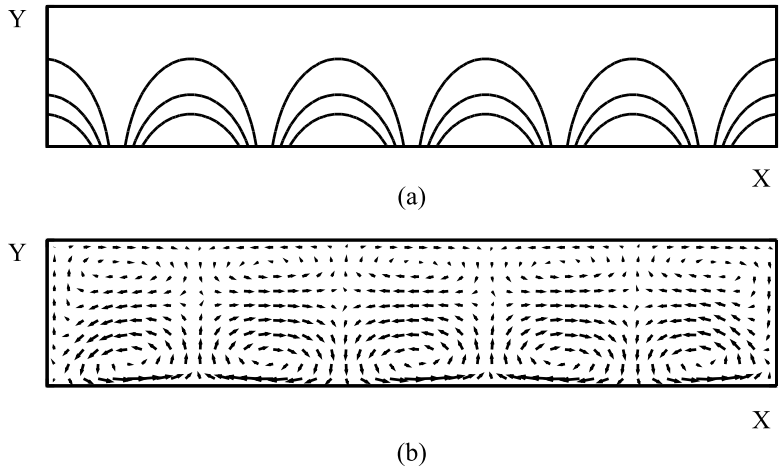

Figure 9.22: Isolines of (a) temperature and (b) velocity field. The vector of acceleration due to the external force field is directed along the *x* axis.

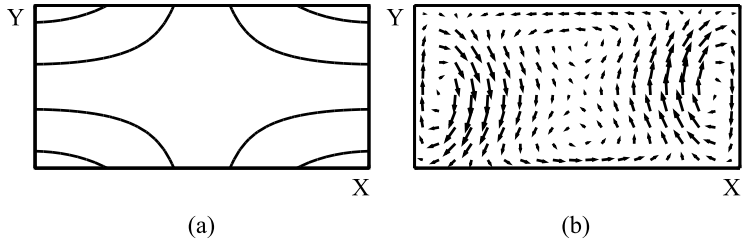

Figure 9.23: Temperature isolines (a) and velocity field (b). The vector of acceleration due to the external force field is directed along the *x* axis.

Two-sided heating

The influence of two-sided heating on the flow structure is illustrated in Figure 9.23, which shows the results calculated for fluid $N.4$ (with the boundary conditions (9.79), (9.81)) during one half-period of heat flux oscillations $n = 1$ at $\eta = 0.01$, $A = 2$, and $\varepsilon = 7.5 \cdot 10^{-4}$. The figure shows the temperature isolines (a) and velocity field (b). A change in the temperature field alters the flow structure in the microconvection model. As shown in Figure 9.23, a structure with four vortices is formed in the cavity, and the most intense vortices are observed near the thermally insulated walls, i. e., in those places where the temperature field has a large gradient (which is seen from condensation of the temperature isolines). The maximum velocity, however, decreases: $V_{\max} = 3.02 \cdot 10^{-5}$ cm/s, whereas $V_{\max} = 1.09 \cdot 10^{-4}$ cm/s for the structure with one vortex. The reason is a smaller difference in temperature, as compared with one-sided heating.

Effect of the aspect ratio A on the microconvective flow

Numerical calculations show that an increase in the aspect ratio leads to an increase in the maximum velocity. Thus, for fluid $N.4$, this increase is $V_{\max} = 1.89 \cdot 10^{-5}, 1.09 \cdot 10^{-4}$, and $6.04 \cdot 10^{-4}$ cm/s for $A = 1, 2,$ and 5, respectively. This effect is related to the increase in specific power of heating and difference in temperature over the domain, which also increases with increasing A. Moreover, for different values of A, the formation of the flow structure with two vortices in the microconvection model occurs at different times: the greater the value of A, the later the instant of formation of this structure, compared to the instant when the heat flux reaches the extreme value on the boundary. This can be related to flow inertia, which prevents instantaneous thermal expansion as the heat flux on the boundary changes its direction to the opposite one.

The results calculated for fluids $N.1$, $N.2$, and $N.3$ differ only quantitatively. The maximum physical velocities $V_{\max}$ for these fluids at $\eta = 0.01$, $n = 1$, and $\Theta = 50$ K/cm are given in Table 9.11.

Thus, for typical substances and geometric configurations of physical systems used in experiments on convection under microgravity conditions and space material science, we considered the effect of thermal expansion of the fluid on convection at extremely low Rayleigh numbers, which is related to spatial nonuniformity of the thermal field on the reservoir boundary. Based on numerical results obtained in [63], we can conclude that the spatial nonuniformity of the external thermal field can contribute to convection in experiments with accelerations reachable on modern space vehicles, which are lower than the on-ground acceleration by a factor of 10^5 to 10^6, and this contribution is appreciably different from that predicted by the Oberbeck–Boussinesq model.

At the same time, microconvection phenomena can be effectively studied in experiments under conditions of spatial nonuniformity of heating. This approach supplements the approach based on using external actions rapidly changing in time [80]. The approach proposed in [63] has the advantage of forming configurations of physical systems which facilitate the emergence of stable, easily predictable qualitative changes in convection modes generated by thermal expansion of the fluid.

Table 9.11: Maximum velocity $V_{\max}$, cm/s.

Fluid	$A = 1$	$A = 2$
$N.1$	$7.82 \cdot 10^{-7}$	$5.23 \cdot 10^{-6}$
$N.2$	$2.31 \cdot 10^{-6}$	$1.65 \cdot 10^{-5}$
$N.3$	$2.53 \cdot 10^{-6}$	$1.83 \cdot 10^{-5}$

Microconvection of a binary mixture

Gaponenko and Zakhvataev [62] studied microconvective flows of a nonisothermal binary fluid mixture subjected to the Soret effect. The study of natural convection in media with gradients of two and more characteristics with different coefficients of molecular diffusion (temperature, concentrations of chemical species) is interesting for many laboratory and engineering processes. On the other hand, interaction of the gradients of these characteristics forming the distribution of mass density in the gravity field generates convection modes that are much more versatile in terms of their spatial structure, dynamics, and conditions and mechanisms of evolution in time than in the single-species case.

Let us now assume that the physical system is a Newtonian isotropic fluid consisting of two nonreacting species located in an external force field. Let $\mathbf{x} = (x_1, x_2)$ be the Cartesian coordinates, $\varrho_k(\mathbf{x}, t)$ be the mass density of the species k ($k = 1, 2$) at the point $\mathbf{x}$ at the time t, and $\mathbf{v}_k(\mathbf{x}, t)$ be the velocity of the species k. The state of the system is described by the total density field $\varrho(\mathbf{x}, t)$, field of velocity of the center of mass of the fluid element $\mathbf{v}(\mathbf{x}, t) = (v_1, v_2)$, pressure $p^* = p^*(\mathbf{x}, t)$, absolute temperature $\theta(\mathbf{x}, t)$, and mass concentration of one of the species $c(\mathbf{x}, t)$,

$$\varrho = \varrho_1 + \varrho_2; \quad \mathbf{v} = \frac{\varrho_1 \mathbf{v}_1 + \varrho_2 \mathbf{v}_2}{\varrho}; \quad c = \frac{\varrho_1}{\varrho}.$$

The density of the diffusion flux of the substance $\mathbf{J}_c$ is determined as $\mathbf{J}_c = -k_c(\nabla c - \alpha \nabla \theta)$, where the constant coefficients k_c and α characterize diffusion and thermal diffusion (thus, k_c/ϱ is the coefficient of molecular diffusion).

The state equation is taken in the form of a linear dependence of the specific volume of the fluid not only on changes in temperature, but also on changes in chemical species concentrations:

$$\varrho = \varrho_0(1 + \beta T + \gamma C)^{-1}, \quad T = \theta - \theta_0, \quad C = c - c_0. \tag{9.84}$$

After normalization, the equations of convection of a nonisothermal binary mixture can be presented in the form (details of system derivation are described in [62], and also in Section 9.1)

$$\begin{aligned} \operatorname{div} \mathbf{v} &= \varepsilon(1 - s\,\mathrm{Le})\Delta T + \varepsilon\,\mathrm{Le}\,\Delta C, \\ \frac{d\mathbf{v}}{dt} &= (1 + \varepsilon T + \varepsilon C)\,\mathrm{Pr}\{-\nabla p + \operatorname{div} \mathbf{D}\} + \varepsilon\eta\,\mathrm{Pr}\,\mathbf{e}_3(T + C), \\ \frac{dC}{dt} &= (1 + \varepsilon T + \varepsilon C)\,\mathrm{Le}(\Delta C - s\Delta T), \\ \frac{dT}{dt} &= (1 + \varepsilon T + \varepsilon C)\Delta T, \end{aligned} \tag{9.85}$$

where $\mathrm{Le} = \delta/\chi$ is the Lewis number, $\delta = k_c/\varrho_0$ is the diffusion coefficient, and $s = -\alpha\gamma/\beta$ is the separation ratio.

Based on the estimates obtained in [62], we can conclude that the Oberbeck–Boussinesq approximation is inapplicable to describe natural convection under the condition

$$\eta \frac{1+\xi}{1+\xi\,\mathrm{Le}} \le O(1), \tag{9.86}$$

where $\xi = \gamma C_*(\beta T_*)^{-1}$ is the ratio of the characteristic accelerations due to buoyancy forces, which are induced by nonuniformity of the concentration and temperature fields, and C_* is the characteristic difference in concentrations. Under the condition $\mathrm{Le} \ll 1$, which is typical for water solutions and many other liquid solutions, we have $\eta(1+\xi) \le O(1)$ instead of eq. (9.86). If, in addition, $\xi = O(1)$, which is typical for many liquid solutions with changes in concentrations induced by the Soret effect, then the Boussinesq approximation becomes physically invalid under the condition $\eta \le O(1)$. The last condition of applicability of the Boussinesq approximation is similar to the case of a single-species fluid [177].

Results of numerical modeling and discussion

Let us consider two basic problems of microconvection in a rectangular domain $0 \le x \le l$, $0 \le y \le h$ bounded by impermeable solid walls. In the first problem, the domain is insulated: $T_y = 0$ at $y = 0, h$, $T_x = 0$ at $x = 0, l$, and the initial data correspond to a contact of two media with different constant values of temperature and concentration:

$$T = T_1, \quad C = C_1 \quad (0 \le x \le l/2); \quad T = T_2, \quad C = C_2 \quad (l/2 \le x \le l);$$
$$\mathbf{v} = 0 \quad (0 \le x \le l,\ 0 \le y \le h).$$

(A similar problem for an isothermal binary mixture was considered in [161].) In the second problem, a heat flux periodic in time is imposed on the upper and lower boundaries of the domain: $T_y = \Theta\cos(\Omega t)$ at $y = 0, h$, $T_x = 0$ at $x = 0, l$, and the initial conditions correspond to the equilibrium state.

After normalization, the boundary conditions take the form

$$\begin{aligned}
&x = 0: && \mathbf{v} = 0, \quad T_x = 0, && C_x = 0;\\
&x = A: && \mathbf{v} = 0, \quad T_x = 0, && C_x = 0;\\
&y = 0, 1: && \mathbf{v} = 0, \quad T_y = f(t), && C_y = sf(t).
\end{aligned}$$

We have $f(t) \equiv 0$ for the first problem and $f(t) = \cos(\Omega t)$ for the second problem (Ω is the dimensionless frequency).

In problem 1, the initial values of temperature and concentration responsible for the discontinuity of these quantities at $t = 0$ in the middle of the domain $x = A/2$ are defined as 0.5 and −0.5. The vector of external forces is directed along the x axis, $\mathbf{l} = (1, 0)$. The linear size l along the x axis is 1 cm.

In problem 2, the following distributions of the temperature and concentration fields are specified at the time $t = 0$: $T = y - 0.5$ and $C = s(y - 0.5)$. The vector is $\mathbf{l} = (0, 1)$.

For integrating the system of equations, we use a numerical method of calculating microconvective flows in the variables $\omega - \psi$, which was proposed in [80] and was generalized to the case of a binary nonisothermal system. A description of this numerical method can be found in Section 9.1.

Below we present the results obtained in [62] by studying the influence of the governing parameters Ω, ε, Le, and s on the microconvection characteristics at $\eta = 1$, Pr = 13.48, and $A = 2$.

Results of the numerical study of problem 1

The flow structure in problem 1 is determined by volume expansion of the fluid related to the temperature and concentration distributions in the computational domain and has a unidirectional character until thermodynamic equilibrium is established. The process of flow formation at $\varepsilon = 7.5 \cdot 10^{-3}$, $s = 0.38$, and Le $= 0.01$ is illustrated in Figure 9.24, which shows the velocity field and the distributions of temperature and concentration at the time instants $t = 10^2$ (a), $2 \cdot 10^3$ (b), and $14 \cdot 10^3$ (c).

At small values Le ~ 0.01, the concentration field changes much more slowly than the temperature field; therefore, the flow is formed at the initial time mainly owing to changes in the temperature field (Figure 9.24a). When the temperature equilibrium is established in the domain (as seen in Figure 9.24b, c) that the temperature is close to zero in the entire domain, the main factor affecting the microconvective flow is the change in the concentration field. For this reason, more intense convection is observed in regions of more pronounced changes in concentration. In Figure 9.24b we see that the flow structure formation in the middle part of the domain is consistent with the concentration distribution at the time instant considered. Thus, the presence of two characteristics with different coefficients of molecular diffusion in the system leads to the emergence of new qualitative and quantitative effects, as compared with microconvection in a single-species medium.

Figure 9.25 shows the influence of Le on the time evolution of the maximum velocity of the microconvective flow in the computational domain at $\varepsilon = 7.5 \cdot 10^{-3}$ and $s = 0.38$. It is seen that the microconvective flow exists for a longer time than in a pure fluid with decreasing Le. This result completely agrees with the analysis of the exact solution [62].

Figure 9.26 shows the time evolution of the convective flux of the substance F for different values of Le in the cross section $x = 1.8$, where F is determined as

$$F = \int_0^H (\rho \mathbf{v} C)\, dy.$$

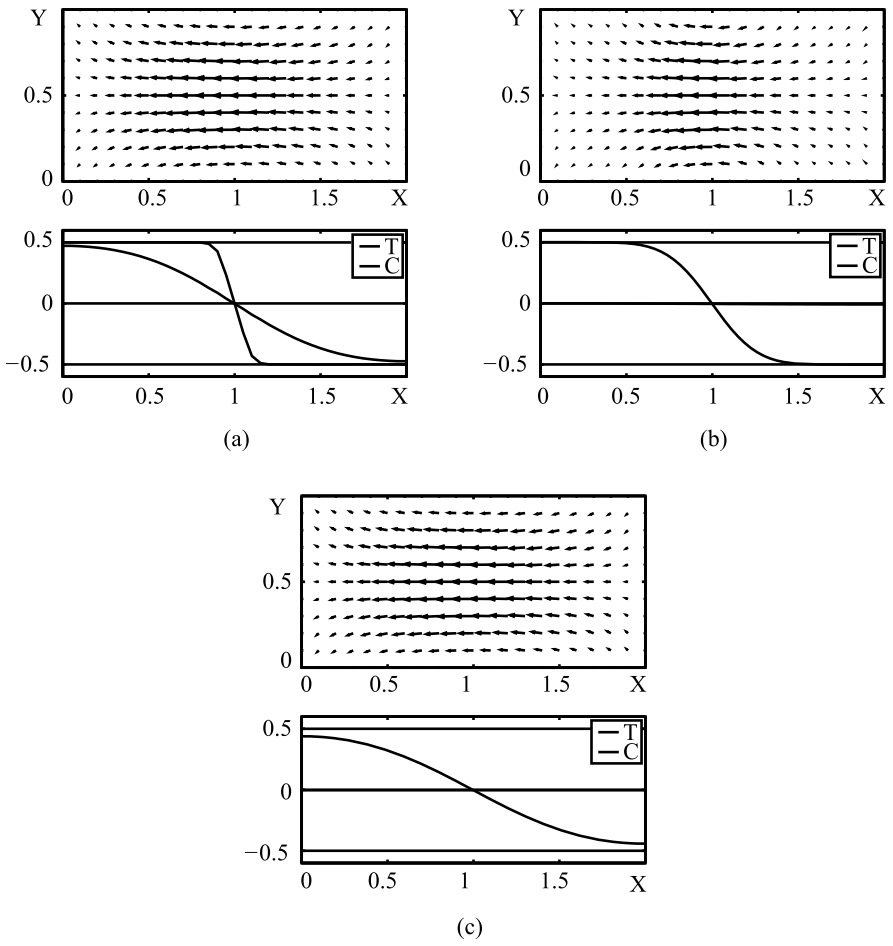

Figure 9.24: Field of velocities and distributions of temperature and concentration along the x axis for different time instants.

For Le ≤ 0.01, it is possible to identify a short-time initial peak of the convective flux of the substance due to thermal expansion and a second peak of F, which is less intense, but more extended, due to changes in the concentration field. A change in Le leads to a change in the intensity and duration of each of these segments. At small values of Le, the concentration field changes in time too slowly, which results in separation of the temperature and concentration effects on the velocity field and, as a consequence, in a second peak of the convective flux. For values of Le close to unity, the second peak of F is absent because the equilibrium states of the concentration and temperature fields are established more or less simultaneously.

The calculated results also show that an increase in the Boussinesq number ε within the framework of problem 1 leads to a proportional increase in the characteris-

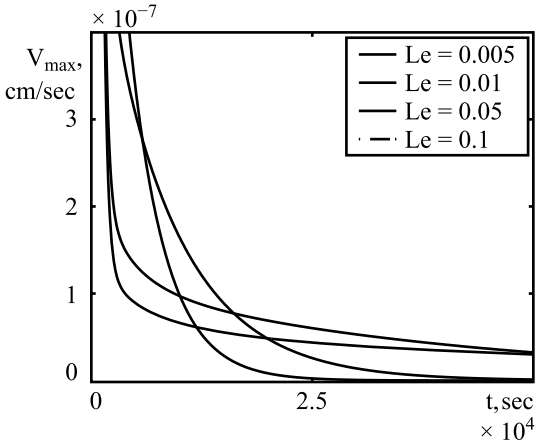

Figure 9.25: Time evolution of the maximum velocity V_{max} for different values of Le.

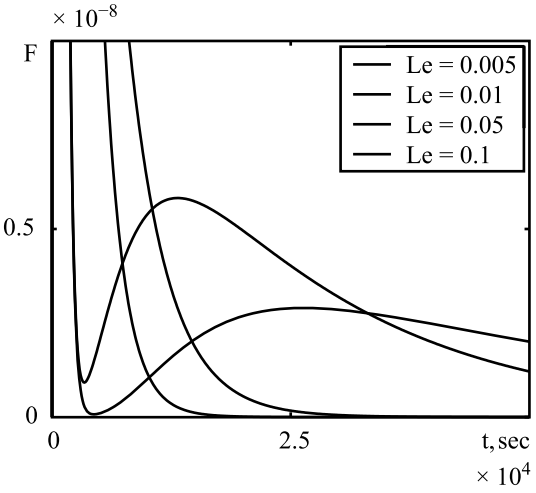

Figure 9.26: Dependence of F [g/(cm s)] on time.

tic velocity in the domain, and an increase in the thermodiffusion parameter s leads to a minor increase in flow intensity (less than 5 % for $s = 1.9$ as compared with $s = 0.38$).

Results of the numerical study of problem 2

The second problem considered in this chapter deals with the influence of unsteady heat fluxes on the flow characteristics in binary nonisothermal systems. As in problem 1, the flow structure is formed here mainly under the action of volume expansion forces.

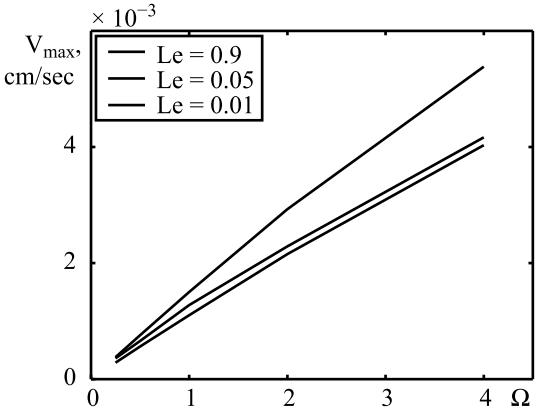

Figure 9.27: Maximum velocity V_{max} vs. the dimensionless frequency Ω.

Figure 9.27 shows the maximum flow velocity as a function of the dimensionless frequency Ω at $\varepsilon = 7.5 \cdot 10^{-3}$, $s = 0.38$, and different values of Le. The microconvection intensity increases with increasing frequency of variations of the external heat flux, and this dependence is close to linear. Similar results are obtained under a pulsed (in time) action of the external heat flux. Thus, if the pulse amplitude is inversely proportional to its duration, then the maximum velocity of microconvection increases in proportion to the pulse amplitude.

The results presented in Figure 9.27 also show that the characteristic velocity of microconvection in unsteady temperature fields increases with increasing Lewis number Le.

In addition to the parameter determining the rate of variations of the external temperature actions, the Boussinesq parameter ε has a significant effect on the microconvective flow. If the external action frequency is sufficiently large, the calculations predict that an increase in ε leads to an approximately linear increase in the maximum velocity of convection.

The influence of the parameters s and Le on microconvection is illustrated in Figure 9.28, which shows a typical dependence of the maximum flow velocity on the separation ratio s for different values of Le at $\varepsilon = 7.5 \cdot 10^{-3}$, and $\Omega = 1$. The results demonstrate that the characteristic velocity of the microconvective flow increases in proportion to s. Moreover, it also increases with increasing Le.

In addition to the basic problems described above, we also studied microconvective effects for other system configurations. Significant qualitative and quantitative differences in the transitional and limiting convection modes calculated by the Oberbeck–Boussinesq and microconvection models were found at low values of $\eta \leq$ 10–100 in wide ranges of the orders of the governing parameters: $\varepsilon = 10^{-6}$–10^{-1}, $\mathrm{Pr} = 10^{-3}$–10^{4}, $\mathrm{Le} = 10^{-4}$–1, $s = -3$–3. At sufficiently small values of η, the mechanism based on volume expansion dominates, and buoyancy forces do not exert any

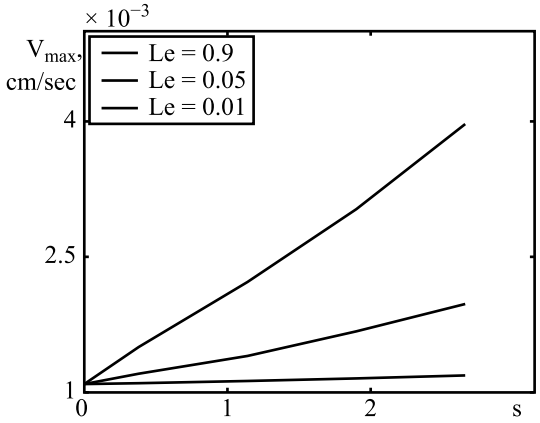

Figure 9.28: Maximum velocity V_{max} versus the separation ratio s for different values of Le.

appreciable influence on convection evolution. For such values of η, the flow structure calculated by the microconvection model is qualitatively different from the Boussinesq convection, and the characteristic velocities of microconvection for the parameter values corresponding to those reached in space experiments can exceed the values predicted by the Oberbeck–Boussinesq model by two orders of magnitude. At the same time, the temperature and concentration fields do not exhibit essential differences from the classical case. These results are similar to conclusions obtained for microconvection in a single-species fluid [79, 80].

Microconvection in thin layers of a binary fluid with a free boundary

The microconvection model constructed in [177] is used to describe convective flows with low values of the microconvection parameter η. In previous sections we considered convective flows where the MM applicability condition ($\eta < 1$) was satisfied, owing to the small gravity force. Another possible example of using this model is the flow in fluid layers with microscopic values of the characteristic linear size l (which is involved into the parameter η as a multiplier to the third power). In this case, the condition $\eta < 1$ is satisfied even at $g = g_0$, where g_0 is the acceleration due to the gravity force on the Earth surface.

An important application of such flows is the case of thin layers of the fluid with a free boundary. Because of the small value of l (and, as a consequence, $\eta \ll 1$), it is possible to neglect the effect of the gravity force and to consider interaction of two basic factors in the fluid: volume expansion and surface tension (Marangoni convection).

The study of convective flows in a fluid with a free boundary with the use of the microconvection model was performed previously in [82, 83, 78]. Problems in cylindrical domains for a single-species fluid with different temperature regimes on the boundary were considered. Qualitative and quantitative differences in results predicted by the

MM and OBM were found already at characteristic sizes of the domain of the order of 1 cm, and the Marangoni numbers were sufficiently high.

Gaponenko [61] considered a convective flow in a rectangular domain with a free boundary in a binary fluid mixture with allowance for the Soret effect. In this case, the nonuniformity of the temperature distribution gives rise to flows induced by volume expansion and gradients of surface tension forces. The free boundary was assumed to be flat and nondeformable. The study of convective flows was performed for microsystems with the characteristic linear size of the order of several micrometers with the use of two models of the fluid: classical OBM and MM. Let us consider some results.

Formulation of the problem and governing equations

The convective flows are studied in a rectangular domain $0 \le x \le l$, $0 \le y \le h$. The following boundary conditions for temperature are considered:

B1: spatially nonuniform heat flux $T_x = \Theta \cos(y\pi/h)$ on the boundaries $x = \text{const}$. The domain boundaries $y = \text{const}$ are assumed to be thermally insulated;

B2: spatially nonuniform heat flux $T_y = \Theta \cos(x\pi/l)$ on the boundary $y = 0$. In this case, the conditions of thermal insulation are imposed on all other boundaries of the domain.

The boundary conditions for concentrations are determined from the condition of a zero diffusion flux of the substance on the boundary. The conditions for velocity on the boundary $y = h$ are the conditions of a free nondeformable surface:

$$\mu \frac{\partial v_1}{\partial y} = \sigma_T \frac{\partial T}{\partial x} + \sigma_c \frac{\partial c}{\partial x}, \quad v_2 = 0.$$

Here, $\sigma_T(\sigma_c)$ is the temperature (concentration) coefficient of surface tension and μ is the dynamic viscosity coefficient. All other boundaries are subjected to the no-slip condition: $\mathbf{v} = 0$.

After normalization, the boundary conditions take the form

$$\begin{aligned}
&\text{B1}: \quad x = 0, x = A: \quad \mathbf{v} = 0,\ T_x = \cos(y\pi), C_x = sT_x.\\
&\qquad y = 0: \quad \mathbf{v} = 0,\ T_y = 0, C_y = 0;\\
&\qquad y = 1: \quad \frac{\partial v_1}{\partial y} = \mathrm{M_T}\frac{\partial T}{\partial x} + \mathrm{M_c}\frac{\partial c}{\partial x}, \quad v_2 = 0, \quad T_y = 0, \quad C_y = 0;\\
&\text{B2}: \quad x = 0,\ x = A: \quad \mathbf{v} = 0,\ T_x = 0,\ C_x = 0.\\
&\qquad y = 0: \quad \mathbf{v} = 0,\ T_y = \cos(x\pi/A),\ C_y = sT_y;\\
&\qquad y = 1: \quad \frac{\partial v_1}{\partial y} = \mathrm{M_T}\frac{\partial T}{\partial x} + \mathrm{M_c}\frac{\partial c}{\partial x}, \quad v_2 = 0, \quad T_y = 0, \quad C_y = 0.
\end{aligned}$$

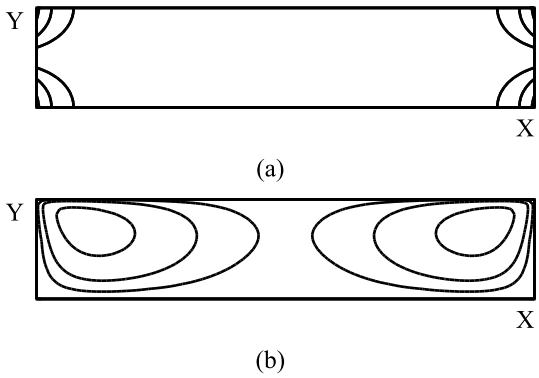

Figure 9.29: Temperature isolines (a) and stream functions (b) for the Oberbeck–Boussinesq microconvection model (condition B1).

In these equations, M_T and M_c are the temperature and concentration Marangoni numbers: $M_T = \sigma_T T^* l/(\mu\chi)$ and $M_c = \sigma_c C^* l/(\mu\chi)$, and $A = l/h$ is the aspect ratio of the computational domain sides.

The system of MM equations for a binary mixture has the form of eqs. (9.85). It is solved by using the variables ω–ψ (vorticity–stream function) for the modified velocity. The main computational procedures are described in Section 9.1.

Results of numerical modeling and discussion

The results presented here were calculated for a model fluid with the parameters taken at a temperature of 300 K: $\chi = 0.00112\,\mathrm{cm}^2/\mathrm{s}$, $\mu = 1.758\,\mathrm{g/(cm{\cdot}s)}$, $\varrho = 0.996\,\mathrm{g/cm}^3$, $\beta = 0.005\,\mathrm{K}^{-1}$, $\sigma_T = -0.08\,\mathrm{dyn/(cm{\cdot}K)}$, Pr = 1625, and Le = 0.01. The gradient of the temperature Θ, the parameter ε, and the Marangoni numbers M_T and M_c were determined on the basis of the characteristic linear size of the domain and the value of T^*. The condition $M_c = 0.5M_T$ was conventionally chosen. The values of the separation ratio were taken in the interval $s = 0$–1.5.

Figures 9.29, 9.30, and 9.31 show the results of flow calculations for the boundary conditions B1 and parameters $\varepsilon = 0.005$ and $T^* = 1\,\mathrm{K}$. The characteristic linear size l was 10, 1, and 0.1 μm ($M_T = -4.063{\cdot}10^{-2}, 10^{-3}$, and 10^{-4}, respectively). The aspect ratio was $A = 5$. The influence of thermodiffusion was ignored ($s = 0$).

The figures show the temperature fields (Figure 9.29a, step between the isolines 0.1), isolines of the stream function of the physical velocity for the OBM (Figure 9.29b), and also the flow structures predicted by the MM (Figure 9.30). Note that the temperature and concentration fields for two models are practically identical, in contrast to the velocities and flow structures. In the OBM, the flow structure and the maximum velocity ($V = 1.26 \cdot 10^{-3}$) remained unchanged as l was varied. Vice versa, the results predicted by the MM show that both the flow structure and the maximum velocity sub-

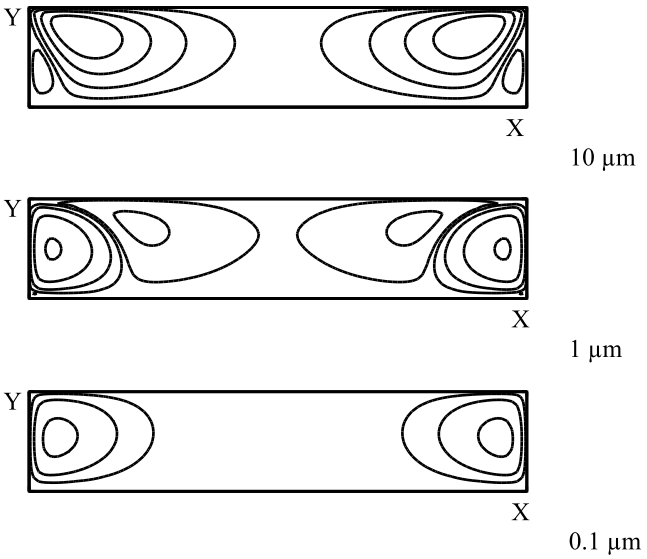

Figure 9.30: Isolines of the stream function for the Oberbeck–Boussinesq microconvection model (condition B1).

stantially depend on l: $1.32 \cdot 10^{-3}$ ($L = 10$ μm), $2.86 \cdot 10^{-3}$ (1 μm), and $29.97 \cdot 10^{-3}$ cm/s (0.1 μm).

It is seen that the dominating factor at low values of l is the volume expansion of the fluid caused by changes in the temperature and concentration fields; the influence of this factor is attenuated with increasing l. Therefore, the flow structures and the maximum velocities in the MM and OBM become close to each other.

Figure 9.31 shows the time evolution of the maximum velocity in the computational domain for different models. It is seen that the maximum velocity in the MM is appreciably higher than that in the OBM. This effect, however, lasts for a short time, and its duration is determined by the value of ε. The maximum velocity in the MM approaches the value predicted by the OBM with time.

Figure 9.32 demonstrates the estimated influence of thermodiffusion on the maximum velocity for $M_T = -4.063 \cdot 10^{-2}$ (a) and $M_T = -4.063 \cdot 10^{-4}$ (b) under the boundary conditions B1. As is seen from the figure, the effect of the separation ratio substantially depends on the Marangoni number M_T. At large values of M_T (i. e., those at which the influence of volume expansion is insignificant), the thermodiffusion effect is more pronounced (see Figure 9.32a), because the concentration gradient along the free boundary increases with increasing s; therefore, the action of surface tension leads to more intense convection. At small values of M_T (Figure 9.32b), there is only a short-time effect of thermodiffusion, which is mainly related to the changes in the concentration field at the initial time, leading to enhancement of the influence of volume expansion owing to the concentration component.

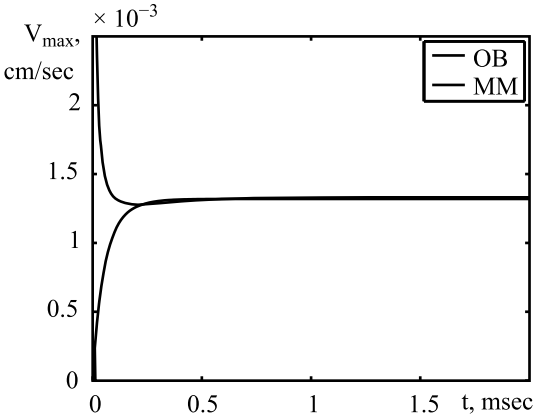

Figure 9.31: Time evolution of the maximum velocity predicted by the OBM and MM (condition B1).

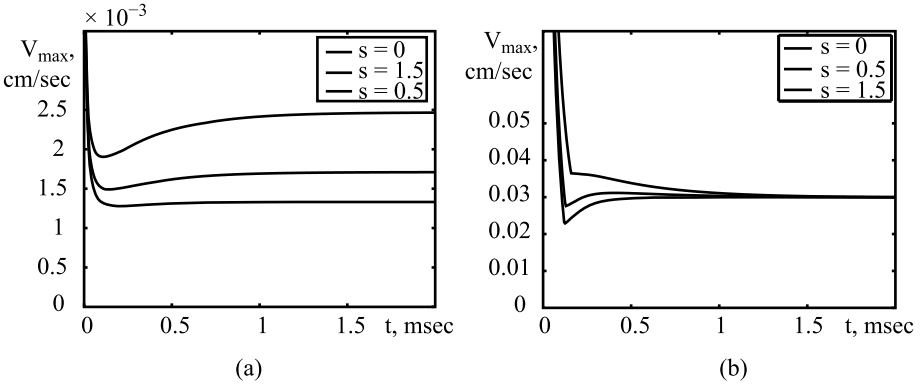

Figure 9.32: Effect of the separation ratio s on the maximum velocity.

Figure 9.33 shows the results of flow calculations under the boundary conditions B2 and parameters $\varepsilon = 0.005$ and $T^* = 1\,\mathrm{K}$. The characteristic linear size h was $0.1\,\mu\mathrm{m}$ ($\mathrm{M} = -4.063 \cdot 10^{-4}$). The figure shows the isolines of the temperature field (a) (the step between the isolines is 0.4), and the isolines of the stream function of the physical velocity predicted by the OBM (b) and MM (c). Under the boundary conditions B2, the value $h = 0.1\,\mu\mathrm{m}$ is the greatest value at which the differences between the OBM and MM results are still observed. In this case, the maximum velocity is $1.29 \cdot 10^{-2}$ (OBM) and $1.33 \cdot 10^{-2}$ (MM).

Thus, based on the results presented in this section we can conclude that convective flows can form in thin layers of the fluid with a free boundary under the action of volume expansion, which is taken into account in the microconvection model. In fluids with inhomogeneous compositions, the thermodiffusion effect should be additionally taken into account.

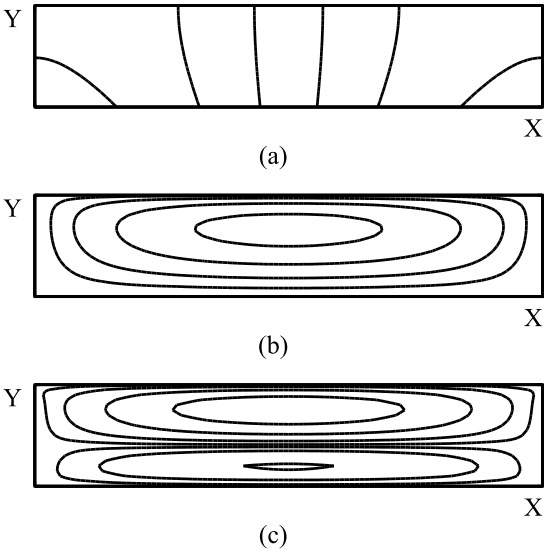

Figure 9.33: Temperature isolines (a) and stream functions (b and c) under the condition of nonuniform heating from above (condition B2).

9.5 Convection in miscible fluids

It is well known that the emergence of fluid flows can depend on processes that occur in domains close to the interface between the fluids. For instance, capillary forces arising on the interface in immiscible fluids can lead to convection. Beginning in the 19th century, such processes for immiscible fluids have been intensity studied because of numerous applications.

Capillary phenomena are much less adequately investigated in miscible fluids, where the thermodynamically stable interface between the phases does not exist and the system tends to a homogeneous equilibrium state by means of diffusion. In 1901, Korteweg assumed that such effects could also be observed for miscible fluids with a nonuniform distribution of density (concentration or temperature). The interface of miscible fluids is characterized by the presence of regions with high concentration gradients, which can exist for long times at low diffusion coefficients (in this case, it would be more correct to say the "transitional zone" instead of the "interface"). As was demonstrated in [111], stresses σ_K can arise in such zones; the action of these stresses is similar to the action of surface tension. Such stresses were estimated in [242] as

$$\sigma_K = K\frac{(\Delta C)^2}{\delta}, \tag{9.87}$$

where K is a parameter characterizing the intensity of the arising stress, C is the con-

centration of mass of one species, ΔC is a typical change in concentration inside the transitional zone, and δ is the transitional zone thickness.

Convection induced by such stresses in binary systems was studied both experimentally and theoretically [24, 4, 163, 164, 102]. Numerical simulations of convective flows in binary systems were considered in [167, 34], where the main task was to define the initial concentration distribution in a manner such that the resultant flow structure would be most convenient for conducting a full-scale experiment.

It should be noted that the volume forces arising in the transitional zone of miscible fluids are very small; therefore, the convective flow induced by such forces is suppressed by natural convection under standard conditions. Thus, it is obvious that this phenomenon should be studied under microgravity conditions on board space laboratories. Optimal configurations for physical experiments on studying convection in miscible fluids were considered in [34].

This model describes various capillary phenomena, in particular, capillary waves, which are formed when the curvature of the interface between two fluids changes in space, thus, generating a difference in pressure. Below we study waves called interphase waves to distinguish them from capillary waves. These waves also refer to capillary phenomena, but have different manifestations and propagation mechanisms.

Let us consider a flat interphase surface between two fluids and assume that the thickness of this surface changes in space. Then, the effective interphase stress (9.87), which is inversely proportional to the interface thickness and therefore also changes in space, generates forces directed along the interface. These forces can change the interface shape and initiate convection in the neighboring fluid. This effect is experimentally observed if the effective stress (9.87) is locally changed by adding a chemical substance or heating the interface, which alters the interface thickness or the amount of the admixture inside the transitional zone.

In this section we describe the results [26], which show that interphase waves can be described by the Navier–Stokes equations with additional terms of Korteweg's stress. To study such a problem, we seek a numerical solution of a simplified model problem and also of a problem posed in a plane geometrical formulation. The model problem is obtained by using the thickness of the transitional zone of the interface as a small parameter. As a result, we can reduce the initial plane problem dimension, study its properties and its solutions in detail, for example, for analyzing the fluid behavior on the interface. A numerical study of the model problem reveals the existence of interphase waves. They propagate with a velocity proportional to the interface stress and can reflect from the walls, thus, changing their direction, penetrate into each other, or intersect each other.

Qualitatively identical results were obtained for the problem in the plane geometrical formulation, but in this case the waves decay faster due to the influence of the interface boundaries.

Formulation of the problem and governing equations

In the problems considered below, the physical system is under isothermal conditions. The system is a viscous weakly compressible fluid consisting of two nonreacting species. The fluid fills a rectangular domain $0 \le x \le L_x$, $0 \le y \le L_y$ whose boundary Γ consists of solid impermeable walls (x and y are the Cartesian coordinates). The influence of buoyancy forces is ignored.

Assuming the viscosity and diffusion coefficients to be constant, we write the expression for the components of the Korteweg's stress tensor $\mathbf{S}$ arising in the transitional zone between the two fluid species [24]:

$$S_{11} = \left(\frac{\partial C}{\partial y}\right)^2, \quad S_{12} = S_{21} = -\frac{\partial C}{\partial x}\frac{\partial C}{\partial y}, \quad S_{22} = \left(\frac{\partial C}{\partial x}\right)^2.$$

Taking into account the above-described factors acting on the system, we can present the convection equations in the form

$$\begin{gathered} \varrho \frac{dC}{dt} = k_c \nabla^2 C, \\ \varrho \frac{d\mathbf{v}}{dt} = -\nabla p + \frac{\mu}{3}\nabla(\operatorname{div}\mathbf{v}) + \mu\Delta\mathbf{v} + K\operatorname{div}\mathbf{S}, \\ \frac{d\varrho}{dt} + \varrho\operatorname{div}\mathbf{v} = 0. \end{gathered} \tag{9.88}$$

The state equation is taken as a dependence of the fluid density ϱ on concentration $\varrho = \varrho_0(1 - \gamma(C - C_0))$, where $\varrho_0 > 0$ is the characteristic value of density, γ is the concentration coefficient of density, and C_0 is the constant mean value of concentration.

Using the Boussinesq approximation, passing to dimensionless variables, and choosing h, h^2/ν, ν/h, $\varrho_0\nu^2/h$, and C_* as the scales of length, time, velocity, pressure, and characteristic change in concentration, we obtain the following system of equations from eqs. (9.88):

$$\begin{gathered} \frac{dC}{dt} = \mathrm{Sc}^{-1}\Delta C, \\ \frac{d\mathbf{v}}{dt} = -\nabla p + \Delta\mathbf{v} + K_c\operatorname{div}\mathbf{S}, \\ \operatorname{div}\mathbf{v} = 0. \end{gathered} \tag{9.89}$$

Here, the dimensionless variables are denoted in the same manner as the dimensional ones. The dimensionless parameters are defined as $\mathrm{Sc} = \nu/d$, $K_c = K(C_*)^2/(\varrho_0\nu^2)$, where $\nu = \mu/\varrho_0$ is the kinematic viscosity and $d = k_c/\varrho_0$ is the diffusion coefficient.

The boundary conditions are the no-slip condition for the fluid on the solid boundaries and the absence of the substance flux through the boundary:

$$\mathbf{v} = 0, \quad \nabla C_n|_\Gamma = 0. \tag{9.90}$$

Model problem

Let us consider a simplified problem where the fluid motion is studied only inside the transitional zone. In this case, as was shown in [26], it is possible to formulate the problem and study the properties of its solution with a smaller number of variables than in the initial full system of equations. For this purpose, we write eqs. (9.89) in the form

$$\frac{\partial C}{\partial t} + u_1 \frac{\partial C}{\partial x} + u_2 \frac{\partial C}{\partial y} = d\Delta C, \tag{9.91}$$

$$\frac{\partial u_1}{\partial t} + u_1 \frac{\partial u_1}{\partial x} + u_2 \frac{\partial u_1}{\partial y} = -\frac{1}{\varrho} \frac{\partial p}{\partial x} + \nu \Delta u_1 - K \frac{\partial C}{\partial x} \Delta C, \tag{9.92}$$

$$\frac{\partial u_2}{\partial t} + u_1 \frac{\partial u_2}{\partial x} + u_2 \frac{\partial u_2}{\partial y} = -\frac{1}{\varrho} \frac{\partial p}{\partial y} + \nu \Delta u_2 - K \frac{\partial C}{\partial y} \Delta C, \tag{9.93}$$

$$\frac{\partial u_1}{\partial x} + \frac{\partial u_2}{\partial y} = 0. \tag{9.94}$$

We align the orthogonal coordinate axes x and y so that the x axis is directed along the transitional zone separating the miscible fluids, and the y axis is perpendicular to it. In order to study the solution behavior inside the transitional zone, we extend the domain along the y axis by introducing an internal variable $\eta = y/\varepsilon$. Equating terms of the order of ε, we find from eq. (9.91) that C is a linear function of η; we assume that $C = \eta z(x,t)$. Equation (9.91) is presented in the form

$$\frac{\partial z}{\partial t} + u_1 \frac{\partial z}{\partial x} + u_2 z \frac{1}{\varepsilon \eta} = d \frac{\partial^2 z}{\partial x^2}. \tag{9.95}$$

As follows from eq. (9.93), u_2 is also a linear function of η. In addition, we assume that the last term in the left-hand side of eq. (9.95) is also a quantity of the order of ε. Otherwise the concentration does not satisfy the equation of motion. We thus have $u_2 = \varepsilon \eta w(x,t)$, and eq. (9.95) takes the form

$$\frac{\partial z}{\partial t} + u_1 \frac{\partial z}{\partial x} + wz = d \frac{\partial^2 z}{\partial x^2}. \tag{9.96}$$

Substituting the expression for u_2 into eq. (9.93), we obtain

$$\frac{\partial w}{\partial t} + u_1 \frac{\partial w}{\partial x} + w^2 = -\frac{1}{\eta \varepsilon^2 \varrho} \frac{\partial p}{\partial \eta} + \nu \frac{\partial^2 w}{\partial x^2} - \frac{K}{\varepsilon^2} z \frac{\partial^2 z}{\partial x^2}. \tag{9.97}$$

We transform the resultant equation. An analysis of the last term in the right-hand side of this equation allows us to conclude that the value of K is proportional to ε^2. We assume that $K = \varepsilon^2$. The pressure p is presented as a sum of two terms, one of which is independent of η: $p = \varrho(p_1(x,y,t) + \pi(x,t))$. Taking into account eq. (9.94), we find that $\partial u_1/\partial x$ is also independent of η. Let us assume that $u_1 = u(x,t) + \phi(\eta)$. In this case, we

obtain $\phi = 0$ from eq. (9.96) under the condition that $\partial z/\partial x \neq 0$. Then, from eq. (9.92) we find the equation for the function u (see eq. (9.99) below) and also the equation

$$\frac{\partial p_1}{\partial x} + \varepsilon^2 \eta^2 \frac{\partial z}{\partial x} \frac{\partial^2 z}{\partial x^2} = 0.$$

As z is independent of η, we can conclude that p_1 has the second order with respect to η. Let us assume that $p_1 = \varepsilon^2 \eta^2 G(x,t)/2$.

We obtain the following system of equations:

$$\frac{\partial z}{\partial t} + u \frac{\partial z}{\partial x} + wz = d \frac{\partial^2 z}{\partial x^2}; \tag{9.98}$$

$$\frac{\partial u}{\partial t} + u \frac{\partial u}{\partial x} = -\frac{\partial \pi}{\partial x} + \nu \frac{\partial^2 u}{\partial x^2}; \tag{9.99}$$

$$\frac{\partial G}{\partial x} + 2 \frac{\partial z}{\partial x} \frac{\partial^2 z}{\partial x^2} = 0; \tag{9.100}$$

$$\frac{\partial w}{\partial t} + u \frac{\partial w}{\partial x} + w^2 = -G + \nu \frac{\partial^2 w}{\partial x^2} - z \frac{\partial^2 z}{\partial x^2}; \tag{9.101}$$

$$\frac{\partial u}{\partial x} + w = 0. \tag{9.102}$$

The same system can be derived if we seek for the solution of eqs. (9.91)–(9.94) in the form

$$u_1 = u(x,t), \quad u_2 = yw(x,t), \quad C = \frac{y}{\sqrt{K}} z(x,t),$$

$$p = \varrho\left(\frac{1}{2} y^2 G(x,t) + \pi(x,t)\right)$$

and equate terms with identical powers of y.

Integrating eq. (9.100), we obtain

$$G(x,t) = G_0(t) - \left(\frac{\partial z}{\partial x}\right)^2. \tag{9.103}$$

Assuming that

$$F = -\frac{\partial \pi}{\partial x} - z \frac{\partial z}{\partial x},$$

we present system (9.98)–(9.102) in the form

$$\frac{\partial z}{\partial t} + u \frac{\partial z}{\partial x} - z \frac{\partial u}{\partial x} = d \frac{\partial^2 z}{\partial x^2}; \tag{9.104}$$

$$\frac{\partial u}{\partial t} + u \frac{\partial u}{\partial x} - z \frac{\partial z}{\partial x} = F + \nu \frac{\partial^2 u}{\partial x^2}; \tag{9.105}$$

$$\frac{\partial F}{\partial x} = G_0 + 2\left(\left(\frac{\partial u}{\partial x}\right)^2 - \left(\frac{\partial z}{\partial x}\right)^2\right). \tag{9.106}$$

Thus, the model problem is problem (9.91)–(9.94) in the band $0 \le x \le 1$, $-\infty < y < \infty$ with the boundary conditions $x = 0, 1:\ u_1 = u_2 = 0$, $\partial c/\partial x = 0$. The boundary conditions for the new variables are

$$x = 0, 1:\ u = 0, \quad \frac{\partial u}{\partial x} = 0, \quad \frac{\partial z}{\partial x} = 0. \tag{9.107}$$

System (9.104)–(9.107) contains unknown functions z, u, and F. It includes two second-order equations, one first-order equation, and six boundary conditions. The function $G_0(t)$ is defined in a manner that the boundary conditions are satisfied.

Numerical method of solving the model problem

To obtain a numerical solution, we write system (9.103)–(9.106) in the form

$$\frac{\partial z}{\partial t} + u\frac{\partial z}{\partial x} - z\frac{\partial u}{\partial x} = d\frac{\partial^2 z}{\partial x^2}; \tag{9.108}$$

$$\frac{\partial u}{\partial t} + u\frac{\partial u}{\partial x} - z\frac{\partial z}{\partial x} = F_0 + xG_0 + M + \nu\frac{\partial^2 u}{\partial x^2}; \tag{9.109}$$

$$M = 2\int_0^1 \left[\left(\frac{\partial u}{\partial x}\right)^2 - \left(\frac{\partial z}{\partial x}\right)^2\right] dx. \tag{9.110}$$

Let us consider numerical discretization of system (9.108)–(9.110). For this purpose, we introduce a uniform grid x_i $(i = 1, \dots, N)$ with a step $\Delta x = 1/(N-1)$. In solving the system of equations, we use the finite-difference scheme

$$\begin{aligned}&\frac{z_i^{n+1} - z_i^n}{\tau} + \frac{u_i^n + |u_i^n|}{2\Delta x}\left(z_i^{n+1} - z_{i-1}^{n+1}\right) + \frac{u_i^n - |u_i^n|}{2\Delta x}\left(z_{i+1}^{n+1} - z_i^{n+1}\right)\\ &\quad - z_i^n\frac{u_{i+1}^{n+1} - u_{i-1}^{n+1}}{2\Delta x} = d\frac{z_{i+1}^{n+1} - 2z_i^{n+1} + z_{i-1}^{n+1}}{\Delta x^2};\end{aligned} \tag{9.111}$$

$$\begin{aligned}&\frac{u_i^{n+1} - u_i^n}{\tau} + \frac{u_i^n + |u_i^n|}{2\Delta x}\left(u_i^{n+1} - u_{i-1}^{n+1}\right) + \frac{u_i^n - |u_i^n|}{2\Delta x}\left(u_{i+1}^{n+1} - u_i^{n+1}\right)\\ &\quad - z_i^n\frac{z_{i+1}^{n+1} - z_{i-1}^{n+1}}{2\Delta x} = \nu\frac{u_{i+1}^{n+1} - 2u_i^{n+1} + u_{i-1}^{n+1}}{\Delta x^2} + F_0 + x_iG_0 + M_i^n.\end{aligned} \tag{9.112}$$

Here, the subscript i refers to discretization in space, and the superscript n refers to discretization in time.

To solve system (9.111)–(9.112), we use the method of vector sweeping [205]. We give the general scheme of implementation of this method, which was proposed in [26]. Let

$$\mathbf{x}_i = \begin{pmatrix} u_i \\ z_i \end{pmatrix}; \tag{9.113}$$

$$\mathbf{y} = \begin{pmatrix} F_0 \\ G_0 \end{pmatrix}. \tag{9.114}$$

We present system (9.111)–(9.112) in the form

$$u_1 = 0, \quad u_N = 0; \tag{9.115}$$

$$-\mathbf{C}_1 \cdot \mathbf{x}_1 + \mathbf{B}_1 \cdot \mathbf{x}_2 + \mathbf{D}_1 \cdot \mathbf{y} = -\mathbf{e}_1; \tag{9.116}$$

$$\mathbf{A}_i \cdot \mathbf{x}_{i-1} - \mathbf{C}_i \cdot \mathbf{x}_i + \mathbf{B}_i \cdot \mathbf{x}_{i+1} + \mathbf{D}_i \cdot \mathbf{y} = -\mathbf{e}_i, \quad i = 2, \dots, N-1; \tag{9.117}$$

$$\mathbf{A}_N \cdot \mathbf{x}_{N-1} - \mathbf{C}_N \cdot \mathbf{x}_N + \mathbf{D}_N \cdot \mathbf{y} = -\mathbf{e}_N. \tag{9.118}$$

In the case considered, we have

$$\mathbf{B}_1 = \mathbf{C}_1 = \mathbf{A}_N = \mathbf{C}_N = \mathbf{I}, \quad \mathbf{D}_1 = \mathbf{D}_N = 0, \quad \mathbf{e}_1 = \mathbf{e}_N = 0,$$

$$\mathbf{A}_i = \begin{pmatrix} \frac{\nu}{\Delta x^2} + \frac{u_i^n + |u_i^n|}{2\Delta x} & -\frac{z_i^n}{2\Delta x} \\ -\frac{z_i^n}{2\Delta x} & \frac{d}{\Delta x^2} + \frac{u_i^n + |u_i^n|}{2\Delta x} \end{pmatrix},$$

$$\mathbf{B}_i = \begin{pmatrix} \frac{\nu}{\Delta x^2} - \frac{u_i^n - |u_i^n|}{2\Delta x} & \frac{z_i^n}{2\Delta x} \\ \frac{z_i^n}{2\Delta x} & \frac{d}{\Delta x^2} - \frac{u_i^n - |u_i^n|}{2\Delta x} \end{pmatrix},$$

$$\mathbf{C}_i = \begin{pmatrix} \frac{2\nu}{\Delta x^2} + \frac{1}{\Delta t} + \frac{|u_i^n|}{\Delta x} & 0 \\ 0 & \frac{2d}{\Delta x^2} + \frac{1}{\Delta t} + \frac{|u_i^n|}{\Delta x} \end{pmatrix},$$

$$\mathbf{D}_i = \begin{pmatrix} 1 & (i-1)\cdot\Delta x \\ 0 & 0 \end{pmatrix}, \quad \mathbf{e}_i = \frac{\mathbf{x}_i^n}{\Delta t} + \begin{pmatrix} M_i^n \\ 0 \end{pmatrix}.$$

System (9.116)–(9.118) consists of N equations and $N+1$ variables. It is solved in three stages.

First stage: transformation of system (9.116)–(9.118) from the tetradiagonal to the tridiagonal form. Let

$$\mathbf{x}_{i-1} = \mathbf{F}_i \cdot \mathbf{x}_i + \mathbf{H}_i \cdot \mathbf{y} + \mathbf{g}_i, \quad i = 2, \dots, N. \tag{9.119}$$

It follows from eqs. (9.116) and (9.119) that

$$\mathbf{F}_2 = \mathbf{C}_1^{-1} \cdot \mathbf{B}_1, \quad \mathbf{g}_2 = \mathbf{C}_1^{-1} \cdot \mathbf{e}_1, \quad \mathbf{H}_2 = \mathbf{C}_1^{-1} \cdot \mathbf{D}_1. \tag{9.120}$$

Further, using eqs. (9.117) and (9.119), we obtain

$$\mathbf{F}_{i+1} = (\mathbf{C}_i - \mathbf{A}_i \cdot \mathbf{F}_i)^{-1} \cdot \mathbf{B}_i; \tag{9.121}$$

$$\mathbf{g}_{i+1} = (\mathbf{C}_i - \mathbf{A}_i \cdot \mathbf{F}_i)^{-1} \cdot (\mathbf{A}_i \cdot \mathbf{g}_i + \mathbf{e}_i); \tag{9.122}$$

$$\mathbf{H}_{i+1} = (\mathbf{C}_i - \mathbf{A}_i \cdot \mathbf{F}_i)^{-1} \cdot (\mathbf{A}_i \cdot \mathbf{H}_i + \mathbf{D}_i), \quad i = 1, \dots, N-1. \tag{9.123}$$

Using eqs. (9.118) and (9.119), we find

$$\mathbf{x}_N = (\mathbf{C}_N - \mathbf{A}_N \cdot \mathbf{F}_N)^{-1} \cdot (\mathbf{A}_N \cdot \mathbf{H}_N + \mathbf{D}_N) \cdot \mathbf{y} + (\mathbf{C}_N - \mathbf{A}_N \cdot \mathbf{F}_N)^{-1} \cdot (\mathbf{A}_N \cdot \mathbf{g}_N + \mathbf{e}_N). \tag{9.124}$$

Thus, the transformation of the system from the tetradiagonal form (9.116)–(9.118) to the tridiagonal form (9.119), (9.124) is finalized.

Second stage: transformation of system (9.119), (9.124) from the tridiagonal to the bidiagonal form. Let

$$\mathbf{x}_i = \mathbf{Q}_i \cdot \mathbf{y} + \mathbf{p}_i, \quad i = N, \dots, 1. \tag{9.125}$$

It follows from eq. (9.124) that

$$\mathbf{Q}_N = (\mathbf{C}_N - \mathbf{A}_N \cdot \mathbf{F}_N)^{-1} \cdot (\mathbf{A}_N \cdot \mathbf{H}_N + \mathbf{D}_N); \tag{9.126}$$

$$\mathbf{p}_N = (\mathbf{C}_N - \mathbf{A}_N \cdot \mathbf{F}_N)^{-1} \cdot (\mathbf{A}_N \cdot \mathbf{g}_N + \mathbf{e}_N). \tag{9.127}$$

From eqs. (9.119) and (9.125), we obtain

$$\mathbf{Q}_{i-1} = \mathbf{F}_i \cdot \mathbf{Q}_i + \mathbf{H}_i, \quad \mathbf{p}_{i-1} = \mathbf{F}_i \cdot \mathbf{p}_i + \mathbf{g}_i, \quad i = N, \dots, 2. \tag{9.128}$$

Third stage. Using eqs. (9.115) and (9.125), we find $\mathbf{y}$ on the computational domain boundaries $i = 1, N$:

$$\mathbf{y} = \begin{pmatrix} Q_{(11)1} & Q_{(12)1} \\ Q_{(11)N} & Q_{(12)N} \end{pmatrix}^{-1} \cdot \begin{pmatrix} -p_{(1)1} \\ -p_{(1)N} \end{pmatrix}. \tag{9.129}$$

After that, using eqs. (9.125) and (9.129), we determine $\mathbf{x}_i$ for $i = 1, \dots, N$.

Numerical results of the model problem

Here we describe the results of numerical modeling of problem (9.104)–(9.107). The initial conditions for the functions u and z have the form $u = 0, z = f + \exp(-k(x-0.5)^2)$, which corresponds to the case with a local change in the concentration gradient in the transitional layer of a quiescent miscible fluid.

Figure 9.34a–c shows the time evolution of the z-component of the solution for $f = 0$ and $k = 100$. If the values of d and ν are sufficiently large, the perturbations rapidly decay, and the solution takes the form of a spatially homogeneous distribution (Figure 9.34a). If d remains unchanged and ν is sufficiently small, the solution consists of two waves which propagate in the opposite directions, reflect from the walls, move toward each other, and then repeat this process periodically with a gradual decrease in their amplitudes (Figure 9.34c). If d is much smaller than ν, the wave structure differs from the previous case. The solution evolves in the same manner at the beginning, but the sign of the transported perturbations becomes different after wave reflections from the walls: the minimum of the quantity z is observed rather than its maximum (Figure 9.34b).

Figures 9.35 and 9.36 show the concentration isolines $C = yz$ and the stream functions $\psi = yu$ in the time interval where the solution interacts with the domain

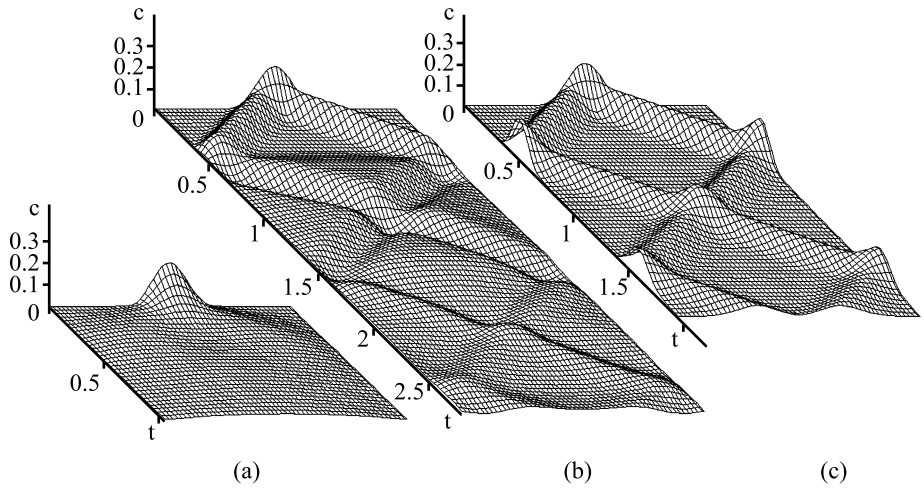

Figure 9.34: Evolution of the solution: (a) $d = 10^{-2}$, $v = 10^{-2}$; (b) $d = 10^{-5}$, $v = 10^{-3}$; (c) $d = 10^{-2}$, $v = 10^{-3}$.

boundaries for the first time. The isolines of the functions show the instants before (Figure 9.35) and after (Figure 9.36) wave reflections from the walls for different values of d. Note that the linear dependence on y, chosen as the form in which the solution is sought, implies that the stream function isolines are not closed. For the case with $v < d$, (Figure 9.35a) displays two vortices propagating to the opposite sides from the domain center. When they reach the computational domain boundary, they are reflected from the boundary and simultaneously change the directions of their rotation (Figure 9.36a). Then, returning to the domain center, the vortices interact with each other, thereby vanishing; after that, the vortices are formed again and propagate to the opposite sides. This process is periodically repeated with a gradual decrease in amplitude.

At $v > d$ (Figures 9.35b and 9.36b), the vortices propagate in the same manner, but there are four vortices in the vicinity of the domain boundary, two vortices on each side (Figure 9.35b).

The values of the parameters f and k used in the initial conditions for the function z can also affect the solution behavior. Figure 9.37 shows $z(x,t)$ as a function of f: $f = 1$ (a) and $f = 2$ (b) (the remaining calculation parameters have the values $k = 500$, $d = 10^{-5}$, and $v = 10^{-3}$). It is seen from the figure that the initial perturbations propagate faster at $f = 2$ than at $f = 1$. As applied to the initial problem (9.91)–(9.94), the results obtained show that an increase in f corresponds to a decrease in the transitional zone thickness. On the other hand, the effective stress (9.87) is inversely proportional to the transitional zone thickness. Therefore, the wave propagation velocity is proportional to the effective stress (9.87) in the interphase transitional zone.

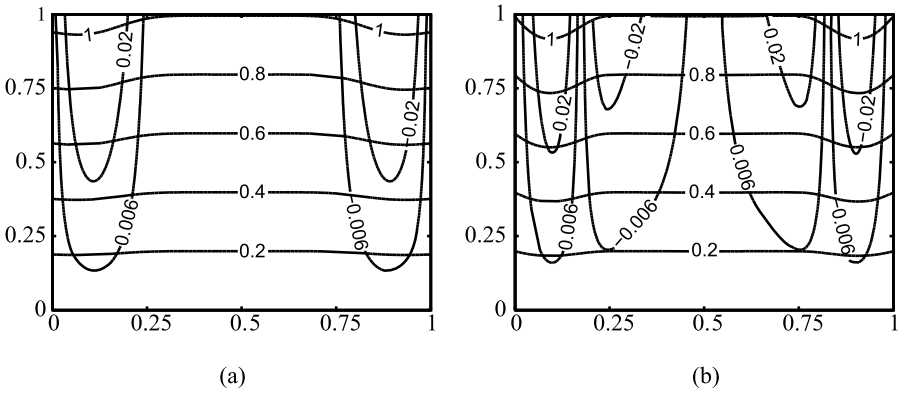

Figure 9.35: Isolines of concentration and stream function after 0.4 s: (a) $d = 10^{-2}$, $\nu = 10^{-3}$; (b) $d = 10^{-5}$, $\nu = 10^{-3}$.

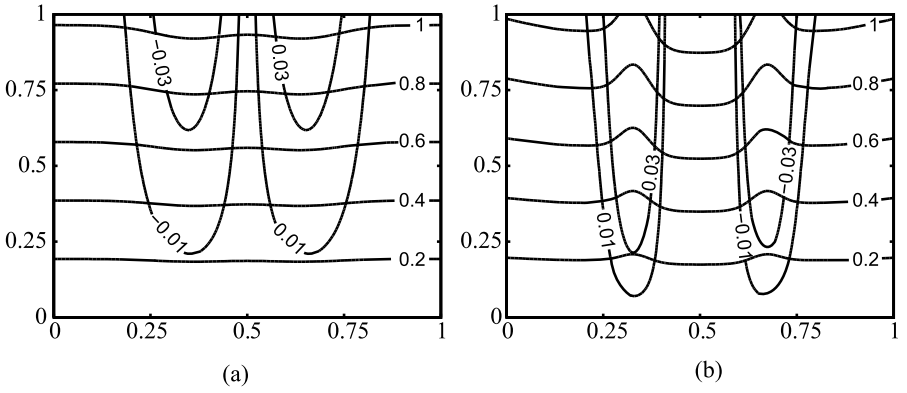

Figure 9.36: Isolines of concentration and stream function after 0.8 s: (a) $d = 10^{-2}$, $\nu = 10^{-3}$; (b) $d = 10^{-5}$, $\nu = 10^{-3}$.

Figure 9.38 illustrates the effect of the quantity k on the solution. Two cases are calculated: (a) $k = 500$ and (b) $k = 50$ ($f = 2$, $d = 10^{-2}$, and $\nu = 10^{-3}$). It is seen that the initial perturbations propagate faster at $k = 50$ than at $k = 500$; moreover, the solution decays more slowly.

Numerical study of the plane problem in the full formulation

Problem (9.89), (9.90) was solved with the use of the stream function and vorticity variables, as applied to the governing equations

$$\frac{dC}{dt} = \mathrm{Sc}^{-1}\Delta C,$$
$$\frac{d\omega}{dt} = \Delta\omega + K_c\{C, \Delta C\}, \tag{9.130}$$

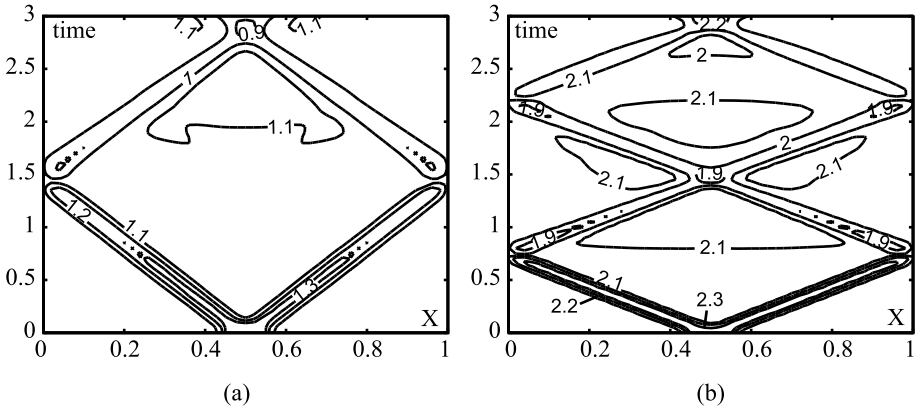

Figure 9.37: Isolines of the function $z(x,t)$ for different values of f: (a) $f = 1$; (b) $f = 2$.

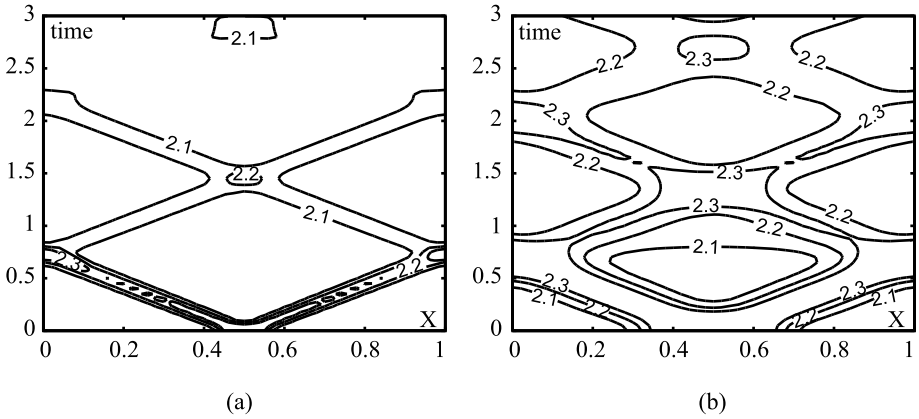

Figure 9.38: Isolines of the function $z(x,t)$ for different values of k: (a) $k = 500$; (b) $k = 50$.

$$\Delta\psi = -\omega,$$

where $\{g,h\} = \partial g/\partial x\, \partial h/\partial y - \partial g/\partial y\, \partial h/\partial x$. This system was numerically solved by the method of alternating directions.

The problem was considered in a rectangular domain $0 \le x \le 1.5$; $0 \le y \le 3$ with the boundary conditions (9.90). The initial conditions correspond to a contact of two quiescent species separated by a transitional zone that has a prescribed shape:

$$u_1 = u_2 = 0,$$

$$c(x,y) = \begin{cases} 0 & \text{at } 0 \le y < y_1, \\ m^4 - 4(m^3 - m^2) & \text{at } y_1 \le y \le y_2, \\ 1 & \text{at } y_2 < y \le 6, \end{cases}$$

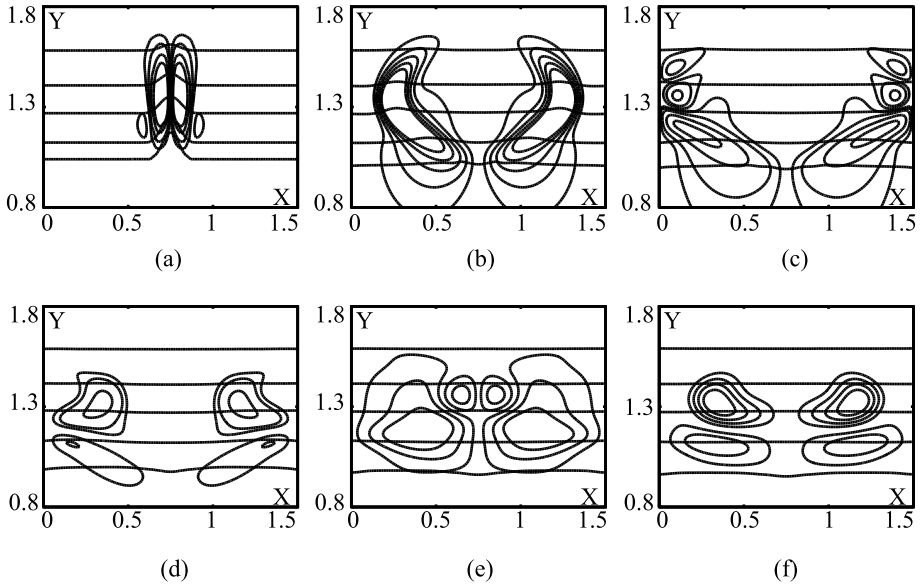

Figure 9.39: Isolines of concentration and stream function at different time instants: (a) $t = 0.05$; (b) $t = 0.95$; (c) $t = 1.45$; (d) $t = 2.0$; (e) $t = 2.95$; (f) $t = 3.6$.

where the function $m(y)$ determines the vertical profile of concentration in the transitional zone $m(y) = (y - y_1)/(y_2 - y_1)$, y_1 is the function of the lower boundary of the transitional zone, which depends on the x coordinate, and $y_2 = 1.75$ is the coordinate of the upper boundary of the transitional zone. The results presented below demonstrate the influence of the perturbation of the lower boundary of the transitional zone, which is defined by changing the function y_1, on the structure and properties of the arising flow. The parameters were taken to be $K_c = 1$ and $\mathrm{Sc} = 10^2$.

Figure 9.39 shows the results calculated in the case where the function y_1 has the form $y_1(x) = f + g\exp[-k(x - 1.5)^2]$, $f = 1$, $g = 0.3$, $k = 50$. Such initial conditions for concentration model a perturbation of the thickness of the transitional zone between two species. The perturbation shape is seen in Figure 9.39a: the thickness of the transitional zone at the center is smaller than in the remaining parts of this zone. Note that the value of z is greater at the transitional zone center and smaller at the periphery if the initial conditions for concentration are presented in the form $c = yz$. Therefore, the choice of the initial conditions corresponds to the model problem considered above.

Changes in the transitional zone thickness defined by the initial conditions generate volume forces acting along the interface of the miscible species in the fluid. As a result, two symmetric vortices are formed near the perturbed region (Figure 9.39a). They begin to move from the domain center to its boundaries (Figure 9.39b). Concentration perturbations propagate together with the vortices. The velocity of their propagation is nonuniform over the transitional zone thickness: the greatest velocity is

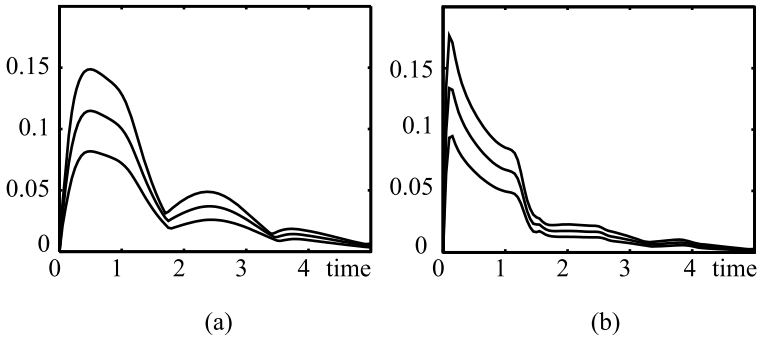

Figure 9.40: Time evolution of the maximum stream function for different parameters of the transitional zone thickness perturbation function: (a) $k = 5$; (b) $k = 50$ ($g = 0.3$ (dotted line), $g = 0.4$ (dashed line), and $g = 0.5$ (solid line)).

observed inside the transitional zone, and the smallest velocity is observed near the upper and lower boundaries. This phenomenon is explained by the results obtained for the model problem, which showed that the propagation velocity increases with increasing f. In the full problem, the quantity f corresponds to the concentration gradient in the vertical direction inside the transitional zone, where its greatest value is determined by the initial conditions. It is seen in Figure 9.39b that the maximum velocity of perturbations is observed in the middle part of the transitional zone (at $y = 1.3$). The nonuniformity of propagation of perturbations over the transitional zone cross section also explains the fact that the shape of the propagating vortices resembles a lens.

Further dynamics of flow evolution are similar to those obtained in the model problem. After the impact on the domain boundary, the vortices change their structures and the directions of their rotation (Figure 9.39c). Then, the vortices move toward the domain center (Figure 9.39d), meet there, intersect each other, and again begin to move toward the domain boundary (Figure 9.39e, f).

Figure 9.40 shows the dependence of the maximum stream function on time for different values of k and g, which characterize the magnitude of the imposed perturbation of the transitional zone thickness. It is seen that the stream function increases with increasing g, i. e., the flow intensity depends on the degree of the local change in the transitional zone thickness. In addition, the figure shows a sequence of decaying oscillations, where the minimum values correspond to time instants when the propagating vortices are reflected from the computational domain boundaries.

The next version of the initial conditions is similar to the previous one. The difference is the fact that the transitional zone at the center has a greater thickness than in the remaining parts (Figure 9.41a), rather than a smaller thickness as previously (Figure 9.39a). The formation and propagation of vortices shown in Figure 9.41 differs

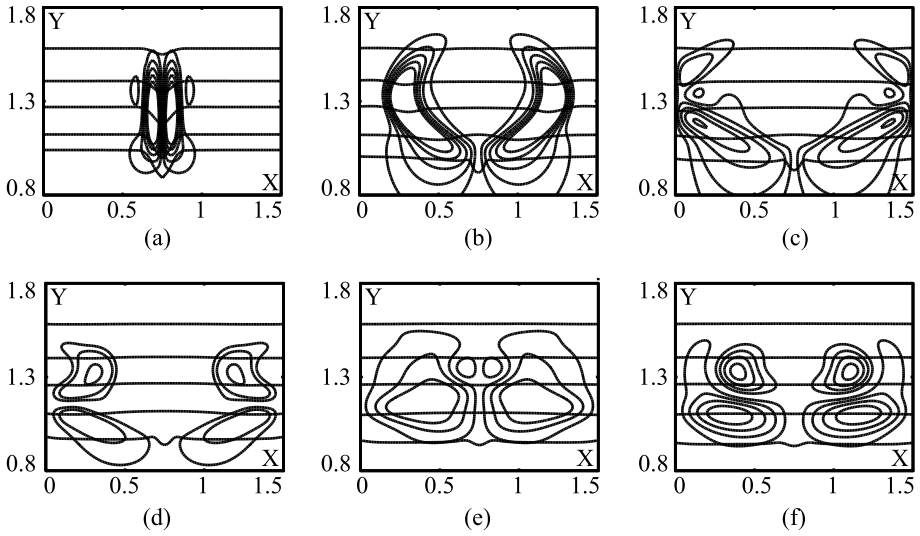

Figure 9.41: Isolines of concentration and stream function ($f = 1$, $g = 0.3$, $k = 50$). The time instants are the same as those in Figure 9.39.

little from the pattern in Figure 9.39. This similarity, however, is not obvious; here it is even unexpected, because these two cases are the opposite ones in the initial analysis.

It is known that interphase surface tension is inversely proportional to the transitional zone thickness (9.87). Therefore, in the case with the initial conditions corresponding to the results in Figure 9.41, surface tension is smaller at the center of the transitional zone than in the remaining parts. It can be expected that the fluid motion is directed from the center to the periphery. In the case with the initial conditions shown in Figure 9.39, interphase surface tension has the greatest value at the center. Therefore, the fluid is expected to move from the boundaries toward the center. The results of numerical simulations, however, predict the opposite situation: the concentration perturbation and the vortices move from the center to the domain boundaries. An explanation for this behavior can be found from Figure 9.39a, b. Two intense localized vortices are formed at the initial stage of flow evolution; these vortices change the transitional zone thickness, so that this contradiction is eliminated. Therefore, the vortices in Figures 9.39 and 9.41 rotate in the opposite directions.

Figure 9.42 shows the results for the initial conditions with two perturbations of the transitional zone thickness imposed simultaneously. The initial perturbations have different magnitudes; therefore, the intensity of the pair of vortices in the left part of the domain is smaller than that of the right-hand pair of vortices. This choice of the initial conditions allows us to observe intersection of two vortices. This intersection is most clearly seen in Figure 9.42c, where the small vortex,

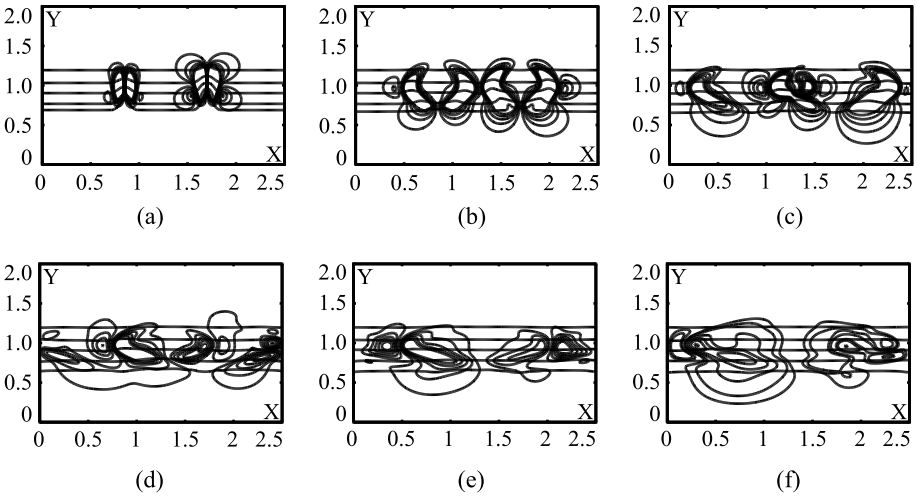

Figure 9.42: Isolines of concentration and stream function ($f = 1$, $g_1 = 0.3$, $g_2 = 0.5$, $k = 50$). Two local perturbations of the transitional zone thickness are imposed at the initial time.

which was on the left at the beginning, passes through the more intense vortex on the right.

The next version of the initial conditions for the function $y_1(x)$ has the form

$$y_1(x) = \begin{cases} 1, & 0 \le x < 0.3,\ 1.2 < x \le 1.5, \\ [1 + (x - 0.3)^2(0.5 - x)^2]/0.055, & 0.3 \le x \le 0.5, \\ 1.15, & 0.5 < x < 1, \\ [1 + (x - 1)^2(1.2 - x)^2]/0.055, & 1 \le x \le 1.2. \end{cases}$$

In this case, the solution behavior differs from the previously considered regimes. Two large vortices are formed at the initial time and fill the entire width of the computational domain (Figure 9.43a, b). Then they begin to change their structure. Firstly, each of these vortices decomposes into three vortices (Figure 9.43d); the largest vortex is located in the lower part of the transitional zone. After that, the intensity of the central vortex starts to grow (Figure 9.43e), and then the largest vortex is again observed in the lower part of the transitional zone (Figure 9.43g).

Thus, another type of the solution behavior is observed which differs from those considered previously. The perturbations also propagate here in the transitional zone, but in the direction perpendicular to it. This motion is repeated periodically with a decaying amplitude (Figure 9.44).

Another type of the initial conditions was considered for the problem where the transitional zone has a rounded rather than flat shape. Such a configuration is typical for the case where a drop of one species of the miscible fluid is surrounded by the other species.

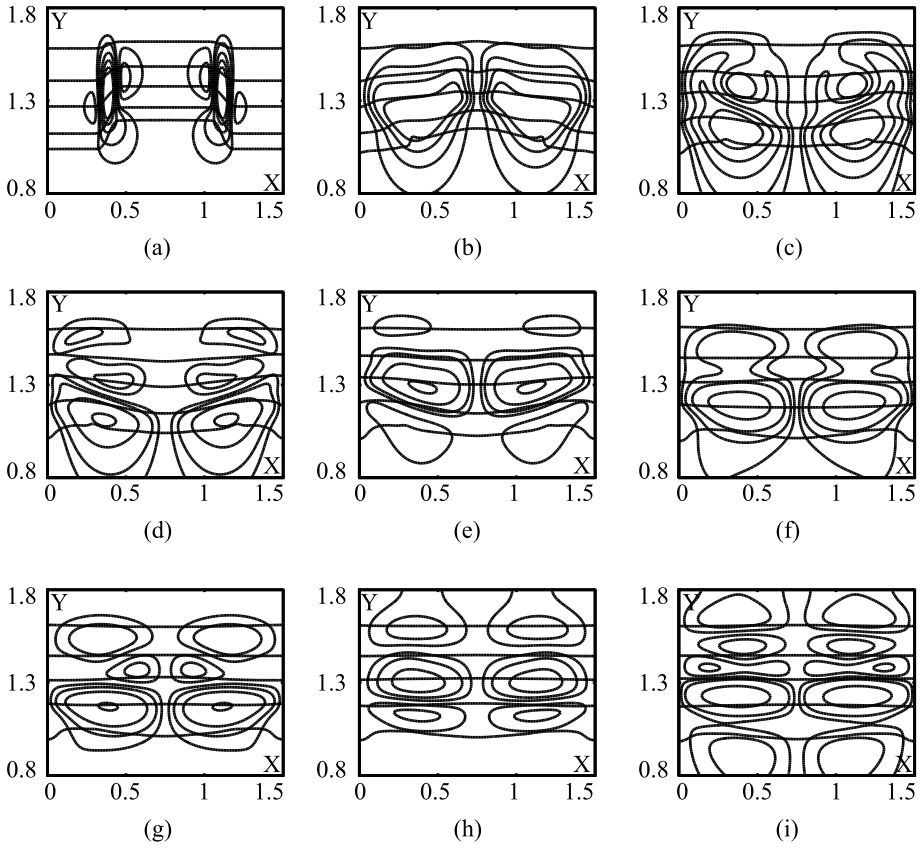

Figure 9.43: Isolines of concentration and stream function at different time instants: (a) $t = 0.05$; (b) $t = 0.65$; (c) $t = 1.5$; (d) $t = 1.7$; (e) $t = 2.05$; (f) $t = 3.0$; (g) $t = 3.25$; (h) $t = 3.8$; (i) $t = 4.55$.

Figure 9.45 shows that a pair of vortices is formed in the case of a local perturbation of the transitional zone; this pair of vortices moves along the drop surface with time. In this case, the convective flow intensity depends on the curvature of the transitional zone.

Figures 9.46 and 9.47 show the results for three different values of the curvature radius. The smaller the curvature, the greater the stream function (see Figure 9.47 up to the time $t = 0.27$).

Note that the curvature of the transitional zone near the boundaries begins to change in view of the boundary conditions of the absence of concentration fluxes. This is the reason for the formation of additional vortices in this part of the computational domain, which become more intense than those formed due to the initial perturbation of the transitional zone thickness, especially if the curvature is large (Figure 9.46: $t = 0.6$; Figure 9.47: $t > 0.3$).

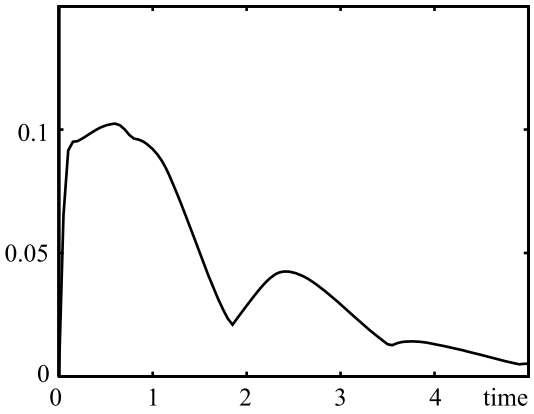

Figure 9.44: Time evolution of the maximum stream function.

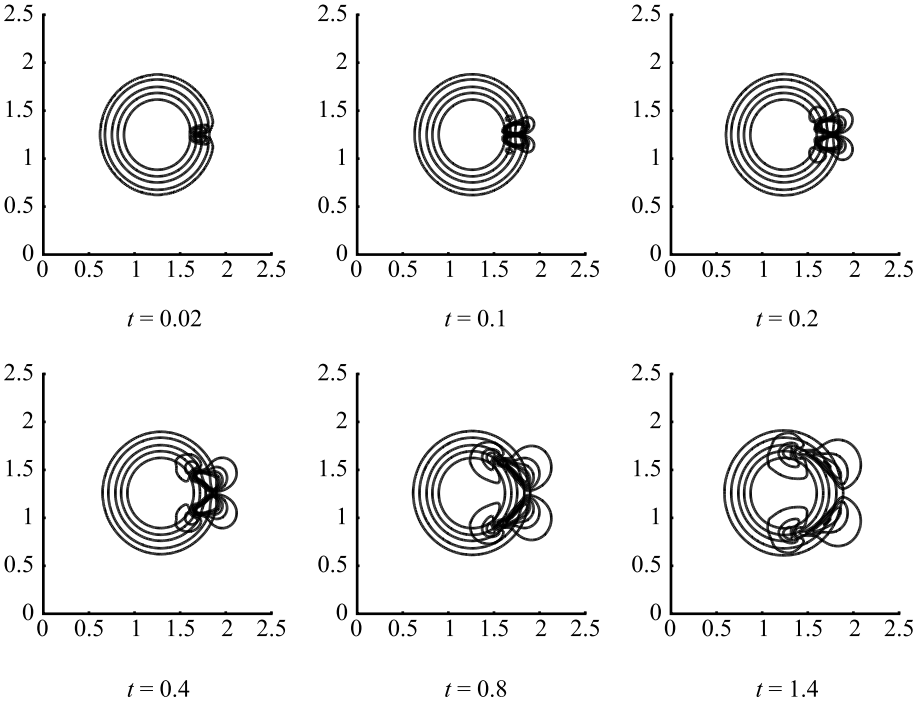

Figure 9.45: Isolines of concentration and stream function, $R = 0.3$ (R is the radius of curvature).

All problems considered above as well as the results of solving them were obtained for parameters where the nature of the examined phenomenon is manifested most clearly.

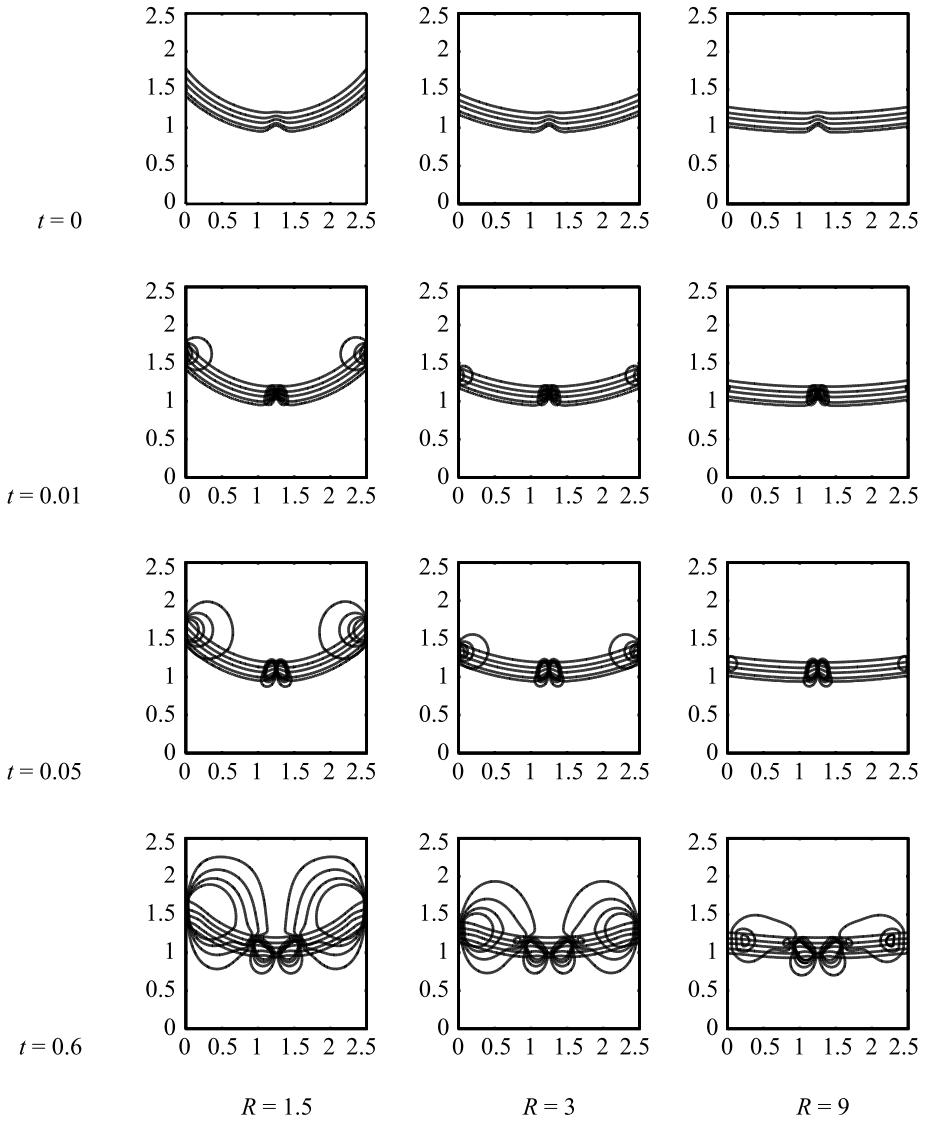

Figure 9.46: Isolines of concentration and stream function for different values of R.

Let us now give an example of solving problem [167], where the following physical parameters of the fluid are used: $K = 10^{-9}$ N, $\varrho_0 = 10^3\,\mathrm{kg/m^3}$, $d = 10^{-10}\,\mathrm{m^2/s}$, $\nu = 10^{-5}\,\mathrm{m^2/s}$, $\gamma = 0.2$, $C_* = 1$, and $h = 10^{-2}$ m, which corresponds to the dimensionless parameters $\mathrm{Sc} = 10^5$ and $K_c = 10^{-2}$.

The computational problem is related to studying convective flows in the case where the transitional zone has the thickness $\delta = \delta(x)$, which increases linearly from 0.5 to 4.5 mm along the x axis. The problem is considered in a rectangular domain

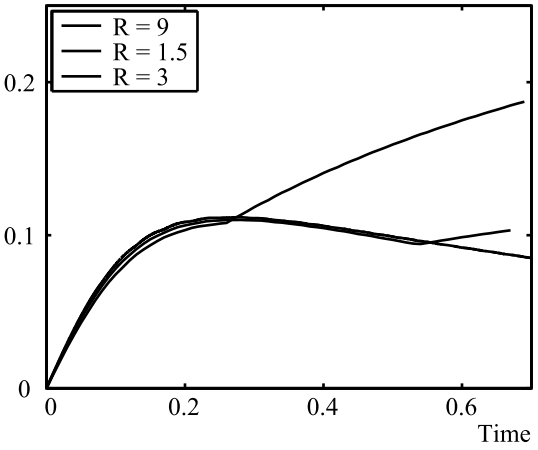

Figure 9.47: Time evolution of the maximum stream function for different values of R.

$L_x = 3$ cm, $L_y = 6$ cm. The initial conditions for the concentration C have the form

$$C(x,y) = \begin{cases} 0, & 0 \le y < 3 - \frac{\delta}{2}, \\ 0.5 - 1.5(\frac{3-y}{\delta}) + 2(\frac{3-y}{\delta})^3, & 3 - \frac{\delta}{2} \le y \le 3 + \frac{\delta}{2}, \\ 1, & 3 + \frac{\delta}{2} < y \le 6. \end{cases}$$

The distribution of the concentration C at the initial time is shown in Figure 9.48a. Two symmetric vortices are formed in the computational domain with time; the centers of these vortices are located in the vicinity of the narrow part of the transitional zone (Figure 9.48b). At the initial time these vortices have the greatest intensity, which decreases because of the increase in the transitional zone thickness under the action of convective transfer and diffusion of the admixture. At the same time, it is seen that the positions of the vortex centers change with time: they move along the transitional zone, similar to the situation considered above for the model regimes (Figures 9.39 and 9.41).

Thus, in this problem, which is most suitable for conducting a physical experiment, manifestation of the action of Korteweg's stresses can be detected not only as the formation of vortices of a given configuration, but also as their motion along the transitional zone, which is the manifestation of the wave nature of propagation of perturbations.

Let us also note that the considered initial conditions for concentration can be used to study convective flows formed owing to volume expansion of the fluid with the use of the microconvection model. Studying the joint action of volume expansion of the fluid and forces generated by Korteweg's stresses, however, requires a preliminary analysis of the physical properties of the fluid. Thus, for example, for water and water-based solutions the maximum velocities predicted by the MM have the order of

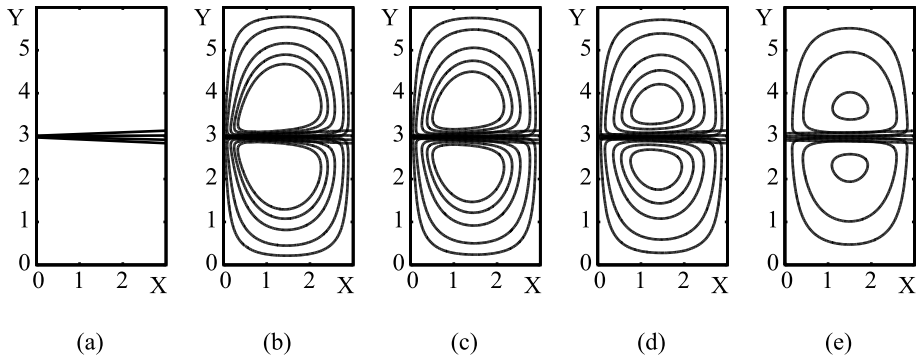

Figure 9.48: Isolines of concentration and stream function at different time instants (in seconds): (a) $t = 0$; (b) $t = 10$; (c) $t = 100$; (d) $t = 250$; (e) $t = 1000$.

10^{-5} cm/s [63], whereas flows with the maximum velocities of $3 \cdot 10^{-4}$ cm/s can be obtained in such systems if only Korteweg's stresses are taken into account. It is for this reason that we used here the Boussinesq model for studying convective flows, because this model ensures simpler numerical investigations. The action of volume forces of fluid expansion was ignored.

10 Convective flows in tubes and layers

Convective flows in tubes and layers are studied in this Chapter with the use of the group-theoretical approach [181, 186, 187]. This approach allows three-dimensional motions of a nonuniformly heated fluid to be studied in terms of solutions of two-dimensional (or, sometimes, one-dimensional) problems. The flow domain is unbounded along one or two coordinates. Typical examples are the classical solutions obtained by Ostroumov [153] and Birikh [35]. They describe steady flows in an infinite vertical tube and an infinite horizontal band, respectively. If the tube or band length is much greater than its cross-sectional size, however, these solutions ensure good approximations of the main part of the flows, which is confirmed by experimental data and results of numerical modeling. In this Chapter, we construct analogs of the Birikh solution in a tube with an arbitrary cross section and in a rotating circular tube. In the second case, the fluid experiences the action of both the centripetal force and the transverse gravity force. The above-mentioned solutions are invariant solutions of the Oberbeck–Boussinesq equations. The set of exact solutions is extended in plane or axisymmetric problems, where the streamwise temperature gradient is an arbitrary function of time (in contrast to Ostroumov's and Birikh's solutions where this gradient is constant). The problem of deformation of a viscous layer by thermocapillary forces is considered in the last Section of Chapter 10. The solution of this problem is described by a partially invariant solution of the Navier–Stokes equations. Thermal convection in a horizontal channel in the presence of a longitudinal temperature gradient varying with time in accordance with the exponential law is studied. An attempt is made to describe the delay of thermocapillary convection onset owing to the existence of a film on the fluid surface. The difference in the convection flow structures in the cases of fixed and destroyed films is shown. An exact solution for the plane-parallel flow under a surface with the friction proportional to the velocity at a constant longitudinal temperature gradient is derived. The solution of the time-dependent problem for the model with the Bingham properties of the fluid surface is obtained using a difference method.

10.1 Group-theoretical nature of the Birikh solution and its generalizations

Birikh [35] constructed exact solutions to the system of the Oberbeck–Boussinesq equations, which has the following form in generally accepted notations:

$$\mathbf{v}_t + \mathbf{v}\cdot\nabla\mathbf{v} = -\rho^{-1}\nabla p + \nu\Delta\mathbf{v} - \beta\theta\mathbf{g}, \quad \nabla\cdot\mathbf{v} = 0, \quad \theta_t + \mathbf{v}\cdot\nabla\theta = \chi\Delta\theta. \tag{10.1}$$

In what follows, we use individual notations for the x, y, and z coordinates and for the corresponding velocity components u, v, and w and assume that $\mathbf{g} = (-g, 0, 0)$.

https://doi.org/10.1515/9783110655469-010

The class of the Birikh solutions of system (10.1) describes plane steady flows with $u = v = 0$, $p = -A\rho g\beta xz + q$, $\theta = -Az + T$, $A = \text{const}$ (in what follows, this constant is assumed to be positive), and the functions w, T, and q depend only on x, being polynomials of the third, fifth, and sixth powers, respectively. The solutions found in [35] are remarkable not only because of their simplicity, but also owing to clear physical interpretation. One of them describes the flow in a band $-h < x < h$ where both boundaries are solid walls; in the second case, the upper boundary of the band is a free rigid surface subjected to the action of thermocapillary forces. The streamwise velocity component w in the first Birikh solution has the form

$$w = \frac{\nu}{h}\frac{G}{6}(s - s^3), \tag{10.2}$$

where $G = \frac{Ag\beta h^4}{\nu^2}$ is the Grashof number and $s = \frac{x}{h}$. The same component in the second Birikh solution is given by the formula

$$w = \frac{\nu}{24h}\left[G(-4s^3 + 3s^2 + 6s - 1) + G_\sigma(3s^2 + 2s - 1)\right], \tag{10.3}$$

where $G_\sigma = \frac{3A\text{æ}h^2}{\rho\nu^2}$ is the Marangoni number and $\text{æ} > 0$ is the temperature coefficient of surface tension (2.21). Note that the flow rate through the band cross section in solutions defined by Eqs. (10.2) and (10.3) is equal to zero. This allows us to use the Birikh solutions to describe convection in horizontal channels whose length is much greater than their width, with the vertical boundaries being solid walls. The asymptotic character of the second solution was confirmed by experiments aimed at studying capillary-gravitational convection in a long horizontal cavity and by the numerical solution of a two-dimensional steady problem for system (10.1) with boundary conditions modeling the conditions of the above-mentioned experiments [109].

Group-theoretical nature of the Birikh solutions was revealed in paper [106]. A generalization of the Birikh solutions to a three-dimensional unsteady case was given in [182]. Our considerations are based on the following observations: the solutions obtained in [35] are invariant solutions of system (10.1) with respect to a three-parameter Lie group generated by the infinitesimal operators ∂_t, ∂_y, and

$$Z = -A^{-1}\partial_z + \rho\beta gx\partial_p + \partial_\theta. \tag{10.4}$$

(The fact that the operator Z is admitted by system (10.1) follows from the results obtained in [76].) If we now take a one-parameter group with operator (10.4), we obtain a class of invariant solutions of system (10.1) of rank 3, whereas the Birikh solutions have rank 1. All invariant Z-solutions of system (10.1) have the representation

$$\begin{aligned} &u = u(x,y,t), \quad v = v(x,y,t), \quad w = w(x,y,t),\\ &p = -A\rho\beta gxz + q(x,y,t), \quad \theta = -Az + T(x,y,t), \end{aligned} \tag{10.5}$$

where the functions u, v, w, q, and T satisfy a system of differential equations with three independent variables x, y, and t.

Before writing this system, we pass to dimensionless variables in system (10.1). The most natural interpretation of solutions (10.5) is the flow of a viscous heat-conducting fluid in a horizontal cylindrical tube, which is induced by nonuniform heating of the tube surface. Let us denote the tube cross section by Ω and choose the width h of the domain Ω in the x direction as the characteristic linear scale. The basic similarity criteria in the problem considered are the Grashof number Gr and the Prandtl number Pr defined by the formulas

$$\mathrm{Gr} = \frac{A\beta g h^4}{\nu^2}, \quad \mathrm{Pr} = \frac{\nu}{\chi}. \tag{10.6}$$

We choose $\tau = h^2/\nu$ as the characteristic time scale and pass to new sought functions u', v', w', q' and T', defining them as

$$\begin{gathered} u = \frac{\nu}{h}\,\mathrm{Pr}\,\mathrm{Gr}^2\,u', \quad v = \frac{\nu}{h}\,\mathrm{Pr}\,\mathrm{Gr}^2\,v', \quad w = \frac{\nu}{h}\,\mathrm{Gr}\,w', \\ q = \rho\beta g A h^2\,\mathrm{Pr}\,\mathrm{Gr}\,q', \quad T = Ah\,\mathrm{Pr}\,\mathrm{Gr}\,T'. \end{gathered} \tag{10.7}$$

The new sought functions depend on the dimensionless variables $x' = x/h$, $y' = y/h$, and $t' = t/\tau$.

By virtue of Eqs. (10.1), (10.5), and (10.7), the new sought functions satisfy the equations

$$\begin{gathered} u_t + \lambda(uu_x + vu_y) = -q_x + \Delta_2 u + T, \quad v_t + \lambda(uv_x + vv_y) = -q_y + \Delta_2 v, \\ w_t + \lambda(uw_x + vw_y) = -x + \Delta_2 w, \quad u_x + v_y = 0, \\ \mathrm{Pr}\,T_t + \lambda\,\mathrm{Pr}(uT_x + vT_y) - w = \Delta_2 T, \end{gathered} \tag{10.8}$$

where the primes are omitted and the notations $\lambda = \mathrm{Pr}\,\mathrm{Gr}^2$ and $\Delta_2 = \partial^2/\partial x^2 + \partial^2/\partial y^2$ are used. By virtue of Eqs. (10.5) and (10.7), any solution of system (10.8) generates a solution of the original equations (10.1). In particular, the Birikh solution is obtained if we assume that $u = v = 0$ in Eqs. (10.8) and that the functions w, q, and θ are independent of y and t. A systematic search for exact solutions of system (10.8) is based on its group properties. This system admits the operators

$$\begin{gathered} X_0 = \partial_t, \quad X_\gamma = \gamma\partial_y + \lambda^{-1}\frac{d\gamma}{dt}\partial_v - \lambda^{-1}\gamma\frac{d^2\gamma}{dt^2}\partial_q, \quad X_\delta = \delta\partial_q, \\ X_\alpha = -\,\mathrm{Pr}\,\frac{d^2\alpha}{dt^2}\partial_x - \lambda^{-1}\,\mathrm{Pr}\,\frac{d^3\alpha}{dt^3}\partial_u + \mathrm{Pr}\,\frac{d\alpha}{dt}\partial_w + x\left(\lambda^{-1}\,\mathrm{Pr}\,\frac{d^4\alpha}{dt^4} + \alpha\right)\partial_q + \alpha\partial_T, \end{gathered}$$

where α, γ, and δ are arbitrary functions of t of the class C^∞. Note that the operators X_0, X_γ, and X_δ are "inherited" by system (10.8) from the original system (10.1), whereas X_α is a "redundant" operator.

In its structure, system (10.8) resembles the system of the Navier–Stokes equations in a plane case, supplemented with two parabolic equations. Thus, we can naturally pose the following initial-boundary problem: find a solution u, v, w, q, T of system (10.8) in a cylinder $Q_N = \{x, y, t : (x, y) \in \Omega,\ 0 < t < N\}$, which satisfies the initial conditions

$$u = u_0(x, y), \quad v = v_0(x, y), \quad w = w_0(x, y), \quad T = T_0(x, y), \quad \text{at } (x, y) \in \Omega,\ t = 0, \tag{10.9}$$

the no-slip conditions for velocities

$$u = v = w = 0 \quad \text{at } (x, y) \in \Sigma = \partial\Omega,\ t \in (0, N) \tag{10.10}$$

and one of the following conditions for temperature:

$$\frac{\partial T}{\partial n} = a(x, y, t), \quad (x, y) \in \Sigma,\ t \in (0, N) \tag{10.11}$$

or

$$T = b(x, y, t), \quad (x, y) \in \Sigma,\ t \in (0, N) \tag{10.12}$$

Here, u_0, v_0, w_0, T_0, a, and b are given functions of their arguments, and $\partial/\partial n$ is the derivative along the external normal to the curve Σ. We do not discuss here whether problems (10.8)–(10.11) or (10.8)–(10.10), (10.12) are well-posed or not. We only note that they satisfy theorems of unique global solvability in classes of functions that are natural extensions of the classes of well-posedness of a two-dimensional unsteady problem for the Navier–Stokes equations [114].

Along with problems (10.8)–(10.11) and (10.8)–(10.10), (10.12), it is of interest to consider steady problems for system (10.8) under the assumption that $u_t = v_t = w_t = T_t = 0$. In this case, conditions (10.9) are not imposed, and the functions a and b in conditions (10.11) and (10.12) are independent of t. The theorems of existence of generalized solutions without constraints on the value of the corresponding norms of the functions a and b are valid for both steady problems; for small values of the parameter λ, the theorems of uniqueness are also valid. Moreover, the components u, v, w, q, and T of the steady solution are analytical functions of the parameter λ at the point $\lambda = 0$. Below we calculate the principal terms of the corresponding series in the case where the domain Ω is a circle of a unit radius with the circle center at the origin, and condition (10.11) is homogeneous. The following boundary-value problem is posed:

$$\begin{gathered}\Delta_2 u - q_x + T = 0, \quad \Delta_2 v - q_y = 0, \quad u_x + v_y = 0,\\ \Delta_2 w - x = 0, \quad \Delta_2 T + w = 0 \quad \text{at } x^2 + y^2 < 1,\end{gathered} \tag{10.13}$$

$$u = v = w = 0, \quad \frac{\partial T}{\partial n} = 0 \quad \text{at } x^2 + y^2 = 1. \tag{10.14}$$

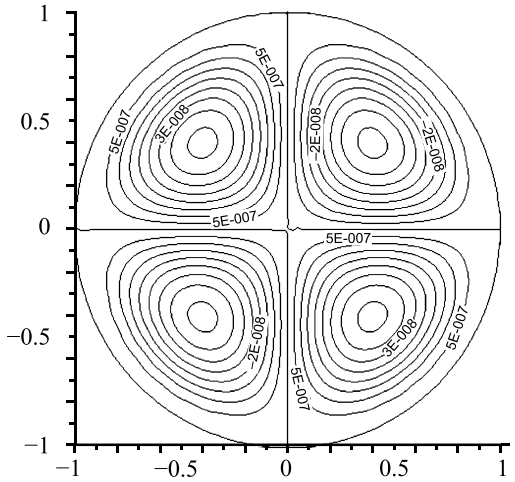

Figure 10.1: Level lines of stream function ψ.

The solution of problem (10.13), (10.14) is given by the explicit formulas

$$\psi = \frac{r^2 \sin 2\varphi}{2^{13} \cdot 3^2 \cdot 5}(2r^6 - 15r^4 + 24r^2 - 11), \quad w = \frac{r \cos \varphi}{8}(r^2 - 1),$$
$$T = -\frac{r \cos \varphi}{192}(r^4 - 3r^2 + 4), \tag{10.15}$$
$$q = \frac{r^2}{2^{10} \cdot 3^2 \cdot 5}[10(2r^4 - 9r^2 + 24) + 3(5r^4 - 20r^2 + 9)\cos 2\varphi].$$

Here, ψ is the stream function related to u and v as $u = \psi_y$ and $v = -\psi_x$; $r = (x^2 + y^2)^{1/2}$ and $\varphi = \arctan(y/x)$ are the polar coordinates. The functions ψ and q are normalized so that $\psi = q = 0$ at $x = y = 0$. In this case, the function u is odd with respect to x and even with respect to y, the function v is even with respect to x and odd with respect to y, the functions w and T are odd with respect to x and even with respect to y, and the function q is even with respect to x and y. The flow domain $x^2 + y^2 < 1, z \in \Re$ is divided into four subdomains by the planes $x = 0$, $y = 0$; each subdomain is filled by nested cylindrical stream surfaces $\psi(x, y) = \text{const}$, $z \in \Re$ (Figure 10.1).

The trajectories of the fluid particles have a helical character. The fluid in the upper and lower halves of the tube moves in the negative and positive directions of the z axis, respectively (let us recall that the temperature is a linear decreasing function of z by virtue of Eq. (10.5)). Note that the component w of solution (10.15) satisfies the equality

$$\int_{\Omega} w dx dy = 0 \tag{10.16}$$

(here, Ω is a circle $x^2 + y^2 < 1$). This equality, which is similar to the "condition of flow closedness" in [35], gives us hope that a three-dimensional analog of the Birikh

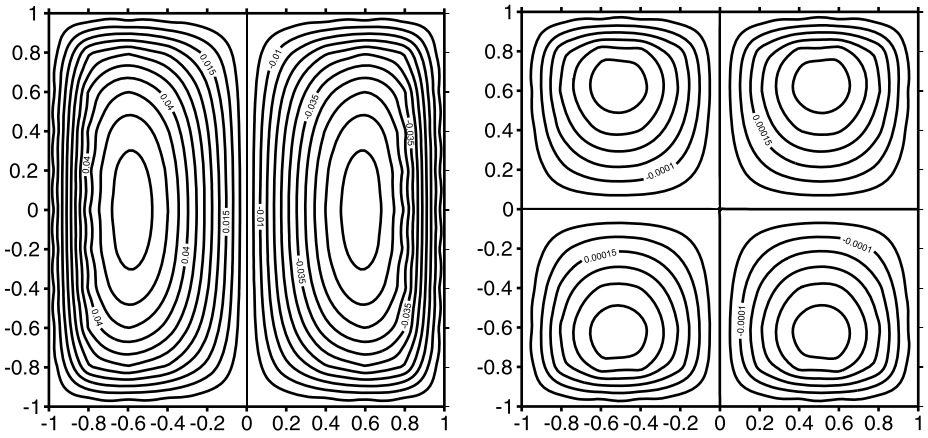

Figure 10.2: (a) Level lines for w. Parameters: Pr = 7, Gr = 1, moment of time $t = 3$; (b) Level lines for vortex ω. Parameters: Pr = 7, Gr = 1, moment of time $t = 3$.

solution ensures an adequate approximation of the steady flow far from the end faces of a long horizontal cylinder, which is induced by a linear distribution of temperature along the side surface. Obviously, condition (10.16) is also satisfied for steady flows if the domain Ω is symmetric about the y axis. In the general case, this condition can be satisfied by slightly changing the structure of the invariant solution by adding the term $C\partial_p$ with an appropriate constant C to operator (10.4).

For a square domain Ω, the initial-boundary problems (10.8)–(10.12) were solved numerically in [2]. The calculations were performed for the Prandtl number equal to 7 and different values of the Grashof number. The motion started from the quiescent state. The functions T_0 and b involved into conditions (10.9) and (10.12) for temperature were chosen to be equal to zero.

If the Grashof number is small, then the solution of the initial-boundary problem reaches a steady state retaining a typical four-vortex structure of the level lines of the stream function ψ. Figure 10.2(a) shows the isolines of the velocity component w of this steady regime. The isolines of the projection $\omega = -\triangle_2 \psi$ of the velocity rotor onto the z axis for Gr = 1 are plotted in Figure 10.2(b).

As the Grashof number increases, the steady regime loses its stability. The arising unsteady motion is accompanied by changes in the topology of the level lines of the stream function ψ with time. This fact is illustrated in Figures 10.3(a)–(d), which show the level lines for the Grashof number Gr = 59 and dimensionless times $t = 0.7, 1.7, 2.3,$ and 3.0.

A steady problem for system (10.8) was also studied in [122]. There, the domain was taken to be a square or a rectangle with the width-to-height ratio equal to 4. Lyubimova et al. [123] constructed an asymptotic of the steady solution at low Prandtl

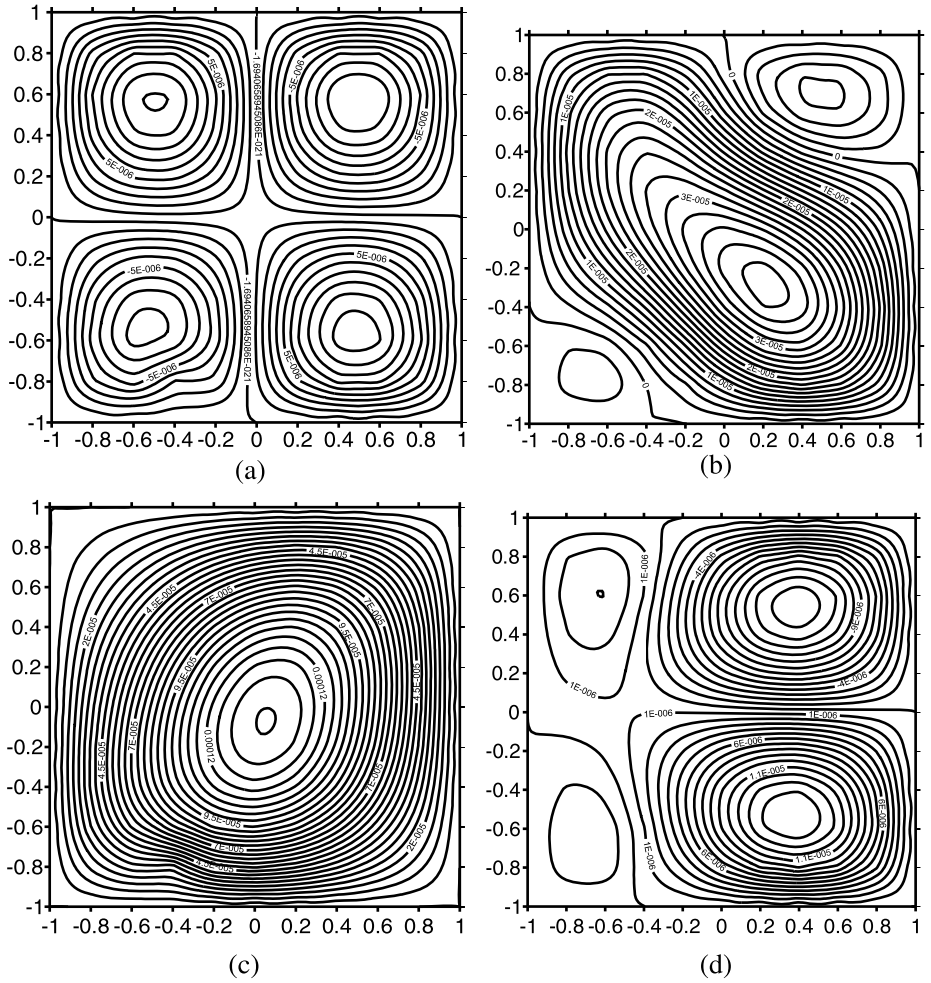

Figure 10.3: (a) Pr = 7, Gr = 59, t = 0.7; (b) Pr = 7, Gr = 59, t = 1.7; (c) Pr = 7, Gr = 59, t = 2.3; (d) Pr = 7, Gr = 59, t = 3.0.

numbers and studied its stability within the framework of the linear approximation. The following modes were found in the problem spectrum: stationary hydrodynamic, sidewall stationary hydrodynamic, oscillating spiral, and stationary spiral modes. Depending on the problem parameters, this or that mode becomes particularly dangerous. It was demonstrated [122] that a vertical magnetic field is a factor stabilizing the steady flow of the mentioned type.

Exact numerical solutions of type (10.5) of system (10.1), which describe flows with an interface of two fluids in an infinite channel with a rectangular cross section, were studied in [87, 88]. The a priori unknown cylindrical interface is sought as an equilibrium capillary surface with a given contact wetting angle. If this is a right angle, then

this surface is planar. Results calculated for a two-layer fluid with a flat interface in a channel with a rectangular cross section were reported in [87, 88]. In such situations, the parameters of the contacting fluids can be appreciably different: e. g., one of them can be a gas. The channel walls are thermally insulated. The source of motion is the thermocapillary effect on the interface. The calculations reveal a large variety of vortex structures formed in the channel cross section.

It should be noted that the condition for normal stresses on the interface is satisfied approximately in the solution constructed in the above-cited papers, whereas all the remaining boundary conditions are satisfied exactly. The smaller the capillary number $\mathrm{Ca} = \rho\nu u_*/\sigma_0$ (where u_* is the characteristic velocity of the flow in the channel cross section and σ_0 is the characteristic value of the surface tension coefficient), secures the smaller the induced error. A similar situation is observed for the second Birikh solution, where the condition for the normal stress on the free boundary is also satisfied approximately. In contrast, this and other boundary conditions on the interface in the solution of the problem of a two-layer fluid flow in an inclined channel with a streamwise temperature gradient are satisfied exactly [146]. The reason is the fact that the conditions on the interface follow from conservation laws. At the same time, in recording the conditions on the free boundary, the response of the gas medium to the liquid is expressed by prescribing the pressure and temperature of the fluid on the free surface (instead of the latter, a condition of the third kind for the liquid temperature with a specified gas temperature is often formulated).

To conclude, we should note that the steady solution of system (10.8) under conditions (10.10) and one of the homogeneous conditions (10.11) or (10.12) can be called a three-dimensional analog of the first Birikh solution. Unfortunately, it does not possess simplicity inherent in its prototype. The problem is not only the nonlinearity of system (10.8), but also the fact that addition of the variable y gives rise to two nonzero velocity components u and v (let us recall that we have $u = 0$ in the Birikh solution independent of y). On the other hand, rich group properties of system (10.8) allow us to construct its invariant and partly invariant solutions of lower dimensions, which are related to the first Birikh solution in a certain sense.

Generalization of the second Birikh solution with the free boundary to a three-dimensional case is more complicated. The nature of the invariant solution (10.5) is such that the natural conditions on the free surface can be satisfied only if this surface is the plane $x = 0$. In this case, however, the corresponding problem for system (10.8) becomes overdetermined. The following question is interesting, though difficult: Is it possible to satisfy the "redundant" boundary condition on the free boundary $x = 0$ by choosing an appropriate right-hand side of condition (10.11) or (10.12)? Experimental implementation of the three-dimensional analog of the Birikh solution is also of great interest, including its implementation under microgravity conditions. A typical feature of the class of flows discussed here is the possibility of transporting passive admixtures to large distances along the tube under the combined action of the streamwise temperature gradient and the transverse force of gravity (the value of the gravity

force can be very small). We can estimate the streamwise velocity w from Eqs. (10.6) and (10.7), assuming that w' is of the order of unity; then, we obtain $w \sim A\beta g h^3/\nu$. Assuming that $h = 5\,\text{cm}$, $\nu = 10^{-2}\,\text{cm}^2/\text{s}$, $\beta = 0.4 \cdot 10^{-3}\,\text{K}^{-1}$, $A = 1\,\text{K/cm}$, and $g = 0.2\,\text{cm/s}^2$, we obtain the estimate $w \sim 1\,\text{cm/s}$.

10.2 An axial convective flow in a rotating tube with a longitudinal temperature gradient

The solution describing the established planar motion of a liquid in a horizontal band under the effect of a longitudinal temperature gradient and transverse gravity force is well known [35]. The asymptotic character of this exact solution is confirmed by the results of [109], where the problem of convection in a long horizontal cuvette with a constant temperature gradient being held on its side boundaries was investigated by experimental and numerical methods. The generalization of a plane flow to the case of motion in a cylindrical channel of an arbitrary cross section is given in [182]. Other generalizations of this solution and a detailed bibliography are contained in review [7]. We consider below the convection in a rotating round tube excited by the interaction of the centripetal force and thermal flow along the tube axis. In the simplest case, when the transverse gravity force is absent and the motion is steady-state, the solution is expressed in elementary functions. There are two generalizations of this solution. In the first of them, the motion retains the axial symmetry but is time-dependent because the rotation rate of the tube is variable. The second generalization describes the established motion with a cylindrical interface. Both these problems are linear and effectively one-dimensional. One more generalization corresponds to the joint effect of the centripetal force and the transverse force of gravity. The appearing problem becomes nonlinear, but it is reduced to the solution of a set with two spatial variables. In this case, the velocity field has three nonzero components. This paragraph is based on the results of paper [37].

Equations of motion

The problem of thermal gravitational convection of a liquid in a round rotating tube is considered in the Oberbeck–Boussinesq approximation. Let r, φ, z be the cylindrical coordinates, a be the tube radius and $\omega(t)$ be the angular velocity of its rotation around the z axis. In addition to the centripetal force, the liquid is affected by the weight force with the acceleration $(-g(t)\sin\varphi, -g(t)\cos\varphi, 0)$. If $g = \text{const}$, this force can be identified with the gravity force. Further, u and w denote the radial and axial components of the velocity vector, v is the difference between the circular velocity and the velocity of rotation of the liquid as the solid ωr, p is the deviation of the pressure from its equilibrium value $\rho(-gr\sin\varphi + \omega^2 r^2/2)$, and θ is the deviation of the temperature from the average value $\bar{\theta}$. The liquid is characterized by the following parameters: density ρ at

temperature θ, kinematic coefficient of viscosity ν, thermal diffusivity χ, and thermal expansion coefficient β. These parameters are considered below as constants.

In the accepted notation, the equations of motion are written in the form [68]

$$\begin{aligned}
&u_t + uu_r - \frac{v}{r}u_\varphi + \omega u_\varphi + wu_z - 2\omega v - \frac{v^2}{r} = \\
&\quad = -\frac{1}{\rho}p_r + \nu\left(u_{rr} + \frac{1}{r}u_r + \frac{1}{r^2}u_{\varphi\varphi} + u_{zz} - \frac{2}{r^2}v_\varphi - \frac{u}{r^2}\right) + (g\sin\varphi - \omega^2 r)\beta\theta, \\
&\dot{\omega}r + v_t + uv_r + \frac{v}{r}v_\varphi + \omega v_\varphi + wv_z + 2\omega u + \frac{uv}{r} = \\
&\quad = -\frac{1}{\rho r}p_\varphi + \nu\left(v_{rr} + \frac{1}{r}v_r + \frac{1}{r^2}v_{\varphi\varphi} + v_{zz} + \frac{2}{r^2}u_\varphi - \frac{v}{r^2}\right) + g\cos\varphi\beta\theta, \\
&w_t + uw_r + \frac{v}{r}w_\varphi + \omega w_\varphi + ww_z = -\frac{1}{\rho}p_z + \nu\left(w_{rr} + \frac{1}{r}w_r + \frac{1}{r^2}w_{\varphi\varphi} + w_{zz}\right), \\
&u_r + \frac{u}{r} + \frac{1}{r}v_\varphi + w_z = 0, \\
&\theta_t + u\theta_r + \frac{v}{r}\theta_\varphi + \omega\theta_\varphi + w\theta_z = \chi\left(\theta_{rr} + \frac{1}{r}\theta_r + \frac{1}{r^2}\theta_{\varphi\varphi} + \theta_{zz}\right)
\end{aligned} \tag{10.17}$$

(the dot denotes differentiation with respect to t). Equations (10.17) are derived under the assumption that the centripetal force has the same order as the gravity force. In some technical equipment the rotation velocity is so high that this force significantly exceeds the gravity force. Moreover, the Oberbeck–Boussinesq model fails to describe convection if the centripetal acceleration is very large. Asymptotic approach for analysis of convective flows in a circular fast-rotating tube of finite length was realized in paper [211].

Group property of equations (10.17)

Immediate verification shows that the transformation at which all independent variables and velocity components remain invariable, while the pressure and temperature are transformed by formulas

$$p' = p + c\rho\beta\left(gr\sin\varphi - \frac{\omega^2 r^2}{2}\right), \quad \theta' = \theta + c, \tag{10.18}$$

where c is the constant, does not vary system (10.17). The transformation of one-parameter group (10.18) corresponds to the infinitesimal operator

$$X_1 = \rho\beta\left(gr\sin\varphi - \frac{\omega^2 r^2}{2}\right)\frac{\partial}{\partial p} + \frac{\partial}{\partial\theta}.$$

In addition, system (10.17) admits operators

$$X_2 = \frac{\partial}{\partial z}, \quad X_3 = G\frac{\partial}{\partial p}$$

where G is an arbitrary smooth function of t; and, consequently, their linear combination $X = X_2 + X_3 - AX_1$ where A is the constant. The general view of the invariant solution of system (10.17) with respect to operator X is as follows:

$$\begin{aligned} &u = u(r,\varphi,t), \quad v = v(r,\varphi,t), \quad w = w(r,\varphi,t),\\ &p = \left[-A\rho\beta\left(gr\sin\varphi - \frac{\omega^2 r^2}{2}\right) + \rho G\right]z + q(r,\varphi,t),\\ &\theta = -Az + T(r,\varphi,t). \end{aligned} \tag{10.19}$$

Functions u, v, w, q, and T satisfy the following system of equations:

$$\begin{aligned} &u_t + uu_r + \frac{v}{r}u_\varphi + \omega u_\varphi - 2\omega v - \frac{v^2}{r} =\\ &\quad = -\frac{1}{\rho}q_r + \nu\left(u_{rr} + \frac{1}{r}u_r + \frac{1}{r^2}u_{\varphi\varphi} - \frac{2}{r^2}v_\varphi - \frac{u}{r^2}\right) + (g\sin\varphi - \omega^2 r)\beta T,\\ &\dot{\omega}r + v_t + uv_r + \frac{v}{r}v_\varphi + \omega v_\varphi + 2\omega u + \frac{uv}{r} =\\ &\quad = -\frac{1}{\rho r}q_\varphi + \nu\left(v_{rr} + \frac{1}{r}v_r + \frac{1}{r^2}v_{\varphi\varphi} + \frac{2}{r^2}u_\varphi - \frac{v}{r^2}\right) + g\cos\varphi\beta T,\\ &w_t + uw_r + \frac{v}{r}w_\varphi + \omega w_\varphi =\\ &\quad = A\beta\left(gr\sin\varphi - \frac{1}{2}\omega^2 r^2\right) - G + \nu\left(w_{rr} + \frac{1}{r}w_r + \frac{1}{r^2}w_{\varphi\varphi}\right),\\ &u_r = \frac{u}{r} + \frac{1}{r}v_\varphi = 0,\\ &T_t + uT_r + \frac{v}{r}T_\varphi + \omega T_\varphi - Aw = \chi\left(T_{rr} + \frac{1}{r}T_r + \frac{1}{r^2}T_{\varphi\varphi}\right). \end{aligned} \tag{10.20}$$

Formulation of the initial boundary problems for system (10.20)

The following interpretation of solution (10.19) is most natural. The liquid fills the round rotating tube with a constant axial temperature gradient being held on its surface. The velocity vector satisfies the no-slip condition on the boundary of the flow region. The initial velocity and temperature distribution should be specified in the time-dependent problem. In addition, the axial pressure gradient and transverse gravity force may be specified.

The form of solution (10.19) limits the selection of the initial data. In particular, all three components of the initial velocity field should be the functions of two variables r and φ alone. Let Ω be a circle $r < a$, Γ be its boundary, Q_l be a cylinder, $(r,\varphi) \in \Omega$, $0 < t < l$, and B_l be the lateral surface of the cylinder. Let us state problem (A): find a solution of system (10.20) in the domain Q_l satisfying the boundary conditions

$$u = v = w = 0, \quad T = 0, \quad (r,\varphi,t) \in B_l, \tag{10.21}$$

and initial conditions

$$u = u_0, \quad v = v_0, \quad w = w_0, \quad T = T_0, \quad (r, \varphi) \in \Omega, \quad t = 0, \tag{10.22}$$

where u_0, v_0, w_0, and T_0 are the specified functions of r and φ satisfying the fitting condition with the continuity equation,

$$u_{0,r} + \frac{u_0}{r} + \frac{1}{r} v_{0,r} = 0$$

The following problem (B) is the steady-state analog of problem (A):

$$\begin{aligned}
&uu_r + \frac{v}{r} u_\varphi + \omega u_\varphi - 2\omega v - \frac{v^2}{r} = \\
&\quad = -\frac{1}{\rho} q_r + \nu\left(u_{rr} + \frac{1}{r} u_r + \frac{1}{r^2} u_{\varphi\varphi} - \frac{2}{r^2} v_\varphi - \frac{u}{r^2}\right) + (g \sin\varphi - \omega^2 r)\beta T, \\
&uv_r + \frac{v}{r} v_\varphi + \omega v_\varphi + 2\omega u + \frac{uv}{r} = \\
&\quad = -\frac{1}{\rho r} q_\varphi + \nu\left(v_{rr} + \frac{1}{r} v_r + \frac{1}{r^2} v_{\varphi\varphi} + \frac{2}{r^2} u_\varphi - \frac{v}{r^2}\right) + g \cos\varphi \beta T, \\
&uw_r + \frac{v}{r} w_\varphi + \omega w_\varphi = \\
&\quad = A\beta\left(gr \sin\varphi - \frac{1}{2}\omega^2 r^2\right) - G + \nu\left(w_{rr} + \frac{1}{r} w_r + \frac{1}{r^2} w_{\varphi\varphi}\right), \\
&u_r + \frac{u}{r} + \frac{1}{r} v_\varphi = 0, \\
&uT_r + \frac{v}{r} T_\varphi + \omega T_\varphi - Aw = \chi\left(T_{rr} + \frac{1}{r} T_r + \frac{1}{r^2} T_{\varphi\varphi}\right), \\
&\quad (r, \varphi) \in \Omega, \\
&\quad u = v = w = 0, \quad T = 0, \quad (r, \varphi) \in \Gamma.
\end{aligned}$$

Here, the quantities ω, g, and G are constants.

Problem (10.20)–(10.22) is the analog of the well-studied two-dimensional problem for the Navier–Stokes equations (see, for example, [114]). Let us assume that the following conditions are fulfilled:

$$\omega \in C^{(1+\alpha/2)}[0, l], \quad G \in C^{\alpha/2}[0, l], \quad 0 < \alpha < 1.$$

In this case, for each $l > 0$, problem (A) has, besides the unique solution, in which functions u, v, w, T, and T belong to the Hölder class $C^{(2+\alpha,1+\alpha/2)}[\bar{Q}_l]$, $\nabla p \in C^{(\alpha,\alpha/2)}[\bar{Q}_l]$. The validation of this statement follows the known procedure [114] and is not given here. Its key element is the presence of the energy identity, which allows one to obtain the a priori evaluation of the solution. As for problem (B), it is only possible to prove the local solvability of the problem. Let quantities $|g|$, $|\omega|$, and $|G|$ be sufficiently small. Then problem (B) has at least one isolated solution, and its norm in the corresponding Hölder class is also small. Such a situation is typical of standard boundary problems of the dynamics of a viscous liquid.

Motions with rotational symmetry

Let us assume that $g = 0$ and the functions u_0, v_0, w_0, and T_0 involved into conditions (10.22) are independent of the polar angle φ. Then problem (A) admits a rotationally symmetric solution, in which all desired functions are also independent of φ, and it has no other solutions (not possessing symmetry; see the end of the previous section).

By virtue of the continuity equation (fourth equation of system (10.20)) and the symmetry condition, we have $u = kr^{-1}$, where $k = k(t)$. If we exclude the presence of sources and sinks on the tube axis, then $k = 0$. Equations of problem (A) become linear in this case. We will present them in a sequence convenient for their solution:

$$w_t = -\frac{1}{2} A\beta\omega^2 r^2 - G + \nu\left(w_{rr} + \frac{1}{r} w_r\right), \tag{10.23}$$

$$T_t - Aw = \chi\left(T_{rr} + \frac{1}{r} T_r\right), \tag{10.24}$$

$$\dot{\omega} r + v_t = \nu\left(v_{rr} + \frac{1}{r} v_r - \frac{v}{r^2}\right), \tag{10.25}$$

$$q_r = \frac{\rho v^2}{r}. \tag{10.26}$$

We can see that the circular and axial velocity components can be determined independently, while the temperature distribution is determined only by component w. Each of the initial boundary problems for Eqs. (10.23)–(10.25) can be solved by the Fourier method. The procedure of their solution has a routine character, and we do not discuss it.

Let us attach the initial and boundary conditions to Eq. (10.23)

$$w(r, 0) = w_0(r), \quad 0 \leqslant r \leqslant a, \tag{10.27}$$

$$w(a, t) = 0, \quad 0 \leqslant t \leqslant l, \quad |w| < \infty, \quad r \to 0, \tag{10.28}$$

as well as the additional condition of the nonzero flow rate through the tube cross section

$$\int_0^a w(r, t) r dr = 0, \quad 0 \leqslant t \leqslant l. \tag{10.29}$$

At specified functions ω and G, problem (10.23), (10.27)–(10.29) is overdetermined. However, we can formulate an inverse problem, i. e., find the function G and the solution of Eq. (10.23) at a specified function ω so that conditions (10.27)–(10.29) are fulfilled. There are the reasons to assume that the solution of such a problem will approximate well the solution of the convection problem in the main part of a long closed rotating cylinder at a linear temperature distribution of its boundary along the axial

coordinate. The results [114], where the convection problem in a long horizontal cuvette with a constant temperature drop being held at its lateral boundaries, support this assumption. They confirm the asymptotic character of the exact solution found in [35].

An inverse problem close to the formulated one was considered in article [166]. It was devoted to the time-dependent Poiseuille flow in a cylindrical tube with an arbitrary cross section with a specified flow rate depending on time, while the temperature gradient (the analog of function G) was subjected to determination.

To solve the inverse problem to (10.23), (10.27)–(10.29), let us multiply both parts of Eq. (10.23) by r and integrate the obtained equality by r in the interval $(0, a)$. Taking into account conditions (10.28) and (10.29), we obtain

$$G(t) = -\frac{1}{4} A\beta\omega^2(t) + \frac{2\nu}{a} w_r(a,t). \tag{10.30}$$

Relation (10.30) can be interpreted as a linear operator equation for the function G. Indeed, let us assume that the function $G \in C^{\alpha/2}[0,l]$ is specified, $0 < \alpha < 1$. Let the conditions of fitting be fulfilled for the input data of problem (10.23), (10.27), (10.28):

$$\omega \in C^{\alpha/2}[0,l]; \quad w_0 \in C^{2+\alpha}[0,a];$$
$$\frac{dw_0}{dr} = 0, \quad r = 0;$$
$$\nu\left(\frac{d^2w_0}{dr^2} + \frac{1}{r}\frac{dw_0}{dr}\right) = \frac{1}{2} A\beta\omega^2(0)a^2 + G(0), \quad r = a.$$

It follows from the general results of the theory of parabolic equations [116] that problem (10.23), (10.27), (10.28) has the unique solution $w \in C^{2+\alpha,1+\alpha/2}([0,a]\times[0,l])$. At specified ω and ω_0, let us determine the linear operator assigning the value of $w_r(a,t)$ to function $G(t)$. This operator acts from space $C^{\alpha/2}[0,l]$ into space $C^{(1+\alpha)/2}[0,l]$; it is the continuous Volterra-type operator. From here, an unambiguous dependence of Eq. (10.30) in space $C^{\alpha/2}[0,l]$ follows. Note that inverse problem (10.23), (10.27), (10.28) is reduced to finite dimensional if $\omega(t)$ is a trigonometric polynomial or finite sum of exponents $\exp(\lambda nt)$, where $\lambda = \text{const}$ and n is the integer.

Steady-state rotationally symmetrical flows

Let us consider the steady-state solutions of system (10.23), (10.24). It is convenient to pass to dimensionless variables to analyze them. The following scales are used: the tube radius a as the length scale, χ/a for velocity, $r\nu\chi/a^2$ for pressure, and Aa for temperature. Let us retain the previous notation of dimensionless quantities. In the above-mentioned scales, the general steady-state solution of system (10.23), (10.24)

can be presented in the form

$$w = \mathrm{Ra}\left(\frac{r^4}{32} + c_1\frac{r^2}{4} + c_2\ln r + c_3\right),$$
$$T = -\mathrm{Ra}\left[\frac{r^6}{32\cdot 36} + c_1\frac{r^4}{64} + c_2\frac{r^2(\ln r - 1)}{4} + c_3\frac{r^2}{4} + c_4\ln r + c_5\right],$$

where $\mathrm{Ra} = \beta A\omega^2 a^5/\nu\chi$ is the Rayleigh number, while the dimensional constant $G = \beta A\omega^2 a^5 c$.

If the tube is completely filled with liquid, it is natural to lay the conditions of finiteness of velocity and temperature. This gives $c_2 = 0$ and $c_4 = 0$. Two boundary conditions on the tube wall $r = a:\ w = 0$ and $T = 0$ along with the condition for full rate Q of the liquid through the tube section

$$\int_0^1 rwdr = \frac{Q}{2\pi}$$

determine the three remaining constants in the general solution. After simple calculations, we obtain

$$w = \frac{\mathrm{Ra}}{96}(1 - 4r^2 + 3r^4) + \frac{Q}{2\pi}(1 - r^2),$$
$$T = \frac{\mathrm{Ra}}{9\cdot 128}(1 - r^2)^3 + \frac{Q}{8\pi}(3 - 4r^2 + r^4),$$
$$\frac{\partial p}{\partial z} = -\frac{\mathrm{Ra}}{6}(1 - 3r^2) - \frac{8Q}{\pi}.$$

The case when the tube with a longitudinal temperature gradient is filled with two different liquids is of special interest. The presence of the interface between the liquids leads to the appearance of the surface thermocapillary force that forces the liquid to move along the tube. A rather complex convective flow with several controlling parameters, which is described by elementary functions, is formed in the rotating tube under the effect of the centripetal force (Figure 10.4).

Let the denser liquid occupy the region $r_* < r < 1$, while the lighter liquid occupies the region $0 < r < r_*$. Marking the solution of Eqs. (10.23) and (10.24) for the external liquid by index 1 and for the internal liquid by index 2, we write the general solution in the form

$$r_* < r < 1:\ w_1 = \mathrm{Ra}\left(\frac{r^4}{32} + c_1\frac{r^2}{4} + c_2\ln r + c_3\right),$$
$$0 < r < r_*:\ w_2 = \mathrm{Ra}\left(\frac{r^4}{32} + c_6\frac{r^2}{4} + c_7\ln r + c_8\right),$$
$$T_2 = -\mathrm{Ra}\left[\frac{r^6}{32\cdot 36} + c_6\frac{r^4}{64} + c_7\frac{r^2(\ln r - 1)}{4} + c_8\frac{r^2}{4} + c_9\ln r + c_{10}\right],$$
$$T_1 = -\mathrm{Ra}\left[\frac{r^6}{32\cdot 36} + c_1\frac{r^4}{64} + c_2\frac{r^2(\ln r - 1)}{4} + c_3\frac{r^2}{4} + c_4\ln r + c_5\right].$$

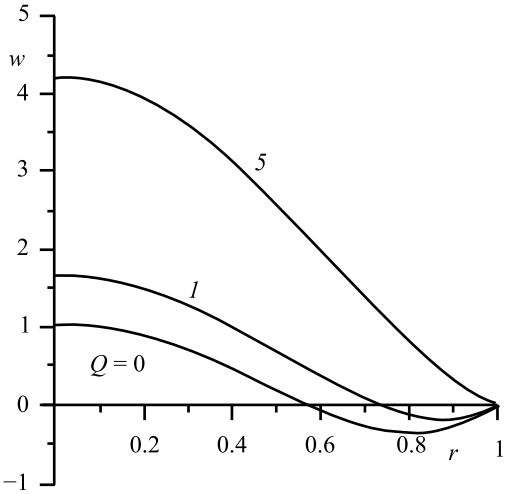

Figure 10.4: Velocity profile of the convective flow for different values of flow rate Q and Ra = 100.

To determine the constants, five continuity conditions at the interface between liquids should be added in this solution to the two conditions formulated above on the tube axis and the two conditions on the wall:

$$r = r_* : \; w_1 = w_2, \quad \frac{dw_1}{dr} - \eta \frac{dw_2}{dr} = \mathrm{Ma},$$
$$\frac{\partial p_1}{\partial z} = \frac{\partial p_2}{\partial z} - \mathrm{Ma}\,\frac{1}{r_*},$$
$$T_1 = T_2, \quad \frac{dT_1}{dr} = æ \frac{dT_2}{dr}, \quad \text{where } \mathrm{Ma} = \frac{d\sigma}{dT}\frac{Aa^2}{\eta_1 \chi_1}.$$

Here, Ma is the Marangoni number determined by the characteristics of the external liquid and $\sigma(T)$ is the surface tension coefficient on the interface, and the relative dynamic viscosity $\eta = \eta_2/\eta_1$ and thermal conductivity $æ = æ_2/æ_1$ of the liquids are introduced.

Let us formulate the condition for the pressure specifying the overall flow rate:

$$\int_0^{r_*} r w_2 dr + \int_{r_*}^{1} r w_1 dr = \frac{Q}{2\pi}.$$

Ten mentioned conditions form the linear set of equations for the determination of coefficients of the general solution. The velocity profiles of the convective flow calculated for $r_* = 0.5$ and different values of the Marangoni number and flow rate are presented in Figure 10.5. As follows from the form of the solution, the Rayleigh number is the scale factor; when constructing the plots, it equals 1.

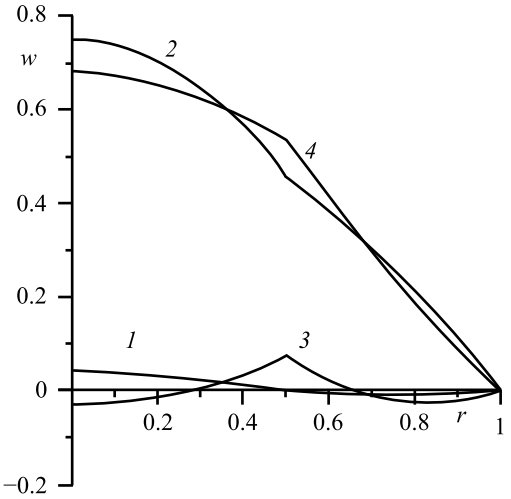

Figure 10.5: Velocity profiles of the convective flow in the two- liquid system with $r_* = 0.5$: (1) Ma = 0, $Q = 0$; (2) Ma = 0, $Q = 1$; (3) Ma = 1, $Q = 0$; and (4) Ma = 1, $Q = 1$.

10.3 Unsteady analogs of the Birikh solutions

New exact solutions of the Oberbeck–Boussinesq equations are constructed, which describe the motions in a horizontal band and in a rotating circular tube. These solutions generalize solutions constructed in [35, 37]. It is important that the streamwise temperature gradient depends on time. Results of this paragraph are based on the results of paper [185].

10.3.1 Introduction

The object of our study is the Oberbeck–Boussinesq equations

$$\mathbf{v}_t + \mathbf{v}\cdot\nabla\mathbf{v} = -\rho^{-1}\nabla p + \nu\Delta\mathbf{v} - \beta\theta\mathbf{g}, \quad \nabla\cdot\mathbf{v} = 0, \quad \theta_t + \mathbf{v}\cdot\nabla\theta = \chi\Delta\theta, \tag{10.31}$$

which describe convective motions of a viscous incompressible heat-conducting fluid in the gravity field with the acceleration $\mathbf{g} = (-g, 0, 0)$. Unlike (4.60), equations (10.31) are given in dimensional variables. Now we assume that $g = \text{const}$, but this constraint will be further eliminated. In system (10.31), $\mathbf{v}$ is the velocity vector, p is the deviation of pressure from the hydrostatic value, θ is the deviation of temperature from its mean value, ρ is the mean density of the fluid, ν is the kinematic viscosity coefficient, β is the volumetric coefficient of thermal expansion, and χ is the thermal diffusivity. In that follows, the quantities ρ, ν, β, and χ are assumed to be constant.

System (10.31) is nonlinear, it has a high order and does not refer to any classical type. For this reason, exact solutions of this system are extremely important for

decreasing the dimension and the order of the reduced equations; sometimes, the equations may become linearized. An example of such a solution is the solution obtained by Birikh [35], which describes a steady convective flow in a horizontal band. The solution constructed in this paper extends the Birikh solution to the case where the streamwise temperature gradient depends on time. A similar generalization can be obtained for the solution of the problem of axial convective motion in a rotating tube [37] and also of the problem of motion of two immiscible fluids with a plane or cylindrical interface [7, 85, 86, 194].

A systematic analysis of exact solutions is based on the use of methods of the group analysis of differential equations [155]. As applied to system (10.31), the group analysis was performed by Katkov [106] who considered a plane steady case and by Goncharova [76] who studied the general case and, moreover, examined the problem of the group classification of convection equations with temperature-dependent transfer coefficients. The group nature of the Birikh solution was discovered in [106, 182]. Pukhnachev [182] generalized the Birikh solution to a three-dimensional case. Other applications of theoretical-group methods in convection problems were described in [10, 18, 20].

Solutions of system (10.31) found in [35, 7, 86, 194] admit an interpretation in the form of flows in a plane horizontal or inclined channel. Pukhnachev [182] considered unsteady motion of the fluid in a horizontal cylindrical tube. All these solutions are united by the following circumstance: the temperature field can be represented in the form $\theta = -Az + T$, where $A = \text{const}$, and the function T is independent of the streamwise coordinate z. For the first time, solutions of the Oberbeck–Boussinesq equations possessing this property were found by Ostroumov [153] in studying the problem of stability of the equilibrium state of the fluid in a vertical tube with a streamwise temperature gradient. In this problem, the arising secondary flows have a simple nature: the horizontal components of velocity in these flows are equal to zero, and the vertical component of velocity and temperature are found from a linear system of equations. A natural question arises: Is it possible to cancel the assumption $A = \text{const}$, but still retain a comparatively simple flow structure? An affirmative answer is given to this question below for the case of a plane flow in a horizontal band. This generalization admits a solution with rotational symmetry, which was constructed in [37]. An analog of the Ostroumov solution for the case with $\theta_z \neq \text{const}$, however, cannot be constructed.

10.3.2 Plane motion in a horizontal band

We consider a plane layered motion in a horizontal band of width h. In what follows, the horizontal and vertical coordinates are denoted by z and x; the projections of the vector v onto the z and x axes are denoted by w and u, respectively. The third component of the velocity v is equal to zero, and the remaining sought functions u, w, p, and

θ are independent of the variable y. The gravity force with the acceleration g acts in the negative direction of the x axis. The layered character of motion is ensured by the equality $u = 0$. Then, it follows from the second equation of system (10.31) that the function w is independent of the variable z.

Under the assumptions made above, the Oberbeck–Boussinesq equations are substantially simplified and transform to

$$w_z = 0, \quad w_t = \nu w_{xx} - \rho^{-1} p_z, \quad p_x = \rho g \beta \theta, \quad \theta_t + w\theta_x = \chi(\theta_{xx} + \theta_{zz}). \tag{10.32}$$

System (10.32) is overdetermined. Its steady version was studied by Birikh [35]. He demonstrated that the function w in the steady case is a cubic polynomial and the remaining sought functions can be represented in the form $\theta = -Az + T(x)$, $p = -A\rho g\beta xz + q(x)$, where T and q are polynomials of the fifth and sixth powers, respectively. It was found later [106] that the Birikh solution has a theoretical-group nature; it is an invariant solution of system (10.31) with respect to the group with the basis operators $\partial_z - A(\partial_\theta + \rho g\beta x\partial_p)$, ∂_t, ∂_y ($A = \text{const}$) admitted by this system. The issue of compatibility of system (10.32) is resolved in the general form below. It turns out that the set of solutions of this system, supplemented with the equalities $u = v = 0$, is not confined to the invariant solutions of the original Oberbeck–Boussinesq equations.

It follows from the first two equations of system (10.32) that p depends linearly on the variable z; from the third equation of this system, it also follows that the function θ possesses the same property. Let us assume that

$$w = w(x,t), \quad \theta = -A(x,t)z + T(x,t), \quad p = -B(x,t)z + q(x,t). \tag{10.33}$$

Substituting Eqs. (10.33) into system (10.32), we obtain

$$A_t = \chi A_{xx}, \quad B_x = \rho g\beta A, \quad w_t = \nu w_{xx} + \rho^{-1} B, \quad T_t = \chi T_{xx} + Aw, \quad q_x = \rho g\beta T. \tag{10.34}$$

In contrast to system (10.32), the number of equations in system (10.34) coincides with the number of the sought functions. This system is recurrent, and its consecutively solved equations are linear with respect to the new sought functions. The term Aw in the fourth equation of the system, however, induces an element of nonlinear interaction of the temperature and velocity fields.

System (10.34) is considered in the domain $D = \{x,t : -h < x < 0, t > 0\}$. The solution of the first equation of system (10.34) is uniquely determined by imposing the initial and boundary conditions. Knowing the function A, we take a quadrature and find the function B from the second equation of this system. After that, the system for determining the functions w, T, and q becomes closed. In particular, for the function w, we have

$$w_t - \nu w_{xx} = g\beta \int_{-h}^{x} A(s,t)ds - \rho^{-1} C(t), \quad (x,t) \in D. \tag{10.35}$$

Here, C is a given function of t, which defines the additional term in the linear dependence of pressure on the variable z, which is not related to the convection process. Equation (10.35) requires the initial condition

$$w = w_0(x), \quad -h \leqslant x \leqslant 0, \quad t = 0, \tag{10.36}$$

and the boundary conditions, which can be naturally taken as the no-slip conditions

$$w = 0, \quad x = -h \quad \text{and} \quad x = 0, \quad t > 0. \tag{10.37}$$

The solution of problem (10.35)–(10.37) is determined uniquely. We do not discuss here the properties of smoothness of this solution: they can be obtained on the basis of the well-known results of the theory of linear parabolic equations [116] with ensuring the necessary smoothness of the functions A, w_0, and Q. Now we can find the function T from the solution of the initial-boundary problem for the fourth equation of system (10.34) and, after that, the function q from the last equation by taking a quadrature.

Note that the first equation of system (10.34) always has the solution $A = \text{const}$. If, in addition, the function w is independent of t, we obtain the classical Birikh solution [35]. If $A(x, t)$ is an arbitrary solution of the heat conduction equation, we obtain a new class of solutions of the Oberbeck–Boussinesq equations that describe unsteady convective motions in a band, which possesses broad functional arbitrariness. It should also be noted that the assumption about a constant value of g was not used in deriving Eq. (10.35). Assuming that $g = g(t)$, we obtain the next generalization of the Birikh solution.

In addition to problem (10.35)–(10.37), it is of interest to consider a problem where the flow rate of the fluid through the band cross section is specified instead of the function $C(t)$:

$$\int_{-h}^{0} w(x, t)dx = Q(t). \tag{10.38}$$

The function C in problem (10.35)–(10.38) is also a sought function, in addition to the function w. Therefore, this problem refers to the class of inverse problems. It is a one-dimensional analog of the problem considered in [166]. Using the methods of this work, we can prove the unique solvability of problem (10.35)–(10.38) in appropriate Hölder classes. As this problem is one-dimensional, however, another approach is more convenient here, which is based on reducing this problem to the Volterra operator equation.

To solve the inverse problem, we integrate Eq. (10.35) with respect to x on the interval $(-h, 0)$. Using equality (10.38) and introducing the notation

$$\begin{gathered} \rho g \beta h^{-1} \left\{ \int_{-h}^{0} \left[\int_{-h}^{x} A(s, t)ds \right] dx \right\} - \rho h^{-1} Q'(t) = f(t), \\ C(t) = f(t) + \rho \nu h^{-1} \left[w_x(0, t) - w_x(-h, t) \right], \end{gathered} \tag{10.39}$$

we obtain the relation (10.39) which can be treated as a linear operator equation with respect to the function C. Let the specified functions $A(x,t)$ and $Q(t)$ belong to the following Hölder classes: $A \in C^{2+\alpha,1+\alpha/2}([-h,0]\times[0,l])$ and $Q \in C^{1+\alpha/2}[0,l]$, $0<\alpha<1$. Let the conditions of smoothness and compatibility for the input data of problem (10.35)–(10.37) be satisfied:

$$w_0 \in C^{2+\alpha}[-h,0], \quad w_0(-h) = w_0(0) = 0, \quad \nu w_0''(0) = C(0),$$
$$\nu w_0''(-h) = C(0) - g\beta \int_{-h}^{0} A(x,\ 0)dx = 0.$$

It follows from the general results of the theory of parabolic equations [116] that problem (10.35)–(10.37) has a unique solution $w \in C^{2+\alpha,1+\alpha/2}([-h,0],[0,l])$. Let us determine a linear operator that puts the function $w_x(0,t)-w_x(-h,t)$ into correspondence to the function $C(t)$. This operator acts from the space $C^{\alpha/2}[0,l]$ to the space $C^{(1+\alpha)/2}[0,l]$ and is a continuous Volterra-type operator. From here, there follows unique solvability of Eq. (10.39) in the space $C^{\alpha/2}[0,l]$ for any $l>0$.

10.3.3 Layered motion of immiscible fluids

Let us consider a system of two immiscible fluids separated by the interface $x=0$. The parameters of the fluid moving in the band $0<x<h_1$, $z\in\mathrm{R}$ are indicated by the subscript "1," and the parameters of the fluid moving in the band $-h_2<x<0$ are indicated by the subscript "2." In the plane motion considered here, the velocity components u_1 and u_2 are equal to zero, and the velocity components w_1 and w_2 are independent of z. Following the construction performed in Section 10.3.2, we seek for solutions of the Oberbeck–Boussinesq equations in the form

$$w_i = w_i(x,t), \quad \theta_i = -A_i(x,t)z + T_i(x,t), \quad p_i = -B_i(x,t)z + q_i(x,t), \quad i=1,2. \tag{10.40}$$

Here, A_i and T_i can be arbitrary solutions of the heat conduction equations

$$A_{i,t} = \chi_i A_{i,xx}, \quad T_{i,t} = \chi_i T_{i,xx}, \quad i=1,2, \tag{10.41}$$

related by the conditions of the thermal contact on the interface

$$A_1 = A_2, \quad k_1 A_{1,x} = k_2 A_{2,x}, \quad x=0, \quad t>0. \tag{10.42}$$

The functions A_i and B_i, T_i and q_i $(i=1,2)$ are related by

$$B_i(x,t) = \rho_i g\beta_i \int_0^x A_i(s,t)ds - C_i(t), \quad q_i = \rho_i g\beta_i \int_0^x T_i(s,t)ds, \tag{10.43}$$

where C_i are still arbitrary functions of t. Hereinafter, the density, viscosity, thermal expansion coefficient, thermal diffusivity, and thermal conductivity of the ith fluid are denoted by $\rho_i, \nu_i, \beta_i, \chi_i$, and k_i, respectively. As previously, these parameters are assumed to be positive constants. No other constraints are imposed on these parameters *a priori*. If we want to ensure stability of stratification, however, we should take $\rho_1 < \rho_2$.

Let us introduce the notations $D_1 = \{x, t : 0 < x < h_1, t > 0\}$ and $D_2 = \{x, t : -h_2 < x < 0, t > 0\}$. The functions w_1 and w_2 satisfy the equations

$$w_{i,t} - \nu_i w_{i,xx} = g\beta_i \int_0^x A_i(s,t)ds - \rho_i^{-1} C_i(t), \quad (x,t) \in D_i, \ i = 1,2. \tag{10.44}$$

For system (10.44), we impose the initial conditions

$$w_1 = w_{0,1}(x), \quad 0 \leqslant x \leqslant h_1, \quad t = 0; \quad w_2 = w_{0,2}(x), \quad -h_2 \leqslant x \leqslant 0, \quad t = 0, \tag{10.45}$$

the no-slip conditions on the solid boundaries of the flow domain

$$w_1 = 0, \quad x = h_1, \quad t \geqslant 0; \quad w_2 = 0, \quad x = -h_2, \quad t \geqslant 0, \tag{10.46}$$

and the conditions on the interface, which were formulated in the general form in [10, 18, 20]. One of them is the condition of velocity continuity

$$w_1 = w_2, \quad x = 0, \quad t > 0. \tag{10.47}$$

Another condition requires the jump of the normal stress on the interface to be equal to capillary pressure proportional to the mean curvature of the interface. In the case of a flat interface examined here, the normal stress is continuous. Moreover, by virtue of the equalities $u_1 = u_2 = 0$, we obtain $p_1 = p_2$ at $x = 0$. The last condition combined with Eqs. (10.40)–(10.43) yields the equality $C_1 = C_2 \equiv C$. One more dynamic condition has the form

$$\rho_1 \nu_1 w_{1,x} - \rho_2 \nu_2 w_{2,x} = æA, \quad x = 0, \quad t \geqslant 0, \tag{10.48}$$

where $A(t)$ is the common value of the functions A_1 and A_2 on the line $x = 0$, and æ = const > 0 is the coefficient in the equality

$$\sigma = \sigma_0 - æ(\theta - \bar{\theta}), \tag{10.49}$$

which expresses the dependence of the surface tension coefficient on temperature (here, σ_0 and $\bar{\theta}$ are positive constants). By virtue of Eqs. (10.40) and (10.49), condition (10.48) means that the difference in the shear stresses on the interface is equal to the tangent of the derivative of the surface tension coefficient. Finally, the kinematic condition on the interface is satisfied identically, which is a common property of layered motions.

Let the functions A_1, A_2, and C be known. Then, Eqs. (10.45)–(10.48) define a well-posed problem for system (10.44). If this problem is solved, we can find the functions T_i from the equations

$$T_{i,t} = \chi_i T_{i,xx} + A_i w_i, \quad i = 1, 2$$

under the corresponding initial and boundary conditions. After that, taking quadratures, we reconstruct the functions q_1 and q_2 from Eqs. (10.43).

10.3.4 Unsteady axial convection in a rotating tube

Let the fluid fill a circular tube of radius a rotating around its axis with an angular velocity $\omega(t)$. Let us denote the cylindrical coordinates by r, φ, z, and let the tube axis coincide with the z axis. In what follows, u and w are the radial and axial components of the velocity vector, v is the difference between the angular velocity and the velocity of fluid rotation as a solid ωr, p is the deviation of pressure from its equilibrium value $\rho\omega^2 r^2/2$, and θ is the deviation of temperature from its mean value $\bar{\theta}$. We consider only the case of rotationally symmetric motions. This means that all sought functions are independent of the angle φ. In the above-accepted notations, the equations of rotationally symmetric motion in the field of centripetal forces are written in the following form [37]:

$$\begin{gathered}
u_t + uu_r + wu_z - 2\omega v - \frac{v^2}{r} = -\frac{1}{\rho}p_r + \nu\left(u_{rr} + \frac{1}{r}u_r - \frac{u}{r^2} + u_{zz}\right) - \omega^2\beta r\theta, \\
v_t + uv_r + wv_z + 2\omega u + \dot{\omega} r + \frac{uv}{r} = \nu\left(v_{rr} + \frac{1}{r}v_r - \frac{v}{r^2} + v_{zz}\right), \\
w_t + uw_r + ww_z = -\frac{1}{\rho}p_z + \nu\left(w_{rr} + \frac{1}{r}w_r + w_{zz}\right), \\
u_r + \frac{u}{r} + w_z = 0, \\
\theta_t + u\theta_r + w\theta_z = \chi\left(\theta_{rr} + \frac{1}{r}\theta_r + \theta_{zz}\right).
\end{gathered} \tag{10.50}$$

Birikh and Pukhnachev [37] considered the solutions of system (10.50) where the function w is independent of the variable z, and the function θ has the form $\theta = -Az + T(r, t)$, where $A = \text{const}$. Below, we study solutions of a more general form where

$$w = w(r, t), \quad v = v(r, t), \quad \theta = -A(r, t)z + T(r, t), \quad p = -B(r, t)z + q(r, t). \tag{10.51}$$

Then, it follows from the penultimate equation of system (10.50) and from the assumption of the absence of sinks and sources on the tube axis that $u = 0$. The study

of compatibility of the remaining equations of system (10.50) with Eqs. (10.51) yields the following results. The function A satisfies the radial heat conduction equation

$$A_t = \chi\left(A_{rr} + \frac{1}{r}A_r\right). \tag{10.52}$$

The function v satisfies the equation

$$v_t + \dot{\omega}r = \nu\left(v_{rr} + \frac{1}{r}v_r - \frac{v}{r^2}\right). \tag{10.53}$$

For the function w, we obtain the equation

$$w_t - \nu\left(w_{rr} + \frac{1}{r}w_r\right) = g\beta\int_0^r sA(s,t)ds - \frac{1}{\rho}C(t), \tag{10.54}$$

where C is an arbitrary function of t. For the function T, we have the equation

$$T_t = \chi\left(T_{rr} + \frac{1}{r}T_r\right) + Aw. \tag{10.55}$$

It should be noted that Eqs. (10.52)–(10.54) are linear; therefore, problems similar to that considered in Section 10.3.1 can be studied for these equations. Equations (10.52) and (10.53) are not related to each other. If the function A is found, then the functions w and T are obtained from the consecutively solved Eqs. (10.54), (10.55). For known A, T, and v, the functions B and q are determined by the equalities

$$B(r,t) = \rho g\beta\int_0^r sA(s,t)ds - C(t), q(r,t) = \rho\left\{\int_0^r\left[2\omega(t)v(s,t) + \frac{v^2(s,t)}{s} + g\beta sT(s,t)\right]ds\right\}. \tag{10.56}$$

Thus, we obtained an essentially unsteady analog of the solution studied in [37]. It should also be noted that an inverse problem similar to that formulated in Section 10.3.1 can be considered for Eq. (10.54) in addition to the direct problem.

10.3.5 Motion of immiscible fluids in a rotating tube

The problem considered in Section 10.3.4 admits extension to the case of motion of two immiscible fluids with a cylindrical interface. The solution of the convection equations in this case is sought in the form similar to Eq. (10.51):

$$w_i = w_i(r,t), \quad v_i = v_i(r,t), \quad \theta_i = -A_i(r,t)z + T_i(r,t), \quad p_i = -B_i(r,t)z + q_i(r,t), \quad i = 1,2. \tag{10.57}$$

Here, A_i $(i = 1, 2)$ are the solutions of the radial heat conduction equations with the coefficients χ_i related by the heat balance conditions

$$A_1 = A_2, \quad k_1 A_{1,r} = k_2 A_{2,r}, \quad r = b, \quad t \geqslant 0.$$

We denote the coinciding values of the functions A_1 and A_2 on the interface by A. Without writing all equations of our problem, we formulate the relations that determine the velocities of axial motion of the contacting fluids.

Let the interface equation have the form $r = b = \text{const} < a$, where a is the tube radius. The characteristics of the fluid located in the cylinder $r < b$ are indicated by the subscript "1," and the characteristics of the fluid filling the cylindrical layer $b < r < a$ are indicated by the subscript "2." Let us assume that $\rho_1 < \rho_2$ to avoid the Rayleigh–Taylor instability. Let us denote $D_1 = \{r, t : 0 < x < b, t > 0\}$ and $D_2 = \{r, t : b < r < a, t > 0\}$. The functions w_1 and w_2 satisfy the equations

$$w_{i,t} - \nu_i \left(w_{i,rr} + \frac{1}{r} w_{i,r} \right) = g\beta_i \int_b^r s A_i(s,t)\,ds - \frac{1}{\rho_i} C_i(t), \quad (r,t) \in D_i, \; i = 1, 2, \tag{10.58}$$

the initial conditions

$$w_1 = w_{0,1}(r), \quad 0 \leqslant r \leqslant b, \quad t = 0; \quad w_2 = w_{0,2}(r), \quad b \leqslant r \leqslant a, \quad t = 0, \tag{10.59}$$

the no-slip condition on the tube surface

$$w_2 = 0, \quad r = a, \quad t \geqslant 0, \tag{10.60}$$

the condition of boundedness of w_1 as $r \to 0$, the condition of velocity continuity on the interface

$$w_1 = w_2, \quad r = b, \quad t \geqslant 0, \tag{10.61}$$

and the condition of the balance of shear stresses with allowance for the thermocapillary effect on the interface

$$\rho_1 \nu_1 w_{1,r} - \rho_2 \nu_2 w_{2,r} = æ A, \quad r = b, \quad t \geqslant 0. \tag{10.62}$$

Here, æ is the coefficient in dependence (10.49) of surface tension on temperature. The functions C_i involved into the right-hand sides of Eq. (10.57) arise in the course of obtaining a solution of system (10.50) in the form (10.57). They are related to the functions A_i and B_i by the equalities

$$B_i(r,t) = \rho_i g \beta_i \int_0^r s A_i(s,t)\,ds - C_i(t), \quad i = 1, 2. \tag{10.63}$$

These functions specify additional terms in the linear dependence of pressure on the axial coordinate, which do not have a convective nature. In contrast to the plane problem considered in Section 10.3.2, the functions C_1 and C_2 do not coincide here. The reason is the presence of an additional term (capillary pressure) in the condition of equality of the normal stresses on the interface. By virtue of the equalities $u_1 = u_2 = 0$, this condition is written in the form

$$p_1 = p_2 + b^{-1}\sigma, \quad r = b, \quad t \geqslant 0.$$

Let us substitute Eqs. (10.57) for the functions p_1 and p_2 and Eq. (10.49) for the function σ into the last equality, use equalities (10.63), and then find linear terms with respect to z in the resultant equality. Thus, we obtain

$$C_1 = C_2 + æb^{-1}A, \quad t \geqslant 0.$$

One of the functions (C_1 or C_2) can be prescribed arbitrarily.

Thus, we obtained a closed formulation (10.58)–(10.62) of the problem of determining the axial velocities in a rotating two-layer system under the combined action of the centripetal force and axial gradients of temperature and pressure. As in the problem considered in [37], the temperature in each layer is a linear function of the axial coordinate z. In contrast to [37], however, the coefficient in this dependence is not constant: it is a linear function of the variable z and arbitrary function of the variable t. This dependence possesses functional arbitrariness. In particular, we can specify the temperature on the tube surface in the form

$$\theta_2 = -\gamma(t)z + \delta(t), \quad r = b, \quad t \geqslant 0,$$

where γ and δ are arbitrary functions of time.

10.3.6 Three-dimensional analogs of the Birikh solution

In our further considerations, S is a bounded domain on the plane x, y, and Ω is a cylinder: $\Omega = \{x, y, z : (x, y) \in S,\ z \in \mathrm{R}\}$. Pukhnachev [182] found a class of solutions of the system of the Oberbeck–Boussinesq equations (10.31), which describes unsteady motions in a cylinder. These solutions are a three-dimensional analog of the Birikh solution and have the form (10.5), where $A = \text{const}$. Solutions (10.5) of system (10.31) are invariant solutions of rank 3 with respect to the operator $\partial_z - A(\partial_\theta + \rho g \beta x \partial_p)$ admitted by this system.

A natural question arises: Is it possible to obtain generalizations of solutions (10.5) to the case where the coefficient A is not a constant? It turns out that this can be achieved only with appreciable simplification of the kinematic system of the flow.

We seek for the solutions of system (10.31) supplemented with the relations

$$v_z = 0, \quad \theta = -A(x,\ y,t)z + T(x,y,t), \quad p = -B(x,y,t)z + q(x,y,t). \tag{10.64}$$

These solutions include solutions of the form of Eqs. (10.5), but not only these solutions. Substituting Eqs. (10.64) into system (10.31), we obtain the relations

$$\begin{gathered} u_t + uu_x + vu_y = -\rho^{-1}q_x + \nu(u_{xx} + u_{yy}) + g\beta T + z(\rho^{-1}B_x - g\beta A), \\ v_t + uv_x + vv_y = -\rho^{-1}q_y + \nu(v_{xx} + v_{yy}) - z\rho^{-1}B_y, \\ w_t + uw_x + vw_y = -\rho^{-1}B + \nu(w_{xx} + w_{yy}), \\ u_x + v_y = 0, \\ T_t + uT_x + vT_y - wA - z(A_t + uA_x + vA_y) = \chi(T_{xx} + T_{yy}) - z\chi(A_{xx} + A_{yy}). \end{gathered} \tag{10.65}$$

Equating the coefficients at the first and zeroth powers of z in Eqs. (10.65) to zero, we obtain

$$B_x = \rho g\beta A, \quad B_y = 0, \quad A_t + uA_x + vA_y = \chi(A_{xx} + A_{yy}), \tag{10.66}$$

$$\begin{gathered} u_t + uu_x + vu_y = -\rho^{-1}q_x + \nu(u_{xx} + u_{yy}) + g\beta T, \\ v_t + uv_x + vv_y = -\rho^{-1}q_y + \nu(v_{xx} + v_{yy}), \\ w_t + uw_x + vw_y = -\rho^{-1}B + \nu(w_{xx} + w_{yy}), \quad u_x + v_y = 0, \\ T_t + uT_x + vT_y - wA = \chi(T_{xx} + T_{yy}). \end{gathered} \tag{10.67}$$

It follows from the first two equations of system (10.66) that the function A is independent of y. This fact allows us to rewrite the third equation of system (10.66) in the form

$$A_t + uA_x = \chi A_{xx}. \tag{10.68}$$

There are two options. Either we have $u_y \neq 0$, and then $A = \text{const}$, which yields solutions (10.5). If $u_y = 0$, then the function v depends linearly on y by virtue of the penultimate equation of system (10.67). In what follows, we consider the case where this dependence is homogeneous; therefore, we have

$$u = u(x,t), \quad v = -yu_x. \tag{10.69}$$

Substituting Eqs. (10.69) into Eqs. (10.67), we obtain

$$\begin{gathered} u_t + uu_x = -\rho^{-1}q_x + \nu u_{xx} + g\beta T, \quad y(u_{xt} + uu_{xx} - u_x^2) = \rho^{-1}q_y + \nu y u_{xxx}, \\ w_t + uw_x - yu_x w_y = -\rho^{-1}B + \nu(w_{xx} + w_{yy}), \\ T_t + uT_x - yu_x T_y - wA = \chi(T_{xx} + T_{yy}). \end{gathered} \tag{10.70}$$

It follows from the second equation of system (10.70) that the function q is a squared function of the variable y; moreover, it follows from the first equation of this

system that the function T possesses the same property. Considering the last equation of system (10.70), we see that the function w is also a squared function of y. For simplicity, we further assume that the dependences of the functions q, T, and w on the variable y are even:

$$q = \xi y^2 + \phi, \quad T = \eta y^2 + \vartheta, \quad w = \varsigma y^2 + \psi. \tag{10.71}$$

Here, $\xi, \phi, \eta, \vartheta, \varsigma$, and ψ are the sought functions of the variables x and t. The equations for determining these functions are obtained by substituting Eqs. (10.71) into system (10.70). After simple transformations, we obtain the following system of equations;

$$u_{xxt} + uu_{xxx} - u_x u_{xx} = \nu u_{xxxx} + 2g\beta\eta, \quad \eta_t + u\eta_x - 2u_x\eta - \varsigma A = \chi\eta_{xx}, \tag{10.72}$$

$$\varsigma_t + u\varsigma_x - 2u_x\varsigma = \chi\varsigma_{xx},$$

$$\vartheta_t + u\vartheta_x - \psi A = \chi(\vartheta_{xx} + 2\eta), \quad \psi_t + u\psi_x = -\rho^{-1}B + \nu(\psi_{xx} + 2\varsigma), \tag{10.73}$$

$$\xi_x = \rho g\beta\eta, \quad \phi_x = \rho(g\beta\vartheta - u_t - uu_x). \tag{10.74}$$

Relations (10.68), (10.72) form a closed system of quasi-linear equations for determining the functions A, u, η, and ς of the variables x and t. Three equations are parabolic, and the remaining equation (the first equation of system (10.72)) is of a composite type. If the functions A, u, η, and ς are found, then the functions ϑ and ψ are determined from the system of linear parabolic equations (10.73). After that, the remaining functions ξ, ϕ, and B are reconstructed by using quadratures from Eqs. (10.74) and the first equation of system (10.66) with accuracy to arbitrary additive functions of time. Two of them do not affect the velocity field, while the third one (involved into the definition of B) participates in generating the axial velocity w.

We further assume that the tube cross section S is a rectangle: $S = \{x, y : |x| < h, |y| < d\}$. Let us formulate the initial-boundary problem for system (10.68), (10.72).

On the upper and lower sides of the rectangle S, i. e., at $x = \pm h$, we can naturally impose the no-slip conditions, which are written in the following form by virtue of Eqs. (10.69), (10.71):

$$u = 0, \quad u_x = 0, \quad \varsigma = 0, \quad x = |h|, \quad t \geqslant 0. \tag{10.75}$$

As the temperature conditions, we specify the values of the functions A and η on the horizontal sides of S, assuming for simplicity that these values coincide on both sides:

$$A = \gamma(t), \quad \eta = \delta(t), \quad |x| = h, \quad t > 0. \tag{10.76}$$

The problem formulation is closed by setting the initial conditions

$$A = A_0(x), \quad u = u_0(x), \quad \eta = \eta_0(x), \quad \varsigma = \varsigma_0(x), \quad |x| \leqslant h, \quad t = 0. \tag{10.77}$$

Problem (10.68), (10.72), (10.75)–(10.77) is rather complicated. The theorem of uniqueness of the classical solution is established for it comparatively simply. The lack of *a priori* estimates prevents obtaining the theorem of existence of the solution "as a whole." The existence of the solution of this problem on a small time interval can be proved by the methods developed in [116].

An advantage of the solution obtained is the possibility of specifying a streamwise temperature gradient on the horizontal boundaries of the channel as an arbitrary function of time. An unavoidable defect is the failure to satisfy the natural no-slip boundary conditions on the vertical boundaries of the channel. Physical realization of this solution requires special distributions of velocity and temperature on the lines $y = \pm d$, which should be correlated with Eqs. (10.69), (10.71).

10.3.7 On the Ostroumov solutions

Ostroumov [153] found a class of solutions of convection equations, which describe flows in cylindrical tubes induced by a streamwise temperature gradient. Let S be a bounded domain of the plane x, y, and let Ω be a cylinder with a cross section S and generatrices parallel to the z axis. In this Section, it is convenient to assume that the gravity force with the acceleration g acts in the negative direction of the z axis.

Under the assumptions made above, Eqs. (10.31) are written in the coordinate form as

$$\begin{gathered} u_t + uu_x + vu_y + wu_z = -\rho^{-1}p_x + \nu(u_{xx} + u_{yy} + u_{zz}), \\ v_t + uv_x + vv_y + wv_z = -\rho^{-1}p_y + \nu(v_{xx} + v_{yy} + v_{zz}), \\ u_t + uu_x + vu_y + wu_z = -\rho^{-1}p_z + \nu(u_{xx} + u_{yy} + u_{zz}) + \rho g\theta, \\ u_x + v_y + w_z = 0, \\ \theta_t + u\theta_x + v\theta_y + w\theta_z = \chi(\theta_{xx} + \theta_{yy} + \theta_{zz}). \end{gathered} \tag{10.78}$$

Equations (10.78) admit the operator $\partial_z - A(\partial_\theta + \rho g\beta z\partial_p)$, where $A = \text{const}$. This allows us to construct the invariant solutions of this system in the form

$$\begin{gathered} \mathbf{v} = \big(u(x,y,t), v(x,y,t), w(x,y,t)\big), \quad p = -\rho g\beta A z^2/2 + q(x,y,\ t), \\ \theta = -Az + T(x,y,t). \end{gathered} \tag{10.79}$$

Substituting Eqs. (10.79) into Eqs. (10.78), we obtain the system

$$\begin{gathered} u_t + uu_x + vu_y = -\rho^{-1}q_x + \nu(u_{xx} + u_{yy}), \\ v_t + uv_x + vv_y = -\rho^{-1}q_y + \nu(v_{xx} + v_{yy}), \\ u_x + v_y = 0, \end{gathered} \tag{10.80}$$

$$\begin{gathered} w_t + uw_x + vw_y = \nu(w_{xx} + w_{yy}) + \rho gT, \\ T_t + uT_x + vT_y - Aw = \chi(T_{xx} + T_{yy}). \end{gathered} \tag{10.81}$$

We see that the functions u, v, and q satisfy the equations of plane motion of a viscous incompressible fluid whose theory is well developed. If the functions u and v are known, then the remaining sought functions w and T are determined from the system of linear equations (10.81).

System (10.80) has a trivial solution $u = v = 0, q = q(t)$. In this case, Eqs. (10.81) are simplified; in the steady case, they lead to spectral problems where the temperature gradient A plays the role of the spectral parameter. The simplest problem corresponds to the boundary conditions of the first kind:

$$w = 0, \quad T = 0, \quad (x, y) \in \partial S.$$

Other problems correspond to the condition of the second kind for the function T and to the conditions of the thermal contact of the convective fluid with the ambient solid medium. These problems were studied in [153, 68]. Stability of the Ostroumov steady solutions was examined in [68].

If we take any time-dependent solution of system (10.80) as the coefficients u and v of the linear system (10.81), we obtain a family of solutions of Eqs. (10.31), which can be called unsteady analogs of the Ostroumov solution. Such generalization of these solutions, however, is based on the assumption that the quantity $\theta_z = A$ is constant. An attempt to replace this quantity by a function of the variables x, y, and t is not successful. We propose the reader to prove this statement.

10.3.8 Concluding remarks

a). The solutions of plane and axisymmetric problems of convection, which are given in Sections 10.3.2–10.3.4, are essential generalizations of the known solutions [35, 37] to the case where the axial temperature gradient is an arbitrary function of time. In contrast to the Birikh solution, the theoretical-group nature of these solutions has not been clarified yet, which should not be considered as a drawback of these solutions.

b). The inverse problem similar to that examined in Section 10.3.2 can be considered for a two-layer flow described in Section 10.3.3. In this case, it is possible to specify the flow rate of only one fluid as a function of time, because the streamwise pressure gradients are identical in both layers.

c). Thermogravitational and thermocapillary convective flows in horizontal layers under the action of a streamwise temperature gradient (including unsteady flows) were realized in experiments [107, 108].

d). Problem (10.68), (10.72), (10.75)–(10.77) admits appreciable simplification if $\varsigma_0 = 0$ in Eqs. (10.77). In this case, the function ς is identically equal to zero. A system of two equations (10.72) is obtained for the functions u and η. If the solution of this system is known, then the function A is found from the linear equation (10.68).

e). The problem of convection in a gap between two non-coaxial cylinders is an example of an unsteady analog of the Ostroumov solution. The inner cylinder rotates around its axis with a given angular velocity, which may be time-dependent.

10.4 Model of viscous layer deformation by thermocapillary forces

A three-dimensional non-stationary flow of a viscous incompressible liquid is investigated in a layer driven by a nonuniform distribution of temperature on its free boundaries. If the temperature given on the layer boundaries is quadratically dependent on horizontal coordinates, external mass forces are absent, and the motion starts from rest, then the free boundary problem for the Navier–Stokes equations has an "exact" solution in terms of two independent variables. Here the free boundaries of the layer remain parallel planes and the distance between them must be also determined. In present paper, we formulate conditions for both the unique solvability of the reduced problem globally in time and the collapse of the solution in finite time. We further study qualitative properties of the solution such as its behavior for large time (in the case of global solvability of the problem), and the asymptotics of the solution near the collapse moment in the opposite case. This paragraph is based on the results of paper [175].

Formulation of the problem

We consider thermocapillary motion of a viscous incompressible liquid bounded entirely by free surfaces. The domain occupied by liquid is denoted by Ω_t and its boundary is denoted by Γ_t. The liquid density ρ and kinematic viscosity ν are taken to be constant, and the surface tension σ is taken to be a linear function of temperature θ:

$$\sigma = \sigma_0 - æ(\theta - \theta_0), \tag{10.82}$$

where σ_0, æ and θ_0 are positive constants. We suppose further that the motion starts from rest and that external mass forces do not act on the liquid. Moreover, we assume that the temperature at the free surface $\theta_\Gamma(\mathbf{x}, t)$ is a known function of the coordinates $\mathbf{x} = (x, y, z)$ and time t. Hence, the mathematical formulation of the problem is reduced to determination of the domain Ω_t, $0 < t < T$ and the solution $\mathbf{v}(\mathbf{x}, t) = (u, v, w)$, $p(\mathbf{x}, t)$ of the Navier–Stokes equations

$$\mathbf{v}_t + \mathbf{v} \cdot \nabla \mathbf{v} = -\rho^{-1} \nabla p + \nu \Delta \mathbf{v}, \quad \nabla \cdot \mathbf{v} = 0 \tag{10.83}$$

in this domain, satisfying the initial conditions

$$\Omega_0 \quad \text{is given}, \quad \mathbf{v}(\mathbf{x}, 0) = 0, \quad \mathbf{x} \in \Omega_0 \tag{10.84}$$

and the conditions on the free surfaces

$$-p\mathbf{n} + 2\rho\nu D \cdot \mathbf{n} = -2K\sigma\mathbf{n} + \nabla_\Gamma \sigma, \tag{10.85}$$

$$\mathbf{v} \cdot \mathbf{n} = V_n, \quad \mathbf{x} \in \Gamma_t, \quad 0 < t < T. \tag{10.86}$$

The following notation is used in Eqs. (10.85), (10.86): $\mathbf{n}$ is the unit external normal to the surface Γ_t, $D = [\nabla\mathbf{v} + (\nabla\mathbf{v})^*]/2$ is the strain rate tensor, K is the mean curvature of the surface Γ_t, $\nabla_\Gamma = \nabla - \mathbf{n}(\mathbf{n} \cdot \nabla)$ is the surface gradient, and V_n is the velocity of displacement of the surface Γ_t in the direction of $\mathbf{n}$. Substituting the expression for σ in the form of Eq. (10.82) with $\theta = \theta_\Gamma(\mathbf{x}, t)$ into Eq. (10.85), we obtain a closed formulation of the free boundary problem for the Navier–Stokes equations.

The solvability conditions for the initial boundary-value problem (10.83)–(10.86) are derived in Mogilevskii & Solonnikov [137]. Investigated in Andreev & Pukhnachov [19] are the invariance properties of this problem; the group classification of this problem relative to an "arbitrary element" $\theta_\Gamma(\mathbf{x}, t)$ is satisfied there too. Examples of exact solutions of the equations of thermocapillary motion are presented in Birikh [35], Napolitano [146], Gupalo & Ryazantsev [93], Andreev & Adamev [8] and Andreev et al. [18] (Ch. 7, see also the references therein). It should be noted that the majority of these exact solutions describe stationary flows determined by a system of ordinary differential equations. A solution of plane nonstationary flow for system (10.83) describing thermocapillary flow in a strip is given in Andreev & Pukhnachov [19]. It assumes the dependence $\theta_\Gamma = \theta^* + l(t)x^2$, where $\theta = \text{const}$ and l is an arbitrary function of t. This solution is derived via a system of equations with two independent variables. The possibility of the decrease of order of the problem considered in Andreev & Pukhnachov [19] results from the fact that its solution is a partially invariant solution [156] of the plane analogue of (10.83). The solution studied in the present paper is a natural generalization of the previous solution for the case of thermocapillary motion in a layer. It corresponds to the temperature distribution on the boundaries of the layer

$$\theta_\Gamma = \theta^* + l(t)x^2/2 + m(t)y^2/2, \tag{10.87}$$

where l and m are arbitrary functions of t. The further considerations are based on the following statement, which can be checked directly. If

$$\begin{gathered} u = (f+g)x, \quad v = (f-g)y, \quad w = -2\int_0^z f(\zeta, t)\,d\zeta, \\ p/\rho = \nu w_z(z,t) - \int_0^z w_t(\zeta, t)\,d\zeta - \frac{1}{2}w^2(z,t) + \chi(t), \end{gathered} \tag{10.88}$$

where $f(z,t)$, $g(z,t)$ are the solutions of the system of equations

$$\begin{aligned} f_t + f^2 + g^2 - 2f_z \int_0^z f(\zeta,t)d\zeta &= \nu f_{zz}, \\ g_t + 2fg - 2g \int_0^z f(\zeta,t)d\zeta &= \nu g_{zz} \end{aligned} \tag{10.89}$$

and χ is an arbitrary function of t, then the functions $\mathbf{v} = (u,v,w)$, p satisfy the Navier–Stokes equations (10.83). (Note that the solution (10.88) of the system (10.83) can be determined as usual as a partially invariant solution with rank two and defect two relative to the four-parameter Lie group generated by translations and Galilean translations along the x- and y-axes [131].)

Let us show that the solution (10.88) can be interpreted as a solution describing thermocapillary motion in the layer $|z| < s(t)$ where the temperature distribution is prescribed on its boundaries (10.87). In fact, in this case $K = 0$, $\nabla_\Gamma \sigma = (-æxl(t), -æym(t))$, and the condition (10.85) will be satisfied at $z = s(t)$ if the functions f and g satisfy

$$\begin{aligned} f_z(s(t),t) &= -k\big[l(t) + m(t)\big], \quad 0 < t < T, \\ g_z(s(t),t) &= -k\big[l(t) - m(t)\big], \quad 0 < t < T, \end{aligned} \tag{10.90}$$

where $k = æ/(\rho\nu) = \text{const} > 0$ and the function $\chi(t)$ is chosen in the form

$$\chi = \nu w_z(s(t),t) + \int_0^{s(t)} w_t(\zeta,t)d\zeta + \frac{1}{2}w^2(s(t),t).$$

Further, we assume that

$$f_z(0,t) = g_z(0,t) = 0, \quad 0 < t < T \tag{10.91}$$

and continue the functions f, g (determined initially for $0 < z < s(t)$, $0 < t < T$) to the domain $-s(t) < z < 0$ in an even way. Then condition (10.85) will be satisfied at the lower boundary of the layer $z = -s(t)$ too. If we demand the condition

$$\frac{ds}{dt} = -2\int_0^{s(t)} f(z,t)dz, \quad 0 < t < T \tag{10.92}$$

then we can satisfy the condition (10.86) on both boundaries of the layer. Finally, we assume that

$$s(0) = a > 0 \tag{10.93}$$

(which corresponds to the definition of the initial position of the layer) and

$$f(z,0) = g(z,0) = 0, \quad 0 \leqslant z \leqslant a. \tag{10.94}$$

Then the initial conditions (10.84) will be satisfied.

Conditions for existence and non-existence of solution

Here the solvability conditions for the problem (10.89)–(10.94) are formulated and the qualitative properties of its solution are determined. Note that we are interested only in classical solutions of the above-mentioned problem. The input data of the problem (i. e. the functions $l(t)$ and $m(t)$) must be subjected to some conditions of smoothness and compatibility to ensure the existence of such solutions. Further, we assume that these functions are defined for all $t > 0$, moreover

$$l(t), m(t) \in C^{(1+\alpha)/2}[0, \infty), \quad 0 < \alpha < 1, \tag{10.95}$$

$$l(0) = m(0) = 0, \tag{10.96}$$

where $C^{(1+\alpha)/2}[0, \infty)$ denotes the space of functions continuous on the semiaxis $t \geqslant 0$ and satisfying the Hölder conditions with exponent $(1 + \alpha)/2$ on any compact set. The following notation is used below: S_T is the domain $\{z, t : 0 < z < s(t), 0 < t < T\}$, $C^{2+\alpha,1+\alpha/2}(S_T)$ is the Hölder class used in the theory of parabolic equations (its definition can be found in [137]).

Proposition 10.1. *Let the conditions (10.95), (10.96) be satisfied. Then one can find $T > 0$ such that the problem (10.89)–(10.94) has the unique solution $f(z, t)$, $g(z, t)$, $s(t)$; moreover $f, g \in C^{2+\alpha,1+\alpha/2}(S_T)$, $s \in C^{2+\alpha/2}[0, T]$.*

The proof of this proposition has a purely technical character. It is based on the transition from the Eulerian coordinate z to the Lagrangian coordinate ζ in the problem (10.89)–(10.94). The connection between the Lagrangian and Eulerian coordinates is determined in terms of the solution of the Cauchy problem

$$z_t = -2\int_0^z f(\xi, t)d\xi \quad \text{when } t > 0,$$

$$z = \zeta \quad \text{when } t = 0.$$

Here the domain S_T maps into the rectangle $\Pi = \{\zeta, t : 0 < \zeta < a, 0 < t < T\}$ and equations (10.89) turn into the following equations for the functions $F(\zeta, t) = f[z(\zeta, t), t]$, $G(\zeta, t) = g[z(\zeta, t), t]$:

$$\begin{aligned} F_t + F^2 + G^2 &= \nu \exp\left[2\int_0^t F(\zeta, \tau)d\tau\right]\left\{\exp\left[2\int_0^t F(\zeta, \tau)d\tau\right]F_\zeta\right\}_\zeta, \\ G_t + 2FG &= \nu \exp\left[2\int_0^t F(\zeta, \tau)d\tau\right]\left\{\exp\left[2\int_0^t F(\zeta, \tau)d\tau\right]G_\zeta\right\}_\zeta. \end{aligned} \tag{10.97}$$

The equality

$$z_\zeta = \exp\left[-2\int_0^t F(\zeta, \tau)d\tau\right]$$

was used in the derivation of (10.97). The above-mentioned solution of the Cauchy problem satisfies this equality. Then the boundary conditions (10.90) are rewritten in the form

$$\begin{aligned} F_\zeta(a,t) &= -k\big[l(t)+m(t)\big]\exp\left[2\int_0^z F(a,\tau)d\tau\right], \quad 0<t<T,\\ G_\zeta(a,t) &= -k\big[l(t)-m(t)\big]\exp\left[2\int_0^z F(a,\tau)d\tau\right], \quad 0<t<T. \end{aligned} \tag{10.98}$$

The conditions (10.91), (10.94) give the following conditions for the functions F and G:

$$F_\zeta(0,t) = G_\zeta(0,t) = 0, \quad 0<t<T, \tag{10.99}$$

$$F(\zeta,0) = G(\zeta,0) = 0, \quad 0 \leqslant \zeta \leqslant a. \tag{10.100}$$

As a result we obtain the initial boundary value problem (10.98)–(10.100) in a fixed domain for the system of quasilinear integro-differential parabolic equations of the second order (10.97). Its local unique solvability in Hölder classes follows from general results of the theory of parabolic equations [117] and can be determined, for example, by the method of successive approximations; the convergence of this method is guaranteed for sufficiently small T. If the function $F(\zeta,t)$ is known then the function $s(t)$ determining the position of the free boundary in the plane z,t is given by the formula

$$s(t) = \int_0^a \exp\left[-2\int_0^t F(\zeta,\tau)d\tau\right]d\zeta.$$

Hence the kinematic condition on the free boundary (10.92) is satisfied automatically.

So solvability of problem (10.89)–(10.94) on a small time interval demands that the functions $l(t)$, $m(t)$ only satisfy the smoothness condition (10.95) and compatibility condition (10.96). As will be shown below, these conditions are insufficient for the solvability of the global problem.

Proposition 10.2. *Assume that*

$$l(t)+m(t) \geqslant 0 \quad \textit{for } t \geqslant 0. \tag{10.101}$$

*Moreover the inequality (*10.101*) is strict on some interval* $(0,\tau)$. *Then the "life span"* t_* *of solution of the problem (*10.89*)–(*10.94*) is finite.*

Proof. Let us consider the functions

$$\bar f(t) = \frac{1}{s(t)}\int_0^{s(t)} f(z,t)dz, \quad h = f - \bar f$$

so that quantity $\bar{f}$ is the mean value of the function $f(z,t)$ for any fixed t in the interval $[0,s(t)]$ and the mean value of the function $h(z,t)$ is equal to zero on this interval for any $t > 0$. The relation (10.92) will take the form

$$\frac{ds}{dt} = -2\bar{f}s, \tag{10.102}$$

so that knowledge of the function t determines completely the evolution of the free boundary in the problem (10.89)–(10.94).

We obtain the identity

$$\frac{d\bar{f}}{dt} = -\bar{f}^2 - \frac{1}{s}\int_0^s (g^2 + 3h^2)dz - \frac{\nu k(l+m)}{s} \tag{10.103}$$

after integration of the first equation (10.89) with respect to z over the interval $[0,s(t)]$ and taking into account the conditions (10.90)–(10.92). Further we may suppose without loss of generality that the number τ used in the formulation of Proposition 10.2 is less than the life span t_* of the solution of the studied problem. As follows from (10.103) and the conditions of Proposition 10.2, the function $\bar{f}$ decreases monotonically on the interval $[0,t_*)$ and (10.94) gives $\bar{f}(0) = 0$. So using (10.102) one can conclude that $s(t) \geqslant a$ when $0 \leqslant t < t_*$.

Integration of the identity (10.103) over the interval $(0,\tau)$ and elimination of necessarily nonpositive terms from the right-hand part of the resulting equality lead to the chain of inequalities

$$0 > \bar{f}(\tau) \geqslant -\nu k \int_0^\tau \frac{l(t)+m(t)}{s(t)}\,dt \geqslant -\frac{\nu k}{a}\int_0^\tau [l(t)+m(t)]dt = -\gamma,$$

where $\gamma = \text{const} > 0$, in accordance with the condition of Proposition 10.2. (The sharpness of the left inequality is guaranteed by this condition too.) The estimate $\bar{f}(t) \leqslant (1+\gamma\tau-\gamma t)^{-1}\bar{f}(\tau)$ follows from this fact and inequality $d\bar{f}/dt \leqslant -\bar{f}^2$ which follows from (10.103). So far as $\bar{f}(\tau) < 0$, this estimate means that the solution of the problem (10.89)–(10.94) is destroyed at finite period of time $t_* \leqslant \gamma^{-1} + \tau$. □

Actually, Proposition 10.2 contains the necessary condition for global solvability of the problem (10.89)–(10.94). The determination of sufficient conditions for the existence of its solution for all $t > 0$ demands more effort. The main point here is obtaining the estimate for the maximum modulus of the functions f and g in the domain S_T for all $T > 0$. In the case when such an estimate is obtained, the proof of solvability of the problem (10.89)–(10.94) can be achieved globally by the proof scheme in Andreev et al. [18] (Ch. 7, Theorem 1), using the method developed by Ladyzhenskaya et al. [117].

The specific character of our free boundary problem lies in the fact that its solution can cease to exist as t grows for two reasons. The first reason is demonstrated in Proposition 10.2. The existence of the function $\bar{f}(t)$ obtained in the process of its proof and

equations (10.102) imply that $s \to \infty$ when $t \nearrow t_*$. The vanishing of the function $s(t)$ at finite time t^* is the other reason. This possibility explains the conditional character of Proposition 10.3 formulated below. Henceforth, generic positive quantities (generally speaking, depending on T) are denoted by C_k ($k = 1, 2, \ldots$).

Proposition 10.3. *Let the following inequalities be satisfied:*

$$l(t) \leqslant m(t) \leqslant 0 \quad \text{for } t \geqslant 0. \tag{10.104}$$

Then either

(a) One can find $t^* < \infty$ such that $s(t) > 0$ for $0 \leqslant t < t^*$ and $s \to 0$ when $t \nearrow t^*$. In this case, the estimates

$$\left|f(z,t)\right| \leqslant C_1, \quad \left|g(z,t)\right| \leqslant C_2 \quad \text{when } (z,t) \in \bar{S}_T \tag{10.105}$$

are valid ($T > 0$ is an arbitrary number smaller than t^*);

(b) The inequality $s(t) > 0$ is satisfied for any finite $t > 0$. Then the estimates (10.105) are valid in the domain $\bar{S}_T$ for any $T > 0$.

Proof. Let us introduce the functions $\lambda = f + g$, $\mu = f - g$. It follows from (10.89) that these functions satisfy the equations

$$\begin{aligned} \lambda_t + \lambda^2 - 2\lambda_z \int_0^z f(\zeta,t)d\zeta &= \nu\lambda_{zz}, \\ \mu_t + \mu^2 - 2\mu_z \int_0^z f(\zeta,t)d\zeta &= \nu\mu_{zz} \end{aligned} \tag{10.106}$$

in the domain S_T. Initial and boundary conditions for the system (10.106) are obtained from (10.90), (10.91), (10.94), and have the form

$$\lambda_z\big(s(t),t\big) = -2kl(t), \quad \mu_z\big(s(t),t\big) = -2km(t), \tag{10.107}$$

$$\lambda_z(0,t) = \mu_z(0,t) = 0, \quad 0 < t < T, \tag{10.108}$$

$$\lambda(z,0) = \mu(z,0) = 0. \tag{10.109}$$

If we note that the first and the second equations in (10.106) can be considered as linear in the functions λ and μ, we may apply the maximum principle [57] to the solution of the initial-boundary value problems (10.107)–(10.109) for these equations. In accordance with this principle, the non-negativity of the right-hand sides of the conditions (10.107) provided by the inequalities (10.104) and the homogeneity of the conditions (10.108), (10.109) imply the non-negativity of the functions λ and μ in the domain S_T, where $T < t^*$ in case (a) and T is an arbitrary positive number in case (b). This means that

$$f \geqslant 0 \quad \text{and} \quad |g| \leqslant f \quad \text{for } (z,t) \in \bar{S}_T. \tag{10.110}$$

Hence, the proof of the first inequality (10.105) will imply the proof of the second. Moreover, the function $s(t)$ decreases monotonically for $t > 0$ by virtue of (10.102), (10.110), so that this fact, together with (10.106), implies the estimate

$$s(t) \leqslant a \quad \text{if } t \in [0, T]. \tag{10.111}$$

Finding uniform pointwise estimates of functions f_z, g_z in the domain $\bar{S}_T$ is the next step of the proof. It is evident that it is sufficient for this purpose to obtain similar estimates for the functions $\xi = \lambda_z$, $\eta = \mu_z$. As follows from (10.106)–(10.109), these functions are the solutions of the first initial-boundary value problems for the linear parabolic equations

$$\begin{aligned} \xi_t - 2\xi_z \int_0^z f(\zeta, t)\,d\zeta + 2g\xi &= \nu\xi_{zz}, \\ \eta_t - 2\eta_z \int_0^z f(\zeta, t)\,d\zeta + 2g\eta &= \nu\eta_{zz}, \end{aligned} \tag{10.112}$$

$$\xi(s(t), t) = -2kl(t), \quad \eta(s(t), t) = -2km(t), \tag{10.113}$$

$$\xi(0, t) = \eta(0, t) = 0, \quad 0 < t < T, \tag{10.114}$$

$$\xi(z, 0) = \eta(z, 0) = 0, \quad 0 \leqslant z \leqslant a. \tag{10.115}$$

Now we note that the function g is non-negative in the domain $\bar{S}_T$. Indeed, this function satisfies a linear uniform parabolic equation (the second equation (10.89)) and conditions (10.90), (10.91), (10.94). Due to the condition (10.104), the right-hand side of the second equality (10.90) is non-negative for $0 < t < T$ that involves the non-negativeness of g on the base of the maximum principle. The estimates below are also valid by applying the maximum principle to the solutions of the problems (10.112)–(10.115) and inequalities (10.104) and $g \geqslant 0$ in $\bar{S}_T$:

$$\begin{aligned} 0 \leqslant \xi = \lambda_z \leqslant C_3 &= \max_{0 \leqslant t \leqslant T} [-2kl(t)], \\ 0 \leqslant \eta = \mu_z \leqslant C_4 &= \max_{0 \leqslant t \leqslant T} [-2km(t)]. \end{aligned}$$

So we conclude from these estimates and the definition of λ and μ that

$$0 \leqslant f_z \leqslant C_5 \quad \text{and} \quad |g_z| \leqslant f_z \quad \text{for } (z, t) \in S_T \tag{10.116}$$

with $C_5 = C_3 + C_4$.

From the inequalities (10.116), the maximal value of the function $f(z, t)$ at some fixed t is achieved at the point $z = s(t)$ belonging to the free boundary of the domain S_T. Hence, one must obtain an estimate from above of the function $f(s(t), t)$ for

the completion of the proof of Proposition 10.3. With this aim, let us consider the obvious representation

$$f(s(t),t) = \bar{f}(t) + \frac{1}{s(t)} \int_0^{s(t)} z f_z(z,t)dz. \tag{10.117}$$

The second term of the right-hand side is estimated from the inequalities (10.111), (10.116):

$$\frac{1}{s(t)} \int_0^{s(t)} z f_z(z,t)dz \leqslant \frac{aC_5}{2}. \tag{10.118}$$

An upper estimate of $\bar{f}(t)$ is based on the inequality

$$\frac{d\bar{f}}{dt} \leqslant \frac{\nu k(l+m)}{s},$$

following from (10.103). Integration of this inequality from zero to $t \leqslant T$ with $\bar{f}(0) = 0$, and replacing the functions $-l(t)$, $-m(t)$ with their maximal values on the interval $[0,T]$, implies

$$\bar{f}(t) \leqslant \frac{\nu C_5}{2} \int_0^t \frac{d\tau}{s(\tau)} \quad \text{for } t \in [0,T]. \tag{10.119}$$

Using estimates (10.118), (10.119) and representations (10.117), we conclude that

$$f(s(t),t) \leqslant \frac{C_5}{2}\left[\int_0^t \frac{d\tau}{s(\tau)} + a\right] \quad \text{if } 0 \leqslant t \leqslant T.$$

Here, (a) $T < t^*$, and (b) $T > 0$ is arbitrary. □

Remark. Proposition 10.3 holds if condition (10.104) is replaced by

$$m(t) \leqslant l(t) \leqslant 0 \quad \text{for } t \geqslant 0. \tag{10.120}$$

This follows from the invariance of the Navier-Stokes equations with respect to the transform $x' = -y$, $y' = x$, $u' = -v$, $v = u$.

Qualitative properties of solutions

It will be shown below that all the hypothetical possibilities considered in Proposition 10.3 can be realized. So as not to overload the paper, we consider two simple cases of the behavior of the functions $l(t)$ and $m(t)$ defining the "destiny" of the solution of our problem.

Proposition 10.4. *Let the solution of the problem (10.89)–(10.94) be determined in some domain S_T. Suppose that the conditions (10.104) are satisfied, and moreover,*

$$l(t) = m(t) = 0 \quad \text{when } t \geqslant \tau \tag{10.121}$$

and $l+m \not\equiv 0$ when $0 \leqslant t \leqslant \tau$. Then the problem (10.89)–(10.94) is solvable in the domain S_T for any $T > 0$, and the following estimates are valid: either

$$s = C_6 t^{-2} + O(t^{-3}) \quad \text{when } t \to \infty, \tag{10.122}$$

$$f = t^{-1} + O(t^{-2}), \quad g = O(t^{-2}) \quad \text{when } 0 \leqslant z \leqslant s(t), \tag{10.123}$$

or

$$\begin{aligned} &s = C_7 t^{-1} + O(t^{-2}) \quad \text{when } t \to \infty, \\ &f = g = t^{-1}/2 + O(t^{-2}) \quad \text{when } 0 \leqslant z \leqslant s(t). \end{aligned} \tag{10.124}$$

The last situation is possible only in the case $l = 0$ or $m = 0$ for all $t \geqslant 0$.

Proof. First, note that Proposition 10.1 implies that in any case, one can find the existence time τ of the solution of problems (10.89)–(10.94). So far as the conditions of Proposition 10.3 are satisfied, the inequalities

$$\lambda = f + g \geqslant 0, \quad \mu = f - g \geqslant 0 \tag{10.125}$$

are valid in the domain $\bar{S}_T$. Moreover, at least one of the functions λ, μ is not identically equal to zero on the upper boundary of this domain, i. e. at $t = \tau$, $0 \leqslant z \leqslant s(\tau)$; otherwise, we arrive at a contradiction with the condition $l+m \not\equiv 0$, $0 \leqslant t \leqslant \tau$ (the functions λ and μ satisfy this condition as the solutions of the problem (10.106)–(10.109) by virtue of the strict maximum principle [57]). So we can conclude from this and (10.125) that $\bar{f}(\tau) > 0$.

Now we can use the identity (10.103), where the last right-hand term is absent for $t \geqslant \tau$, as follows from (10.121). The inequality $d\bar{f}/dt \leqslant -\bar{f}^2$ follows from this identity and integration of this inequality from $t = \tau$, taking account of the positiveness of $\bar{f}(\tau)$, implies the estimate

$$\bar{f}(t) \leqslant \frac{\bar{f}(\tau)}{1 + (t-\tau)\bar{f}(\tau)} \quad \text{when } t \geqslant \tau. \tag{10.126}$$

In accordance with (10.102), the upper estimate of $\bar{f}(t)$ implies a lower estimate of the function $s(t)$. Thus, (10.102), (10.126) give

$$s(t) \geqslant \frac{s(\tau)}{[1 + (t-\tau)\bar{f}(\tau)]^2} \quad \text{when } t \geqslant \tau. \tag{10.127}$$

The global existence theorem is valid for the problem (10.89)–(10.94) on the ground of Proposition 10.3 and inequality (10.127).

Now let us obtain the asymptotic representations (10.122)–(10.124). With this aim, we use the formulation of the problem (10.89)–(10.94) in Lagrangian coordinates (10.97)–(10.100), where the boundary condition (10.98) is homogeneous for $t \geqslant \tau$ by virtue of the assumption (10.121). We introduce the functions $\Lambda(\zeta, t) = \lambda(z, t)$, $M(\zeta, t) = \mu(z, t)$ and obtain the initial-boundary value problem

$$\begin{aligned} \Lambda_t + \Lambda^2 &= \nu \exp\left[\int_0^t (\Lambda + M)dt\right]\left\{\exp\left[\int_0^t (\Lambda + M)dt\right]\Lambda_\zeta\right\}_\zeta, \\ M_t + M^2 &= \nu \exp\left[\int_0^t (\Lambda + M)dt\right]\left\{\exp\left[\int_0^t (\Lambda + M)dt\right]M_\zeta\right\}_\zeta, \end{aligned} \tag{10.128}$$

in the semistrip $\Sigma_\tau = \{\zeta, t:\ 0 < \zeta < a, t > \tau\}$,

$$\Lambda_\zeta(a, t) = M_\zeta(a, t) = 0, \quad t > \tau, \tag{10.129}$$

$$\Lambda_\zeta(0, t) = M_\zeta(0, t) = 0, \quad t > \tau, \tag{10.130}$$

$$\Lambda(\zeta, \tau) = \Lambda_0(\zeta), \quad M(\zeta, \tau) = M_0(\zeta), \quad 0 \leqslant \zeta \leqslant a. \tag{10.131}$$

Here the functions Λ_0, M_0 are defined by the equalities

$$\Lambda_0(\zeta) = \lambda[z(\zeta, \tau), \tau], \quad M_0(\zeta) = \mu[z(\zeta, \tau), \tau], \tag{10.132}$$

where τ is a parameter, and the connection between the Lagrangian coordinate ζ and the Eulerian coordinate z is given by the formula

$$z(\zeta, \tau) = \int_0^\zeta \exp\left[-2\int_0^t F(\rho, \sigma)d\sigma\right]d\rho, \quad 0 \leqslant \zeta \leqslant a, \quad t \geqslant 0.$$

The boundedness of $F(\zeta, t) = f(z, t)$ for $\zeta \in [0, a]$ and any finite $t \geqslant 0$ is guaranteed by the solvability of the problem (10.89)–(10.94) globally. This provides the mutual uniqueness of correspondence between the variables ζ and z.

The existence of solutions of system (10.128) not depending on ζ is the remarkable peculiarity of this system. Such solutions are compatible with the boundary conditions (10.129), (10.130). This circumstance permits us to use them as barrier functions for the solution of the problem (10.128)–(10.130). We choose these functions in the following form:

$$\begin{aligned} \Lambda^- &= \frac{\lambda_{\min}}{1 + \lambda_{\min}(t - \tau)}, \quad \Lambda^+ = \frac{\lambda_{\max}}{1 + \lambda_{\max}(t - \tau)}, \\ M^- &= \frac{\mu_{\min}}{1 + \mu_{\min}(t - \tau)}, \quad M^+ = \frac{\mu_{\max}}{1 + \mu_{\max}(t - \tau)}, \end{aligned}$$

where $\lambda_{\min}$ ($\lambda_{\max}$) and $\mu_{\min}$ ($\mu_{\max}$) are the minimal (maximal) values of functions $\lambda(z, \tau)$ and $\mu(z, \tau)$ in the interval $0 \leqslant z \leqslant s(\tau)$.

Here we use the condition of Proposition 10.4, $l(t) + m(t) \not\equiv 0$ for $0 \leqslant t \leqslant \tau$. We may assume without loss of generality that one can find an interval (t_1, t_2), $0 \leqslant t_1 \leqslant< t_2 \leqslant \tau$ such that the strict inequality

$$l(t) < 0 \quad \text{when } t_1 < t < t_2 \tag{10.133}$$

is satisfied. At the same time, the function $m(t)$ can vanish identically (note that both functions l and m are nonpositive for $t \geqslant 0$ in accordance with condition (10.104)). The case when $l = 0$ for all $t \geqslant 0$ and the inequality analogous to (10.133) is satisfied for the function $m(t)$ is considered in a similar way.

First, let us consider the special case $m = 0$ for all $t \geqslant 0$. Then the second condition (10.107) is homogeneous and implies the equality $\mu = 0$ in the domain $\bar{S}_T$ for any $T > 0$ from the uniqueness theorem for the solution of the initial boundary value problem (10.106)–(10.109) for the function μ. This means that the functions f and g coincide for all $z \in [0, s(t)]$, $t \geqslant 0$.

On the other hand, the values of the function λ are strictly positive on the upper boundary $t = \tau$, $0 \leqslant z \leqslant s(\tau)$ of the domain S_T in consequence of inequality (10.133) and the strict maximum principle applied to the solution of the problem (10.106)–(10.109) for the function λ. So $\lambda_{\min} = \min \lambda(z, \tau) > 0$. Now let us consider the function $P^- = \Lambda - \Lambda^-$. By virtue of (10.128)–(10.130), it is the solution of the following problem:

$$P^-_t + (\Lambda + \Lambda^-)P^- = \nu \exp\left(\int_0^t \Lambda dt'\right)\left[\exp\left(\int_0^t \Lambda dt'\right)P^-_\zeta\right]_\zeta, \quad (\zeta, t) \in \Sigma_T,$$

$$P^-_\zeta(0, t) = P^-_\zeta(a, t) = 0, \quad t > \tau,$$

$$P^-(\zeta, t) = \Lambda_0(\zeta) - \lambda_{\min}, \quad 0 \leqslant \zeta \leqslant a$$

(here we take into account that $\lambda[z(\zeta, \tau), \tau] = \Lambda_0(\zeta)$ in accordance with (10.132)). It follows from the maximum principle that $P^-(\zeta, \tau) \geqslant 0$ in the semistrip $\bar{\Sigma}_T$; this fact implies the estimate

$$\Lambda(\zeta, \tau) \geqslant \frac{\lambda_{\min}}{1 + \lambda_{\min}(t - \tau)} \quad \text{for } (\zeta, t) \in \bar{\Sigma}_T$$

by virtue of definition of this function.

The inequality

$$\Lambda(\zeta, t) \leqslant \frac{\lambda_{\max}}{1 + \lambda_{\max}(t - \tau)} \quad \text{for } (\zeta, t) \in \bar{\Sigma}_T$$

is obtained in a similar way. Then we rewrite this inequality in terms of $\lambda(z, t)$, and take into account that $\lambda = 2f$, $f = g$ by virtue of $\mu = 0$, so that

$$\frac{\lambda_{\min}}{1 + \lambda_{\min}(t - \tau)} \leqslant 2f(z, t) \leqslant \frac{\lambda_{\max}}{1 + \lambda_{\max}(t - \tau)} \quad \text{when } 0 \leqslant z \leqslant s(t), \quad t \geqslant \tau.$$

The correctness of asymptotics (10.124) for the functions f and g is obtained; consequently the asymptotics for the function s follows immediately from (10.102).

Let us pass to the analysis of general case where the inequality (10.133) is satisfied in parallel with

$$m(t) < 0 \quad \text{when } t_3 < t < t_4, \tag{10.134}$$

where t_3 and t_4 are some numbers from the interval $[0, \tau]$. First of all we see that the inequality (10.134) implies $\mu_{\min} = \min \mu(z, \tau) > 0$. This fact permits us to prove the non-negativity of the functions $Q^- = M - M^-$, $Q^+ = M^+ - M$ in the domain $\bar{\Sigma}_T$, and to obtain the estimates

$$\frac{\mu_{\min}}{1 + \mu_{\min}(t - \tau)} \leqslant M(\zeta, t) \leqslant \frac{\mu_{\max}}{1 + \mu_{\max}(t - \tau)} \leqslant M(\zeta, t) \quad \text{for } (\zeta, t) \in \bar{\Sigma}_T.$$

The last inequalities take the following form in terms of the functions f and g ($\mu = f - g$):

$$\frac{\mu_{\min}}{1 + \mu_{\min}(t - \tau)} \leqslant M(\zeta, t) \leqslant f(z, t) - g(z, t) \leqslant \frac{\mu_{\max}}{1 + \mu_{\max}(t - \tau)}$$
$$\text{when } 0 \leqslant z \leqslant s(t),\ t \geqslant \tau.$$

These upper and lower estimates $\Lambda(\zeta, t)$ imply the following inequalities for the function $\lambda = f + g$:

$$\frac{\lambda_{\min}}{1 + \lambda_{\min}(t - \tau)} \leqslant M(\zeta, t) \leqslant f(z, t) + g(z, t) \leqslant \frac{\lambda_{\max}}{1 + \lambda_{\max}(t - \tau)}$$
$$\text{when } 0 \leqslant z \leqslant s(t),\ t \geqslant \tau.$$

As a result, we come to the relations $f + g = t^{-1} + O(t^{-2})$, $f - g = t^{-1} + O(t^{-2})$ when $t \to \infty$, $0 \leqslant z \leqslant s(t)$. This fact proves the correctness of the asymptotic representations (10.123) for the general case, when the both functions $l(t)$ and $m(t)$ take negative values even at some part over the interval $(0, \tau)$. The use of (10.102) and (10.123) gives the required asymptotics (10.122) of function $s(t)$. □

Proposition 10.5. *Let us suppose that solution of problems (10.89)–(10.94) is defined in the domain S_T. If the inequality (10.104) and the condition*

$$l + m = -A/vk = \text{const} < 0 \quad \textit{when } t \geqslant \tau \tag{10.135}$$

are satisfied then one can find such finite $t^* > 0$ that $s(t) > 0$ for $0 \leqslant t < t^*$ and $s \to 0$ when $t \nearrow t^*$.

Proof. Let us use the identity (10.103), and rewrite it in terms of the functions f and g:

$$\frac{d}{dt} \int_0^s f dz + \int_0^s (3f^2 + g^2) dz = -vk(l + m). \tag{10.136}$$

We introduce the functions

$$U(t) = \int_0^{s(t)} f(z,t)dz, \quad V(t) = \int_0^{s(t)} g(z,t)dz. \tag{10.137}$$

Using the Cauchy–Bunyakovsky inequality and condition (10.135), we obtain from (10.136) a differential inequality for the function U:

$$\frac{dU}{dt} \leqslant -\frac{3U^2}{s} + A \quad \text{when } t \geqslant \tau. \tag{10.138}$$

Note that the inequality $U(\tau) = U_0 > 0$ is valid by virtue of the conditions of Proposition 10.5. Moreover, the function $U(t)$ is non-negative for $t \geqslant \tau$ and cannot vanish as long as $s(t) > 0$. These statements follow from the strict maximum principle applied to the functions $f+g, f-g$ (see the beginning of the Proof of Proposition 10.4). Then it follows from (10.102), (10.137) that $ds/dt < 0$ for these values of t. This fact permits us to rewrite the inequality (10.138) in more convenient form by introducing the function $U^2 = W(s)$:

$$\frac{dW}{ds} - \frac{3W}{s} \geqslant -As \quad \text{if } s > s(\tau) = s_0.$$

Integration of the last inequality leads to the result

$$W(s) \geqslant \frac{sA}{2}\left(1 - \frac{s^2}{s_0^2} + \frac{2U_0^2 s^3}{As_0^3}\right) \equiv \frac{sA}{2} R^2(s),$$

and, moreover, $R(s) \geqslant C_8 > 0$ for $s \in [0, s_0]$. The estimate below is obtained from this fact and the relation $ds/dt = -2W^{1/2}(s)$ following from (10.102), (10.137) and the definition of function W:

$$\int_0^{s_0} \frac{dr}{R(r)\sqrt{2Ar}} \geqslant t - \tau.$$

The integral entering this estimate converges when $s \to 0$. This fact guarantees finiteness of the value of t^* corresponding to the vanishing-time of the function s, and we obtain the following estimate of t^*:

$$t^* \leqslant \frac{1}{\sqrt{2A}} \int_0^{s_0} \frac{ds}{R(s)\sqrt{s}} + \tau. \qquad \square$$

The interest in investigating the behavior of solution of the problem (10.89)–(10.94) near the moment t^* follows from this proposition. The simplest solution of this question can be found in the case when both functions $l(t)$ and $m(t)$ take constant values beginning with some t.

Proposition 10.6. *Let the conditions of Proposition* 10.5 *be satisfied. Moreover, assume that*

$$l - m = -B/\nu k = \text{const} \quad \text{when } t \geqslant \tau \tag{10.139}$$

with $|B| \leqslant A$. *Then the following relations are valid as* $t \nearrow t^*$:

$$\frac{s}{(t^* - t)^2} \to 4A\big(1 + \sqrt{1 - 8\beta^2/9}\big), \tag{10.140}$$

$$\frac{U}{t^* - t} \to A\big(1 + \sqrt{1 - 8\beta^2/9}\big), \tag{10.141}$$

$$\frac{V}{t^* - t} \to \frac{4B}{3}, \tag{10.142}$$

where $\beta = B/A$ ($|\beta| \leqslant 1$) *and the functions* $U(t)$, $V(t)$ *are defined by* (10.137).

Proof. The identity (10.135) and the analogous identity

$$\frac{d}{dt}\int_0^s g\,dz + 4\int_0^s fg\,dz = -\nu k(l - m), \tag{10.143}$$

obtained by integration of the second equation (10.89) by z over the interval $[0, s(t)]$ with the use of relations (10.90)–(10.92) are the basis of the proof. Both identities are considered for the values $t \geqslant \tau$, when their right-hand sides are constant by virtue of conditions (10.135), (10.139).

Let us denote the mean value of function $g(z,t)$ on the interval $0 \leqslant z \leqslant s(t)$ as $\bar{g}(t)$ and put $j(z,t) = g - \bar{g}$. The identities (10.136), (10.143) can be rewritten in the form

$$\begin{aligned} &\frac{dU}{dt} + \frac{3U^2 + V^2}{s} + \int_0^s (3h^2 + j^2)\,dz = A, \\ &\frac{dV}{dt} + \frac{4UV}{s} + \int_0^s hj\,dz = B \quad \text{when } t \in [\tau, t^*) \end{aligned} \tag{10.144}$$

with the help of these functions and the functions $\bar{f}(t)$, $h(z,t) = f - \bar{f}$ introduced before. (Here we use the evident equalities $U = s\bar{f}$, $V = s\bar{g}$ following from (10.137) and definition of functions $\bar{f}$ and $\bar{g}$.)

The system (10.144) is not closed for the functions U and V; however, this fact does not prevent us from finding the asymptotics of its solution near the moment t^* when $s(t^*) = 0$. The point is that the integral terms of (10.144) tend to zero quickly when $t \nearrow t^*$. The proof depends upon the representations

$$\begin{aligned} f(z,t) &= \bar{f}(t) + \int_{b(t)}^z f_z(\zeta,t)\,d\zeta, \\ g(z,t) &= \bar{g}(t) + \int_{c(t)}^z g_z(\zeta,t)\,d\zeta, \end{aligned} \tag{10.145}$$

where $b(t)$ and $c(t)$ are points from the interval $[0, s(t)]$ where the function $f(z,t)$ ($g(z,t)$) takes its mean value as a function of z. Using the uniform estimates (10.116) of the functions $|f_z|$, $|g_z|$ which are valid by virtue of (10.104), and remembering the definitions of the functions h, j, we arrive at the inequalities

$$|h| \leqslant C_5 s, \quad |j| \leqslant C_5 s \quad \text{when } 0 \leqslant z \leqslant s(t), \quad \tau \leqslant t \leqslant t^*.$$

Now if the system (10.144) is rewritten in the form

$$\begin{aligned} \frac{dU}{dt} + \frac{3U^2 + V^2}{s} + \Phi(t) &= A, \\ \frac{dV}{dt} + \frac{4UV}{s} + \Psi(t) &= B, \end{aligned} \tag{10.146}$$

where

$$\Phi = \int_0^{s(t)} [3h^2(z,t) + j^2(z,t)]dz, \quad \Psi = \int_0^{s(t)} h(z,t)j(z,t)dz$$

then the estimates

$$|\Phi| \leqslant C_9 s^3, \quad |\Psi| \leqslant C_9 s^3 \quad \text{when } \tau \leqslant t \leqslant t^* \tag{10.147}$$

with $C_9 = 4C_5^2/3 = \text{const}$ will be valid for the functions $\Phi(t)$, $\Psi(t)$.

It follows from the strict monotonicity of function s on the interval $[t, t^*)$ obtained in Proposition 10.5 that we may convert the dependence on s to t, and consider Φ and Ψ as functions of the variable s; $\Phi[t(s)] = \varphi(s)$, $\Psi[t(s)] = \psi(s)$(s), where $0 \leqslant s \leqslant s_0 = s(\tau)$. The further reasoning is based on the transformation of (10.146) into a third-order system with the help of the change of variables

$$U = (As)^{l/2} q(\rho), \quad V = (As)^{1/2} r(\rho), \quad \rho = \ln(l/s). \tag{10.148}$$

Substitution of (10.148) into (10.146) and recalling that $ds/dt = -2U$ leads to the system of equations

$$\begin{aligned} 2q\frac{dq}{d\rho} + 2q^2 + r^2 &= 1 - \frac{\varphi(s)}{A}, \\ 2q\frac{dr}{d\rho} + 3qr &= \beta - \frac{\psi(s)}{A}, \\ \frac{ds}{d\rho} &= -s, \quad \rho \geqslant \rho_0, \end{aligned} \tag{10.149}$$

where $\rho_0 = \ln(l/s_0)$, $\beta = B/A = \text{const}$, $|\beta| \leqslant 1$ by virtue of the conditions of Proposition 10.6. Our aim is to investigate the behavior of the solution of the Cauchy problem

$$q(\rho_0) = q_0, \quad r(\rho_0) = r_0, \quad s = \exp(-\rho_o) = s_0 \tag{10.150}$$

for the system (10.149) when $\rho \to \infty$, where

$$q_0 = (As_0)^{-1/2} \int_0^{s_0} f(z,t)dz, \quad r_0 = (As_0)^{-1/2} \int_0^{s_0} g(z,\tau)dz.$$

Moreover, it is assumed that the functions f and g are already determined in the domain S_τ so that $|r_0| \leqslant q_0$, $q_0 > 0$ on the basis of (10.110), (10.137) and (10.148) (note that conditions of Proposition 10.6 guarantee the satisfaction of the inequalities (10.104), providing estimates (10.110)). The inequalities

$$q(\rho) > 0, \quad |r(\rho)| \leqslant q(\rho) \tag{10.151}$$

for any finite $\rho \geqslant \rho_0$ also follow from these relations, but here they play the role of *a priori* estimates for solution of the Cauchy problem (10.149), (10.150).

First, note that the trajectory of the dynamical system (10.149) emerging from the point (q_0, r_0, s_0) cannot leave the limits of the cylindrical sector $K_N = \{q, r, s : 0 < q^2 + r^2 < N^2, |r| < q, 0 < s < s_0\}$ of phase space $\mathcal{R}^3$ (where N is sufficiently large) when $\rho \geqslant \rho_0$. It is sufficient for the proof of this statement to check that no outgoing points of the system (10.149) are situated on the boundary of the domain K_N. In fact, the rectangles $q = r$, $0 \leqslant s \leqslant s_0$ and $q = -r$, $0 \leqslant s \leqslant s_0$ cannot contain outgoing points in view of inequalities (10.151). The upper segment of K_N, i. e. the circular sector $0 \leqslant q \leqslant N$, $|r| \leqslant q$, $s = s_0$, consists of ingoing points in accordance with the third equation of system (10.149). The lower segment of K_N cannot contain outgoing points, since it corresponds to the value $\rho = \infty$.

Now one must check the absence of exit points on the cylindrical part of the boundary K_N, i. e. on the set $H_N = \{q, r, s : q^2 + r^2 = N^2, |r| \leqslant q, 0 \leqslant s \leqslant s_0\}$. The field of directions of the dynamical system (10.149) is characterized by the vector $\mathbf{l}$ with components $(2q)^{-1}[1 - 2q^2 - r^2 - A^{-1}\varphi(s)]$, $(2q)^{-1}[\beta - 3qr - A^{-1}\psi(s)]$, $-s$. The scalar product $\mathbf{l} \cdot \mathbf{n}$ of $\mathbf{l}$ and the unit external normal $\mathbf{n} = (\cos\omega, \sin\omega, 0)$ to the surface H_N, where $\omega = \operatorname{arctg}(r/q)$, gives

$$\mathbf{l} \cdot \mathbf{n} = -N(1 + \sin^2\omega) - \frac{[A^{-1}\varphi(s) - 1]\cos\omega + [A^{-1}\psi(s) - \beta]\sin\omega}{(2N\cos\omega)}$$

Since $|\omega| \leqslant \pi/4$ on the surface H_N, $\varphi \leqslant C_9 s_0^3$ $|\psi| \leqslant C_9 s_0^3$ by virtue of (10.147), and $|\beta| \leqslant 1$, one can obtain the inequality $\mathbf{l} \cdot \mathbf{n} < 0$ on the surface H_N by choosing N larger than $\max[(1 + A^{-1}C_9 s_0^4)^{1/2}, (q_0^2 + r_0^2)^{1/2}]$, and that the point (q_0, r_0, s_0) belongs to the set $\bar{K}_N$. Then both inequalities (10.151) and the *a priori* estimate

$$q \leqslant N \quad \text{when } \rho \geqslant \rho_0 \tag{10.152}$$

are valid for the solution of the Cauchy problem (10.149), (10.150).

Let us return to the system (10.149). It has the unique equilibrium point

$$\begin{aligned} q = q^* &\equiv 0.5\big(1 + \sqrt{1 - 8\beta^2/9}\big)^{1/2}, \\ r = r^* &\equiv 2^{-1/2}\,\mathrm{Sgn}\,\beta\big(1 + \sqrt{1 - 8\beta^2/9}\big)^{1/2}, \quad s = 0 \end{aligned} \tag{10.153}$$

in the domain K_N. Linearization of (10.149) near the equilibrium point leads to the system

$$\frac{dQ}{d\rho} = -2Q - \frac{r^*}{q^*}R,$$
$$\frac{dR}{d\rho} = -\frac{3r^*}{2q^*}Q - \frac{3}{2}R, \quad \frac{dS}{d\rho} = -S.$$

The eigenvalues of the matrix of this system are

$$\lambda_{1,2} = \frac{-7q^* \pm \sqrt{(q^*)^2 + 24(r^*)^2}}{2q^*}, \quad \lambda_3 = -1.$$

Since $q^* > 0$ and $|r^*| \leqslant q^*$, and $|\beta| \leqslant 1$ all eigenvalues λ_i $(i = 1, 2, 3)$ are negative. The equilibrium point $(q^*, r^*, 0)$ of system (10.149) is stable in accordance with the Lyapunov theorem.

The proof of the fact that trajectory of the dynamic system (10.149) starting from the point (q_0, r_0, s_0) at the "moment" $\rho = \rho_0$ finishes at $\rho \to \infty$ at the equilibrium point $(q^*, r^*, 0)$ will complete the proof of Proposition 10.6. From this fact, (10.140)–(10.142) are derived without any problems. By virtue of the third equation (10.149), the projection of the desired trajectory on the plane $s = 0$ approaches asymptotically (by virtue of the third equation (10.149)) as $\rho \to \infty$ the trajectory of two-dimensional dynamical system

$$\begin{aligned} \frac{dq}{d\rho} &= (2q)^{-1}(1 - 2q^2 - r^2), \\ 2q\frac{dr}{d\rho} &= (2q)^{-1}(\beta - 3qr) \end{aligned} \tag{10.154}$$

emerging from the point (q_0, r_0) at $\rho = \rho_0$; denote this trajectory by L. As was proved before, the curve L is contained in a circular sector $\bar{D}_N = \{q, r : q^2 + r^2 \leqslant N^2, |r| \leqslant q\}$.

Now let us suppose that $|\beta| < 1$. Then vector

$$\mathbf{m}(q, r) = \big((2q)^{-1}(1 - 2q^2 - r^2),\, (2q)^{-1}(\beta - 3qr)\big)$$

does not vanish on the boundary of the domain $D_{N,\varepsilon} = \{q, r : \varepsilon^2 < q^2 + r^2 < N^2, |r| < q\}$, where the number $\varepsilon > 0$ is chosen less than $q_0 > 0$. (Note that for $|\beta| < 1$ and sufficiently small ε all points of the "arch" $q^2 + r^2 = \varepsilon^2$, $|r| \leqslant q$ are ingoing points for system (10.154), so that the trajectory L does not fall outside the limits of not only the

sector $\bar{D}_N$ but also the domain $\bar{D}_{N,\varepsilon}$ for $\rho \geqslant \rho_0$.) Since $m \neq 0$ on the boundary of the domain $D_{N,\varepsilon}$ we may calculate the rotation of the vector field $\mathbf{m}(q,r)$ on this boundary. Simple calculations show that this rotation is equal to unity. Since $q = q^*, r = r^*$ is the unique singular point of the field $\mathbf{m}$ in the domain $\bar{D}_{N,\varepsilon}$ and the index of this point is equal to unity, then system (10.154) has no limit cycles in the domain $\bar{D}_{N,\varepsilon}$. So it follows that point (q^*, r^*) is the limit point of curve L when $\rho \to \infty$.

Now let $\beta = 1$ (case $\beta = -1$ is considered in a similar way). Here the vector $\mathbf{m}$ vanishes on the boundary of the domain $\bar{D}_{N,\varepsilon}$: $\mathbf{m}(1/\sqrt{3}, 1/\sqrt{3}) = 0$. If at the same time $q_0 = r_0 = 1/\sqrt{3}$, then the trajectory L consists of one point. If $q_0 = r_0 \neq 1/\sqrt{3}$, $\varepsilon \leqslant q_0 \leqslant N$ then the line L is a part of a segment of the straight line $q = r$. In this case, the dependence $q(\rho)$ is defined from solution of the Cauchy problem

$$\frac{dq}{d\rho} = (2q)^{-1}(1 - 3q^2) \quad \text{when } \rho > \rho_0, \quad q(\rho_0) = q_0.$$

It is evident that $q \to q^* = 1/\sqrt{3}$ when $\rho \to \infty$. If the point (q_0, r_0) lies strictly inside the domain $\bar{D}_{N,\varepsilon}$ then we can narrow down a little the opening angle of this domain and achieve the situation when vector field $\mathbf{m}$ has no zeros on the boundary of the domain $\varepsilon^2 < q^2 + r^2 < N^2$, $|r| < (1-\delta)q$ containing the point (q_0, r_0) (the last fact can be ascertained for small enough $\delta > 0$). Now the above reasoning about the rotation of the field in can be repeated almost literally. So now we have shown that the relations

$$q \to q^*, \quad r \to r^* \quad \text{when } \rho \to \infty, \tag{10.155}$$

hold under the conditions of Proposition 10.6. Concerning $\rho = \ln(l/s)$, this follows from (10.155) and definition of q^* and r^* (10.153), with account of equations (10.148), that

$$\begin{aligned} &\frac{U}{(As)^{1/2}} \to 0.5\left(1 + \sqrt{1 - 8\beta^2/9}\right)^{1/2}, \\ &\frac{V}{(As)^{1/2}} \to \left[0.5\left(1 - \sqrt{1 - 8\beta^2/9}\,\right)\right]^{1/2} \quad \text{when } s \to \infty. \end{aligned} \tag{10.156}$$

The first of this relations means that $ds/dt \to -[As(1 + \sqrt{1 - 8\beta^2/9}\,)]^{1/2}$ when $t \nearrow t^*$ by virtue of the equation $ds/dt = -2U$. The limit equality (10.140) follows from this fact and then the relations (10.141), (10.142) can be obtained from (10.156). □

This proposition deserves some comment. The reason for introducing the functions $U(t)$, $V(t)$ is the following: these functions remain bounded in the limit $t \nearrow t^*$ in contrast to the functions $\bar{f}(t)$, $\bar{g}(t)$; moreover, $U = O(t^* - t)$, $V = O(t^* - t)$ when $t \nearrow t^*$. On the other hand, the equalities below follow from the formulae $U = \bar{f}s$, $V = \bar{g}s$, relations (10.140)–(10.142) and representations (10.145) by virtue of equations (10.116):

$$\begin{aligned} f(z,t) &= \frac{1}{4(t^* - t)} + O(t^* - t)^2, \\ g(z,t) &= \frac{3}{8\beta(t^* - t)}\left(1 - \sqrt{1 - 8\beta^2/9}\,\right) + O(t^* - t)^2 \quad \text{when } t \nearrow t^*, 0 \leqslant z \leqslant s(t). \end{aligned} \tag{10.157}$$

Thus, formulae (10.140), (10.157) imply that smooth joining of free boundaries of the layer takes place in the moment t^*, although the longitudinal components of the liquid velocity grow infinitely when $t \nearrow t^*$.

Discussion and conclusion

(a) The system (10.89) admits solutions with $f = g$, $f = -g$ and $g = 0$. In accordance with (10.88), the first two cases describe plane flows. These cases can be realized if one puts $m = 0$ and $l = 0$ in (10.87). The case $g = 0$ corresponds to the equality $l = m$ for all $t \geqslant 0$. In this case, the solution of the problem (10.89)–(10.94) describes axisymmetric motion.

(b) Proposition 10.2 gives sufficient conditions for blow-up of the solution of problems (10.89)–(10.94) in finite time t_*. Note that this phenomenon has a purely inertial character; viscous forces cannot prevent it, although these forces guarantee the space regularity of the solution.

The question about the structure of the solution singularity near the moment t_* is still open. This question is studied in detail in Galaktionov & Vazquez [60] for the plane analogue of the discussed problem. More precisely, (10.89) with $g = f$ is considered in Galaktionov & Vazquez [60]; there the modified problem with free boundary (10.90)–(10.94) is investigated — one puts $l = m = 0$ in the condition (10.90) and substitutes condition (10.94) for f by the following:

$$f(z, 0) = f_0(z), \quad 0 \leqslant z \leqslant a.$$

(We shall call this problem P.)

Let the function f_0 satisfy the natural smoothness and compatibility conditions and also the inequality $f_0 \leqslant 0$ for $z \in [0, a]$ and some "steepness condition" [60]. Then the solution f, s of problem P has the asymptotics

$$s(t) \sim \frac{\pi}{2\sqrt{\alpha(t_* - t)}}, \quad f(z, t) \sim -\frac{\cos^2(z\sqrt{\alpha(t_* - t)})}{t_* - t}$$

when $t \nearrow t_*$, $0 \leqslant z < s(t)$, where $\alpha = \text{const} > 0$.

(c) Sufficient conditions for solvability of problem P for all $t \geqslant 0$ are determined in Pukhnachov [170]. Also constructed in this paper is a class of its exact solutions of the form

$$f = a(t) + b(t)\cos[\pi n z / s(t)], \tag{10.158}$$

where n is a natural number and functions a, b, s form the solution of a dynamical system. The significance of the solutions (10.158) consists of the fact that these solutions represent the leading terms of both the blow-up of solutions of problem P when $t \nearrow T_*$ and its regular solutions when $t \to \infty$.

(d) Let us consider the problem (10.89)–(10.94) for the case $l + m = 0$ where the function $l(t)$ is non-negative and $l > 0$ at some interval $0 < t_1 < t < t_2 < oo$. Then the statement of Proposition 10.2 is valid, although its proof requires some small modification. The case $l = -m$ is interesting from the physical point of view in so far as tangential stress applied to the free boundary in the x-direction has the same magnitude but opposite sign to that applied in the y-direction. In this case, the analysis of problems (10.89)–(10.94) shows that the layer thickness $2s(t)$ is a monotonically increasing function of time, and there exist some $t_* < \infty$ such that $s \to \infty$ when $t \nearrow t_*$.

Indeed, now the boundary condition (10.90) for the function f is uniform, while the right side of the same condition for the function g is strictly negative within the interval (t_1, t_2). On the basis of the maximum principle, we have $g^2 > 0$ when $t_1 < t < t_2$, $0 \leqslant z \leqslant s(t)$. At once, we consider the first equation (10.89) as a linear parabolic equation with coefficients f and $-2\int_0^z f d\zeta$ before f and f_z, respectively, and with a source $-g^2$. Remembering that the function $f(z,t)$ satisfies the uniform boundary and initial conditions (10.90), (10.94), we conclude that $f < 0$ when $t \in (t_1, t_2)$, $z \in [0, s(t)]$ in view of the maximum principle. It means that the mean value $\bar{f}(t)$ of the function f in the interval $[0, s(t)]$ is negative if $t \in (t_1, t_2)$. As was shown in the proof of Proposition 10.2, the inequality $\bar{f}(\tau) < 0$ implies the estimate $\bar{f}(t) \leqslant (1 + \gamma\tau - \gamma t)^{-1}\bar{f}(\tau)$ where $t > \tau \in (t_1, t_2)$, $\gamma = \text{const} > 0$. On account of (10.102), this estimate guarantees the required property $s \to \infty$ when $t \nearrow t_* \leqslant \tau + \gamma^{-1}$. We emphasize that this effect has a purely nonlinear character.

(e) Here we suggest some comments on Proposition 10.4. The exceptional case described by formulae (10.125) corresponds to plane motion. If the equality $l = 0$ or $m = 0$ is broken at some arbitrarily small interval of time then the solution of the problem (10.89)–(10.94) is symmetrized with growth of t, as follows from relations (10.124) (note that $g = 0$ for axisymmetric motion). The essential distinction between plane and three-dimensional regimes of thinning of the layer is demonstrated by the asymptotics of function s: in the first case $s \sim t^{-1}$ and in the second case $s \sim t^{-2}$ when $t \to \infty$.

(f) Let us consider the problem of thermocapillary motion of viscous liquid in a layer with linear dependence of the free boundary temperature on the space coordinates,

$$\theta_\Gamma = A(t)x + B(t)y.$$

It is not difficult to see that its solution can be obtained in the form

$$u = u(z,t), \quad v = v(z,t), \quad w = 0, \quad p = 0, \quad s = a = \text{const}.$$

The functions u, v are determined as solutions of the second initial boundary value problem for the linear equation of heat conduction (the details are omitted).

Thus, a linear distribution of temperature on the plane free boundary of a viscous layer does not lead to a thickness change. It is natural to suppose on the basis of this observation that the main change of the layer thickness under the action of thermocapillary forces takes place near the critical points of the temperature field on free surface. This concept can be considered as an additional motivation for the investigation of solutions of the Navier–Stokes equations of the form (10.88). The unboundedness of functions u and v when $x, y \to \infty$ is the evident defect of this solution. However, we can consider it as a solution describing the local behavior of liquid in vicinity of critical points of the temperature field on the free boundary.

(g) The problem (10.82)–(10.87) can be referred to as a "non-coupled" problem of thermocapillary convection. It originates from the assumption that the temperature is a given function at the free boundary. A more complicated "coupled" problem deals with the boundary condition of second or third kind for the temperature. Let us suppose that the free boundary is thermo-insulated. Then the condition (10.87) should be replaced by

$$\theta_z(s(t), t) = 0, \quad 0 < t < T. \tag{10.159}$$

In this case, we have the temperature representation

$$\theta = \varphi x^2 + \psi y^2 + \omega$$

where $\varphi(z, t)$, $\psi(z, t)$, $\omega(z, t)$ are determined from the parabolic system coupled with the equations (10.89) via boundary conditions including (10.159). The plane analogue of this problem was studied numerically in Andreev & Pukhnachov [19].

(h) To identify a physical system that might correspond to the solution of the problem (10.82)–(10.87), let us consider a liquid film of mean initial thickness a and the diameter d suspended in a solid frame at the presence of gravity with the acceleration g. It is clear that following relations should be satisfied: $a \ll d$, $d \sim (2\sigma_0/(\rho g))^{1/2} = L$ where L is the capillary constant and σ_0 is a characteristic value of the surface tension coefficient. This gives an upper estimate for a. The lower estimate limiting the applicability of our approach is $a \gg \lambda$, where λ is the thickness of the double diffusional electric layer. In this case, we can neglect the disjoining pressure in the film.

Now let us introduce the dimensionless parameter $q = \rho g \beta a^2/æ$ where β is the volumetric coefficient of thermal expansion and æ is the parameter in relation (10.82). If $q \ll 1$, we can ignore the contribution of the buoyancy in a formation of the velocity field and, therefore, eliminate from consideration the heat equation in the context of our problem.

As an example, we consider a pure water film at low gravity ($g = 1\,\mathrm{cm/s^2}$) near the temperature 298 K; in this case, $L = 12\,\mathrm{cm}$. If we choose $a = 0.1\,\mathrm{cm}$, $d = 5\,\mathrm{cm}$, $\lambda = 10^{-6}\,\mathrm{cm}$ then inequalities $\lambda \ll a \ll d$ will be true as well as $q \ll 1$ (in fact, here

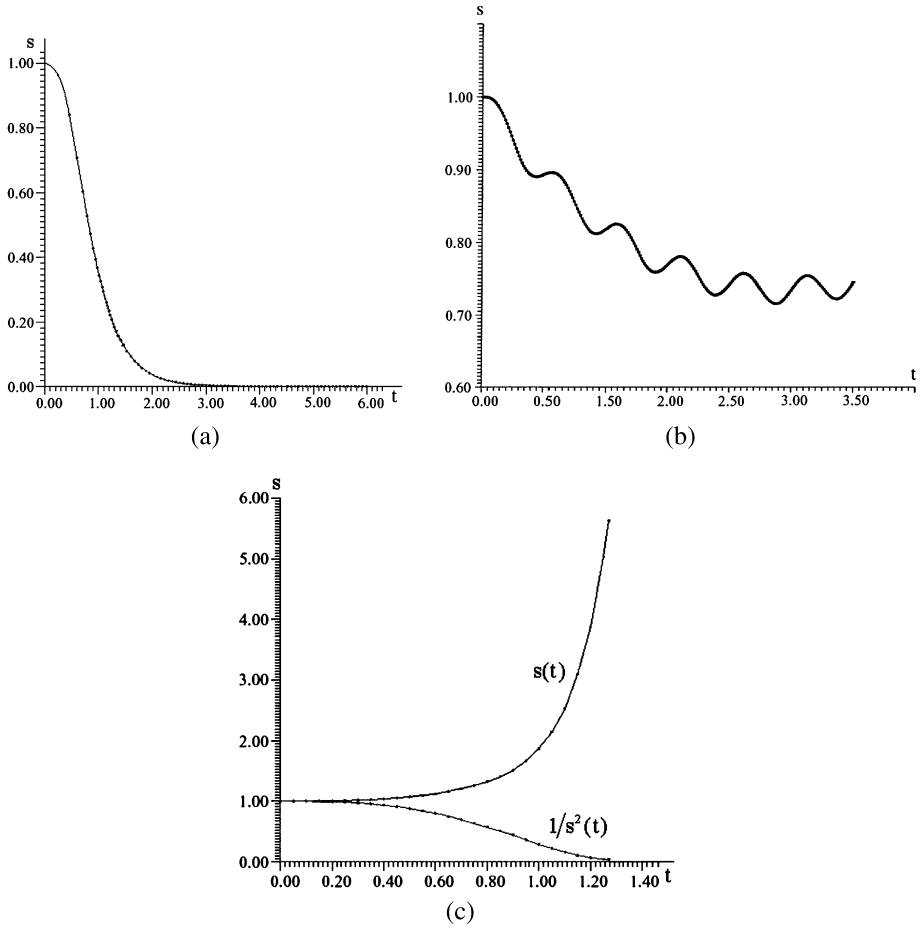

Figure 10.6: Behavior of dimensionless layer thickness with time. (a) $l = m = 5te^{-3t}$; (b) $l = 0.5\sin(12.52t)$, $m = \sin(12.52t)$; (c) $l = 1 - \frac{1}{(1+t)^2}$, $m = 2 - \frac{2}{(1+t)^2}$.

$q = 1.6{\cdot}10^{-5}$). In addition, we note that the characteristic time of the problem is of order $[ap/æ(l_* + m_*)]^{1/2} = \tau$, where l_* and m_* are the maximum values of the functions l and m, respectively. Putting $l_* = m_* = 10^{-2}$ K/cm^2, we obtain $\tau = 5.6$ s.

(i) Problem (10.89)–(10.94) was solved numerically in papers [188, 84]. Below there are given the results of numerical simulation [188]. The figures show the ratio of the layer thickness to its initial value as a function of dimensionless time. The time scale is chosen as $a^2\nu^{-1}$. Figures 10.6(a) and (b) correspond to the case where the problem solution is regular, although the functions l and m do not satisfy the conditions of Propositions 10.3–10.6. Figure 10.6(c) demonstrates the solution blow-up within a finite time, in accordance with Proposition 10.2. The main term of the asymptotic of the function s at $t \longrightarrow t_*$ is $C_{10}(t_* - t)^{-1/2}$.

10.5 Convective flow in a horizontal channel with non-Newtonian surface rheology under time-dependent longitudinal temperature gradient

The experiments of K. G. Kostarev and his co-authors [36, 135] showed that in narrow channels at a local surfactant egress onto the surface the Marangoni convection occurs only at a fairly high surfactant concentration gradient. The delay of the onset of the surface motion can also be observed, when thermocapillary convection is excited by a point heat source in a horizontal channel with a bounded free surface, if only its surface has not been thoroughly cleaned [136]. The threshold nature of the convection onset is attributed to the presence of an uncontrolled surfactant film kept by the channel walls. In this connection, it seems helpful to develop the models of thermocapillary convection in the presence of a temperature gradient along the free surface with the threshold excitation of the convection flow.

In this study, thermal convection is considered in a horizontal channel with a longitudinal temperature gradient. For an infinitely wide channel with a stationary temperature gradient the problem in the conventional formulation has a simple exact solution with threshold-free convection onset [35, 10]. The actuality of this asymptotic solution was demonstrated in the experiments [109, 107]. In [185, 21] this solution was generalized to include the case of a time-dependent longitudinal temperature gradient. The flow in a channel of finite width and its stability at low Prandtl numbers was considered in [123]. An advection flow in a square channel of finite length was studied in [124], again at low Prandtl numbers. In those studies, the fluid surface was free from a surfactant film and thermocapillary flow was attained immediately after the generation of tangential stresses along the surface.

Under actual conditions the threshold nature of the onset of the Marangoni convection is governed by the rheological properties of the surface: its motion begins, when the tangential stresses become greater than a certain threshold value determined by the surfactant film durability. This property of the surface can be described introducing the tangential resistance to the fluid flow with a stepwise stress dependence of the resistance. For a wide layer in the case of a stationary gradient this problem has a simple exact solution with a single velocity component along the temperature gradient. In the unsteady case the solution can be particularly simply constructed using the finite difference method.

10.5.1 Formulation of the problem

The materials in this paragraph are based on the results of article [38]. We will consider a convective viscous flow in a wide horizontal channel (band) with a temperature gradient along its horizontal z axis. The origin of the upward directed x axis is

on the lower plane. In the Oberbeck–Boussinesq approximation the convection equations admit the solution of the form [10]:

$$\mathbf{v} = \mathbf{k}w(x,t), \quad T = -A(x,t)\cdot z + \Theta(x,t), \quad p = -B(x,t)\cdot z + q(x,t). \tag{10.160}$$

Here, w is the fluid flow velocity which has only one direction, T is the temperature deviation from a certain mean value, and p is the pressure deviation from the hydrostatic pressure in an isothermal fluid.

We will formulate the problem in the dimensionless form. We will scale the distances on the layer width h, time on h^2/ν, the velocity component w on ν/h, the pressure on $\nu^2\rho/h$, and the temperature on $A_0 h$, where ν and ρ are the kinematic viscosity and the density of the fluid and A_0 is a maximum value of the longitudinal temperature gradient. In these variables the functions introduced in (10.160) satisfy the following equations

$$\begin{aligned}
\frac{\partial A}{\partial t} &= \frac{1}{\mathrm{Pr}}\frac{\partial^2 A}{\partial x^2}\\
\frac{\partial B}{\partial x} &= \mathrm{Gr}\cdot A\\
\frac{\partial w}{\partial t} &= \frac{\partial^2 w}{\partial x^2} + B\\
\frac{\partial \Theta}{\partial t} &= \frac{1}{\mathrm{Pr}}\frac{\partial^2 \Theta}{\partial x^2} + A\cdot w\\
\frac{\partial q}{\partial x} &= \mathrm{Gr}\cdot\Theta\\
\mathrm{Gr} = \frac{g\beta A_0 h^4}{\nu^2}, &\quad \mathrm{Pr} = \frac{\nu}{\chi}
\end{aligned} \tag{10.161}$$

A solution of the form (10.160) has already been considered in subsection 10.3.2. Below, the equations that describe this solution are rewritten in dimensionless variables. The dimensionless parameters of the problem Gr and Pr contain the thermal expansion coefficient β and the fluid temperature conductivity χ, as well as the gravity acceleration g.

Equations (10.161) are linear with respect to the unknown functions and can be successively solved. However, the presence of the term $A\cdot w$ in the fourth equation introduces an element of the nonlinear interaction between the velocity and temperature fields into the problem.

We will now dwell on the boundary conditions for system (10.161). We assume that the lower boundary of the layer is solid, so that the velocity on it vanishes

$$x = 0: \quad w = 0. \tag{10.162}$$

On the upper surface the mechanical properties of a surfactant film should be taken into account. The experiment has shown that at low tangential stresses on the

boundary the film remains almost immobile but it breaks down, as a certain limiting value is reached by the tangential stresses, whereupon it behaves as a free surface and the Marangoni convection starts in the threshold way. To describe such film properties it is convenient to introduce on the upper boundary a surface resistance α_d with a thresholdwise dependence of the resistance on the tangential stress. We can write the condition for the tangential stress in the following dimensional form:

$$x = h: \quad \alpha_d w = -\eta \frac{\partial w}{\partial x} + \frac{\partial \sigma}{\partial z}. \tag{10.163}$$

Here, η is the dynamic viscosity of the fluid and σ is the surface tension coefficient. It is assumed that the surface velocity is proportional to the tangential stress value. The resistance coefficient itself depends on this. It is large, when the tangential stresses have not reached a certain limiting value P_0, and it becomes small (vanishes) after the moment when the film has broken up and the surface has become free. With account of the temperature dependence of the surface tension, condition (10.163) takes the following dimensionless form:

$$x = 1: \quad \alpha w = -\frac{\partial w}{\partial x} + \mathrm{Ma}\,\mathrm{Pr}^{-1} \cdot A(1,t), \tag{10.164}$$

$$\mathrm{Ma} = -\frac{\partial \sigma}{\partial T}\frac{A_0 h^2}{\eta\chi}, \quad \alpha = \frac{\alpha_d h}{\eta}.$$

We will write the conditions for the temperature in the form:

$$x = 0: \quad A = 1 - e^{-\gamma t}, \quad \Theta = 0, \tag{10.165}$$

$$x = 1: \quad A = 1 - e^{-\gamma t}, \quad \frac{\partial \Theta}{\partial x} = 0. \tag{10.166}$$

The first condition means that on the layer boundaries the longitudinal temperature gradient increases with time from zero to a limiting value, the same for the entire boundary and included in the time unit as the characteristic time $1/\gamma$.

The function $B(x,t)$ in Eq. (10.161) contains the parameter $C(t)$ determining the fluid flow rate through the channel cross-section, which can be obtained, for example, from the flow closeness condition

$$\int_0^1 w(x,t)\,dx = 0. \tag{10.167}$$

To completely formulate the initial and boundary value problem (10.161), (10.162), and (10.164)–(10.167) we must specify the initial state of the system. We will consider the case in which at the initial moment of time the fluid is at rest and has everywhere the same temperature

$$t = 0: \quad w = 0, \quad A = 0, \quad \Theta = 0. \tag{10.168}$$

10.5.2 Limiting steady flow

We will consider the limiting steady flow attained after a lapse of a large time interval. In the steady case Eqs. (10.161) are reduced to the system

$$\frac{d^2w}{dx^2} = -\mathrm{Gr}\cdot x + c,$$
$$\frac{d^2\Theta}{dx^2} = -\mathrm{Pr}\cdot w$$

with the boundary conditions

$$x = 0: \quad w = 0, \quad \Theta = 0,$$
$$x = 1: \quad \alpha w = -\frac{dw}{dx} + \mathrm{Ma}\,\mathrm{Pr}^{-1}, \quad \frac{d\Theta}{dx} = 0.$$

The solution of this problem satisfying the flow closeness condition is as follows:

$$w_0 = -\frac{\mathrm{Gr}}{12}\left(2x^3 - \frac{3(\alpha+5)}{\alpha+4}x^2 + \frac{(\alpha+6)}{\alpha+4}x\right) + \frac{\mathrm{Ma}\cdot\mathrm{Pr}^{-1}}{\alpha+4}(3x^2 - 2x),$$
$$\Theta_0 = \frac{\mathrm{Gr}\,\mathrm{Pr}}{24}\left(\frac{\alpha+6}{\alpha+4}\cdot\frac{x^3}{3} - \frac{\alpha+5}{\alpha+4}\cdot\frac{x^4}{2} + \frac{x^5}{5}\right) + \frac{\mathrm{Ma}}{\alpha+4}\left(\frac{x^3}{3} - \frac{x^4}{4}\right).$$

The surface $x = 1$ moves at the velocity

$$w_0 = \frac{\mathrm{Gr}}{12(\alpha+4)} + \frac{\mathrm{Ma}\cdot\mathrm{Pr}^{-1}}{\alpha+4}.$$

On the surface there arise the tangential stresses P proportional to the longitudinal temperature gradient

$$P = \frac{\alpha}{\alpha+4}\left(\frac{\mathrm{Gr}}{12} + \frac{\mathrm{Ma}}{\mathrm{Pr}}\right).$$

As this gradient increases, the surface stress reaches a critical value P_0 at which the surfactant film breaks down, the surface friction coefficient sharply diminishes, and the fluid surface is set into motion at a velocity similar in value with

$$w_0 = \mathrm{Gr}/48 + 0.25\,\mathrm{Ma}\,\mathrm{Pr}^{-1}.$$

The convective addition to the surface temperature is as follows:

$$\Theta_0 = \frac{\mathrm{Gr}\,\mathrm{Pr}}{320} + \frac{\mathrm{Ma}}{48}.$$

The quantities w_0 and Θ_0 are proportional to the temperature gradient applied.

We note that at the Prandtl number of the order of 10 the contribution of the gravitational convection to the motion is almost the same as that of the Marangoni convection. In the experiment the critical temperature gradient at which the surfactant film breaks down can be determined from a sharp variation in the surface behavior.

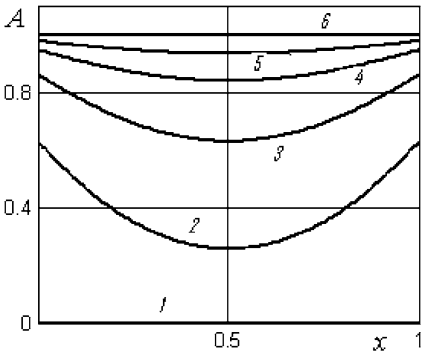

Figure 10.7: Distribution of the longitudinal temperature gradient A along the layer depth at the moments of time $t = 0, 1, 2, 3, 4$, and 10 (*1*–*6*) for Pr = 7 and $\gamma = 1$.

10.5.3 Unsteady convection

We will consider the time variation in the convection flow structure at a variable temperature gradient. We will use the problem formulation described in Section 10.1 in which the temperature gradient increases from zero and reaches a limiting value for a time $1/\gamma$ (we recall that it is the viscous time that is taken as the time unit). In the calculations the condition (10.163) on the free surface was replaced by the condition

$$\left|-\eta\frac{\partial w}{\partial x}+\frac{\partial \sigma}{\partial z}\right| < P_0: \quad w = 0; \quad \left|-\eta\frac{\partial w}{\partial x}+\frac{\partial \sigma}{\partial z}\right| \geqslant P_0: \quad \eta\frac{\partial w}{\partial x} = \frac{\partial \sigma}{\partial z}.$$

This approximation is capable to describe the delay of the onset of thermocapillary convection observed in the experiment [136].

The initial and boundary value problem (10.161), (10.162), (10.164)–(10.168) was solved using a difference method based on an implicit scheme. The solution of the first equation (10.161) is uniquely determined by preassigning the initial condition (10.168) and the boundary conditions (10.165) and (10.166). Knowing the function A we determine by quadratures the function B from the second equation of system (10.161)

$$B(x,t) = \mathrm{Gr}\int_0^1 A(s,t)ds - C(t),$$

where $C(t)$ is an arbitrary function of time determined by Eq. (10.167). Thereupon the system for determining the functions w, Θ, and q becomes closed.

In the problem under consideration the function C is unknown, together with w. Because of this, this problem pertains to the class of inverse problems. Its numerical solution was obtained using the parameter sweeping method for loaded differential equations [41].

In Figure 10.7 the distribution of the longitudinal temperature gradient along the layer depth is presented for different moments of time. As might be expected, at Pr = 7

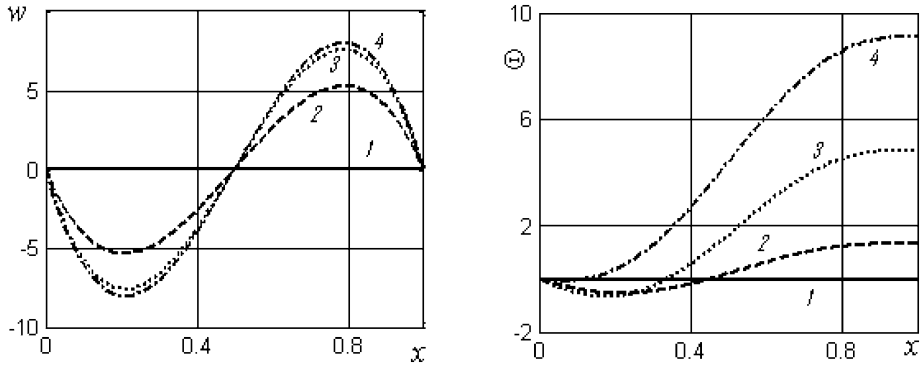

Figure 10.8: Distributions of the velocity w and the convective addition to the temperature Θ along the layer depth; t = 0, 2, 4 and 10 (*1–4*) for P_0 = 500.

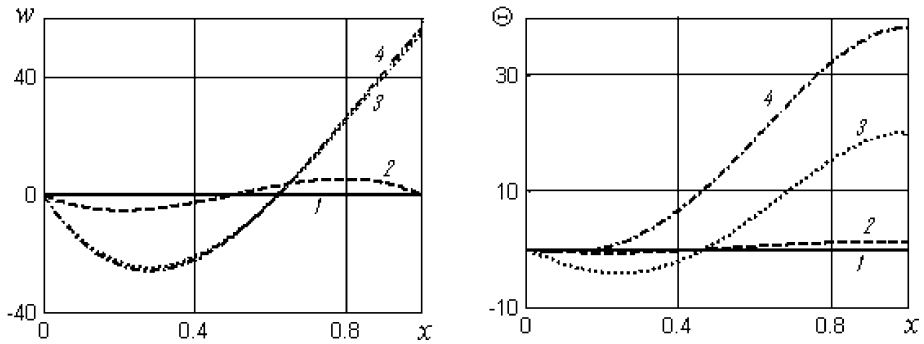

Figure 10.9: Same as in Figure 10.8 for P_0 = 200.

a homogeneous-in-depth temperature gradient is attained for the time $t \sim 7$, that is the unit time based on the temperature conductivity coefficient.

In Figure 10.8 we have plotted the distributions of the velocity and the convective addition to the temperature along the layer depth for the case in which the maximum tangential stress attained, as the convection flow develops, is not greater than the threshold value (P_0 = 500). Here and in what follows, the problem parameter values were taken as follows: Pr = 7, Ma = 10^3, Gr = 10^3, and γ = 1.

As in the case of a solid boundary, the convection flow develops approaching the limiting thermogravitational flow with a cubic velocity profile. In the limiting case the convective addition to the longitudinal temperature gradient is asymmetric about the channel mid-section, owing to the temperature origin adopted.

In the case of a less durable surfactant film (P_0 = 200) the observable convection flow evolution is different. It is presented in Figure 10.9.

At t = 2.7 the surface film breaks down under the action of the tangential stresses and the fluid surface is set into motion. The variations of the velocity of the fluid sur-

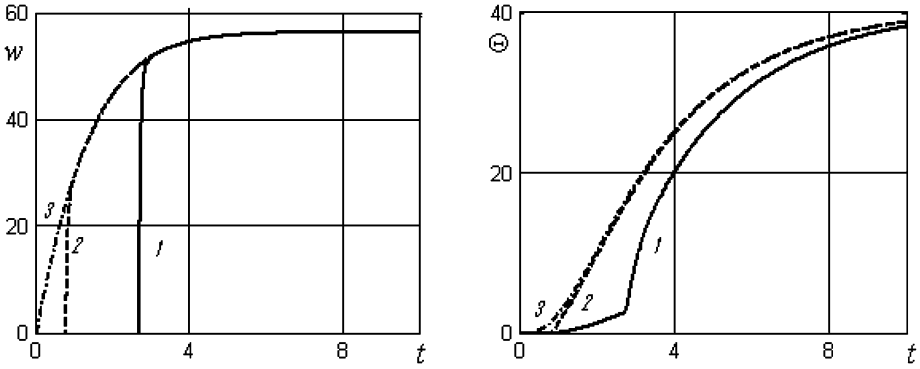

Figure 10.10: Variation in the fluid surface motion velocity w and the convective addition to the temperature Θ for $P_0 = 200$, 100, and 10 (*1–3*).

face motion and the convective addition to the free surface temperature are presented in Figure 10.10 for various values of the threshold stress P_0.

For films with a small limiting stress the change in the convection flow regime takes place at smaller times, when a sufficient temperature gradient is attained. With time the surface velocity and the convective addition to the surface temperature, limiting for the given Grashof and Marangoni numbers, are gradually attained; for the calculated case they are 56.5 and 42.7, respectively.

Summary

A mathematical model describing the development of thermal convection in a horizontal layer, in which a longitudinal temperature gradient gradually increases with time, is developed. It is assumed that on the fluid surface there is a film which breaks down at a certain value of the tangential stress $-\partial w/\partial x + \mathrm{Ma}\,\mathrm{Pr}^{-1} \cdot A(1,t) = P_0$, so that the gravitational convection is supplemented with the Marangoni convection. The limiting steady convection regimes are considered. It is shown that with increase in the temperature gradient the regime changeover must happen. The numerical experiment shows how this changeover proceeds. The limiting regime of thermocapillary convection obtained in the numerical model well agrees with the analytical stationary solution.

Bibliography

[1] A. A. Abramov, *Transfer of boundary conditions for a system of ordinary differential equations (variant of the sweeping method)*, Zh. Vych. Mat. Mat. Fiz., 1, no. 3 (1961), pp. 542–545.

[2] O. V. Admaev, *Numerical experiment for the generalization of the Birikh solution*, in: Proc. Intern. Conf. Lavrent'ev Readings on Mathematics, Mechanics, and Physics, Book of abstracts, Novosibirsk, August 23–27 (2010), pp. 55–56.

[3] A. A. Amsden and F. H. Harlow, *A simplified MAC technique for incompressible fluid flow calculation*, J. Comput. Phys., 6, no. 2 (1970), pp. 322–325.

[4] D. M. Anderson, G. B. McFadden, and A. A. Wheeler, *Diffuse interface methods in fluid mechanics*, Ann. Rev. Fluid Mech., 30 (1998), pp. 139–165.

[5] D. Anderson, J. Tannehill, and R. Pletcher, *Computational hydromechanics and heat transfer*, Hemisphere, New York (1984).

[6] V. K. Andreev, *Invariant solutions of thermodiffusion equations*, in: Proc. III Intern. Conf. Symmetry and Differential Equations, Inst. Comp. Math., Sib. Branch, Russian Acad. of Sci., Krasnoyarsk (2002), pp. 13–17.

[7] V. K. Andreev, *Birikh solutions of convection equations and some generalizations*, Preprint, no. 1-10, Inst. Comp. Math., Sib. Branch, Russian Acad. of Sci., Krasnoyarsk (2010), 68 pp.

[8] V. K. Andreev and O. V. Admaev, *Axisymmetric thermocapillary flow in cylinder and cylindrical layer*, in: Hydromechanics and Heat/Mass Transfer in Microgravity (1992), pp. 169–172.

[9] V. K. Andreev and V. B. Bekezhanova, *Development of thermal convection under low gravity*, in: Joint Xth European and VIth Russian Symposium on Physical Science in Microgravity, St. Petersburg, Book of abstracts (1997), pp. 10–11.

[10] V. K. Andreev and V. B. Bekezhanova, *Stability of the non-isothermal fluids*, Monograph, The Siberian Federal University, Krasnoyarsk (2010), 356 pp.

[11] V. K. Andreev and V. B. Bekezhanova, *Emergence of microconvection in a plane layer*, Preprint No. 1-01, Inst. Comp. Math., Sib. Branch, Russian Acad. of Sci., Krasnoyarsk (2001), 38 pp.

[12] V. K. Andreev and V. B. Bekezhanova, *On an invariant solution of microconvection equations*, in: Proc. Workshop Mathematical Modeling in Mechanics, Inst. Comp. Math., Sib. Branch, Russian Acad. of Sci., Krasnoyarsk (1999), pp. 34–47. (Deposited at VINITI 05.07.1999, no. 1999-B99).

[13] V. K. Andreev and V. B. Bekezhanova, *Stability of the equilibrium of a flat layer in a microconvection model*, J. Appl. Mech. Tech. Phys., 43, no. 2 (2002), pp. 43–53.

[14] V. K. Andreev and V. B. Bekezhanova, *On stability of a steady flow in a vertical layer in a microconvection model*, Izv. Ross. Akad. Nauk, Mekh. Zhidk. Gaza, 2 (2004), pp. 57–68.

[15] V. K. Andreev, V. B. Bekezhanova, and Yu. Gaponenko, *Studying the flows and their stability in microconvection models*, Vych. Tekhnol., 9 (2004), pp. 7–21.

[16] V. K. Andreev, V. E. Zakhvataev, and E. A. Ryabitskii, *Thermocapillary instability*, Nauka, Moscow (2000), 280 pp.

[17] V. K. Andreev, O. V. Kaptsov, V. V. Pukhnachov, and A. A. Rodionov, *Application of group-theoretical methods in hydrodynamics*, Nauka, Novosibirsk (1994), 319 pp.

[18] V. K. Andreev, O. V. Kaptsov, V. V. Pukhnachov, and A. A. Rodionov, *Applications of group theoretical methods in hydrodynamics*, Kluwer Acad. Publ., Dordrecht, Boston, London (1998), 408 pp.

[19] V. K. Andreev and V. V. Pukhnachov, *Invariant solutions of the medium equations*, in: Numerical Methods of Mechanics of Continuous Media (collected papers), 14, no. 5 (1983), pp. 3–23.

[20] V. K. Andreev, Yu. A. Gaponenko, O. N. Goncharova, and V. V. Pukhnachov, *Advanced mathematical models of convection*, Fizmatlit, Moscow (2008), 368 pp.

https://doi.org/10.1515/9783110655469-011

[21] V. K. Andreev, Yu. A. Gaponenko, O. N. Goncharova, and V. V. Pukhnachov, *Mathematical models of convection*, De Gruyter Studies in Mathematical Physics, De Gruyter, Berlin–Boston (2012), 432 pp.

[22] V. K. Andreev and I. I. Ryzhkov, *Group properties of thermodiffusion equations in the plane case*, in: Proc. All-Russia school-conference for young scientists Chebotarev Readings on Problems of Modern Group Analysis and its Applications in Nonlinear Mechanics, Kazan' (2004), pp. 11–18.

[23] V. K. Andreev and E. A. Ryabitskii, *Origination of microconvection in a flat layer with a free boundary*, J. Appl. Mech. Tech. Phys., 45, no. 1 (2004), pp. 22–30.

[24] L. K. Antanovskii, *Microscale theory of surface tension*, Physical Review E, 54, no. 6 (1996), pp. 6285–6290.

[25] S. N. Antontsev, A. V. Kazhikhov, and V. N. Monakhov, *Boundary-value problems of mechanics of inhomogeneous fluids*, Nauka, Novosibirsk (1983), 319 pp.

[26] S. Aristov, N. Bessonov, Yu. Gaponenko, and V. Volpert, *Interfacial waves in binary fluids*, in: Pattern and Waves, St. Petersburg, 2003, pp. 79–97.

[27] I. A. Babushkin, G. P. Bogatyrev, A. F. Glukhov, et al., *Experimental study of heat convection on the Mir orbital station*, in: Proc. VII Russian Symp. Microgravity Mechanics. Results and Prospects of Basic Research of Gravity-Sensitive Systems, Moscow, April 11–14, 2000, pp. 99–122.

[28] C. Baiocchi and V. V. Pukhnachev, *Problems with one-sided constraints for Navier-Stokes equations and the dynamic contact angle*, J. Appl. Mech. Tech. Phys., 31, no. 2 (1990), pp. 185–197.

[29] G. K. Batchelor, *An introduction into fluid dynamics*, Cambridge Univ. Press, London (1987).

[30] V. B. Bekezhanova *Stationary solution of the equations of microconvection in a vertical layer*, J. Appl. Mech. Tech. Phys., 42, no. 3 (2001), pp. 437–444.

[31] V. B. Bekezhanova, *Stability of a steady flow with an exponential distribution of temperature in the microconvection model*, Preprint No. 2-02, Inst. Comp. Math., Sib. Branch, Russian Acad. of Sci., Krasnoyarsk (2002), 22 pp.

[32] R. D. Bengyria and M. C. Derassier, *On the linear stability of Benard-Marangoni convection*, Phys. Fluids A, 1, no. 7 (1989), pp. 1123–1127.

[33] E. I. Berezovskii, T. L. Perelman, and E. A. Romashko, *On convective instability in a system of two unbounded horizontal layers of immiscible fluids*, Inzh.-Fiz. Zh., 27, no. 6 (1974), pp. 1098–1108.

[34] N. M. Bessonov, J. A. Pojman, V. A. Volpert, and B. D. Zoltowski, *Numerical simulations of transient interfacial phenomena in miscible polymer systems*, in: AIAA-2003-1157, Microgravity Science and Space Processing, 41st AIAA Aerospace Sciences Meeting and Exhibit: Proc. of the conference, 6–9 January, 2003, Reno, NV, USA.

[35] R. V. Birikh, *Thermocapillary convection in a horizontal layer of liquid*, J. Appl. Mech. Tech. Phys., 3 (1966), pp. 69–72.

[36] R. V. Birikh, M. O. Denisova, and K. G. Kostarev, *The development of Marangoni convection induced by a local addition of a surfactant*, Fluid Dynamics, 46, no. 6, (2011), pp. 890–900.

[37] R. V. Birikh and V. V. Pukhnachov, *Axial convective flow in a rotating tube with a streamwise temperature gradient*, Dokl. Akad. Nauk, 436, no. 3 (2011), pp. 323–327.

[38] R. V. Birikh, V. V. Pukhnachev, O. A. Frolovskaya, *Convective flow in a horizontal channel with non-Newtonian surface rheology under time-dependent longitudinal temperature gradient*, Izvestiya Rossiiskoi Akademii Nauk, Mekhanika Zhidkosti i Gaza, 50, no. 1 (2015), pp. 192–198.

[39] N. N. Bogolubov and Yu. A. Mitropolskii, *Asymptotic methods in the theory of nonlinear oscillations*, Nauka, Moscow (1974), 503 pp.

[40] B. S. Bokshtein, *Thermodiffusion*, Soros. Obraz. Zh., 4 (1999), pp. 40–43.
[41] E. A. Bondarev and A. F. Voyevodin, *Difference method for solving initial-boundary-value problems for loaded differential and integrodifferential equations*, Differ. Uravn., 36, no. 11 (2000), pp. 1560–1562.
[42] Yu. K. Bratukhin and S. O. Makarov, *Hydrodynamic stability of interphase surfaces*, Izd. Perm. Gos. Univ., Perm' (2005), 239 pp.
[43] Yu. K. Bratukhin and S. O. Makarov, *Interphase convection*, Izd. Perm. Gos. Univ., Perm' (1994), 328 pp.
[44] D. R. Chenoweth and S. Paolucci, *Natural convection in an enclosed vertical air layer with large horizontal temperature differences*, J. Fluid Mech., 169 (1986), pp. 173–210.
[45] P. Colinet, J. C. Legros, and M. G. Velarde, *Nonlinear dynamics of surface-tension-driven instabilities*, Wiley-VCH (2001), 527 pp.
[46] S. H. Davis and G. M. Homsy, *Energy stability theory for free-surface problems: buoyancy-thermocapillary layers*, J. Fluid Mech., 98, no. 3 (1980), pp. 527–553.
[47] P.-G. De Gennes, *Wetting: statics and dynamics*, Usp. Fiz. Nauk, 151, no. 4 (1987), pp. 619–681.
[48] W. Dörfler, O. Goncharova, and D. Kröner, *Fluid flow with dynamic contact angle: numerical simulation*, ZAMM, 82, no. 3 (2002), pp. 167–176.
[49] B. A. Dubrovin, S. P. Novikov, and A. T. Fomenko, *Modern geometry. Methods and applications*, Nauka, Moscow (1979), 760 pp.
[50] V. E. B. Dussan, *On the spreading of liquids on solid surfaces: Static and dynamics contact lines*, Annual Rev. Fluid Mech., 11 (1979), pp. 371–400.
[51] V. E. B. Dussan and S. H. Davis, *On the motion fluid–fluid interface along a solid surface*, Fluid Mech., 65 (1974), pp. 71–95.
[52] A. B. Ezerskii, *Dynamics of defects in hexagonal lattices emerging under the Benard-Marangoni convection*, In: Synergetics. Laboratory Works on Nonlinear Physics, Udm. Inst., Izhevsk (1999), pp. 51–74.
[53] M. V. Fedoryuk, *Asymptotics integrals and series*, Nauka, Moscow (1987).
[54] G. M. Fikhtengolts, *Fundamentals of mathematical analysis. Vol. II*, Gos. Izdat. Tekh.-Teor. Lit., Moscow (1956), 464 pp.
[55] R. Finn, *Equilibrium capillary surfaces*, Springer-Verlag, New York (1986).
[56] C. Fletcher, *Computational techniques for fluid dynamics*, Springer-Verlag, Heidelberg (1988).
[57] A. Friedman, *Partial differential equations of parabolic type*, Prentice Hall (1964).
[58] A. V. Fursikov and O. Yu. Emanuilov, *Local exact controllability of the Boussinesq equations*, Vestn. Ros. Univ. Dr. Narodov, Ser. Matem., 3, no. 1 (1996), pp. 177–194.
[59] W. Fushchych and R. Popowych, *Symmetry reduction and exact solutions of the Navier–Stokes equations. II*, Nonlinear Mathematical Physics, 1, no. 2 (1994), pp. 158–188.
[60] V. A. Galaktionov and J. L. Vazquez, *Blow-up for a class of solutions with free boundaries for the Navier-Stokes equations*, Adv. Diff. Eq., 4 (1999), pp. 297–321.
[61] Yu. A. Gaponenko, *Numerical modeling of convection in thin fluid layers with a free boundary*, in: Proc. Intern. Conf. Mathematical Models and Methods of Their Study, Krasnoyarsk State University, Krasnoyarsk (2001), pp. 155–159.
[62] Yu. A. Gaponenko and V. E. Zakhvataev, *Microconvection in a binary system*, Izv. Ross. Akad. Nauk, Mekh. Zhidk. Gaza, 1 (2003), pp. 67–79.
[63] Yu. A. Gaponenko and V. E. Zakhvataev, *Non-Boussinesq heat convection under microgravity conditions with nonuniform heating*, J. Appl. Mech. Tech. Phys., 43, no. 6 (2002), pp. 823–829.
[64] P. Germain, *Cours de Mecanique des Milieux Continus*, Masson et Cie, Editeurs, Paris (1973).

[65] G. Z. Gershuni, A. K. Kolesnikov, J. C. Legros, and B. I. Myznikova, *On the vibrational convective instability of a horizontal, binary-mixture layer with Soret effect*, J. Fluid Mech., 330 (1997), pp. 251–269.
[66] G. Z. Gershuni and E. M. Zhukhovitskii, *On convective instability of the thermal skin layer*, Prikl. Mat. Mekh., 27, no. 5 (1963), pp. 779–783.
[67] G. Z. Gershuni and E. M. Zhukhovitskii, *On the convective instability of a thermal boundary layer*, J. Appl. Mech. Tech. Phys., 6 (1965), pp. 34–36.
[68] G. Z. Gershuni and E. M. Zhukhovitskii, *Convective stability of an incompressible fluid*, Nauka, Moscow (1972), 392 pp.
[69] G. Z. Gershuni and E. M. Zhukhovitskii, *Monotonic and vibrational instability of a two-layer system of immiscible fluids heated from below*, Dokl. Akad. Nauk SSSR, 265, no. 2 (1982), pp. 302–305.
[70] G. Z. Gershuni and E. M. Zhukhovitskii, *On instability of the equilibrium state of a system of horizontal layers of immiscible fluids heated from above*, Izv. Akad. Nauk SSSR, Mekh. Zhidk. Gaza, 6 (1980), pp. 28–34.
[71] G. Z. Gershuni, E. M. Zhukhovitskii, and A. A. Nepomnyashchii, *Stability of convective flows*, Nauka, Moscow (1989), 320 pp.
[72] G. Z. Gershuni, E. M. Zhukhovitskii, and L. E. Sorokin, *On stability of a plane-parallel convective flow of a binary mixture*, Prikl. Mat. Mekh., 44, no. 5 (1980), pp. 823–830.
[73] G. Z. Gershuni, E. M. Zhukhovitskii, and L. E. Sorokin, *On stability of a convective flow of a binary mixture with thermodiffusion*, Prikl. Mat. Mekh., 46, no. 1 (1982), pp. 66–71.
[74] G. Z. Gershuni, E. M. Zhukhovitskii, and Yu. S. Yurkov, *Stability of a steady convective flow induced by internal heat sources*, Prikl. Mat. Mekh., 34 (1970), pp. 470–480.
[75] S. K. Godunov, *On the numerical solution of boundary-value problems for systems of linear ordinary differential equations*, Usp. Mat. Nauk, 16, no. 3 (1961), pp. 171–174.
[76] O. N. Goncharova, *Group classification of equations of free convection*, in: Dynamics of Continuous Media (Collected Papers), no. 79, Inst. Hydrodynamics, Sib. Branch, Acad. of Sci. of the USSR, Novosibirsk (1987), pp. 22–35.
[77] O. N. Goncharova, *Mathematical models of convection under microgravity conditions*, Doctor's dissertation, Novosibirsk (2005), 243 pp.
[78] O. N. Goncharova, *Microconvection in a domain with a free boundary*, Vych. Tekhnol., 5, no. 2 (2000), pp. 14–25.
[79] O. N. Goncharova, *Microconvection in weak force fields. A numerical comparison of two models*, J. Appl. Mech. Tech. Phys., 38, no. 2 (1997), pp. 219–223.
[80] O. N. Goncharova, *Calculation of microconvection in an extended rectangle*, Vych. Tekhnol., 5, no. 5 (2000), pp. 26–37.
[81] O. N. Goncharova, *Exact solutions of linearized microconvection equations in an infinite band*, in: Proc. VII Russian Symp. Microgravity Mechanics. Results and Prospects of Basic Research of Gravity-Sensitive Systems, Moscow, April 11–14 (2000), pp. 234–247.
[82] O. N. Goncharova, *Numerical simulation of microconvection in domains with free boundaries*, J. Appl. Mech. Tech. Phys., 38, no. 3 (1997), pp. 386–390.
[83] O. N. Goncharova, *Numerical modelling of convection of isothermally incompressible fluid under low gravity in domain with free boundary*, Vych. Tekhnol., 9, no. 5 (2004), pp. 3–13.
[84] O. N. Goncharova and O. A. Kabov, *Deformations of a viscous heat conducting free liquid layer by the thermocapillary forces and tangential stresses: analytical and numerical modeling*, Microgravity Sci. Technol., 22 (2010), pp. 407–414.
[85] O. N. Goncharova and O. A. Kabov, *Mathematical and numerical modeling of convection in a horizontal layer under co-current gas flow*, Int. J. Heat Mass Transfer, 53 (2010), pp. 2795–2807.

[86] O. N. Goncharova and O. A. Kabov, *Gravitational-thermocapillary convection in a horizontal layer with a co-current gas flow*, Dokl. Akad. Nauk, 426, no. 2 (2009), pp. 183–188.

[87] O. N. Goncharova and V. V. Pukhnachov, *Construction of exact solutions of three-dimensional problems of convection*, in: Modern Problems of Applied Mathematics and Mechanics: Theory, Experiment, and Practice [electronic resource], Intern. Conf. Devoted to the 90th Anniversary of Academician N.N. Yanenko, Novosibirsk, Russia, May 30–June 4 (2011), Inst. Comput. Technol., Sib. Branch, Russian Acad. of Sci., Novosibirsk (2011), Number in State Register 0321101160, Access at: http://conf.nsc.ru/files/conferences/niknik-90/fulltext/39133/48751/ONG_VVP.pdf, 6 pp.

[88] O. N. Goncharova, O. A. Kabov and V. V. Pukhnachov, *Solutions of special type describing the three dimensional thermocapillary flows with an interface*, Int. J. Heat Mass Transfer, 55, no. 4 (2012), pp. 715–725.

[89] D. D. Grey and A. Giorgini, *The validity of the Boussinesq approximation for liquids and gases*, Int. J. Heat Mass Transfer, 19, no. 5 (1976), pp. 545–551.

[90] V. A. Griaznov and V. I. Polezhaev, *Investigation of some difference schemes and approximating boundary conditions for the numerical solution of heat convection equations*, Preprint No. 40, Inst. Appl. Math., Moscow (1974), 66 pp.

[91] P. G. Grodzka and T. C. Bannister, *Heat flow and convection demonstration experiments aboard Apollo 14*, Science, 176 (1972), pp. 506–508.

[92] P. G. Grodzka and T. C. Bannister, *Heat flow and convection experiments aboard Apollo 17*, Science, 187 (1975), pp. 165–167.

[93] Yu. P. Gupalo and Ju. S. Ryazantsev, *On thermocapillary motion of a liquid with free surface at nonlinear dependence of surface tension on temperature*, Izv. Akad. Nauk SSSR, Mekh. Zhidk. Gaza, 5 (1988), pp. 132–137.

[94] F. H. Harlow and J. E. Welch, *Numerical calculation of time-dependent viscous incompressible flow with free surface*, Phys. Fluids, 8, no. 12 (1968), pp. 2182–2189.

[95] I. Hashim and S. K. Wilson, *The onset of Benard-Marangoni convection in a horizontal layer of fluid*, Int. J. Engineering Science, 37 (1999), pp. 643–662.

[96] C. W. Hirt and J. L. Cook, *Calculating three-dimensional flows around structures and over rough terrain*, J. Comput. Phys., 10, no. 2 (1972), pp. 324–340.

[97] H. E. Huppert and J. S. Turner, *Double-diffusive convection*, J. Fluid Mech., 106 (1981), pp. 299–329.

[98] N. H. Ibragimov and G. Unal, *Lie groups in turbulence*, Lie Groups and their Applications, 1, no. 2 (1994), pp. 98–103.

[99] V. Kh. Izakson and V. I. Yudovich, *Emergence of convection in a fluid layer with a free boundary*, Izv. Akad. Nauk SSSR, Mekh. Zhidk. Gaza, 4 (1968), pp. 23–28.

[100] E. Jahnke, F. Emde, and F. Losch, *Tables of higher functions*, McGraw-Hill, New York (1960).

[101] D. D. Joseph, *Stability of fluid motions*, Springer-Verlag, Berlin–Heidelberg–New York (1976).

[102] D. D. Joseph and Y. Y. Renardy, *Fundamentals of two-fluid dynamics. Part 2. Lubricated transport, drops and miscible fluids*, Springer, New-York (1992), 445 pp.

[103] N. N. Kalitkin, *Numerical methods*, Nauka, Moscow (1978), 512 pp.

[104] L. V. Kantorovich and V. I. Krylov, *Method of the approximate solution of partial differential equations*, Moscow (1936), 528 pp.

[105] A. P. Kartashev and B. L. Rozhdestvenskii, *Ordinary differential equations and fundamentals of variational calculus*, Nauka, Moscow (1986), 272 pp.

[106] V. L. Katkov, *Exact solutions of some problems of convection*, Prikl. Mat. Mekh., 32, no. 3 (1968), pp. 482–487.

[107] A. G. Kirdyashkin, *Thermogravitational and thermocapillary flows in a horizontal liquid layer under the conditions of a horizontal temperature gradient*, Int. J. Heat Mass Transfer, 27, no. 8 (1984), pp. 1205–1218.

[108] A. G. Kirdyashkin, *Thermocapillary periodic motions*, Preprint No. 8, Inst. Geology Geophysics, Sib. Branch, Acad. of Sci. of the USSR, Novosibirsk (1985), 35 pp.

[109] A. G. Kirdyashkin, V. I. Polezhaev, and A. I. Fedyushkin, *Thermal convection in a horizontal layer with lateral heating*, J. Appl. Mech. Tech. Phys., 24, no. 6 (1983), pp. 876–881.

[110] N. E. Kochin, *Vector calculus and fundamentals of tensor calculus*, Nauka, Moscow (1965), 426 pp.

[111] D. J. Korteweg, *Sur la forme que prennent les équations du mouvement des fluides si l'on tient compte des forces capillaires causées par des variations de densité considérables mais connues et sur la théorie de la capillarité dans l'hypothèse d'une variation continue de la densité*, Archives Néerlandaises des Sciences Exactes et Naturelles, 6 (1901), pp. 1–24.

[112] N. S. Koshliakov, E. B. Gliner, and M. M. Smirnov, *Basic differential equations of mathematical physics*, Fizmatgiz, Moscow (1962).

[113] V. F. Kovalev and V. V. Pustovalov, *Lie algebra of renormalization group admitted by initial value problem for Burgers equation*, Lie Groups and their Applications, 1, no. 2 (1994), pp. 104–120.

[114] O. A. Ladyzhenskaya, *Mathematical issues of dynamics of a viscous incompressible fluid*, Nauka, Moscow (1970), 288 pp.

[115] O. A. Ladyzhenskaya and N. N. Uraltseva, *Linear and quasi-linear equations of the elliptical type*, Nauka, Moscow (1973), 576 pp.

[116] O. A. Ladyzhenskaya, V. A. Solonnikov, and N. N. Uraltseva, *Linear and quasi-linear equations of the parabolic type*, Nauka, Moscow (1967), 736 pp.

[117] O. A. Ladyzhenskaya, V. A. Solonnikov, and N. N. Uraltseva, *Linear and quasilinear parabolic type of equations*, Amer. Math. Soc. (1998).

[118] L. D. Landau and E. M. Lifshitz, *Theory of elasticity*, Pergamon Press, Oxford–New York (1970).

[119] L. D. Landau and E. M. Lifshitz, *Course of theoretical physics. Vol. 6. Fluid dynamics*, Pergamon Press, Oxford-Elmsford, New York (1987).

[120] Yu. V. Lapin and M. Kh. Strelets, *Internal flows of gas mixtures*, Nauka, Moscow (1989), 368 pp.

[121] B. K. Larkin, *Heat flow to a confined fluid in zero gravity*, Progr. Astronaut. Aeronaut., 20 (1967), pp. 819–832.

[122] D. V. Lyubimov, T. P. Lyubimova, A. B. Perminov, D. Henry, and H. Ben Hadid, *Stability of convection in a horizontal channel subjected to a longitudinal temperature gradient. Part 2. Effect of the magnetic field*, J. Fluid Mech., 635 (2009), pp. 297–319.

[123] T. P. Lyubimova, D. V. Lyubimov, V. A. Morozov, R. V. Scurdin, H. Ben Hadid, and D. Henry, *Stability of convection in a horizontal channel subjected to a longitudinal temperature gradient. Part 1. Effect of the aspect ratio and Prandtl number*, J. Fluid Mech., 635 (2009), pp. 275–295.

[124] T. P. Lyubimova and D. A. Nikitin, *Three-dimensional advection flows in a square horizontal cylinder with heat-conducting lateral boundaries*, Vych. Mekh. Sploshnykh Sred 4, no. 2 (2011), pp. 72–81.

[125] N. I. Lobov, D. V. Lyubimov, and T. P. Lyubimova, *Convective instability of a system of horizontal layers of immiscible fluids with a deformable interface*, Izv. Ross. Akad. Nauk, Mekh. Zhidk. Gaza, 2 (1996), pp. 32–39.

[126] G. I. Marchuk, *Splitting methods*, Nauka, Moscow (1988), 264 pp.

[127] G. S. Markman and V. I. Yudovich, *Numerical study of the emergence of convection in a fluid layer under the action of time-periodic external forces*, Izv. Akad. Nauk SSSR, Mekh. Zhidk. Gaza, 3 (1972), pp. 81–86.
[128] G. E. Mase, *Theory and problems of continuum mechanics*, Schaum's Outline Series, McGraw-Hill (1970).
[129] S. V. Meleshko, *Group classification of equations of two-dimensional motions of the gas*, Prikl. Mat. Mekh., 58, no. 4 (1994), pp. 56–62.
[130] S. V. Meleshko, *Generalization of the equivalence transformations*, Nonlinear Mathematical Physics, 3, nos. 1-2 (1996), pp. 170–174.
[131] S. V. Meleshko and V. V. Pukhnachev, *One class of partially invariant solutions of the Navier-Stokes equations*, J. Appl. Mech. Tech. Phys., 40, no. 2 (1999), pp. 208–216.
[132] F. S. Meshcheryakov and S. A. Ulybin, *Thermodynamics. Phenomenological thermomechanics*, Khimiya, Moscow (1994), 352 pp.
[133] J. M. Mihaljan, *A rigorous exposition of the Boussinesq approximation applicable to a thin layer of fluid*, Astrophys. J., 136, no. 3 (1962), pp. 1126–1144.
[134] Yu. A. Mitropolskii and G. P. Khoma, *Mathematical justification of asymptotic methods of nonlinear mechanics*, Naukova Dumka, Kiev (1983), 215 pp.
[135] A. Mizev, M. Denisova, K. Kostarev, R. Birikh, and A. Viviani, *Threshold onset of Marangoni convection in narrow channels*, EPJ ST, 192, no. 1 (2011), pp. 163–173.
[136] A. I. Mizev and A. V. Shmyrov, *Nonsoluble surfactant effect on the development of thermocapillary convection*, in: Convection Flows. Collection of Scientific Studies. Issue 6 [in Russian], Perm (2013), p. 216.
[137] I. Sh. Mogilevskii and V. A. Solonnikov, *On the solvability of an evolution free boundary problem for the Navier-Stokes equations in the Holder spaces of functions*, in: Mathematical problems related to the Navier-Stokes equations. Series on Advances in Mathematics for Applied Sciences, vol. 11 (1992), pp. 105–181.
[138] A. S. Monin and A. M. Yaglom, *Statistical hydrodynamics. Part I*, Nauka, Moscow (1965), 640 pp.
[139] V. B. Moseenkov, *Qualitative methods of studying problems of convection of a viscous weakly compressible fluid*, Inst. Mathematics, National Acad. of Sci. of Ukraine, Kiev (1998), 280 pp.
[140] A. D. Myshkis (ed.), *Microgravity hydromechanics*, Nauka, Moscow (1976), 504 pp.
[141] A. D. Myshkis, V. G. Babsky, N. D. Kopachevsky, et al., *Low-gravity fluid mechanics. Mathematical theory of capillary phenomena*, Springer-Verlag, Berlin (1987), 583 pp.
[142] K. A. Nadolin, *About the Oberbeck–Boussinesq approximation in the Rayleigh–Bénard problem* Izv. Ross. Akad. Nauk, Mekh. Zhidk. Gaza, 5 (1995), pp. 3–10.
[143] K. A. Nadolin, *Convective instability of a horizontal layer with temperature oscillations on the free boundary*, Izv. Vuzov Sev.-Kavk. Regiona, Estestv. Nauki (2003), pp. 269–273.
[144] K. A. Nadolin, *Convection in horizontal layer under the inversion of specific volume*, Izv. Ross. Akad. Nauk, Mekh. Zhidk. Gaza, 1 (1989), pp. 43–49.
[145] A. M. Nakhushev and V. N. Borisov, *Boundary-value problems for loaded parabolic equations and their use to predict groundwater levels*, Differ. Uravn., 13, no. 1 (1977), pp. 105–110.
[146] L. G. Napolitano, *Plane Marangoni-Poiseuille flow of two immiscible fluids*, Acta Astronautica, 7, no. 4 (1980), pp. 461–478.
[147] L. G. Napolitano, *Thermodynamics and dynamics of surface phases*, Acta Astronautica, 6, no. 9 (1979), pp. 1093–1112.
[148] A. A. Nepomnyaschy, *On long-wave convective instability in horizontal layers with a deformable boundary*, in: Convective Flows, Perm. Ped. Inst., Perm' (1983), pp. 25–31.
[149] A. A. Nepomnyaschy, M. G. Velarde, and P. Colinet, *Interfacial phenomena and convection*, Chapman and Hall, CRC (2002), 365 pp.

[150] B. I. Nikolaev and A. A. Tubin, *On stability of a convective flow of a binary mixture in a plane thermodiffusion column*, Prikl. Mat. Mekh., 35, no. 2 (1971), pp. 248–254.
[151] D. A. Nikulin and M. Kh. Strelets, *Numerical modeling of unsteady natural convection of a compressible gas in a closed non-adiabatic domain*, Teplofiz. Vys. Temp., 22, no. 5 (1984), pp. 906–912.
[152] V. V. Ostapenko, *Difference scheme of high-order convergence on an unsteady shock wave*, Sib. Zh. Vych. Mat., 2, no. 1 (1999), pp 47–56.
[153] G. A. Ostroumov, *Free convection under conditions of an internal problem*, Gostekhizdat, Moscow-Leningrad (1952), 256 pp.
[154] L. V. Ovsiannikov, *Introduction into mechanics of continuous media*, Izd. Nov. Gos. Univ., Novosibirsk, Part 1 (1976), 76 pp.; Part 2 (1977), 70 pp.
[155] L. V. Ovsiannikov, *Group analysis of differential equations*, Nauka, Moscow (1978), 400 pp.
[156] L. V. Ovsiannikov, *Group analysis of differential equations*, Academic Press, New York (1982).
[157] L. V. Ovsiannikov, *Symmetry of barochronous motions of the gas*, Sib. Mat. Zh., 44, no. 5 (2003), pp. 1098–1109.
[158] L. V. Ovsiannikov, *On the optimal systems of subalgebras*, J. Lie Groups and Their Appl., 1, no. 2 (1994), pp. 18–26.
[159] S. Paolucci, *On the filtering of sound from the Navier–Stokes equations*, Sandia Nat. Lab. Rep. SAND 82 (December, 1982).
[160] V. M. Paskonov, V. I. Polezhaev, and L. A. Chudov, *Numerical modeling of heat and mass transfer processes*, Nauka, Moscow (1984), 286 pp.
[161] P. S. Perera and R. F. Sekerka, *Nonsolenoidal flow in a liquid diffusion couple*, Phys. Fluids, 9, no. 2 (1997), pp. 376–391.
[162] C. Peter-Garcia and G. Carneiro, *Linear stability analysis of Benard-Marangoni convection in fluids with a deformable free surface*, Phys. Fluids A, 3, no. 2, (1991), pp. 292–298.
[163] P. Petitjeans, *Une tension de surface pour les fluides miscibles*, CRAS, Série II b, 322 (1996), pp. 673–679.
[164] P. Petitjeans, *Fluides non miscible/fluides miscibles: des similitudes intéressantes*, CRAS, Série II b, 325 (1997), pp. 587–592.
[165] I. G. Petrovskii, *Lectures on the theory of ordinary differential equations*, 7th edition, Izd. Mosk. Gos. Univ., Moscow (1984), 295 pp.
[166] K. Pileckas and V. Keblikas, *On existence of the unsteady Poiseuille solution*, Sib Mat. Zh., 46, no. 3 (2005), pp 649–662.
[167] J. A. Pojman, R. Texier-Picard, and V. A. Volpert, *Convection induced by composition gradients in miscible systems*, CRAS, Série II b, 330 (2002), pp. 353–358.
[168] V. I. Polezhaev, M. S. Bello, N. A. Verezub, et al., *Convective processes in microgravity*, Nauka, Moscow (1991), 240 pp.
[169] A. D. Polyanin and A. V. Manzhirov, *Handbook of integral equations*, CRS, Boca Raton, Fl (1998).
[170] V. V. Pukhnachov, *On a problem of viscous strip deformation with a free boundary*, C.R. Acad. Sci. Paris, 328, no. 1 (1999), pp. 357–362.
[171] V. V. Pukhnachov, *Motion of a viscous fluid with free boundaries*, Izd. Nov. Gos. Univ., Novosibirsk (1989), 96 pp.
[172] V. V. Pukhnachov,. *Hierarchy of models in thermal convection*, in: Boundary-Value Problems of Mathematical Physics and Related Issues of the Theory of Functions, Zap. Nauch. Sem. POMI, vol. 288 (2002), pp. 152–177.
[173] V. V. Pukhnachov, *Invariant solutions of the Navier-Stokes equations that describe motions with free boundaries*, Dokl. Akad. Nauk SSSR, 202, no. 2 (1972), pp. 302–305.

[174] V. V. Pukhnachov, *Lectures on the dynamics of a viscous incompressible fluid. Part 1*, Izd. Nov. Gos. Univ., Novosibirsk (1969).
[175] V. V. Pukhnachov, *Model of viscous layer deformation by thermocapillary forces*, Eur. J. Appl. Math., 13, no. 2 (2002), pp. 205–224.
[176] V. V. Pukhnachov, *Microconvection in a vertical layer*, Izv. Ross. Akad. Nauk, Mekh. Zhidk. Gaza, 5 (1994), pp. 76–84.
[177] V. V. Pukhnachov, *Model of convective motion under microgravity conditions*, in: Modeling in Mechanics (Collected Papers), Inst. Theor. Appl. Mech., Sib. Branch, Russian Acad. of Sci., Novosibirsk, 6(23), no. 4 (1992), pp. 47–56.
[178] V. V. Pukhnachov, *Steady problem of microconvection*, in: Dynamics of Continuous Media (Collected Papers), Inst. Hydrodynamics, Sib. Branch, Russian Acad. of Sci., vol. 111 (1996), pp. 109–116.
[179] V. V. Pukhnachov, *Thermal convection in a rotating fluid layer under microgravity conditions*, Izv. Vuzov. Sev.-Kavk. Regiona. Estestv. Nauki (2003), pp. 1–6.
[180] V. V. Pukhnachov, *Thermocapillary convection in weak force fields*, Preprint No. 178-88, Inst. Thermophys., Sib. Branch, Acad. of Sci. of the USSR, Novosibirsk (1988).
[181] V. V. Pukhnachev, *Exact solutions of the hydrodynamic equations derived from partially invariant solutions*, J. Appl. Mech. Tech. Phys., 44, no. 3 (2003), pp. 317–323.
[182] V. V. Pukhnachov, *Group-theoretical nature of the Birikh's solution and its generalizations*, in: Proc. of the Conference Symmetry and Differential Equations, Krasnoyarsk (2000), pp. 180–183.
[183] V. V. Pukhnachov, *Solvability of initial boundary-value problem in nonstandard model of convection*, Zap. Nauch. Sem. POMI (St. Petersburg Division of Steklov Mathematical Institute), St. Petersburg, vol. 233 (1996), pp. 217–226.
[184] V. V. Pukhnachov, *Thermocapillary convection under low gravity*, Fluid Dynamics Trans., Warsaw, 14 (1989), pp. 145–204.
[185] V. V. Pukhnachov, *Unsteady analogs of the Birikh solution*, Izv. Alt. Gos. Univ., 62, no. 1/2 (2011), pp. 62–69.
[186] V. V. Pukhnachov, *Group-theoretical methods in the convection problems*, in: Application of Mathematics in Technical and Natural Sciences, edited by M. D. Todorov and C. I. Christov, American Institute of Physics, CP1404, Melville, NY (2011), pp. 31–42.
[187] V. V. Pukhnachov, *Convective flows in long tubes*, Bulletin of Lobachevsky State University of Nizhni Novgorod, 4, no. 5 (2011), pp. 2445–2447.
[188] T. P. Pukhnachova, *Numerical solution of a problem of viscous layer deformation by the thermocapillary forces*, in: Proc. Conf. Symmetry and Differential Equations, Krasnoyarsk (2000), pp. 183–186.
[189] V. V. Pukhnachov and V. A. Solonnikov, *On the dynamic boundary angle*, Prikl. Mat. Mekh., 46, no. 6 (1982), pp. 961–971.
[190] G. D. Rabinovich, *Separation of isotopes and other mixtures by thermodiffusion*, Atomizdat, Moscow (1981), 144 pp.
[191] G. D. Rabinovich, R. Ya. Gurevich, and G. N. Bobrova, *Thermodiffusion separation of fluid mixtures*, Nauka i Tekhnika, Minsk (1971), 243 pp.
[192] Y. Renardy and D. D. Joseph, *Oscillatory instability in a Benard problem of two fluids*, Phys. Fluids, 28, no. 3 (1985), pp. 788–793.
[193] Y. Renardy and M. Renardy, *Perturbation analysis of steady and oscillatory onset in a Benard problem with two similar liquids*, Phys. Fluids, 28, no. 9 (1985), pp. 2699–2708.
[194] I. V. Repin, *Steady flows of a two-layer fluid*, Master Dissertation, Krasnoyarsk State University, Krasnoyarsk (2003), pp. 1–35.
[195] P. J. Roache, *Computational fluid mechanics*, Hermosa, Albuquerque (1976).

[196] A. A. Rodionov, *Group analysis of microconvection equations and one nonclassical equation*, in: Proc. Workshop Mathematical Modeling in Mechanics, Inst. Comp. Math., Sib. Branch, Russian Acad. of Sci., Krasnoyarsk (1999), pp. 169–180. (Deposited at VINITI 05.07.1999, No. 1999-B99).

[197] A. A. Rodionov, *Some exact solutions of microconvection equations*, in: Symmetry and Differential Equations, Krasnoyarsk (2000), pp. 186–189.

[198] S. Rosenblat and D. M. Herbert, *Low-frequency modulation of thermal instability*, J. Fluid Mech., 43, no. 2 (1970), pp. 385–398.

[199] E. A. Ryabitskii, *Thermocapillary instability of the equilibrium state of a plane layer in the presence of a vertical temperature gradient*, Izv. Ross. Akad. Nauk, Mekh. Zhidk. Gaza, 3 (1992), pp. 19–23.

[200] I. I. Ryzhkov, *Invariant solutions of the thermal-diffusion equations for a binary mixture in the case of plane motion*, J. Appl. Mech. Tech. Phys., 47, no. 1 (2006), pp. 79–90.

[201] I. I. Ryzhkov, *Optimal system of subalgebras for thermodiffusion equations*, Vych. Tekhnol., 9, no. 1 (2004), pp. 95–104.

[202] I. I. Ryzhkov, *On the normalizers of subalgebras in an infinite Lie algebra*, Communications in Nonlinear Science and Numerical Simulation, 11, no. 2 (2006), pp. 172–185.

[203] I. I. Ryzhkov, *Symmetry analysis of the thermal diffusion equations in the planar case*, in: Proc. 10th International Conference on Modern Group Analysis, Larnaca, Cyprus (2005), pp. 182–189.

[204] I. I. Ryzhkov and V. K. Andreev, *Group classification and exact solutions of thermodiffusion equations*, Differ. Uravn., 41, no. 4 (2005), pp. 508–517.

[205] A. A. Samarskii and E. S. Nikolaev, *Methods of solving grid equations*, Nauka, Moscow (1978), 599 pp.

[206] A. A. Samarskii and P. N. Vabishchevich, *Numerical methods of solving convection-diffusion problems*, Editoral URSS, Moscow (1999), 247 pp.

[207] A. A. Samarskii, P. N. Vabishchevich, and P. P. Matus, *Difference schemes with operator multipliers*, Inst. Math. Model., Russian Acad. of Sci., Inst. Math., National Acad. of Sci. of Belorus', Minsk (1998), 442 pp.

[208] L. I. Sedov, *Mechanics of continuous media*, 4th edition, Nauka, Moscow, vol. 1 (1983), 536 pp.; vol. 2 (1984), 560 pp.

[209] J. Serrin, *On the uniqueness of compressible fluid motion*, Archive for Rat. Mech. and Anal., 3, no. 3 (1959), pp. 271–288.

[210] I. G. Shaposhnikov, *On the theory of convective phenomena in a binary mixture*, Prikl. Mat. Mekh., 17, no. 5 (1953), pp. 604–606.

[211] V. Shtern, V. Zimin, and F. Hussain, *Analysis of centrifugal convection in rotating pipes*, Phys. Fluids, 13, no. 8 (2001), pp. 2296–2309.

[212] A. F. Sidorov, V. P. Shapeev, and N. N. Yanenko, *Methods of differential relations and its applications in gas dynamics*, Nauka, Novosibirsk (1984), 272 pp.

[213] V. I. Smirnov, *A course in higher mathematics, Vol. 2: Advanced calculus*, Addison-Wesley, Reading (1964).

[214] B. L. Smorodin, *Convection of a binary mixture under conditions of thermal diffusion and variable temperature gradient*, J. Appl. Mech. Tech. Phys., 43, no. 2 (2002), pp. 217–223.

[215] V. A. Solonnikov, *A priori estimates for solutions of second-order differential equations of the parabolic type*, Tr. Mat. Inst. Im. V.A. Steklova, LXX (1964), pp. 133–212.

[216] V. A. Solonnikov, *Differential properties of the solution of the initial-boundary problem for a linearized system of the Navier-Stokes equations*, Tr. Mat. Inst. Im. V.A. Steklova, LXX (1964), pp. 221–291.

[217] D. R. Sood and H. G. Elrod, Jr., *Numerical solution of the incompressible Navier-Stokes equations in doubly connected regions*, AIAA J., 12 (1974), pp. 636–640.
[218] A. Tani, *On the first initial-boundary value problem of compressible viscous fluid motion*, Publ. Res. Math. Sci. Kyoto Univ., 13 (1977), pp. 193–253.
[219] E. L. Tarunin, *Computational experiment in free convection problems*, Izd. Irkut. Univ., Irkutsk (1990), 225 pp.
[220] E. L. Tarunin, *On the choice of the approximating formula for vorticity on the solid boundary in solving problems of viscous fluid dynamics*, Chisl. Metody Mekh. Sploshnoi Sredy, 9, no. 7 (1978), pp. 97–111.
[221] R. Temam, *Navier-Stokes equations. Theory and numerical analysis*, North-Holland, Amsterdam (1977).
[222] A. N. Tikhonov, A. B. Vasilieva, and A. G. Sveshnikov, *Differential equations*, Nauka, Moscow (1980), 231 pp.
[223] D. J. Tritton, *Physical fluid dynamics*, Oxford University Press (1988), 519 pp.
[224] F. G. Tricomi, *Integral equations*, Interscience, New York (1957).
[225] C. Trusdell, *First course in rational continuum mechanics*, The Johns Hopkins University, Baltimore (1972).
[226] N. B. Vargaftik, *Handbook on thermophysical properties of gases and liquids*, Nauka, Minsk (1972).
[227] G. Venezian, *Effect of modulation on the onset of thermal convection*, J. Fluid Mech., 35 no. 2 (1969), pp. 243–254.
[228] A. F. Voevodin, *Methods of fractional steps for the Stokes and Navier-Stokes equations in closed singly connected and doubly connected domains*, in: Dynamics of Continuous Media (Collected Papers), Inst. Hydrodynamics, Sib. Branch, Acad. of Sci. of the USSR, Novosibirsk, vol. 113 (1998), pp. 22–26.
[229] A. F. Voevodin and O. N. Goncharova, *Calculation of free convection in a changing field of the gravity force*, in: Dynamics of Continuous Media (Collected Papers), Inst. Hydrodynamics, Sib. Branch, Acad. of Sci. of the USSR, Novosibirsk, vol. 67 (1984), pp. 21–28.
[230] A. F. Voevodin and S. M. Shugrin, *Methods of solving one-dimensional evolutionary systems*, Nauka, Novosibirsk (1993), 368 pp.
[231] O. V. Voinov, *Wetting hydrodynamics*, Izv. Akad. Nauk SSSR, Mekh. Zhidk. Gaza, 5 (1976), pp. 76–84.
[232] O. V. Voinov, *Dynamics of wetting of a solid by liquid: movement of thin film*, in: Encyclopedia of Surface and Colloid Science, Marcel Dekker Inc., New York (2002), pp. 1546–1559.
[233] S. Wiegand, *Thermal diffusion in liquid mixtures and polymer solutions*, J. Phys.: Condens. Matter., 16 (2004), pp. 357–379.
[234] H. Y. Wong, *Handbook on essential formulae and data on heat transfer for engineers*, Longman (1977).
[235] S. Yanase and K. Kohno, *The effect of a salinity gradient on the instability of natural convection in a vertical fluid layer*, J. Phys. Soc. Japan, 54, no. 10 (1985), pp. 3747–3756.
[236] C. S. Yih and C. N. Li, *Instability of unsteady flows or configurations. Part 2. Convective instability*, J. Fluid Mech., 54, no. 1 (1972), pp. 143–152.
[237] V. I. Yudovich, *Convection of an isothermally incompressible fluid*, Deposited at VINITI 28.05.99, no. 1699–99, 41 pp.
[238] V. I. Yudovich, *Method of linearization in the hydrodynamic theory of stability*, Rostov-na-Donu (1984), 192 pp.
[239] V. F. Zaitsev and A. D. Polianin, *Handbook on ordinary differential equations*, Fizmatlit, Moscow (2001), 576 pp.

[240] V. E. Zakhvataev, *Models of convection of weakly nonisothermal liquids and gases under microgravity conditions*, in: Proc. Intern. Conf. Mathematical Models and Methods of Their Study, vol. 1, Krasnoyarsk State University, Krasnoyarsk (2001), pp. 259–264.
[241] A. Zebib, G. M. Homsy, and E. Meiburg, *High Marangoni number convection in a square cavity*, Phys. Fluids, 28, no. 12 (1985), pp. 3467–3476.
[242] Ya. B. Zeldovich, *On surface tension of the interface of mutually solvable fluids*, Zh. Fiz. Khimii, 23 (1949), pp. 931–935.

Index

basic thermodynamic identity 20, 32
binary mixture 153, 154, 158, 186, 259, 309, 310, 317
Boussinesq parameter 49, 100, 142, 216, 226, 234, 237, 241, 246, 248, 254, 261, 314

coefficient of thermodiffusion 154
coefficient of volume viscosity 47
complex decrement 232, 233, 237, 240, 248, 252, 253
compressibility parameter 65, 68
conditions of Thom or Woods type 271
continuity hypothesis 1, 2, 4
convective acceleration 6
convective stability 194, 201, 202
convergence criterion 264, 272, 290, 291

diffusion 86, 153, 154, 163, 164, 258, 259, 309, 311, 316, 320, 322, 338
dissipation parameter 49
dissipative function 19, 23, 47, 49, 62, 65, 66, 75, 113, 114
Dufour effect 258, 260
dynamic condition on an interface 31, 39
dynamic viscosity coefficients 19, 316

energy condition on an interface 40
equations of convection in a rotating fluid 211
equations of convection in a weakly compressible fluid 71, 79, 92
equivalence transformation 63, 65, 115, 149, 151, 153, 158, 159, 161, 164, 172

factor-system 113, 116, 120–123, 179, 187
first law of thermodynamics 14
free boundary 25, 26, 41, 42, 44, 50, 52, 113, 148, 149, 152, 153, 187–191, 193–195, 201, 221, 235–237, 240, 242, 244, 284, 286–288, 291–300, 315, 316, 318, 319

Galileo number 205, 207, 210, 237, 304
Gibbs–Duhem equation 33
Grashof number 50, 183, 221, 226, 248, 252, 253, 255

heat flux vector 13
high-frequency acoustic oscillations 74, 79

interface 25–27, 29, 31–36, 39–44, 50–52, 113, 141, 147, 148, 151–153, 193, 201–204, 206, 207, 209, 210, 320, 321, 331
invariant solution 93, 96, 123, 124, 134, 141, 153, 177, 178
isothermally incompressible fluid 45–47, 52, 71, 72, 75, 80, 81, 92, 100, 258, 268, 294, 301
iteration parameter 263, 270, 280, 289, 296, 297

kinematic condition on an interface 31
Korteweg stresses 321, 322, 338, 339
Krylov–Bogolyubov averaging technique 142

Lie group 115, 153
long-wave instability 207, 211

Marangoni number 237, 240–245, 284, 286, 316–318
mean curvature 29, 32, 147, 189, 203, 235
method of alternating directions 262, 266, 268, 270, 330
microconvection model 51, 61, 74, 92, 100–102, 104, 140, 142, 146, 221, 231, 234, 236, 252–254, 257, 259, 261, 265, 268–271, 274, 277–279, 282–284, 289–291, 293–297, 299, 301, 304, 305, 307, 308, 314, 315, 317–319, 338
microconvection parameter 50, 56, 66, 74, 228, 237, 248, 254, 261, 268, 281, 304, 315
model of convection of a viscous heat-conducting fluid 50
modified pressure 49, 54, 55, 75, 260, 285, 302
modified velocity 73–75, 260, 261, 264, 268, 269, 278, 317
monotonic instability 197, 199, 200, 208, 211

neutral curves 200, 201, 207–210, 241–243, 253, 255
Newtonian fluids 18, 25, 35, 81, 257
no-slip condition 35, 43, 44, 53, 56, 62, 73, 78, 93, 94, 104, 132, 141, 181, 189, 212, 217, 245, 246, 259, 261, 268, 287, 288, 303, 316, 322
normal stresses 10, 40, 53, 203, 296

Oberbeck–Boussinesq model 269–271, 274–279, 282, 283, 286, 289, 292–297, 299–301, 305, 308, 314, 315

partially invariant solution 122, 152, 217
Prandtl number 49–51, 64, 66, 140, 183, 205, 207, 214, 217, 219, 228, 237, 243, 244, 248, 261, 273, 281, 284, 303

Rayleigh number 50, 55, 75, 85, 183, 186, 201, 205, 207, 208, 211, 216, 220, 221, 228, 234, 237, 241, 246, 281, 284, 308

Schmidt number 183
second law of thermodynamics 15, 22
shear stresses 10, 11, 40, 53
similarity criteria 63–65
smooth solution 71, 104
Soret effect 153, 309, 310, 316
stability 33, 92, 154, 155, 185, 186, 193, 194, 196, 201, 202, 205, 207–211, 216, 217, 221, 225, 228, 231, 233, 241–244, 252, 254, 262, 291, 292, 299
stream function 74, 220, 259–262, 268, 269, 272, 277–279, 284–288, 295, 317–320, 327–329, 331–339
stress tensor 4, 10, 13, 15, 16, 18, 27, 28, 147, 148, 203
surface phase energy 32
surface phase entropy 32
surface phase free energy 32
sweeping with parameters 280, 281, 297

temperature coefficient of surface tension 33, 147, 294
thermal conductivity coefficient 16, 17, 113, 147, 217, 235, 245
thermal diffusivity 21, 49, 64, 114, 115, 154, 194, 205, 259, 301
thermally inhomogeneous and weakly compressible convection 89
thermogravitational convection 50
trajectories of fluid particles 92, 100, 101, 142, 269

volume and surface forces 2
vorticity 74, 259–262, 264, 265, 268, 269, 271, 272, 277, 280, 281, 284–288, 290, 295, 296, 317, 329

wave vector 196, 206
Weber number 205, 207, 208, 210, 237, 244

De Gruyter Studies in Mathematical Physics

Volume 53
Vladimir K. Dobrev
Invariant Differential Operators: Volume 4: AdS/CFT, (Super-)Virasoro, Affine (Super-)Algebras, 2019
ISBN 978-3-11-060968-4, e-ISBN (PDF) 978-3-11-061140-3,
e-ISBN (EPUB) 978-3-11-060971-4

Volume 52
Alexey V. Borisov, Ivan S. Mamaev
Rigid Body Dynamics, 2018
ISBN 978-3-11-054279-0, e-ISBN (PDF) 978-3-11-054444-2,
e-ISBN (EPUB) 978-3-11-054297-4

Volume 51
Peter Galenko, Vladimir Ankudinov, Ilya Starodumov
Phase-Field Crystals: Fast Interface Dynamics, 2019
ISBN 978-3-11-058597-1, e-ISBN (PDF) 978-3-11-058809-5,
e-ISBN (EPUB) 978-3-11-058653-4

Volume 50
Sergey Lychev, Konstantin Koifman
Geometry of Incompatible Deformations: Differential Geometry in Continuum Mechanics, 2018
ISBN 978-3-11-056201-9, e-ISBN (PDF) 978-3-11-056321-4,
e-ISBN (EPUB) 978-3-11-056227-9

Volume 49
Vladimir K. Dobrev
Invariant Differential Operators: Volume 3: Supersymmetry, 2018
ISBN 978-3-11-052663-9, e-ISBN (PDF) 978-3-11-052749-0,
e-ISBN (EPUB) 978-3-11-052669-1

Volume 48
Jared Maruskin
Dynamical Systems and Geometric Mechanics: An Introduction, 2018
ISBN 978-3-11-059729-5, e-ISBN (PDF) 978-3-11-059780-6,
e-ISBN (EPUB) 978-3-11-059803-2

www.degruyter.com